IPP Max-Planck-Institut für Plasmaphysik

Annual Report 2003

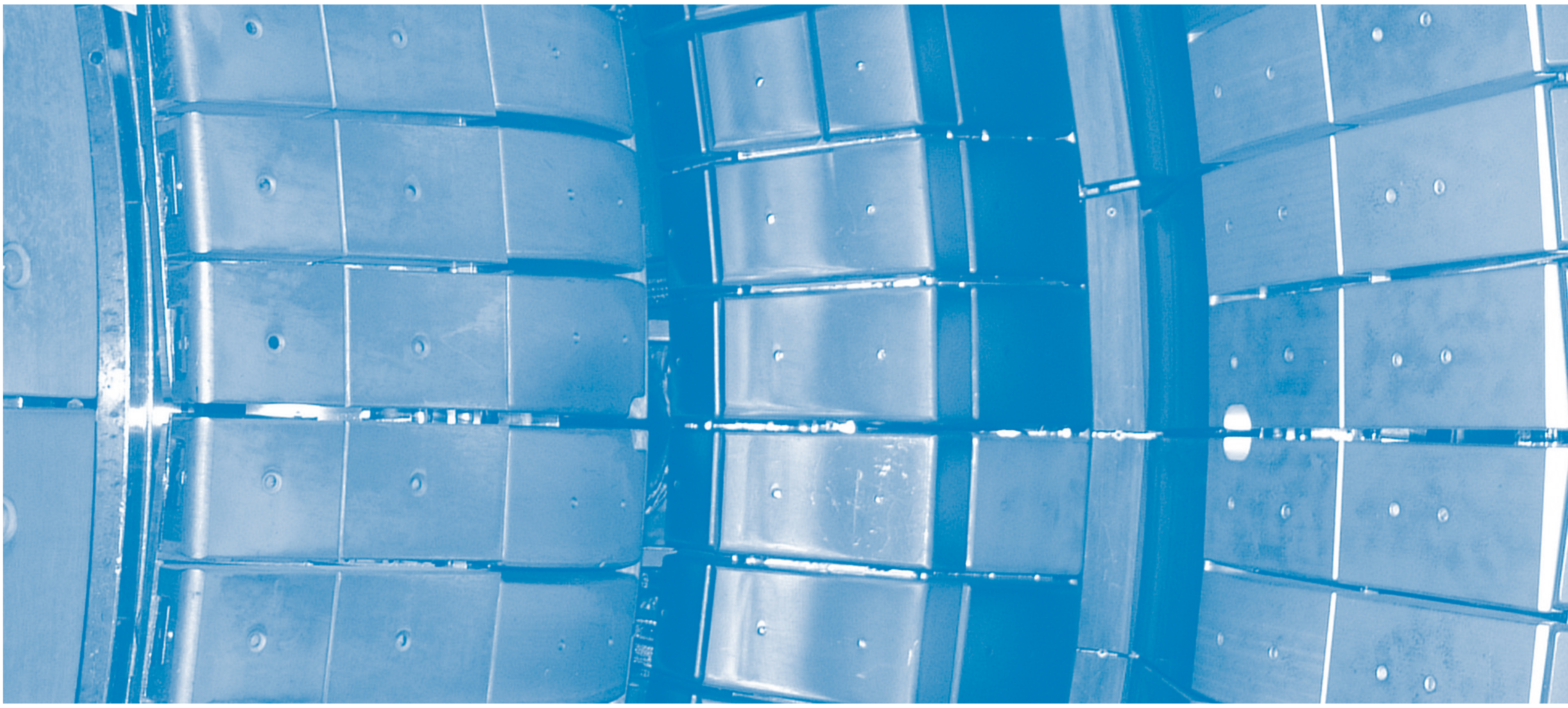

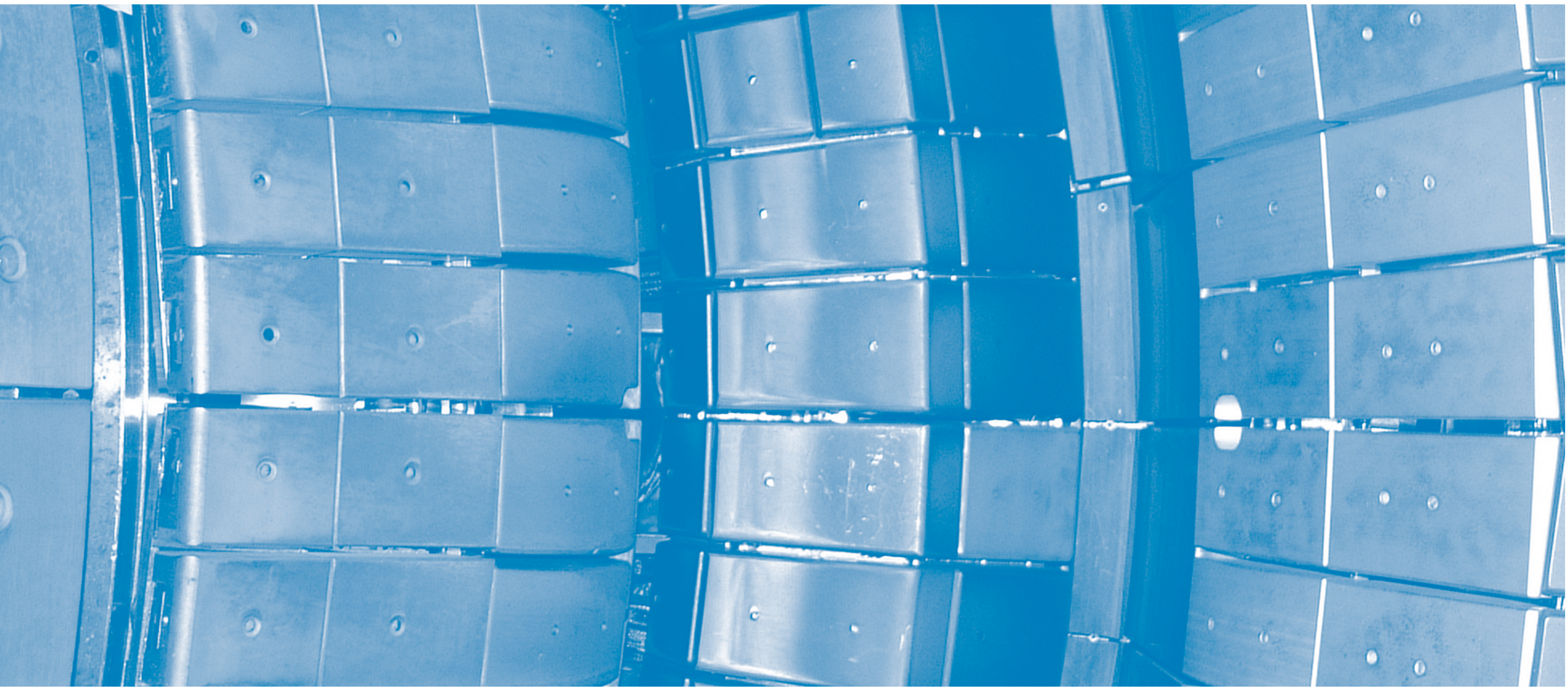

View from top into the ASDEX Upgrade divertor showing the present mix of W-tiles on the inner and outer entrance baffle.
central part: strike points
left and right parts: C-tiles on the roof baffle

Max-Planck-Institut
für Plasmaphysik

EURATOM Association

Annual Report 2003

The Max-Planck-Institut für Plasmaphysik is an institute of the Max Planck Gesellschaft, part of the European Fusion Programme (Euratom) and an associate member of the Helmholtz-Gemeinschaft Deutscher Forschungszentren.

Alexander M. Bradshaw

The Max-Planck-Institut für Plasmaphysik (IPP) carries out fundamental research in high temperature plasma physics and related areas. These investigations form the scientific basis for the realisation of a future fusion power plant using the magnetic confinement concept. Research concentrates on the two main types of fusion experiment, tokamak and stellarator, as well as on theory, plasma-surface interactions and materials. The experiments on the ASDEX Upgrade tokamak in Garching are directed towards the next step in fusion research, the planned international tokamak experi-ment ITER. Construction of the WENDELSTEIN 7-X stellarator in Greifswald progresses steadily; completion is foreseen for 2010. This device is being built to demonstrate that the stellarator is a viable option for the step after ITER, namely, the construction of a demonstration fusion power plant.

Since ASDEX Upgrade was opened to more extensive use by other European fusion research institutes (the "Associations") in 2002, contributions from our partners have become more numerous and more important. In 2003 the number of Associations represented on the ASDEX Upgrade programme committee increased to ten. More-over, new hardware for diagnostics has been installed on ASDEX Upgrade by several of our European partners, thus opening up exciting new possibilities for joint research. Numerous papers and conference contributions by non-IPP authors testify to these developments. IPP physicists have continued to make major contributions to the preparation and implementation of the experimental campaigns on the Joint European Torus (JET) in Culham, UK. More than thirty IPP scientists have been seconded to JET, three of them as Task Force Leaders. The strong support given by IPP to the European ITER contributions is reflected in the good progress made on the development of an RF source for the NNBI system and in the R&D work for diagnostics and heating systems.

In the area of plasma-facing components the percentage of surface covered with tungsten-coated tiles on ASDEX Upgrade has been further increased in order to demonstrate the viability of this alternative wall material for ITER. So far, no deleterious effect of the tungsten on plasma operation has been found and preparations for completely covering the interior with tungsten are proceeding.

Following the shutdown of WENDELSTEIN 7-AS in July 2002 the analysis of the extended database has concentrated on the understanding of the newly discovered high density H-mode (HDH-mode) with its favourable properties and of the surprisingly high ·{β}-values obtained in the presence of the island divertor modules. A comparison of the conventional ELM-free H-mode followed by the HDH-mode in the same discharge demonstrates the completely different impurity transport properties.

There has been substantial progress in the construction of the successor experiment, WENDELSTEIN 7-X. The first coils were successfully tested in Saclay and the first non-planar coil was delivered to IPP Greifswald. The characteristics of the superconducting coils are those expected from the properties of the superconducting NbTi filaments. The first plasma vessel segments and the first ports have been completed and delivered. The Thales Maquette and the CPI gyrotron - the first high-power steady-state 140 GHz gyrotrons - have also arrived in Greifswald. The Maquette gyrotron, powered by the recently commissioned solid-state high-voltage power supply, is now operated routinely. The assembly tools and scaffolding have been constructed and the first assembly trials performed. More than half of the modular and planar coils, of the vessel and cryostat components and of the ports are in various stages of fabrication. The assembly and installation of the coil power supplies has begun and will be completed by the end of 2004.

Last but not least, there is good news concerning ITER: the international negotiators met at the ministerial level in the US in December 2003 and concluded that there are two excellent sites for ITER (in Europe and in Japan), but that a further evaluation is needed before a decision based on consensus can be made. At the time of this Annual Report going to press, the comparative assessment of the two sites by the six ITER partners continues. Moreover, it was decided at the ministerial meeting that a so-called "broader project approach to fusion power" should be explored.

On behalf of the Directorate and the Scientific Board I would like to take this opportunity of thanking our staff for their dedication, for the research results obtained and for the very high quality of their work generally throughout the year.

Projects & Research Fields

University Contributions to IPP Programme

Publications

Appendix

Projects & Research Fields

ASDEX Upgrade

Head of Project: Dr. Otto Gruber

Overview

1.1 Scientific Aims and Operation

The design of the tokamak fusion experiment ASDEX Upgrade (AUG) combines the successful divertor concept of ASDEX with the requirements of a next step fusion reactor, in particular the need for an elongated plasma shape and poloidal magnetic field coils outside the toroidal magnetic field coils. As a result, AUG is close to ITER in its magnetic geometry and in particular the relative length of both divertor legs compared with the plasma dimension. The flexible heating system consists of neutral beam (NBI), ion cyclotron resonance (ICRF) and electron cyclotron resonance (ECRF) injection, as envisaged for ITER, with a total heating power of 28 MW, ensuring that the energy fluxes through the plasma flux surfaces are equivalent to those in ITER. The scientific programme gives priority to the preparation of the design, physics basis and discharge scenarios of ITER. The studies are guided by five Task Forces consisting of

- Confinement and performance of the ITER base-line scenario, the ELMy H-mode and improved H-mode scenarios leading to enhanced performance, long pulse and possibly steady-state operation,
- Scenarios and physics of advanced tokamak plasma concepts with both internal transport barriers (ITB) and mainly non-inductive current drive,
- H-mode pedestal physics and ELM mitigation and control,
- Magnetohydrodynamic (MHD) stability, active stabilisation of β limiting instabilities as well as avoidance and mitigation of disruptions,
- Scrape-off layer and divertor physics with the aim of optimising power exhaust and particle control (ash removal) and optimization of first wall material with emphasis on tungsten.

The similarity of ASDEX Upgrade to ITER makes it particularly suited to testing control strategies for shape, plasma performance and MHD modes. Additionally, the similarity in cross-section to other divertor tokamaks is important in determining size scalings for core and edge physics. This collaborative work was enhanced in the JET operation under EFDA during the last years. In particular, the physics programme of 2003 was based on the conclusions and findings of the last years, new ITER requirements and tokamak concept improvement (see section 1.2). Our programme has a strong impact on the ITPA “High Priority Physics Research Areas” and the “Physics R&D Needs for the EU Fusion Programme” (SWG-2002). Several items described below have been further investigated in Joint Experiments at all major tokamaks as proposed by the ITPA Topical groups and approved in the framework of the IEA Implementing agreements. In summary, the ASDEX Upgrade programme is embedded in a framework of national (see section on University contributions to IPP programme) and international collaborations (see section 10 on International Co-operation).

The AUG Programme Committee enables the Associations to take more responsibility for our programme. This body defines the Task Forces responsible for the different elements of the ASDEX Upgrade programme, nominates the Task Force Leaders and approves the experimental programme. At present, it comprises 10 members from the associations and 9 from IPP. Furthermore, the bodies that work out the programme proposals, are now open for external participants and remote participation in these meetings is possible. With this structure, we have achieved a compromise between the increased international participation and the flexibility that has so far been typical for the AUG programme.

During the 2003 experimental campaign, ASDEX Upgrade operated routinely with NBI powers up to 17.5 MW, which allowed studies of the influence of heat deposition on energy and particle transport, of MHD stability and of fast particle effects. The ICRF heating system is now capable of routinely delivering up to 5 MW even in ELMing H-mode discharges. Even 7 MW could be launched after some conditioning discharges. This capability was used, through comparison with NBI heating, to separate the effects of heating, deep particle refuelling, toroidal momentum input and localisation of power deposition. The present ECRF system was kept available up to a coupled power of 1.6 MW allowing pure electron heating (ECRH) and current drive (ECCD), electron transport studies and MHD mode control of sawteeth and neo-classical tearing modes (NTM). Both RF systems allow the control of particle and impurity transport via the heat deposition profile. Provisions for current drive and for active control of current profiles in advanced scenarios were available with more perpendicular on-axis or off-axis tangential NBI and ECRF using steerable mirrors. Stationary discharges with up to 10 s flat-top allowed steady state investigations not only on the transport and MHD time scales but also for more than five current diffusion times, still a unique feature for tokamks with ITER plasma geometry.

The operation regarded the hardware upgrades from 2002, namely the extension of the tungsten coated first wall area based on the positive experience with tungsten plasma facing components so far, and the equipment of the ICRH antennas with new straps. The heat shield tiles on the high field side limiter were replaced by larger tungsten coated tiles being capable of higher heat loads. Additionally, first wall parts at the low field side were covered by tungsten so that the total tungsten covered surface was about 15 m^2 corresponding to 40% of the first wall. The shaping capability was extended up to triangularities $\delta = 0.55$ at the separatrix (with elongations $\kappa \leq 1.8$) exceeding the ITER operational range and allowing for studies on the influence of plasma shape on performance as well as on similarity experiments with medium and small aspect-ratio devices. The Div IIb divertor geometry is still adapted to these plasma shapes.

Major points of our experimental programme have been the investigation of the particle transport, electron transport, exploration of confinement and maximised plasma pressure in improved H-modes, active MHD stability control and Alfven Eigenmodes. This is combined with the stability and transport in the H-mode edge, the combination with tolerable and controlled ELMs, wall interaction physics and tungsten as wall material.

1.2 Summary of Main Results

Both ion and electron temperature ($T_{i,e}$) profiles in conventional H- modes on AUG are generally stiff and limited by a critical temperature gradient length L_T=T/∇T normalized to the major radius R as given by ion temperature gradient (ITG) and trapped electron (TEM) driven turbulence. Electron cyclotron heating and modulation experiments revealed the electron temperature profile stiffness, as predicted by TEM turbulence, under dominant electron heating conditions in low density L-mode discharges with T_i>>T_e. In H-modes with T_e>T_i the electron temperature profile is even more resilient and the TEM threshold is higher.

Density profiles are not stiff, and confinement improves with density peaking. The particle transport and hence the density profile shapes are governed by anomalous transport due to ITG and TEM driven turbulence predicting both on- and off-diagonal contributions to the particle flux. These terms are influenced by the collisionality and the heat deposition profile. The often observed density peaking decreases with increasing collisionality, as both inward and outward contributions to the anomalous particle flux decrease, but the decrease of the inward contribution is stronger. Therefore, at high collisionality the neo-classical inward Ware pinch becomes comparable to the anomalous off-axis pinch terms. The observed density profile peaking with off-axis deposition and profile broadening with central RF deposition was explained by a link between particle fluxes and heat fluxes: on-axis deposition leads to a high central heat flux and consequently an increased central particle out-flux. This is substantiated by drift wave theory showing a change of the thermodiffusive flux contribution, which is usually directed inward for ITG instabilities, but can lead to an outward pinch with enhanced electron heating and hence dominating TEMs. A corresponding impurity transport behaviour was observed for tungsten and other injected impurities.

A main focus has again been the stationary improved H-mode scenarios developed since 1998 at ASDEX Upgrade combining high β_N >3, improved confinement ($H_{98\text{-}P} \leq 1.4$) and operation both at low densities with ITER relevant collisionality as well as high density operation close to the Greenwald density limit for optimal divertor operation. In the high density branch at plasma configurations near double null a combination with tolerable type II ELMs is achieved. These integrated scenarios have a low central magnetic shear with q_0 above, but near one, in the centre avoiding sawteeth and (3, 2) NTMs remain small at highβ. Both β_N and H factors increase with triangularity and the performance measure β_N $H_{98\text{-}P}$ / q_{95}^2 is nearly independent of the edge safety factor over a range $q_{95} \approx 3.3$ to 4.2. The total non-inductively driven current exceeds 50% of the plasma current making this improved H-mode a serious candidate for a long pulse stationary integrated reactor scenario with "hybrid" current drive consisting of non-inductive and a small amount of inductive drive. This year the scenario was further developed in common q-scan experiments with DIII-D and successfully demonstrated at JET providing a more robust extrapolation to ITER.

In the experiments with ion ITBs and strong reversed shear a core region with nearly zero current density, a “current hole”, was found, as already observed at larger devices. An optimised heating scenario in the current ramp-up using counter-ECCD followed by NBI resulted in simultaneous electron and ion ITBs with central temperatures of 8 to 10 keV which survived the first small ELM activity for some hundred ms´s.

After successfully removing (3,2) and (2,1) NTMs by DC ECCD in the respective magnetic islands to replace the missing bootstrap current, the influence of the width of the absorbed ECCD power compared with the island width was investigated. The remaining NTM amplitudes increase with increasing absorption width. Another tool to control NTMs is the reduction of seed islands by controlling the sawtooth frequency and amplitude using NBI, ECRH and co- / counter ECCD both inside and outside the sawtooth inversion radius. Prevention of NTMs could be demonstrated. Finally the impact of NTMs on confinement can be reduced by transition to the low amplitude (3,2) FIR-NTM regime with coupled (3,2), (4,3) and (1,1) modes. This transition was actively controlled by triggering (4,3) tearings using co-ECCD at the (4,3) surface.

Active control techniques used to ameliorate ELM energy deposition or to avoid ELMs entirely was a major task this year. At high densities, q_{95}>3.5 and closeness to magnetic double null configuration, small type II ELMs combine low power loading with only a modest reduction in confinement. Another way to mitigate ELMs is to control their frequency and amplitude by injecting small high-frequency deuterium pellets. Reliable type I ELM triggering by each pellet was demonstrated up to a frequency of 80 Hz without detrimental confinement reduction. This pellet-triggering scheme has been integrated in a high performance radiative feedback scenario in order to avoid radiation collapses. The non-linear evolution of ELM structure was investigated by its footprint on the target heat load structures using a new thermography system. Finally, steady ELM-free H-modes can be obtained with counter NBI, the “QH-mode”.

Toroidicity induced Alfven Eigenmodes (TAE) due to fast particles are destabilized in ASDEX Upgrade using ICRH with unstable toroidal mode numbers n=3 to 6 which propagate in the current direction, i.e. the ion diamagnetic drift direction. Their characterization in terms of amplitudes, frequency and toroidal, poloidal and radial mode structure was established.

The scaling of energy and particle losses of type I ELMs was assessed as well as their precursor structures. The power loading and the time scales of ELMs significantly influence the choice of the first wall and divertor material in ITER. On AUG the power deposition on the divertor structures accounts for only about 50% of the ELM energy losses in the midplane. This is comparable to that found for the total plasma and poloidal energy losses in disruptions. The ELM power load to the non-divertor first wall structures was measured to be below 25%, while the rest is radiated. As the divertor power loading profiles during disruptions are rather broad, the peak power loads in disruptions are even below those during ELMs.

Finally, the plasma operation with tungsten coverage of large wall areas shows tungsten concentrations below 10^{-5}. In discharges with improved core confinement a tailored central RF heating was always sufficient to control the impurity content accompanied by only a modest reduction of energy confinement. Increased W-concentrations in low ELM frequency discharges were overcome by controlling the ELM frequency with pellet injection.

1.3 ASDEX Upgrade Technical Enhancements and Programme in 2004

The programme in 2004 will be executed in co-operation with the EU Associations and in close connection with the JET programme and the ITPA joint experiments. Main emphasis will be on the dimensionless scaling of confinement and maximum stable β and dominant reactor-relevant ICRH in the improved H-modes. Current profile can be controlled and sustained in a flexible way, where the off-axis NBI current drive still needs consolidation. NTM control, disruption avoidance and mitigation, and ELM control using triggering by pellets and vertical position oscillations and QH-mode are further issues. The tungsten coverage of all relevant structures has the highest priority in the present AUG hardware extension programme. Another 13.6 m^2 of newly tungsten coated tiles have been mounted in the shutdown period August–December 2003, including the complete upper divertor.

A new fast control and data acquisition system will be in operation at the end 2004. The upgrading of the ECRF power to 4 MW at tuneable frequencies between 104 and 140 GHz is underway. The four launchers were already installed in the 2003 shut-down. To reach the ultimate ideal MHD limits in addition to profile control, the introduction of a stabilizing wall at the low field side close to the plasma in combination with active feedback coils working on the resistive time scale of the wall are under consideration and have been supplemented by 3D MHD stability calculations.

In this annual report, sections 2- 6 are concerned with stationary improved H-modes, active control of core MHD modes, ELM pace making and mitigation, toroidicity induced Alfven Eigenmodes and progress in particle transport understanding. In section 7 the ASDEX Upgrade technical and heating systems are described. Section 8 deals with electron heat and impurity transport, type I ELM physics, QH-mode operation, zonal flow and radial electric field shear measurements and plasma regime identification. Section 9 covers SOL and divertor physics, ELM structure, and power loads during ELMs and disruptions.

Stationary advanced scenarios at ASDEX Upgrade

For “steady state” operation of tokamaks, with significant fusion power gain, so-called “advanced scenarios” are required. Currently it is planned to use a hollow current density distribution, leading to the formation of transport barriers (ITB´s) in the core of the plasma to achieve improved confinement. Yet, after nearly a decade of intensive research, no convincing demonstration of steady state operation in reactor relevant conditions has been obtained in this regime.

Since 1998 ASDEX Upgrade has developed a new stationary regime of operation with improved core confinement for both electrons and ions in combination with an H-mode edge. Initially, the pressure increase in the core was attributed to a formation of an internal transport barrier. However, quickly after, detailed transport analyses showed that in such a regime the temperature profiles remain in the so-called stiff regime; the gradients do not exceed a critical temperature gradient length set by the turbulence in the plasmas and hence no ITB is produced. This new regime was called “Improved H-Mode”. Further developments of this regime in recent years by ASDEX Upgrade and DIII-D are now known under the common name “ITER Hybrid Scenario”. Key to this regime is to obtain a different stationary profile of the safety factor (q-profile) with a central q-profile near 1 and with very low magnetic shear - a hybrid of the non-inductive, reversed shear, scenario with internal transport barriers, and the q-profile of standard H-modes.

The specific q-profile for the hybrid scenario is obtained by heating during the current rise phase of the discharge, at moderate input power in order to avoid a reversed q-profile or the formation of an ITB. In the subsequent main heating phase, no strong neoclassical tearing modes (NTMs) occur due to the absence of sawteeth. Hence the plasma pressure can be increased to $\beta_N \sim 3$. Despite operating at $q_{95}{\sim}4$ compared to standard H-modes ($q_{95}=3$), the capability of operation at $\beta_N \sim 3$ allows hybrid discharges to achieve values for $(H_{89}\beta_N /q_{95}^2) \sim 0.40$, providing a possible route to long pulse operation with Q=10 in ITER. Operating at lower plasma current compared to the ITER reference scenario, the hybrid scenario could reduce the potential for damage in the case of disruptions (sudden terminations of the plasma discharge) and could lengthen the duration of the discharge, through reduced flux consumption.

ASDEX Upgrade has demonstrated operation of this regime at 80% to 90% of the Greenwald density limit, in discharges with $\delta=0.43$, with a confinement ($H_{98}(y,2)$ = 1.1-1.2) while sustaining $\beta_N = 3.5$ (see annual report for 2001). In these conditions, non-inductive current fractions of typically ~50%, in combination with benign MHD modes in the core (fishbones and NTMs) maintain a inherently stationary q-profile on the current relaxation time scale. With these encouraging results from ASDEX Upgrade, international collaboration, coordinated under auspices of the ITPA (International Tokamak Physics Agreement) was started in 2003, to provide more insight into the physics of the performance improvement and the use of this regime in a reactor. Discussions within the steady-state operation and energetic particles and the transport and internal transport barrier topical groups of the ITPA stimulated proposals to establish the regime in more devices (like JET) and to map the existence domain of this type of discharge as a function of q_{95} and density in experiments in ASDEX Upgrade and DIII-D.

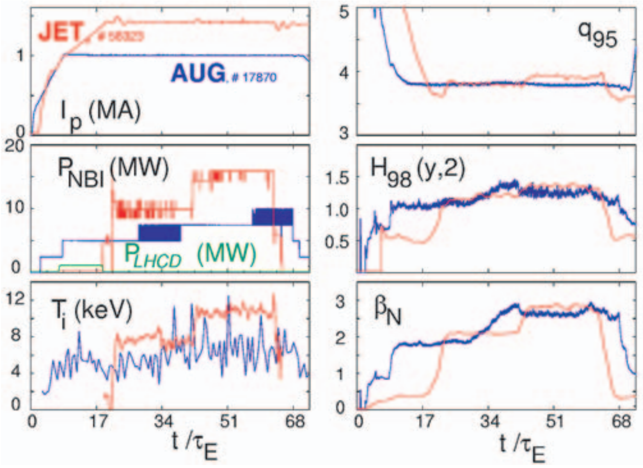

Figure 1: Matched hybrid scenario discharges in AUG and JET, showing that similar values for H_{98}(y,2) and β_N can be achieved. For the x-axis the time duration is normalised to the energy confinement time during the high β phase of the discharges (115 ms for AUG and 210 ms for JET).

The results of the JET experiments show that by matching the plasma shape, q-profile and ρ* of ASDEX Upgrade, the hybrid scenario can be obtained at JET. ASDEX Upgrade concentrated on matching the plasma shape used in the JET experiments as to make a better comparison with the JET results. Figure 1 shows a JET discharge at 1.4MA/1.7T and an ASDEX Upgrade discharge at 1MA/2.1T with matched plasmas shapes. For these discharges the q-profile can also be matched enabling similar values for confinement and β to be obtained. In this figure the time axis is normalised to the energy confinement time during the high β phase. For these two discharges the shape of the density profile and temperature profiles are also similar.

Both DIII-D and ASDEX Upgrade started with documenting the hybrid regime by variation of q_{95}. This was done at fixed plasma current (I_p), and varying the toroidal field (B_t) as the confinement in H-mode plasmas has only a weak dependence on B_t ($\tau_E \propto B_t^{0.15}$). As the q-profile plays an important role a variation of q_{95} will for example corroborate the role of MHD modes. In ASDEX Upgrade stationary operation of the hybrid scenario at the maximum β was documented for three different values for q_{95} (3.3, 3.9 and 4.3). In these experiments the maximum beta is limited by the occurrence of "large" (2,1) NTM modes. The amount of neutral beam power that can be applied at q_{95}=4.3 is substantially higher compared to q_{95}=3.3. At the lower value of q_{95}=3.3, sawteeth can not be suppressed and NTM modes were triggered at $\beta_N \sim 2.5$. The trend that the β limit increases with q_{95} is also reported from DIII-D which made a similar scan in q_{95}. In these experiments the fusion figure of merit, $(H_{89}\beta_N/q_{95}^2) \sim 0.4$ is be obtained at q_{95}~4.3, while results indicate that with early heating even plasmas at low q_{95}~3.3 could exceed the ITER design values for Q=10, mainly because ITER assumes a conservative β limit at this q_{95} of $\beta_N \sim 1.8$.

Data of various experiments from discharges with internal transport barriers and from the hybrid regime have been collated to form an international database. This database has been used to plot progress made over the past few years and to compare different advanced scenario regimes. ASDEX Upgrade has contributed a significant fraction (> 30%) of the data to this international database. An example of a comparison between ITB discharges and hybrid scenarios is given in Figure 2. The requirements for ITER are indicated. From the experimental results obtained, the hybrid scenario comes close to these ITER requirements, while the discharges with ITB´s do not achieve the required density or the required performance in stationary conditions. Thus discharges with ITB´s provide no firm basis for satisfying ITER's second major goal of reaching Q=5 under fully non-inductive conditions.

With the success of the international collaboration and the important role of ASDEX Upgrade, future experiments will concentrate on: (i) investigating the reason for the confinement improvement in hybrid scenarios, (ii) a more detailed study into the benign MHD behaviour in this regime, (iii) continue experiments in defining the optimum parameter range for the regime (q_{95}, density, or heating scheme), (iv) proceed with experiment having $T_e \sim T_i$ and the use of radio frequency heating which is more similar to power heating and (v) to push regime towards ITER parameters (ρ^*,β_N).

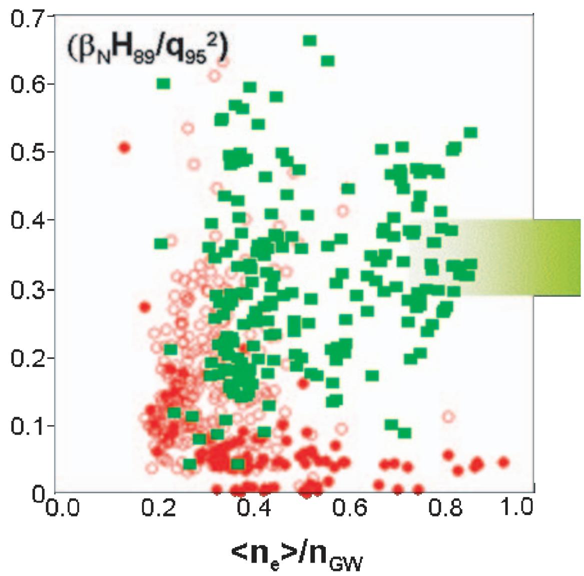

Figure 2: Overview of advanced scenario results from ASDEX Upgrade and other tokamaks in the international database. Open red circles are ITB discharges with a duration < $10\tau_E$, closed red circles are ITB discharges with a duration > $10\tau_E$, and the closed green squares are stationary hybrid discharges. Plotted is the achieved figure of merit ($H_{89}\beta_N/q_{95}^2$) against line averaged density normalized to the Greenwald density limit for H-modes. Indicated by the green shaded box is the requirement for ITER.

Sawtooth tailoring and active control of core localized MHD

The avoidance of neoclasssically driven tearing modes (NTMs), their removal, or the mitigation of their impact on confinement was a major task in last year´s programme. As sawteeth are the main trigger for generating seed islands to trigger NTMs, their possible modification and avoidance has been investigated.

For the neutral beam injection it has been found that the most tangential beams with the most off-axis deposition strongly increase the sawtooth period. This cannot be explained simply by fast particle effects. The off-axis beams have the least fast trapped particle production. The gradient of the perpendicular and parallel fast particle pressure, calculated with the ASTRA transport code, does not have a strong influence on the sawteeth. The influence of the NBI deposition location, also shown with ASTRA, is similar for different beam sources, showing a completely different behaviour. The long relaxation time after the change from an off-axis beam to an on-axis one strongly indicates a resistive process being relevant. The most probable explanation is that the flattening of the q-profile stabilizes the sawteeth resulting in a longer sawtooth period.

The influence of the electron cyclotron resonance heating (ECRH) and co/counter current drive (ECCD) to the main plasma current on the sawtooth period was investigated in mainly neutral beam heated plasmas (P_{NBI}=5MW). The deposition has been scanned systematically from far on the high field side (HFS) to the low field side (LFS) by variations of B_t and has been verified with the TORBEAM beam tracing code.

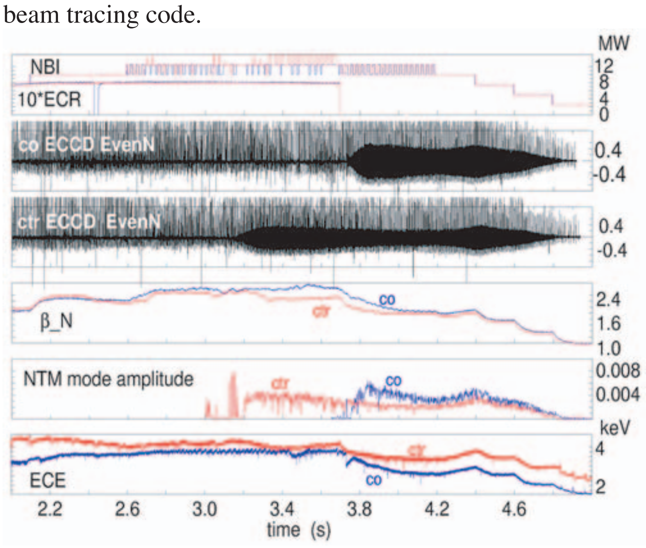

Figure 3: Co-and counter-ECCD with four gyrotrons (2MW). Prevention of the (3, 2) NTM achieved for the entire co-ECCD pulse.

For co-ECCD deposited inside the sawtooth inversion radius a destabilization of the sawteeth is observed. This can be explained by the simple picture of changing the q-profile at the q=1 surface. For deposition slightly inside the q=1 surface, the current gradient increases and with it q' which has a destabilizing effect on the sawtooth period. A strong increase in the sawtooth period is observed for off-axis deposition outside the inversion radius and complete stabilization was observed throughout the entire ECR pulse. The sawteeth could be stabilized without increasing the central q over one. An ASTRA simulation showed a decrease of the shear at the q=1 surface which is expected for ECR deposition slightly outside the q=1, decreasing the current gradient at the q=1 surface. For a scan from the HFS to the LFS with counter-ECCD, the reverse effect is observed. A strong increase in the sawtooth period is found inside the sawtooth inversion radius.

This scheme of sawtooth suppression has been used in order to avoid NTMs. The main result of these experiments was achieved with P_{NBI}=12.5MW and off-axis co-ECCD deposition. According to the magnetic field scans with co ECCD at lower power, a narrow maximum in the sawtooth period is found with respect to B_t. The increased Shafranov shift with higher heating power changing the relative ECR deposition has to be compensated by a correction of the main toroidal field. To ensure high β_N values, poloidal β feedback control has been applied. An NTM could be prevented throughout a complete ECR pulse (see Figure 3). Instability like a mixture of small sawteeth with fishbones might eventually appear in such pulses. The position of the (1, 1) mode, determined with the soft X-ray diagnostic, is positioned further outside the plasma centre. Sawteeth are prevented in this case, very likely due to this flattening in the q-profile. The seed island by the small sawteeth/fishbones is not big enough to trigger an NTM. In the reference discharge, performed with counter-ECCD to achieve comparable profiles, an NTM is triggered in the middle of the ECR pulse. It has to be proven that this important result can be reproduced and thus consolidated. This type of sawtooth control is furthermore in use for transport investigations with and without sawteeth. In discharges with pellet induced ELMs it is used to avoid sawteeth. An application in so-called advanced scenarios is planned.

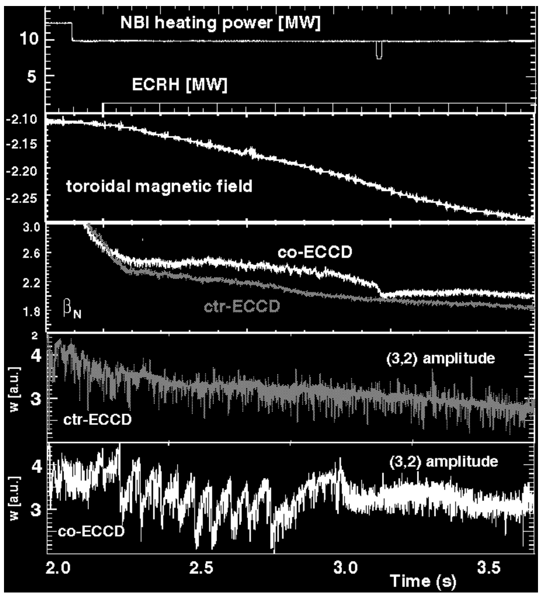

Figure 4:Time traces of P_{heat} ,β_N, and NTM amplitude with co- (black) and counter-ECCD (grey) respectively. A ramp in B_t is performed to find the optimum location of the ECCD to trigger FIR-NTMs. A clear FIR behaviour is seen between 2.3 and 2.8 s in case of co-ECCD.

Considering an already excited NTM, there are the possibilities of either stabilizing, i.e. removing the NTM by local current drive within the island's O-point or trying to reduce the impact on confinement in the presence of an NTM. The stabilisation scheme with co-current drive at the resonant surface has already been presented for the (3/2) and the (2/1) NTM in last year's report. A complete stabilisation of these modes could be achieved. A more detailed exploration of the possibility of NTM stabilisation in ITER has been performed during the last year.

As the stabilisation efficiency of the ECCD is reduced for small islands W compared to the deposition width d, i.e. for W<d, it is not clear, if the mode can be fully stabilized with continuous ECCD. It might be necessary to use a modulated ECCD scheme for small islands, driving only current in the O-point of the island. A dedicated scan of the ratio W/d has been started by changing the launching angle of the ECCD antenna varying the deposition width d for the (3/2)-NTM stabilisation. The completion of this scan is an important task for the 2004 programme.

In last year's report the FIR-NTM operational regime was described. In this regime the averaged NTM amplitude and hence the confinement reduction due to the mode is reduced by frequent interruptions, i.e. amplitude drops, by a non-linear three wave coupling of the (3/2) NTM, (1/1) and an ideal (4/3) mode activity. The short growth time and the required high plasma pressure suggests the (4/3) mode to be an ideal mode close to its marginal limit. A flattening of the q-profile in the vicinity of the q=4/3 surface should destabilise this mode also at lower β_N .

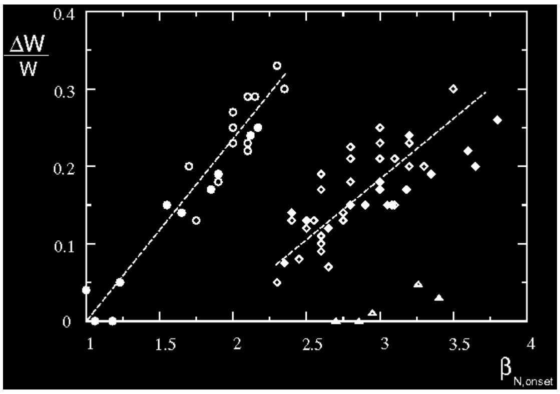

Figure 5: Comparison of reduction in energy confinement due to (3,2) NTMs on ASDEX Upgrade (open symbols) and JET (full symbols) with (circles) and without (diamonds) reaching the FIR regime. Very good agreement is seen, both in the relative confinement degradation as well as in the β_N value above which FIR-NTMs cause less energy losses. The ITER hybrid discharges at JET are marked with triangles and lead to a further recovery.

Applying ECCD close to the (4/3) surface it is, as predicted, possible to artificially trigger a (4/3) activity and get to the FIR regime at arbitrary β values. By applying the local current drive in the vicinity of the q=4/3 surface, q' can be reduced and the ideal (4/3) mode can be triggered. In Fig. 4 a comparison between co- and counter-ECCD with a magnetic field ramp is shown.

This scenario has been established at ASDEX Upgrade with co-ECCD and at JET with lower hybrid current drive. In Fig. 5 the achievable recovery in confinement in the FIR-regime is shown. The ITER hybrid scenario at ASDEX Upgrade, DIII-D and JET with a naturally flat central q-profile shows in the presence of NTMs a similar reduction of the effective (3/2)-NTM amplitude and hence confinement degradation with a NTM. At JET in the ITER hybrid scenario with lower hybrid current drive a more or less continuous reduction in the NTM amplitude could be achieved resulting in an even larger confinement recovery (see Fig. 5). The analysis and the artificial triggering of the (4/3) ideal mode has led to a deeper understanding of the FIR regime of NTMs.

ELM pace making and mitigation by pellet injection

The favourable performance of the H-mode is necessary for a compact and cheap reactor design. Its advantage, the formation of an edge transport barrier, also, unfortunately drives ELMs, causing periodic expulsion of plasma energy and particles. With their short duration, type-I ELMs can generate large energy losses from the main plasma, leading to unacceptably high heat power loads on first wall elements. A possible solution to the problem currently being explored is the ELM mitigation, aiming to break the deadlock in the relation between the plasma energy content W and the energy loss per ELM ΔW_{ELM} . An escape from the deadlock can be realized if action on $\Delta W_{ELM} \sim f_{ELM}^{-1}$ is possible. Applying a tool driving the external ELM frequency f_{ELM}^{ext} beyond the intrinsic value f_{ELM}^{0} can reduce the according ΔW_{ELM} below a desired safe level while keeping W sufficiently high.

Injection of cryogenic D pellets was found to reliably trigger ELMs; the trigger mechanism works almost instantly. Hence, the pellet ELM trigger technique was used last year, showing that ELM frequency control was possible and that mitigation was feasible. Improvement of our hardware equipment allowed us to operate with significantly reduced pellets sizes and accordingly higher values of f_{ELM}^{ext} and f_{ELM}^{0} using target scenarios well inside the type I ELM regime.

To satisfy operational concerns, ELM pace making has to fulfil three basic requirements:

- potential to impose external ELM control and enhancement of f_{ELM} beyond f_{ELM}^{0} , - keep good plasma performance, - reduction of ΔW_{ELM}

A scan of the pellet frequency f_{Pel} was performed in the steady state phase stable operation of a type-I ELMing discharge with an intrinsic ELM frequency $f_{ELM}^{0} \approx 30$ Hz. For a duration of 1.4 s, pellet trains at a selected $f_{Pel} =$ 20.8, 41.7, 62.5 or 83.3 Hz were injected. The result is shown in Figure 6, displaying an averaged f_{ELM} before, during (shaded area) and after the pellet sequence. A transient increase of f_{ELM} beyond the level of f_{ELM}^{0} is obvious. An enhancement $f_{ELM} > f_{ELM}^{0}$ was already achieved for the nominal f_{Pel} (indicated by the solid arrow) slightly above or even below f_{ELM}^{0} . In these cases, a mixture of intrinsic and externally triggered ELMs is observed during the control phases. Once $f_{Pel} \approx 1.5$ x f_{ELM}^{0} is reached, full control with $f_{Pel} = f_{ELM}$ is obtained. This is demonstrated by the fraction of pellet controlled ELMs (number of pellet triggered ELMs/number of ELMs) reaching unity. For the maximum available pellet rate, an enhancement of $f_{ELM} \approx 2.8 \times f^0_{ELM}$ is finally achieved. Thus, ELM pace making was demonstrated in the range 1 - 2.8 x f^0_{ELM}, with the maximum value only prescribed by technical limitations and the range 1 - 1.5 x f^0_{ELM} still showing intrinsic ELMs.

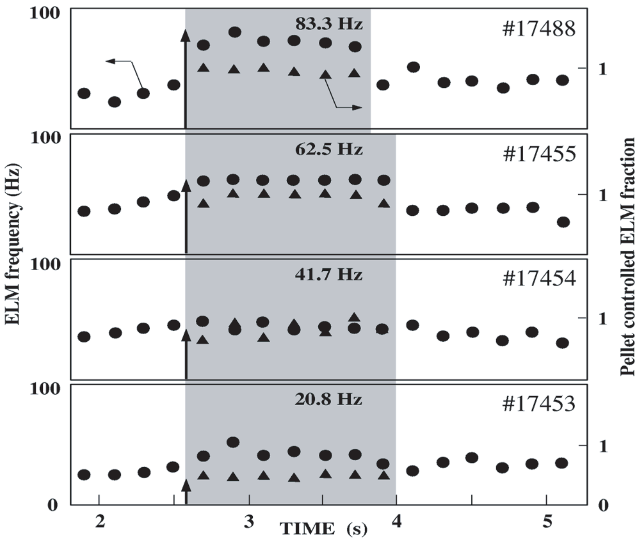

Figure 6: Demonstration of ELM pace making by pellets. Pellet phases (shaded areas) at different nominal frequencies (solid arrows) show up higher ELM frequencies (dots) than pre- and post-pellet reference phases. For highest pellet frequencies complete external control is established as indicated by the fraction of pellet controlled ELMs (triangles, number of pellet triggered ELMs/number of ELMs).

Successful frequency controlling by pace making is only useful for operational application if imposed burdens are bearable. The main concern is the impact of the pellet strings on the plasma confinement - either as a secondary effect of the fuelling, or by a persistent change of the parameters in the edge region. In order to clarify the extent of pellet induced confinement losses, the previously described scan of f_{Pel} was analyzed. Results are shown in Figure 7. Its upper part shows the evolution of the discharge with a nominal f_{Pel} = 83.3 Hz applied in more detail. Clearly, the effect of the pellet string $\bar{n}_e$, W_{MHD} and the ELM behaviour can be realized. Due to some missing pellets, the real pellet and hence the ELM frequency averaged over the pellet sequence is 68 Hz. Two different reference phases were performed. The initial pre-pellet phase after equilibration of the discharge had no auxiliary particle source at all ($\Phi = 0$). During the post-pellet phase, a constant gas bleeding rate of Φ_{Gas} = 8 x 10^{20} D/s was applied, as it was thought to simulate approximately the gas input to the vessel imposed by the pellets ($\Phi_{Pel} \approx 2.5 \times 10^{19}$ D x f_{Pel} [1/s].) Data for all three phases was extracted as shown in Figure 7a) during stationary phases. They are compiled in Figure 7b). Data for the pre- (squares) and post-pellet (triangles) phases, as well as for the pellet (dots) phase are plotted versus the (averaged) ELM frequency realized. It turns out f^0_{ELM} = 30 ± 10 Hz shows some variation from shot to shot. Nevertheless, some impact of the gas puff can be realized. Besides a clear enhancement of the density level, a tendency towards a reduced confinement and enhanced f^0_{ELM} with respect to the $\Phi = 0$ case is visible. Clearly, pellets are still causing some fuelling and also a reduction in confinement. However, this confinement reduction is quite modest, a least-square-fit to the data (dashed black line, including pre-pellet phases representing f_{Pel} = 0) yield a correlation $W_{MHD} \sim f^{-0.16}_{ELM}$. Such confinement loss faced when driving up the ELM frequency by pace making is significantly less severe than when acting via engineering parameters. For such approaches, massive confinement degradation $W_{MHD} \sim f^{-0.6}_{ELM}$ is predicted from the empirical scaling derived for AUG and JET data. Indeed, confinement reduction pretty close to this scaling prediction (dashed grey line) was observed in a case where f^0_{ELM} was increased by a gas puff ramp. Trajectories for this discharge obtained with gradually increasing Φ_{Gas} are given as solid grey lines in Figure 7b). An according discharge with Φ_{Gas} = 0 and pellet pace making achieved a higher f_{ELM} for matched W_{MHD} and $\bar{n}_e$ values (black star).

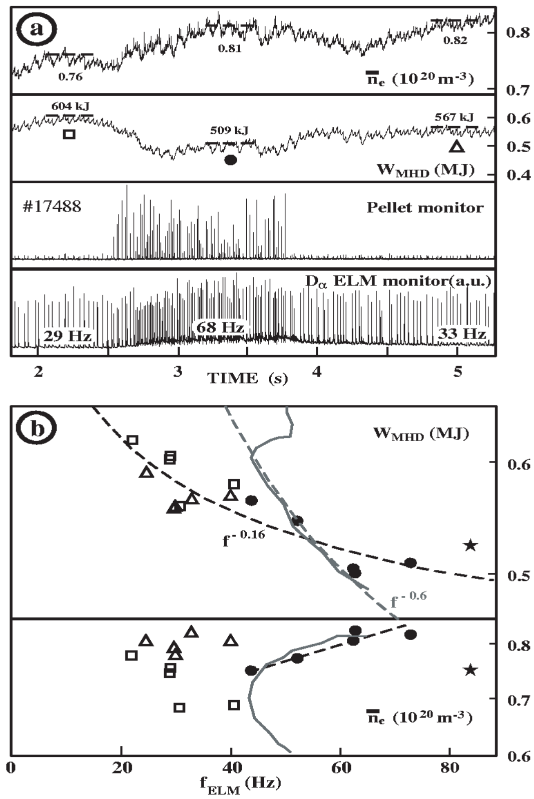

Figure 7: (a) Temporal evolution of a type-I ELMy discharge containing a pellet pace making sequence averaged f_{Pel} = 68 Hz ($\Phi_{Pel} \approx 17 \times 10^{20}$ D/s). Pre-pellet reference phase without any external fuelling, post-pellet reference phase with modest gas bleeding Φ_{Gas} = 8 x 10^{20} D/s. Data extracted for steady state pre- (squares), post- (triangles) and pellet (dots) phases. (b) Data compiled from f_{pel} scan showing a mild degradation of confinement with increasing f_{ELM} for pellet pace making ($W_{MHD} \sim f^{-0.16}_{ELM}$). Increase of f^0_{ELM} by gas puffing (solid grey line) causes confinement reduction close to $W_{MHD} \sim f^{-0.6}_{ELM}$ predicted from empirical scaling (dashed grey line). Black star: matched discharge with pellet pace making employed.

To answer the concluding question whether there is an amelioration of the ELM impact in cases where f_{ELM} is enhanced with respect to f^0_{ELM} , a matching experiment was performed. The same discharge scenario as used for the f_{Pel} scan was employed. One of this pair of discharges contains a pellet train of maximum repetition rate comprising a phase showing f_{Pel} = f_{ELM} = 83.3 Hz chosen as pellet triggered ELM reference. A gradually increasing gas puff was employed during the other discharge. The intention was to obtain and identify a phase in this discharge with the plasma parameters preferentially in the edge region matched to those of the pellet reference. Indeed, a phase showing almost perfect matching serving as intrinsic ELM reference was achieved. Results from this matching experiment are included in Figure 7b). During the pellet sequence, a slight density rise and modest confinement reduction is observed while the energy loss per ELM is significantly reduced. Also, the normalized collisionality ν^*_{Ped} is enhanced due to the higher n_e^{Ped} and lower T_e^{Ped} . In the reference discharge, the gradual increase of Φ_{Gas} causes an ongoing increase of $\bar{n}_e$, n_e^{Ped} and ν^*_{Ped} while W_{MHD} and T_e^{Ped} are decreasing. There is only little impact on ELM frequency and losses, only in the phase shortly before the discharges undergo a back transition to type-III ELMy H-mode f_{ELM} shows a modest increase while losses per ELM are reduced. In this phase, an almost perfect match of the plasma parameters with respect to the pellet phase is realized. While the plasma parameters and also the electron density and temperature profiles are virtually identical in the matching phase, there is a striking difference in the ELMing behaviour. f^0_{ELM} = 51 Hz realized in the gas puffed discharge is less than $f_{ELM} = 83\ Hz$ imposed by ELM pace making. Moreover, pace making results in a smoother evolution of W_{MHD} and less pronounced ELM losses. By the successful matching it is clearly proven that an ELM frequency different to the intrinsic one can be imposed by pace making. Thus, indeed at least in case $f_{ELM} > f^0_{ELM}$ the ELM frequency can be established as an independent free parameter for a given plasma configuration and the deadlock between plasma confinement and ELM magnitude can be resolved. Moreover, it also becomes clear that the ELM frequency and magnitude is not prescribed by the edge parameters n_e^{Ped}, T_e^{Ped} (and thus of course also the pedestal pressure p_e^{Ped}) and ν^*_{Ped} .

5 Toroidicity induced Alfvén Eigenmodes

The understanding of plasma instabilities is of great importance for the optimisation of the design and future operation of a fusion tokamak reactor. Alfvén instabilities are particularly important due to the fact that the charged fusion products (_ particles) which provide the plasma heating have a birth velocity v_α=1.3x10^{7}ms^{-1}, larger than the Alfvén velocity v_A=B/√ρ≈10^{7}ms^{-1}. Toroidicity induced Alfvén Eigenmodes (TAE) are destabilised in ASDEX Upgrade using ICRH. Unstable TAE are observed in the magnetic probes, reflectometer and soft X-rays cameras when the ICRH power exceeds P_{ICRH} > 2.5 MW in both conventional and advanced scenarios. The most unstable TAE have toroidal mode numbers (n=3, 4, 5, 6) and experiments with reversed I_p and B_t showed that the TAE propagate in the current direction, i.e. the ion diamagnetic drift direction, confirming that these modes are destabilised by the ICRH produced energetic ions. The characterisation of the TAE is reported, focussing on the identification of the toroidal, poloidal and radial mode structure. The data is compared with the ideal MHD model.

5.1 TAE Amplitude and stability threshold

The most suitable diagnostic for the detection and identification of TAE are the magnetic probes. TAE are in general global modes, which extend towards the plasma edge and can be detected in the vacuum using magnetic sensors. Low amplitude intermittent TAE were observed in the magnetic probes measuring the vacuum magnetic field perturbations, when the ICRH power exceeds P_{ICRH}>2.5 MW at low density ($\bar{n}_e$=2-3x10^{19}m^{-3}). TAE with amplitudes larger than δB/dt>0.08 T/s are clearly seen in the signals, which correspond to vacuum field perturbations of δB/B > 2x10^{-7}. By increasing the ICRH power, a larger number of modes are observed simultaneously. At the maximum ICRH power obtained in these experiments P_{ICRH}~5 MW, 6 TAE are observed simultaneously. The highest amplitude perturbations measured in the magnetic probes are of the order of δB/dt=3-4 T/s, which corresponds to vacuum field perturbations of δB=0.025mT or δB/B~10^{-5}. However, the TAE amplitude is strongly modulated by the occurrence of other plasma instabilities, such as the sawtooth and ELMs. In the case of the sawtooth, it is known that the crashes remove the fast particles from the core, therefore, removing the drive for the TAE. This explains the strong reduction of the TAE amplitude after each sawtooth crash. On the other hand, the amplitude increases after each ELM collapse. This could be due to the change in the propagation of the TAE in the plasma edge, when the edge plasma parameters are strongly affected by the ELM or due to a change in the distribution function of the fast particles reinforcing the TAE drive.

5.2 Frequency of the TAE instability

The TAE frequency in the plasma frame of reference is obtained from the measured frequency in the laboratory frame of reference using the Doppler correction given by the plasma toroidal rotation f_{ROT} and the TAE toroidal mode number (n), f_{LAB}=f_{TAE}+n f_{ROT}. This simple relation is able to explain the frequency splitting between the different TAE toroidal harmonics observed in JET and DIII-D. In both cases, Δf_{TAE}=($f_{TAE\ (n)}$-$f_{TAE\ (n-1)}$) is largely independent of n. After subtracting the Doppler shift f_0=f_{TAE} - n Δf_{TAE}, all frequencies nearly coincide and f_0 can be inferred as the TAE mode frequency in the plasma rest frame. In the DIII-D case, Δf_{TAE} is comparable to the bulk plasma toroidal rotation measured using spectroscopy. In the JET case, Δf_{TAE} is comparable to the rotation of the n=1 sawtooth precursor, which is also closely linked to the bulk plasma toroidal rotation. In ASDEX Upgrade, Δf_{TAE} is also largely independent of n and when the Doppler shift is subtracted f_0=f_{TAE} - n Δf_{TAE} all frequencies also nearly coincide. The resulting frequency (f_0) is comparable with the TAE gap frequency $f_A=V_A/2qR_0$. However, in contrast with the results discussed above from JET and DIII-D, the differences between the frequency of two adjacent toroidal mode numbers $\Delta f_{TAE}=(f_{TAE\ (n)}-f_{TAE\ (n-1)})$ >10kHz cannot be explained solely by toroidal plasma rotation, which is less than f_{ROT}<2 kHz (V_{ROT}<20 km/s) for ICRH only heated plasmas.

5.3 Toroidal mode number analysis

The analysis of the toroidal mode number (n) is particularly important, since the TAE destabilisation is linked to the breaking of toroidal symmetry by the wave fields in the interaction with the energetic ions. The most unstable toroidal mode numbers are given by the balance between the instability drive proportional to n, which saturates for large n due to finite orbit widths effects, and the various damping mechanisms. Due to toroidal symmetry of the tokamak plasma and weak non-linear coupling between different toroidal harmonics, the TAE have well defined toroidal mode numbers.

The toroidal mode number of the TAE perturbation can be calculated using the magnetic fluctuation measurements from 'Mirnov' sensors located at different toroidal positions. These measurements are sensitive to phase offsets in the signal amplification hardware. Therefore, an appropriate calibration of the signal responses around the TAE frequency need to be carried out before accurate TAE toroidal mode numbers are obtained using the toroidal array of magnetic probes. After the appropriate calibration, the TAE toroidal mode number can be calculated very accurately, even for TAE with low measured amplitudes $\delta B/B \sim 2 \times 10^{-7}$. TAE toroidal mode numbers for the discharges with forward and reversed I_p and B_t are shown in Figures 8 and 9, respectively. The convention is that positive toroidal mode numbers signifies propagation in the counter clockwise direction, as viewed from the top of the machine. This is the normal direction of I_p in ASDEX Upgrade. Therefore, with the normal current (counter clockwise direction) #16161, the TAE modes propagate in the same direction (positive mode numbers), i.e. the ion diamagnetic drift direction. With reversed current (clockwise direction) #17677, the TAE modes propagate in the opposite direction (negative mode numbers), but again the ion diamagnetic drift direction. This is consistent with the fact that TAE are destabilised by the ICRH produced energetic ions, extracting the free energy from the radial gradients of the fast particle distribution function.

In discharge #16161, an n=-1 is also observed, which propagates in the opposite direction to the other 5 modes (n=1, 3, 4, 5, 6) as seen in Figure 8. The observed amplitude of the n=-1 and n=1 modes is around δB~0.1 T/s an order of magnitude smaller than the n=3, 4, 5 modes which is around δB~1 T/s. TAE modes propagating in the direction opposite to the ion diamagnetic drift direction are seen in ASDEX Upgrade, if the ICRH power exceeds P_{ICRH} >5MW in conventional scenarios. It is possible that at these levels of ICRH power, particle with large energy and orbit widths are generated. Large orbits lead to non-standard distribution functions and TAE propagating in both directions can be destabilised.

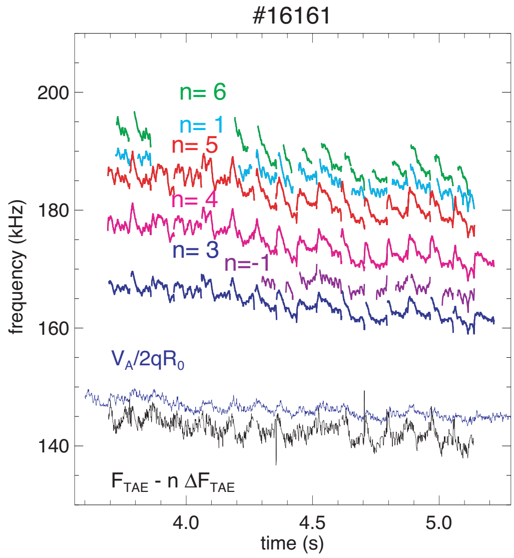

Figure 8:Frequency of the TAE modes observed with different toroidal mode numbers as a function of time, compared with $f_0=f_{TAE}-n\ (f_{(n)}+f_{(n-1)})$ for n=4 and the Alfvén frequency at q=1.5.

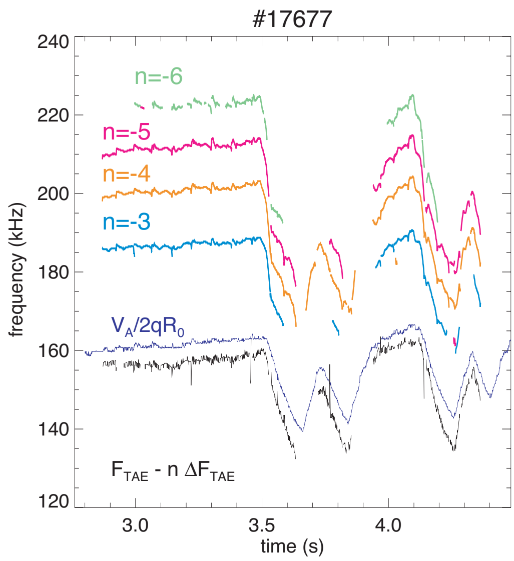

Figure 9:Frequency of the TAE modes observed with different toroidal mode numbers as a function of time, compared with $f_0=f_{TAE}-n\ (f_{(n)}+f_{(n-1)})$ for n=4 and the Alfvén frequency at q=1.5.

5.4 Poloidal mode number analysis

The poloidal mode structure of the TAE is more complex, because the TAE are created by toroidal coupling of two adjacent poloidal harmonics. Toroidal coupling across the plasma radius generates higher harmonics towards the plasma edge resulting, in a rather different poloidal structure compared with the structure at the rational surface where the mode is generated. Different poloidal harmonics behave differently while propagating in the vacuum, with the higher mode numbers decaying very rapidly. The poloidal wave number measured is largely independent of the toroidal mode number. However, the wave number changes sign, i.e. propagation in the poloidal plane changes direction, when the current and field are reversed. When, TAE propagating in both toroidal directions are destabilised in the same discharge, the poloidal wave numbers also change sign. This result confirms that all modes have the same helicity, consistent with the magnetic field configuration.

5.5 Radial mode structure

In ASDEX Upgrade, the radial extent of the TAE eigenfunction can be obtained by combining the information from magnetic sensors "Mirnov probes", microwave reflectometer and soft X-ray emission. The magnetic data provides information on the vacuum magnetic field perturbation outside the plasma. The reflectometer gives information on the perturbation in several radial positions, corresponding to the fixed frequency microwave beam cut-off layers. For the discharges used in these experiments, 4 channels were available on the high field side and 4 channels on the low field side. However, due to the limitation of the homodyne detection system used in these channels, only qualitative amplitude information could be obtained. Therefore, most information is obtained from the horizontal soft X-rays camera C, the only camera installed with fast diodes capable of detecting the high frequency TAE perturbations. Camera C is installed in the outer mid-plane (low-field side), with horizontal lines of sight. Measurements of the soft X-ray emission provides line integrated information on the plasma perturbations caused by the instabilities. The TAE eigenfunction is expected to have a short radial wavelength, especially in the high shear region at the edge, beyond the resolution of the soft X-ray cameras. However, preliminary information on the main features of the eigenfunctions can be obtained using the present diagnostic setup. In the discharge analysed in detail (#17806), the measured TAE amplitude for channels 18-24 in the core region is $\delta\Gamma$=10-40W/m^2, significantly larger than the background fluctuation level, which is around $\delta\Gamma$=5W/m^2. A detailed comparison between the camera C soft X-ray emissivity fluctuation profile and the modelled TAE perturbation calculated using the MISHKA code was performed. The measured emissivity fluctuations $\delta\Gamma$ can be related to the local MHD fluctuations by integrating along the lines of sight. MHD model shows the existence of two n=3 TAE modes in this plasma configuration with distinct radial mode structures: the usual global n=3 TAE, which crosses several continuum gaps and the core localised n=3 TAE, located in a single continuum gap. Comparison between the global eigenfunction and the measured soft X-ray emissivity fluctuations profile, shows good agreement for all channels 16-30. Therefore, it can be concluded that the modes observed are global TAE. The maximum amplitude of the perturbation in the region covered by the soft X-ray camera is 0.39mm, corresponding to a magnetic perturbation of $\delta B/B=10^{-4}$ in the plasma core.

6 Particle Transport

The study of particle transport has received particular attention by the fusion community over the last year. The predictions of fusion gain and plasma performance for the next step devices are found to depend crucially on the shape of the density profile. The reliable prediction of the shape of the density profile in a burning plasma is, therefore, an important task to be accomplished. In tokamaks the density profile is regularly observed to be peaked, even in the absence of any central particle source. The observed peaking suggests, therefore, the existence of an off-diagonal pinch term in the particle flux. The neoclassical theory predicts the existence of such a pinch term, the Ware pinch, which is directed inward, but which turns out to be too small to explain the observed peaking under the majority of plasma conditions. Also the anomalous transport, in particular that ascribed to micro-instabilities like ion temperature gradient (ITG) and trapped electron (TEM) modes, predicts out-of-diagonal terms in the expression of the anomalous particle flux. These out-of-diagonal terms can be ascribed to two different mechanisms, which have been proposed separately in the literature, but which both arise directly from the quasi-linear particle flux computed from a simple fluid model describing both ITG and TEM instabilities. One mechanism is usually called thermodiffusion, and provides a contribution to the particle flux proportional to the logarithmic gradient of the electron temperature. The other mechanism provides the curvature pinch, whose magnitude is related to the peaking of the current density profile. The curvature pinch is dominant in practically all of the plasma regimes, and predicts therefore a density peaking which increases with the current density peaking. Such a prediction is in agreement with the experimental observations of density peaking in several tokamaks.

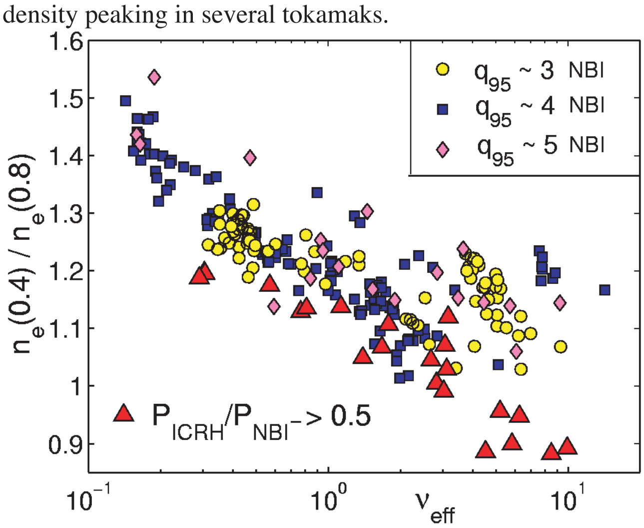

Figure 10: Density peaking vs. $\nu_{eff} = \nu_{ei}/\omega_{De}$.

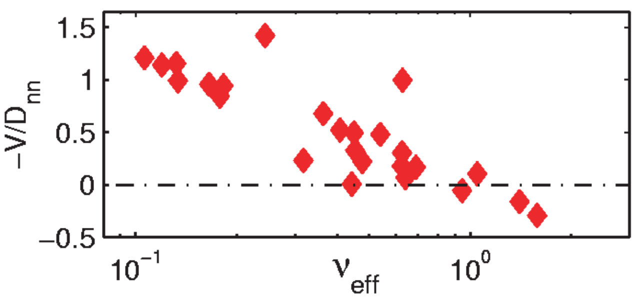

Figure 11: Ratio of the effective total pinch to the diagonal diffusivity versus ν_{eff}

An important parameter in the theory of particle transport is the collisionality. The analysis of the collisionality dependence of density peaking observed in AUG H-mode plasmas shows that density peaking decreases with increasing collisionality. In Figure 10 the density peaking of AUG NBI and NBI + ICRF heated plasmas is plotted as a function of the collisional parameter $\nu_{eff} = \nu_{ei} / \omega_{De}$, where ν_{ei} is the usual ion electron collision frequency, and ω_{De} is the curvature drift frequency. The latter is used in the normalisation since it provides an estimate of the growth rate of ITG and TEM plasma micro-instabilities. The experimental behaviour illustrated in Figure 10 has been explained by investigating the dependence of the anomalous particle transport on collisionality. It has been shown that both inward and outward contributions to the total anomalous particle flux decrease with increasing collisionality, but that inward contributions decrease more than outward contributions, leading to a flattening of the density profile at high collisionality. This is shown in Figure 11, in which the ratio of the incremental out-of-diagonal contributions to the particle flux to the incremental diagonal term, computed with the gyro-Landau-fluid GLF23 transport model, is plotted as a function of the effective collisionality ν_{eff} . Such a ratio provides an estimate of the predicted logarithmic density gradient, which is found to decrease with increasing ν_{eff} . This explanation has been confirmed by a large set of transport simulations applying transport models both including and not including the effect of collisions. Good agreement has been found only in transport simulations involving a collisional transport model, like GLF23, whereas a density peaking independent of collisionality has been found with a collisionless transport model, like the reactive Weiland model. Modified versions of the GLF23 model, describing the same reactive collisionless physics of the Weiland model, have been applied, and have delivered the same results as the Weiland model, in disagreement with the experimental behaviour.

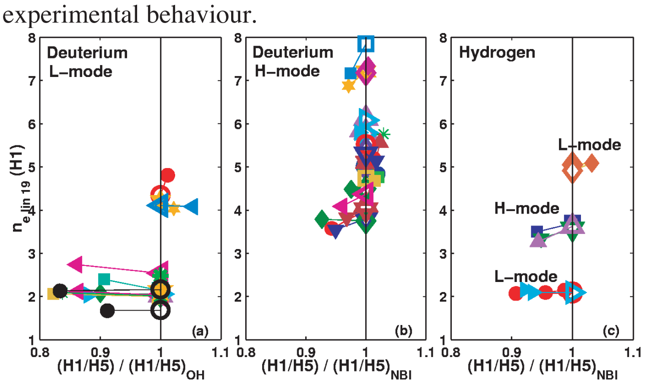

Figure 12: Line average density as a function of the relative peaking for Deuterium plasmas in L-mode (a), Deuterium plasmas in H-mode (b) and Hydrogen plasmas in both L-mode and H-mode (c). The relative peaking is defined as the ratio of the central (H1) to the peripheral (H5) chord interferometer signal, normalised to the value during the non-EC heated phase, namely OH or NBI phase. Solid lines connect symbols representing different heating phases within the same shot.

Density profiles are also observed to be affected by external heating. In particular under many circumstances it has been observed that density peaking decreases when central electron heating is applied. However this observation is not general and opens the question on the effect of central electron heating provided by _-particles in a burning plasma. In order to clarify this phenomenon, the effect of central ECH on the density profiles has been analysed in both Deuterium and Hydrogen plasmas and in both L- and H- confinement modes. The results of this study are presented in Figure 12. Here density peaking during the phase with ECH, normalised to the peaking during the non-EC heated phase, is plotted on the x-axis, while the line average density is on the y-axis. The non-EC heated phase is represented by an open symbol on the straight x=1, while the ECH phase is represented by a full symbol, a displacement towards lower values on the x-axis from the open to the full symbols describes the occurrence of density flattening due to central ECH. In general density flattening with central electron heating is observed only at low densities. An explanation of this experimental behaviour is indicated by the inspection of the expression of the thermodiffusive contribution to the total anomalous particle flux. We have observed that the thermodiffusive coefficient is a function of the frequency of the unstable mode. Hence the thermodiffusive contribution, which is usually directed inward for ITG instabilities, can change sign in the instability domain of the TEM, becoming outwards when the mode is propagated in the electron drift direction. In this framework, a mechanism can be identified which leads to flatter profiles when the plasma is in the instability domain of dominant TEMs, and the electron to ion temperature ratio is increased by the application of central ECH. Indeed the mode frequency increases with the temperature ratio, and so does the thermodiffusive coefficient. In this way central electron heating can produce a measurable effect of density flattening. Instead, when the dominant plasma instability is an ITG, the thermodiffusive term is predicted to be small and directed inwards. In this case the effect of central electron heating on the density profile is predicted to be small, leading to a slight peaking. These theoretical predictions agree with the experimental diagrams presented in Figure 12. Detailed calculations with the gyrokinetic code GS2 identifying the mode with the largest linear growth rate in the plasma, have shown that plasmas exhibiting density flattening in response to central ECH are usually dominated by TEM instabilities. In particular, in L-mode at intermediate densities (Figure 12a) no flattening with central ECH is observed. Here the destabilisation of an ITG as dominant mode is found in the gyrokinetic calculations and it is confirmed by experiments with modulated ECH, which yield that with increasing density the electron heat transport becomes less dependent on the electron temperature gradient. This observation, which indicates that transport arises from ITG instabilities when increasing densities in an L-mode plasma, is explained by the stabilising effect of collisions on the TEM instability, which are otherwise dominant at lower density (and lower collisionality), where both density flattening with central ECH and a strong dependence of transport on the electron temperature gradient in modulated ECH experiments are observed. For the same reason, H-mode plasmas at the

lowest densities (Figure 12b and 12c) exhibit small density flattening with central ECH, and are found in the TEM instability domain, due to the small collisionality and the consequent large density gradients of these plasmas.
The collisionality in a burning plasma will be at least one order of magnitude smaller than collisionalities usually achieved in present tokamak experiments at the same densities. This is because present experiments at densities close to the density limit have much lower temperatures than corresponding burning plasma, due to the lower additional heating power available. From the first part of this study, one can expect that density profiles in a reactor will be more strongly peaked than previously assumed. Although a burning plasma has dominant central electron heating, the present study indicates that this does not lead to density flattening as long as the dominant instability is an ITG. The peaking of the density profile in a reactor is expected to sit close to the value at which the TEM instability becomes dominant.

7 Technical Systems

In 2003, the experiment was in operation for 81 days performing 1619 pulses in total. Only 61 days were dedicated to physics to allow for commissioning and calibrating of technical systems. In particular, the new active damping equipment to avoid flywheel oscillations of the generators EZ3 and EZ4 was installed. There was one unscheduled opening in April for calibrating the MSE diagnostic. Eroded tiles were thereby detected and exchanged. Locally disturbed edge shading caused by misalignment of one of the target modules gave rise to the tile erosion.
The summer opening from early August to late November was mainly dedicated to the mounting of the high-speed ECRH launching mirrors in SE5. The mirrors work meanwhile as specified. Additionally the tungsten-coated area facing the plasma was increased by 13.6 m^2. At the end of 2003 about 75% of the whole plasma facing component surface is W-coated. The upper outer divertor target plates were reinforced to allow for a maximum disruptive halo current of 600 kA in total. Water-cooling of the last two poloidal limiters next to the NBI-Ports was added-on to reduce the re-cooling time during pulse intervals.

7.1 Machine core

In the following the improvements of the vacuum vessel, the pumping-systems and the power supply are described.
Vacuum vessel: Before the 2002/2003 campaign all of the central column (heat shield) tiles were replaced by tungsten coated double tiles, which reduced the number of leading edges and prevented misalignment through independent movement of the substructure. Additionally, the inner divertor baffle and the upper passive stabiliser loop were covered with W-coated tiles. The W-coating had the thickness of 1 μm and was produced by arc deposition at Plansee AG. In the summer opening of 2003 further areas were W-coated in the same way: the upper, outer divertor target plate and the complete outer retention and transition modules. Altogether, 1200 tiles received a new W-coat, whereby 500 old tiles could be re-used to keep the costs low.

Pumping systems: For the renewed 14 turbo molecular pumps (TMP) the degree of automatic control and safety was increased. The root pumps were equipped with a bypass. In case of their failure, limited operation with only the roughing pumps is thus possible. The valves of the TMPs are not fail-safe. To be able to close them in case of a break down of the central supply of compressed air a buffer vessel of sufficient size for closing the valves was installed.
Helium pumping catalysed by Argon frosting was assessed with the cryo pumps. The tests could be run at low cryo panel temperatures. At 3.3 K the required ratio of Ar/He atoms is 30:1 and rises for 4.2 K to 100:1. A low cryo panel temperature is thus of great advantage. This was also observed in 2002 for the case of hydrogen pumping. Only deuterium can be adequately pumped at 4.2 K.
Power Supply:
The technical design for extending the experimental power supply by compact flywheel generator units (rating: 8 MVA / 36 MJ) was finalised. In order to avoid the experimental programme being disturbed by sub synchronous oscillations in the large flywheel generators, an external damping module was developed and submitted for patent. It consists of a six-pulse thyristor bridge, which is connected to a magnet coil acting as buffer storage of magnetic energy. The thyristor converter is feedback controlled with the measured natural frequency of the rotor shaft system. Thus, torsional vibrations and resonances can be damped efficiently with low additional power. The control of the damping circuit allows the attenuation factor of the rotating shaft assembly to be adjusted electronically, as shown in Fig. 13.

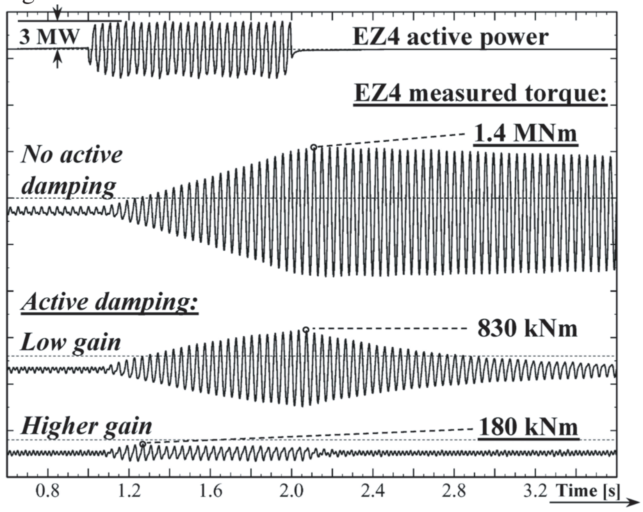

Figure 13:Active damping of a torsional resonance in the shaft assembly of flywheel generator EZ4. The torsional stress in the rotor shaft system can be drastically reduced if the thyristor controlled damping circuit is operated at high gain (lowest curve).

Since April 2003, two active damping circuits have been routinely operated at low gain in order to suppress sub synchronous resonance phenomena in the generator shaft assemblies.

7.2 Data Acquisition and Remote Participation

The diagnostic system has been extended to seamlessly integrate the new PCI-bus based real-time diagnostics. The same configuration and control tools used to set-up traditional CAMAC devices and measuring channels now also apply to PCI devices and real-time channels. The PCI-bus time to digital converters (TDCs) developed in 2002 has been put forward into more diagnostics. Having set-up a TDC based central timer (CT) the build-up of the new timing system is nearly complete.
The H.323 video conference rooms have been used successfully in weekly operations meetings as well as to broadcast conference rehearsals, lectures and executive meetings. Using the new Radvision MCU (multipoint control unit) of the Deutsche Forschungs Netz (DFN) has raised audio quality from the G711 to the G722 standard providing a more comprehensible system for the non-native English speaking participants of the meetings. Unfortunately this higher standard is not supported by many low cost software H.323 clients (e.g. MS Netmeeting), which still stick to the low quality G711 encoding. The recommendation is to participate at the H.323 sessions using at least a desktop H.323 hardware solution, e.g. the Polycom via Video or similar.
Remote access to data (using the MDSplus or the AFS client) and computer systems (using secure connections) have become standard techniques to analyse measurements from remote and to collaborate with the on-site personnel. Weekly summaries of the various task forces are collected from all contributors as PDF files to be presented, e.g. during the “Monday morning meetings”.

7.3 Neutral Beam Heating

As in former years, Neutral Beam Injection (NBI) acted as the standard plasma heating system. In addition two of the beams are being used as "diagnostic beam" for the MSE and CXRS diagnostic, respectively. The NBI system was operated routinely at maximum parameters (2.5 MW (D^0) per beam; altogether 20 MW) with a high availability. Towards the end of the 2003 campaign, however, one of the sources developed a water leak in an extraction grid and had to be taken off. Further technical problems encountered during operation were occasional high voltage break-downs across a modulator tube and a high duct loading from stray particles of the second injector. Both problems have been addressed during the summer shut down in parallel to the regular maintenance work.
Both NBI systems were re-commissioned after the shut-down period and have been available for plasma experiments since the beginning of the present experimental campaign.
During the recent experimental campaign a feed back control with respect to the plasma β was introduced as a further possibility to optimize plasma performance. The control computer determines on-line the NBI heating power necessary to maintain a pre-set β value. In order to vary the heating power in small steps on-off modulation of individual beams is applied.

7.4 Ion Cyclotron Heating

In the summer of 2003, damage was found on some of the bellows in the water supply to the antenna. The location (far behind limiter, only near the two antenna closest to the NBI injectors), the extent of the damage (also nearby diagnostics had seen large heat loads) and the analysis of videos of specific plasma discharges, pointed to injected ions as the cause of the damage. The bellows were replaced and a protective cover of graphite tiles installed.
In previous years the tubes of three generators have been refurbished. This year some problems occurred with the refurbishment of the tube of a fourth generator. At present it is not causing any problems, as two more tubes from the ASDEX/Wendelstein generators remain.
The delivery of the AFT ferrite tuners, which are meant to provide for one double system automatic matching to the load variations during a discharge, was further delayed. Delivery is now foreseen for 2004.

7.5 Electron Cyclotron Resonance Heating

The existing ECRH system with 140 GHz / 2 MW / 2 s was used regularly in the experiments. However, one gyrotron got a leak and was replaced by a gyrotron from W7AS. Another gyrotron had a short across the filament which we could burn away with short high current pulses (600 A / 0.5 sec). Presently the system is again available at full power.
A new ECRH system with 105 – 140 GHz / 4 MW / 10 s is presently under construction, as described in last year’s annual report. But the delivery of the first two gyrotrons, one two frequency gyrotron and one step tuneable gyrotron, has been further delayed. They are now expected to come in 2004. The launchers for these two beams have been constructed, tested and installed into the torus. Each microwave beam is directed from an open-ended waveguide via a fixed focusing mirror to the steerable launching mirrors. These can be rotated around a horizontal axis so that the direction of the beam gets a toroidal component for current drive applications. This is a slow motion and it can only be set in-between successive shots. The mirrors can be rotated by 180° so that the reflecting surface looks towards the vessel wall in cases where ECRH is not required. The poloidal steering of the beam is fast with a speed of 100°/s. It will be used for a fast feedback control of the power deposition in experiments on suppression of neoclassical tearing modes.
The broad frequency band of the new system requires us to study the frequency dependence of the transmission line components. Two polariser mirrors, with $\approx \lambda/8$ and $\approx \lambda/4$ groove depths, can be used in the whole frequency interval, provided they are designed for the centre frequency of 122.5 GHz. The polarisers, designed for the existing 140 GHz system do not allow all of the necessary polarisations at the low frequency of 105 GHz to be set.
For the frequency step tuneable beam we are designing, in co-operation with FZ Karlsruhe, a tuneable double disc diamond window. The individual discs are resonant at both 105 GHz and 140 GHz. But for frequencies within these limits the space between the discs needs to be evacuated to handle the high electric field. The distance between the discs will be only a few millimetres so that the

instantaneous bandwidth allows a frequency drift of ≈ 200 MHz during a pulse.

8 Core Plasma Physics

8.1 Tungsten as intrinsic impurity

Before the 2002/2003 campaign all the tiles of the central column (heat shield, HS), the inner divertor baffle and the upper passive stabilizer loop were exchanged for tungsten coated tiles. This W-surface comprised 14.6m^2 and represented about 40% of the whole plasma facing components (PFC).

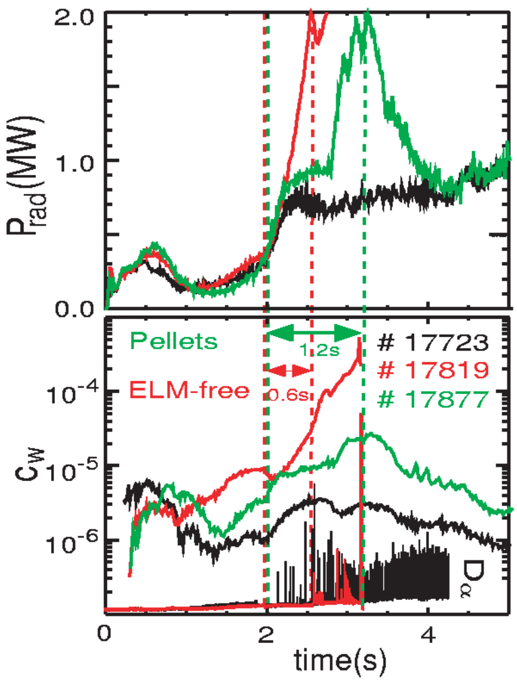

Figure 14: Temporal evolution of P_{rad} and W concentration c_W in similar discharges $P_{aux} \leq 5MW$ as a consequence of degrading conditioning. #17723 (black) was performed directly after a boronisation. #17819 (red / dark grey) disrupted due to a radiation collapse, whereas #17877 (green / light grey) could be stabilised by ELM pace-making through pellets. The bottom D_α traces demonstrate the prolongation of the ELM-free phase.

Despite the large area of the new W-PFC the expected strong reduction of C in the plasma discharges was not observed. The CFC guard limiters in the main chamber were still a strong primary source and, according to influx measurements, a dynamical C-source quickly built up on the central column, giving cause of C-recycling. The central W concentrations are mainly governed by the central impurity transport, which strongly depends on the local heat fluxes in the plasma, as could be shown recently with Si trace-injections (see sect. 8.2). Another critical parameter for the W inventory is the transport near the edge, which has been known for a long time from ELM-free H-Modes. A new observation here is the indication for a feed back loop which leads to an unstable situation in the case of the operation near the L-H threshold. There, the ELM-frequency is low and during the time in-between ELMs, impurities penetrate the plasma much more easily, leading to increased impurity concentration and radiation. In contrast to C, which under normal plasma conditions mostly radiates in the SOL, a substantial amount is radiated within the separatrix when heavier species (mid-Z as well as W) are involved. This leads to a reduced power flux crossing the pedestal region and consequently results in a lower ELM frequency, closing the feedback loop. Fig.14 shows the evolution of plasma radiation and W-concentration C_w in 'Standard H-Mode' discharges, run once daily. During the low power phase, the ELM-free period is prolonged from initially 250ms to above 600ms. This leads to increased W-concentrations and to the feedback-loop described above. A remedy is a faster increase in heating power, which leads to higher ELM frequency and much lower radiation and c_w was reduced. Another possibility to break the self-amplifying cycle is to enforce ELM activity by pellet injection (see sect. 4). In discharge #17877 a train of small pellets was injected at 80Hz from 2.0s - 3.2s. Although the confinement was degraded only by about 10% c_w remained low, demonstrating the subordinated role of the W source. In contrast to operation in an 'all-carbon' device, there is a strong difference between W-limiter and divertor operation, as demonstrated in a discharge with divertor-limiter-divertor transitions. The strong bulk W-contamination is suppressed immediately after the re-transition to divertor operation. The discharge proved that the W-surfaces are still visible to the plasma after half a year of operation. From the almost identical W-level before and after the shift, a strong coverage by low-Z elements could be excluded, which is in line with the post mortem analysis of W-tiles. The W-influx from the HS was estimated from Langmuir probe data using the yields measured during the W-divertor experiment. As soon as the separatrix is lost and the plasma is limited at the HS, the temperature and density rise, leading to an increase of the W influx by almost a factor of 100 which is reflected in the increase of c_w. The transient limiter phases during ramp-up and ramp-down were found to dominate the gross erosion of tungsten at HS. DIVIMP simulations using background plasma from B2-modelling reveal that the eroded tungsten from the HS is predominantly re-deposited close to its source. The remaining fraction of W leaves the computational grid mostly at the low-field side and the amount of W reaching the divertor is negligible. Transport away from the source region is mainly caused by the ion temperature gradient force in competition with friction and the parallel electric field. The erosion is significantly increased by W self sputtering while, on the other hand, prompt re-deposition only has a very moderate effect due to the low local plasma densities. Comparing simulations for the limiter and the flat-top phases, one finds that the modelled fraction of the discharge integrated net erosion migrating into the divertor is in agreement with the campaign integrated experimental data on W deposition in the divertor, determined by ion beam surface analysis.

8.2 Influence of the Heating Profile on Impurity Transport

The transport of silicon has been investigated for various heat deposition profiles in H-mode discharges. The variation of the heating profile was achieved by using different densities in NBI heated plasmas, by adding central or off-axis ECRH to the NBI, and by using pure ICRH with on-axis or off-axis power deposition. The transport coefficients were evaluated from the soft X-ray profile evolution after Si laser blow-off. For sawtoothing plasmas, only the Si transport between the crashes was considered.
In the central part of the plasma (approximately inside of $r \approx a/4$), the diffusion coefficient D is either mainly neoclassical or anomalous depending on the heating method. For all investigated scenarios with NBI heating and off-axis ECRH or off-axis ICRH, the diffusion coefficient is approximately neoclassical, and the effective heat diffusion coefficient χ_{eff} is below the neoclassical ion heat diffusion $\chi_{i,neo}$ in the plasma core. When central ECRH is added, χ_{eff} is above $\chi_{i,neo}$, and D strongly increases by a factor of 3-10, i.e. Si transport becomes predominantly anomalous. For central ICRH, D is above the neoclassical level by a factor of 2. Further outward, D is always anomalous and increases towards the plasma edge. A clear scaling of D in terms of χ_{eff} was found, where D is about equal or above χ_{eff}. A strong inward drift parameter v/D is only observed in the central part and only for cases, when the diffusion coefficient is neoclassical. With central wave heating, the drift parameter decreases to small values, thus, offering a tool to control central impurity accumulation as has previously been demonstrated for the case of tungsten. These findings are also promising with regards to impurity transport in a burning reactor, where α-heating provides a centrally peaked power deposition profile.

8.3 Z_{eff} behaviour

The line-averaged value of Z_{eff} in H-mode discharges has been found to decrease with increasing line-averaged electron density. This trend is roughly inversely proportional to $\overline{n}_e$ and holds for co-NBI as well as for ctr-NBI discharges. In the latter case, QH-mode discharges are described by the same trend leading to the conclusion, that the higher impurity content is a consequence of the low electron density. The radial profiles of Z_{eff} in ELMy H-mode discharges are in most cases flat. Apart from discharges with impurity accumulation, one exception with slightly peaked Z_{eff} profiles arises in the case of off-axis NBI heating. This can be explained by the low thermal diffusivity in the plasma centre and the assumption, that particle transport is coupled to energy transport.

8.4 ECRH power deposition

Our ECRH system, working at the second harmonic X-mode, is designed to produce a very localised electron heating even in a situation where we deposit off-axis by poloidal beam steering. However, since our ECE diagnostic is using the second harmonic emission, we cannot measure the temperature response in the immediate deposition volume, rather we have to measure it on a remote place on the same flux surface, and thus rely on a rapid distribution of the energy on this surface.
The temperature response also depends on the electron heat diffusivity and the variation of other heat sources, or sinks due to their temperature dependence. For the experimental determination of the deposition profile we therefore used an Ohmic discharge with off-axis cw ECRH heating in which the electron heat diffusivity is considerably reduced in the central region. Into this region we deposited another ECRH pulse and studied the switch-on/off process, or the response to modulated heating. The temperature evolution of the switch-on/off cases was compared with a simulation performed with the ASTRA transport code, using the Weiland model of turbulent electron heat transport combined with neoclassical transport. The simulation was tested to reproduce the cw-heated discharge. Then the deposition profile of the probing beam was varied in the simulation until a satisfactory agreement with the measurement was obtained.
In a second approach to determine a deposition profile width we compared the frequency dependence of amplitude and phase of the temperature modulation in the deposition centre in discharges with modulated ECRH with an analytic expression derived for homogeneous plane plasma. In both cases the deposition profile as determined remote from the immediate absorption volume is up to a factor of 2 broader than the calculated absorption profile.

8.5 Electron heat transport

8.5.1 Low density L-modes with $T_e >> T_i$

Studies in ECRH heated L-modes with $T_e >> T_i$ suggested that electron heat transport increases above a threshold $(R/L_{Te})_{crit}$. This means, in particular, that the propagation speed of heat pulses excited by power modulation is expected to increase abruptly by a large factor when R/L_{Te} evolves from below to just above $(R/L_{Te})_{crit}$. New discharges, designed to scan R/L_{Te} around $(R/L_{Te})_{crit}$ exhibit the expected change. This may be considered as direct evidence of the existence of the threshold $(R/L_{Te})_{crit}$.
The strongly non-linear response of plasma transport around the threshold, is expected to excite a secondary heat wave. This aspect has been addressed in experiments in which R/L_{Te} has been modulated around the threshold between two ECRH depositions slightly separated in space and modulated out of phase with respect to each other. The analyses indicate that R/L_{Te} could indeed be modulated and the expected secondary heat wave has been found, confirming the existence of the threshold.
These properties of electron heat transport are expected to be general for such discharges with large values of $T_e >> T_i$ and rather low collisionality. Therefore, experiments were performed using cold pulses excited at the plasma edge by laser blow-off impurity injection. The characteristics of the cold pulses propagating inwards have been investigated in plasmas heated by ECRH deposited at different radial positions. The propagation of the perturbation is fast outside of the ECRH deposition, where R/L_{Te} is high, whereas it is slow inside of the deposition where R/L_{Te} is much lower. This behaviour is in agreement with experiments carried out previously with ECRH heat pulses and confirms the existence of a threshold, above which

transport increases, is a general property. Transport modelling confirms that indeed very different values of the diffusivity are required on each side of the ECRH deposition to describe the propagation of the heat pulses.
Finally, the possible existence of a heat pinch inside off-axis ECRH depositions has been investigated. Despite very low heat flux in this central region of the plasma quite peaked T_e profiles are observed and the power balance analysis yields negative electron transport, which might be related to the existence of an inward heat pinch. Modulation data support this possibility.

8.5.2 H-modes with $T_e < T_i$

The electron heat transport in low density H-modes heated by NBI has been investigated using ECRH combining both steady state and transient response analysis by ECRH power modulation. Due to the low coupling, most of the NBI power is delivered to the ions, while only 20-25% to the electrons. T_i is higher than T_e and T_e/T_i is approximately 0.8 at mid radius. The power in the electron channel is more than doubled when the ECRH is added, while the power in the ion channel is increased by less than 30%. Power balance and transient response analysis of these discharges reveal very resilient T_e profiles. Moreover, the sudden jump of the heat pulse diffusivity at R/L_{Te}~6 hints at the existence of a threshold in $\nabla T_e/T_e$ above which transport is strongly increased. Comparison of the heat diffusivities, normalised to $T_e^{3/2}$, between NBI-heated plasmas, with $T_i>T_e$, and EC-heated L-modes, with $T_e>T_i$ [annual report 2002], shown in Figure 15, suggests that these different plasmas have quite similar stiffness factors.

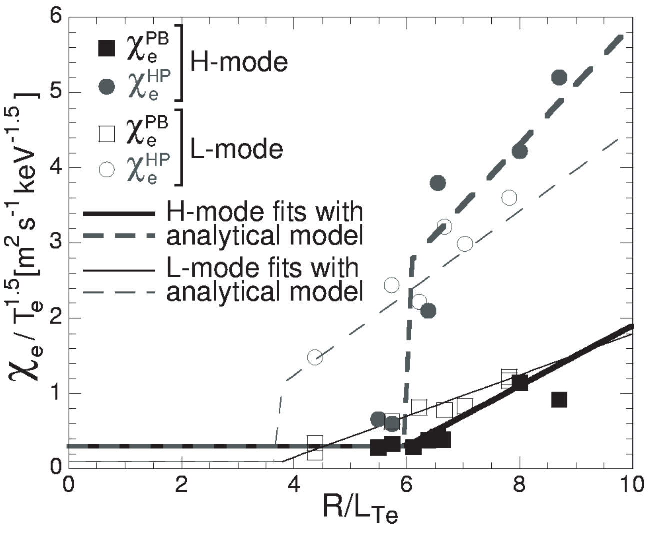

Figure 15: Comparison of power balance and heat pulse diffusivities between NBI-heated H-modes and pure EC- heated L-modes.

8.6 “Current Holes” and ITBs with $T_e \approx T_i$

ITB experiments with NBI into the current ramp-up phase have produced extremely reversed q-profiles. A core region with a very small or zero current density, as determined from Motional Stark Effect (MSE) diagnostic measurements, characterizes these so-called 'current hole' plasmas (zero poloidal field within the error bars of the MSE diagnostic). A new scenario uses counter ECCD on-axis early in the current ramp-up phase (t=0.2s) with 0.9MW as a more effective way to produce 'current holes' similar to the effect of LHCD at JET. The electron temperature T_e show sawtooth-like crashes between t=0.6-0.85s (collapsing electron ITBs, see Fig. 16) similar to the JET 'current hole' discharges. After the start of NBI (t=0.85s) an electron and an ion ITB with $T_e \approx T_i$ develop for about 300ms and decay (t=1.15s) well after the start of the regular ELM activity at t=0.99s. ASTRA simulations show the development of a small 'current hole'.

8.7 Plasma Regime Identification

The rising demands on plasma performance control to optimize dedicated plasma regimes have led to the development of an improved real-time plasma regime identification algorithm. Discriminant analysis has been applied to identify several different regimes. As input a set of plasma parameters averaged over a time slice in a discharge is used. The data set consists of all observations over different discharges and time slices and the assignment of this time slice to a particular regime. Discriminant analysis yields coefficients allowing the classification of a new observation. With 5 plasma variables, a failure rate of 1.3 % for predicting the L-mode and H-mode confinement regime was achieved. With 5 plasma variables, a failure rate of 5.3 % for predicting the H-mode and improved H-mode confinement regime was achieved. The small difference in failure rate when taking the full data set or a random 60 % sample of the data set shows that the regime identification procedure is robust when applied to data not used in the training set. Furthermore, when performing discriminant analysis on a random 60 % sample of the data set, it is found that the prediction failure rate on the remaining 40 % of the data set or on the whole data set is to within error bars the same. A comparison of the formal Bayesian and frequentist approaches of assigning the probability did not show an essential difference in the prediction failure rate for this data set.

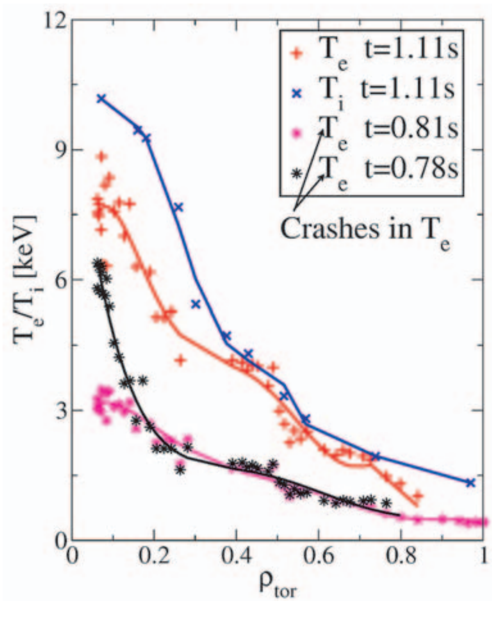

Figure 16: Temperature profiles during ITB´s of #17542.

8.8 Energy and particle losses of type-I ELMs

The energy loss produced by ELM bursts can increase erosion of the divertor targets to the point where component lifetime becomes unacceptably short. A basic observation in several devices is that the ELM energy loss can generally become larger with increasing pedestal stored energy and is reduced with increasing plasma density. Mitigating the heat load onto the divertor target simultaneously without deterioration of the energy confinement is a crucial issue in recent ELM studies.

Characteristics of ELM energy and particle losses in type-I ELMy H-mode plasmas are investigated by a large data set with as many independent variations in engineering parameters as possible. The data set shows that the ELM energy loss decreases with the pedestal density or collisionality. However, elevated triangularity leads to lower ELM frequency and larger ELM energy loss significantly exceeding that simply expected from the increased pedestal pressure in high triangularity plasmas at a fixed power. The observed larger ELM energy drop at higher triangularity involves the ELM perturbations of the electron temperature profile across an ELM that extend radially more inward, suggesting that there is a direct effect of plasma shape on ELM energy losses. It is found that the fraction of ELM power loss does not remain constant but the increased pedestal collisionality enhances the transport level between ELMs and reduces the ELM power loss. When the particle flux near the separatrix is enhanced, the increase of ELM frequency and the reduction of ELM power loss caused by the increased collisionality lead to the reduction of ELM energy loss so that the energy balance can be sustained.

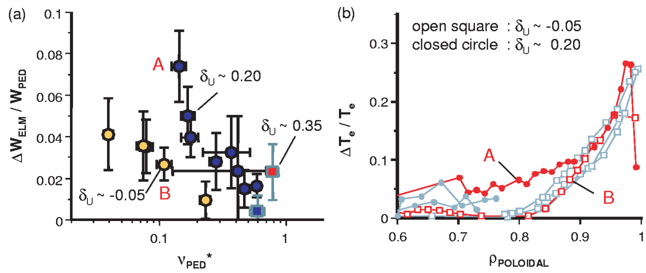

Figure 17: (a) Relation between $\Delta W_{ELM}/W_{ped}$ and ν^*_{ped} for a variety of triangularity. (b) Relative changes to T_e profile due to an ELM.

8.9 Type I ELM precursor

The comparison between measurements with co- and counter-NBI led to a significant improvement in the understanding of high and low frequency coherent magnetic fluctuations related to type I ELMs. These MHD modes had been recently described for the first time in ASDEX Upgrade and are characterised by a frequency in the range 300-500 kHz and are consequently different form the low frequency (5-10 kHz) magnetic precursors normally seen in discharges with counter NBI heating. New experiments confirm that type I ELM precursors are normally locked in co-NBI heated discharges, and can be seen with a non-zero rotation frequency only in counter-NBI shots. The low frequency oscillation is a true ELM precursor in the sense that it grows in amplitude until the ELM happens. In contrast, the high frequency oscillation described above does not always grow up to an ELM, in fact it saturates or even decreases in amplitude, before the ELM happens. With the help of additional information given by ECE data it is possible to see that the main effect of the high frequency oscillation is to clamp the increase of the edge electron temperature. Since it is well known that the pressure gradient can saturate prior to an ELM and stay constant for some time before the ELM happens, these new measurements are suggestive that the high frequency oscillation is linked to this clamping of the pressure gradient. The existence of low and high frequency MHD events suggests an interpretation in the framework of the peeling-ballooning model. The high frequency magnetic activity seems to be related more strictly to the increase (and eventual saturation) of edge electron temperature and can be connected with the ballooning limit, while the low frequency modes are directly related to the ELM crash itself and can be connected with the peeling mode.

8.10 Integrated high performance radiative feedback scenario with ELM frequency control by pellets

A high performance scenario has been developed for simultaneous feedback control of the divertor neutral particle density and the divertor temperature using impurity puffing. The repetitive injection of small pellets is used to sustain a minimum ELM frequency, which turned out to be essential to avoid a radiative run-away situation. The ´effective´ divertor temperature is obtained from online measurements of the thermoelectric currents flowing between the inner and outer divertor, which measures the difference in the divertor temperatures. Divertor temperature as a control quantity turned out to be superior for type-I ELM conditions compared to the radiative power measured by bolometry. Adding external ELM triggering by small pellets avoids a radiative run-away situation which is often observed in the vicinity of the H-L power threshold: Radiation rise in between type-I ELMs leads to a further delay of the next ELM, with ongoing radiation increase until a short H-L transition occurs. The pellet triggered ELMs suppress the excessive impurity density and radiation build up, while their contribution to D fuelling remains small. This type of discharge represents a fully controlled integrated exhaust scenario, applicable in a future full-tungsten ASDEX Upgrade tokamak.

8.11 "Quiescent H-Mode" experiments

The “Quiescent H-mode” (QH-mode) regime, originally discovered in DIII-D and then reproduced in ASDEX Upgrade in 2002 has been further studied in a campaign with reversed plasma current (for counter-current neutral beam injection). After a fresh boronisation, the lowest Z_{eff} values observed so far in QH-mode, Z_{eff} =2.5, have been obtained. At comparable density, lower impurity content is seen in the 2003 campaign, indicating the importance of impurity influx which can be influenced by vessel conditioning. There is no systematic difference between Z_{eff} in ELMy and QH-mode phases for the same density for counter-NBI.

Equilibrium calculations with prescribed scrape-off-layer currents and sufficient freedom in the current profile parametrisation to reconstruct the edge current are made with the CLISTE code. No significant difference of the mainly bootstrap-driven edge current is found between ELMy and QH-mode phases. This indicates that the ELM suppression does not require a reduction of the edge bootstrap current, e.g. due to high edge collisionality.

The behaviour of the Edge Harmonic Oscillation (EHO) is studied with variations of edge safety factor q_{95}. In an in-shot toroidal field ramp (Fig. 18), the q=4 surface is brought from the pedestal top into the gradient region. The EHO fundamental, initially at n=1, m=5, switches between m=5 and m=4 between t=3.0 – 3.2 s and then remains at n=1, m=4. During the field ramp, the resonance of several ECE channels is shifted radially, all showing that the EHO activity is localised in the edge gradient region. This suggests that the EHO is pressure gradient or bootstrap current driven.

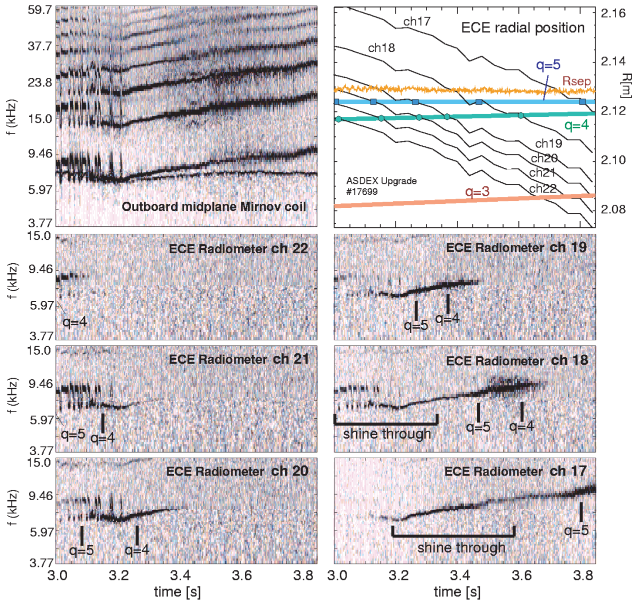

Figure 18: Evolution of the edge harmonic oscillation (EHO) in a Quiescent H-mode discharge with a toroidal field ramp. The EHO switches poloidal mode numbers so as to remain localised in the edge gradient region.

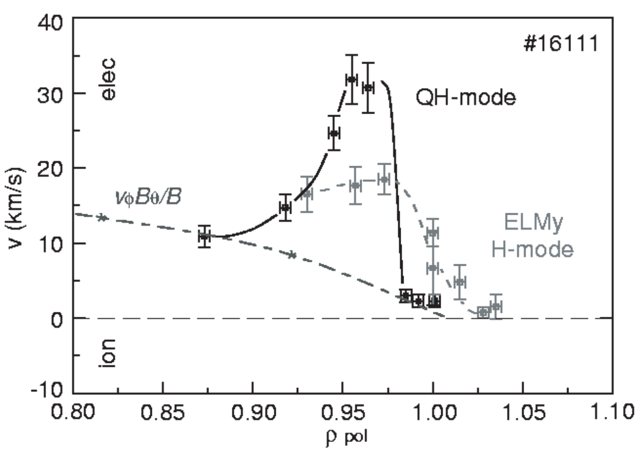

Figure 19: $v_\perp$ radial profile from Doppler reflectometer showing enhanced E_r during Quiescent H-mode.

During the QH-mode, stepped frequency Doppler reflectometry measurements show an enhancement in the perpendicular rotation velocity ($v_\perp$) across the pedestal compared to a normal ELMy H-mode phase, as shown by the radial profile in Fig. 19. The peak in $v_\perp$ (e.g. the negative E_r well) associated with the H-mode barrier is factor of two higher in the QH phase and substantially narrower (commensurate with a narrower pressure profile) indicating larger electric fields and stronger radial shearing in E_r compared to the ELMing phase. Although the enhanced E_r will certainly affect the edge particle orbits and losses, there is as yet no MHD theory to link the E_r shear (normally associated with turbulence reduction) with the ELM suppression.

8.12 Zonal flows and GAM oscillations

In Doppler reflectometry the Doppler shifted frequency f_D is directly proportional to the E×B velocity, hence the diagnostic can, potentially, provide a direct measurement of fluctuations in the radial electric field E_r with high spatial and temporal resolution. The reflectometer has a radial resolution of a few mm, however, the finite spot size of the reflectometer beam limits the poloidal resolution to longer wavelength E_r fluctuations. Nevertheless, this is ideal for the study of m=n~0 zonal flows (poloidal plasma flows with finite radial extent). Zonal flows are of major interest since they are predicted to moderate drift-wave turbulence, and hence edge transport. Fig. 20(a) shows a typical f_D spectra, from an L-mode discharge at ρ_{pol} ~0.96, with a dominant peak around 10 kHz on a broad-band incoherent background. The frequency of the peak scales with the square-root of the local T_e, Fig. 20(b), with a value close to the expected Geodesic Acoustic Mode (GAM) frequency. The GAM is not always detected. The amplitude of the GAM varies strongly with radial position, and is only observed inside the separatrix close to the top of the density pedestal. So far only ohmic and L-mode shots have been analysed. Further measurements are in progress to define the GAM properties and behaviour in varying discharge scenarios, particularly across the L-H transition.

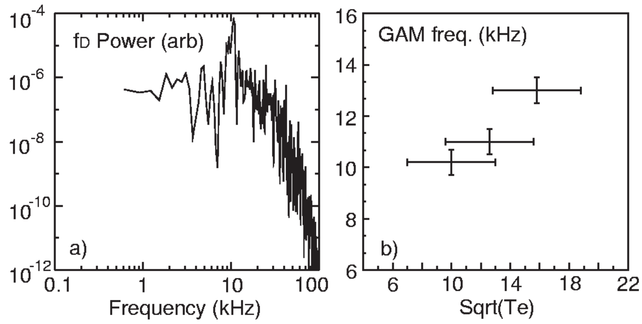

Figure 20: (a)Typical E_r fluctuation spectrum from Doppler reflectometer showing GAM/zonal flow. (b) Spectral peak frequency scales with $\sqrt{T_e}$.

8.13 Radial Electric Field Shear using Correlation Doppler Reflectometry

Correlation Doppler reflectometry is a new diagnostic technique, which can provide information on turbulent properties, such as the instantaneous radial electric field shear (E_r shear). In this technique, two microwave reflectometer beams are launched into the plasma from the same tilted antenna. By repetitively sweeping the launch frequencies of the beams with a constant fixed frequency difference, two simultaneous radial profiles of the perpendicular rotation velocity ($v_\perp$) can be constructed from the Doppler frequency shift in the reflectometer signal. Since $v_\perp$ is directly proportional to the ExB velocity, the E_r profiles for each channel can be determined. Taking the instantaneous radial derivative of the two E_r profiles gives a profile of the E_r shear. An example of an instantaneous E_r shear profile for an H-mode discharge is shown in Fig 21. The shear is mainly concentrated at the edge and everywhere in the core it is zero. Around the region of the H-mode pedestal, a negative shear of -1.5 up to -4 MV/m^2 is typically measured. It is believed that the large negative shear in H-mode may be responsible for the confinement improvement and the reduction of anomalous transport.

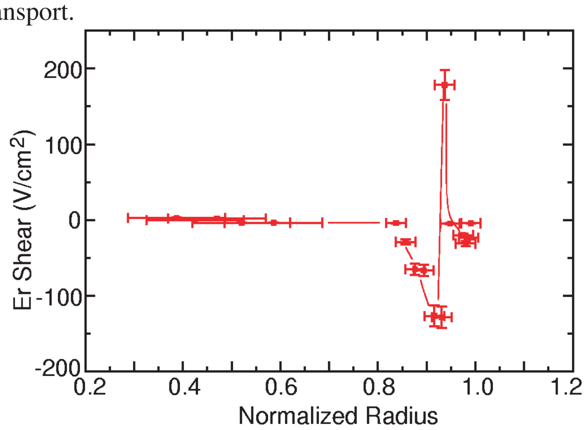

Figure 21: The instantaneous radial electric field shear for an H-mode.

8.14 Edge Ti Measurements

A neutral lithium beam, routinely used to measure electron densities at the plasma edge, is now also used as a source for charge exchange with fully stripped impurity ions which locally enhances the Doppler-broadened line emission. Temperatures have been measured for carbon (CVI, 529.2 nm) and helium (HeII, 486.5 nm) in ohmic, L-mode and type-I ELMy H-mode plasmas. The temperatures of carbon and helium ions agree within their respective experimental error bars in discharges where both could be measured.
In low density ohmic and ECRH heated L-mode plasmas, a significant difference between ion and electron temperature has been seen near the separatrix. Both absolute values of the temperatures and respective gradients differ by factors of up to two. Temperatures from a so-called improved L-mode at densities of 4 x 10^{19} m^{-3} with NBI heating do not show such strong differences between electrons and ions, but rather a steep gradient near the separatrix and, consequently, a pedestal in the ion temperatures. Measurements in ELMy H-mode have to deal with periodic edge perturbations connected with strong spikes in line emission. This was successfully done for low ELM frequencies <60 Hz and long integration times (>2 s). From the recent H-mode measurements, there is strong evidence for a pedestal similar to the improved L-mode. Within the experimental uncertainty, electron and ion temperatures are identical at the pedestal top and do not decouple strongly down the steep gradient region.

9 Scrape-off Layer and Divertor Physics

9.1 Hydrogen gas balance with Div IIb

The retention of hydrogen fuel in fusion devices represents a serious difficulty for the utilisation of future machines, since the accumulation of tritium in the vessel walls can become a major operational problem. A large fraction of the injected gas is normally pumped out from the vessel on short time scales during and after a plasma pulse. A small fraction is retained permanently.
This D gas balance investigation is divided into three phases. The first covers the complete discharge, the second the glow discharge for wall cleaning in between plasma pulses and the third the complete warm up of the cryo-pump during the weekend after every week of plasma operation.
At very low injection levels during pulses, the ratio of pumped to injected deuterium particles R_D clearly exceeds 100 % which indicates that low density plasmas can reduce the long term wall inventory. Above a small amount of gas injection R_D levels off to values around 65 %.
In phase two (5 min He GDC) about 10 % of the injected D is released. In addition, phase three contributes ≤ 10 % deuterium. The number of deuterium particles transported by the most important hydrocarbon molecules like methane, ethane and ethylene has been shown to play a minor role. Within the experimental errors one can conclude that about 10-20 % of the deuterium which is injected into the torus is retained on long time scales in the vessel.

9.2 Scrape-off layer flow measurements

Measurements of plasma flows parallel to the magnetic field, using a Mach probe at the midplane manipulator, were performed in ohmically heated plasma with lower single null plasma configuration with the normal direction of the B_t. A strong plasma flow towards the inner divertor is observed between the separatrix and the outer polidal limiter. Maximal Mach numbers of up to 0.7-0.8 were measured for $\overline{n}_e$ of 2.5x10^{19} m^{-3}. The maximum of the flow is located at about 1 cm out from the separatrix. An increase of the density to 4.4x10^{19} m^{-3} resulted in decrease of the plasma flow down to Mach numbers of about 0.2. Further Mach probe measurements are planned for the experimental campaign in 2004.

9.3 ELMs and ICRH antenna coupling

Fast measurements of coupling characteristics of ICRF antennas during H-mode discharges show that a single ELM leads to a change in coupling of the antennas at different times. The delays between reactions on four antennas indicate a toroidal propagation of the ELM perturbation. The perturbation propagates in the opposite direction to the direction of the I_p (electron diamagnetic drift direction) in accordance with the magnetic measurements of ELMs and ELM precursors. First measurements indicate velocities of the propagation of the order of 100 km/s. Further measurements are planned to find dependencies of the propagation velocity on the pedestal parameters and energy loss from the plasma during ELMs.

9.4 ELM power load outside the divertor

Investigation of ELM energy losses at ASDEX Upgrade and JET revealed that the energy detected in the active divertor accounts for only about 50% of the ELM losses in the midplane. The heat load to non-divertor components in ASDEX Upgrade was measured by diagnostics with high time resolution, such as thermography and Langmuir probes in combination with slow but toroidally and poloidally distributed measurements, such as thermometry and cooling water calorimetry. The total deposited energy to non-divertor components is below 10% of the plasma deposited energy. The main part of this energy is deposited onto the ICRH antenna limiters (see Fig. 22). The fraction of energy received by the central column during the flat top phase is negligible. The radial heat flux deposition profile measured at the protection limiter is the continuation of the heat flux profile measured in the lower divertor. A 2D-pattern of ELM heat deposition is shown in Fig. 22 (right). The fraction of ELM energy deposited onto the ICRH and protection limiters is about 14% of ELM midplane loss. 12% is deposited at the inner column with its large area. In total, about 25% of the ELM mid plane loss is received outside the divertor for low density ($\overline{n}_e / \overline{n}_e^{GW}$ =0.4) shots. The power load to ITER non divertor components becomes 8 MW, if a fraction of ELM transported power of 0.2 is assumed. The missing 25 % of ELM energy released in the midplane is possibly dissipated by enhanced radiation in the scrape-off layer and the divertor region, as investigated by ELM resolved bolometry. The latter shows that the additional radiation during ELMs is between 15% and 40% of the ELM energy, depending on various plasma parameters.

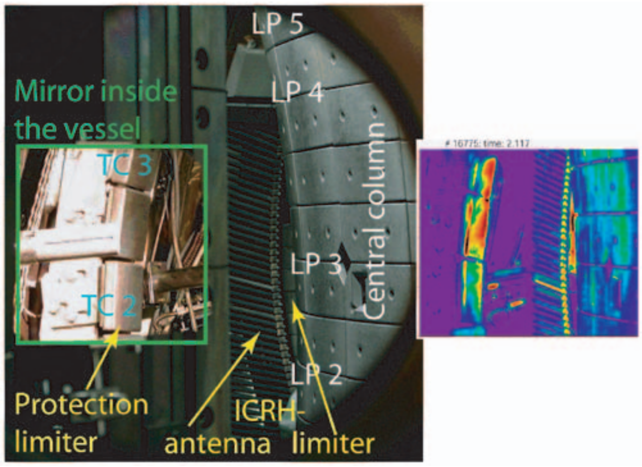

Figure 22: Tangential view into the torus in the visible and IR wavelength region. Main components and diagnostics used are mentioned in the left figure. ELM heat flux pattern calculated from the IR measurement is shown in the right figure. The heat flux double structure at the limiter is due to the limiter geometry.

9.5 Type-I ELM target heat load structures

Complex power deposition structures on the divertor target plates during type-I ELMs have been discovered by fast (few ms) two-dimensional (40 cm x 40 cm) infrared thermography. On the outer target plate there appear, statistically distributed, several laterally displaced, non-axisymmetric, inclined stripes in addition to the usual axisymmetric power deposition line near the separatix. They are mostly well separated from each other and from the main strike zone as presented in Figure 23.

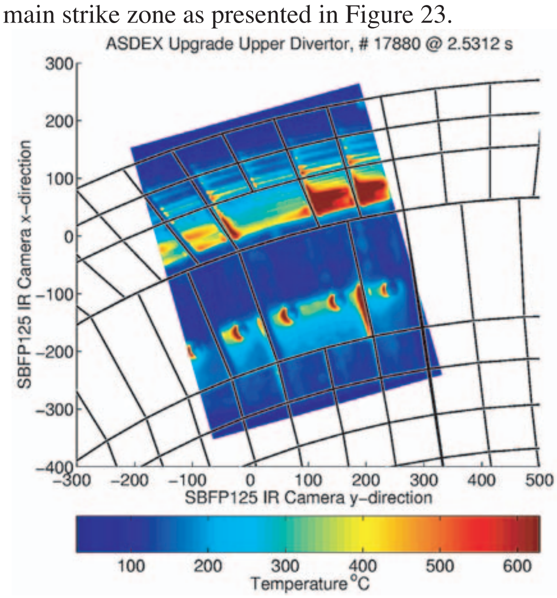

Figure 23: Camera view of the target heat load pattern in the upper divertor. The target tile arrangement is superimposed. The outer strike zone corresponds to the upper three tile rows.

These structures are interpreted as footprints of approximately field aligned, helical perturbations at the low field side of the main plasma edge, related to the non-linear ELM evolution. Based on this picture and in conjunction with extensive field line tracing studies, the ELM related global mode structure can be derived from the target load pattern, yielding on average toroidal mode numbers in a range of 8-24.

9.6 Fast ion losses and limiter load

Low field side limiter glow is frequently observed with NBI and/or ion cyclotron minority heating. It is attributed to fast ions, generated either directly in the edge region ('NBI first orbit loss'), or in the core and transported to the edge by classical ripple-banana diffusion and via interaction with MHD-modes. The maximum energy deposition occurs, where the particle drift surfaces first intersect material walls. The local power load, though marginally tolerable with carbon limiters, may become a problem with tungsten coated limiters, and should be avoided or minimized in next step experiments.

In order to better understand these effects, and to exploit the information on core transport and MHD contained in the fast ion propulsion, a code package has been developed and a fast particle detector is being designed. The code package simulates the ionization pattern of the NBI system (FAFNER), computes the guiding centre trajectory of the fast ions inside the separatrix (HAGIS), taking into account collisions and MHD perturbations and follows the full particle orbit in the edge (GOURDON) until wall or detector incidence (Figure 24). The detector, to be mounted on the mid plane manipulator, is based on the α particle detector design used in TFTR and further developed for W7-AS.

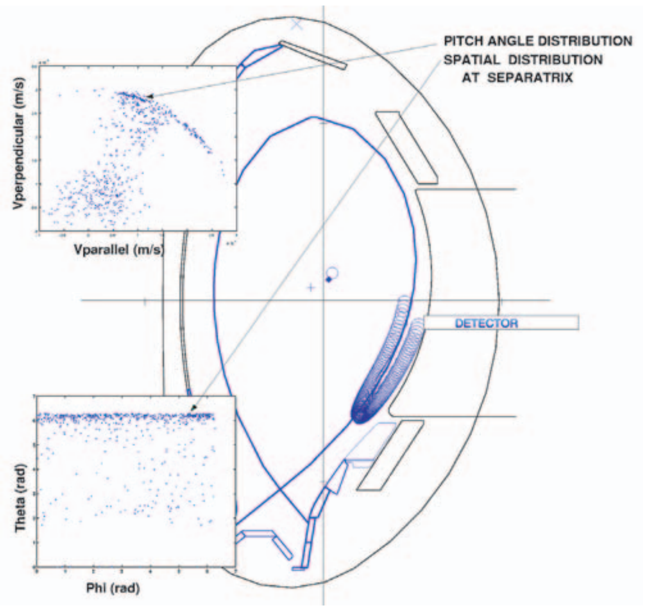

Figure 24:ASDEX Upgrade poloidal cross section together with the phase space distribution of fast particles on the last closed flux surface (HAGIS-GOURDON interface; see inserts). A typical GOURDON particle orbit from the separatrix to the detector is also shown.

9.7 Energy deposition in disruptions

The extension and the time scale of the energy deposition on PFCs during disruptions remains a relevant issue of investigation and discussion since it significantly influences the choice of the first wall and divertor material in a future ITER.

The energy deposition during recent disruptions has been analysed from a statistical point of view. The database built for the analysis contained 44 discharges with complete measurements of the power deposition on the lower divertor plates. The 30 discharges pertain to the divertor II-lyra configuration; the later 14 ones to the divertor II-b geometry. By visual inspection of a large number of time histories of the spatially integrated power, we find that there is no one typical time history but a variety of them. The power density profiles are very broad and extend outside of the divertor region. The amount of energy deposited onto the divertor plates may change from disruption to disruption. Therefore it is necessary to look at the statistical distribution of the power deposited onto the divertor and its different parts. The amount of energy deposited on the lower divertor during the whole disruption (E_{div}) is on average 30 % (and can reach 45 %) of the total pre-disruptive energy of the plasma ($E_{tot}= E_{th}+E_{mag}$). During the 4 ms centred about the thermal quench time, the energy deposited on the lower divertor (E^{th}_{div}) is on average 90 % (and can reach 200 %) of the thermal energy. This suggests that during this time a fraction of the magnetic energy has already dissipated. Figure 25 shows a histogram of the mean amount of energy per unit surface, for discharges with the divertor II-lyra configuration and for the different divertor regions and disruption phases. Similar results have been obtained for the divertor II-b.

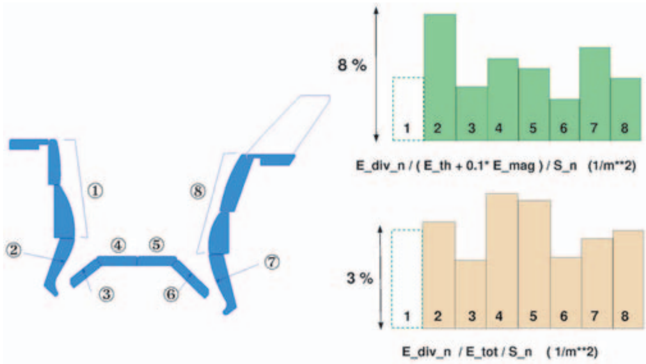

Figure 25: Left: Divertor II-lyra geometry and its 8 regions.Right: Histogram of the power per unit surface deposited on the different divertor regions (30 disruptions) during the thermal quench phase (upper part) and whole disruption (lower part).

The thermography measurements on region n. 1 are not correct and therefore have been disregarded. We conclude that the strike point modules (regions n. 2 and 7) are more loaded than the other parts of the divertor during the thermal quench and that the energy is nearly uniformly distributed during the current quench.

9.8 Tungsten Limiter Tests

During the last campaign, tungsten limiter tests were performed with a W-coated CFC probe on the midplane manipulator, positioned in front of the ICRH protection limiters, but still about 3 cm away from the separatrix. The power flux deposited on the test limiter is calculated by

solving the heat conduction equation with the measured time dependent surface temperature as boundary condition.
The test limiter was exposed to deuterium plasmas in H-mode discharges with about 1s NBI heating of 5 MW, selecting different combinations of NBI sources (with different injection angle and toroidal location) in subsequent shots. The calculated time averaged power flux to the probe was up to the order of 25 MW/m^2. Strong localized erosion of W was found at the front edge on top of the probe. SEM images show that such an erosion is mainly due to arcing occurring in many micrometer-scale hot spot areas. These results show a strong dependence of the deposited power and erosion of W on the injection angle of the NBI beams, a fact which emphasizes the influence of fast ion losses on the low field side limiters.

9.9 Modelling of Tungsten Erosion

The transient limiter phases during ramp-up and ramp-down were identified by spectroscopy and Langmuir probe measurements to dominate the gross erosion of tungsten at the central column (HS). B2-Eirene modelling of stationary limiter plasma could provide a good plasma background for the simulation of impurity transport processes during these phases. DIVIMP simulations using this background plasma reveal that the eroded tungsten from the HS is predominantly re-deposited close to its source. The remaining fraction of W leaves the computational grid mostly at the low-field side and the amount of W reaching the divertor is negligible. The simulations reveal that transport away from the source region is mainly caused by the ion temperature gradient force in competition with friction and the parallel electrical field. The erosion is significantly increased by W self sputtering while, on the other hand, prompt re-deposition only has a very moderate effect due to the low local plasma densities. Comparing simulations for the limiter and the flat-top divertor phases, one finds that the modelled fraction of the discharge-integrated net erosion migrating into the divertor is in agreement with the campaign integrated experimental data on W deposition detected there by ion beam surface analysis.

9.10 Hydrocarbon photon efficiencies and chemical erosion in the divertor

The investigation of the photon efficiency (D/XB) dependencies of CD/CH molecules on the local plasma parameters continued in 2003. The variation of photon efficiencies with plasma edge conditions was studied by introducing CH_4 and CD_4 in deuterium/hydrogen plasma pulses. To obtain a broad range of temperatures and densities at the puffing location, strike-point scans were performed. (D/XB) $CH \leftarrow CH_4$ shows a positive dependence on the density and a negative dependence on the temperature in L-mode hydrogen discharges, whereas weaker dependences are found in H-mode deuterium discharges. A parametric dependence on just density and temperature is not sufficient to fit all the data sets. D/XB values directly measured and obtained from the correlation analysis (Fig. 26(a)) are used to obtain the erosion yield profile. Typical erosion yield values of 0.3÷0.5 % are found in the outer divertor for H-mode deuterium discharge (Fig. 26(b)), whereas shortly after boronization, yields as low as 0.1% have been observed.

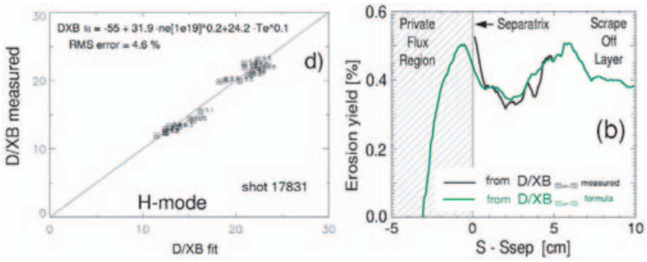

Figure 26: (a) D/XB correlation plots in H-mode discharge and (b) erosion yield profile as a function of the distance from the separatrix.

10 International Co-operations

10.1 DOE – ASDEX Upgrade Activities

The activities ranged from sharing data, carrying out theoretical studies and computations, and joint work on demonstrating new advanced mode operations (such as QH mode and EDA mode). The interaction among the U.S. and ASDEX Upgrade scientists has increased substantially through the International Tokamak Physics Activity (ITPA), through joint work on JET, and through a joint workshop with the IEA Large Tokamak Agreement. About 8 scientists from each side were involved directly in personnel exchanges this year between the U.S. (DIII-D, C-MOD, ORNL, and PPPL) and ASDEX Upgrade in experiments, theory and modelling. Some of the collaborative work is carried out off-site, at home laboratories, in data analysis and modelling work. The collaboration with South Korea is being integrated into the existing collaborations. Thereby, the basis will expand substantially, if the South Korean long-pulse and superconducting tokamak KSTAR starts operating. There were also personnel exchanges and joint workshops from South Korea to U.S. Labs.
The ASDEX Upgrade programme is aimed at establishing and expanding the physics basis for ITER-FEAT and at tokamak concept improvement. The U.S. Fusion programme aims, amongst other things, at increased understanding of tokamak physics. Both of these goals have many common research interests. For example, both ASDEX Upgrade and DIII-D have been at the forefront of research on feedback stabilisation of ‘Neoclassical Tearing’ modes using ECH system and on development of reactor-relevant advanced hybrid scenarios. ASDEX Upgrade and C-Mod share close interest on high-Z wall materials, wall recycling and impurity transport whereas DIII-D will stay with graphite walls. All three tokamaks are keenly interested in plasma fuelling, particle transport and density limits. The main heating and current drive methods are based on NBI, ICRH and ECRH at ASDEX Upgrade and DIII-D, while Alcator C-Mod relies on ICRH and LHCD. RWM stabilisation has been pioneered at DIII-D and is also being considered for ASDEX Upgrade. NSTX with its low aspect ratio complements these investigations in many

fields and looks for off-axis FWCD and RWM stabilisation. At KBSI the buildings for KSTAR have been completed and assembly started in May 2003. Prototype coil tests of both external and internal PF coils have started.
The 18th meeting of the IEA Executive Committee was held at St. Petersburg, Russia, July 8, 2003. The collaboration is expected to continue in 2004 through co-ordinated research among the major world tokamaks with enhanced interaction through multilateral arrangements such as the ITPA and other IEA tokamak agreements. A slightly higher level of activity in direct exchanges is expected, resulting from the participation of Korean scientists.

10.2 University of Cork

The collaboration with University College Cork in the area of MHD equilibrium reconstruction, equilibrium database generation, ITB formation and sustainment criteria, fast q profile recovery from MSE data and the new topic of improved current profile identification from TAE´s and other MHD activity continued in 2003.
The CLISTE interpretive equilibrium code was further extended to interpret tile current measurements of SOL poloidal currents. Work is in progress to incorporate line integrated density measurements into the cost function.
A new equilibrium database was generated with detailed spatial structure in the Grad-Shafranov source profiles. To preserve the dimensions of the coefficients used in the realtime control system, a simple principal component analysis no longer suffices and linear combinations of the magnetic input signals with maximal predictive power for the set of plasma parameters needed by the control algorithm are required.
Fast recovery of the q profile from MSE data using an extension of the method of Function Parameterization is functioning successfully offline, with good agreement between FPJ and CLISTE recoveries of the q profile. The incorporation of the algorithm into the realtime control hardware environments is in progress.

10.3 Centro de Fusão Nuclear

The continuing collaboration with CFN on the measurement of density profiles and fluctuations using swept microwave reflectometers has seen, during 2003, the conversion of the second fluctuation channel (Q-band) to heterodyne with IQ detection to permit the separation of phase and amplitude components. Density profile capabilities were extended to higher densities ($n_e \sim 1\times10^{20}m^{-3}$) with the commissioning of a W-band swept channel, including the installation of a new O-mode antenna. Testing is still in progress but initial results are promising. Sections of the control software have also been substantially upgraded to unify operation and monitoring tasks using a client/server approach. The profile analysis codes have been improved with the inclusion of routines for automatic profile initialization using the two X-mode channels (in preparation for hardware upgrades).
Numerical studies using a 2D FDTD full-wave code have also assisted in understanding of the reflectometer response, specifically in the optimization of the bust-mode technique.
On the physics side, further progress has been made in the study of ELM dynamics as well as ELM energy and particle losses. Asymmetries were found between the density profile behaviour on the high-field and low-field-sides suggesting that the trigger of the ELM is related to the ballooning instability. A dependence of the ELM particle losses with the ELM affected depth was also found. Reflectometry has also contributed to the study of type-I ELM pace making and mitigation by pellet injection in H-mode discharges. This involved studying the density profile evolution during different pellet injection phases, as well as turbulence properties around the pellet deposition region. CFN has also provided co-ordination of MHD experiments (via Taskforce V) and undertaken studies on TAE behaviour, which are detailed in section 5.

10.4 TEKES

The co-operation between IPP and Helsinki University of Technology (HUT) and VTT Processes laboratory (Espoo, Finland) continued with emphasis on four main topics:
1. Re-deposition of carbon is studied by controlled injection of $^{13}CH_4$ marker gas. Sample tiles from all in-vessel areas have been removed after the 2003 experimental campaign and are now being analysed at VTT by Secondary Ion Mass Spectrometry (SIMS).
2. Tiles with C-Re-C multilayer structure, prepared at VTT, were exposed during the previous ASDEX Upgrade campaign at different in-vessel positions and are now analysed at IPP and VTT to measure the thickness and composition of eroded or deposited layers.
3. The dynamics of ELMs is studied at HUT (in collaboration with EPFL-CRPP Lausanne and University of Latvia), with current focus on the existence of deterministic chaos in ELM time series.
4. Monte-Carlo calculations of the beam ion slowing down distribution are made at HUT with the ASCOT code to assess the fast particle distribution in stationary ELM-free "Quiescent H-mode" discharges. These calculations are intended to help clarify the origin of the observed MHD behaviour in this scenario.
5. Edge stability calculations are performed at HUT using GATO and IDBALL codes for cases of Quiescent H-mode and ELMy H-mode plasmas before and after an ELM crash, the latter to study time-dependent ELM dynamics.

10.5 NCSR Demokritos, Athens, Greece

The reciprocating Langmuirprobe system (LPS), designed and constructed by NCSR Demokritos for the lower divertor of ASDEX Upgrade, has been refurbished and adapted to the actual divertor IIb, which is compatible with a larger variety of plasma shapes. For many of these plasmas, the probe track can approach the lower X-point, lying on the 'first' separatrix for bottom single null equilibria, but on the 'second' one for upper single null configurations. Experiments will start early in 2004.

10.6 KFKI-Research Institute for Particle and Nuclear Physics

The collaboration between KFKI-RMKI and IPP aims at investigating hydrogen isotope pellet and plasma interaction. To detect the spatial distribution and time evolution of the visible radiation of the cloud of pellets ablating in plasmas, a fast observation system was built in 2002 and was

further developed in 2003. The system presently consists of three fast digital cameras. Using images of observations from two different directions, the 3D pellet trajectory and velocity distribution were reconstructed for different pellet velocities and sizes. It was found that during the ablation in the hot plasma the pellet is accelerated both in the radial and toroidal directions. The most likely explanation for this acceleration is the rocket effect caused by the asymmetric heating of the pellet surface. The pellet cloud distribution was measured with high spatial and temporal resolution. According to the results of a numerical mode calculating the intensity of the line radiation, the Bremsstrahlung and the recombination radiation of the cloud particles, the mixture of the D_α line radiation and the Bremsstrahlung were detected on the camera images. Therefore both the ablation cloud surrounding the pellet and the drifting cloud (plasmoid) accelerated in the direction of the major radius can be seen on the images.
The code calculating the pellet ablation and cloud expansion was improved by including a neutral gas shielding model. This model takes into account the shielding of the spherically expanding neutral cloud formed close to the pellet surface.

10.7 EURATOM-ENEA-CNR Association, Milan

The contributions to the electron transport investigations are included in Section 8.5.

Scientific Staff

Experimental Plasma Physics Division E1: N. Berger, U. Brendel, A. Carlson, A. Cierpka, T. Eich, H.U. Fahrbach, J.C. Fuchs, O. Gehre, A. Geier, L. Giannone, O. Gruber, G. Haas, T. Härtl, A. Herrmann, J. Hobrik, L. Horton, K. Iraschko, M. Kaufmann, B. Kleinschwärzer, H. Kollotzek, P.T. Lang, P. Leitenstern, C. Li, A. Manini, K. Mank, K.F. Mast, D. Meisel, D. Merkl, V. Mertens, H.W. Müller, P. Müller, Y.-S. Na, J. Neuhauser, J. Neumann, E. Oberlander, G. Prausner, G. Reichert, V. Rohde, W. Sandmann, M. Sator, G. Schall, H.-B. Schilling, G. Schramm, K.-H. Schuhbeck, S. Schweizer, J. Schweinzer, H.-P. Schweiss, U. Seidel, O. Sigalov, C. Sihler, A. Sips, J. Stober, B. Streibl, G. Tardini, W. Treutterer, M. Troppmann, T. Vierle, S. Vorbrugg, M. Wolf, E. Posthumus-Wolfrum.
Tokamak Physics Division: C. Angioni, M. Apostoliceanu, G. Becker, A. Bergmann, R. Bilato, K. Borrass, M. Brambilla, A. Chankin, Y. Chen, D. Coster, T. Dannert, K. Dimova, S. Günter, V. Igochine, F. Jenko, O. Kardaun, A. Kendl, J. Kim, R. Kochergov, C. Konz, K. Lackner, P. Lauber, P. Martin, P. Merkel, Y. Nishimura, G. Pautasso, A.G. Peeters, G. Pereverzev, S. Pinches, E. Poli, T. Ribeiro, S. Riondato, W. Schneider, E. Schwarz, B. Scott, M. Spannowsky, D. Strintzi, E. Strumberger, C. Tichmann, Q. Yu.
Experimental Plasma Physics Division E2: C. Aubanel, K. Behler, H. Blank, A. Buhler, G.D. Conway, R. Drube, K. Engelhardt, M. Garcia Munoz, L. Höllt, H. Höhenöcker, M. Jakobi, A. Keller, S. Klose, B. Kurzan, A. Lohs, M. Maraschek, H. Meister, R. Merkel, A. Mück, H. Murmann, G. Neu, M.-G. Pacco-Düchs, G. Raupp, J. Schirmer, W. Suttrop, K.-H. Steuer, H. Urano, D. Wagner, D. Zasche, T. Zehetbauer, H. Zohm.
Experimental Plasma Physics Division E4: K. Behringer, R. Dux, W. Engelhardt, J. Fink, J. Gafert, J. Harhausen, B. Heger, A. Kallenbach, C. Maggi, R. Narayanan, R. Neu, D. Nishijima, T. Pütterich, R. Pugno, I. Radivojevic, S.-W. Yoon.
Technology Division: W. Becker, V. Bobkov, F. Braun, H. Faugel, P. Franzen, D. Hartmann, B. Heinemann, M. Kick, K. Kirov, W. Kraus, F. Leuterer, F. Monaco, M. Münich, J.-M. Noterdaeme, S. Obermayer, R. Riedl, F. Ryter, W. Schärich, E. Speth, A. Stäbler, F. Wesner, R. Wilhelm, E. Würsching.
Plasma Diagnostics (Berlin): D. Hildebrandt, M. Laux, W. Schneider.
Garching Computer Centre: P. Heimann, J. Maier, H. Reuter, M. Zilker.
Materials Research: M. Balden, I. Bizyukov, H. Bolt, J. Chen, K. Krieger, H. Maier, M. Mayer, J. Roth, M.Y. Ye.
Central Technical Services: F. Ascher, H. Eixenberger, T. Franke, M. Huart, C. Jacob, C.-P. Käsemann, K. Klaster, M. Kluger, J. Maier, H. Nguyen, J. Perchermeier, G. Raitmeir, I. Schoenewolf, F. Stobbe, H. Tittes, F. Zeus.
University of Augsburg: U. Fantz.
IPF University of Stuttgart: G. Gantenbein, E. Holzhauer, W. Kasparek, T. Kubach, P. Lindner, U. Schumacher.
FZ Jülich: A. Kirschner.
ERM/KMS, Brussels, Belgium: A. Lyssoivan.
RISØ, Roskilde, Denmark: H. Bindslev, F. Meo.
UKAEA Culham, Abingdon, England: R. Buttery, H. Meyer, M. Valovic.
HUT, Espoo, Finland: O. Dumbrjas, V. Hynönen, T. Kurki-Suonio, S. Saarelma.
VTT, Espoo, Finland: E. Vainonen-Ahlgren, J. Likonen.
NCSR Demokritos, Athens, Greece: M. Tsalas, N. Tsois.
KFKI, Budapest, Hungary: S. Bató, K. Gál, S. Kálvin, G. Kocsis, G. Veres.
University of Cork, Ireland: M. Foley, P. McCarthy, E. Quigley.
IFP, ENEA-CNR, Milano, Italy: C. Capuano, S. Cirant, A. Jacchia, E. Lazzaro, P. Mantica.
Consozio RFX-ENEA, Padua, Italy: T. Bolzonella, M. Cavinato, R. Lorenzini, M. Valisa, B. Zaniol.
Riga University, Riga, Latvia: V. Kuzovkov, G. Zvejnieks.
FOM, Nieuwegein, Netherlands: M. de Baar.
IST, Lisbon, Portugal: D. Borba, L. Cupido, L. Fattorini, S. da Graca, M.-E. Manso, L. Meneses, I. Nunes, T. Ribeiro, J. Santos, F. Serra, A. Silva, F. Silva, P. Varela.
IOFFE, St. Petersburg, Russian Federation: S.V. Lebedev.
CIEMAT, Madrid, Spain: F. Tabares.
CRPP, Lausanne, Switzerland: T. Goodman, J. Lister, O. Sauter.
EFDA Close Support Unit, Garching: A. Loarte, R. Sartori, G. Saibene.
Guests: C.V. Atanasiu, G. Miron, Inst. of Atomic Physics, Romania; H. Summers, University of Strathclyde, Glasgow, Scotland.

JET Co-operation

Head of Project: Prof. Dr. Michael Kaufmann

1 Introduction

The JET Work Programme is executed under the framework of the European Fusion Development Agreement. Scientific exploitation of JET is carried out by Task Forces with members from all EURATOM Fusion Associates whereas the technical operation is under the responsibility of UKAEA.
In 2003, six experimental campaigns (C8-C12) of more than 110 experimental days were executed. The campaign C9 addressed several issues pertaining to the direction of the magnetic field and plasma current. The second half of 2003 was mainly devoted to the exploitation of the upgraded NBI system (C10, C12). A trace tritium campaign (C11) was focussed on transport studies in ITER relevant scenarios.
In parallel to the execution of campaigns new hardware systems (JET enhancements) have been prepared which will be implemented in the 2004 shutdown.
Thirty IPP scientists were seconded to JET in 2003. Three JET Task Forces (TF) were under leadership of IPP experts. New results of ASDEX Upgrade (AUG) experiments influenced significantly the 2003 JET Programme. Below are described areas where IPP physicists have made major contributions to the execution and analysis of specific experiments on JET as well as to JET enhancements.

1.1 Task Force S1

IPP contributed to experiments described below and was involved in the commissioning of the new pellet track (V-HFS). The latter is thought to allow deeper fuelling of the central plasma. Technical problems in the summer restart prevented scientific exploitation of the new system.

1.1.1 Search of type-II ELMs in JET using ASDEX Upgrade recipes

The search for a pure type-II edge, which would be very advantageous for ITER, has been a major topic in the TF S1 programme. One ingredient is thought to be the closeness to a double-null (DN)-configuration as demonstrated by ASDEX Upgrade. Three different quasi-double-null (QDN) configurations have been tested at JET in 2003 at maximum plasma currents of 2.5 MA, 2.0 MA and 1.5 MA.
In the 2.5 MA shape the closeness to double null had no obvious effect on the ELM behaviour. For $q_{95} = 3$ mixed type-I/II ELMs with good confinement were observed at the Greenwald density (n_e^{GW}). For q_{95} above 3.5, confinement and achievable density decreased and only 0.8 n_e^{GW} could be reached. Therefore it was not possible to access the operational range of type-II ELMs with $n_e > 0.8\ n_e^{GW}$ and $q_{95} > 3.5$-4.
Following experience from AUG the 2.0 MA shape was tested as a further attempt with a larger wall clearance and with the upper X-point well within the vessel. Experiments with this shape have only been done with $q_{95} = 4$. Again the density was clamped at 0.8 n_e^{GW}. Nevertheless a reduction of type-I ELM size and an increase in frequency and inter-ELM activity was seen when approaching QDN, but no complete suppression.
After these failures to find pure type-II ELMs, a dimensionless identity approach has been conducted. Unfortunately, a perfect match to the AUG QDN shape at high triangularity (δ) was impossible. The 1.5 MA shape which was finally used had the upper and lower triangularity inverted. At 0.8 MA and $q_{95} = 4$ these shape indeed showed steady-state edge pedestals without ELMs. The core plasma, however, was not steady-state since it showed a strong central density peaking followed by loss of sawteeth which triggered the accumulation of impurities and high central radiation losses. Such a behaviour is quite commonly observed at high δ, high density discharges and it may not be related to the specific edge conditions. Unfortunately these quiet pedestal phases where not observed at 1.2 MA and 1.5 MA. At 1.2 MA it was possible to combine the experiment with the high β_{pol}-scheme from JT-60U and to achieve a stable small ELM regime with $q_{95} = 6$ and 17 MW of NBI heating ($\beta_{pol} > 1.6$), which is only relevant for ITER if q_{95} can be reduced.

1.1.2 Tritium transport in high-δ, high density ICRH heated discharges.

High density discharges moderately heated with NBI show a slow peaking of the density profile with constant pedestal values. This behaviour is most pronounced at high δ. On AUG and JET it has been observed that the peaking is stopped or even reduced when NBI is partially substituted by central ICRH. One explanation assumes a correlation between the heat conductivity and particle diffusivity. The first is increased in the ICRH case (due to the stiff T-profiles and unchanged pedestal) leading to an increase in D. If this is the case tritium should arrive earlier in the plasma center with ICRH. In contrast, if a change in the particle pinch is responsible for the different peaking, this pinch must be reduced with ICRH which should then delay the T transport.
Only 20% of the 13 MW of NBI heating could be substituted by central ICRH. Following the above model this would lead to an average increase of D by roughly 20% in the confinement region and therefore a reduction of the T propagation by a similar amount. This has indeed been

observed in one pair of discharges. Unfortunately they suffered from (4,3) or (5,4)-NTMs which on the other hand do increase the T propagation. A detailed analysis is therefore necessary to check whether these two effects can be disentangled.

1.1.3 Ion temperature modulation

Experiments were carried out to investigate the properties of ion heat transport by means of power modulation. This method allows to measure the propagation of heat pulses which yields the so-called perturbative heat diffusivity. This quantity delivers a direct measure of the dependence of transport upon temperature gradient around a given working point.

Deuterium discharges were heated by NBI and ICRF in the scheme using ^{3}He minority. The ICRF power was modulated, at 4 Hz or 6 Hz. ICRF is assumed to heat dominantly the ions for ^{3}He concentration of about 10%. The resulting modulation in the ion temperature could be detected with a good signal to noise ratio, which allows to estimate the perturbative heat diffusivity. Comparing this quantity to the diffusivity derived from power balance suggests that ion heat transport might be governed by turbulence increasing significantly above a threshold of the normalized temperature gradient. This is consistent with the profile resilience observed in general. Transport modelling is foreseen to assess these results in detail.

In addition, a scan of the ^{3}He concentration performed in these experiments also allowed to investigate the direct electron heating by ICRF due to mode conversion.

1.2 Task Force S2

IPP contributed to Task Force S2 in areas of operation support, scientific coordination of experiments and data analysis. The main topics for these activities in 2003 are described below.

1.2.1 Confirmation of ASDEX Upgrade´s ‘improved H-mode’ scenario by JET.

The aim of the experiments at JET in 2003 were to establish improved H-mode conditions at 1.4 MA / 1.7 T with similar non-dimensional parameters compared to AUG in stationary conditions. In the experiments plasma shapes with a low triangularity δ=0.2 and δ=0.44 were used to match configurations in AUG.

The current rise phase in JET was optimised using LHCD at ~1 MW to set-up a q-profile with low central shear and q_0 close to 1. By careful timing the start of the neutral beam heating, sawteeth can be suppressed throughout the heating phase. Figure 1 shows pulse 58323, where the initial NBI heating phase uses feedback control to maintain β_N close to 2. After 4.5s of NBI heating the request for β_N is increased to 2.8, just within reach of the maximum available heating power. In these conditions, T_{i0} = 11 keV and T_{e0} = 5 keV are obtained at $\langle n_e\rangle / n_e^{GW} = 0.5$, with neoclassical tearing modes at q=3/2 and 4/3 or fishbone activity in the core occurring without degradation of confinement.

In these conditions peaked density profiles are obtained with $n_{e0}/\langle n_e\rangle \sim 1.3$, at both triangularities (δ=0.2 and δ=0.44) with $\langle n_e\rangle / n_e^{GW} = 0.87$ at δ=0.44. The calculated non inductive current contributions for pulse 58323 add up to 46% of the total plasma current. At 1.4 MA / 1.7 T $\rho^*=7 \cdot 10^{-3}$ is obtained, with the figure of merit for fusion gain, $H_{89} \cdot \beta_N / q_{95}^2$, reaching values up to 0.42 at q_{95}=3.85.

Results in JET are in agreement with results from AUG, concerning plasma performance, density and temperature profile shapes, MHD activity, non-inductive current fractions, range of ρ^* ($6 \cdot 10^{-3} < \rho^* < 9 \cdot 10^{-3}$) and $H_{89} \cdot \beta_N / q_{95}^2$ between 0.35 and 0.5. These JET experiments, in combination with detailed parameter scans at AUG and DIII-D, have been given high priority by the ITPA for collaborative experiments in 2003.

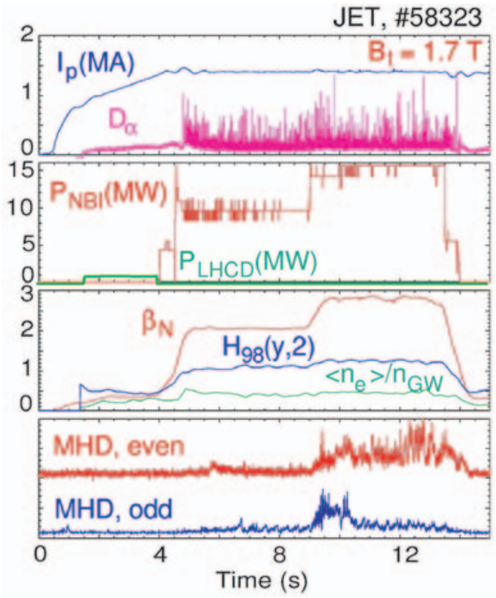

Figure 1: Pulse 58323 at JET is similar to improved H-modes obtained at ASDEX Upgrade.

1.1.2 Modelling of current profile control in JET with neutral beams

For real-time current profile control at AUG, it is planned to use neutral beam injection as an actuator for the control of the current density at three radial positions and poloidal β. In a similar way, the current profile control could be obtained in JET, using six NBI sources. An analysis method used for system identification at AUG has been applied to ASTRA simulations of JET discharges. Although parameters for control are now available, the NBI heating system at JET has less variation of the NBI deposition profile compared to AUG. Hence, priority will be given to demonstrate q-profile control with NBI in AUG before detailed experiments are proposed for JET.

1.1.3 High β_{pol} experiments at JET

The aim of the high poloidal β experiments at JET was to maximise the bootstrap fraction in stationary discharges at low plasma current (1 MA or 1.2 MA at a toroidal field of 2.7 T), using the maximum input power available (NBI: 20 MW, ICRH: 6 MW). By operating at densities close to the Greenwald density limit, these experiments resemble closely experiments done at high β_{pol} at AUG in 2000. The new JET results show that the maximum $\beta_{pol} \sim 1.8$ can be sustained in stationary conditions, and β_{pol} ~ 2.2 transiently. The maximum bootstrap fraction in these experiments was limited to ~ 30% for β_{pol} ~ 1.8, with still ~ 50% of the current driven by the ohmic transformer. Future work in this scenario will concentrate on changing the plasma profiles to obtain a different bootstrap current distribution. The bootstrap current will be increased by more peaked pressure profiles (ITB´s) in combination with reversed q profiles.

1.3 Task Force E

The previously assumed uniformity of Beryllium sources has been investigated spectroscopically by comparing line intensities of singly charged Be ions from different locations. It turned out that the primary Be source distribution in the main chamber as well as the secondary Be re-erosion source in the divertor show significant spatial variations. The connection of these no uniformities to Be migration patterns will be investigated in future studies in more detail.
In order to determine experimentally the flow velocities of intrinsic impurities (e.g., C) in the outer upper SOL, the Doppler shifts were obtained from the high resolution spectra of the lines of sight of KY6 (Lithium-Beam-Diagnostic) using a refined Zeeman analysis which takes into account the geometry and other specific features of the KY6B-diagnostic. The results demonstrate the capability of the analysis technique, and show, in general, a wide variety of different behaviours of the C-flows that depend, e.g. on density, NBI-power, L- or H-mode, and strongly on the location of the valve used for gas-puffing. In particular, a significant reduction of C-flows is observed for the cases of reversed toroidal magnetic field.
A fast particle balance for ELMs was performed using the ionisation gauge. It could be shown that a pronounced density decay observed for certain conditions is caused mainly by effects following the ELM (L-phase, type-III ELMs) and that desorption contributes to the pressure rise in the divertor.
Further work was devoted to evaluation of power load profiles with the IR camera, planning and execution of quiescent H-mode experiments and analysis of DOC discharges with the EDGE2D/NIMBUS package.
The JET Edge Modelling activities were coordinated during the year by IPP[1)].

1.3.1 Search for "Quiescent H-Mode" in JET

The "Quiescent H-mode" (QH-mode) regime, originally discovered in DIII-D and reproduced in AUG is characterised by good H-mode performance (H>1), and the complete absence of ELMs. Nevertheless, it allows stationary operation without impurity accumulation. The QH-mode regime is obtained with neutral beam injection in a direction opposite to the plasma current (counter-NBI), high clearance between plasma and main chamber walls, and low divertor recycling, i.e. minimum gas fuelling and good pumping. In the used JET shape the outer and inner plasma-wall gaps were increased from typically 3-5 cm to 15 cm at midplane. The experiment was preceded by an extended He glow of 4 hours and four-head Beryllium evaporation.
Longest ELM-free phases were found in discharges performed right after the wall conditioning procedure. Stationarity during the ELM-free phases was proven by a constant radiated power and a constant plasma density ($4 \cdot 10^{19}$ m^{-3}, corresponding to 0.4 n_e^{GW}). The effective charge Z_{eff} ranged between 4 and 5 and originated mostly from light impurities. The H-mode performance was adequate, with a confinement factor H_{98y}=1.0-1.1, and similar in ELMy and ELM-free phases.
In QH-mode, ELMs are replaced by pronounced continuous MHD activity, most prominently the "Edge Harmonic Oscillation" (EHO), an edge localised MHD mode with a fundamental toroidal mode number n=1 and higher harmonics. This MHD mode was also observed in the JET experiment and appears continuously during ELM-free phases, as seen both in fast magnetic measurements and in density fluctuations detected by the X-mode microwave reflectometer. The latter measurement confirms the localisation of the EHO at the plasma edge. The EHO is also observed in ELMy phases in between ELMs, but then only in bursts of a few ms duration.
These results indicate that "Quiescent" H-mode with the same signatures as those seen in DIII-D and AUG can be obtained in JET. However, more physical insight is needed to establish it more robustly in JET.

1.4 Task Force H

The domain of investigations of TF H are heating, current drive and plasma rotation physics, launching and deposition issues and optimisation of the systems.
The expertise of IPP in the area of influencing the sawtooth behaviour with ECRH was complemented by similar work using ICCD. Sawteeth could be stabilized and destabilized.
At AUG it was shown that off-axis NBI injection does not drive current at the expected location. In cooperation with UKAEA experiments were devised and performed to investigate the reasons for this apparent lack of off-axis current drive. Using tritium off-axis NBI with various levels of on-axis deuterium NBI, the possible transport of the off-axis fast ions could be investigated for different levels of additional power and thus of profile stiffness. At high q_{95}, no inward transport of the energetic particles was observed, neither at low heating power nor at high power. At low q_{95}, an inward transport of the off-axis fast particles was observed.
IPP scientists participated in the experiments on ELMs, where a toroidal delay of the ELM appearance was found, in the opposite direction to the plasma rotation.
The dependence of ICRH coupling on the plasma shape for triangular plasmas was studied experimentally. Here IPP provided theoretical support.
Experiments on RF plasma production and wall conditioning, in the presence of a magnetic field are very relevant for ITER and W7-X, where regular glow discharges cannot be used, because of the magnetic field. After experiments on TEXTOR and Tore Supra, the method was tested on AUG as a cooperative endeavour between IPP and TEC. This team was essential in getting this method operational at JET.

[1] For more details see section ‘Tokamak Physics’

1.5 Task Force M

In the field of neoclassical tearing modes (NTMs), experiments have confirmed the improvement in confinement in the so-called frequently interrupted regime (FIR-NTMs), especially in the ITER hybrid scenario (high q_0, see fig. 2). New results on JET including the effects of ELMs have reconciled the transition threshold to the FIR regime with that observed on AUG, helping to unify understanding of the subject.

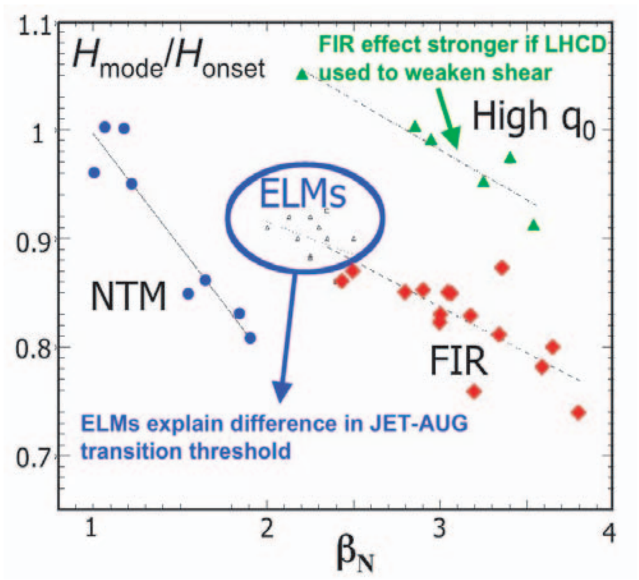

Figure 2: Confinement degradation by NTMs and FIR Modes in JET .

NTM power-ramp down studies have shown that the 2/1 NTM has a lower marginal β threshold than the 3/2 NTM. This raises concerns that 2/1 suppression will be demanding and that it may be better to look at avoidance strategies such as sawtooth control. Contributions to the ITPA cross-device 3/2 and 2/1 NTM meta-stability scaling identity experiments have been made, that have taken place on JET, DIII-D and AUG. The cross-machine data is very consistent and the trend in ρ* predicts a low meta-stability threshold for ITER.

Experiments directed at destabilising monster sawteeth, such as those that are expected to arise as a result of fast alpha-particle stabilisation in a reactor, were planned and executed in close collaboration with TF H. A monster sawtooth scenario was developed and through the application of -90° ICCD close to the inversion radius it was demonstrated that the sawteeth could be destabilised. This is an important technique to avoid NTMs that are triggering by the creation of sufficiently large seed islands due to sawtooth crashes.

Contributions to the development and exploitation of a new JET scenario enabling investigations of resistive wall modes (RWMs) were made, which are predicted to form the β-limit to the ITER steady-state scenario. Experiments using the saddle coils and error field correction coils (EFCCs) have shown error field amplification with plasma pressures above the no-wall β-limit.

IPP participated in the development of a pioneering diagnostic technique for observing Alfvén eigenmodes (AE), enabling Alfvén cascade modes to be resolved in un-precedented detail as compared to magnetic measurements.

In addition, MHD experts have analysed the experimental data in support of the other task forces at JET. In particular, providing information on the evolution of the safety factor and identifying detrimental MHD events as they occur. Publicly available data analysis tools have also been developed, enabling easy inter-shot identification of MHD activity.

1.6 'JET-EP' Enhancements

The JET Enhanced Performance (EP) Programme consists of 17 projects which are currently being executed and are due to be completed within the major 2004 shutdown. IPP has been involved in five JET enhancements and is the leading Associate for two diagnostic enhancements.

For the ITER-like ICRH antenna project IPP contributed to the testing of components for the transmission line.

1.6.1 Bolometer Diagnostic KB5

The new vertical (KB5V) and horizontal (KB5H) cameras will not only replace the existing bolometer diagnostic, but will allow high resolution measurements in the divertor region. The project began the year considerably behind schedule. This was due to a late discovery in 2002 of inadequacy in disruption stress design of KB5V, which coerced a redesign thereby postponing work on KB5H. Nonetheless, technical specifications for the Electronics and Bolometer Cameras (multiple tender) were produced and the KB5V Final Design Review held early enough that Calls for Tender (CfT) could be issued in March. Of the three responses for the camera CfT, PINK Vakuum of Wertheim was chosen to receive the contract. Expected delivery dates of the cameras (summer 2004) show that this enhancement is fully on track.

1.6.2 Lost Alpha Particle Diagnostic

The scintillator probe system will give information about the gyro radii (40 mm to 140 mm) and pitch angle (30° to 86°) of fast ions and charged fusion products in various plasma scenarios. The probe has to be positioned close to the plasma edge in order to avoid ion orbit blocking by limiting in-vessel components. The major technical challenge was to find a design being capable to withstand the structural and thermal loads caused by disruptions and neutral beam injection adjacent to the scintillator probe, respectively. The final design review was submitted in September.

Scientific Staff

S. Bäumel, R. Bilato, V. Bobkov, X. Bonnin, K. Borrass, A. Chankin, G.D. Conway, D.P. Coster, R. Dux, T. Eich, J. Fink, J.C. Fuchs, J. Gafert, A. Geier, S. Günter, G. Haas, J. Hobirk, L.D. Horton, A. Kallenbach, O. Kardaun, K. Krieger, P.T. Lang, M. Laux, A. Lorenz, M. Maraschek, M. Mayer, K. McCormick, H. Meister, D. Merkl, A. Mück, Y-S. Na, R. Neu, J-M. Noterdaeme, A. Peeters, G. Pereverzev, S.D. Pinches, R. Pugno, F. Ryter, J. Schweinzer, A.C.C. Sips, J.K. Stober, W. Suttrop, G. Tardini, D. Wagner, A. Werner, F. Wesner, W. Zeidner, H. Zohm

ITER Co-operation Project

Head: Dr. Lorne Horton

1 Introductory Remarks

In 2003, the developments towards the realization of ITER moved towards their conclusion with the selection of Cadarache, France as the preferred European site and the withdrawal of the proposed Canadian site. Moreover, China, Korea and the US have (re)joined the activities, bringing the number of participants to six and reducing the potential cost burden on individual members. The ITPA (International Tokamak Physics Activity) has proven to be a bottom-up forum for physicists worldwide to establish the physics base for ITER and other burning plasma experiments. IPP contributes actively to this activity, mainly by providing input from the ASDEX Upgrade tokamak, which carries out a broad physics programme that is mainly directed towards the preparation of ITER (see the corresponding section of this Annual Report). In addition, the stellarator community is now contributing to the ITPA, including experts from the WENDELSTEIN Team. The ITER construction project has been divided into procurement packages and the international negotiations on the division of these packages between the partners are now well advanced. IPP has expressed a strong interest in various fields, ranging from diagnostics design and procurement to developing and procuring the sources of the NNBI system. Moreover, building on its traditional strength in plasma physics, IPP aims at playing an important role in the EU accompanying physics programme during ITER construction with its facilities ASDEX Upgrade and W7-X, both of which will be available to the EU associations for experimental work.

2 Prediction of ITER Performance

The prediction of ITER performance is mainly carried out in the framework of the ITPA activity, both through contribution of ASDEX Upgrade data into the various databases as well as analysis of these.

In order to improve upon simple power-law scalings such as ITERH-98P(y,2), which has been used as a reference for the ITER FEAT design, two approaches were pursued: (a) interaction models to the ITERH.DB3v10 dataset with additional timeslices from ASDEX Upgrade, JET and JT-60U. With respect to ITERH-98P(y,2), four terms are added on a logarithmic scale, one of these describing the roll-over near the Greenwald limit and another utilising the plasma shape factor $F_q = q_{95}/q_{eng}$ related to the plasma triangularity. The other two terms describe interaction between current density, electron density and power flux across the separatrix. Similar to a simple power-law based on the deuterium subset, this interaction scaling leads to some 15%, i.e. about one technical standard deviation, lower prediction for (type III) ELMy confinement in ITER-FEAT inductive reference discharge than the point prediction of ITERH-98P(y,2). (b) two-term power-law scalings based on a separate analysis of the plasma core and pedestal energy content, which appeared in Nuclear Fusion and lead to similar predictions of the confinement time in ITER-FEAT as ITERH-98P(y,2), but are not tailored to describe a roll-over with less favourable confinement near the Greenwald limit. Moreover a re-analysis of the ITERH.DB 12 dataset was made expressing the confinement time scalings in dimensionless parameters, ρ^*, β and ν^*, while using temperatures as predicted by a scaling to avoid a spurious correlation illustrated by F. Galton (1889). A preliminary joint analysis at an ITPA meeting in San Diego indicated the presence of systematic deviations from a simple power-law, which are to be pursued further.

After being presented at the IAEA conference in Lyon, a paper on the comparison of ITER performance predictions has appeared in Nuclear Fusion. The three methods are based on (a) global confinement analysis, followed by 1/2-D temperature profile integration; (b) dimensionless similarity experiments from JET and DIII-D; (c) performance predictions from four theory-based models (Multi-mode, Weiland, IFS/PPPL, GLF23). From this investigation it is concluded that (i) a reduction of helium fraction markedly increases the operating window for achieving $Q > 10$; (ii) a pedestal temperature in the range of 3.0 - 5.5 keV is projected to be expected in ITER and also to be required for achieving a predominance of alpha particle heating at the reference operating point; (iii) predictions by the three alternative methods yield a similar range for the ratio Q between fusion power and net input power: $6 < Q < 12$ when n_e/n_G, with Greenwald density $n_G = I/\pi a^2$, varies in the range 2/3 - 1.

The accompanying paper of the ITER Physics Basis Overview presentation by V.S. Mukhovatov at St. Petersburg in the framework of the ITER Transitional Arrangements (ITA) has appeared in PPCF. The overview summarises more or less the established state-of-the-art in confinement and plasma transport (including issues at high density), heating power threshold for achieving (ELMy) H-mode, power and particle control, ELM's, sawteeth, NTM's, disruptions, improved H-mode and hybrid scenarios, TAE's and fast particle physics, and refers to a related plasma diagnostics IAEA paper by A.E. Costley et al.

The L-mode database in the ITPA framework has been extended with data from ASDEX Upgrade, FT-U, HL-1M and NSTX. Interestingly, the ratio between L-mode and H-mode thermal energy scaling appears to depend on aspect ratio as well as Larmor radius, the latter in accordance to a theoretical difference between Bohm (L-mode) and gyro-Bohm (H-mode) transport. A further extension of the L-mode database, especially with respect to hydrogen discharges, serves to improve the comparison between L-mode and H-mode scaling and to predict performance of ITER FEAT during hydrogen operation.

Fourteen fundamental issues on statistics, briefly formulated by Sir D.R. Cox during his Bernoulli Lecture at Groningen University, have been analysed and the results were published as a view of Groningen statisticians in International Statistical Review (with discussion). The ensuing collaboration with W. Schaafsma et al. on the subject of Distributional Inference, which lies at the root of predicting epistemic probabilities of future events, is continued; the work on Classical Methods of Statistics, with physically motivated datasets from ASDEX Upgrade, has been brought to a temporary conclusion with a book submission to Springer-Verlag.

3 Design of ITER Technical Systems

3.1 Diagnostics

The area of diagnostics remains a focus of IPP's ITER activities. An EFDA contract (EFDA/03-1117) for the development of a radiation hard bolometer foil has been signed. In co-operation with UCSD (Prof. F. Hellman, D. Queen), the production of a platinum foil on a silicon nitride insulator is planned. The neutron cross-section of platinum is a factor of 9 smaller than gold and therefore the new foils should be able to be operated successfully for a longer period at constant neutron flux before the resistive meander is damaged. Pin compatibility with the present foils allows a simple exchange of the foils in the currently used housing to allow tests of the new foil to be carried out in ASDEX Upgrade.

The development of the thermography diagnostic for the divertor and the main chamber is being done in cooperation with CEA-Cadarache. In 1997, the IPP proposed a wavelength multiplexing system for divertor surface temperature monitoring. The modified divertor geometry in ITER-FEAT requires a redesign of this proposal. This is being done by the ITER IT (K. Itami, 30th EPS conference). In parallel to the wavelength multiplexing approach, the conventional optics layout has to be investigated and brought up to the same level of design as the wavelength approach to allow a final decision on the thermography diagnostic design, in particular vis-à-vis the technique based on optical fibers which is being studied in a contract between EFDA and CEA-Cadarache. This is the aim of a contract between IPP and EFDA.

3.2 Heating systems

A major field of support for ITER is the contribution to the R&D for heating systems, based on the experience gained on the IPP fusion experiments. Main contributions are given in the fields of NNBI, ICRH and ECRH. For the latter, the design and testing of the remotely steered launcher is being carried out by the IPP sub-association IPF Stuttgart and is described in the corresponding section of this Annual Report.

3.2.1 Design of the ITER Upper ECRH Launcher – Physics Integration

In 2003, IPP became the leading Association in the physics integration activity concerning the ITER upper ECRH launcher design. The task here is to evaluate the performance of different design options with respect to the physics aims of the ECRH system. For the upper launcher, the main task is NTM stabilisation. Here, only the current deposited within the island counts so that the figure of merit is the ratio of driven current to deposition width. In a first step, the ECRH modelling codes used by the Associations involved in the task were compared. Very good agreement was found between TORBEAM developed at IPP and ECWGB (CNR Milano). The agreement is less good, but still acceptable, for the BANDIT-3D code (UKAEA, Culham), mainly due to a different methodology used in this code (ray tracing and Fokker-Planck absorption / current drive as opposed to beam tracing and an analytical model for absorption and CD).

Next, a series of ITER equilibria typical for high performance operation was established. These include an li scan I scenario 2 (the standard H-mode Q=10 scenario) as well as a hybrid scenario (scenario 3) and a low q case (scenario 5). It was found that the resonant surfaces q=1.5 and q=2 surfaces can be reached, for a fixed toroidal angle of 20 degrees, with a poloidal steering range of ± 8 degrees. This is an important input for the design team since such a large steering range is at the limit of the presently foreseen option. Furthermore, at 20 MW absorbed ECCD power, the predicted driven current density is of the order of the local bootstrap current density at q=1.5 whereas it exceeds the bootstrap current density at q=2 by up to a factor of 2. From this it can be concluded that the present system is marginal for the q=1.5 surface, but has some reserve for q=2.

3.2.2 ITER NNBI System

In 2003 the development of a large-area RF source for negative hydrogen ions, an official EFDA task agreement, has made significant progress. The project is aiming at demonstrating ITER-relevant ion source parameters, i.e. a current density of 20 mA/cm^2 accelerated D- ions from a PINI-size extraction area for pulse lengths of up to 1 hour. The final results are expected by mid 2005.

The investigations of Cs-free experiments were stopped in spring, because it became clear from theoretical studies that it would be very difficult indeed to achieve the required yields. Instead attention was redirected towards surface processes, in which hydrogen ions and neutrals, impinging on a surface of low work function, yield a flux of negative hydrogen ions leaving the surface. The most widely spread method of achieving low work function is the technique of depositing thin Cs layers onto internal Molybdenum or Tungsten surfaces. Although this technique has been found to be rather difficult with respect to reproducibility, Cs evaporation experiments were resumed. A new type of oven was used, that seemed to promise a more reproducible and well-controlled way. The major achievements can be summarised as follows.

(i) With Cs evaporation the source can be operated at a much lower pressure than previously experienced and the H- current density does not decrease any more with pres-

sure. This is in agreement with the physics expectations from surface processes in contrast to volume ones.
(ii) Despite the new oven design, reproducibility can still be optimised. Nevertheless under non-optimum conditions current densities of up to 20 mA/cm^2 accelerated H- in the right pressure range have been achieved.
(iii) Short pulses in deuterium have been possible despite the neutron production by closing the experiment hall and using a remote control room: up to 17 mA/cm^2 accelerated D- ions have been reached. The co-extracted electron current can be reduced to values lower than the ion current by increasing the filter strength (see fig. 1). The time evolution in fig. 1 is mainly governed by improving the Cesium distribution in the source. The recorded neutron flux is 40 times lower than estimated from positive ion experiments.

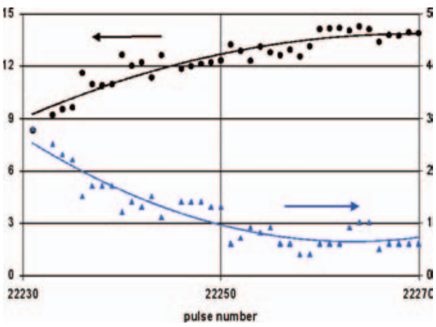

Figure 1: Evolution of the calorimetric D$^-$ current density and electron to ion current ratio in a configuration with an increased filter field.

(iv) The accompanying electron current can be largely suppressed by choosing a sufficiently strong magnetic filter in combination with modest positive electric biasing of the plasma grid (≈ 15 V) . In hydrogen operation the ratio Ie/I- was as low as 0.25, in deuterium 0.6. The ITER requirement is ≤1.
(v) Increasing the extraction area by roughly a factor two (150 cm^2) results in the same calorimetric ion current density in hydrogen, compared to the small extraction area (70 cm^2) see fig. 2. One has to take into account, that the larger area is being investigated on a different test bed ("MANITU" = Multi-Ampere Negative Ion Test Unit) where many aspects are slightly different from the small testbed BATMAN (different ion optics, Rf power supply, Cs reproducibility, diagnostics etc.). The investigations are ongoing.

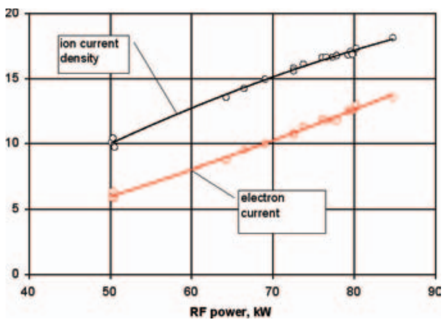

Figure 2: H$^-$ and electron yields with increased (150 cm^2) extraction area as a function of RF power.

Diagnostic development includes Langmuir probes, though complicated due to the magnetic filter field and by the RF field that introduces noise pickup. Spectroscopic measurements in collaboration with Augsburg University have yielded the knowledge of the electron temperature, H_0 density, distribution function of vibrationally excited $H_2(v^*)$, and the gas temperature. This allows computing the H- density from pure volume processes. It has been shown to be unacceptably low. On the other hand, non-hydrogen plasma constituents and in particular the Cs / Cs$^+$ densities have been investigated and give valuable clues in this respect. A laser detachment system to measure the H$^-$ concentration is still suffering from low signals.
Modelling studies concern the plasma dynamics in the driver / expansion region as well as the plasma / extraction boundary under the influence of magnetic, electrostatic and space charge fields, a problem much more complex than the analogue one of positive ions. The latter work is being done in collaboration with Lublin University, Poland.
The very encouraging results quoted above represent the achievement of almost all of the essential ITER NBI requirements. What remains to be shown is the extrapolation to larger size and to 3600 s pulse length. In preparing those activities, the procurement of a high voltage power supply and a RF power supply for c.w. operation are under way. Furthermore a cryo pumping system is being developed in collaboration with FZ Karlsruhe. It is a cryo sorption pump similar to the type that is presently being tested for ITER. In context with long pulses and deuterium operation the required neutron shield has turned out to be much simpler than previously thought. Also the design of a large-area plasma source (about half ITER-size) for the demonstration of size scalability has been finished (see fig. 3) All those components are scheduled to enter commissioning towards the end of this year.
Experiments with a hollow cathode arrangement are being pursued in the frame of a Diploma work.

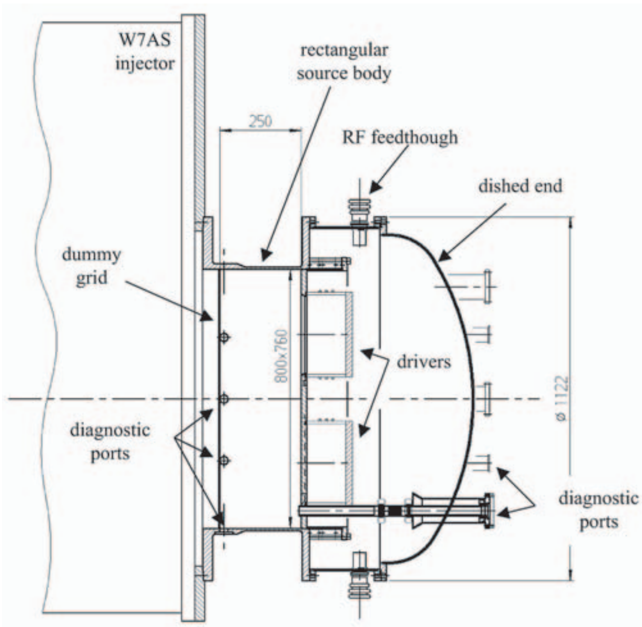

Figure 3: Layout of the half size ITER prototype source consisting of a 800 x 760 mm x mm source body, a height adjustable back plate which houses the drivers and a vacuum enclosure of drivers and back plate.

3.2.3 Developments for the ITER ICRH System

Work is underway, under an EFDA R&D contract, for the development of c.w. capable RF generators. To this end, the test stand in Garching (a section of resonant transmission line) has been put into service. Ceramic spacers and electrical spring contacts have been successfully tested for c.w. operation. AlN was found to be a material that combines the desired properties: low electrical loss, high heat conductivity, non-toxicity. Forthcoming are tests of a ceramic spacer of Al_2O_3, sliding contacts, transmission lines without cooling of the inner conductor and a mock-up of the in-vessel transmission lines.

3.3 Hydrocarbon Erosion, Transport and Deposition

3.3.1 Carbon Erosion Mitigation by Beryllium Layer Formation in ITER

The chemical erosion of C components poses a significant limitation to the ITER operation time due to reduction of component lifetime and an intolerable Tritium inventory due to co-deposition of eroded C species. Due to the large amount of Be in the ITER main chamber wall the Be plasma impurity level in the divertor is expected to be in the order of a few percent. This Be will be deposited onto the divertor C components and may form a protective layer reducing erosion and thus alleviating the use of C in ITER.

The formation of Be layers deposited from a Be seeded D plasma was investigated at the PISCES-B facility at UC-San Diego. In the experiments a C target was exposed to D plasma with varying Be concentrations in the range from 0.01 to 0.3 %. The C physical and chemical erosion was monitored spectroscopically and through weight loss measurements after exposure. It was found that in steady state the C surface became covered almost entirely with Be. The Be plasma concentration required to cover the C surface and thus suppress C erosion was found to always be << 1% even at temperatures of 1280K where Be diffusion and radiation enhanced sublimation resulted in strong Be loss from the surface. This resulted in a reduction of both the physical and chemical erosion of C which scaled linearly with Be surface coverage indicating the observed reduction being a pure coverage effect while the chemistry of the erosion process is not influenced by the layer.

To extrapolate the results gathered at the PISCES-B facility to ITER conditions computer simulation codes were developed to model the formation of shielding Be layers on C surfaces. The model includes erosion, implantation, diffusion and re-deposition of the eroded species. The developed codes well reproduced the PISCES-B results, which were used to benchmarked the computer models. Currently efforts are undertaken to extrapolate the results to ITER.

3.3.2 Hydrocarbon Transport and Deposition

A series of experiments dedicated to the analysis of transport and deposition of hydrocarbon molecules has been performed at the plasma generator PSI-2. As a source of hydrocarbons, defined amounts of CH4 and C2H4 were blown into the plasma. After injection the molecules undergo a series of ionisation and dissociation reactions. By means of an optical interference technique the thickness of deposited layers on temperature controlled collector surfaces (outside the plasma column) was measured in situ for different plasma conditions as a function of temperature of the collector. Such experiments were performed for hydrogen and deuterium discharges with different plasma parameters to study their influence on hydrocarbon decomposition and film formation. In order to avoid erosion by atomic hydrogen, similar experiments were conducted in argon discharges. It was found that the flux of atomic hydrogen mainly determines whether net-deposition or net-erosion occurs. Furthermore, global and local deposition and their dependence on electron density could be studied by injecting the hydrocarbon at two different positions. hydrogen

Staff

Performance predictions: O. Kardaun, ITER Transitional Arrangement physics cooperation group, ITPA Confinement and Pedestal Database cooperation group

Diagnostics: A. Herrmann, L. Giannone

ECRH Physics Integration: E. Poli, G. Ramponi (CNR Milano), G. Saibene (EFDA CSU Garching), F. Volpe (UKAEA), H. Zohm

NNBI: M. Bandyopadhyay (IPR Gandhinagar, India), A. Encheva, H. Falter, U. Fantz, P. Franzen, B. Heinemann, D. Holtum, W. Kraus, Ch. Martens, P. McNeely, R. Riedl, W. Schärich, J. Sielanko (University of Lublin, Poland), E. Speth, A. Tanga

ICRH: W. Becker, D. Birus, F. Braun, H. Faugel, D. Hartmann, J.-M. Noterdaeme, J. Wendorf, F. Wesner

Erosion studies: K. Schmid, R.P. Doerner (Center for Energy Research, UCSD), M.J. Baldwin (Center for Energy Research, UCSD), J. Roth

Deposition studies: W. Bohmeyer, G. Fussmann, A.V. Markin (Institute of Physical Chemistry, RAS, Moscow), D. Naujoks, H.-D. Reiner **ITER Transitional Arrangement physics cooperation group:**

V.S. Mukhovatov, G. Bateman, A.N. Chudnovskiy, A.E. Costley, J.G. Cordey, G. Federici, Y.V. Gribov, O.J.W.F. Kardaun, A.S. Kukushkin, A.H. Kritz, T. Onjun, A. Pankin, G.V. Pereverzev, F.W. Perkins, A.R. Polevoi, V.D. Pustovitov, M. Shimada, Y. Shimomura, T. Sugie, M. Sugihara, G. Vayakis, I.A. Voitsekhovich, J. Weiland, O.V. Zolotukhin.

ITPA Confinement and Pedestal Database cooperation group:

G. Bateman, G. Becker, M. Bell, G. Bracco, R. Budny, C. Bush, A. Chudnovskiy, J. Connor, J.G. Cordey, A.Coté, Z. Cui, J. DeBoo, A. Dnestrovskij, Yu. Dnestrovskij, T. Fukuda, M. Greenwald, Y. Gribov, G. Hammett, T. Hatae, T. Hoang, L. Horton, W. Houlberg, A. Hubbard, F. Imbeaux, G. Janeschitz, Y. Kamada, O. Kardaun, S. Kaye, A. Kirk, S. Konovalov, A. Kritz, A. Kukushkin, A. Kus, S. Lebedev, V. Leonov, Y. Liu, D. Meade, Y. Martin, D. McDonald, Y. Miura, J. Ongena, T. Osborne, M. Osipenko, G. Pacher, H. Pacher, G. Pereverzev, F. Perkins, A. Polevoi, C. Roach, M. Romanelli, F. Ryter, R. Sartori, K. Shinohara, J. Snipes, A. Stäbler, J. Stober, L. Sugiyama, W. Suttrop, A. Sykes, T. Takizuka, K. Thomsen, K. Tsuzuki, H. Urano, M. Valovic, M. Walsh.

WENDELSTEIN 7-AS

Head: Dr. Rolf Jaenicke

1 Overview

After shutdown of the experiments on the W7-AS stellarator in July 2002 analysis of the extended database gained during the last experimental period was continued. Efforts concentrated especially on understanding of the newly discovered ”High Density H-mode“ (HDH-mode) with its favourable properties and of the surprisingly high $\langle\beta\rangle$-values obtained in the presence of the island divertor modules.

Discharges where a conventional ELM-free H-mode (H*-mode) is followed - after an additional gas puff - by the HDH-mode supply valuable hints on the different impurity transport properties. The EMC3/EIRENE code developed for interpretating the island divertor results were further improved by comparing its predictions with the experimental results - especially to allow extrapolation to the conditions of the successor experiment, W7-X. The MHD stability of the high-β discharges was further investigated including stability studies in special cases and comparative experiment/theory investigations on Alfvén modes. Additionally, equilibrium calculations with the PIES code were started at PPPL, Princeton, to get a more consistent picture of the magnetic field topology in high-β discharges.

2 Experimental and theoretical results

2.1 Divertor related studies

2.1.1 Impurity transport with the island divertor

With the W7-AS island-divertor configuration essentially three operational modes can be established under high-power ($P_{nbi} \geq 1$ MW) and high-density ($n_e > 10^{20}$ m^{-3}) conditions: With increasing density one encounters: a) Normal Confinement (NC: peaked n_e, T_e and p_{rad} profiles, whereby P_{rad} increases with time; ELMs can be present at higher n_e), b) the Quiescent H-mode (H*: no ELM activity; flat n_e profile, peaked T_e profile, hollow p_{rad} profile, whereby P_{rad} increases rapidly with time – generally leading to radiation collapse), and c) the High Density H-mode (HDH: no ELMs; n_e and T_e profiles similar to H*, but p_{rad} peaked outside the transport barrier and stationary). In contrast to NC, both H* and HDH exhibit energy confinement times in excess of standard stellarator scalings. Equally important and of primary interest here is the behaviour of impurity confinement, i.e. the different impurity accumulation profiles for NC and H*, and the observed impurity-flushing for HDH, where Thomson scattering measurements of density and temperature profiles do not show a significant difference within the error bars between H* and HDH.
Initial ad hoc simulations of core impurity transport pointed to a significant reduction of the inward convective velocity for HDH plasmas in contrast to NC, rather than a change in diffusion coefficient. In principle, a simple physical explanation is provided by neoclassical theory, which indeed predicts a smaller inward velocity for the flatter HDH n_e profiles. However, the same physics also dictates that the steep n_e profiles at the plasma edge must lead to a strong inwards-directed ”convective edge layer”. Thus, impurities would be driven to the edge as a result of the flat n_e profiles and then effectively held there inside the transport barrier, leading to very long confinement times. Since this is in contradiction to observation, high edge diffusion had to be artificially invoked in the peripheral region in order to counteract the neoclassical inwards convection and to match the strikingly small confinement times τ_{imp} observed in HDH. Aside from yielding small τ_{imp}, this transport model can also approximately reproduce p_{rad} profile shapes as well as C^{6+} distributions measured by Li-beam CXS in NC and HDH plasmas. A further result is that impurity transport in H* emerges as being basically neoclassical, without any anomalous edge diffusion as in HDH. Interestingly, the deduced transport coefficients show remarkable agreement with neoclassical values, derived for axisymmetric devices, concerning both their radial profiles as well as absolute values - except for the high edge diffusion.
Within the discussed HDH impurity transport model, anomalous edge diffusion is a central and essential feature. Nonetheless, in back-to-back comparisons between H* and HDH, no direct indications of an increase in edge turbulence or mode activity have been apparent. This includes analysis of signals from: Mirnov coils placed at the wall as well as near the separatrix, Langmuir probes at the target plates and near the separatrix, examination of density fluctuations via a microwave reflectometer in the n_e gradient region, soft x-ray tomography and various H_α viewing channels. Thus, the nature of the conjectured enhanced diffusion is unknown and not yet capable of being extrapolated to other situations. On W7-AS, HDH has been found only for impurities in the Pfirsch-Schlüter regime (ν*>1). But H* can also be established for ν*>1, albeit at a

lower value than for HDH, so high collisionality per se is not a singular criterion for attainment of HDH.

2.1.2 EMC3-EIRENE code modelling

After extension of the EMC3-EIRENE code to island-divertor configurations with ergodic structures, a dedicated numerical transport study on detachment in W7-AS was carried out by varying the separatrix density and the input power through the separatrix. Modelling reproduced the experimental observation that (partial) stable detachment in W7-AS exists only above a critical value of the target-to-separatrix distance Δx as an increasing function of the connection length L_c. This indicates that sufficiently strong parallel transport is a pre-condition for stable detachment. Furthermore, the code simulations showed that by increasing the separatrix density after the detachment transition, which is characterised by a shift of the radiation front to the X-point just in front of the targets, two completely different carbon radiation patterns develop for stable and unstable detachment. In the stable large-Δx and small-L_c cases, the radiation zone moves away from the divertor region towards the X-points located in the inboard side of the torus, whereas in the unstable small-Δx or large-L_c cases the radiation zone stays in the divertor region while moving radially into the plasma core. The predicted inboard-X-point carbon radiation picture for stable detachment was verified by the 2D patterns of CII radiation from a CCD camera viewing vertically through the plasma in the divertor region and indirectly by target thermography showing high local heat fluxes on the target region magnetically connected to the outboard side of the torus. According to the code simulations and a linear stability analysis, the detachment instability is associated with the loss of neutral gas screening due to very low temperature in the strongly radiating divertor region.

2.2 High-β experiments

The data of the high-β programme of W7-AS gathered in the past years were further investigated to improve understanding of this operational regime. This was done with respect to the overall performance, including stability studies in special cases and comparative experiment/theory investigations on Alfvén modes. Additionally, equilibrium calculations with the PIES code were started at PPPL, Princeton, to get a more consistent picture of the magnetic field topology in high-β discharges, including the effect of the control coils at high external rotational transform values ι_{ext}.

During operation of W7-AS continuous progress in the achievable volume-averaged $\langle\beta\rangle$-values was made. Most of the progress was due to upgrades in the neutral beam (NB) heating power, which finally reached 3.5 MW through-port input power of a purely co-injecting system. Additional improvement was possible by installation of correction coils and island divertor modules. The correction coils were used to compensate the boundary islands at high-ι in order to increase the plasma volume for higher NBI absorption and higher global confinement. They allowed access to high-ι configurations ($\iota_{ext} \approx 0.5$) where the Shafranov shift is smaller (ι-effect), and where the island divertor modules contributed to reduce the impurity radiation in these high density discharges. The progress is documented in Fig.1 by comparing estimated $\langle\beta\rangle$-values versus ι for the campaigns before divertor installation and change in the NBI system with those thereafter. A proper evaluation of the β-values involves equilibrium calculations where the volume is adjusted according to the in-vessel components functioning as limiters. The $\langle\beta\rangle$-values calculated with NEMEC are usually higher than the ones in Fig.1 but only a subset of these discharges was analysed this way. The highest $\langle\beta\rangle$-values reached 3.4%. The most striking features in Fig.1 are 1) that for $\iota < 0.35$ no improvement can be identified, 2) the strong increase for medium up to 0.4 with following saturation and decay at the higher ι-values and 3) the overall extension of the accessible ι range. The present conjecture is that the limitation at lower ι may be attributed to an equilibrium β-limit roughly increased by a factor of 2 compared with a classical stellarator. At medium and high ι the increased heating efficiency together with the beneficial effect of the correction coils and the divertor installation (reduced impurity radiation) are thought to be effective. The decay in $\langle\beta\rangle$ at high ι may result from the correction coils becoming less effective in compensating the boundary islands because the responsible error fields increase with ι.

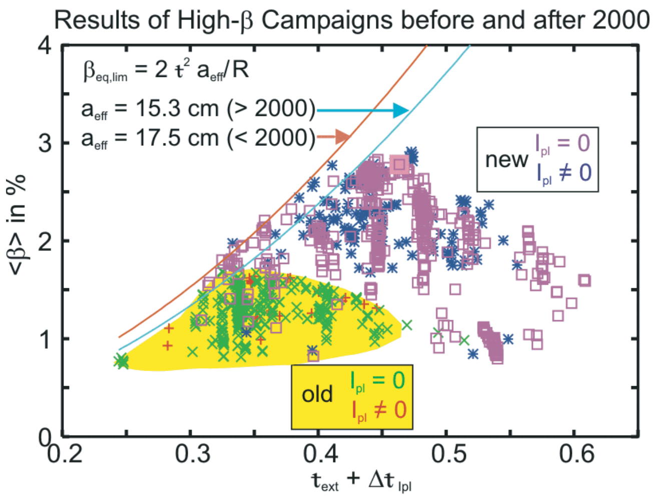

Figure 1: Plot of estimated $\langle\beta\rangle$-values versus sum of external ι_{ext}-value and $\Delta\iota_{Ipl}$ (derived from the total net toroidal plasma current I_{pl} at minor radius a_{eff}). Here, $\langle\beta\rangle$ is estimated from the diamagnetic energy, the magnetic field on axis and an estimated volume indicative for the different limiting structures in the corresponding time periods before and after divertor installation. The yellow region indicates the range (green & red symbols) accessible before divertor installation

The last point is investigated in a collaboration with PPPL, Princeton, using the PIES code, which does not assume the existence of flux surfaces. First preliminary results show ergodisation of the magnetic field at the boundary at high β-values, which is stronger without the usage of the correction, coils, reducing the available plasma volume (Fig. 2). A comparison with NEMEC equilibrium calculations, where flux surfaces are assumed, shows that NEMEC may deliver an upper boundary for the volume. However, further studies are required.

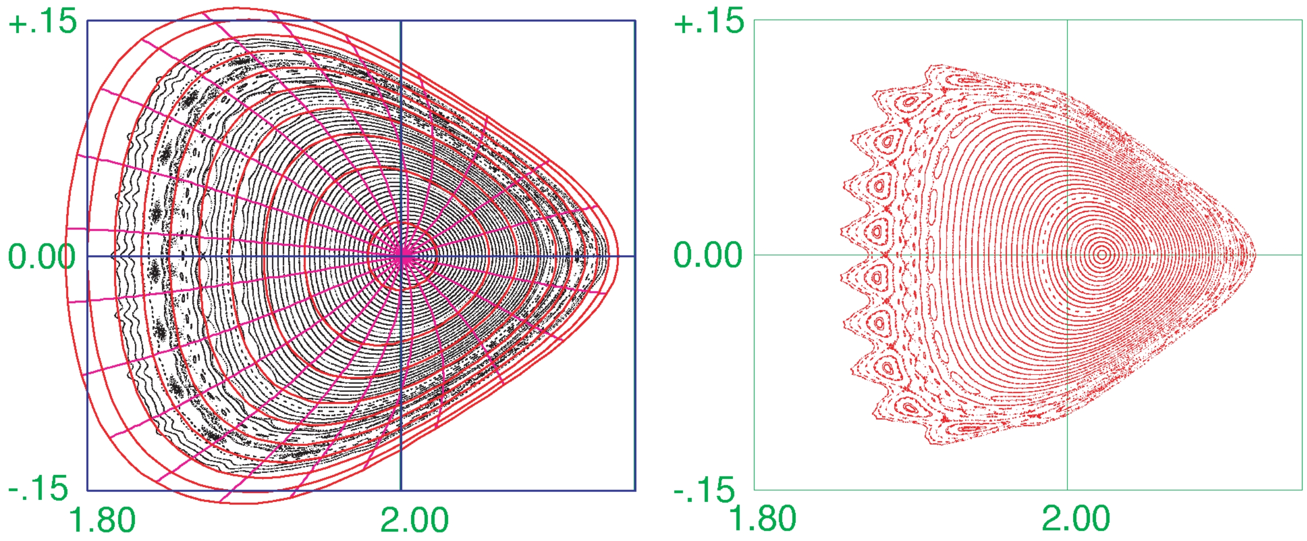

Figure 2: Poincare plots from 2 PIES runs for W7-AS at ι_{ext} = 0.5 with and without control coils effective (left/right). The ⟨β⟩-values reached in these runs are 2% (left) and 1.8% (right). The runs aimed at modelling the discharges #53052 (left) and #53053 (right). For #53052 flux surfaces of a NEMEC equilibrium calculation have been put on top for comparison

An interchange-stability study involved investigating the influence of NBI-driven, bootstrap and ohmic current densities for net-toroidal current-free discharges, since the individual current densities might be large due to the pure co-injecting NBI. However, only marginal changes in the stability boundaries were found at high-β because the changes in the driving and damping terms in the ideal and resistive interchange criterion balanced each other.

The investigations of Alfvén modes were continued. Good agreement is observed when comparing measured frequencies with predicted ones from numerical codes like the COBRA Alfvén-continuum code and the CAS3D code. The calculations give strong evidence that also stellarator specific Alfvén modes have been observed, like helicity- or mirror-induced ones. The studies will continue to clarify operational boundaries for the existence of Alfvén modes and their impact on high-β startup scenarios.

2.3 Doppler reflectometry study of the LH transition

Doppler reflectometry provides a local measurement of the propagation velocity of density turbulence $v_\perp(k_\perp)$ and simultaneously of changes in their fluctuation amplitude $\tilde{n}$ $(k_\perp)$. The antenna system and signal detection of the Doppler reflectometer at W7-AS are optimised for maximum temporal resolution to get an insight into the dynamics of bifurcations in turbulent transport, e.g. the transition between L- and H-mode.

For example, Fig. 3 shows three spectra selected from a time window around an H- to L- back-transition which occurs after the NBI heating has been switched off. Frequency spectra of the returning microwave radiation are obtained with a 15 channel spectrum analyser from which the parameters $v_\perp$ and $\tilde{n}$ are deduced. The individual filter bandwidths are indicated by horizontal bars. Note the log scale of the vertical axis. Each spectrum is integrated over 4 µs and fitted to Gaussian line shapes as expected from the antenna characteristics. The spectrum measured in the H-mode (blue dots) shows high rotation (Doppler shift) and low turbulence level (displayed by the amplitude of the frequency-shifted signal). 4 ms prior to the back-transition (green dots) rotation has already started to decrease and turbulence increases. The frequency shift of 3.7 MHz corresponds to $v_\perp = 27$ km/s. In the L-mode (red dots) the fluctuation level is increased by more than an order of magnitude and the propagation velocity of the turbulence is low. The radial position chosen by the microwave frequency (85 GHz) is located 2 cm inside the separatrix, which is at about the maximum ExB shear as measured from spectroscopy. According to the Bragg condition the tilt angle of the antenna selects perturbations with poloidal wavelength $\Lambda_\perp \approx 0.8$ cm.

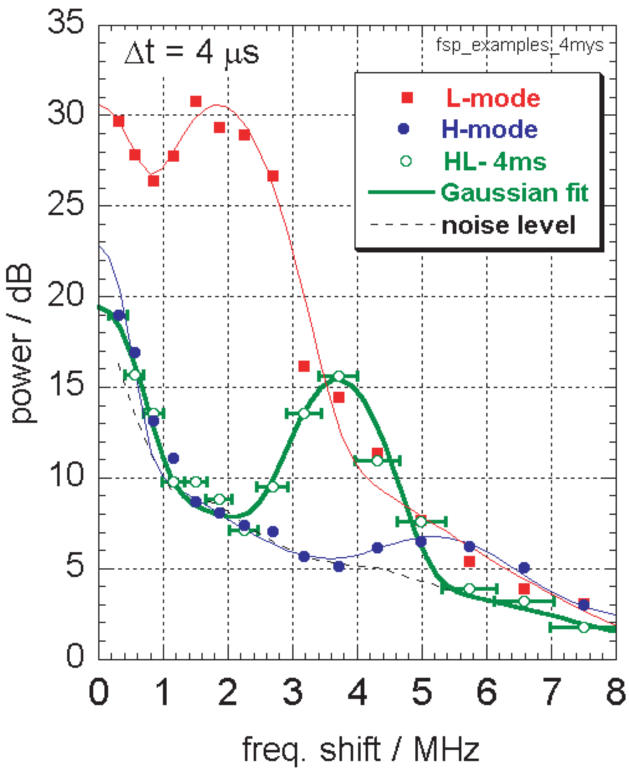

Figure 3: Doppler reflectometry spectra measured around an H- to L- back-transition in W7-AS

Scientific Staff

Contributions were from: R. Burhenn, Y. Feng, J. Geiger, M. Hirsch, E. Holzhauer[11)], G. Y. Kolesnichenko[2)], V. V. Lutsenko[2)], K. McCormick, A. Reiman[3)], D. A. Spong[4)], F. Sardei, A. Weller,Y. V. Yakovenko[2)], M. Zarnstorff[3)]

3 IEA Implementing Agreement

3.1 Objectives of the agreement

The objective of the Implementing Agreement for Cooperation in Development of the Stellarator Concept, first concluded in 1985, is to ”improve the physics base of the Stellarator concept and to enhance the effectiveness and productivity of research and development efforts relating to the Stellarator concept by strengthening co-operation among Agency member countries“. To achieve this, it was agreed to exchange information, conduct workshops, exchange scientists, do joint theoretical, design and system studies, coordinate experimental programmes in selected areas, exchange computer codes, and perform joint experiments. In 2000 the Agreement was extended until June 2005. The contracting parties are EURATOM, the U.S. DoE, Japan, and Australia. In September 1994, Russia became an Associate Contracting Party. In 2002, the Ukraine also joined the Implementing Agreement.

3.2 Status of the Agreement

In 2003, there was one meeting of the Executive Committee during the 14th International Stellarator Workshop in Greifswald (Sept. 22 - 26, 2003).

3.3 Report on 2003 Activities

The international collaboration in neoclassical theory was continued with V. Tribaldos (CIEMAT), S. Murakami and A. Wakasa (NIFS), W. Kernbichler (TU-Graz), S. Kasikov and V. Nemov (IPP-Kharkov), D. Mikkelsen and R. White (PPPL) and D. Spong (ORNL). Different codes were applied to various stellarator configurations, and very good agreement for the mono-energetic particle diffusion coefficients was obtained. Further work will concentrate on benchmarking of the bootstrap current coefficient for the different stellarator configurations.

A collaboration for updating the energy confinement time scaling (with respect to ISS95) was started with H. Yamada (NIFS), E. Ascasibar (CIEMAT), J. Harris (ANU), F. Sano (Kyoto University), J. Talmadge (Wisconsin), U. Stroth (U. of Kiel) and D. Mikkelsen (PPPL). New data mainly from LHD and W7-AS will be taken into account. Advanced delta-f Monte Carlo techniques for calculating, for example, the NBI power deposition were analysed in collaboration with V. Tribaldos (CIEMAT) and S. Murakami (NIFS). The kinetic stability of the NBI slowing-down distribution functions for the neutral beams at W7-AS was analysed with A. Shalashov and E. Suvorov (IAP Nizhny Novgorod) for interpreting the collective Thomson scattering data (experimental campaign at W7-AS in 2002). N. Marushchenko visited CIEMAT for two weeks to implement the ray-tracing code of V. Tribaldos for W7-X. M. Kobayashi (NIFS) visited Greifswald to implement the EMC3-EIRENE code for the edge physics of LHD. The collaboration with D. Reiter (IPP-Juelich) concentrated on implementation of the EMC3-EIRENE code at Textor. The collaboration on the HINT equilibrium code with T. Hayashi (NIFS) was continued. At the international stellarator workshop (Greifswald) a joint development IPP-PPPL on a predictive stellarator transport code was discussed (with D. Mikkelsen).

Within the stellarator theory division the following physicists visited IPP Greifswald: Roman Zagorski (U. of Warsaw) for ”3D finite-difference modelling of ergodic edge transport“, Detlef Reiter (FZ Juelich) for ”3D Monte Carlo modelling of edge transport with ergodic effects“, Aleksander Shyshkin (Nat. Science Center, Kharkov) for ”Impurity transport in a Helias configuration“, Vladimir Rozhansky and Ilya Senichenkov (U. of St. Petersburg) for ”Pellet modelling for stellarators and tokamaks“, from Kurchatov Institute Mikhail Mikhailov for ”Work on bs current and high beta in quasi-isodynamic stellarators“, Maxim Isaev for ”Investigations on coil systems for optimized torsatrons“, Alexey Subbotin for ”Extension of set of physics issues in stellarator optimizer“ and Alexander Zvonkov for ”Investigations on equilibria with vanishing rotational transform“, Yaroslav Kolesnichenko and Vadym Lutsenko (U. of Kiev) for ”Investigations on fast-particle-driven MHD modes“ and, from NIFS, Chihiro Suzuki for ”Investigations on bs driven kink instabilities in CHS-qa“, Noriyoshi Nakajima for ”Investigations on MHD growth rates in LHD, W7-AS, W7-X“ and Masaykji Yokoyama for ”Investigation on maximum-J in stellarator configuration“.

3.4 Conferences and Workshops

The 14th International Stellarator Workshop was held at Greifswald in September 2003 with a total number of 180 participants from Europe, Japan, Russia, Ukraine, the US and Australia representing worldwide stellarator research. The workshop was followed by the IAEA Technical Meeting on Innovative Concepts and Theory on Stellarators from Sept 29 to Oct 1, 2003.

1) Guest from IPF Stuttgart (Germany)
2) Guest from NUCRESI, Kyiv (Ukraine)
3) Guest from PPPL, Princeton (USA)
4) Guest from ORNL, Oak Ridge (USA)

WENDELSTEIN 7-X Construction

Head: Dr. Manfred Wanner

1 Introduction

The WENDELSTEIN 7-X (W7-X) Construction project is responsible for the design, manufacture, and assembly of the W7-X stellarator, the heating systems, the power supplies, the cooling system, and the system control.
The main components of the stellarator are the superconducting magnet system to confine the plasma, the cryostat to insulate the cryogenic parts, the plasma vessel to enclose the plasma, the ports to observe and heat the plasma, and the plasma-facing components to control the energy and particle exhaust. Steady-state plasma heating is based on powerful ECR sources. In addition, the plasma temperature and density can be increased by pulses of ICR or NBI heating. The superconducting coils are energised with high current by dedicated supplies and kept at a temperature of about 4 K by a helium refrigeration plant. Safe operation of the magnet system is ensured by fast detection of quenches and subsequent shut-down. A total input power of about 48 MW has been installed to operate the magnet system, supply the ECR, ICR and NBI heating systems, and provide power for cryogenic refrigeration. Waste heat is removed by circulating water which is re-cooled by cooling towers.

Production of most of the W7-X components made significant progress in 2003. The first non-planar and planar coils were delivered to the test facilities in Saclay and have successfully passed acceptance tests at nominal current. The segments of the first half-module of the plasma vessel and the first ports were delivered to Greifswald. The prototype gyrotron (“Maquette”) was commissioned at Greifswald by the ECRH team. The orders for the thermal insulation of the cryostat, the divertor target plates and the wall protection and the helium refrigeration plant have been placed with industry.

The mechanical problems which evolved in 2002 during detailed analysis of the magnet system were solved by local stiffening of the coil support structure and modifications of the fixture elements between the coils and the support structure.

Preparation of assembly of W7-X was continued, and all tools required for assembly of the half modules and the modules of the magnet system are ready for use. The actual dimensions of each winding package and of all coils are continuously checked and analysed to make sure that the required accuracy of the magnetic configuration of W7-X is achieved.

The technique for assembling and joining the modules in the torus hall was re-assessed to achieve maximum symmetry of the magnet configuration and allow installation of supply lines and some basic diagnostics at an early date. As a result, the magnet modules together with the lower half of the outer vessel will be successively placed at their nominal positions on the machine foundation. Before the final connections are made between the modules, the modules will be precisely adjusted within a few millimetres of each other.

The DEMO cryostat, which represents a 1/8 sector of W7-X, was dismantled; the components will be used to practise specific steps of assembly.

The design of the basic machine was strongly supported by engineers and scientists from the experimental divisions E3 and E5, the technology division TE and the technical services TD at Greifswald. In addition, Garching’s engineers from the central technical services ZTE and from the experimental division E1 in Garching contributed to design of the machine, testing of components, analysis of the structure and fabrication of the in-vessel components. The project also benefited from significant support by engineers from ENEA, EFDA, ITER, CEA and CIEMAT. Magnet experts from Atominstitut Wien followed the coil production processes. The University of Rostock and the University of Applied Sciences at Neubrandenburg are supporting the project with specific tasks. Co-operation continued with the D.V. Efremov Scientific Research Institute of Electrophysical Apparatus in St. Petersburg to perform the structural analysis of the complete magnet system and characterise components at cryogenic temperatures.

FZK is contributing the complete ECRH system for W7-X. After successful completion of the development programme together with European industry, CRPP and IPP in 2002, the first prototype gyrotron ("Maquette") was refitted and operated at Greifswald for pulses of up to one second on a test load. A second gyrotron from an American supplier also successfully passed works acceptance tests and is being installed at the branch institute. The orders for the series gyrotrons and the associated superconducting magnets were placed.

Forschungszentrum Jülich (FZJ), which already contributes to the Diagnostics for W7-X project, enhanced its co-operation. FZJ designs, manufactures and mounts the superconducting bus bar system connecting the coils and current leads and contributes to specific system engineering and welding aspects.

2 Basic Machine

2.1 Magnet System

The main components of the magnet system are the superconducting coils, the coil support structure, the inter-coil support elements and the power supplies.

2.1.1 Superconductor

The superconducting cable is composed of 243 strands enclosed by an aluminium jacket. A total of 360 conductor lengths, typically 120 to 180 m long, are required to wind all superconducting coils. The conductor is being manufactured by the EAS/EMS (formerly VAC/EM) consortium. The conductor is meanwhile being produced in a routine way. By the end of 2003 almost all strands were produced and 70 % of the required conductor was delivered. All steps of conductor production are controlled by IPP inspectors.

2.1.2 Superconducting Coils

The non-planar coils are being manufactured by the Babcock-Noell Nuclear (BNN)/Ansaldo consortium. Winding of the coils is being performed in parallel on three winding lines at Ansaldo and two winding lines at BNN's subcontractor, ABB. By the end of 2003, 21 winding packages were delivered for coil integration and an additional 15 were in different stages of production. The Swedish subcontractor, Österby Gjuteri AB, cast, heat-treated and machined 62 half-shells of the coil casings, 21 of them being already delivered.
Integration of all non-planar coils is being done at BNN's production site at Zeitz. First each winding package is positioned between the two halves of the casings. For precise positioning each winding package is equipped with four reference pins on each side. Next the winding package is embedded in quartz sand and epoxy resin. During injection of the quartz sand the casing is heated to approx. 100 °C, while the winding package is kept at ambient temperature. During re-cooling of the casing the winding package is pre-stressed. This stress is released during cool-down to cryogenic temperatures due to the different thermal contraction of the casing and the winding package.
After embedding, the coil casing and the connection areas are machined to the required precision on a five-axis CNC machine. This operation takes place at the company PEM in Schwarzenberg. During a subsequent survey the positions of the coil fixtures and reference pins and the contour of the surface of the casing are checked against the CAD model. The accuracy achieved is within 0.5 mm for the reference pins and coil fixtures, 2 mm for the inner surface and 5 mm for the outer surface of the casings. Oversizing of the cast half-shells called for considerable machining to bring the contour of the coil within the required tolerance range. With the experience gained, the half-shells can be cast closer to the final size in future.
Finally, the cooling system is mounted to the casing. This involves covering the surface of the casing with strips of highly conductive copper and mounting the cooling loops. The copper strips reduce eddy current heating of the coils in case of rapid shut-down of the magnet system. The strips are welded to the casing and contacted to the helium cooling pipes by soldering. Finally, the temperature and strain sensors are mounted.
Prior to delivery each coil is subject to a factory test which comprises a pressure and flow test, an integral helium test in a vacuum chamber and an electrical test of the insulation.

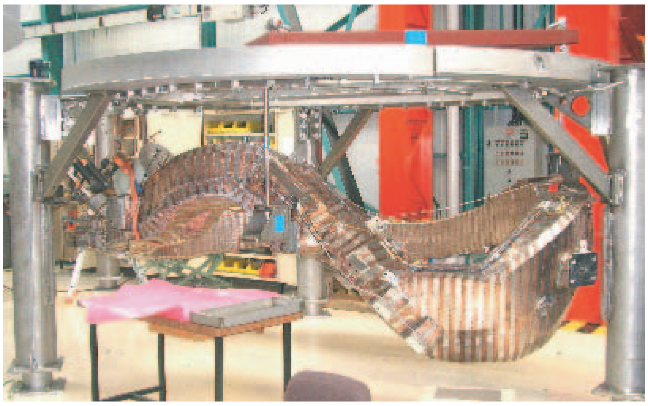

Figure 1: First non-planar coil in a test rig at Saclay

The first non-planar coil was delivered to the test facility at Saclay in June 2003 followed by further coils in July and August (Fig. 1).

The necessary modifications of the mechanical structure of the coil system had a major impact on the design of the support elements on the coil casings. As a consequence, the welds between some support elements and the casing had to be enforced and the number and size of bolts fixing the support elements to the support structure needed to be modified. Implementation of the new design led to a delay in delivery of further coils until the beginning of 2004. Ten coils which had already been completed will be repaired by cutting and replacing the support elements. The welding processes for replacing the elements are carefully controlled to avoid overheating the epoxy embedding and superconductor and to minimise distortions of the casing.

In order to study the evolution of eddy currents and heating of the coil cases during ramp-up and rapid shut-down, a numerical model was developed by the University of Rostock.

After production all superconducting coils will be tested under operational conditions at the Low Temperature Laboratory of Commissariat à L'Énergie Atomique (CEA) in Saclay. During several tests with the DEMO coil the facility was checked and procedures were practised. Cool-

down of the first non-planar coil started at the end of August and was finished within ten days, demonstrating the improved cooling of the casing. The nominal current of 17.6 kA was reached without problems. The quench was detected at a temperature of 6.1 K. This temperature is in very good agreement with the predictions from the data of the virgin strands and shows that the degradation of the conductor during manufacture is minimal. No helium leak was detected within the specified range of 10^{-7} mbarxlxs^{-1}.
The high-voltage test, however, revealed partial discharges at voltages significantly below the specified test voltage of 9 kV. The cause of the partial discharge was identified in the design of the quench detection cables, which need to be replaced. Since the inductive voltage during a rapid ramp-down of a single coil is only 400 V, the tests could be safely continued with the existing cables.
In December, the second non-planar coil was successfully cooled down together with the first planar coil. Operating both coils individually up to a quench showed that the specified margins of operation are fully achieved.

Manufacture of the 20 planar coils at Tesla Engineering was continued. Sixteen winding packages have been produced and five were integrated in the casings by the end of 2003. The first coil was completed and dispatched to Saclay in October 2003.
Since the facilities of Tesla for leak tests and metrology were not appropriate, IPP is leak testing all winding packages as well as the coils. This is being done by a new leak test method examined by Forschungszentrum Karlsruhe. This technology uses SF_6 to pressurise the superconductor and the helium cooling pipes. Leaks are accumulated in a plastic bag around the coil and detected by laser spectroscopy.
Surveys of the coil connections, the positions of the reference pins and the contour of the casings are being performed by JET experts at Tesla by the photogrammetry technique.

2.1.3 Accuracy and Correction of the Magnetic Field

The accuracy of the magnetic configuration of W7-X depends on the accuracy of coil production and the accuracy achieved during assembly. In particular, coils of the same type need to be reproduced very carefully. Small statistical deviations of coils from the ideal coil shapes or small non-symmetric misalignments of the coils cause magnetic field perturbations with a periodicity different from the five-fold periodicity of the device and result in additional magnetic islands. As a general rule, non-symmetric disturbances of the magnetic field $\Delta B/B_{00}$, where B_{00} is the toroidal field on axis, must be below $1x10^{-4}$.
As an example, a perturbation field is assumed which is generated during assembly by a statistical distribution of coil axes inclined at angles of up to 0.1 degree. The main error components with values normalised to B_{00} are the m=1, n=-1 component with $\Delta B/B=2.73x10^{-4}$ followed by the m=2, n=-2-component with $\Delta B/B=0.53x10^{-4}$, as can be seen from the Poincaré plot of the field at the triangular cross-section in Fig. 2. The perturbation splits the common separatrix of the five “natural” islands into five nested single islands, with the largest separatrix enclosing all others and separating the m=1, n=-1 island.
In general, Fourier components of the magnetic field associated with high m and n numbers decrease faster with increasing distance from the generating currents; they thus have smaller amplitudes and introduce smaller islands. Furthermore, only resonant Fourier components of the error field disturb the periodicity of the magnetic field, and so in practice only a small number of components need be considered in the analysis.

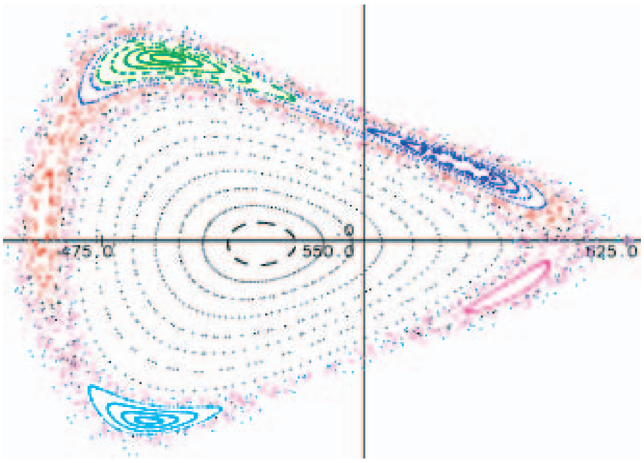

Figure 2: Poincaré plot of the model error field at the triangular cross-section

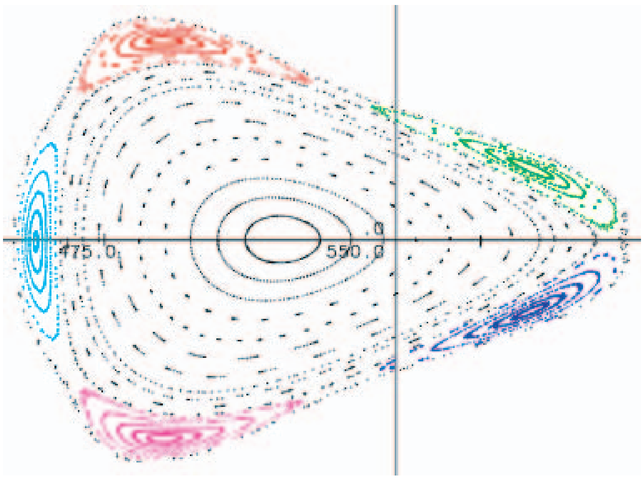

Figure 3: Compensation of the model error field by proper alignment of the five modules

The real geometry provided by the metrology of the individual winding packages forms the basis for calculating the relevant Fourier components of the error field. During assembly, shifts or inclination of individual coils from their nominal positions generate distinct perturbing Fourier spectra. Because of the three degrees of freedom concerning shift and inclination one gets a set of six spectra for each coil. The same argument holds for coil assemblies of the half-modules or of complete modules. Since the geometrical deviations and the resulting field perturbations are small, the spectra can be linearly superimposed. A numerical optimisation code was written to optimise alignment. This field correction procedure is to be performed as an accompanying action during assembly. Figure 3 shows a Poincaré plot where the model perturbation of Fig. 2 is corrected by proper alignment of all five modules. The offsets of the individual modules which are necessary to correct the field are quite small; the largest shift is 2.4 mm and the largest inclination is 0.05° with respect to the vertical axes.

2.1.4 Structural Analysis of the Magnet System

The mechanical analyses of the W7-X structures were performed by means of a global FEM model developed at IPP Garching. This model represents one semi-module of W7-X and includes five non-planar coils, two planar coils, a sector of the coil support structure with the central coil supports and all inter-coil supports (narrow supports at the inboard side, lateral supports along the outboard side of the non-planar coils and planar supports between the non-planar and planar coils). In particular, the bolted connections between the coil central support elements and the central ring extension elements required very detailed analysis.

Three major plasma scenarios were analysed, viz. the standard, high-jota and low-shear cases. From these calculations the maximum deformation in the coil system during operation, the maximum stresses in the coil casings and the central ring and the resultant forces and moments acting on the support structure elements were determined.
In addition, specific mechanical analyses were performed to support the design and testing of individual W7-X components. In particular, the welding seam thickness of the joints between the support elements of the planar and non-planar coil casings was verified. Furthermore, stresses in the coil casings and winding packages during the embedding process and deformation of the coils during cool-down to 4 K and operation in the self-field at nominal current during the Saclay tests were analysed in collaboration with Efremov Institute.
As a result of the detailed structural analysis of the magnet system the design was modified to take the forces and moments during operation. The concept of fixing the coils with bolts is being maintained, but the four M30 bolts initially proposed for connecting the non-planar coils and the support structure are being increased case by case to six or nine. In one case the four M30 bolts are replaced by a central M76 bolt, in another case by a central M90 bolt. By increasing the bolt length to approx. 500 mm the stresses in the bolts can be safely handled. The shear forces at the interfaces between the coil connections and the support ring are taken by enforced shoulders and friction.
In order to limit deformation of the coils by the electromechanical forces, lateral supports are fixed between adjacent coils.

2.1.5 Coil Support Structure

The coil support structure is being manufactured by the Spanish contractor, Equipos Nucleares, S.A. (ENSA), and consists of ten identical sectors with a total weight of 72 t to span a central pentagon. Ten cylindrical supports carry the weight of the support structure and provide the thermal barrier between the cold structure and the base plate. The coil support structure is made of steel plates and cast steel elements for the coil fixtures. As a result of the structural analysis the support ring was stiffened in some areas and the coil connection blocks were modified to cope with the new requirements for the larger number and different sizes of the screws.
The sectors of the coil support structure are joined by bolts. All interfaces of the structure are precision-machined. The two sectors of a module are directly bolted to each other. Fixing of the bolts between different modules of the support structure will not occur till symmetric alignment of all W7-X modules during final assembly of the torus. This requires precisely machined interlayers between the sectors of the coil support structure. The design changes have been agreed with ENSA.

The inter-coil supports are welded to the coil casings. Particular attention is given to the narrow support elements where the coils contact each other. These contact elements are subject to tilting and sliding under forces of up to 1.5 MN. Aluminium, bronze and diamond-coated steel elements are being considered as candidate materials. A dedicated test facility is being set up to test samples of the material under realistic conditions.

2.1.6 Magnet Power Supply

The five types of non-planar and two types of planar coils are energised by power supplies providing direct currents of up to 20 kA at voltages of less than 30 V. The Swiss contractor, ABB, selected the concept of twelve-pulse rectifiers to ensure that the currents are stabilised with an accuracy of $2x10^{-3}$.
Fast and reliable discharge of the superconducting magnets in case of quenching is realised by a fast circuit which short-circuits the coils and dumps the magnet energy to nickel resistors. These resistors feature a high heat capacity and a strong increase of the resistance with temperature. At the start of the shut-down the resistance is small what keeps the switching voltages low. During discharge the resistor heats up. The subsequent increase of the resistance has a positive effect on the discharge time of the magnet system.
Production of all components was successfully completed by appropriate works acceptance tests. The test of the nickel resistors was performed at the Garching institute using existing power supplies. The results for the temperature increase of the resistors matched well with the predictions. The control concept for the ten power supplies was designed in detail and took into account the required detection of grounding defects in the electronic circuits. The racks for the local control system were installed and programming was started.
The first module of the power supplies and the protection system was installed in Greifswald in autumn and is being commissioned.

2.1.7 Current Leads

Fourteen current leads each able to carry 20 kA connect the seven groups of superconducting coils with the power supplies. The concept is based on conventional current leads designed for lower than nominal current but operated at higher current during nominal operation. As a consequence, the warm end is considerably heated and needs to be water-cooled. In this way the heat conduction along the current leads and hence the cooling requirements are reduced during stand-by periods. The basic specification is complete. Tendering is planned for 2004.

2.2 Cryostat

The cryostat provides thermal protection of the magnet system and gives access to the plasma. Its main components are the plasma vessel, the outer vessel, the ports and the thermal protection. German Deggendorfer Werft und Eisenbau GmbH (MAN DWE) are responsible for manufacturing the plasma vessel, the outer vessel and the thermal insulation.

The plasma vessel is composed of ten half-modules. Each half-module is cut into two parts to allow stringing of the innermost coil during assembly. For each half-module of the plasma vessel 20 steel rings are precisely bent to the required shape and carefully welded to represent the changing cross-section of the vessel. Between all major steps of manufacture, compliance with the narrow tolerances of the vessel is controlled by laser tracking metrology. Vacuum tightness of the welds was checked by an integral helium leak test of the vessel segments. Precise cutting of the holes for the ports is performed by the water jet technique. The water jet was also used to mark the routing of the coils for the magnetic diagnostic. Water pipes are welded around the vessel to allow control of its temperature during plasma operation and for bake-out. By the end of 2003, approx. 50 % of the required rings were shaped and welded and the two sectors required for assembly of the first half-module were delivered to Greifswald (see Fig. 4).

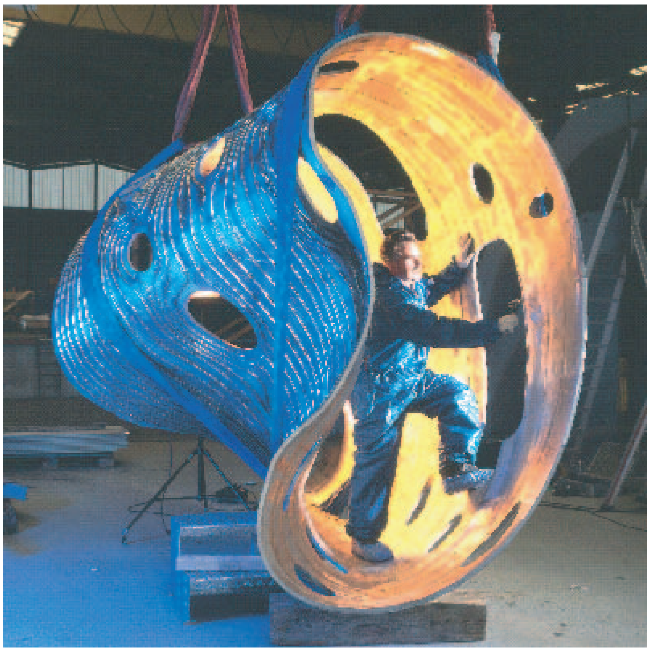

Figure 4: Half-module of the plasma vessel

The outer vessel of W7-X is assembled from five lower and upper half-shells. All upper and lower half-shells of the outer vessel have been welded. Following detailed structural analysis some ports closed by flanges had to be modified. Cutting of the openings will start at the beginning of 2004. To allow final symmetric alignment of the W7-X modules a fitting ring will be used between the sectors of the outer vessel.

A total of 299 ports are used for evacuating the plasma vessel for plasma diagnostics and plasma heating and for feeding supply lines and sensor cables. All ports are surrounded by water pipes to control their temperature. The ports are manufactured by the Swiss company, Romabau. The first two ports were delivered at the end of 2003.

Efficient insulation of the cold magnet system requires careful protection against thermal radiation by cooled metallic shields, high vacuum and multi-layers of reflecting metallic foils. The shields are kept at temperatures between 40 K and 70 K by cold helium gas.

The contract for the thermal insulation was also placed with MAN DWE. Subcontractor Linde AG is responsible for the cryogenic layout, development and assembly of the multi-layer insulation. IPP, MAN DWE and Linde AG are closely co-operating in design of the main components. A novel technique using dyeless forming has been successfully applied to shape panels for the stainless-steel shield according to the complicated contour of the plasma vessel. Kapton was selected for the multi-layer insulation because of its resistivity to elevated temperatures during bake-out. FEM calculations of the eddy currents, the induced forces, and the temperature distribution in the thermal shields were continued to support the detailed design. Routing of the cryogenic supply lines in the cryostat was continued.

2.3 In-vessel Components

2.3.1 Design and Construction of the Plasma-facing Components

Three different types of surfaces face the W7-X plasma: The divertor target plates are hit predominantly by hot particles from the plasma and have to withstand heat loads of up to 10 MW/m_. Baffles, which influence the fluxes and density of neutralised particles in front of the target plates and improve the pumping efficiency, need to be designed for heat loads of 0.5 MW/m_. The wall protection of the plasma vessel mostly interacts with neutral particles and radiation from the plasma boundary and receives heat loads of up to 0.2 MW/m_. To keep the reflux of impurities from the wall to the plasma at acceptable limits all plasma-facing surfaces have to be covered with low-Z material.

For economic reasons the area of the divertor targets was reduced from about 30 m_ to about 20 m_. This was achieved by increasing the angle of incidence of the particles on the target elements from 2° to typically 3° at the expense of a higher local heat load. In the new design, each of the ten horizontal targets consists of two zones subject to heat loads of up to 10 MWm^{-2} which are separated by an intermediate area of 0.6 m_ with convective heat loads of 1 MWm^{-2} only. The new design still preserves the full range of magnetic field configurations and plasma parameters to be studied. FEM simulations have shown that the maximum heat load on the targets is still within the acceptable range of 10 MWm^{-2} for stationary and 15 MWm¯_ for transient operation. Each of the ten divertors requires 89 highly loaded target elements. The target elements consist of precipitation-hardened CuCrZr alloy heat sinks armoured with tiles of SEPCARB® NB31 carbon fibre composite. The carbon fibre composite is joined with the heat sink by the active metal casting technique (AMC®) and electron beam welding. The contract for the fabrication of the target elements was placed in December with Plansee AG, Austria. The CFC material is provided by SNECMA Propulsion Solide, France. A first batch of about 150 kg of CFC has been delivered.

The designs of the divertor baffles, of intermediate target areas and specific areas of the wall protection with higher heat load use fine-grain graphite tiles clamped to water-cooled CuCrZr heat sinks. The conceptual design of these elements is complete.

The major part of the wall with an area of about 70 m^2 will be protected by double-walled steel panels with integrated cooling loop. They are designed to withstand heat loads of 0.1 MWm^{-2} stationary and 0.2 MWm^{-2} transient. A total of 197 panels of 75 different shapes are required for the wall protection, 210 panels of 21 different shapes for the poloidal and toroidal closures of the divertor, and 40 panels of 4 different shapes for protecting the wall behind the divertor slits. The large number of versions is due to the complex shape of the vessel as well as to specific requirements concerning the diagnostics and heating systems.
A full-scale mock-up of a panel element was successfully tested on the FIWATKA facility at FZK with respect to thermal loads and at IPP Garching to check deformations during pressurisation. For more details refer to the section of the Materials Research Division.
The design specification of the panels for protecting the wall and some ports was completed and the contract for detailed engineering and fabrication of the panels was placed with the MAN DWE/Buco Wärmetauscher consortium (Germany).

A facility for leak tests at elevated temperatures and a high heat load test facility are being installed at the Garching institute to allow testing of the plasma-facing components close to operational conditions.

2.3.2 Pumping

Vacuum pumps are required to evacuate the plasma vessel, to control the density of auxiliary gases injected into the divertor chamber and to pump out neutral particles. Additional cryo-pumps behind the divertor allow the pumping capacity to be increased during high-density plasma discharges.

The cryo-pumps are composed of a cryo-panel cooled with liquid helium, a Chevron baffle, a reflector cooled with liquid nitrogen and an additional baffle cooled with water. Two cryo-pump units will be placed behind the horizontal targets of each divertor. The geometry and the pumping capacity were analysed in keeping with the new geometry of the divertor and the heat loads expected from the plasma. The space restrictions behind the divertor allow lengths of the cryo-units of 780 mm and 400 mm respectively and a height of the Chevron baffle of 180 mm. Helium will be supplied at a temperature of 3.4 to 4 K through dedicated ports. The additional water-cooled baffles are required to shield energetic particles and radiation passing through the diverter slit. An analysis showed that between 2.5% and 9% of the plasma radiation could reach the Chevron baffle if a wall absorption coefficient of 0.8 to 0.9 for thermal radiation is assumed. The additional baffles reduce the D_2 pumping speed in the divertor chamber to 75 $m^3 s^{-1}$, which is still acceptable.

2.3.3 Control Coils

Ten copper coils will be installed in the plasma vessel behind the baffle plates to correct minor field errors, influence the extent and location of the magnetic islands, and allow the power deposition area to be swept across the target plates.

Each coil can be individually supplied with direct currents of up to 3 kA at voltages of up to 30 V which can be modulated at frequencies of up to 20 Hz by dedicated power supplies. All ten power supplies have been delivered and installed by the Spanish contractor, JEMA. Nine units have already passed the final acceptance tests.

The design of the control coils was slightly modified to take into account the new geometry of the divertor target plates. The coils, with dimensions of 2x0.3 m_, will be wound by 8 turns of a hollow copper conductor and cooled by water.
The call for tender resulted in two offers which are currently being evaluated.

2.4 System Control

The W7-X experiment will be controlled by a master control system with local controllers for all subsystems such as magnets, cryogenics, heating units, diagnostics, and data acquisition. The local controllers will run automatically according to predefined routines and parameters, which will be set from the master control system as long as the units have to co-operate.
A central trigger-time-event system (TTE) will serve to distribute the precise system time, triggers and event messages. Local TTE cards in the connected units respond to the central TTE system and have local trigger, time and event-handling capabilities.
In order to structure the experiment and other activities in the system, all periods of operation will be divided into segments of variable duration. A "segment programme" defines the operational rules and parameters which determine the state and activity of each unit in use.

In previous years, work concentrated on basic concepts and development and testing of control techniques. Meanwhile work is focusing on installation of the control room and realisation of the control system.

The distributed PLCs and computers for control and data acquisition will communicate through computer networks using several different communication protocols. A concept for the TCP/IP network in the experimental zone was

worked out and agreed by all groups. An optical fibre backbone was extended into the torus hall and some switch modules necessary for the new network structure were provided.
The master control system comprises devices working at different levels. A safety system will ensure safe co-operation of all components of W7-X and control access to the torus hall by means of interlocks. The basic concept has been defined and a database for possible malfunction and hazards was set up. A safe PLC and a safe interlock bus will be used for maximum flexibility. Another PLC system will provide information about the status of all components and ensure their co-ordinated operation as a precondition of "segment control". A database for all interfaces between the master control system and the local controllers was set up.
Development of the TTE system was continued. The central TTE card was completed. It constitutes the core of a redundant central TTE system which sends precise time information and event messages to all local TTE cards via a dedicated fibre network. The complementary TDC card of ASDEX upgrade, which will be used mainly for experimental data acquisition, has been adopted to allow communication with the TTE system. To facilitate use of the local TTE cards in laboratory applications a specification for a LabView driver was written.
Furthermore, a standardised method was developed to generate segment control software objects from database information in computers running the VxWorks operating system. Concepts were worked out for the central segment control computer system and for the software to be used by the session leader for controlling the discharge and for a "notification server" which will collect error messages from control computers.

The furniture of the control room was delivered. The room for the master control system was equipped with the necessary air cooling and electrical and computer network installations. Electronic and computer equipment will be procured at a later stage, but the concept of all elements required to operate the machine has been defined.

2.5 W7-X Assembly

Assembly of the basic machine is being performed in three main phases. During the first phase half-modules are assembled by stringing five non-planar and two planar coils across the plasma vessel and fixing them to a segment of the coil support structure. During the second phase the half-modules are joined to form a module of the magnet system. The sectors of the coil support structure are bolted, the plasma vessel segments are welded, and the electric bus and helium cooling lines are connected. All these activities are performed in the assembly hall on dedicated mounting devices. After assembly of the magnet modules each unit is moved into the torus hall and lifted into the thermal insulated lower half of the outer vessel. After integration of supports, the assembly is lifted onto its nominal position on the machine foundation and completed. All modules are placed on the foundation before the torus is joined. Prior to joining, minor corrections of the magnet modules of the order of 5 mm can be realised to achieve optimum symmetry of the stellarator.

In 2003 a great deal of auxiliary assembly equipment required to lift, adjust and transport the components with weights of up to 50 t was fabricated, e.g. a second coil-handling unit and several fixtures. Training for specific steps of assembly has started (Fig. 5).

Figure 5: Handling of a non-planar coil with the coil-handling unit

In order to provide space for preparation of the components, an additional pre-assembly hall with an area of 700 m^2 will be realised by 2004 at the site of the branch institute. Facilities for preparing the plasma vessel and the coils for assembly were installed.

The coils have to be electrically connected with each other and with the current leads by a system of superconducting bus lines. Forschungszentrum Jülich (FZJ) is responsible for design, manufacture and mounting of the bus system. The basic design of the bus system was optimised, taking into account routing of some 1100 m of conductor.
Connection between the bus sectors requires approx. 300 disconnectable low-resistance joints. Tests at Paul Scherer Institute, Switzerland, showed resistances of typically 1 nΩ, which is well below the specified resistance of 5 nΩ. Design of the joint housing was improved by FZJ to withstand a pressure of 170 bars. Prototypes manufactured met the requirements.
Welding tests at FZJ helped to determine the shrinkage and the achievable precision of welds during assembly of the coil supports.
The metrology concept was improved to allow prediction of the accuracy achievable during the different steps of assembly. Experience is being exchanged with the metrology experts of JET.

3 Heating Systems

3.1 Electron Cyclotron Resonance Heating

The Electron Cyclotron Resonance Heating (ECRH) system is being developed and built by FZK as a joint project with IPP and IPF Stuttgart. The “Projekt Mikrowellenheizung für W7-X” (PMW) co-ordinates all engineering and scientific activities in the collaborating laboratories and in industry. It is responsible for the realisation and installation of the ECRH system for W7-X. Ten gyrotrons with 1 MW each will provide the required microwave power at 140 GHz in continuous-wave (CW) operation. The W7-X gyrotrons were developed within a European R&D programme as a joint effort of the French company, THALES Electron Devices (TED), and the research laboratories, FZK, IPP, IPF and CRPP-Lausanne. Two prototype tubes were manufactured within this programme. The "Maquette" pre-prototype gyrotron, which constituted the first development step, was delivered to IPP after successful test operation at FZK. Although this tube does not give full-power CW performance, it is used for high-power CW tests of the transmission system and other components. The installation is seen from Fig. 6.

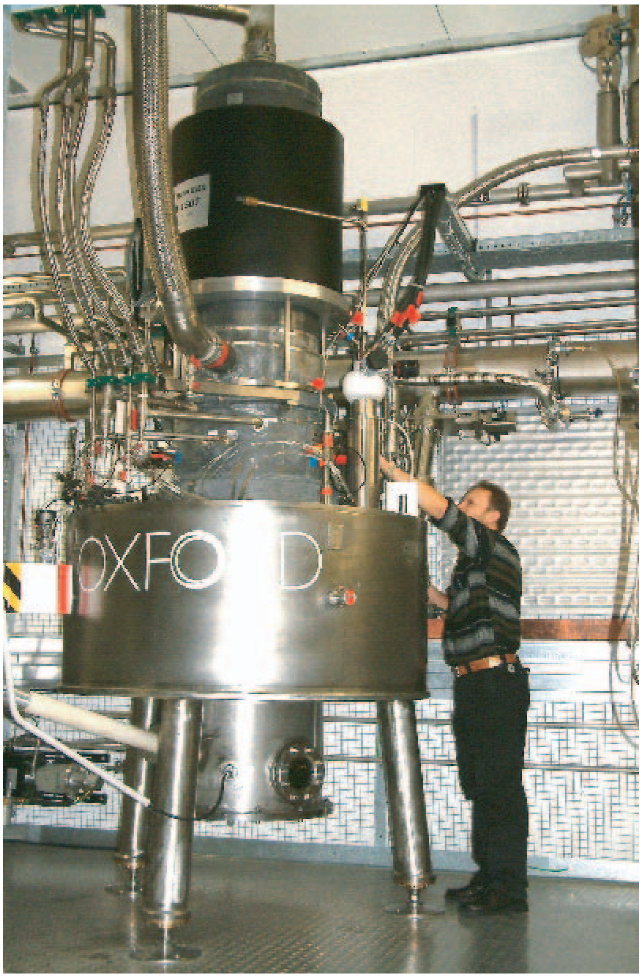

Figure 6: Installation of the "Maquette" Gyrotron in box Bravo 1 at IPP-Greifswald

The “Maquette” was successfully put into operation on 14 November 2003, demonstrating the integrated functioning of all auxiliary systems of the ECRH installation. In particular, the first pre-prototype HV modulator from IPF is operating reliably and safely together with the first HV power supply unit. All auxiliary systems such as gyrotron and transmission line cooling, cryogenic supply, central control system, and network are operational, and are undergoing under integrated tests.

The gyrotron is now operating at a power of 850 kW into a short pulse calorimetric load (<500 ms) and at 650 kW for 1 s into the CW load. The test programme aims at loading the transmission system step by step with increasing power and energy.

The second R&D "Prototype" gyrotron incorporates some improvements on the "Maquette" and was successfully tested on the test stand at FZK. An output power of 890 kW could be achieved for a pulse length of 180 s (which is the limit of the test stand for a beam current of 40 A) and 540 kW for 940 s with reduced beam current. The prototype tube was sent back to the manufacturer after the tests for visual inspection. No severe damage could be observed. The tube was reassembled with some improvements and was shipped back to FZK for the final tests in the first series magnet.

Figure 7: Multi-beam waveguide mirrors and CW loads in the beam duct.

In parallel to the European gyrotron R&D programme IPP had ordered a 140 GHz gyrotron with the same specifications from the U.S. company, CPI. This tube passed the factory acceptance tests. A maximum power of 910 kW was demonstrated in short-pulse operation (1-3 ms), limited by the test-stand power supply. A power of 500 kW was reliably demonstrated in 600 s pulses at reduced beam current. The gyrotron and magnet were shipped to IPP for full-power CW tests. With the “Maquette”, the TED prototype and the CPI tube available, seven more series gyrotrons are needed to complete the installation. A contract for delivery of these tubes was placed with TED in August 2003; the eight superconducting magnetic systems additionally required were ordered from the U.S. company, Cryomagnetics Inc.

The prototype modulator was completed by autumn at IPF Stuttgart; implementation at IPP is scheduled for February 2004. Major components for the series production of nine more modulators have been ordered. Fabrication is planned

in close cooperation of IPF and industry. The water-cooling plant for ten gyrotrons is close to completion, five modules already being operational. The transmission line is an optical system which operates at normal pressure. It consists of single-beam wave guide (SBWG) mirror modules mounted on a common base frame and multi-beam waveguide (MBWG) mirrors. Each SBWG base-frame is connected to a common water-cooling circuit and the SIMATC S7 remote control units in the beam duct.
Installation of the SBWG mirror modules as well as the MBWG mirrors is completed in the beam duct. The B1 beam line ("Maquette" gyrotron) is completely equipped and is now undergoing high-power tests. A newly designed short-pulse calorimeter (<0.5 s) has been installed on the SBWG frame for absolute measurement of the gyrotron output power. For long-pulse (>0.5 s) operation the beam can be steered into a commercial CW microwave load. Two large MBWG mirrors are shown in Fig. 7 together with the CW loads. During the beam alignment procedure the remotely steerable mirror system had already proven its unique advantages and easy handling.
Design of the in-vessel components was continued. Different possibilities for movable launcher mirrors were investigated. The mechanics for bi-axial movement and the connections for cooling water have to be integrated in the very limited port space. The most favoured solution for the mirror drive is push-pull rods with integrated water-cooling. The design was finished by autumn, the detailed design and fabrication of a simplified mock-up launcher will start in 2004. The system will be tested in the ECRH stray radiation test chamber at IPP Garching. The stray radiation of 30 kW will be generated by a modified, former W7-AS gyrotron. The antenna for the isotropic ECRH launch has already been manufactured. Calls for tender for the W7-X torus window units with CVD diamond disks were issued. Detailed FEM calculations for the heat- and stress-loading of the ports showed that without an appropriate heat shield the stresses at the welded joint are severe. The design of armour with the required heat removal capability is under way.

3.2 Ion Cyclotron Resonance Heating

In 2003 it was decided to realise the first stage of the ICRH system as outlined in the preferential support application. This will allow pulsed operation using the equipment from W7-AS: two generators with originally 2 MW of output power for 10 s each, transmission lines and matching circuitry.
This system still requires two different antennas, namely a single-strap antenna that is fully retractable into the port and a double-strap antenna that extends toroidally beyond the port and acts as a limiter for a small subset of possible plasma configurations. Both antennas need to be radially movable. To withstand CW plasma operation and baking of the machine requires that all antenna parts and in-vessel transmission lines can be cooled with water. The basic design of the cooling circuitry has been worked out. Model antennas were measured and their properties compared with fully 3-D calculations in order to optimise the antenna structures and the corresponding in-vessel transmission lines. Vacuum windows for the transmission lines were designed and optimised for low electric fields. Basic tests of a ceramic metal joint are in preparation in collaboration with industry. Testing of electrical sliding contacts for radial movement of the antennas has started.
In a transmission line resonator at Garching all components of the antenna feeders can be studied under realistic conditions. Ceramic spacers and electrical spring contacts have been successfully tested for CW operation. Part of this work is being performed under an EFDA contract to develop CW-capable RF generators. AlN was found to combine low electrical loss, high heat conductivity and non-toxicity. For the future, tests of a ceramic spacer made of Al_2O_3, sliding contacts, transmission lines without cooling of the inner conductor and a mock-up of the in-vessel transmission lines are planned.

3.3 Neutral Beam Injection

Neutral beam injection (NBI) is planned in W7-X for bulk heating of the plasma in the high-density, high-ß regime, eventually with a total beam power of up to 20 MW with 100 kV deuterium beams. This power will be available in two stages. In a first step 5 MW of heating power will be available for 10 s using two injector boxes of the ASDEX Upgrade type.
Activities were slowed down in 2003, since the NBI team is supporting the construction of the basic device. To support the design of the in-vessel components calculations, the beam power loading in the port, and the far side of the torus wall were determined.
Calculations of the magnetic stray field in the entire volume of the NBI boxes showed that the existing design of the titanium evaporators cannot be used for continuous vacuum pumping. Additional supports would be required to limit the movement of the titanium wires under the action of the JxB forces. Cryo-pumps are being considered, as an alternative.
The acceptance tests of the first high-voltage power supply, PS1, were completed for NBI conditions. By adding some damping resistors and modifying the filters the ripple could be kept within limits.

4 Auxiliary Systems

4.1 Refrigeration System

The refrigeration concept takes into account that the superconducting coils will be energised at nominal current only for about 700 hours per year and at maximum current only for about 50 hours per year. During the remaining time the plant is in different standby modes. As a consequence, the refrigeration requirements of W7-X vary considerably. To allow economic operation the excess plant capacity during standby modes (e.g. overnight) will be used to liquefy helium into a 10,000 l storage tank. During W7-X operation helium is taken from the storage tank to boost the refrigeration power.
The contract for the refrigeration system was placed with Linde Kryotechnik AG, Switzerland. The scope of supply comprises the compressors, the helium purification system, the cold box with expansion turbines and cold compressors, the sub-cooler with helium circulation pumps, the cryogenic transfer lines between the refrigerator and W7-X, and the coolant distribution valve box. The refrigeration

capacity complies with the requirements of the divertor cryo-pumps. The interfaces for later installation of a distribution box for the divertor cryo-pumps will be provided.
The refrigerator is designed to keep the W7-X magnet system at 3.9 K but interfaces are prepared for later upgrading of the plant to 3.4 K. The distribution of the cooling power during peak power operation of the magnet system at 3 T is as follows (the values correspond to 4.5 K entropy equivalent):

superconducting coils	1500 W
housing and support	2470 W
cryo-pumps	620 W
thermal shields	970 W
current leads	3130 W
losses (transfer lines, circulators)	1900 W
total	10590 W

This cooling power is provided by the refrigerator proper and liquid helium withdrawal from the storage tank. The compressor motor power is 1.55 MW, which corresponds to a refrigeration power of roughly 5000 W without liquid support.

The liquid nitrogen system of the branch institute consists of a 30,000 l tank and a distribution system. In 2003 approx. 45,000 l of liquid nitrogen was provided for the ECRH system, the cryo-laboratory and other users within the institute.

4.2 HV Power Supply

The power requirements of W7-X amount to approx. 48 MW and will be provided by the local 20 kV grid and a dedicated 110 kV junction of the Mecklenburg-Vorpommern grid. The ECR, ICR and NBI heating systems will be supplied with DC power spanning the ranges 18-130 kV und 50-160 A. Five power supply modules PS1 to PS5 are required to supply the heating units. Each module is again split into two half-modules. To deliver a voltage of 130 kV two half-modules of a module are operated in series. In a first step, eight half-modules using the advanced pulse step modulation (PSM) technique were ordered from the Thales/Siemens consortium.

In 2003 the works tests, the routine test and the acceptance tests for the first two half-modules of PS1 were successfully completed. Since December PS1 has been used for testing the ECRH system.
The two half-modules of the PS2 unit required replacment of the transformers, which was completed in November. Commissioning of these units has started. The installation of the half-modules of the PS3 unit has started.

Staff

W7-X Construction Division

Engineering Team: Y. Bozhko, J. Boscary, T. Bräuer, Ch. P. Dhard, J.-H. Feist, W. Gardebrecht, M. Gasparotto, H. Grote, B. Hein, H. Laqua, J. Ludvik[1], H. Modrow, M. Nagel, H. Niedermeyer, J. Reich, H. Renner, K. Riße, K. Rummel, T. Rummel, J. Schacht, F. Schauer, D. Sharma[2], S. Y. Shim[3], A. Spring, M. Wanner, L. Wegener
Technical Team: H. Bau, A. Benndorf, A. Berg, H.-J. Bramow, R. Brockmann, A. Brückner, M. Czerwinski, H. Dutz, M. Fricke, F. Füllenbach, G. Gliege, M. Gottschewsky, S. Heinrich, A. Hölting, U. Kamionka, T. Kluck, E. Köster, C. Kopplin, U. Krybus, F. Kunkel K. Lang, H. Lentz, B. Missal, T. Mönnich, I. Müller, F. Nankemann, A. Opitz, M. Pietsch, S. Pingel, S. Raatz, D. Schinkel, A. Schütz, U. Schultz, M. Schweitzer, K.-U. Seidler, F. Starke, H. Viebke, O. Volzke, A. Vorkö-per, A. Wölk

Contributing Divisions and Institutes

E1, E3, E5, MF, PD, ZTE/TD: T. Andreeva, F. Ascher, M. Balden, J. Baldzuhn, D. Birus, B. Böswirth, R. Brakel, H. Braune, B. Brucker, D. Döring, H. Ehmler, D. Eichner, H. Eixenberger, M. Endler, V. Erckmann, T. Franke, H. Greuner, H. Greve, P. Grigull, K. Gallowski, S. Geißler, M. Haas, E. Harmeyer, D. Hartmann, G. Heilmaier, B. Heinemann, K. Hertel, D. Hildebrandt, J. Hofner, F. Hollmann, D. Holtum, R. Holzthüm, M. Huart, Ch. Jacob, N. Jaksic, A. John, L. Jonitz, C. P. Käsemann, R. Kairys, F. Kerl, M. Kick, J. Kißlinger, K. Klaster, J. Knauer, R. Krampitz, B. Kursinski, H. Laqua, C. Li, J. Maier, G. Marlow, M. Marquardt, G. Matern, P. McNeely, B. Mendelevitch, G. Michel, M. Müller, F. Noke, S. Obermayer, J. Ogasa, J. Perchermeier, K. Pfefferle, G. Pfeiffer, H. Pirsch, F. Purps, S. Radau, T. Richert, R. Riedl, P. Rong, N. Rüter, N. Rust, J. Sachtleben, W. Schärich, F. Schneider, I. Schoenewolf, R. Schroeder, T. Schulz, S. Schweizer, O. Sellmeier, St. Siche, J. Simon-Weidner, M. Sochor, E. Speth, M. Steffen, B. Streibl, J. Tretter, T. Vierle, K. J. Voigt, M. Weißgerber, J. Wendorf, F. Wesner, M. Winkler, G. Zangl, H. Zedler
Forschungszentrum Karlsruhe FZK (IHM, IMF I, ITP, PMW): A. Arnold, E. Borie, G. Dammertz, I. Danilov, W. Fietz, S. Fink, U. Fuhrmann, A. Goetz, P. Grundel, R. Heidinger, W. Herz, H. Hunger, S. Illy, M. Huber, P. Komarek, H.-R. Kunkel, W. Leonhardt, R. Lukits, A. Meier, D. Mellein, G. Neffe, B. Piosczyk, M. Schmid, W. Spiess, J. Szczesny, M. Thumm, R. Vincon, X. Yang, G. Zahn
Institut für Plasmaforschung (IPF) Stuttgart: H. Babilon, P. Brand, G. Gantenbein, M. Grünert, H. Hailer, W. Kasparek, H. Kumric, M. Krämer, F. Müller, G. A. Müller, R. Munk, H. Salzmann, H. Schlüter, R. Schütz, K. Schwörer, R. Wacker, D. Wimmer
Forschungszentrum Jülich B. Giesen, A. Charl, G. Czymek, F. Harberts, O. Neubauer, U. Reisgen, M. Sauer, W. Schalt, J. Schruff, J. Wolters

[1] Doctoral fellow
[2] Postdoc
[3] Guest from Korea Basic Science Institute

WENDELSTEIN 7-X Diagnostics

Head: Prof. Dr. Hans-Jürgen Hartfuß

1 Overview

Work concentrated on the list of level-0 diagnostics, the set of highest priority, indispensable for the start-up of WENDELSTEIN 7-X and the first years of operation, defined to deliver scientific data as well as the signals used for machine control and its safe operation.

Detailed time schedules for the individual diagnostics of the level-0 category are being worked out . Schedules include research, development, design and construction of the individual diagnostics planned as well as the development to be done within the two temporary working groups on stray radiation tests (3.1, see below) and plasma facing optical components (3.2). The whole time interval until the start-up of WENDELSTEIN 7-X has been considered.

However, since the late phase is strongly linked to the assembly of the machine, only rough estimates are possible at the moment for this interval. Detailed planning has been done for the first two to three years of diagnostics development. The other two main points, collision and feasibility studies on one hand and detailed design of those diagnostic components to be integrated into the WENDELSTEIN 7-X vessel on the other hand, characterize as in the years before, other important activities within the group of designers. In regular meetings all space request in the torus hall is being thoroughly discussed and reservations are fixed. Be-cause of the accessibility demanded and the large amount of space needed, additional floors, platforms and frames need to be designed and to be installed in the hall in time harmonized with the machine assembly. Other activities in progress consider discussion and definition of the start-up scenarios for WENDELSTEIN 7-X since experimental needs determine the set of diagnostics and vice versa the available diagnostics determine the experimental program to be conducted. In summary the progress made in developing individual diagnostics is still in agreement with the time schedules. However, due to a lack of manpower, the total set of level-0 diagnostics, as agreed to be ready in the start up phase of WENDELSTEIN 7-X, can probably not be realized without collaboration with external partners.

2 Reports of Expert Groups

The activities of the nine subgroups as well as of the two temporary working groups and the technical coordination group of the project are briefly summarized by the responsible persons in the following chapters.

2.1 Fluctuations (M. Endler)

The subgroup defines all kinds of turbulence diagnostics for WENDELSTEIN 7-X. The planning for the use specifically of Langmuir probes for fluctuation measurements has been continued. Furthermore, the data analysis method to obtain simultaneously several fluctuating quantities from the characteristics of fast swept Langmuir probes has been improved and the analysis of data from W7-AS has been continued in order to gain experience with this kind of measurement. In order to further develop the technique of optically imaging fast phenomena, a fast framing CCD camera was used to study fast phenomena in the edge of the TJ-II stellarator with high spatial and temporal resolution, in collaboration with CIEMAT.

2.2 Plasma Edge and Divertor (P. Grigull)

The activities on plasma edge and divertor diagnostics were adapted to the available resources by primarily focusing on a highest-priority set which comprises Langmuir probes, target thermography, coolant calorimetry and neutral gas gauges. Concerning Langmuir probes, a full-scale prototype of target-integrated pop-up arrays has been designed, constructed and mechanically tested. In addition, a variety of manipulator types has been studied with respect to their applicability for fast-reciprocating probes in WENDELSTEIN 7-X. The final design of both probe types will be completed in autumn 2004. The electronics for position control and data acquisition has been conceptually designed. Coolant calorimetry is in the conceptual design phase. The types of temperature sensors and flow meters as well as the electronics for data acquisition have been defined. The number and positions of sensors are presently being discussed with respect to their suitability to supervise – in combination with thermography – the divertor targets with regard to thermal overload. The thermographic system has been conceptually designed.

Thermographic measurements using radiation between 0.5 and 5 µm have been applied on all significant magnetic fusion devices in order to supervise and diagnose the power loading of plasma facing components with a spatial resolution of some millimeters. Two and three dimensional

numerical codes (e.g. THERM code) were developed to derive power fluxes arriving at the internal components from the temporal evolution of the measured surface temperature distribution.
The accuracy of temperature readings and values of the derived power fluxes has been examined at surface heat loading of various materials for application to the WENDELSTEIN 7-X project.
The experiments involving well defined heat pulses by laser radiation have been performed on carbon target materials including fine grained graphite and carbon fibre composites of different surface roughness and surface impurity contamination obtained after plasma exposure. Heat fluxes with densities up to 100 MW/m^2 and with durations up to 20 ms were applied.
The surface temperature excursion during and after the laser heat pulses was measured by three different cameras operating in the wavelength region between 0.4 and 1 µm (Si-sensor), 3-5 µm (InSb-sensor) or 8-15 µm (VOx-microbolometer).
In order to validate the accuracy of the measured surface temperature evolutions thermographic temperatures are compared with corresponding values of analytical and numerical solutions of the three-dimensional heat diffusion equation.
In particular in the shorter wavelength regions (0.4-1 µm and 3-5 µm) significant deviations between the experimentally observed evolutions of the surface temperature and the calculated results are found already on samples having original surface roughness before plasma exposure. Measurements with improved spatial resolution show an extremely non-uniform heating of the surface correlated with its morphology (see Fig.1). This effect causes an overestimation of the averaged temperature measured with lower spatial resolution at shorter wavelengths. Although temperature measurements with insufficient spatial or temporal resolution are more accurate in the longer wavelength region (8-15 µm) they still demonstrate a substantial deviation of the measured results from the predicted behaviour for both materials, the CFC material and the fine grained graphite at surface heat loading indicating a much lower mean value of the thermal conductivity at the surface than in the bulk material.
In addition the experiments demonstrate that the measured temperature excursion is strongly changed after surface modification by erosion and deposition processes occurring during plasma exposure. Even contamination layers with a thickness smaller than 300 nm influence the measured temperature.
These uncertainties of the temperature measurements make it difficult to supervise plasma-facing components as divertor target plates in real time. Without additional information they might lead to an overestimation of the power flux densities obtained by the evaluation of thermographic measurements during plasma experiments.

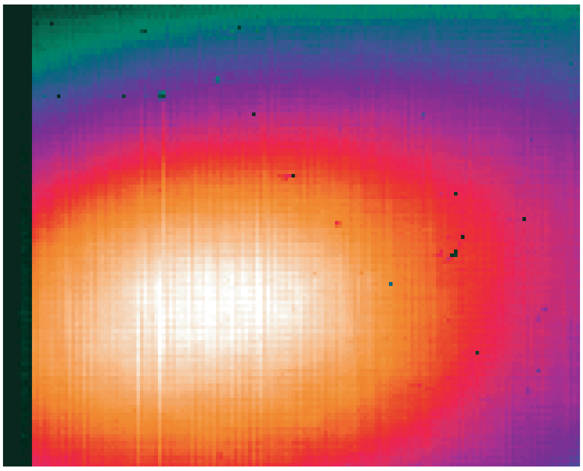

Figure 1: Thermal images taken by the InSb-camera during similar laser heat pulses at oblique incidence with a spatial resolution of 30 mm /pixel

The temperature scaling is different for Figure 1 and Figure 2: T_{ave} denotes the averaged temperature in the marked area which would be obtained in measurements with a spatial resolution of 0.4 mm. The material is polished fine grained graphite (T_{ave} =600 K).

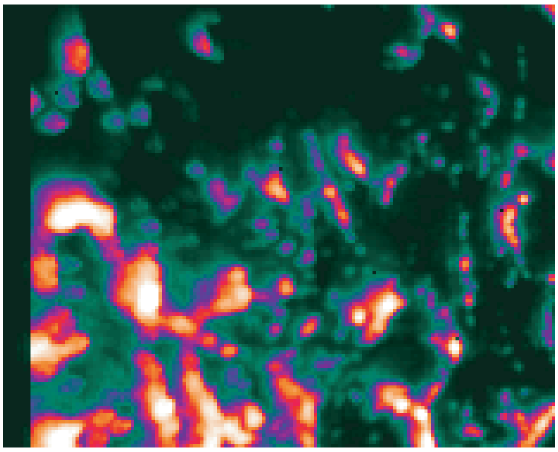

Figure 2: Same as in Figure 1, however, the material is CFC as used in the plasma experiments (T_{ave} =745 K).

2.3 Microwave Diagnostics
(M. Hirsch)

Main activities concentrated on the definition of the infrastructure necessary for the diagnostic systems developed within this group, a multichannel interferometer, the interfero-polarimeter based on the Cotton-Mouton effect, the reflectometers and the ECE radiometer.
Detailed time schedules taking into account personnel resources were elaborated for all four diagnostics as well as for the stray radiation test chamber being set into operation by members of this group (see section 3.1). All in-vessel components of the microwave diagnostics have been checked with respect to possible conflicts between their sightlines and divertor components. The retro-reflectors of the multi channel interferometer are identified as critical components since they need cooling as well as protection

during conditioning phases of the machine. The optimization of interferometer sightlines with the aim to gain maximum information on the density profile in the complex WENDELSTEIN 7-X geometry was continued in collaboration with the University of Helsinki. A first approach of sightlines has been suggested using the full port geometry and a set of reference profiles. A design with four channels and one with eight channels have been compared. The optimization of the chord geometry with respect to the full set of possible magnetic configurations and plasma parameters is the topic of upcoming work.

As a research and development program a two-colour (CO_2 and He:Ne) single channel test interferometer was brought into operation in the laboratory. In a first step, vibration compensation by the dual frequency arrangement could be verified.

The Cotton-Mouton polarimeter as already used at the W7-AS experiment has been set up in the laboratory as a first step of a conceptual design study for the planned interfero-polarimeter and to further optimize the optical set-up.

Work on reflectometry concentrated on the positioning of in-vessel antennas and reflectometry related microwave systems in the tours hall around the machine port A21 were not much space is available.

Concerning ECE, it is planned that main components of the multi channel radiometer of W7-AS will be used at WENDELSTEIN 7-X too. Work concentrated on the detailed characterization of these components, on fixing of a position outside the torus hall where the microwawe components will be installed, and on the design of the transmisson line and the in-vessel antennas, mirrors and their optical arrangement.

2.4 Charge Exchange Diagnostics

(J. Baldzuhn)

A Neutral Beam Diagnostic Injector is envisaged for the Neutral Particle measurements on WENDELSTEIN 7-X. It is planned to develop, construct and test such an Injector (RUDI) at the Budker In-stitute in Novosibirsk, Russia. After definition of the hardware and software components for RUDI, agreement was found between Budker and IPP concerning the details for a develop-ment contract. The control and steering electronics for RUDI, as well as the ion source will be developed at FZ Jülich (FZJ).

The tender procedure for the high voltage power supply for RUDI was started in the begin-ning of 2003, and finished with an offer from Budker Institute within the predefined price margin. After successful completion of that administrational part, the contract for the develop-ment of the high voltage power supply was signed by the end of 2003. In the middle of 2003, a tender action for an appropriate quantity of stainless steel was started, such that required 13 tons of steel will be ready for delivery to Novosibirsk in January of 2004.

During a meeting at FZJ, agreement was found between the partners FZJ, Budker and IPP, that a phase of close collaboration has to follow during the next years. In this way, the development of RUDI will be accomplished, as well as the associated Neutral Particle Analysis and the Charge Exchange Spectroscopy in the beam of RUDI.

be ordered at the end of 2004.

2.5 Spectroscopy

(R. König)

The design of a prototype immersion tube suitable for the simultaneous installation of periscopes for UV, visible and IR divertor observation has begun. A design concept for a water cooled front end of the tube with integrated water cooled windows and a water cooled rotating shutter has being outlined and the detailing of the design started. The development of the water-cooled windows was taken up by the temporary working group 'Plasma Facing Optical Components' (TAG PFOC). The integration of the tube's front end into the design of the three cooled liner panels of the vacuum vessel which merge at this location and with the tube liner, insuring the observation angle of 110° required to be able to observe the entire divertor has been completed.

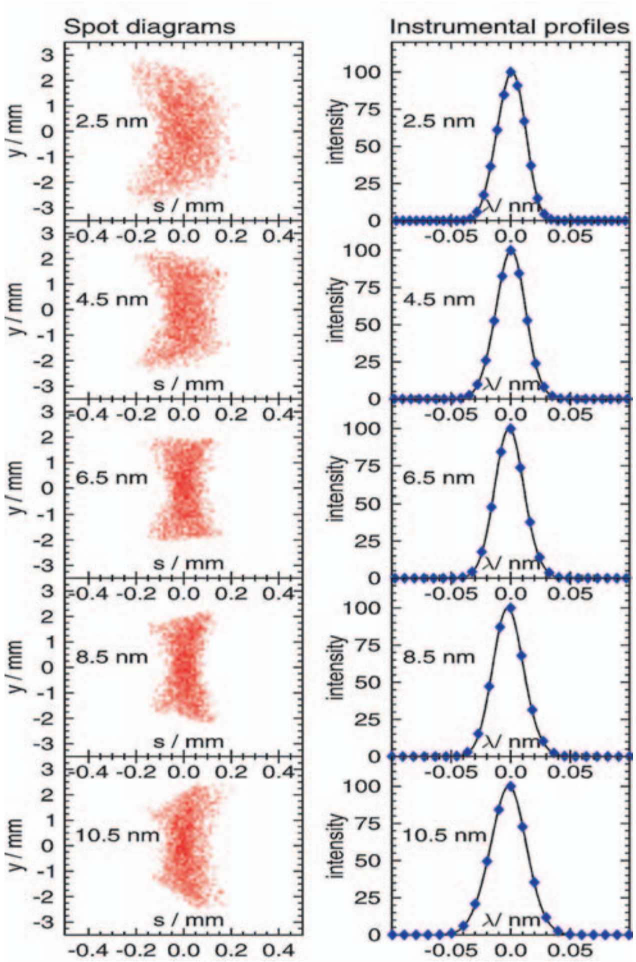

Figure 3: Spot diagrams and line width for grating no. 1

The second focal point of our work was the specification of the details of a set of four high-efficiency VUV/XUV spectrometers, which will be used for plasma impurity monitoring and impurity transport studies on WENDELSTEIN 7-X. This system is being largely developed by FZ-Jülich in close collaboration with the WENDELSTEIN 7-X spectroscopy group. The new HEXOS system (High Efficiency XUV Overview Spectrometer system) covers the wavelength range from 2.5

nm to 160 nm, divided into four subsections with some overlapping, thus achieving a complete coverage of prominent spectral lines from the relevant impurity elements. Taking into account spectrometer geometries and detector geometries, toroidal holographic diffraction gratings were numerically optimised to maximise the total throughput while maintaining good spectral resolution (figure 3). The performance of the spectrometers was tested and optimised by means of ray tracing calculations. In order to prove the potential for line identification as well as the expected levels of signal intensity and noise figures of the new systems, spectra were simulated using the impurity transport code STRAHL (tab.1). Under typical plasma conditions on WENDELSTEIN 7-X the new spectrometers will allow to clearly identify all relevant impurity elements in the plasma. The large collected photon flux results in a high accuracy for the measured line intensities even when operating the spectrometers at spectra rates of 1000/sec.

A fast piezo-valve for the thermal He-beam which can be installed in vacuum directly behind the target plate of the divertor has been designed, constructed and successfully tested in the laboratory at FZ-Jülich and has finally been installed on TEXTOR for further tests under true working conditions. The new design ensures that the gas reservoir can be kept sufficiently small so that the beam can be modulated.

A diploma thesis based on experiments performed on W7-AS has been completed which proved that the concept of using a set of micro-spectrometers to determine robust Z_{eff} profiles from Bremsstrahlungs measurements over a wide spectral range and which makes use of a Bayesian data analysis procedure can be successfully employed.

Spectrometer No.	1	2	3	4
Wavelength range nm	2.5 – 10.5	9.0 – 24.0	20.0 – 66.0	60.0 – 160.0
Wavelength resolution (from imaging only) / nm	0.026	0.04	0.09	0.18
Detected line width / nm	0.031	0.05	0.13	0.26
Illuminated solid angle of entrance beam / 10^{-5} sterad	3.6	22	88	92
Effective etendue[6)] / 10^{-5} mm^2 sterad	3.0	10	20	21

Tab. 1: Calculated intensities of selected spectral lines

Continuously potential conflicts between diagnostic components and parts of the periphery, like water, heating or pumping pipes, liner panels, etc. have been identified and the design of the components modified in mutual agreement. Also the cut-outs in the divertor target and baffle structures required by some of the divertor diagnostics have been agreed on in accord with the in-vessel components group (KiP).

2.6 Thomson Scattering

(E. Pasch)

For all three Thomson scattering systems placeholders in the torus hall were rendered. However, work of the diagnostics development is focused on the bulk system. This system must be qualified for analysing time resolved plasma profiles with high spatial resolution. Because of interaction with plasma facing components, the main concern was the development of a concept for the detection optics. The designing work of the total detection optics showed, that an additional port, AEN 31 port, is needed to optimise the optical imaging. Therefore port AEN 31 is now additionally reserved for the bulk Thomson scattering system. To cover the whole plasma profile two observation optics, one in port AEM 31 and the other one in port AEN 31, are provided. To reduce calibration uncertainties in particular at the plasma centre, an overlap of the radial observation points (along the laser beam) is considered.

2.7 SX- and Electromagnetic Diagnostics

(A. Weller)

New more substantiated time schedules have been worked out, in particular for the prioritised systems which have to be integrated into the vacuum vessel. Design activities concerning the proposed X-ray multi-camera tomography system will started early in 2004. The design of the heat shield protecting the cameras has to be accompanied by heat load and structural analysis calculations. At the same time a solution for mounting the cameras close to the inside vessel wall has to be found. The detailed design will depend on the results of activities already star-ted in the laboratory. The design of the additional flexible camera system equipped with interchangeable filters and of the X-ray pulse height analyser system will commence in 2006.

Concerning the magnetic diagnostics, the saddle-coils are ready for the assembly onto the first vessel module. Some of the fasteners foreseen had to be modified due to interferences with the cooling pipes of the vacuum vessel. A diamagnetic-loop prototype is under construction. The correction of the diamagnetic-loop signals in the divertor section cannot be realised by internal compensation coils in consequence of the re-design of the divertor. Instead, the actual field coil currents have to be used directly requiring a larger electronics R&D effort. Another prototype of the segmented Rogowski-coil has now been successfully tested. One more proto-type is under construction, which is particularly intended for tests of joints between the coil segments. The effect of parasitic vessel currents on the signals was successfully simulated by a finite element code.

2.8 HIBP and Fast Particles

(H. Hartfuss)

As the main component of the heavy ion beam probe (HIBP) diagnostic, a 2-MeV-accelarator has been transferred from the TEXT experiment in Austin, Texas to IPP-Greifswald. The accelerator belongs to the Rensselaer Institute in Troy, N.Y. which will collaborate with IPP in a later phase. The necessary infrastructure has been developed and the authorization procedure started. The accelerator will be operational by mid 2005.

Concerning the fast ion loss detectors, the concept has been reviewed, considering finite plasma pressure as well as the new divertor geometry of WENDELSTEIN 7-X. Helpful in this context is the software developed as a contribution to Jet-EP.

2.9 Neutron Diagnostics (S. Baeumel)

The planned 6 neutron detectors will be developed in cooperation with PTB-Braunschweig and the University of Uppsala in Sweden. Contracts are in preparation.

3 Temporary Working Groups

3.1 ECRH Stray Radiation Test Chamber (H. Hartfuß)

A aluminium vacuum test chamber has been designed, constructed and has been installed at IPP-Garching, dedicated to high power steady state tests of materials and components at the ECRH frequency of 140 GHz. The chamber is designed to operate at microwave power flux densities up to 30 kW/m^2 as expected under certain heating scenarios in WENDELSTEIN 7-X.

The necessary microwave power is delivered from a gyrotron tuned to operate in a pulsed mode continuously. Its output power is guided into the chamber to generate an isotropic power flux. The chamber will be operated in collaboration with the Plasma Physics Institute of CNR in Milano. First measurements will be conducted in the frame of a diploma thesis at the University of Greifswald. The test chamber and the diagnostics installed also serve as a test-bed for concept tests of diagnostic control and data acquisition.

3.2 Plasma facing optical components (R. Koenig)

The working group concentrated on the development of water cooled windows for optical periscopes which can withstand the expected maximum heat loads of up to 50 kW/m^2 which, due to the predominantly short wavelength nature of the radiation emitted by the plasma, will be absorbed within the first millimetre of any window. Detailed ANSYS-code calculations of the heat and stress distribution across the window have been performed at FZ-Jülich for a large number of different window materials required for the various spectral regions covered by the miscellaneous diagnostics so that the most suitable materials for each application could be identified.

Also the dependence of the cooling rate on the window diameter and thickness has been studied. The calculations suggest that CVD-diamond as a very expensive last resort for the few large windows (dia. >150 mm) required can most likely be avoided by using sapphire but that for many of the other materials like ZnSe, ZnS, CaF_2, MgF_2 and quartz, one will be limited to considerably smaller sizes.

A vacuum test chamber, which has been equipped with a vacuum compatible IR heater, has been build. First tests of a low cost, easily ex-changeable window design using Helicoflex gaskets and un-blackened Sapphire and Quartz windows have been successful. It has been demonstrated that the design was watertight and that the window materials behaved roughly as predicted by the ANSYS calculations, with sapphire, as expected, showing excellent heat removal properties. The test windows are now being blackened with Aquadag material to ensure effective absorption of the IR radiation at the surface of the

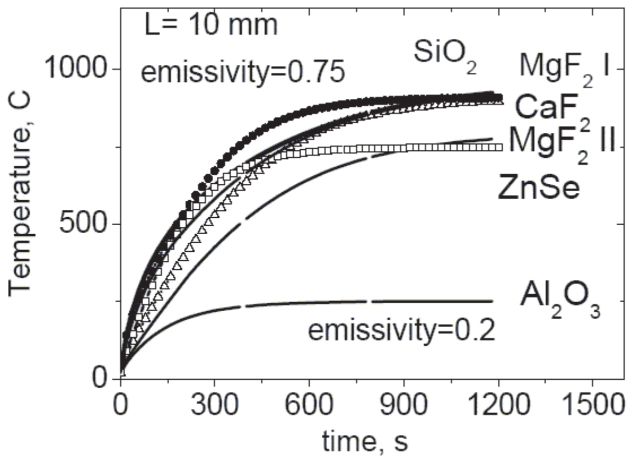

Figure 4: Time dependence of the maximum temperatures of different window materials for a heat load of 50 kW/m^2. Design parameters are: diameter D = 170 mm, thickness L = 10 mm. Emissivity = 0.75 for all materials, except sapphire (Al_2O_3) for which the emissivity is = 0.2.

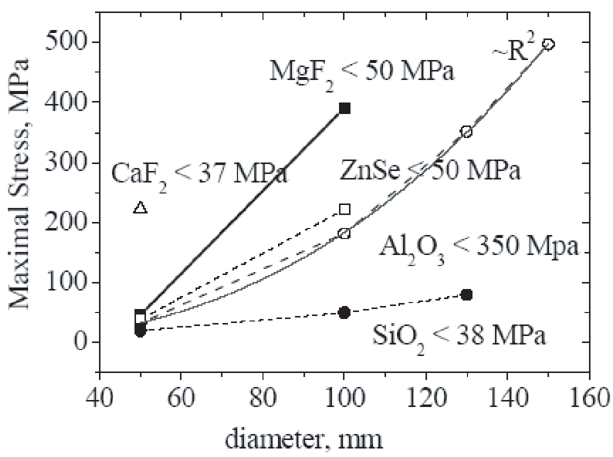

Figure 5: Dependence of the maximum stress on the window diameter for different window materials caused by a heat load of 50 kW/m^2 after 20 minutes at a window thickness of 10 mm.

substrates on the vacuum side of the windows and IR cameras for different wavelength regions as well as other test equipment are presently being installed at the periphery of the test chamber for detailed investigations of the radial heat distribution across the different window materials and a comparison with the ANSYS calculations.

4 Technical Coordination

4.1 Overview

(U. Neuner)

Work on the infrastructure for the diagnostics progressed with the design of the diagnostics electrical power supply system, the detailing of the control system and the concept definition of the cooling system. Positioning of components in the diagnostic hall and in the torus hall carried on, to check for and to eliminate collisions. The vacuum test chamber for heat load experiments of periscopes came into operation, and the ECRH stray radiation test chamber was designed and set up.

The design of a few diagnostics has been further developed in detail. While a prototype of the Langmuir probe array is currently under test, its design had to be adapted to fit the redesigned divertor. For the Rogowski coils a functioning prototype could be found, and the final design is now being completed so that these coils can be included in time into the machine assembly. A number of manipulator scenarios were studied and a suitable solution was selected. The assembly of the saddle coils was prepared, since it is included in the very first step of the WENDELSTEIN 7-X machine assembly.

Scientific Staff

Experimental Division 3: T. Bindemann[1], J. Geiger, H. Hartfuss, R. Jaenicke, J. Knauer, U. Neuner, M. Otte, E. Pasch

Experimental Division 5: S. Baeumel, J. Baldzuhn, R. Burhenn, H. Ehmler, M. Endler, P. Grigull, M. Hirsch, R. Koenig, R. Narayanan[1], K. McCormick, E. Sallander, H. Thomsen, A. Weller, A. Werner, D. Zhang

Plasma Diagnostics Division: D. Hildebrandt, M. Laux, U. Wenzel

FZ-Juelich: W. Biel, G. Bertschinger, A. Kreter, P. Mertens, A. Pospieszczyk, B. Schweer[1]

5 Plasmatheorie

5.1 Predictive Transport Code Development

(Henning Maaßberg)

The development of the predictive transport code (and a related analysis version) for stellarators was continued. The code is based on a system of diffusion equations, namely for the particle and power balances as well as for the radial (ambipolar) electric field and the toroidal current density. The platform-independent GUI framework was implemented (i.e. programs to monitor the task running and to visualise the simulated phenomena) and the following new modules were developed: a straight line ray-tracing module; tools for coordinate transform from real space to magnetic coordinates and a module for the calculation of the metric coefficients. The development of modules for modelling the particle source for pellet injection was also started (collaboration with PPPL).

Finally, a Web-server based on the analysis version of the transport code was implemented, which calculates the (ambipolar) radial electric field profiles within the Baysian error analysis of density and temperature profile fits to measured W7-AS data.

5.1.1 Advanced δf Monte Carlo Code for NBI

For NBI heating, the full slowing-down of the fast ions is typically simulated using a standard f Monte Carlo technique (a standard δf MC technique based on the Maxwellian has no advantage for high energies). This is fairly time expensive since the simulation must be performed on the slowing-down time-scale.

If, however, the radial diffusion and particle losses within the slowing-down are of minor importance, e.g. for the nearly tangential injection in W7-AS or due to the quasi-isodynamic optimization of W7-X, a simple and very fast Fokker-Planck solution with slowing-down on flux surfaces is used for the advanced δf MC technique (in the marker equation). Then, this δf MC simulation determines only the radial diffusion within the slowing-down process on a much faster time scale. A detailed comparison with the full f MC technique demonstrated the advantage of this new approach (collaboration with V. Tribaldos, CIEMAT and S. Murakami, NIFS)

5.1.2 Beam-/Ray-tracing Code for ECRH

Development of a new beam-/ray-tracing (BRT) code was started. Parts were used from the ray-tracing codes of V. Tribaldos (CIEMAT) and F. Volpe as well as the beam-tracing code of E. Poli (AUG). This new code will treat ECRH standard scenarios, e.g. X2 and O2 modes, and also the O-X-B scenario for Bernstein wave heating of very high densities. Especially for the O2 launch (with low optical depth), the hot dielectric tensor in the weakly relativistic limit is used for the tracing. New interfaces for the transform from real space to Boozer coordinates were developed and implemented. For the calculation of the linear current drive efficiency the adjoint approach is used. In addition, the quasi-linear diffusion coefficient will be calculated for the interface to Fokker-Planck or Monte Carlo codes (stochastic mapping technique). The BRT code will be extended laterto include also diffraction effects.

5.1.3 Stochastic Mapping Technique

A new Monte Carlo code based on the stochastic mapping technique (developed at TU-Graz) was implemented for W7-X configurations. The stochastic mapping technique is equivalent to orbit-averaging and is extremely efficient for electron Monte Carlo simulations (orbits are calculated once and stored in the maps). With the coupling to the ray-tracing code, "convective" electron fluxes driven by the ECRH absorption can be calculated and taken into account in the ambipolarity condition for estimating the radial electric field ("electron-root" feature). Furthermore, the full non-linear ECRH absorption can be treated with this technique in addition to the linear and quasi-linear treatment used for W7-AS (EURATOM collaboration with TU-Graz)

[1]postdoc

5.1.4 Function Parametrization for W7-X

In order to provide fast transforms from real space to magnetic coordinates, code developement has started in collaboration with the University College Cork (UCC). Based on previous work at W7-AS, function parametrization of NEMEC-equilibrium calculations are envisaged to provide such a tool. As a starting point a database of 1210 vacuum configurations has been created to investigate its properties (rotational transform, field strength on axis, etc.) The configurations have been chosen randomly out of a 6-dimensional hypercube formed by the 6 coil current ratios of the W7-X coil system with reasonable assumptions for their limits. First parametrizations have been recovered for axis values and a parametrization of island position and width for the low-order natural islands (5/4, 5/5 and 5/6) is being set up to provide additional information about the vacuum configurations. Also, a "back" transformation has been successfully found to relate the axis parameters to the coil currents so as to provide the possibility to derive coil currents from physical properties.

5.1.5 EMC3-EIRENE Modelling

5.1.5.1 Physics of detachment

The new (flux-tube) version of the EMC3-EIRENE code was extended to include the self-consistent treatment of impurities. This opened the way to a detailed modelling of the detachment physics for island-divertor configurations with ergodic structures. In particular, applications to W7-AS showed, in agreement with the experiment, that by increasing the separatrix density after detachment transition a bifurcation in the carbon radiation distribution appears leading to stable or unstable detachment (see W7-AS contributions in this report). Stable detachment is established only if the target-to-separatrix distance, Dx, and the field-line pitch in the island frame are sufficiently large (Fig. 1a), which corresponds to a sufficiently effective parallel transport. These non-trivial requirements for island divertors could be met for W7-AS only by using additional island-enlarging perturbation coils. Besides W7-AS, the code is being routinely applied to TEXTOR-DED (collaboration with D. Reiter and D. Harting, IPP Jülich) and has been recently implemented for W7-X, standard configuration. Implementation for LHD is on the way (collaboration with M. Kobayashi, NIFS).

5.1.5.2 Optimization of the W7-X pumping system

Applications of EMC3-EIRENE to W7-X have been started aiming at the optimisation of the cryopumping system for an efficient particle control consistent with long-pulse operation. A scan of the gap area to the divertor chamber shows that the neutral densities and pumping rates in the divertor chamber have a maximum at a gap of 1 to 1.5 of the design value depending on the divertor pumping efficiency. The establishment of a stationary particle balance crucially depends on the pumping efficiency, which, for a given particle input, sets a lower limit to the plasma density at the separatrix. First code simulations indicate that for the W7-X standard configuration, rotational transform = 5/5, a cross-field diffusion coefficient of 1 m^2s^{-1} and a technically specified pumping efficiency of 20%, a minimum separatrix density between 1 and 2 10^{19} m^{-3} will be required to remove a refuelling rate of 2 10^{21} s^{-1} corresponding to 10 MW NBI heating power.

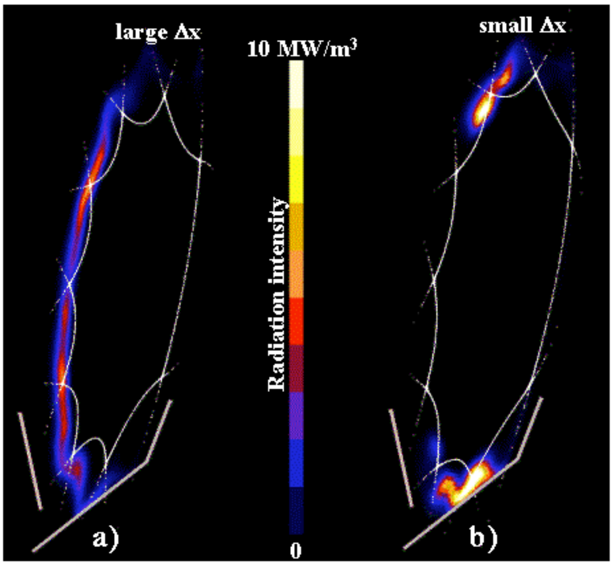

Figure 1: a) Radiation at inboard X-points, stable detachment in experiment
b) Divertor radiation, unstable detachment in experiment

5.1.6 Neoclassical Transport: Tokamak Fits

For a database of tokamak configurations in an extended "standard model" (different τ, r/R and elongation) the 3 mono-energetic transport coefficients (radial transport, bootstrap current and electric conductivity) were calculated using DKES for all collisionalities. Based on the flux-friction relations (due to symmetry) only the bootstrap current coefficient is fitted (and the other Pfirsch-Schlueter contributions) for a good and consistentrepresentation of all coefficients (EURATOM collaboration with TU-Graz).

5.1.7 Neoclassical Transport: Electric Conductivity and Ware Pinch

Using the field line integration technique (t is approximated by a high-order rational) the electric conductivity and the Ware pinch will be formulated first in the collisionless limit. A numerical scheme (coupled diffusion equations in the magnetic moment along the field line) is analysed for finite collisionalities. For the highly localised (in phase space) first-order distribution function, this scheme is expected to have fewer convergence problems than the DKES approach using a Fourier-Legendre expansion (EURATOM collaboration with TU-Graz).

5.1.8 Integrated Data Analysis

Efforts on Integrated Data Analysis were continued. Various profile analyses were performed required for further physics modelling. Special emphasis was placed on coupling transport codes in order to improve data consistency checks and cross validation of different diagnostics and finite beta mappings. The development and exploration of statisticalmodels was continued (Cooperation with Data Analysis Group, CIPS, Fischer, Gori, v. Toussaint).

Meeting the necessity for an appropriate inclusion of systematic errors and the incorporation of interdependencies, conceptual studies for a fully integrated data models for W7-AS employing Bayesian Graphical Models were performed.

5.1.9 International τ_E Scaling

Within a comprehensive international collaboration a revision of the ISS95 confinement data base was agreed and initiated (NIFS, CIEMAT, U-Kyoto, ANU, U-Wisconsin, U-Kiel, and IPP). First data from W7-AS after divertor installation and from the 6th LHD experimental campaign has been included in the revised database.

Stellarator System Studies

Head: Dr. Yuri Igitkhanov

Introduction

During the last year the Stellarator System Study Group has carried out almost exclusively (≥ 90%) tasks associated with WENDELSTEIN 7-X construction and the remaining resources (10%) were used to prove further the credibility of the WENDELSTEIN 7-X as a reactor-relevant machine. This mainly implies engineering and technological tasks related to the coil system, power handling and the maintenance, which have been reconsidered on the bases of WENDELSTEIN 7-X construction experience and ITER technological achievements

1 Contribution to WENDELSTEIN 7-X construction

1.1 Task-Force

In the frame of " Task-Force" for the WENDELSTEIN 7-X coil system the force and momentum distributions for different operational conditions have been recalculated. The net magnetic forces acting on the coils were computed and the points of application of these force vectors have been determined. These calculations were necessary because it was found that the support structure would require further assessment.

1.2 Magnetic stray field

The stray field in the machine hall of WENDELSTEIN 7-X was calculated for all operation regimes. The maximum values of stray field among the different regimes have been documented as an IPP-Report (IPP 13/2, Nov 2003). Additionally, very detailed calculations were carried out at the location of the NBI boxes.

1.3 Calculation of the magnetic field errors

The analysis of the manufacturing errors of WENDELSTEIN 7-X coils has been carried out taking into account the real measurements of coils already fabricated. The estimation of the perturbed magnetic fields has been done for every newly fabricated coil to help in assessment of its acceptability. The numerical code for the calculation of the filament positions of the coils, which can be displaced due to the manufacturing and assembly errors, was developed in order to take into account reference and measured coordinates of the PIN points at different stages of the assembly of W 7-X.

1.4 Ferromagnetics

The support structure below W7-X (basement construction MAFU) is designed from SS and has an overall weight of about 40t. The permissible magnetic permeability has been calculated in order to avoid non-acceptable field disturbances of the vacuum magnetic field inside the plasma region. Furthermore, the ferromagnetic effect of a thin nickel layer on the surface of the vacuum vessel was estimated.

1.5 Angular distribution of the neutron field

Knowledge of the neutron spectra and their dependence along the toroidal angle j of the Wendelstein-7-X torus is of importance and is analysed by using the MCNP transport code. The modelling of the Wendelstein-7-X torus is described in: J. Junker and A. Weller "Neutrons at W7-X" IPP Report IPP 2/341, Oct. 1998 and F.Herrnegger, J. Junker, A.Weller, H.Wobig, " Neutron Field in the W-7X Hall", Fusion Engineering and Design 66-68 (2003), 849-853. The present geometrical model of the torus and the hall assumes a cylindrical wall which extends from R=1770 cm to R=1950 cm. The clear height of the hall is 24 m. Point detectors are located along a circle at R=850 cm and z=150 cm (and also z=0 cm, z=300 cm). The two fusion reactions D(d,n) 3He and D(d,p) 3T have about the same probability; the tritons are produced at 1 MeV, the neutrons at 2.46 MeV. Here the ring source for the neutrons is located at R=550 cm, z=0 cm (cylindrical coordinates with origin at R=0, z=0) and produces Q=1E16 neutrons per second with a Gaussian energy distribution.

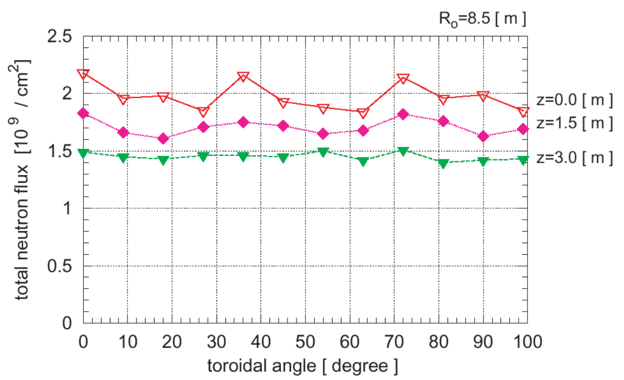

Figure 1: Total neutron flux vs the toroidal angle at various z-values

2 Helias Reactor studies

2.1 Configuration studies

For 3 and 4-period Helias reactor configuration equilibrium and stability have been calculated for different pressure gradient profiles. It was shown, that at finite beta the main properties of the magnetic configuration do not change significantly (the island divertor concept can be used) and the plasma remains stable against Mercier and ballooning modes. The Shafranov shift is sufficiently small for the HSR3/15 and HSR4/18 configurations.
The range of rotational transform values increases for higher beta, so that low-order resonances appear inside the LCMS. For HSR3/15, Mercier and resistive interchange stability criteria for the chosen pressure profiles are satisfied for b=3% and the maximum b is around 4%. In future, the CAS3D code will be applied for stability analysis of both configurations. HSR3/15 needs further optimisation with respect to the bootstrap current, a-particle confinement and rotational transform profile. The main results have been presented at the 30th EPS, St. Petersburg, 2003 and during the Stellarator Workshop, Greifswald, 2003.

2.2 Design considerations

Helias reactor design has traditionally sought configurations with an inherently small bootstrap current and a magnetic field strength at the coils which is low enough to permit NbTi as the superconductor. Unfortunately, these goals become increasingly contradictory as the aspect ratio is decreased. The current 3-field-period reactor conforms to the NbTi technological constraints and it is therefore of interest to determine what ramifications this has for the bootstrap current. Calculations of the bootstrap current coefficient were performed using the DKES code and then convoluted with plausible density and temperature profiles to determine the radial bootstrap current profile.

Total bootstrap currents on the order of 1 MA are predicted, more than an order of magnitude larger than expected in the 5-field-period case. A current of this magnitude is probably unacceptable but a final verdict must await the outcome of equilibrium simulations (NEMEC-MFBE) which account for its presence.

2.3 Analysis of MHD stability

To check the MHD stability at finite beta for HSR4/18 configuration the Terpsichora code will be employed. This work has been started in the frame of cooperation with CRPP-EPFL (Lausanne). The current distribution in the modular and planar coils of HSR4/18 was delivered to Dr. A. Cooper.

2.4 Power supply and protection system

Computer simulation studies were done for the power supply and the protection system for the superconducting coils of the Helias reactor, using the SIMPLORER code. This work was performed in collaboration with A. Wieczorek from the University of Applied Science in Regensburg and reported at the 10th EPE conference in Toulouse and the14th International Stellarator Workshop in Greifswald.

By means of the Finite Element Network method (FEN) the computation of the eddy currents (induced during the transient process in the walls of the coil housing) was reduced to analyses of transient processes in electric networks. In these computations the inductance and resistance data of the nonplanar coils and their coil housings were used. The safety system, inserted between each power supply unit and the coil group, protects the superconducting coils in case of faults. The strong dependence of the resistivity on temperature at cryogenic temperatures is taken into account. The approximation method allows one to study the design of the whole system with a real model of the power supply and the passive structures and to simulate the different kinds of faults that may occur in the confinement system and in the power supply units.

2.5 Physics aspects of a Helias Reactor

Burn control in a Helias power reactor and the High Density Mode (HDH-mode) of operation have been considered. Controlled, steady-state operation of a fusion plasma implies that transport power loss from the core region balances the self-heating from alpha particle power. A thermally stable solution requires that the transport power losses increase more rapidly with temperature than the fusion power. It was shown that a stable burn in the optimised HSR4/18 reactor plasma can be envisaged at expected residual value of neoclassical transport at the edge. (T. Andreeva, C.D. Beidler, Yu. Igitkhanov, E. Polynovskii, H.Wobig "Burn Control in a Helias Power Reactor" at 30st EPS, St.Petersburg, July, 2003, paper P-1.8).

The HDH mode, observed in the W7-AS may occur due to the formation of an Edge Transport Barrier in stellarator plasmas. Analysis shows that the appearance of the ETB depends on the fuelling rate in the initial stage, but steady-state operation depends on the average density value. This value scales with power, and the question arises whether the HDH mode of operation is feasible under reactor conditions. This result was presented at the 14th International Stellarator Workshop, Greifswald, 2003 (Yu. L. Igitkhanov, K. McCormick and P. Grigull "On the High Density modes of operation in W7-AS")

3 International co-operation

International cooperation exist in three domains: a) contacts with ARIES project, b)cooperation with CRPP-EPFL concerning MHD stability, c) the international collaboration on the topic of neoclassical transport in stellarators, recent progress was reported on at the 30th EPS conference in St. Petersburg. Benchmarking of the radial transport properties of a large number of planned and existing devices is nearing completion with satisfactory agreement in all cases.

Scientific Staff

T. Andreeva, C.D. Beidler, E. Harmeyer, F. Herrnegger, Yu. Igitkhanov, J. Kisslinger, H. Wobig

WEGA

Head: Dr. Johann Lingertat

1 Introduction

In 2003, the work of the WEGA group was focused on the compensation of error fields, the improvement of heating efficiency and the installation of new diagnostic equipment. Part of the results obtained is relevant for the W7-X project.

As in 2002 the new technical infrastructure of the institute has been continuously operated and experience has been gained for future W7-X operation.

2 Compensation of error fields

As mentioned in the Annual Report 2002 vacuum magnetic flux surface measurements revealed the existence of non-natural islands of the order m=1 and m=2 caused by error fields. Although the origin of the errors fields can not be derived from flux surface measurements, they can be used for a comparison with code results. In our calculations (Gourdon-code and LMAA field line tracing code) it could be shown that a horizontal shift between the vertical axis of the toroidal and helical field coils of ~3 mm reproduces the experimentally found islands.

Furthermore, calculations show that the error fields can be compensated by introducing a compensation coil. After analysing different types of coils an optimal position for a single planar field coil (∅=34 cm, 36 turns) was determined.

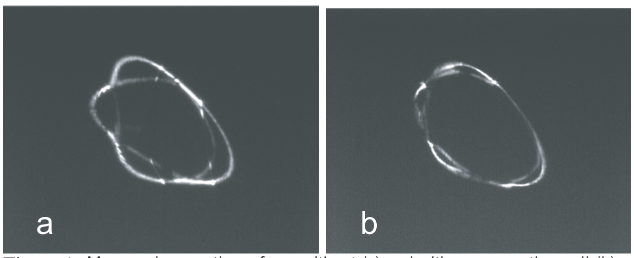

Figure 1: Measured magnetic surfaces without (a) and with compensation coil (b), compensation coil current I_c = 400 A = 0.66 × I_{tor}

In Fig.1 the experimentally determined magnetic flux surfaces for B_0=87.5mT at the resonance $\iota/2\pi$=1/4 are shown. Fig.1a presents the situation without using the compensation coil. For the same magnetic configuration the width of the island can be clearly decreased with the help of the compensation coil as shown in Fig. 1b. While the main purpose of the compensation coil is the suppression of non-natural islands it can also be used to turn the islands poloidally by tilting the coil. In the future it is planned to rotate an island from the X- to the O- point along the tip of a Langmuir probe to measure transport and fluctuations properties inside islands.

3 Optimisation of the heating efficiency

The WEGA plasma is ignited and heated from the low-field side by ECRH at 2.45 GHz (O-mode). Typically, the resonant field of B_o = 87.5mT is located near the centre of the vacuum vessel. Under those conditions the wavelength (λ ~ 12 cm) is comparable to the plasma radius (a ~ 10 cm) and the physics of plasma-wave interaction becomes complicated. Experimentally, we measure densities well above the cut-off density of $n_c = 7.5\times10^{16}\mathrm{m}^{-3}$. For heating of such overdense plasmas, mode conversion into the electrostatic Bernstein wave (EBW) is required.

We assumed the OXB mode conversion process to be relevant in the WEGA device and optimised the antenna accordingly, using the HFSS code. Initially a cylindrical TE_{11} waveguide was used as an antenna. Since the O-X conversion efficiency has a maximum for an angle between magnetic field and wave vector of 45°, the waveguide in a first step was cut at an angle of 45^0. With this antenna the maximum of power is emitted in a direction of 22^0. However, more power is launched in the optimum 45^0 direction. For the second step a special antenna shape was chosen (cylindrical TE_{11} waveguide with two slits on both toroidal sides). Here the directivity pattern has two lobes near the optimum direction, and the efficiency of O-X conversion is higher than in the two previous cases. Indeed the heating efficiency improved. The maximum achievable density at constant heating power increased by more then a factor of 10 above the cut-off density.

A scenario for non-resonant heating has been developed. At present it is possible to ignite and to maintain a plasma in Argon at a magnetic field of 0.5 T. The achievable plasma parameters at 2.45 GHz/6 kW are $n_e \approx 6\times10^{18}\ \mathrm{m}^{-3}$, $T_e \approx 3$ eV at a neutral pressure in the vacuum vessel of ~ 10^{-6} mbar. Such a plasma is well suited as a target for neutral beams in high-β experiments at W7-X.

Staff

D. Aßmus, K. Horvath[1)], J. Lingertat, M. Otte, Y. Podoba[1)] , N. Paschkowski

Guests: D. Keil[3)], O. Lischtschenko[4)], S. Marsen[2)], M. Nitz[2)], S. Pfeifer[3)], A. Vogelsang[4)].

1) International Max Planck Research School, 2 Fachhochschule Stralsund, 3 Fachhochschule Wismar, 4 Universität Greifswald

Plasma-facing Materials and Components

Head: Prof. Dr. Dr. Harald Bolt, Dr. Joachim Roth

During operation of fusion devices the plasma-facing materials are subjected to particle fluxes from the plasma (ions, electrons, atoms) and to electromagnetic radiation. This results in a multitude of complex processes termed “plasma-wall interaction”. Understanding these processes helps to improve the materials used for applications on the first wall of fusion experiments. It also leads to optimised operation conditions and thus to improvement of performance during the plasma discharge. New materials with improved properties in terms of e.g. erosion behaviour and heat flux capability are to be developed and characterised under plasma interactive conditions. Integration of new materials into the plasma-facing components also requires detailed work on interfacial engineering, since dissimilar materials with different functions have to be used. Within the project "Plasma-facing Materials and Components" the areas of plasma-wall interaction studies, material modification under plasma exposure, development of new plasma-facing materials and their characterisation have been merged to form a field of competence at IPP. The work supports exploration and further development of the fusion devices of IPP and also generates basic expertise with regard to PFC-related questions in ITER and fusion reactors. The tasks of the project are:

- Surface processes on plasma-exposed materials,
- Migration of materials in fusion devices,
- Tritium inventory – understanding and control,
- Materials – processing and characterisation,
- Component behaviour.

1 Surface processes on plasma-exposed materials

1.1 Surface Reactions of Carbon on Fe and Ni

We investigated the binary systems C on Fe and Ni using the surface and chemistry-sensitive method, X-ray photoelectron spectroscopy (XPS). Fe(110), Ni(111) and Ni(100) crystal surfaces were used as substrates. The carbon films (thickness up to 4 nm) were deposited at room temperature. In contrast to W, Ti, Be and Si substrates investigated earlier, Ni and Fe show endothermic carbide formation reactions and different behaviour was expected at elevated temperatures. In addition, we investigated the influence of the surface structure on the carbon dissolution and carbide formation. Even with endothermic formation we observed a thin carbide layer at the interface. More carbide is found on Fe(110) than on Ni(100) and Ni(111). A maximum carbide fraction is measured within the first carbon monolayer, as shown in Figure 1. The carbide intensity in the C 1s signal rapidly decreases after further carbon deposition. With increasing temperature the C 1s signal shows carbide decomposition beginning at 470 K independently of substrate or surface structure. The decomposition of the initially formed carbide is due to the metastable character of these carbides. Further annealing leads to carbon diffusion beginning at 670 K both on Fe(110) and Ni(100) and at 770 K on Ni(111) and concomitant additional carbide formation. In the case of Fe(110) the carbide formation reaction is very fast and leads to a thin, fully carbidised C layer. Ni shows dependence of the residual carbon on both the surface structure and the initially deposited layer thickness.

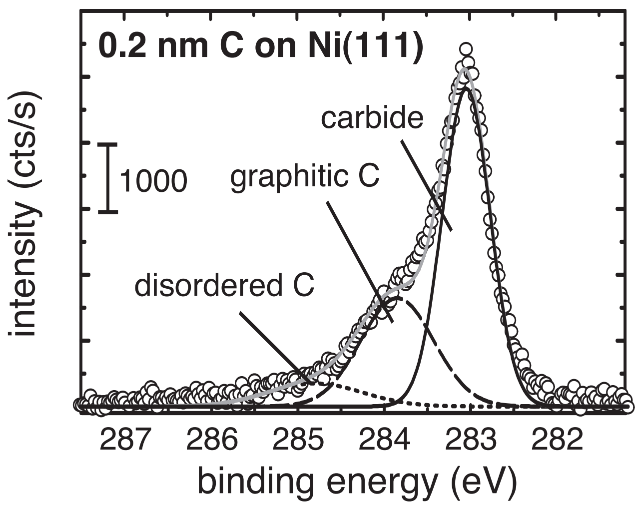

Figure 1: XPS spectra from carbon on nickel showing carbide formation within the first monolayer

1.2 Chemical Erosion of Mixed Ti/C layers by D Impact

Doping carbon materials with Ti atoms largely reduces their chemical reactivity with hydrogen and their chemical erosion. To investigate in detail the processes involved in this reduction, new H-free amorphous Ti/C layers were produced by magnetron sputtering. Their erosion behaviour under 30 eV D impact is similar to that already observed on doped amorphous hydrocarbon layers, for which the CD_4-production yield at elevated temperatures is almost completely suppressed in contrast to the pure C layer.

Erosion measurements below room temperature (T between 77 and 300 K) were required to understand the origin of the reduction better. It was found that the presence of Ti in amorphous C layers under hydrogen impact enhances the hydrogen release. As a consequence, also the erosion at elevated temperatures is largely reduced. For the case of mixed Ti/C layers with 13 at% Ti, the activation energy for hydrogen release is reduced from 1.8 eV (for pure graphite) to 0.9 eV. At low temperatures Ti enrichment at the surface additionally reduces the erosion yield by one order of magnitude at ion fluences of ~10^{23} D/m^2.

1.3 Deep Depth Profiling of Deuterium in Tungsten using Nuclear Reaction Analysis

The nuclear reaction D(^{3}He,p)^{4}He is used to determine the depth profile and the total content of deuterium atoms in near-surface layers of solids. Analysis of the energy spectrum of the resulting α particles provides depth profiles of D for depths ≤1 μm. For this depth range, incident ^{3}He energies around 650 keV corresponding to the maximum of the reaction cross-section can be employed.

The resonance structure of the excitation function for the D(^{3}He,p)^{4}He nuclear reaction cross-section around this energy can also be applied to measure deuterium depth profiles at larger depths by determining the proton yield as a function of the incident energy. These measurements require precise cross-section data, especially at higher energies, while data are available only up to 2.5 MeV.

The energy range provided by the tandem accelerator allows measurement of the nuclear cross-section at ^{3}He energies in the range from 0.55 to 6.0 MeV (Figure 2). An a-C:D film ~55 nm thick deposited on a Si substrate and an Er film ~30 nm thick on a Cu substrate irradiated with 200 eV D ions were used as deuterium targets. Protons emitted from the D(^{3}He,p)^{4}He nuclear reaction were counted by means of a wide-angle surface barrier proton detector positioned at the laboratory scattering angle of 135°.

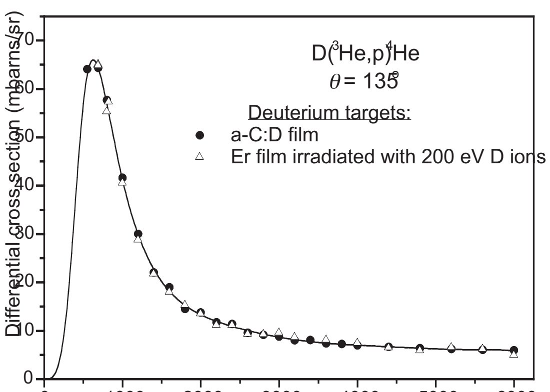

Figure 2: Cross-section of the D(3He,p)4He reaction measured up to 6 MeV

For investigation of hydrogen isotope retention and recycling in tungsten materials, the D(^{3}He,p)^{4}He reaction with variable primary energy is used for depth profiling of deuterium. By increasing the incident ^{3}He energy, the maximum in the cross-section is shifted to larger depths according to the energy loss of the ^{3}He ions in tungsten. A depth distribution $C_D(x)$ is assumed with allowance for the near-surface depth profile obtained from the α-particle spectrum varied by an iterative technique until the calculated proton yields match the proton yields measured experimentally. Depth profiles of D in W up to a depth of >10μm can be obtained with a sensitivity of <0.001 at %.

1.4 Be Diffusion in C

The formation of protective Be layers on C through deposition from a Be-seeded D plasma is governed by erosion, deposition and diffusion of Be in C. Diffusion data for Be in C is limited to tracer diffusion coefficients which cannot be applied to the diffusion of high Be concentrations in C. For concentrations above ~10% the concentration dependence of diffusion cannot be neglected.

The concentration-dependent diffusion coefficient of Be in C can be obtained from Be diffusion profiles in C by applying "Boltzmann-Matano" analysis (BM analysis). Samples consisting of a Be layer with a nominal thickness of several 10 nm on a C substrate were prepared. Two sets of samples were created, differing in the evaporation conditions, which resulted in different O impurity distributions at the Be-C interface. The samples were heated at constant temperatures in the range from 400 K to 1000 K.

For measuring accurate depth profiles in these samples a combination of different techniques was applied. RBS and NRA were used to measure quantitatively the total Be content in these samples. To obtain the depth distribution of Be XPS sputter depth profiles were measured. To apply a depth scale to these profiles, the scale was varied until the Be integrals of the measured profiles corresponded to the total amount of Be as measured by RBS/NRA. With these depth profiles, BM analysis yields the diffusion coefficients shown in Figure. 3 for an annealing temperature of 973 K.

The diffusion in Figure 3 seems to be enhanced by the O at the interface, On the basis of the measured diffusion coefficients it can be concluded that diffusion will only play a role in the formation of shielding Be layers on C for temperatures above 1000 K. No measurable diffusion was found below 973 K.

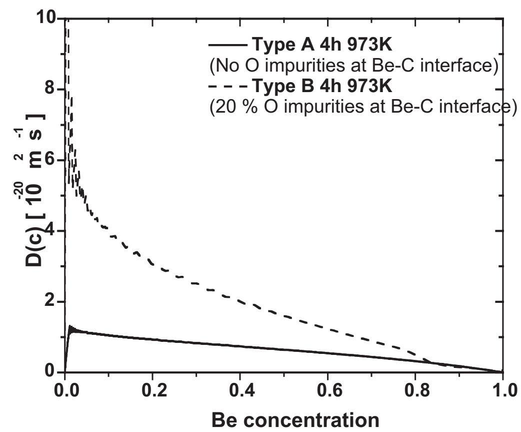

Figure 3: Diffusion coefficients of Be in C for different O impurity concentrations

1.5 Deuterium Retention in Beryllium

Deuterium retention in beryllium is of great importance for the operation of present and future fusion devices using Be as first-wall material. To understand hydrogen retention, experiments in well-defined laboratory experiments are necessary to identify the underlying physical and chemical processes. Retention of implanted deuterium ions in beryllium was investigated by means of accelerator-based nuclear-reaction analysis (NRA). The D(^{3}He,P)^{4}He nuclear reaction with 800 keV ^{3}He was used to measure protons at a scattering angle of 135° for quantification of the retained D. Deuterium was implanted at room temperature into cleaned single-crystal beryllium Be(0001) through D_3^+ ions at 3 keV corresponding to D implantation at 1 keV.

Incremental implantation steps up to a D fluence of 3.9 x10^{17} D/cm^2 were performed with implanted D being measured after each step. After an initial linear D retention yield of 4% of the implanted dose up to an implanted fluence of 5x10^{16} D/cm^2, saturation occurs at a fluence of 2.5x10^{17} D/cm^2 with a retention of 4x10^{15} D/cm^2.

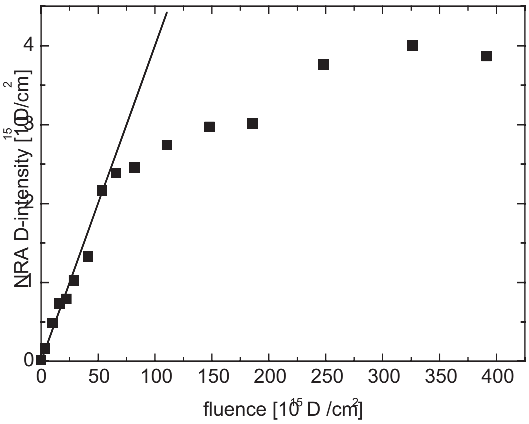

Figure 4: D retention in Be as function of fluence for 1 keV D+ irradiation

1.6 The Dual Beam Experiment

Simultaneous bombardment of metal surfaces by hydrogen isotopes and impurities, e.g. carbon, leads to synergistic effects with plasma-wall interaction properties significantly different to those of pure-hydrogen or pure-carbon bombardment. This process also leads to formation of mixed surface layers whose properties usually differ from the original wall material.

To study various synergistic effects, the dual-beam experiment has been designed and is currently being assembled. This setup consists of the Bombardino vacuum chamber, a Duoplasmatron ion beam system for simulating deuterium flux, a sputter ion beam system for simulating impurity flux and a MeV ion beam line for performing ion beam analysis (IBA). Detectors for the following methods will be installed: PIXE, proton counter for NRA, three RBS detectors at scattering angles of 165°, 135° and 105°.

Ion sources are capable of irradiating targets with fluxes up to 10^{19} m^{-2}s^{-1}. The Duoplasmatron ion source can produce argon and hydrogen ion beams with energies from 0.5 to 10 keV with an energy spread of 25 eV. The sputter ion source produces negative ions from a wide variety of materials. Relevant species for study of plasma-wall interactions are: H_, O_, C_, ^{28}Si_, ^{48}TiH$_3$_, ^{56}Fe_, ^{56}FeC_, ^{58}Ni_, ^{181}TaH_, TaC_, ^{186}W_, ^{184}WC_, etc. For both ion sources a mass-analysing magnet is used for separating the various ion species present in the beam.

2 Migration of Materials in Fusion Devices

2.1 Tungsten Migration in ASDEX Upgrade

In ASDEX Upgrade tungsten-coated graphite tiles are used as plasma-facing components in the main chamber and divertor baffle region. In the 2002/2003 campaign graphite tiles with metallic marker strips were installed at the upper and lower edges and near the midplane of the central column heat shield. Local tungsten redeposition at the inner column was measured by ion beam analysis of the graphite surface of these tiles. Comparing the campaign-integrated W deposition rate to the W erosion rates determined from spectroscopic measurements and post-campaign marker analysis, one finds that approximately 20% of the eroded tungsten is locally redeposited with transport lengths larger than the tile dimensions (≈20 cm). Previous measurements show that approximately 10% of eroded tungsten migrates to the divertor. Therefore, a fraction of two-thirds of eroded tungsten is missing at the surfaces analysed as yet. Two possibilities remain to resolve this observation. Eroded tungsten might be promptly re-deposited close to its origin with transport steps smaller than the typical tile dimensions. Alternatively, a significant fraction of eroded tungsten might be found at not yet analysed surfaces of the low-field-side guard limiters. This would, however, be in striking contrast to the direction of boundary plasma flows, which are generally found to be directed from the low-field towards the high-field side of the plasma.

2.2 Mechanism of Hydrocarbon Layer Formation in Remote Areas of ASDEX Upgrade

Deposition of hydrocarbon layers in remote areas of ASDEX Upgrade (below the divertor IIb roof baffle and in pump ducts) was studied with long-term samples from March – August 2001 and October 2001 – August 2002. The composition of deposited layers and their optical properties were analysed with ion beam techniques and ellipsometry. All deposits form soft hydrocarbon layers consisting mainly of deuterium and carbon with D/C ranging from 0.7 to 1.4. The thickest deposits with a maximum thickness of about 1.3 µm were observed in the inner divertor leg just opposite the inner strike point module. The thickness of deposited layers strongly decreased by about two orders of magnitude with increasing distance from the strike points. About 0.3% of the total deuterium input is trapped below the dome baffle and only about 0.008% in layers deposited in the pump ducts. The layer deposition pattern suggests the following model for hydrocarbon layer formation:

1. Carbon is eroded in the main plasma chamber, transported in the plasma and re-deposited on divertor tiles.
2. Redeposited layers are partly re-eroded by chemical sputtering, and eroded carbon atoms and hydrocarbon radicals are mainly re-deposited in line of sight of the plasma strike points. A small fraction is able to survive more than one wall collision, resulting in some deposition in areas not in the direct line of sight. A very small fraction is able to survive hundreds of wall collisions, resulting in a small deposition in remote areas such as pump ducts.

3 Tritium Inventory – Understanding and Control

3.1 Tritium Inventory in ASDEX Upgrade

Hydrogen isotope inventories in ASDEX Upgrade were measured in the main chamber by analysis of long-term samples retrieved from the vessel after the 2002/2003 experimental campaign. Retained D was quantified by NRA at the accelerator laboratory of IPP. In addition, the implanted tritium isotope originating from D-D reactions in the plasma discharge was quantified by accelerator mass spectroscopy at the Technical University of Munich. The levels of both implanted deuterium and tritium are found to show strong toroidal asymmetries. These asymmetries can be ascribed to local zones of increased charge exchange reactions due to the neutral particle halo along the path of the neutral beam injection. Since this halo extends to the central region of the plasma discharge, the neutral tritons produced in charge exchange reactions with the halo neutrals are not yet thermalised in part and are therefore implanted deeper than hydrogen ions escaping the cooler edge plasma either as ions or charge exchange neutrals. The amount of T implanted beyond the thermal ion range in the samples as a function of the toroidal position illustrates the strong correlation to the location of the neutral beam injectors.

3.2 Chemical Sputtering of Carbon

One of the issues in plasma-wall interaction most critical for a next-step device such as ITER is tritium retention and tritium co-deposition with eroded carbon. The erosion process leading to production of volatile hydrocarbon species through interaction of the plasma species with carbon surfaces was investigated in the MAJESTIX particle-beam experiment. The most important plasma species in this context are energetic particles (ions and neutrals) and thermal hydrogen atoms.

On the basis of experimental results of the erosion of amorphous hydrogenated carbon (a–C:H) films due to combined Ar^+ ion and thermal atomic hydrogen atom impact a model was devised to describe the ion energy and ion species dependence of chemical sputtering in the presence of atomic hydrogen. The agreement between model and data is excellent. Model results for some ion species of particular relevance to fusion plasmas (H^+, D^+, T^+, He^+) that are incident simultaneously with a 100 times higher flux of thermal H^o atoms are shown in Figure 5.

With increasing mass of the projectile, the chemical sputtering yield in relation to the incident ions increases. The differences of the yields for H, D, and T are due to the mass dependent energy transfer to carbon atoms. The significant increase of the yield between T and He is due to the dependence of the nuclear scattering cross-section on the nuclear charge Z. The model for chemical sputtering is to be further tested in the near future by comparison with experimental data using other ion species.

3.3 Hydrogen Permeation and Diffusion Barriers

Control of the radioactive tritium inventory in a fusion reactor requires knowledge of hydrogen isotope diffusion coefficients and solubilities in relevant materials as well as

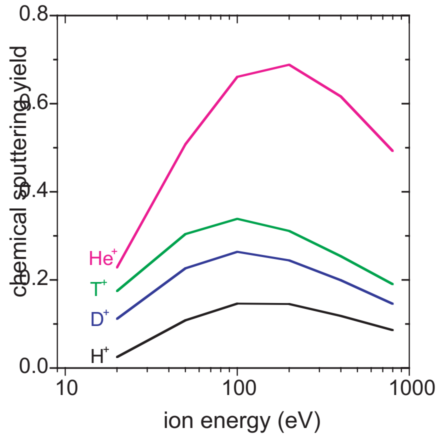

Figure 5: Calculated chemical sputtering yields at 300 K for H^+, D^+, T^+, and He^+

active measures to reduce excessive tritium permeation. In the Materials Research Division the deposition of ceramic Al_2O_3 coatings has already been investigated with respect to their crystal structure for several years. A filtered vacuum arc facility was employed for this purpose.

With this device the deposition of crystallised α-Al_2O_3 was achieved at temperatures well below 700° C. In parallel to this, a setup for direct measurement of gas-driven hydrogen isotope permeation through thin foils has been operated.

By combining both activities, substantial progress concerning hydrogen permeation barriers on a fusion-relevant structural material was achieved: With the vacuum arc facility an α-Al_2O_3 coating was deposited onto a thin foil of the EUROFER low-activation structural material. By subsequently making deuterium permeation measurements on such coated and on uncoated EUROFER foils, it was demonstrated that these coatings reduce the deuterium permeability of the foils by more than three orders of magnitude at a coating thickness of only one μm (Figure 6).

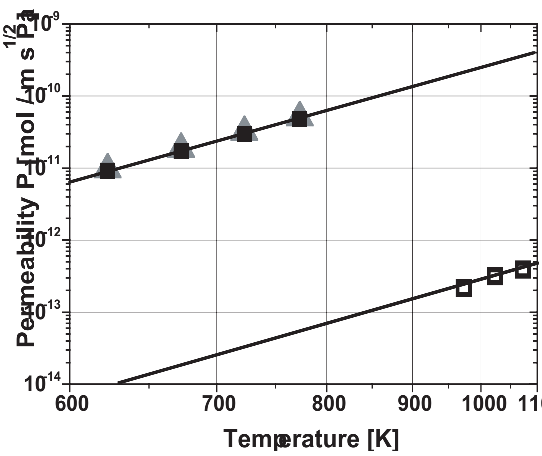

Figure 6: Deuterium permeability as a function of temperature for uncoated EUROFER (solid symbols) and EUROFER coated with 1µm of Al_2O_3 (blank symbols)

3.4 Hydrogen permeation through metals by ion bombardment

Energetic hydrogen ions and atoms are able to penetrate the surface barrier of metals. After slowing down in the material they start to diffuse through the metal lattice. This ion-driven permeation can exceed gas-driven permeation (from the gas phase) by several orders of magnitude. In order to investigate ion-driven permeation of deuterium through candidate first-wall materials, a new experimental set-up was designed and assembled at the Garching high-current ion source. It allows us to measure the flux permeating through thin metal foils (typical thickness in the range 10 – 100 µm) at temperatures between room temperature and 600° C and ion energies from 30 – 3000 eV. The diffusion coefficient, intrinsic hydrogen trap density, and surface recombination coefficient can be determined.

4 Materials – Processing and Characterisation

4.1 W-Si as Plasma-facing Material for Fusion Reactors

Tungsten-silicon compounds (W-Si) may provide a major safety advantage in comparison with pure tungsten (W) in future fusion power reactors.

A potential problem with the use of pure W is the formation of radioactive and highly volatile WO_3 compounds under accidental conditions. A loss-of-coolant event (LOCA) in a He-cooled reactor would lead to a temperature rise to 1100° C due to the nuclear decay heat of the W components. In such a situation additional accidental air ingress into the reactor vessel would lead to strong endothermic formation and subsequent evaporation of WO_3 molecules.

A sub-stoichiometric $WSi_{0.45}$ compound was found to form under air above 600° C a protective SiO_2 film at the surface which seals the reactive W from further air contact and oxidation. In experiments $WSi_{0.45}$ and pure-W films of 1 - 2 µm thickness were sputter-deposited on Inconel substrates. Afterwards these films were subjected to oxidation in synthetic air and the oxidation rates were determined by thermobalance measurements. The oxidation rates of W and $WSi_{0.45}$ are similar at 600° C, but $WSi_{0.45}$ oxidation is two orders of magnitude lower at higher temperatures due to self-passivation. The use of this material would eliminate the above-mentioned concern relating to pure W.

4.2 Metal Matrix Composites

The development of new heat sink materials with high thermal conductivity and sufficient strength under service loading is decisive for the efficiency of future fusion reactors. In the case of the divertor, the maximum allowable working temperature of the currently utilised copper alloy is 350° C under neutron irradiation. To increase efficiency, it is necessary to develop heat sink materials for operation temperatures up to 550° C. Metal matrix composites with a copper matrix for thermal conductivity reinforced with silicon carbide long fibres (SCS6, Textron) for strength were investigated. SiC fibres were electrolytically coated with a 100 µm thick copper layer and hot isostatically pressed in a copper capsule. Push-out tests were applied to investigate the bonding between the fibres and matrix. Single fibres were pushed out of composite specimens with thicknesses between 2 mm and 4 mm by a micro indenter The calculated interfacial shear strength was about 6 MPa. To increase the shear strength, a 100 nm thin titanium interlayer was deposited on the SiC fibres by magnetron sputtering. After electrolytic deposition of matrix copper, heat treatment with very slow rates was applied to form TiC with the carbon surface of the SiC fibres. TiC was verified by ELNES (Energy Loss Near Edge Structure) at MPI of Microstructure Physics. The interfacial shear strength was determined by push-out tests, to be about 60 MPa (10 times higher than without titanium interlayer). The bonding was stronger than the adhesion between SiC and the surface carbon layer of the fibre.

4.3 Low-Z Coatings for the first wall protection of WENDELSTEIN 7-X

In addition to carbon materials on components subjected to high heat flux, 300-500 μm thick vacuum plasma spraying (VPS) of boron carbide (B_4C) is being developed and evaluated as coatings on large actively cooled stainless-steel panels. In order to examine behaviour relevant to the expected plasma-wall interactions and thermomechanical loads, an extensive material characterisation and test programme was executed from 1999 and completed in 2003. The final thermal cycling test of a B_4C-coated full-scale mock-up (laser welded and embossed) was performed at a heat load of 200 kW/m_ and 1,221 cycles in the FIWATKA facility at Forschungszentrum Karlsruhe. The microscopic inspection of the tested prototype showed no cracks or separation of layers.

As result, a coating system with a thickness of 300-500 μm B_4C and an additional stainless-steel interlayer ensures reliable adhesion, erosion resistance and acceptable dielectric properties at 140 GHz. The spraying parameters chosen resulted in homogeneous B_4C layers which are completely bonded to the substrate (Figure 7).

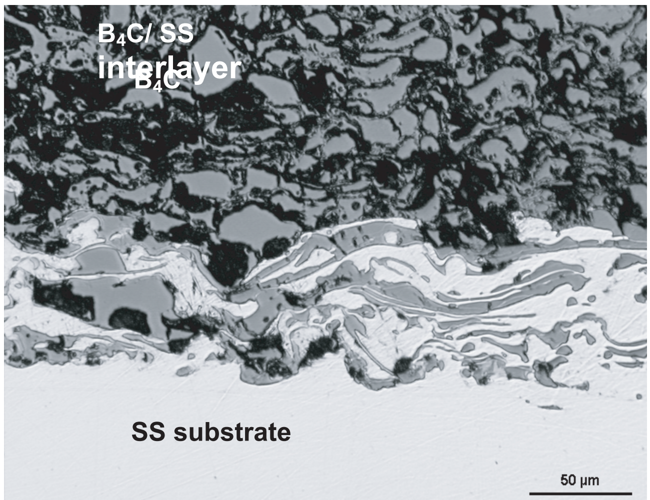

Figure 7: Interface structure of B_4C on stainless-steel

4.4 Plasma-sprayed Tungsten Coatings on Stainless-steel Substrates

Tungsten is a potential candidate as first-wall material for ITER and DEMO to avoid excessive erosion. The expected heat load on these components is in the range of 0.5 to 1 MW/m_. The vacuum plasma spraying (VPS) of W on plasma-facing components offers effective industrial coating of large and complexly shaped components. In collaboration with an industrial partner, Plansee AG (Austria), VPS of W was developed and deposited on stainless-steel 316L and low-activation-steel (EUROFER; F82 H) substrates. Deposition was done on actively cooled substrates (190 mm x 60 mm) with mixed steel/W interlayers to reduce the residual stresses and increase the thickness of the W coating to 2-3 mm. Characterisation of W coatings has been started with regard to their structure and in terms of their fusion-relevant properties (composition and impurities, thermal conductivity, adhesion on the substrate, thermomechanical behaviour). The specimens were prepared for heat flux testing up to 2.5 MW/m_.

5 Component Behaviour

5.1 Micro- and Macroscopic Composite Mechanics

The motivation for developing fibrous metal matrix composite (FMMC) is to locally strengthen the most highly stressed part of a plasma-facing component (PFC). The stresses are generated owing to the misfit in thermal expansion and temperature gradient. In this subproject, a design feasibility study was conducted for a FMMC-reinforced PFC. Dual-scale finite-element analysis (DS-FEA) was conducted.

In the DS-FEA technique, the stress/strain are computed simultaneously on macro and micro scales. Focus was placed on the evolution of local damage in individual microscopic phases under thermal cycling. To this end, an incremental nonlinear micromechanics algorithm was implemented into a commercial finite-element code.

An actively cooled PFC model consisting of W armour/ FMMC interlayer/Cu heat sink was considered. FMMC was assumed to be a long SiC fibre-reinforced copper matrix composite laminate (3 mm thick). ITER-relevant divertor geometry and thermal load (15 MW/m_) were considered for simulation.

Results are as follows: The FMMC interlayer caused only a slight reduction of heat removal capability of the PFC (5 % increase of the surface temperature). The thermal stresses on micro as well as macro scales were significantly alleviated during the heat loading. The sign of the matrix stress was reversed from tensile to compressive on heating. This indicates a possibility of low cycle fatigue. The maximum fibre stress was in the safe state (50 % of the mean fracture strength). Ductile damage in the matrix was restricted to sufficiently low level during the whole load cycle (20 % of the critical damage for crack initiation). This behaviour was attributed to the compressive hydrostatic stress state in the matrix, which suppresses the growth and coalescence of micro-voids. The damage characteristics suggest engineering applicability of the FMMC-PFC concept.

5.2 IPP High-heat-flux Test Facility

Investigation of the thermomechanical behaviour of highly loaded divertor components requires extensive tests with fusion-relevant thermal loads. The ongoing industrial manufacture of the nearly 900 W7-X target elements, calls for effective and realistic heat load tests of complete modules of target elements with outer dimensions of up to 0.6×0.8 m_ to guarantee the required quality and reliable operation as target plates.

In 2003, the activities were concentrated on the construction of the main components of the high-heat-flux test facility. The turbomolecular pumping system with a pumping speed of 8000 l/s H_2, the water-cooled test chamber, the Siemens Simatic S7 operating control system, the diagnostic instrumentation including an infrared camera with high spatial resolution for transient surface temperature measurements, were successfully procured, and assembly of the facility started on time.

Table 1 summarises the technical characteristics of the test facility. The current design includes the possibility of future operation with two individually controlled ion beams.

Max. power of the beam [kW]	1100, (2200)
Max. voltage of the beam [kV]	55
Max. current of the beam [A]	20
Heat flux density, beam centre [MW/m_]	5 - 55
Heated length of component [mm]	200 – 700
Max. length of component [mm]	2000
Component layout	horiz./vert.
Beam spot [∅ mm]	≥ 70
Pulse duration	1 ms to 15 s, (30) s
Max. cooling water temp. [°C]	in: 80, (150)
Max. water pressure [bar]	25, (45)
Max. water flow rate [l/s]	8.5, (> 9)

Table 1:Technical characteristics of the IPP high-heat-flux test facility. Brackets mark values of potential upgrading

Staff

V. Alimov, M. Balden, A. Beikler, M. Ben Hamdane, I. Bizyukov, A. Brendel, R. Brill, B. Böswirth, B. Cieciwa, J. Chen, J. Dorner, W. Eckstein, K. Ertl, M. Fußeder, K. Gehringer, A. Golubeva, H. Greuner, T. Höschen, R. Hoffmann, W. Hohlenburger, A. Holzer, Ch. Hopf, E. Huber, W. Jacob, E. de Juan Pardo, B.Y. Kim, J. Kißlinger, K. Klages, F. Koch, T. Köck, K. Krieger, R. Lang, A. Leinthaler, D. Levchuk, S. Levchuk, S. Lindig, Ch. Linsmeier, H. Maier, K. Marx, G. Matern, P. Matern, M. Mayer, M. Meier, M.A. Miskiewicz, L. Morlaine, I. Quintana Alonso, B. Plöckl, C. Popescu, M. Roppelt, J. Roth, F. Sardei, J. Schäftner, K. Schmid, T. Schwarz-Selinger, M.M. Spychalski, R. Straßer, A. Weghorn, A. Wiltner, M. Ye, J.-H. You

Contributors: W. Bohmeyer, J. Boscary, A. Geier, M. Laux, R. Neu, H. Renner, V. Rohde, S. Schweizer

Theoretical Plasma Physics

Head of Project: Prof. Dr. Sibylle Günter

Tokamakphysics

The role of theory and modelling in magnetic confinement research has substantially changed during the last decade. Up to that time only some areas were amenable to first –principle based approaches (like equilibrium calculations, linear MHD stability, wave physics, purely collisional slowing down of fast particles, neoclassical transport) whereas empirical or semi-empirical approaches had to be used to interpret and extrapolate the turbulent energy and particle transport dominating in most experiments. The development of new theoretical plasma models (gyrokinetic and gyrofluid), the advent of powerful, highly parallel computer systems, and the development of algorithms adapted to these configuration has made the ab-initio solution of the basic equations and the direct modelling of turbulent transport in realistic plasma configurations a credible vision. At the same time, also the simulation of large-scale events is now carried deeply into the non-linear stage, where even calculations starting from strictly axisymmetric tokamak geometry become truly 3-d. The differences between model developments in tokamak and stellarator configurations are therefore expected to fade progressively in the near future. To exploit the unique situation of our institute as a centre both of tokamak and stellarator research, and to utilise to the fullest the possible synergies, the first-principle based model developments within the institute have been united into a project ”Theoretical Plasma Physics”. It combines the corresponding efforts of the Tokamak Physics and the Stellarator Theory Divisions and of the Nachwuchsgruppe ”Computational Studies of Turbulence in Magnetised Plasmas”, and is headed, on a yearly rotating basis, by one theoretician on the board of scientific directors of the institute.

1 Tokamak Physics Division

Heads: Prof. Dr. S. Günter, Prof. Dr. K. Lackner

1.1 Tokamak Edge Physics Group

The efforts to understand the physics in the edge region of the plasma centre around the continuous improvement, extension and application of a large code package SOLPS - incorporating models for all phenomena happening in those plasma regions which have a strong interaction with the walls. In a divertor tokamak the latter encompass the open flux surfaces intersecting the target plates, plus a region of closed flux surfaces which is less clearly defined, but has to comprise at least the layers into which neutral particles can penetrate in significant measure. Central element is a 2-d (axisymmetric) multispecies fluid model of a collisional plasma supplemented by terms describing suitably averaged turbulent transport of particles, momentum and energy. It includes all important ionisation stage of impurities. Neutral particle dynamics is treated by either a Monte-Carlo or a fluid approach, and continuously improving models are used to take into account the surface processes leading to recycling of the main plasma species and the release of impurities. The SOLPS code package has been developed and is used in the frame of an international collaboration, pivoting around the edge physics group in Garching, and comprising, at present, in particular also Prof. Rozhansky's group in St Petersburg, Dr Ralf Schneider's group in IPP-Greifswald and Dr Bonnin in CEA-Cadarache.

Development and applications of the SOLPS edge physics code package

Support of the SOLPS package for groups around the world (including Japan, China, Russia, the USA) as well as within Europe have continued, with increasing contributions to supporting the use of the code within the EFDA-JET framework. Some of the essential activities under this heading are listed below.

Analysis of a new series of AUG shots with the interpretative version of the SOLPS5.0-B2 code, B2.5-I, has started. In preparation to fitting to the full database, a small subset has been examined to optimise the fitting process. Possibilities examined have included fitting to the raw data, fitting to data derived from a *tanh*-fit of the experimental data, fitting of one (constant) transport coefficient for density and temperature, the use of a ”three region model”, and fitting to the pedestal region only versus fitting of the whole profile. An example is shown in the figure below. The same process has also been tested on a JET shot.

In collaboration with the TOK Core Transport Group, the option of using neo-classical transport coefficients has been implemented in B2.

As part of EFDA JET activities, benchmarking comparisons of SOLPS5.0 (B2-Eirene) and EDGE2D-NIMBUS were started. Initial large differences in the results were tracked down to differing assumptions about parallel electron and ion heat flux limits in the two codes packages. When the same assumptions were used in both codes, the remaining differences were significantly smaller. The effort of identifying the causes of the remaining differences is ongoing, as well as the effort to extend the comparisons to cases with drifts.

The SOLPS package has two models for treating neutrals, a fluid neutral model built into B2.5, and the Monte-Carlo model provided by Eirene. The fluid neutral model is less exact but faster, while the Monte-Carlo model is more exact but slower and also introduces statistical noise. For a particular ASDEX Upgrade scenario, the two models have been compared, and the neutral fluid model has been tuned to provide a better match to the Eirene model. In addition, the effects of transport ballooning, parallel heat flux limits and drifts were examined.

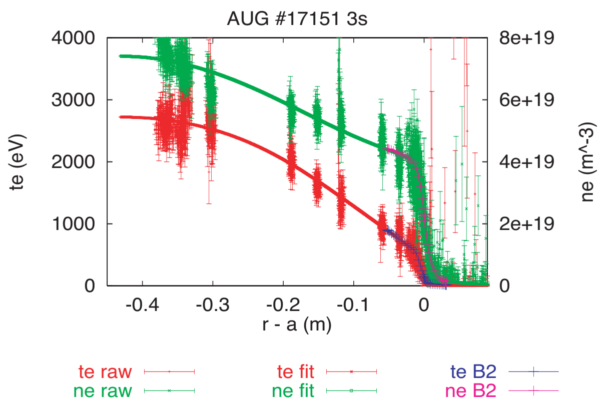

Figure 1: Use of the B2 code in an interpretative mode to fit experimental electron density and temperature profiles. The procedure used in this case is to match a mtanh fit to the experimental data.

SOL turbulence
(in collaboration with the TOK Turbulence Group). The purpose of this work is to compute turbulence in the scrape-off layer (SOL) region of a tokamak plasma using flux tube codes, such as DALF or *GEM* . In this region, the magnetic field lines are open and strongly deformed due to the proximity of the separatrix, as opposed to the closed field lines region. Using similar methods to those behind the construction of the globally consistent flux tube formulation in the referred codes, a flux tube (modified) Hamada coordinate system was constructed, and then calculated for the SOL region of the tokamak ASDEX Upgrade. From this calculation the geometrical information needed for the turbulence codes was obtained. Variations in the perpendicular metric require a model which can treat dynamics down to and below the scale of the ion gyro radius. Consequently, the focus has shifted to the GEM (gyrofluid) code. Since the field lines now end on the divertor plates, the parallel boundary conditions also change, respective to those on closed field lines. A simple model, using Debye sheath physics, was used to yield the particle and energy fluxes to the divertor which provide those conditions. More realistic models for the parallel boundary conditions, namely to include phenomena like neutrals recycling or electron secondary emission are planned.

1.2 MHD Theory Group

During the last decade, the scope of studies of large-scale MHD modes has significantly broadened and shifted away from the original exclusive focus on instabilities defining upper, insurmountable limits to the parameters achievable in toroidal confinement devices. Wider classes of macroscopic instabilities has been found to exist, which are driven either by the spatial distribution of fast particles or by neoclassical transport effects, and are not necessarily catastrophic, but lead to important reductions in heating efficiency or energy confinement. Being of slower growth rate, they sometimes are amenable also to external intervention and feedback control, like the so-called neoclassical tearing modes (NTM). At the same time the inclusion of realistic boundary conditions and finite plasma rotation into the theory has opened up a parameter regime for potential operation, where ideal MHD modes are slowed down in their growth rate to the decay rate of currents induced in structures surrounding the plasma, again making them controllable by feedback systems. The investigations of the MHD theory group have participated in these developments, developing tools for practical performance enhancement, and identifying in this process also analogies and links to other areas of non-linear physics.

Fast-particle-driven instabilities and Gyrokinetic MHD.
This year the principal development phase of a new linear gyrokinetic stability code (LIGKA) was finished and first results were obtained. LIGKA allows to calculate the growth- and damping-rates of fast-particle-driven kinetic MHD modes in a non-perturbative and self-consistent way. Benchmarks with other kinetic codes were started: on the one hand, good agreement of LIGKA with CAS3D-K (in collaboration with A. Koenies) in the drift kinetic limit with zero banana-orbit-width was found. On the other hand, also gyrokinetic results (KIN2DEM, by H. Qin) in circular concentric geometry were reproduced. Furthermore, LIGKA's accurate treatment of particle-trajectories (HAGIS, collaboration with S.D. Pinches) showed that broad banana orbits can reduce the growth rates of TAE-modes driven unstable by a hot ion population.

Resistive Wall Modes and Error Field Amplification
To prepare a possible modification of the ASDEX Upgrade in-vessel structures to accommodate a resistive wall, existing stability codes have been extended to allow for more realistic wall structures.
The vacuum part of the 3D CAS3D MHD stability code has been generalised by replacing the perfectly conducting wall by a resistive wall (in the thin shell approximation) allowing studies of resistive wall modes. Using this code version, low-n modes of ASDEX Upgrade type equilibria have been studied for realistic wall structures, including, e.g. the effect of vessel ports.
In the advanced tokamak scenarios, plasma performance is strongly limited by the external kink mode. This mode can be stabilised by conducting walls and plasma rotation. But, at the same time, error fields (for instance asymmetric perturbations produced by the magnetic coils) can strongly amplify the mode and stop the plasma rotation. The problem is equivalent to the acceleration of the plasma via externally applied rotating fields. The torque due to the error fields can then be calculated directly from the power absorbed by the plasma. We use the linear MHD CASTOR-FLOW code to calculate the power absorption and to investigate the error field amplification. For this purpose, an antenna has been implemented into the CASTOR-FLOW code (integration of the CASTOR-ANTENNA code), which also includes plasma rotation, viscosity and a resistive wall. First calculations show a very good agreement with the existing analytical theory (simple one mode approximation). Further, the computations show that several

resonant surfaces, the plasma geometry, viscosity and a resistive wall strongly influence the results.

Linear and Non-linear Tearing Modes

The stabilisation of NTMs by ECCD has been studied numerically, focusing on the small island case (the wave deposition width is larger than the island width). It is shown that in this case the modulated ECCD has a larger stabilising effect than the non-modulated one. In addition, the slowing-down time of the fast electrons and the initial island width when applying the wave are also found to be important in determining the stabilising effect.

An essential element of progress in these studies was the development of an algorithm for the solution of the heat conduction equation in complex magnetic fields, which allows for an effective separation of parallel and perpendicular heat transport without the need to introduce field-aligned coordinates.

We also investigated the linear stability of drift tearing modes based on two-fluid equations. It was found that, in addition to the electron diamagnetic drift, the electron perpendicular heat conductivity is also very important in determining the mode stability. A new type of unstable mode destabilised by the electron temperature gradient is found in a certain range of electron diamagnetic drift frequency, providing a possible explanation for some experimental observations of spontaneous growing NTMs.

Interpretation of Complex MHD Instabilities

Techniques are readily available for interpreting the diagnostic signature of simple MHD instabilities. Frequently, however, more complex structures are observed. We have developed an MHD interpretation code (MHD-IC), which combines different available diagnostic information to identify, with high radial resolution, the structure of such complex (composite) MHD modes. As a sample application, it was possible to establish the "ideal" character of a (2,2) kink mode, coupled to a (3,2) tearing mode on ASDEX Upgrade. Even advanced, previously existing plasma tomography algorithms had only been able to identify the fact of mode coupling and the location of the modes, whereas the present code can even resolve the parity of the perturbation at the resonant surfaces and hence decide on its ideal or resistive nature.

1.3 Transport Analysis Group

This group is responsible for linking the experimental observations on tokamaks to existing theoretical models. This proceeds by a variety of means: the development of transport codes (ASTRA), the statistical analysis of confinement data banks, and the comparison between observed plasma profiles and the predictions of linear stability criteria for micro-instabilities and semi-analytical models of turbulent transport. The group has, however, also significant competence in kinetic theory and its advanced tools (e.g. collisional Monte Carlo methods), which have recently been used mainly to extend neoclassical theory into regimes where its ordering assumptions (poloidal orbit width small compared to gradient lengths) do not hold. Situations of the latter type have gained significant importance in recent times, with the advent of "advanced" tokamak scenarios (with very small poloidal fields in the centre) and the interest in the onset conditions for neoclassical tearing modes, which can require expressions for the bootstrap current in the small island limit.

This year the analysis of the observed anomalous tokamak transport has concentrated mainly on the electron density pump out phenomenon. This work is described under the ASDEX Upgrade section. Below three topics (bootstrap current in current holes, the polarisation current around moving island structures and the gyro-kinetic stability of Trapped Electron Modes (*TEM*)) of the work on theory development are discussed in more detail.

Finite poloidal orbit effects on neoclassical phenomena

Recently the observation of tokamak discharges with very small or zero poloidal magnetic field in the vicinity of the axis was reported. In such magnetic field configurations large particle orbits exist in the central plasma and the validity of the standard neoclassical theory is questionable. Therefore guiding centre calculations of the bootstrap current were performed. The guiding centre code *PGCC* was augmented and thus turned into a δf- code similar to the code *HAGIS*, but with the toroidal flux as the radial coordinate. The calculation is done in two steps. First the distribution function of the ions is determined taking into account ion-ion collisions. Then the calculation for the electrons is made with electron-electron and electron-ion collisions; for the latter the ion distribution is approximated by a shifted Maxwellian. We find that inside the current hole the bootstrap current does not vanish, although the density and temperature profiles are flat. The particle orbits connect the current hole with the region with strong gradients of density and temperature. Particles on these orbits also "feel" the gradients outside the current hole.

The radial polarisation current due to the time-varying electric field associated with a magnetic island moving with respect to the bulk plasma decreases linearly with the island width W when the island width is comparable with the ion banana width w_b, as shown by Monte Carlo δf-calculations. This reduces its role in determining the threshold for the Neoclassical Tearing Mode (*NTM*) as described by the generalised Rutherford equation, where the polarisation current itself is independent of W. The steepness of this linear drop increases with increasing plasma temperature and island rotation frequency ω. According to the existing analytic theory, the polarisation current should be proportional to ω^2 if the pressure is flat, i.e. it should have only two coincident zeros corresponding to a non-rotating mode, ω=0. Numerical simulations show in contrast four distinct zeros. These zeros occur when the mode frequency approaches some typical frequencies associated with the motion of the plasma ions, like the toroidal precession frequency of the trapped particles, the (inverse of) the time needed by a passing particle to orbit the island, the bounce time. At least two zeros are found to lie in the frequency range predicted for the experiments (around the electron or ion diamagnetic frequency), i.e. they could play a role in the *NTM* evolution.

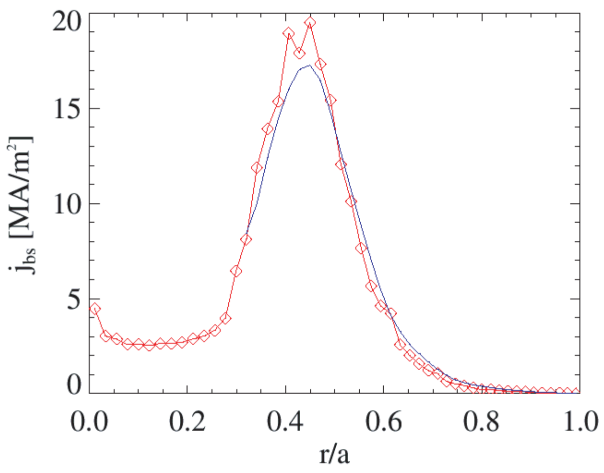

Figure 2: Bootstrap current as a function of normalised radius for standard neoclassical theory (blue) and δf calculations (red)

Analysis of micro instabilities for ASDEX Upgrade discharge parameters.
A large number of linear gyro-kinetic (*GS2*) stability runs have been performed for ASDEX Upgrade relevant parameters to have more insight in electron heat transport. It has been found that under experimental conditions the threshold of the mode is significantly affected by the density gradient, magnetic shear and collisionality. Also the competition between *ITG* and *TEM* can play a role. With increased collisionality the dominant mode changes from *TEM* to *ITG*, which should lead to a significant change in behaviour in the experiments. Including collisionality one can obtain a perfect match of the scaled linear growth rate and heat conduction coefficients obtained from the experiment.

1.4 Wave Physics Group

The core of the activities of the Wave Physics group is devoted to the realistic simulation of radiofrequency heating of toroidal plasmas, by the development of an appropriate suite of codes. The central tool is the full-wave code TORIC, which solves Maxwell equations in toroidal axisymmetric plasmas in the ion cyclotron range of frequencies. TORIC is routinely used not only at IPP, but in several other laboratories in Europe, USA, and elsewhere.It has been coupled to Fokker-Planck solvers for the determination of the distribution function of the heated particles and of the efficiency of radio frequency current drive. In collaboration with Princeton, efforts are underway to include TORIC in the global tokamak simulation package TRANSP. An extension of the functionality of TORIC to cover the Lower Hybrid frequency domain is also pursued in collaboration with the MIT group. Attention has also been given to wave launching problems: the FELICE code uses a variational principle to evaluate the input and radiation characteristics of metallic antennas, and the GRILL code evaluates the launching properties of waveguide arrays.

Modelling of heating and current drive with waves in the ICR frequency range
Several extensions have been made to the full-wave code TORIC, modelling heating and current drive in realistic tokamak geometry: (1) inclusion of large ion Larmor radius effects and absorption at higher ion cyclotron harmonics, with application to Fast Wave heating experiments on the high-β plasmas of spherical tokamaks, (2) coupling to a Fokker-Planck code for the self consistent development of the electron distribution function during fast-wave current drive (3) (in collaboration with Princeton)production of an interface to MHD equilibrium files, in view of coupling TORIC with the TRANSP code for global simulations of tokamak discharges. The applicability of quasilinear theory for the evaluation of radio-frequency current drive in the ion cyclotron frequency range in tokamaks has been investigated in details, taking into account Hamiltonian and collisional stochasticity, and the effects of toroidal geometry.

Plasma equilibrium and stability
Wall Mode Control and Monodromy: Floquet stability of systems of differential equations with piecewise constant periodic coefficients has been studied. In the two-step case the monodromy is the product of two matrix exponentials, which are evaluated either, exactly, using Cayley-Hamilton theorem or, approximately, with the help of Baker-Campbell-Hausdorff formula. The two methods have been applied to a crude model of the "resistive wall mode" with encouraging results. The equilibrium momentum equation for MHD flows and Ohm's law with anisotropic resistivity tensor have been solved simultaneously for velocities parallel to the magnetic field. Axisymmetric solutions inherently free of Pfirsch-Schlüter diffusion can be found if the resistivities are properly chosen. Though such profiles are roughly similar to collisional resistivities profiles and satisfy $\eta_{\perp}>\eta_{//}$, strictly constant resistivities on flux surfaces are not compatible with these solutions.

Drift-kinetic and gyrokinetic theories
Expressions for the electric charge and current densities, including polarisation and magnetisation contributions, have been derived from a Lagrangian for the combined system of Maxwell and general kinetic equations within the framework of gyrokinetic theories. These expressions reduce in the appropriate limit to those obtained previously for drift-kinetic theories.
Gauge-invariant expressions for the variation of the kinetic contribution to the Lagrange density are obtained by a new method. These expressions are then used together with the contribution from the Maxwell fields to obtain the symmetric energy-momentum tensor.

Difference schemes for quasilinear evolution problems
Several efficient integration methods for ordinary initial value problems were considered. They lead to variable-coefficient schemes and/or to exact schemes (functional fitting; principle of coherence, collocation). Conditions for obtaining coefficients independent of time were found. Dependence on the time-step, however, seems to be practically unavoidable. Some of the discussed schemes can be extended to efficient difference schemes for parabolic equations with explosive solutions.

1.5 Turbulence Theory Group

The anomalous transport, which usually dominates the energy and particle confinement in tokamaks and stellarators, is generally believed to be caused by low frequency fluid like drift turbulence. The quantitative understanding of these phenomena is expected to come from computational studies based on the direct solutions of the basic equations, resolving both the macroscopic and the relevant microscopic time and space scales. Within the turbulence theory group we employ both fluid models extended to capture important kinetic effects (Landau damping, finite gyro radius), and kinetic models intended to treat all phenomena at the scales of interest (1 mm to 10 cm, 10 kHz to 1 MHz). The latter models are called gyrokinetic. Both fluid and gyrokinetic models have been recast within the past year for greater accuracy within a wider set of parameter regimes.

GEM -- Gyrofluid Electromagnetic Model.
We have recast the gyrofluid model to attain exact conservation of fluctuation free energy (related to entropy) in the local limit. Exploratory studies show this to have solved some of the problems of the gyrofluid model in the past (see below). Its main application currently is the study of transport of a minority ion species by a bath of existing ion temperature gradient (ITG) or drift (Alfvén) wave turbulence. All species are treated with full finite gyro radius (FLR) effects, and the background is considered inseparable from the turbulence within the dependent variable set. The code finds the meridional flows and currents associated with the equilibrium in the Pfirsch-Schlüter and plateau collisionality regimes. The third species is treated self consistently; all regimes of temperature, mass, and relative composition are accessible. Transport properties of minority hot ions, trace tritium, and edge impurities are to be treated.

Zonal Flows in Edge and Core Parameter Regimes.
In core turbulence parameter regimes, the GEM code is able to reproduce the non-linear threshold upshift caused by zonal flows. As in the kinetic models in the Cyclone study in the USA (an effort made in 1997-2000 to benchmark different turbulence modelling codes, based on a particularly well-diagnosed DIII-D discharge), essentially all of the energy in linear ITG instabilities is transferred conservatively to zonal flows, with the end result a total suppression of small scale activity within about 20 percent of the linear threshold in the parameter R/L_T, the major radius/temperature scale length ratio. Further away from threshold, the turbulence remains strong. A control test showed that geodesic curvature is the main mechanism by which the flow amplitude is kept at moderate levels, regulating but not suppressing the turbulence.

The Collisionless Kinetic Alfvén Problem.
The kinetic Alfvén kernel of our gyrokinetic code GENE has been recast to capture the global Alfvén mode which in a torus is part of any electromagnetic system in a pressure gradient. This component, artificially suppressed by most models, is important in the overall energetic balance of zonal flows, since kinetic Alfvén waves are coupled to electron pressure disturbances at all scales. Ultimately, a numerical scheme must be found which remains stable at moderate to high beta and at large scale, in other words the deep MHD regime. Up to now this difficulty prevents computations from using the complete gyrokinetic model rather than its common δf limit, which dissimilar to the local limit in fluid models. Complete solution of this problem is a prerequisite for gyrokinetic codes to be as well founded as the best of their gyrofluid counterparts.

Gyrofluid Equations with Nonlinear Parameters.
We have generalised the gyrofluid model to relax the local limit using Lagrangian field theory methods in which field as well as thermal/kinetic energy is rigorously conserved to arbitrary order in both FLR and turbulence amplitude. This model will be necessary to capture the core/edge parameter transition within a single computation, and perhaps self-consistent formulation of the pedestal. All pedestal computations to present have at least one artificial element making the pedestal possible. A self-consistent computation free of these elements is a prerequisite for credible prediction of the ITER pedestal width scaling.

New Developments.
The GEM code is being extended to treat the edge/SOL interface. With the upcoming inhomogeneous generalisation the model should be able to treat the entire confinement zone of the plasma completely and self consistently, which would be done for the first time.

Scientific Staff

C. Angioni, M. Apostoliceanu, G. Becker, A. Bergmann, R. Bilato, K. Borrass[1], M. Brambilla, A. Chankin, Y. P. Chen, D. Correa-Restrepo, D. Coster, T. Dannert, K. Dimova, M. Götz, S. Günter, V. Igochine, F. Jenko, O. Kardaun, A. Kendl[2], J.-W. Kim, R. Kochergov, C. Konz, K. Lackner, P. Lauber, P. Martin, P. Merkel, R. Meyer-Spasche, Y. Nishimura[3], G. Pautasso, A. Peeters, G. Pereverzev, D. Pfirsch, S. Pinches, E. Poli, T. Ribeiro, S. Riondato, B. Scott, W. Schneider, E. Schwarz, M. Spannowsky, D. Strintzi, E. Strumberger, G. Tardini, H. Tasso, C. Tichmann, Q. Yu, R. Zille

Guests: C. V. Atanasiu, Institute of Atomic Physics, Romania, M. Foley, University College, Cork, Ireland, P. Lalousis, IESL.FORTH, Heraklion, Greece, P. McCarthy, University College, Cork, Ireland, G. J. Miron, Institute of Atomic Physics, Romania, E. Quigley, University College, Cork, Ireland, J. Tataronis, Universitz of Madison, USA, G. N. Throumoulopoulos, University of Ioannina, Greece, H. Weitzner, Courant Institute of Mathematical Sciences, New York, USA

1 Retired
2 University of Innsbruck
3 U. C. at Irvine

2 Stellarator Theory

2.1 Introduction

In 2003, the work of the Stellarator Theory Division was concentrated on widening the scope of the theoretical work at the Greifswald Branch Institute /176, 223, 324, 647, 831, 865/ and on further development of the stellarator concept, notably for quasi-isodynamic configurations /278, 738/.

2.2 Development of Stellarator Concept

In 2003, the INTAS project No. 592 `Novel approaches to Improve Confinement in 3D Plasma Magnetic Systems' /738/ ended, the collaboration between NFI (Kurchatov), KIAM, Kharkov, CRPP and IPP will of course continue (partly with a WTZ agreement). With a confinement system with qualitatively new confinement properties having been identified[1], the exploration of large aspect ratio cases of this type of configuration has been one further aspect. The result shown in Figs. 1, 2 indicates that high-β MHD-stable configurations different from quasi-helically symmetric ones may exist.

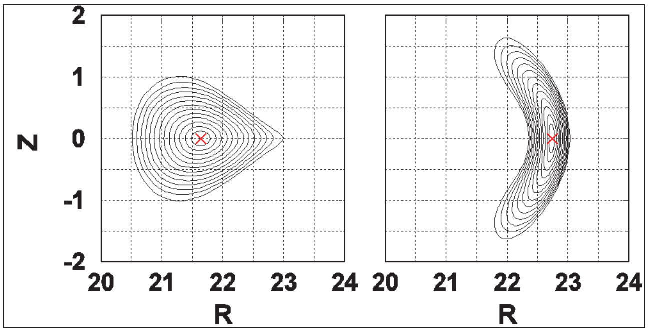

Figure 3 A 9-periodic stellarator with poloidally closed contours of *B* at $\langle\beta\rangle$.0.2

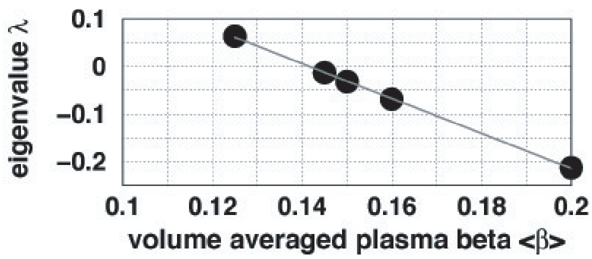

Figure 4 A global ideal-ballooning stability limit of $\langle\beta\rangle$.0.14 is found.

2.3 MHD Theory of Stellarators

2.3.1 Pies with Improved Initial Conditions

The computation of free boundary PIES equilibria was advanced to a pressure of $\langle\beta\rangle$ = 4%. In order to reduce the computational effort, the MFBE procedure developed by E. Strumberger[2] was incorporated in the generation of the PIES starting point. Where previous computations had to rely on an initial guess for the size of the plasma volume, MFBE gives a vastly improved estimate of the plasma boundary, resulting in a starting point for PIES which is much closer to the final solution.

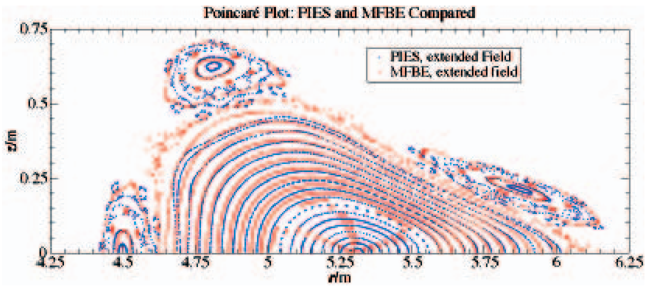

Figure 5 [color online] Poincaré cuts from the PIES field (blue dots) and the extended field of the consistent VMEC equilibrium (red dots).

Fig. 3 shows Poincaré data obtained from the consistent VMEC equilibrium found with MFBE, and from the PIES computation after 1500 iterations. In both cases, the field from plasma currents was extended beyond the original computation domain so as to allow for analysis of the 5/5 islands. It can be seen that the flux surfaces of the two fields agree closely. The PIES solution exhibits some corrugation of the outer flux surfaces absent in the VMEC computation. The axis of the PIES solution is shifted by ~2cm with respect to the MFBE solution. The two computations agree particularly well with respect to the location and size of the 5/5 islands.

2.3.2 Ideal MHD Stability

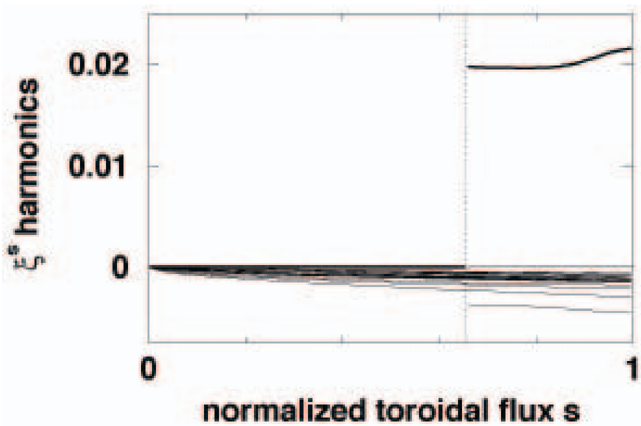

Figure 6 1/1-island scenario for W7-X: the jump in the resonant m=1 n=1 component of the normal displacement represents a surface current that models the island, i.e. can be used to estimate the island-width.

In 2003, besides a number of application studies using the CAS3D code, e.g. of ideal MHD modes in LHD /723/, of the nature of the unstable spectrum /528/, of MHD activity in W7-AS /399, 565/, and of the nature of ballooning modes in low-shear stellarators /276/, the applicability of

[1] Nucl. Fusion **42**, L23 (2002)
[2] Nucl. Fus. **37**, 19 (1997)

ideal MHD stability studies has been extended to include the description of perturbed equilibria[6], in particular islands, which are not present in MHD equilibrium solvers that assume nested magnetic surfaces. The CAS3D code has been extended accordingly /277/ and now provides a method to assess the sensitivity of finite-β plasmas to islands opening at low-order rationals of the rotational transform in the case of error-fields (see Fig. 4).

2.3.3 MHD-Stability with kinetic Effects

Fast particles in toroidal fusion devices have the potential to destabilize modes from the stable part of the MHD spectrum. A kinetic MHD stability code (CAS3D-K)[7] has been developed which is an extension of the 3D ideal MHD stability code CAS3D (see 2.3.2).
To start comparisons with experimental findings calculations for W7-AS shots have been performed. A bulk plasma damping rate has been estimated from a perturbative calculation in analogy to that of the hot particles. Comparing the stabilizing and destabilizing contributions, a stability diagram can be drawn with allows a direct comparison with the experiment.
The 3D-MHD continuum code (CONTI) has been improved being now able to cope with a very large number of Fourier harmonics. As continuum codes are frequently used for experimental data analysis a benchmark with the COBRA code[8] is under way.
If the effects of a finite gyro radius are taken into consideration the Alfvén eigen modes turn into Kinetic Alfvén modes. These global modes may reside even outside the Alfvén gaps and may also be driven unstable by fast particle populations. Based on analytical investigations[9] a numerical investigation of these modes for stellarators has been started in collaboration with a group from (KINR, Ukraine). Eigen frequencies and eigen modes have been obtained in a two-mode model using high order B-spline decomposition. The agreement with the analytical results is satisfactory.

2.4 ITG & Drift Wave Theory of Stellarators

ITG driven instabilities are likely to be one main mechanism to drive turbulence leading to anomalous transport in the core of magnetically confined plasmas. Drift-wave turbulence is held responsible for plasma edge turbulence.

2.4.1 Global linear ITG Modes in 3D geometry

An l=2 stellarator, different tokamak models and the W7-X vacuum configuration have been investigated with respect to ITG modes using the global 3D linear gyrokinetic PIC code EUTERPE[10]. The ITG mode found for W7-X (phase factor m_0=-53, n_0=53) is characterized by a very broad Fourier spectrum; a $\boldsymbol{j}\cdot\boldsymbol{E}$ drive analysis shows that it is driven to 60% by curvature.

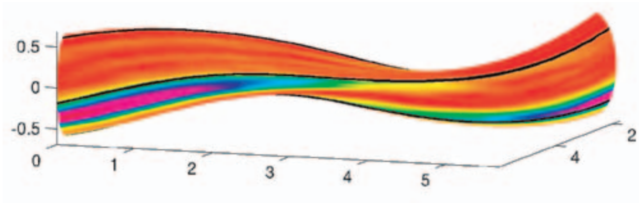

Figure 7 [color online] Modulus of the electrostatic potential for the ITG mode in W7-X.

In order to compare with the gyrokinetic results ITG modes for the above equilibria have been calculated using the newly developed global eigenvalue code in general geometry based on the Braginskii equations.

2.4.2 Global linear stable and unstable electromagnetic modes

Using a gyro-kinetic approach the linearized Vlasov-Maxwell system of equations has been solved in the low frequency limit (i.e. neglecting compressional Alfvén waves) with a δf-particle-in-cell (PIC) method.

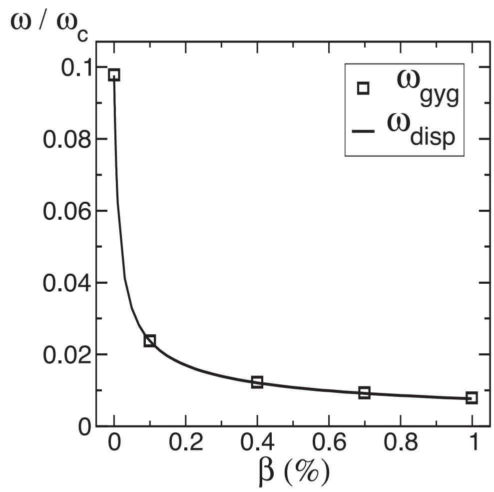

Figure 8 Frequency of the damped shear Alfvén wave in slab geometry over $\beta=(v_{th}/v_A)^2$, no gradients have been applied, k_x=0.1; k_y=0.4; k_z=0.000714; μ=1836.15, the solid line is from the dispersion relation. The data points, shown in squares are from the simulations.

The linear particle-in-cell code GYGLES[11] has been extended to solve also Ampères law. So far, results for slab geometry have been obtained where a comparison with the results of a local dispersion relation is possible. A considerable deviation of the PIC results was a puzzling problem for almost a decade[12]. It is attributed to an insufficient cancellation of certain terms in Amperes law because of the properties of their numerical representation. It had been solved only recently using a split weight scheme and a refined mapping of the fields to the markers[13].

[6] Phys. Plasmas **6**, 831 (1999)
[7] A. Könies, Phys. Plasmas **7**, 1139 (2000)
[8] Y. I. Kolesnichenko, V.V. Lutsenko, H. Wobig, Y. Yakovenko, Phys. Plasmas **9**, 517 (2002)
[9] O.P. Fesenyuk, Y. I. Kolesnichenko, V.V. Lutsenko, H. Wobig, Y. Yakovenko, IAEA Technical Meeting, Greifswald 2003
[10] G. Jost et al., Phys. Plasmas **8**, 3321 (2001)
[11] M. Fivaz, S. Brunner, et al., Comp. Phys. Comm. **111** (1-3):27-47 (1998); R. Hatzky et al., 25th EPS Prague 1998, p. 1804; S. Sorge et al., PPCF **44**, 2471 (2002)
[12] Y. Chen, S.E. Parker, Phys. Plasmas **8** 2095 (2001)
[13] Y. Chen, S.E. Parker, J. Comput. Phys. **189**, 463 (2003)

Using the standard δf-scheme with GYGLES a very good agreement could be obtained even for the more severe case of damped modes. To obtain these results Fourier decomposition in one or two dimensions has been used.

2.4.3 Global ITG turbulence in cylindrical equilibrium with finite β

Turbulence in the geometry of a straight cylinder as a first simplified model of the W7-X stellarator has been investigated. For this purpose, the gyrokinetic global non-linear particle-in-cell code TORB (CRPP/IPP) was started to be modified.

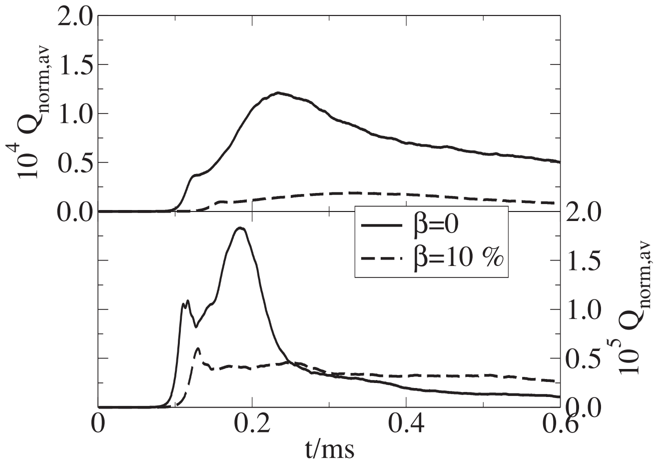

Figure 9 Normalised radial heat flux averaged in the whole cylinder volume $Q_{norm,av}$ for zero and finite β, respectively. The curves in the upper picture were calculated with artificially neglected zonal *E*x*B* flows, whereas for those in the lower picture the formation of these zonal flows was permitted. Note, that the scale factors of the *y* axes differ by a factor of 10 for reasons of presentation.

A magnetic field with a magnetic well according to a finite β pinch equilibrium was implemented. A reduction of linear growth rates of the ITG modes, turbulence level, and heat flux were found.

Special interest was focused on the influence of the magnetic well on the formation of turbulence driven zonal ***E***x***B*** flows, which were found to strongly reduce the ITG fluctuation level and heat transport for a homogeneous magnetic field[14]. In particular, the formation of well localised regions with strongly reduced ITG fluctuation level and heat transport having a behaviour similar to that of transport barriers were observed.

In the case of a finite-β pinch equilibrium, these well localised transport barriers no longer exist. As a consequence, the radial heat flux averaged over the cylinder volume, increases in spite of reduced linear growth rates of the ITG modes. However, a strong reduction of the heat transport compared to the case of artificially suppressed zonal flows remains.

In particular, the turbulent heat flux exceeds the ionic neoclassical heat flux of W7-X, $Q_{neocl,i}.10^{-5} n_0 v_{th,i} T_{i0}$ calculated with an effective field ripple δ_e.0.015, if no zonal flows were included. With zonal flows, the turbulent heat transport level is below the neoclassical one. This shows the PIC method to be a viable tool if extendable to 3D geometry.

[14] S.J. Allfrey et al., *Theory of Fusion Plasmas: Proc. Joint Varenna-Lausanne International Workshop 2002* ed. J. W. Connor, O. Sauter, and E. Sindoni (Bologna: Societá Italiana di Fisica) p. 171

2.4.4 Drift Wave Turbulence in Stellarators

The DALF-Ti code that, in collaboration with B. Scott, has been modified in order to use VMEC calculated equilibria in magnetic (Boozer) coordinates has been used to calculate turbulence in the boundary plasma of axisymmetric configurations with various ι profiles, W7-X and an *l*=2,3 stellarator, respectively.

Increasing ι for the axisymmetric configurations leads to a strong reduction in transport accompanied by an increase of the zonal flow activity. The W7-X configuration shows a strong zonal flow while the small turbulence amplitude is relatively structureless along a field line; the anomalous fluxes obtained are consistent with those found for the corresponding axisymmetric configurations.

2.5 Plasma edge physics

2.5.1 Plasma modeling

A hierarchy of neutral models is now available within the 3D fluid transport code BoRiS: a purely diffusive model, a model with radial diffusion and parallel Navier-Stokes description and a model with full 3D Navier-Stokes. All models were tested together with the system of plasma equations in different test geometries (1D through 3D) /316/. The parallel Navier-Stokes model was found to be a good compromise between numerical effort and the quality of the results as compared to the (correct) full Navier-Stokes model.

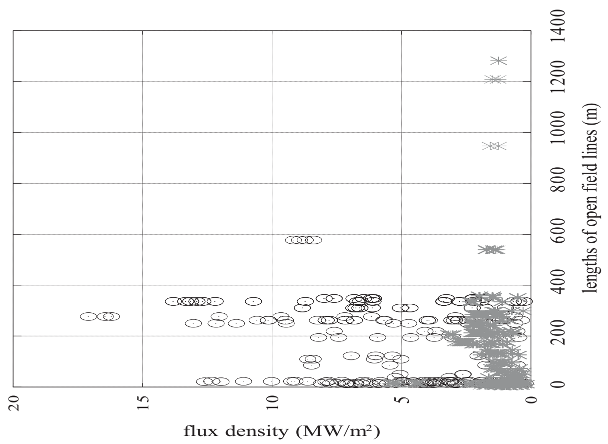

Figure 10 Target power load as a function of field line length for a W7-X vacuum case (circles) and finite β configurations (stars). Both cases are done for 8 MW input power and stay below the engineering limit of about 20 MW/m².

A finite-difference code was used to study the effect of ergodic transport on electron transport in a finite-β W7-X case /330/. An unexpected broadening of the island temperature profile in front of the target was found which reduces the power load strongly (see Fig. 8). This effect is driven by cascading of energy from quite long fieldlines showing ergodic modulation effects towards shorter fieldlines. These shorter fieldlines are shorter than the Kolmogorow length and are not directly affected by ergodicity, but through the influence of radial transport.

A fully kinetic model (PIC MC) including all relevant species (neutrals, ions, electrons) and their reactions was used to study capacitive RF discharges. Depending on neutral gas pressure different plasma conditions appear (determined by the importance of collisions with neutrals). For low neutral densities rather dynamic plasma profiles and distribution functions emerge (stochastic Fermi heating), whereas for high densities quasi-stationary conditions show up. These RF plasmas are then used for the study of plasma crystals, where the dust particles are introduced as additional species in the model. The creation mechanism of these quasi-ordered systems (see Fig. 9) is the force balance between gravitational force and electrostatic electric field force in the sheath allowing a levitation of the dust. Focusing of ion flows in the sheath regions leads to the formation of vertical strip structures (dust molecules). This is driven by the unidirectional interaction towards the plate due to the supersonic background ions (Bohm condition at the sheath entrance).

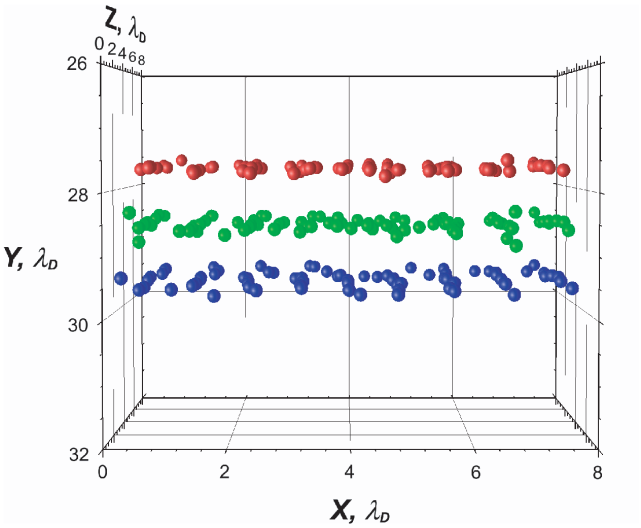

[Figure 11 color online] Side view of a 3D plasma crystal simulation with three layers.

2.5.2 Plasma-wall interaction

A molecular dynamics (MD) code is used to study the transport of interstitials in a graphite crystal. The interstitial trajectories (over a sample size of 100 Å for 100 pico-sec) are analysed to obtain input parameters for our Kinetic Monte Carlo (KMC) code /222/. A first study of the diffusion of hydrogen in porous graphite showed /397/ Levy-flight-type behaviour. The diffusion process proceeds via vacancy jumps towards neighbour atoms, which are thermally activated processes with jump frequencies ω determined by $\omega=\omega_0\cdot\exp\text{-}\Delta E/k_BT$, where ω_0 is the jump attempt frequency and ΔE is the activation energy for this process. There exist two different channels of diffusion for hydrogen isotope interstitials in graphite crystallites: one a high frequency, high migration energy channel which matches the graphite phonon frequencies and the other which is a low frequency, low migration energy channel which shows a $1/m^{1/2}$ mass-dependence for the jump attempt frequencies /397/. The information of the MD code is used within a kinetic Monte Carlo (KMC) code to study the transport and interactions of hydrogen as it diffuses in a realistic porous graphite structure. Experimental results for diffusion in graphite were matched in the trapping/de-trapping dominated regime. It was shown that the diffusion coefficient depends on the structure of the graphite used (void sizes) and the trapping mechanism /397/.

Scientific Staff

X. Bonnin, M. Borchardt, M. Drevlak, R. Kleiber, A. Könies, V. Kornilov, K. Matyash, A. Mishchenko, N. McTaggart, C. Nührenberg, J. Nührenberg, J. Riemann, A. Runov, R. Schneider, S. Sorge, M. Warrier.

Guests: J. Albrecht[15], X. Bonnin[16], W. Cooper[17], S. Ferrando-i-Margalet[14], O. Fesenyuk[18], G. Fuchs[19], K. Gal[20], A. Hatayama[21], C. Hegna[22], U. Heinzmann[23], S. Hudson[24], K. Ichiguchi[25], M. Isaev[26], V. Kalyuzhnyi[27], S. Kasilov[24], E. Kaveeva[28], W. Kernbichler[29], Y. Kolesnichenko[15], L. Kovrizhnykh[30], V. Lutsenko[15], J. Lyon[31], H. Majaniemi[32], B. McMillan[33], P. Merkel[34], M. Mikhailov[23], M. Mikkelsen[21], R. Miklaszewski[35], N. Nakajima[22], M. Nasim[36], S. Okamura[22], P. Popovich[14], T. Rafiq[33], D. Reiter[16], V. Rozhansky[25], E. Salonen[37], M. Samitov[23], I. Senichenkov[25], A. Shishkin[24], O. Shyshkin[38], D. Spong[28], A. Subbotin[23], L. Sugiyama[39], C. Suzuki[22], Y. Suzuki[40], F. Taccogna[41], P. Traskelin[34], A. Ware[42], S. Voskoboynikov[25], Y. Yakovenko[15], M. Yokoyama[22], R. Zagorski[43], M. Zarnstorff[21], A. Zvonkov[23].

[15] DEKRA Akademie Stralsund
[16] CEA Cadarache
[17] CRPP
[18] Institute for Nuclear Research Kyiv
[19] FZ Jülich
[20] KFKI Budapest
[21] Keio University Yokohama
[22] University of Wisconsin
[23] Universität Rostock
[24] PPPL
[25] NIFS
[26] Kurchatov Institute Moscow
[27] National Science Centre Kharkov
[28] State Technical University St. Petersburg
[29] Universität Graz
[30] Russian Academy of Sciences
[31] Oak Ridge National Laboratory
[32] University Joensuu
[33] Australian National University
[34] IPP Garching
[35] IAEA
[36] Chalmers University Göteborg
[37] University Helsinki
[38] Kharkov National University
[39] MIT
[40] Kyoto University
[41] Universita di Bari
[42] University of Montana
[43] Institute of Plasma Physics and Laser Microfusion, Warsaw

3 Nachwuchsgruppe Computational Studies of Turbulence in Magnetised Plasmas

Head: Dr. Wolf-Christian Müller

3.1 Nonlinear energy dynamics in magnetohydro- dynamic turbulence

The phenomenologies of magnetohydrodynamic (MHD) turbulence which are currently under discussion (Komogorov, Iroshnikov-Kraichnan, Goldreich-Sridhar) lead into conceptual dead-ends. Their common problem is the mere postulation of a dominant energy-cascading process without deeper theoretical justification. By falling back on statistical closure theory, we have built a phenomenological framework which seems to correctly describe the nonlinear energy transfer of kinetic and magnetic energy in incompressible MHD turbulence. The basic concept is a dynamic equilibrium of magnetic-field generation by turbulent motions and equipartition due to shear-Alfvén-waves. The new phenomenology is more closely linked to the underlying first-principles than the standard models mentioned above but does not have a significantly increased formal complexity compared to them. The theory is now being extended to become a more general phenomenological description of turbulent MHD energy dynamics.

3.2 Phase transitions of Yukawa systems

Many-particle systems whose constituents interact via potentials of Debye-type, _ (r)~exp(-r/_)/r, are of interest to, e. g., plasma physics, elementary particle physics, and chemistry. These Yukawa systems are particularly attractive for numerical simulations since they allow to eliminate large timeßscale differences between interacting particles by approximating the _fast_ particles as an adiabatic Boltzmann fluid. An existing particle-in-cell (PIC) code was extended to study liquid-solid phase transitions of Yukawa systems in simple periodic geometry. Most of the known characteristics of the transitions can reliably be reproduced with the developed simulation code. The detection of small discontinuities in the Helmholtz free-energy as a quantitative indicator of a first-order phase transition is currently under way.

4 Center of Interdisciplinary Plasma Physics

Heads: Prof. Dr. Volker Dose, Prof. Dr. Gregor Morfill

4.1 Theoretical tokamak turbulence studies

Pinch effect studies (in collaboration with W. Dorland, University of Maryland, USA)

The pinch effect in ion temperature gradient or trapped electron mode turbulence, which is caused by the circulating electrons, has been studied further. It turned out that their surprising importance is caused by the potential fluctuations at large parallel scale lengths (of order of $(v_{e,th}/\omega)$ excited by the circulating electrons themselves. These fluctuations appear as large tails in a flux tube representation of the respective linear eigenmodes. Previous perturbative approaches regarded the effects of these potential perturbations as small of second order in the electron mass. A careful analysis shows this to be wrong. It is not possible to compute the perturbations of the electron distribution functions and electric potential in an expansion in the small electron mass. Instead, the electron and potential fluctuations at large parallel scales have to be computed self consistently, whereby no abbreviations are possible. For sufficiently high gradients in the electron parameters, a resonance in the large parallel scale tails is likely, which boosts the particle transport (inward or outward depends on the parameters) and the circulating electron contribution to it very substantially compared to current wisdom.

Saturation of Tokamak Core Zonal Flows (in collaboration with K. Itoh, NIFS, Toki, Japan)

The saturation of zonal flows (ZF) in the core of a tokamak was studied in a turbulence fluid model with the NLET code. Collisionless Landau damping was modelled qualitatively by a phenomenological ion heat conductivity, the qualitative correct linear properties of the poloidal and toroidal rotation in a torus was checked, i. e., the occurrence of undamped stationary ZFs, and of damped oscillating geodesic acoustic modes (GAM). It was found that the perpendicular Reynolds stress continues to drive the ZFs even past their saturation. The ZF growth is instead limited by the parallel Reynolds stress breaking their parallel return flow (or ist kinetic equivalent in a kinetic collisionless model), which incidentally comprises the major part of the ZFs kinetic energy. These findings require an extension of current theoretical models, which require a drop and eventual reversal of the driving perpendicular Reynolds stress upon ZF saturation. Moreover, using numerical turbulence studies, for the first time a phenomenological formula describing the actual dependence of parallel and perpendicular Reynolds stress on the form and amplitude of the ZFs has been found. The individual components can be associated with the effects of negative viscosity, drift wave dispersion and nonlinear, nearly coherent ZF features, which occur in the computations for certain plasma parameters.

Scientific Staff

K. Hallatschek

Centre for Interdisciplinary Plasma Science

Heads: Prof. Dr. Dr. h.c. Volker Dose, IPP, Prof. Dr. Dr. h.c. Gregor Morfill, MPE

1 Plasma Technology

The Low-temperature Plasma Physics group (LTPP group) at IPP is concerned with the application of low-temperature plasmas for surface treatment, such as deposition of thin films, erosion, and surface modification. The main focus is on the investigation of plasma-surface interaction processes of hydrogen and hydrocarbon plasmas (e.g. CH_4) with hydrocarbon layers. These processes play an important role in the transport of carbon in the boundary layers of fusion experiments. The main activities in 2003 were to investigate deposition of amorphous, hydrogenated carbon films (a-C:H) from pulsed discharges and to study the synergistic interaction of ions and neutral radicals relevant to deposition and erosion of hydrogenated carbon films.

1.1 Synergistic Erosion of C:H Surfaces by Energetic Argon Ions and Thermal Hydrogen Atoms

Erosion of hard a-C:H films by simultaneous exposure to an Ar^+ ion beam and a beam of thermal, atomic hydrogen was investigated by in-situ real-time ellipsometry. Experiments were performed at room temperature and the energy of the Ar^+ ions was varied between 20 eV and 800 eV, as communicated in the last report.

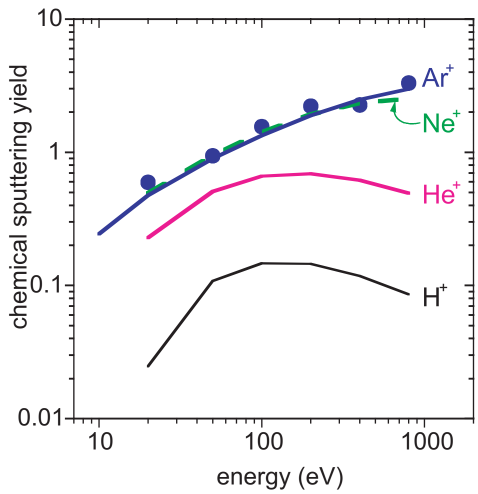

Figure 1: Comparison of experimental data (blue circles) and model results (blue line) for the chemical sputtering of carbon due to simultaneous exposure to argon ions and atomic hydrogen. Model results for other types of ions (H, He, and Ne) are also shown.

On the basis of these experimental results and a proposed microscopic mechanism for chemical sputtering, a model was devised to describe the ion energy and ion species dependence of chemical sputtering in the presence of atomic hydrogen. Model results for a variety of ion species (H^+, He^+, Ne^+, Ar^+) are shown in Fig. 1 and compared with the data for Ar^+/H. The agreement between model and data is excellent.

In addition, the flux dependence, i.e. the dependence of the chemical sputtering yield, Y(Ar|H), on the H atom to Ar^+ ion flux ratio R (= j_H/j_{Ar}), was investigated for an argon ion energy of 200 eV. Y decreases with decreasing R. The data can be well described by a simple rate equation model. The model suggests that saturation of Y occurs only for very high values of R (R > 1000, saturation value of Y ≈ 3).

1.2 Inductively-coupled Plasma Device for In-situ Growth Studies (PAUKE)

In a new plasma experiment set up in 2001, the plasma is produced by inductive coupling at a frequency of 13.56 MHz. In this device, the deposition of a-C:H layers from pulsed discharges is investigated. A self-bias voltage can be applied to the substrate holder with a second RF generator to tune the energy of the impinging ions. Growth and erosion of layers are investigated by real-time, in-situ ellipsometry. Furthermore, the setup is equipped with a mass spectrometer and a plasma monitor for measuring the neutral species and ion flux densities to the sample surface. Measurements were performed with a plasma on-time $\tau_{on} = 3$ ms and varying plasma off-times τ_{off} for different fluxes of the source gas, different pressures, and different self-bias voltages between 20 and 260 V.

The measured growth rate times the total length of a pulse yields the thickness gain per pulse, which can be converted into the number of carbon atoms incorporated per pulse. The parameter that governs the plasma chemistry is the mean energy per source gas molecule, it being determined by the power of the RF generator, P_{ICP}, the duty cycle, *d.c.*, and the flux of the source gas, Φ_{source}:

$$< E > / molecule = P_{ICP} \cdot d.c. / \Phi_{source}$$

Some results for the number of carbon atoms incorporated per pulse are plotted in Fig. 2. The plot contains data from a large variety of different experiments where the process parameters P_{ICP}, *d.c.*, and Φ_{source} were changed over a wide range It is quite remarkable that in spite of this large variation all measurements for a certain pressure lie on the same curve. The carbon incorporation shows a maximum around 20 eV/molecule. This coincides with the maximum in the density of heavier hydrocarbon species (C_xH_y, x>1) measured by mass spectrometry. The decrease following the maximum is caused by the depletion of the source gas.

Quantitative measurements of ion and methyl radical fluences to the substrate show that only 10% of the growth can be caused by these species. The observed growth can only be explained by highly reactive radicals, which do not need any surface activation of the film for incorporation. These species can be formed directly from the source gas (preferentially for low <E>/molecule, where the source gas density is still high) and from heavier hydrocarbons.

In particular, the highly reactive radicals C and CH also have a high reaction rate coefficient for gas phase recombination with CH_4. One should therefore expect substantially lower growth for higher pressures. This can also be clearly seen in Fig. 2.

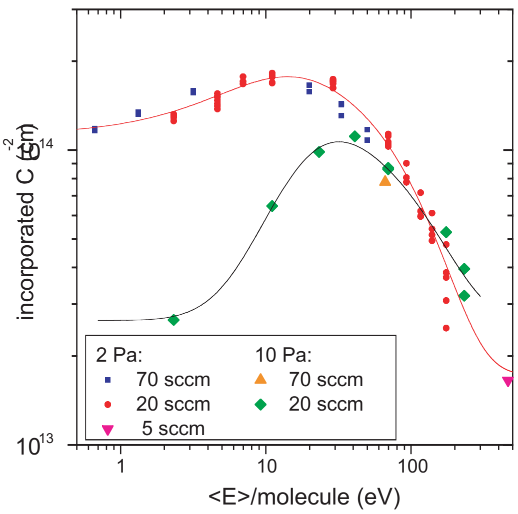

Figure 2: Incorporated carbon atoms per pulse for a pulsed ICP discharge (source gas : CH_4) as a function of the mean energy per source gas molecule. The lines are guides to the eye. (In this graph no distinction was made for different self-bias voltages.)

1.3 Inductively-coupled Plasma Device for Plasma Diagnostics (PUMA)

A new low-temperature plasma device was installed. Following the development of an inductively-coupled plasma device for in-situ growth studies in 2001 this setup is mainly devoted to plasma diagnostics. The device is designed as an all-metal UHV experiment. An energy-dispersive mass spectrometer (Plasma Process Monitor PPM 422, Pfeiffer, Germany), a multi-grid retarding field analyzer (home-made), and a Langmuir probe are the main diagnostics applied to measure the fluxes of ions, stable neutrals, and radicals reaching the electrode surface as well as the particle energy distributions. The chamber and electrode geometry resemble the GEC (gaseous electronic conference) reference cell and are identical to the PAUKE setup. The plasma device as well as the diagnostics were installed and first experiments to characterize the Plasma Process Monitor were performed. The final aim is to combine the quantitative results obtained from both experiments to develop a well-founded description of the processes during growth and erosion of a-C:H films.

1.4 Particle Growth Experiment

In a collaboration between the experimental groups, 'Complex Plasmas' at MPE and 'Low-temperature Plasma Physics' at IPP, a new experiment for the growth of carbon microparticles in a hydrocarbon plasma was constructed and commissioned during 2001.

The behaviour of particle clouds and particle growth in reactive plasmas is studied in this experiment applying a capacitively-coupled RF discharge. We use a three-electrode assembly with the electrodes, 10 cm in diameter, being horizontally oriented. To change the plasma conditions in the levitation region, a gridded electrode is put between two RF electrodes. The particles are levitated between this gridded and the lower electrode. To collect the particles directly from the particle clouds, we use a NFP (negatively charged fine-particle) collector.

In CH_4/H_2 plasmas at 20 Pa, we observed the formation of a particle cloud some 10 minutes after igniting the plasma. Most of the particles levitated are amorphous carbon flakes, delaminated from the surface of the upper two electrodes. However, a few particles are of spherical shape. This indicates that these particles are produced by another process. These spherical samples are assumed to be produced by nucleation and growth in the plasma volume. The evolution of the particle number depends on the gas composition and temperature of the apparatus. We find that dilution by hydrogen and heating of the electrodes can suppress production of particles from the electrode surfaces.

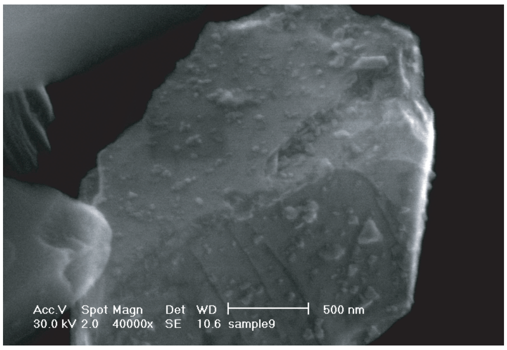

Figure 3: SEM image of diamond particle after 8 h of plasma exposure, showing nucleation of new diamond particles on the surface.

Particles generated in the plasma without introducing seed particles are mainly amorphous carbon, but we also find a few nano-diamond particles for the following growth conditions, CH_4: 1 sccm, H_2: 20 sccm, temperature of electrodes: 800 K. This means the mechanism of layer or particle growth changes in both the plasma-production and particle-levitation regions, especially in the latter. If diamond seed particles (average size ~2.8 micron) are added to the plasma, we observe nucleation of new particles on their surface as shown in Fig. 3 (size up to 100 nm after 8 hours of plasma exposure at 800 K).

1.5 Quantitative Mass Spectrometry

Identification and quantification of components in a gas mixture from quadrupole mass spectra are challenging tasks due to the fragmentation of molecules in the ionization source. Present methods provide only poor and sometimes unphysical results such as negative concentrations. Over the last few years a novel method of decomposing complex multi-component mass spectra based on Bayesian probability theory was developed in collaboration with the data analysis group. This advanced method consistently treats the data and all other information such as calibration measurements or expert knowledge. Point estimates for the species concentrations as well as confidence intervals are determined. In addition to the concentrations, the procedure allows one to derive improved values of the cracking coefficients of all contributing species together with the margin of confidence. It even works for those components for which no calibration measurements exist or cannot be performed, which is the case for reactive radicals or hazardous chemicals. Therefore, this method is suited to disentangling mixtures which contain radicals in addition to stable molecules, a problem often encountered in mass-spectrometric analysis of low temperature plasmas.
The algorithm was extended with a so-called model comparison module. It now allows one to decompose even mixtures containing an unknown number of constituents. Applying the principle of Occam's razor, the method penalizes complicated models for increasing the number of species unless they are supported by the data. As a result, it provides the actual number of species reflected by the data instead of decreasing the misfit between data and model. This feature makes it superior to all existing algorithms. The method was applied to disentangle mass spectra for methane, ethane, and acetylene discharges. Signals of 34 mass channels produced by 10 different stable species were considered, ranging up to 60 amu. Uncommon species such as C_4H_2 were identified. In this example, Bayesian model comparison proved its power to extract information about trace gas elements in the overwhelming parent gas atmosphere.

2 Data Analysis

The Data Analysis group at IPP is concerned with analyzing measured data to obtain most reliable results. The reliability achieved depends on the uncertainties of all measured data, the uncertainties of parameters entering the measurement descriptive model, and the quality of the physical model. A ubiquitous problem in data analysis is to identify and quantify sources of uncertainties of a measurement system and describe the data with a model including all uncertainties in order to obtain a robust result. This can only be achieved if all information relevant to the inference problem is combined in one concise formalism. Bayesian probability theory (BPT) provides a general and consistent frame for combining various kinds of information taking into account the degree of uncertainty of data and models.

2.1 Integrated Data Analysis

Integrated Data Analysis (IDA) of fusion diagnostics is the combination of various diagnostics to obtain validated physical results. IDA requires a systematic and formalized error analysis of all (statistical and systematic) uncertainties involved in each diagnostic. BPT allows systematic combination of all information entering the diagnostic model that considers all uncertainties of the measured data, the calibration measurements, and the physical model. Prior physics knowledge of model parameters and handling of systematic errors is provided. A central goal of integration of redundant or complementary diagnostics is to remedy inconsistencies and reduce estimation uncertainties of physical results by exploiting interdependencies.

The systematic error analyses of the Nd:YAG and ruby Thomson scattering diagnostics were continued with critical assessment of the electron cyclotron emission (ECE) diagnostic (A. Dinklage, E. Pasch, J. Knauer, D. Hartmann, H.-J. Hartfuss, W7-X). The hot-cold calibration data and the noise-tube re-calibration data were combined with the ECE data to obtain a consistent error analysis. BPT generalizes classical error propagation laws which are based on multi-normal distributions. The interdependences of calibration quantities and physical quantities result in asymmetric posterior probability density distributions (pdfs) for the electron temperature which have an impact on best estimates and uncertainty measures.

The complete statistical model of the diagnostics allows one to quantify the influence of different error sources on the reliability of the results. This has an impact on both diagnostic improvement and design of setups and experimental procedure. Development of diagnostic optimization approaches on the basis of an entropy measure is in progress.

For continuously working fusion devices timely provision of significant physics quantities is desirable for interventions in running physics programmes. Capabilities of real-time performance of Bayesian analysis codes were explored.

2.2 Spatial Tritium Distribution in ASDEX Upgrade

Measurement of the toroidal and poloidal distributions of tritium in the ASDEX Upgrade walls by secondary ion mass spectroscopy was continued. The total tritium content as well as the depth distribution were recovered by deconvolving the SIMS transfer matrix from the data. Prominent toroidal and poloidal distribution variations were found and interpreted (in collaboration with J. Neuhauser, AUG, and E. Nolte, TU München).

2.3 Neural Networks for Speckle Interferometry in ASDEX Upgrade

Neural networks are famous for their advantageous flexibility for problems where insufficient information prevents a proper physical model from being set up. The drawback is that this flexibility can cause over-fitting which denies the opportunity to generalize neural networks. Many approaches to regularizing neural networks are based on ad-hoc arguments. Employing the principle of transformation invariance, we derived a general prior pdf for a class of feed-forward networks. This prior also affords cell pruning. By means of Bayesian model comparison the optimal network complexity was estimated for the analysis of speckle interferometry data.

2.4 Bremsstrahlung Background Estimation at WENDELSTEIN 7-AS and ASDEX Upgrade

Spectroscopic bremsstrahlung intensity measurements are superposed with line emission intensities. Separation of the bremsstrahlung background from the line intensities is achieved with a Bayesian mixture model. Robust estimation of the bremsstrahlung amplitude benefits from joint analysis of all data points including those containing line intensities. The Bayesian treatment allows a critical assessment of measurement uncertainties which results in a consistent and improved estimation uncertainty of the effective ionic charge (Z_{eff}). The method was developed and applied for the WENDELSTEIN 7-AS and ASDEX Upgrade bremsstrahlung diagnostics (cooperation with R. König and M. Krychowiak from W7-AS and H. Meister from ASDEX Upgrade).

2.5 Sputtering Yield

Bayesian parameter estimation was employed to determine the parameters of empirical fit formulae for the energy and angular dependences of the physical sputtering yield. In fusion devices most of the particles hitting the first wall have low energy, attracting interest in the behaviour of the sputtering yield close to the threshold energy. While former formulae failed in that respect, the new approach gives a good description in the whole energy (and angular) range. With this method the full variety of ion-target combinations will be treated to facilitate obtaining a consistent view of the sputtering properties.

2.6 Reaction Cross-sections

Reaction cross-sections and rate constants are parameters of a rate equation model for the interaction of CH_3 and H with amorphous hydrocarbon surfaces. Instead of stating the result of the parameter estimation traditionally as single numbers with uncertainties, it was much more informative to have a look at the Bayesian posterior distributions for the model parameters. Comparison of the posterior with the prior distributions revealed the amount of information that was contained in the analysed data set.

2.7 Bayesian Group Analysis of PECVD Data

A ubiquitous goal in plasma-enhanced chemical vapour deposition (PECVD) is to describe the correlation between film properties and categorical and quantitative input variables. The correlations within the high-dimensional parameter space are described with a multivariate model. Bayesian group analysis is employed to assess the grouping structures of the set of data vectors. This allows one to identify sub-groups or meta-groups of predefined groups of data sets, e.g. with respect to source gases. Outliers can be identified by the necessity to form a separate group. The Bayesian approach consistently allows missing data to be handled. The grouping probabilities are compared with classical approaches for likelihood ratio tests and the Akaike information criterion and a Bayesian variant called the Bayesian information criterion. The method was applied to PECVD data of rare-earth oxide film deposition and hydrocarbon film deposition to study the evidence for grouping structures attributed to categorical quantities such as rare-earth components or source gases and quantitative variates such as bias voltage.

2.8 Entropic Priors

The problem of assigning probability distributions which objectively reflect the prior information available about experiments is still an open problem. We employed the Maximum Entropy method in order to translate the information contained in the known form of the likelihood into a prior distribution for Bayesian inference. The evolving entropic prior leads to results which differ from those known in standard statistics.

2.9 Source Detection and Background Estimation on ROSAT All-Sky Survey Data

BPT is applied to separate celestial sources and background intensity on ROSAT All-Sky Survey x-ray photon distributions. The coexistence of background and sources is described with a probabilistic two-component mixture model where one component describes background contribution only and the other component describes background plus signal contributions. The background is due to cosmic, diffuse x-ray emission plus instrumental background. The bivariate Thin-Plate spline modelling the background map is estimated without censoring pixel data containing source intensity. The robust one-step approach allows one to obtain consistent uncertainties of background and source properties. The detection sensitivity of faint and extended sources is enhanced in relation to the Standard Analysis Software System (cooperation with W. Voges and G. Boese from MPE).

Scientific Staff

M. Bauer, R. Fischer, S. Gori, F. Guglielmetti, K. Hallatschek, Ch. Hopf, W. Jacob, H. Kang, A. von Keudell, M. Meier, B. Plöckl, K. Polozhiy[1], R. Preuss, Th. Schwarz-Selinger, U. von Toussaint, J.S. Yoon.

1 [1]Kharkov State University, Ukraine

Plasma Diagnostics

Head: Prof. Dr. G. Fussmann

1 Introduction

Since its establishment in 1992, the Plasma Diagnostics Division at IPP is engaged on activities, experimental and theoretical investigations in Berlin and research on the ASDEX Upgrade and WENDELSTEIN 7-AS fusion machines at Garching. The division is now re-formed and split into two parts: One part is integrated at the Humboldt University, Berlin, where the PSI-2 plasma generator and the EBIT electron beam ion trap experiment are re-established. The second has moved to the Greifswald Branch of IPP and continues to participate in the WENDELSTEIN 7-X stellarator project. The activities of the Plasma Diagnostics Division reported here comprise the PSI-2 and EBIT experiments as well as modelling calculations of hydrocarbon transport. For work is devoted to development of the WENDELSTEIN 7-X project (experimental testing of techniques for thermographic target control in the UHV laboratory), we refer to the respective sections of this report.

2 PSI-2 Plasma Generator

One topic of investigation at PSI-2 was measurement of the heat flux using a newly developed probe. The probe could be operated as sensor for direct measurement of the heat flux or as Langmuir probe for measurement of the ion and electron current densities, electron temperature and plasma potential. Heat flux measurements were made for different orientations of the sensor surface to the magnetic field direction and as a function of the plasma density and electron temperature as well as plasma composition (H^+, D^+, He^+ and Ar^+ ions) and magnetic field strength. The plasma parameters (electron density and temperature, floating potential) were obtained by operating the heat flux sensor as Langmuir probe. From the analysis of the data it was possible to infer the sheath energy transmission and ion energy reflection coefficients. Particularly significant in these measurements was a strong asymmetry in the angular distribution of the electron and ion flux density depending on the orientation of the sensor surface. This asymmetry can be understood from a consistent picture of the dynamics of gyrating particles in the magnetized plasma. To study hydrocarbon transport in a well-defined plasma environment, erosion/deposition measurements were made using controlled gas injection (CH_4, C_2H_4) and wafers or cavities as collectors. The growth rate at which a-CH layers are formed on the heated collectors was measured by (*in situ*) optical diagnostic methods for surface characterization. It was found that the flux of atomic hydrogen has a large effect on the erosion/deposition behaviour. There are indications that the presence of atomic hydrogen leads to net erosion of the a-CH layers. This effect was particularly significant for discharges in hydrogen when the temperature of the collector was raised above 100?C. In contrast, for discharges in argon the process of deposition prevailed, resulting in formation of a-CH layers on the collector surface. Theoretical analysis of the erosion/deposition processes was made using the ERO 3-D Monte Carlo code, which was adapted to the conditions of the PSI-2 plasma generator. This theoretical work is reported in sec. 4. Investigation of the flow behaviour of a plasma in contact with a material surface is in progress. This item is connected with the question whether the plasma flow in front of a neutralizer plate is sonic or supersonic. In the experiment the change of flow induced by a magnetic nozzle was studied. Using LIF techniques, we measured the 1D distribution function of Ar^+ ions at different axial positions parallel to the magnetic field direction. It was found that 75 cm away from the target plate the ion distribution function is close to a Maxwellian, but with a small asymmetry leading to Mach numbers of as low as $M \approx 0.1$. Close to the target, however, it approaches a one-sited Maxwellian with $M \approx 0.5$. This number is significantly lower than the value predicted by theory for the magnetic configuration of the present experiment ($M \approx 2.5$). Attempts to enhance the flow velocity by reducing the neutral gas pressure in front of the target (by enforced pumping) were successful. However, the deviation from the (one-sited) Maxwellian became in this case even more pronounced and a temperature could not be safely assigned any more. Mach numbers in the range 1 to 2.4 can be inferred from the experimental data.

3 Electron Beam Ion Trap (EBIT)

In 2003, the activities of the EBIT group focused on extraction and transport of ions to the gas target, EUV spectra of argon and xenon, visible spectroscopy of Ar ions, and general EBIT physics studies. Investigation of sawtooth oscillation was continued. Previous measurements for Ar and Ba (see Annual Report 2002) were extended to Ar /Xe and Ar/Kr mixtures. The sawtooth behaviour in EBIT is caused by the feedback between low-Z and high-Z ions. This explanation is confirmed by the new measurements. Theoretical analysis of the effect was made by solving sets of coupled rate equations for the ion density and temperature taking all charge states of each component into account. In an earlier attempt at first interpretation only a representative sequence of ionization stages was considered. Covering all rungs of the charge ladder resulted in faster oscillations and a very strong current dependence of the effect similar to the time profiles measured. Theoretical analysis suggests that the experimental thresholds for switching the sawtooth activity on and off correspond to the bifurcation points of the many-particle system (Hopf bifurcation).

The EBIT device was recently extended to allow the extraction of ions for collision experiments with an external gas target. First experiments were performed with 5q keV highly charged Ar ions (Ar^{q+}, q = 16-18) colliding with neutral argon atoms. The charge exchange process was investigated by recording the characteristic x-ray spectrum of the stabilizing ion after electron capture. For the conditions of the experiment, the (static) Over Barrier Model predicts capture into the n=8 shell from which the electron can decay via various cascade routes, depending on the ℓ-substate. Theoretical line emission spectra resulting from capture into different ℓ-substates (ℓ = s, p, d, …, j) were simulated. The relative intensities within the spectra vary greatly, and by comparing the experimental and theoretical spectra one can get information about the details of the capture process. The next steps will be to improve the detection system and slow the extracted ions down to gain control over the ℓ-sensitive capture.

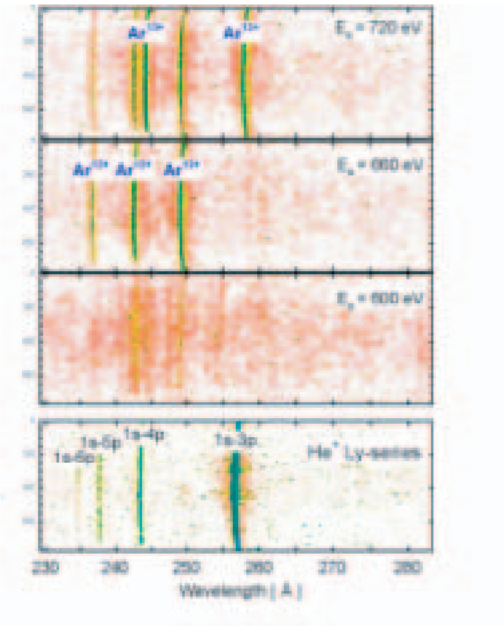

Figure 1: EUV spectra (CCD images) of highly charged argon ions obtained with the grazing incidence spectro-meter. In the lower graph a calibration spectrum is shown.

Investigation of EUV spectra from highly charged argon and xenon ions in the range 100 to 700 Å was continued. Such experimental data are of great importance because Ar is used for diagnostic measurements of high-temperature fusion plasmas and Xe can be considered as promising candidate for cooling purposes in future large tokamaks, such as ITER. The ions in EBIT were sampled using electron beam energy increments of as low as 50 eV. More than 100 spectral features from Ar and Xe have been observed at the Berlin EBIT. Identification of Ar lines is almost complete. Figure 1 is an example showing how Ar^{12+} and Ar^{13+} lines between 230 and 280 Å can be distinguished by stepwise variation of the electron beam energy.

4 Modelling of Hydrocarbon Transport

To clarify the complex deposition and erosion processes occurring in PSI-2 during gas injection, modelling calculations were made with the ERO code applying conditions, which correspond to the conditions of the experiment. A flow of molecules from a 1-mm-diameter 25-mm-long nozzle is considered. The motion of the molecules inside the nozzle was described in the molecular flow regime via consecutive adsorption-desorption cycles predicting at the exit a 200 °C hot beam of $2.2{\cdot}10^{17}$ molecules per second. This beam is directed towards the collector plate, thereby crossing the full plasma column. In the plasma the molecules are dissociated and ionized producing a broad spectrum of C_xH_y and $C_xH_y^+$ hydrocarbon species, as well as H, H_2 and C. Taking into account electron-impact ionization and dissociation of C_xH_y, dissociative excitation, electron-impact ionization and electron recombination of $C_xH_y^+$ as well as charge and atom exchange in collisions of protons and C_xH_y, the number of particles sticking onto the collector plate was calculated. The deposition efficiency increases with increasing plasma density. This is because the rate at which methane molecules are decomposed down to carbon is proportional to n_e. On the other hand, if the density is low the plasma appears to be almost transparent for the nonsticking methane molecules. Compared with CH_4, the deposition rate is faster for the injection of C_2H_4 since in this case more radicals (C_2H_3, C_2H) are produced that can stick onto the collector. In general, however, the ERO code predicts much lower deposition rates (factor 4-5) than observed in the experiment. The measured rates turn out to be unexpectedly high especially for low-density conditions.

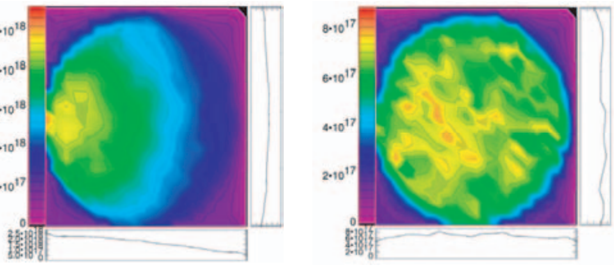

Figure 2: Calculated deposition pattern (C atoms/m^2 s) for injection of C_2H_4 into a deuterium plasma (discharge current I = 400 A, $n_e = 9{\cdot}10^{18}\,m^{-3}$) with (left) and without (right) inclusion of the radial electric field

In the experiment, a shift of the deposition maximum relative to the centre of the collector plate was observed. This effect could be confirmed by the modelling calculations. It is caused by the **E**x**B** drift of the produced ions, leading to plasma rotation. The effect becomes important especially in the case of higher densities, when the reaction probability increases. Figure 2 presents the calculated deposition pattern for the cases with and without radial electric field.

Staff

F. Allen, P. Bachmann, C. Biedermann, W. Bohmeyer, N. Ezumi1[1], D. Hildebrandt, B. Jüttner[2], H. Kastelewicz[2], B. Koch, M. Laux, A. Markin[3], D. Naujoks, R. Radtke, H.-D. Reiner, D. Schröder, A. Stareprawo, D. Sünder, U. Wenzel

1 - Guest, Nagano College of Technology, Japan
2 - Humboldt University, Berlin
3 - Guest, Ac. Sci. Inst. of Chemistry, Moscow, Russia

Energy and System Studies

Head: Dr. Thomas Hamacher

1.0 Objectives

The energy and system studies group evaluates possible future developments of the energy system. Special emphasise is put on the possible role of fusion in the very long-term. Therefor the studies need to consider a time horizon far beyond the next fifty years. This needs of course very special care of the methodologies applied. Developing these methodologies is one of the major focus of the group. It turns out that the geographical scale has to be the whole world. This is necessary to have a good understanding of resources, demand development and environmental impact. On the other side smaller scale and more technical investigations are necessary. The local level shows specificity's, which could be easily overlooked working on a global scale. And some very technical issues like the future development of the electricity network need very special considerations.

2.0 Energy models for the long range

Two major studies are carried out in this direction, which are both strongly supported by the European Commission. The first is the Very Long Energy and Environmental Model (VLEEM) and the second are the Socio-Economic Research on Fusion (SERF). General information about both projects can be found in the internet: www.vleem.org and www.efda.org.

2.1 VLEEM

The Very Long Energy and Environmental Model (VLEEM) tries to establish a new methodology based on a back-casting approach. Several pictures of the future are designed which fulfil certain sustainability criteria. The pictures are designed according to paradigms or clusters of possible future technologies. It is assumed that these technology families dominate the energy system in a way like oil and the internal combustion engine dominate the system today. In a second step a possible trajectory from the future end-point to the present system is drawn. Software tools are under design for both steps.

The heart of the software tool will be a GIS based user interface. The idea is that all information and tools can be accessed from this interface. Using a GIS tool makes it simple to assign geographic information to the system. For a variety of future energy conversion technologies – like renewable technologies – the geographic information is crucial.

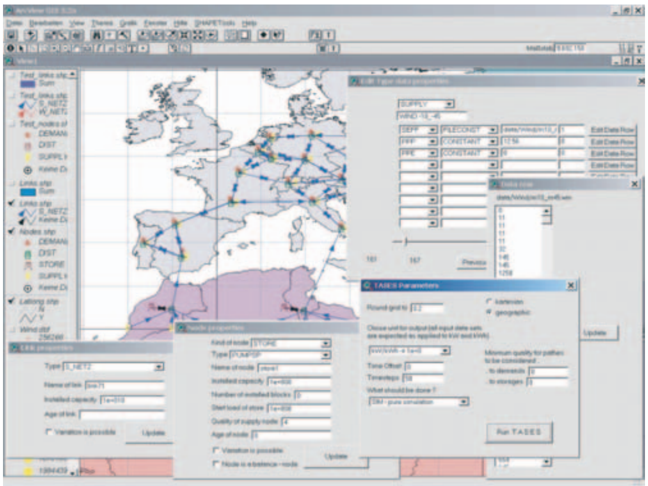

Figure 1: The picture shows the user interface of the TASES software tool, which is developed for the VLEEM project.

The actual back-casting step will be done with the BALANCE tool, which is implemented in GAMS. The model will be forced to reach a certain end-point and to fulfil a number of requested constraints. Again the idea is that the dynamics of the system is not simply simulated with an overall optimisation approach, but that the major decisions and milestones, which would lead to the future system are explicitly mentioned and described.

2.2 Times

The TIMES model generator designed under the auspices of the IEA ETSAP group can be considered to be the state of the art energy model generator.

A global energy model was designed by the IER. The model was implemented at the IPP. A data base describing the underlying technologies is under design and will be finished soon, making more detailed model runs possible. The philosophy of this system is much more in line with conventional economic thinking.

2.3 India

The IPP has co-operation with the Indian Institute of Management in Ahmedabad to investigate the possible development of the Indian energy system. This is of prime importance, because the dynamics of the energy consumption in countries like India are expected to be completely different than the more steady and smooth developments in OECD countries. A demand increase of a factor ten in the electricity sector seems rather likely for India, in other sectors like the transport sector similar growth rates are expected. Very conventional technologies will be applied in these countries, especially coal, if no alternatives like nuclear fusion or cheap solar power are available.

3.0 Fusion in Future energy networks

Future energy systems and especially future energy networks might be completely different than the systems today. The massive introduction of renewable energy technologies, which seems to be one of the possible directions of the energy system, makes it necessary to cope with intermittent nature of wind and solar power plants and the geographical mismatch between sites with huge resources and sites with the equivalent demand. In this project the question is raised how would nuclear fusion fit into these networks. This work is carried out in close collaboration with the university of Rostock.

4.0 Urban energy systems

More and more people of the increasing world population are expected to live in urban areas. The energy system of an urban area is very special, a considerable high demand is requested on a considerable small piece of land. This offers on the one hand the chance to utilise energy very efficient, combined heat and power is a prominent example here. On the other hand it seems difficult due to the space restrictions to supply the energy from energy flows in nature alone. Some sources of high power density are required.

4.1 Augsburg

The activities in Augsburg are done on close collaboration with the Wissenschaftszentrum Umwelt of the University of Augsburg and the chair for Plasmaphysics at the university.

The main focus of the work was to develop a methodology to analyse and forecast the development of urban energy systems.

Four modules make up the approach called URBS. The first module describes and captures the general and overall development of the city, like the population and the settlements, the second focuses on the energy demand, which is partially derived from the first module and partially the result of general considerations like the development of the life style. The third module describes the energy supply system. In a next step, the demand and the supply module will be combined to one. The fourth module captures the environment, both as source of energy and as sink of releases and emissions.

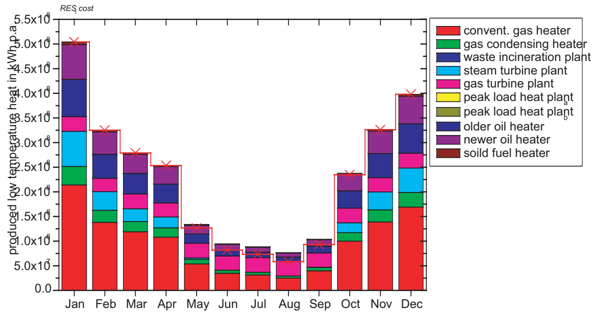

Figure 2: Space heat covers still a big fraction of the end-energy use. New technologies need to be developed to supply the heat in a more sustainable fashion. Shown is the reference case for the city of Augsburg.

In a next step, the demand and the supply module will be combined to one. The fourth module captures the environment, both as source of energy and as sink of releases and emissions. The methodology was in a first step applied to the city of Augsburg. The current energy system can be well described. Different pathways into the future were analysed.

4.2 Greifswald

A first connection with the city of Greifswald was established to develop scenarios and measures for Greifswald to reduce greenhouse gas emissions. The situation in Greifswald is characterised by a very high fraction of district heating, which is powered by modern combined heat and power plants and the fact that the population is still expected to decrease in the coming years. The problem to sustain a infrastructure like the district heat network in times of declining heat demand is a challenging task, if environmental consideration will also be considered.

In co-operation with the Fachhochschule Stralsund two first studies on the situation in Greifswald were completed. One study looked into the potential of bio-gas production in the vicinity of the city and the second described the expected development of the heat demand in one part of the city of Greifswald.

Scientific Staff

Martin Baumann (guest scientist, TU Graz), Prof. Kurt Behringer, Markus Biberacher, Jörg Düweke, Christian Eherer (guest scientist, TU Graz), Tahir Farid, Thomas Hamacher, Stephan Richter

We would especially like to acknowledge the financial support of the Schiedel Stiftung for the guest scientists.

VINETA

Head: Prof. Dr. Thomas Klinger

1 Introduction

The VINETA experiment is a linear, magnetized plasma device, specifically designed to conduct basic research in the physics of discharges, plasma diagnostics development, and electromagnetic waves and instabilities. The current scientific programme is partially embedded in the special collaborative research centre (SFB) 198 "kinetics of partially ionized plasmas" of the German Science Fund (DFG), established in 1993 at Greifswald University.

2 Device and Diagnostics

The conceptual design of VINETA is based on the idea of having maximum flexibility in plasma parameters and magnetic field structure. It consists of four identical modules, each immersed in a set of 8 water-cooled magnetic field coils. The standard configuration provides a homogeneous magnetic field (≤0.1 T) with less than 1% spatial ripple. The individual modules can be operated at different magnetic fields and the coils can be repositioned to obtain well-defined magnetic field gradients along the device axis.

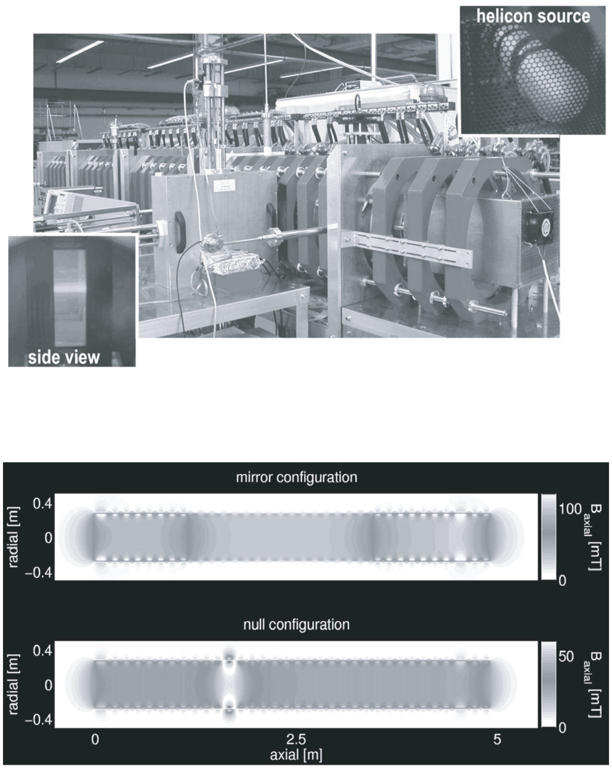

Figure 1: Photo of the VINETA device with a detailed view of the helicon discharge (top). Colour-coded diagram of two different magnetic field configurations (bottom)

In this way, mirror or magnetic separatrix configurations can be established. Figure 1 shows a photo of the device and two different magnetic field configurations.

The VINETA plasma is primarily operated with non-resonant heating via helicon waves, driven in the frequency range 10–30 MHz. This highly efficient heating scheme provides electron densities spanning the range 10^{15}-10^{19} m^{-3} at electron temperatures of typically 3 eV. For the independent control of the electron temperature an additional ECR heating system was recently installed. It utilizes resonant absorption of a right-hand polarized microwave propagating along the magnetic field axis. The microwave source operates at 2.45 GHz and powers ≤ 15 kW.

3 Experimental Programme

3.1 Whistler Waves

Whistler waves in bounded plasmas were the subject of intense research in the context of helicon wave heating. In particular, the effect of plasma boundaries on the dispersion of Whistler waves was an open question. Studies of the magnetic field fluctuation profiles of Whistler waves in VINETA in conjunction with numerical calculation of the full dispersion relation revealed that the plasma density profile fully determines the Whistler wave propagation perpendicular to the ambient magnetic field.

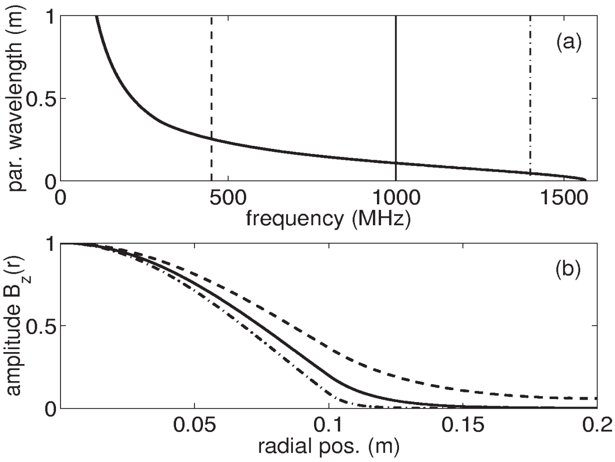

Figure 2: Whistler wave dispersion relation (a) and corresponding radial fluctuation profile (b) for three different frequencies indicated in (a)

This finding stands in contrast to the commonly made assumption that the vessel walls define the boundaries for wave propagation. Furthermore, even for fixed plasma density profile there is a significant frequency dependence, as shown in Figure 2.

3.2 Drift Waves and Drift-Alfvén Waves

The efficient plasma heating in VINETA allows one to investigate drift waves in high-density plasmas. The mid-term perspective is to establish plasma parameters in a regime where drift waves are expected to interact self-consistently with Alfvén waves, so-called drift-Alfvén waves. A key aspect is to reduce the collisionality by increasing the electron temperature $T_e > 10$ eV via ECR heating (work in progress).

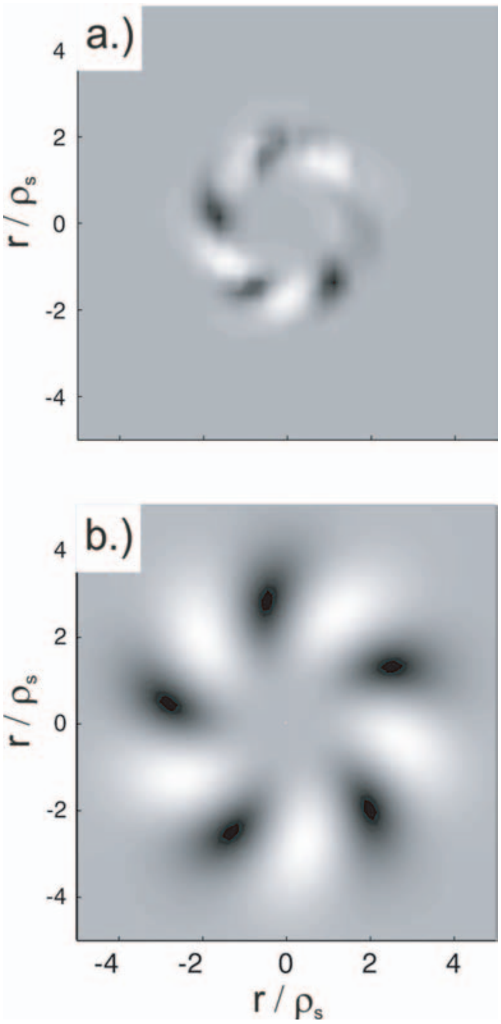

Figure 3: Sheared m=5 eigenmode structures of a drift wave. Shown are (a) measurement and (b) results obtained from a linear numerical model, where radial Coulomb collision profiles are taken into account

Electrostatic coherent drift modes were studied in the collisional VINETA plasmas and detailed comparisons with a non-local linear numerical model were made (in cooperation with Dr. V. Naulin, Risø National Laboratory). Figure 3a shows the measured poloidal structure for a single m=5 drift mode. An interesting feature of the drift mode is its apparently sheared structure, also reproduced by the model. The sheared structures are eigenmode solutions and are caused by the non-homogeneous radial collision profile. Radial velocity shear does not play a role.

3.3 Alfvén Waves

The investigation of Alfvén waves concerns three different aspects: (1) dispersion of kinetic Alfvén waves, (2) ion heating by Alfvén waves, and (3) nonlinear effects such as Alfvén solitons. The kinetic Alfvén wave studies are closely related to the drift-Alfvén programme (see above) and use experimental techniques already developed for Whistler wave investigations. Ion heating by kinetic Alfvén waves is an important topic in space plasma science. In VINETA, this question is addressed by direct measurements of the ion energy distribution function (IEDF) by means of laser-induced fluorescence (LIF). The LIF system at VINETA consists of a 668 nm cw diode laser (output power 60 mW) for high-resolution measurements of the IEDF. Figure 4 shows the IEDF measured in an argon helicon plasma. The next step is to measure perturbations of the IEDF, induced by kinetic Alfvén waves launched into the plasma. This allows one to investigate in detail the interaction between ion kinetics and Alfvén wave dynamics.

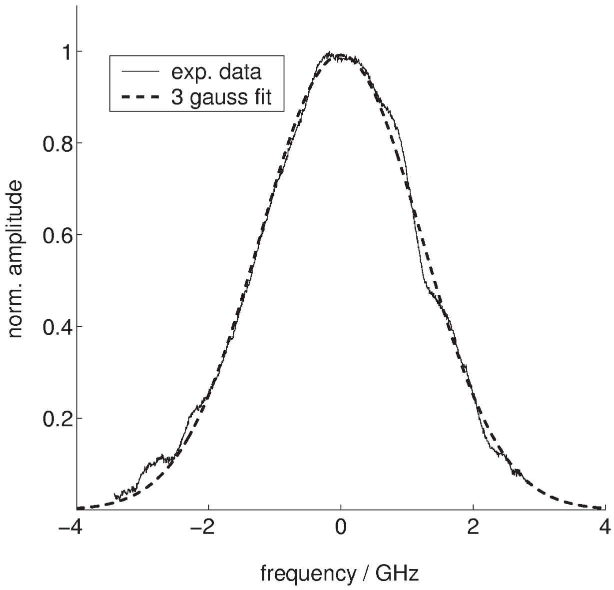

Figure 4: Ion energy distribution function measured by LIF and a multi-Gaussian fit taking Zeemann splitting into account. The resulting ion temperature is 0.2 eV

Scientific Staff

T. Klinger, O. Grulke, K. D. Lee, C. Schröder, A. Stark, J. Zalach

Electron Spectroscopy

Head: Uwe Hergenhahn

1 Introduction

The electron spectroscopy group uses short-wave radiation produced at synchrotron radiation sources for investigations of photon matter interactions that are *i.e.* important diagnostic tools for fusion plasmas.

2 Results

The group currently is working on three projects: Coincident electron-electron and electron-ion spectroscopy of small molecules, circular dichroism in photoionization of chiral molecules and electron spectroscopy of clusters.

2.1 Photoelectron – photoion coincidence measurements

Motivation for this project is the study of chemical transformations on their natural time-scale. Among the fastest processes with respect to the nuclear dynamics involved is the fragmentation of a small molecule provoked when a core electron is resonantly excited into an empty antibonding valence state. By that, both dissociation and relaxation of the electronic shell are initiated and then compete on a similar, femtosecond time-scale. When the nuclear dynamics proceeds quickly enough, a fraction of the molecules is already dissociated when autoionization takes place. This is the case for the deexcitation of the O_2 $1s \rightarrow 3\sigma^*$ resonance, investigated in our work. To study electronic and nuclear relaxation in coincidence, we have combined our high-resolution electron spectrometer with a projective ion spectrometer constructed in the group of Prof. U. Becker, FHI Berlin. This allowed to carry out high-resolution detection of photoelectrons from axis selected molecules. The velocity of the fragments in the atomic region leads to a momentum exchange with the autoionization electrons. Dependent on the electron emission direction relative to the fragment velocity a shift towards lower or higher kinetic energy can occur. By that, we have been able to distinguish electrons that have been emitted in the direction of the other fragment from electrons with other emission directions. We have even distinguished electrons, which after being emitted from one oxygen fragment have been scattered at the other fragment.

2.2 Autoionization of clusters

In weakly bonded systems, such as van-der-Waals clusters, a novel type of autoionization process has been discovered by our group in the preceding year. In this so-called Interatomic Coulombic Decay (ICD), an excited ionized state of the cluster relaxes by a rearrangement of the electronic structure at the initial site of ionization going along with an energy transfer to a neighbouring atom, and subsequent electron emission from this neighbouring site. We have broadened our knowledge of the ICD process now by recording this process in mixed NeAr clusters. Due to the presence of Ne and Ar atoms in the clusters, different electronic final states for ICD are accessible and in electron spectra additional lines pertaining to (Ne $2p^{-1}$)(Ar $3p^{-1}$) final states, as opposed to (Ne $2p^{-1}$)$_2$ final states, occur.

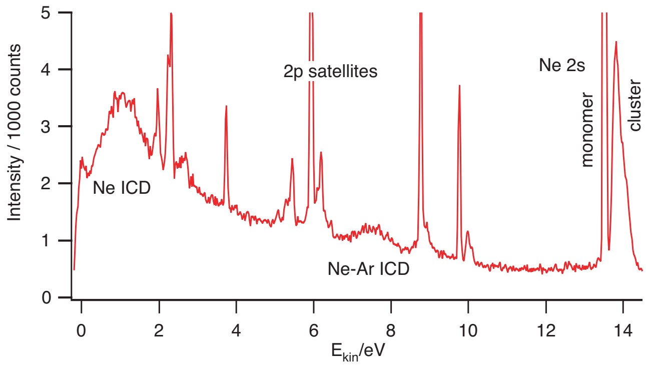

Figure 1: Electron spectrum of free Ne clusters doped with 10-20 % Ar. The occurrence of a broad feature around 6-8 eV kinetic energy identifies IC decay to states with two positive charges, distributed to one Ne and one Ar atom.

2.3 Photoelectron circular dichroism in chiral molecules

The principle of every circular dichroism (CD) measurement is to record the intensity difference of a signal from a handed sample, when it is illuminated with left-handed vs. right-handed circularly polarized light. The relative intensity differences in these measurements are small, typically in the 1/1000 range for conventional CD commonly used in chemistry and biochemistry, and in the percent range in photoelectron circular dichroism, a dichroic effect for radiation in the soft X-ray range recently discovered by our and two other groups. It is therefore highly desirable to have differential methods for measuring these effects at hand. We have done a first successful measurement of photoelectron CD at the BESSY synchrotron radiation source, in which we have employed a fast switch to change the handedness of the polarization each 10-20 s. This will push our detection limit for these effects pushed by an order of magnitude.

Scientific Staff

S. Marburger, O. Kugeler, U. Hergenhahn

Scientific Computing, Data Management and Data Acquisition

Head: Stefan Heinzel

1 Introduction

Rechenzentrum Garching (RZG) traditionally provides supercomputing power and archival services for IPP and other Max Planck Institutes throughout Germany. Besides operation of the systems, application support is given to Max Planck Institutes with high-end computing needs in fusion research, materials science, astrophysics, and other fields. Large amounts of experimental data from the fusion devices of IPP (ASDEX Upgrade, WENDELSTEIN 7-AS, and, later, WENDELSTEIN 7-X), satellite data of MPI of Extraterrestrial Physics (MPE) at the Garching site, and data from supercomputer simulations are administered and stored with high lifetimes. In addition, RZG provides network and standard services for IPP and part of the other MPIs at the Garching site. The experimental data acquisition software development group for the new WENDELSTEIN 7-X fusion experiment and the current ASDEX Upgrade fusion experiment operates as part of RZG.

2 Major Hardware Changes

The IBM pSeries 690 based supercomputer obtained an increased disk capacity of 27 TB and an optimized I/O configuration. Later in 2003 an upgrade of the node interconnect to the new IBM High Performance Switch occurred. The system with 822 IBM Power 4 processors (1.3 GHz), 4.2 TeraFlop/s peak performance and 2 TB of main memory was ranked as top German supercomputer both in the June 2003 and Nov 2003 Top500 lists of the world´s most powerful supercomputers (see www.top500.org).

For non-parallel vectorizing codes, a NEC SX-5 vector system with 3 processors and 12 GB of main memory was available with high single processor performance. As general or dedicated compute servers, besides a 6 processor IBM power 4 system, many rack-based Linux systems with Intel Xeon processors have been installed and operated for general RZG users and for a series of different institutes. Such institute or department servers have been operated and maintained for: IPP, Fritz-Haber-Institute, MPI for Astrophysics, MPI for Polymer Research, MPI for Quantum Optics, MPI of Developmental Biology, MPI of Extraterrestrial Physics, MPI for Biochemistry.

3 Data Management

3.1 Multiple-resident AFS and OpenAFS

RZG developed the OpenAFS client for IBM AIX 5.2 which is used on the new Regatta systems. The major advantage over the IBM supplied AFS client are large file support and the MR-AFS extensions to allow for data-migration commands. On the server side RAID systems which use inexpensive IDE disks, but appear to the host as SCSI disks have replaced the SSA disks. The new RAID systems show better performance at much higher capacities and lower price. They can be used not only with Linux PCs, but with any hard- and software supporting SCSI or fibre channel. Especially for the Regatta systems a high performance AFS solution based on GPFS data transfer protocol is being developed.

3.2 Archival and Backup System

With the huge RAID-systems used by the AFS fileservers the conventional backup by TSM is not sufficient because a restore of the data of a lost RAID system would take days. Therof a new backup concept has been developed for AFS: RO-clones of all volumes are kept on separate servers and updated each night. If a partition is lost a simple fast command converts this RO-clone to the new RW-volume. The file based TSM backup is still useful for restoring of erroneously removed or overwritten files.

Concerning mass storage of data, a basic distinction is made between experiment-type data sets with requirements for long-time conservation and short-lifetime data of the backup type which are replaced by new versions at short intervals. Meanwhile, besides MR-AFS, TSM (Tivoli Storage Manager from IBM) is routinely in use.

One of the GPFS filesystems on the Regatta now is subject to data migration by means of TSM-HSM. These data go onto LTO2 tapes attached to one of the Regatta nodes.

4 Developments for High End Computing

High-performance computing is a key technology for IPP and other Max Planck Institutes. Application development and support for high-end parallel computing is of great importance for disciplines especially in the fields of plasma physics, materials science, and astrophysics. Projects to support new developments in close collaboration with the respective scientists are described in detail.

4.1 Fusion Research

4.1.1 MHDT Code

For efficiency improvement of the general turbulence code MHDT (magneto-hydro-dynamic turbulence) of the group of W.-C. Müller a specific, parallel, three-dimensional FFT was developed. The routine can be used by MPI based programs, but benefits from the shared-memory-feature of the IBM Regatta nodes to avoid the redistribution of data between MPI processes. The highly optimized routines for one-dimensional FFT from the IBM library ESSL have been used as building block. The FFT execution time could be reduced by about 30 % for MHDT.

4.1.2 EUTERPE Code

The three-dimensional geometry of the code implies the solution of a very large set of equations in the form of a sparse matrix equation. This equation was solved by usage of a parallel solver from the PETSc library of PNNL (Pacific North-West National Laboratory). The sparse matrix is time independent and is solved about 1000 times during one simulation run. Therefore direct methods for solving the sparse matrix equation could also be evaluated. The Watson Sparse Matrix Package WSMP from IBM provides such routines both for AIX and Linux. After correction of several problems with WSMP together with the IBM developer, a performance test could be done. Unfortunately a fill factor of about 100 was introduced by the direct method which leads to significant disadvantages compared to the indirect method. By selection of a different solver for the indirect method a performance improvement by a factor of 2 could be achieved.

4.1.3 GYGLES Code

For test purposes the code was equipped with a simple slab geometry. This allowed comparisons with solutions from theoretical considerations. Reasons for marginal inconsistencies were detected and corrected. The technique of “optimized loading” to suppress statistic noise has been applied, as it was already done for the TORB and EUTERPE codes. The expansion of the physical model from electrostatic to electromagnetic simulations required an adaptation and extension of the “optimized loading”.
GYGLES code was ported successfully to the IBM Regatta architecture and adapted to the Intel Linux compiler. The analysis program for GYGLES, TORB und EUTERPE output data was extended and is now available both for AIX and Linux systems.

4.1.4 GENE Code

Recently the GENE turbulence code (of F. Jenko) was used on the LRZ Hitachi SR8000 system in an older version. Now support was given to fully implement the new code version with a modified communication pattern on one Regatta node with 256 GB of main memory. Advice was given for further parallelisation tasks.

4.2 Materials Sciences

4.2.1 WIEN2K Package

In the parallel program package WIEN2K, a quantum mechanical code for the calculation of electron configurations in crystals from the Technical University of Vienna, performance bottlenecks were detected. In one of the subroutines, HNS, sequential code parts were found that had not yet been parallelized by the authors. These parts could successfully be parallelized. The overall performance was improved by 20 %. Run times for a typical problem size (matrix size 15000) on 32 CPUs were as follows:

	Subroutine HNS	Routine LAPW1
original	160 s	642 s
optimized	60 s	537 s

A further complication is introduced by features of the complex WIEN2K script which initiates parallel processing at script level in addition to MPI parallel processing which hit limitations of the Loadleveler batch system which does not support dynamic tasking. For this problem a workaround could be provided, a proper solution, however, requires a design change of the IBM software.

4.2.2 MOLPRO Code

The commercial chemistry code MOLPRO was installed for the IBM AIX System and configured for parallel processing via MPI.

4.3 Astrophysics

4.3.1 Rady/2D

The parallel supernova simulation code Rady/2D (radiation hydro code) was limited to one node (32 CPUs) due to its implementation as shared memory based OpenMP version.
A detailed analysis was done to explore the potential for distributed memory parallelisation with the aim to increase the number of usable CPUs to improve the turn-around time.
2D radiation scales excellently, whereas 1 D radiation and convection including all remaining parts and I/O scale badly (by a factor of 2 as maximum). Since the part which cannot be parallelized with MPI consumes about 13% on one Regatta node, a speedup of 1.6 can be expected at best on 2 nodes. The corresponding code restructuring was done, the estimated speedup achieved. For efficient usage of more than 64 processors a completely new algorithmic approach in a research project will be required.

4.3.2 ZEUS 3D Code

For a special version of the radiation hydrodynamics code ZEUS used at MPA a shared memory parallelisation was done using the OpenMP model.

5 Bioinformatics

For a new project of several Max Planck Institutes RZG started the development of a bioinformatics platform for microbial genome analysis. Existing tools or tools developed by partners are combined in a pipeline in a comfortable way in order to accelerate complex genome analysis in an integrated way.
Furthermore a tool package for automatic gene prediction from the University of Bielefeld was first ported to the RZG environment for SUN Solaris machines, then ported to Linux for usage on a fast Linux compute cluster.

6 Multimedia

6.1 Video Conferencing

MPG and HGF have signed addenda to the general GWiN contracts with the DFN-Verein for using the DFN VideoConferencing Service (DFNVC). This service is available for IPP and all other institutes of the MPG and HGF from December 2003 on.

The IPP videoconferencing (VC) infrastructure consists of 3 Tandberg (T) 6000, 3 x T 880, 5 T 500, 2 T 1000 and 25 desktop systems Polycom ViaVideo. All systems are operable over IP, i.e. the GWiN, alternatively ISDN lines are used for backup of the larger systems. Multipoint conferences are run mostly on the MCUs operated by the DFNVC. The open H.323 GNU gatekeeper and proxy on a dedicated Linux PC are running stable (165 days since last restart, the number of conferences per day is around 20, 5 of them connecting to external gatekeeper zones from all over the world. The current data throughput is ~150 GByte per month. A dedicated PC has be installed in RZGs DMZ and will replace the current system). All internal VC systems of IPP (~40) are registered on the gatekeeper with individual E.164 numbers which are used instead of the IP addresses which stay hidden behind the firewall. The global dialling system (GDS), based on E.164 numbers is used, allowing standardized world-wide connections. TMS (Tandberg Management System) has been installed for scheduling and administration.

AUG is holding regular meetings based on H.323 with European partners in the EFDA. A decision for using H.323 throughout EFDA and possibly ITER is still pending. About 15 EFDA H.323 systems are currently registered with the IPP gatekeeper.

MPGs General Administration is running 5 desktop systems and a videoconferencing room. Another 15 systems have been installed in MPIs of the biological medical section of MPG. The BAR installed 7 room systems in central MPIs to push the acceptance and distribution of H.323 based videoconferencing. The latter systems are registered with the DFNVC gatekeeper and supported by DFNVC and IPPs video group.

7 Developments in Networking

The new network infrastructure is almost completely implemented at IPP. The goal was to use a cabling structure that can easily be adapted to future technologies. The data network realized is therefore based on the concept of a “collapsed backbone”, consisting of switches at a few central locations which directly connect to all endpoints via links based on copper or fibre. This structure drastically enhances overall network performance, for all connections between centralized switches are now at a speed of 1 Gigabit/s (Gigabit Ethernet technology) with the option of implementing even more powerful trunks. Due to the availability of both multi-mode and mono-mode fibre optic cables between the premises it is also possible to adopt upcoming new network technologies such as 10 or 40-Gigabit Ethernet. With this structure we also improved the security and integrity of data because eavesdropping is almost impossible.

For logical security based on the functionality of the internet protocol suite TCP/IP a packet filter firewall at the access point to the internet was implemented, where all the incoming/outgoing packets are checked against a set of blocking or granting rules. Additionally all incoming electronic mail is scanned for viruses and only clean and unobjectionable data (based on known problems) will be passed to the internal network. Spam mail filtering has also been installed. Users can now individually define and set filter threshold values.

Due to the new building for the computer center a bunch of reconfiguration was necessary to converge the physical and logical layers of the network.

8 Data Acquisition and Data Bases for Plasma Fusion Experiments

The major effort of the IPP at the moment is the construction of the new stellerator experiment W7-X in Greifswald. The XDV group is responsible for the development of the data acquisition, archiving and processing system for W7-X. The design of this system is therefore strongly influenced by the design goals of the experiment to operate in long pulses. A large number of diagnostic systems will be implemented to investigate the behavior of the plasma. On the contrary to the previous shot oriented operation, long pulses require continuous sampling, archiving and displaying of collected data. The amount of data, that has to be handled, is some magnitudes higher and requires new techniques for compression, archiving and retrieval.

After verifying the design principles of the data processing system with several prototype implementations a major milestone in the development phase was reached. The primary goal was to achieve a state in the software development, ready to support the first data acquisition stations in measuring and archiving data. Those stations, needed for lab testing of heating subsystems and for the first tests on diagnostic construction, were expected to operate by the middle of this year. To get the future users of the system familiar with the principles of the design a demonstration of all important features was organized. All hardware necessary for the demonstration was moved to Greifswald and set up in a new environment. This included four prototype diagnostic systems, typically for the experiment as well as the data base server and the complete timing system.

All diagnostic systems were equipped with a time measuring board (UTDC), that is necessary for tagging measured data with the global time. The global time and clock was generated by the central timer. The quantities are sent to local systems through a fiber optic star like network. The experiment time is defined by a 64 bit counter, where the least significant bit corresponds to one nanosecond and the resolution of the time was 20 nanoseconds. An accurate clock signal of 25 MHz is used to transfer time values and commands to the local timer (UTDC).

The operating systems, supported in the data acquisition stations were Windows NT, Windows XP and Linux. One diagnostic (BOLO) uses a NI6052E ADC board with a sample rate of 20 KHz for each of the 16 channels. The computer is a main stream Intel PC with a dual processor board and 500 MHz CPU clock. The main memory used is 500 MByte.

At WENDELSTEIN 7-X several surveillance cameras for the plasma and for the divertor will be installed, so we defined as second DAQ station a video system (VIDEO). It consists of a Meteor2 frame grabber and a color video camera. The frame grabber is also equipped with a hardware JPEG compressor.

The third DAQ station is a fast sampling system (FLUK). It uses a Datel PCI416P ADC board equipped with 4 separate analog input channels with a sample rate of 2.5 MHz. It is mainly used to show the limits of the continuous sampling possibilities. This limit is strongly dependent on the computer power and network capabilities and will change during the next generations of PC's.

To show how to integrate legacy systems, a connection to a Siemens S7 SPS for data acquisition was established and incorporated for archiving (fourth DAQ).

As data base server a Sun Enterprise was used with Objectivity as the object oriented data base system. All collected data is archived in the data base as data stream objects. With this setup a data rate to the archive of <=7.8 Mbyte/sec could be maintained for 30 minutes.

The data base also holds all configuration and segment definition data, that was needed to setup the environment for the demonstration. Changes in the setup or segment data can only be done by a special editor. To show the ideas behind this novel technique a generic data base object editor (JOE) was presented.
For controlling the prototype DAQ stations a DAQ control program was demonstrated. It is a graphical user interface (GUI) application and shows the state of all available DAQ stations on the net. This control program can also run a discharge program, described by a text file with lines defining segments by id and duration times.

It is important for remote handling of control- and DAQ stations, to have a messaging system that is independent from console output and direct viewing. Together with the experiment control group a message protocol was defined and presented.

The long duration of a discharge makes it necessary to visualize essential parts of the data during the acquisition process and view the machine state while the program is running. Three of the installed DAQ stations (BOLO, VIDEO and SPS) were configured to send monitor data for viewing. The monitor client for BOLO showed a moving line signal that is updated every 100 milliseconds. The client for VIDEO displayed a reduced picture with an update rate of 30 pictures per minute.

The presentation also included the demonstration of online analysis methods and data retrieval techniques needed for data analysis.

Reaching this milestone, support is now offered to the physicists and engineers for construction of laboratory data acquisition systems. Parallel to this task, the system needs to be developed further and investigated with respect of performance. One important task for the near future is the development of a user friendly editor for the configuration and segment definitions.

Staff

I. Ahlert, A. Altbauer, G. Bacmeister, V. Bludov[1], K. Desinger, R. Dohmen, R. Eisert, S. Gross, A. Hackl, B. Hagemann[1], C. Hanke[1], R. Hatzky, S. Heinzel, C. Hennig[2], A. Jacob, H. Kroiss, G. Kühner[2], H. Kühntopf[2], F. Paulus, J. Schuster[1], K. Lehnberger, H. Lederer, R. Mühlberger, K. Näckel[2], W. Nagel, M. Panea-Doblado, P. Pflüger, F. Pirker, A. Porter-Sborowski, M. Rampp[1], H. Reuter, S. Sagawe[2], H.-G. Schätzko, R. Schmid, A. Schott, H. Schürmann[2], U. Schwenn, T. Soddemann, H. Soenke, K. Stöckigt, R. Tisma, S. Valet[2], Th. V. Weber[2], I. Weidl

Data Acquisition Group:
P. Heimann, J. Maier, J. Reetz, M. Zilker

[1] since Q1 2003
[2] IPP Greifswald

University Contributions to IPP Programme

Lehrstuhl für Experimentelle Plasmaphysik

Head: Prof. Dr. Kurt Behringer

1 Molecular Hydrogen

The presence of hydrogen molecules in the edge plasma of fusion experiments requires simple and reliable diagnostic tools which can be developed and checked best in well defined laboratory plasmas. The well established technique of optical emission spectroscopy (OES) in combination with a collisional radiative (CR) model was further improved. One crucial point in the CR calculations was the assumption that the population within electronic states of one principle quantum number *n* (united atom approximation for each multiplet system separately) follows a Boltzmann distribution. A new and more flexible CR model (*Yacora*) was developed in which these electronic states are resolved using the latest data base for the input cross sections. Since population densities of a variety of electronic states in $n = 3$ are accessible by OES, measurements were compared with calculations. The plasma parameters T_e and n_e of the microwave excited discharge in H_2 and in D_2 are known from other diagnostics. Results for the population of two electronic states, one in the singlet system $I\ ^1\Pi_g$ and one in the triplet system $e\ ^3\Sigma_u^+$, are shown in Fig. 1. The previous model (dashed lines) assumes a population within $n = 3$ according the statistical weights. In the *Yacora* model (full lines), predicted values are lower for $I\ ^1\Pi_g$ whereas a strong enhancement is obtained for $e\ ^3\Sigma_u^+$. The comparison with experimental data (full circles) indicates clearly that the assumption of a statistical population is not justified and that the *Yacora* model should be preferred for the interpretation of molecular radiation.

A further application of the CR model for H_2 and H is the interpretation of Balmer lines in recombining plasmas. Besides population mechanisms within the atom, molecules can contribute also via dissociative excitation mechanisms and dissociative recombination. In case of usual electron-ion recombination (EIR) lower quantum numbers are preferred, whereas the molecular assisted recombination (MAR) process favours higher quantum numbers. As a consequence, population densities are sensitive to contributions of these two channels. Calculations were compared with measurements carried out at the plasma generator PSI-2 (IPP, Berlin). It could be demonstrated that molecules contribute to the plasma recombination. In collaboration with the MAGNUM-PSI pilot experiment (Rijnhuizen, Netherlands) and the UMIST Linear System (Manchester, UK), the comparison of calculations with measurements clearly identifies EIR and MAR dominated regimes.

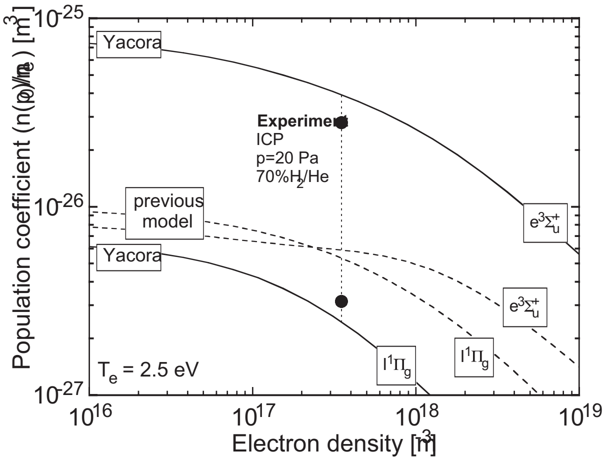

Figure 1: Comparison of experimental data with calculations from two CR models, the *Yacora* model and the previous model for two electronic states.

2 Hydrocarbons

The diagnostic technique, which provides a correlation of CH_4 and C_2H_y particle fluxes with CH and C_2 radiation, respectively, was further developed in hydrocarbon plasmas. In particular, intensity ratios can be used to monitor particle ratios, a method, which will be very valuable for monitoring the release of higher hydrocarbons from carbon, surfaces in hydrogen plasmas. Therefore, the method was checked first in different hydrocarbon plasmas with He and Ar as background gas. Measured intensity ratios of C_2 radiation at 516 nm to CH radiation at 431 nm are shown in Fig. 2. As expected, a strong increase (factor ten) from CH_4 plasmas to plasmas of the C_2-group is observed. Plasmas with Ar enhance the formation of C_2 particles, i.e. higher C_2H_y dissociation, although T_e is lower than with He. Detailed investigations on the basis of a 0-dim dissociation model (*Medicus*) showed that the C_2H radical plays the key role in the formation of C_2 from C_2H_y and that metastable states of Ar are responsible for an enhanced dissociation by excitation transfer.

In collaboration with the Material Research division of the IPP, the time dependence of erosion yields of doped graphite was measured spectroscopically in hydrogen plasmas (ICP discharge). A clear decrease of erosion (factor

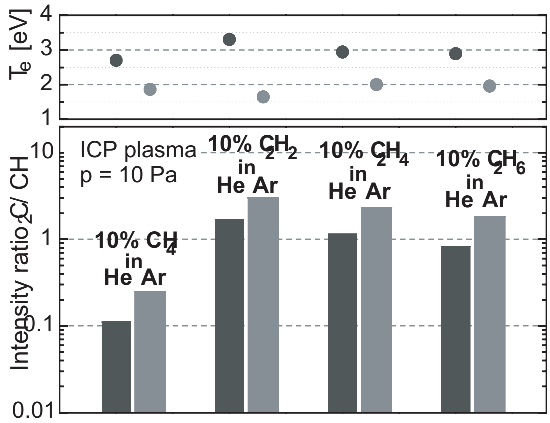

Figure 2: Intensity ratio of radiation of the C_2 Swan band and CH A -X transition in different gas mixtures.

two) with time, i.e. fluence, is observed, which is caused by an enrichment of carbides (TiC, SiC) at the surface. Absolute values are in reasonable agreement with ion beam data only if the erosion yield in plasma experiments is related to the hydrogen ion flux although the neutral particle flux is dominant in these plasmas.

3 Diagnostic applications

One of the main activities of the Augsburg group was the application of diagnostic methods, which were developed and checked at the University, to other low temperature plasmas. Measurements were carried out with the mobile spectroscopic equipment at the plasma generator PSI-2 (IPP, Berlin), the WEGA stellarator (IPP, Greifswald) and the negative ion source BATMAN (IPP, Technology division). Recombining and ionising plasmas in hydrogen and deuterium were characterised in the PSI-2 generator. A method for H^- detection based on recombination of H^- and Ne^+ resulting in excited neon states was tested and shows promising results. At the WEGA experiment plasma parameters, like gas temperature, T_e, n_e, ionisation and dissociation degree, of helium, argon and hydrogen plasmas were determined with spectroscopic methods and compared with results from Langmuir probes. OES shows systematically a factor of three low electron densities and slightly lower temperatures than probes.

The spectroscopic characterisation of the RF source for negative hydrogen ions (BATMAN) was systematically continued. Plasma parameters in two plasma regions of this source, driver region and expansion region near the extraction grid, were measured. Dominant formation and loss mechanisms for H^- particles were identified. In the driver a hollow profile in n_e and a peaked profile in T_e was observed. Main emphasis was given to experiments with a cesium seeded source which enhance negative ion formation via surface processes. The upper part of Fig. 3 shows the variation of the RF generator power and the Cs oven temperature for the evaporation of Cs. As can been seen in the lower part of Fig. 3, the normalised signals of extracted H^- and electron current density correlate well with the radiation of a Cs neutral line (at 455 nm) and the Balmer line (H_γ), respectively. The first correlation is due to the enhanced Cs amount in the discharge and the second correlation is due to the variation of plasma parameters, namely a decrease in n_e in this case. A next step will be the spectroscopic quantification of the Cs amount.

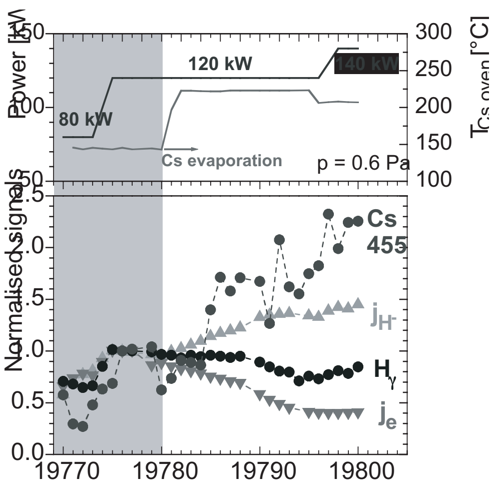

Figure 3: Experimental campaign at the plasma source for negative ions (BATMAN).

4 Publications and Lectures

(in completion to publications of IPP division E4)

U. Fantz, B. Heger, D. Wünderlich, R. Pugno and ASDEX Upgrade Team*: Photon Efficiency (S+D)/XB of Hydrogen Molecules at Low Electron Temperatures*, J. Nucl. Mater. **313-316** (2003) 743-747.

K. Matyash, R. Schneider, A. Bergmann, W. Jacob, U. Fantz and P. Pecher*: Modeling of Hydrocarbon Species in ECR Methane Plasmas*, J. Nucl. Mater. **313-316** (2003) 434-438.

V.P. Veremiyenko, R. Engeln, U. Fantz, W.J. Goedheer, B. de Groot, M.G. von Hellermann, G.J. van Rooij, and N.J. Lopes Cardozo: *Determination of T_e and n_e from Atomic Spectroscopy in Low Temperature (Detached Divertor) Plasmas*, Proceedings of the 30th EPS (2003).

P.K. Browning, U. Fantz, K.J. Gibson and B. Mihaljcic*: Recombination Regimes in the UMIST Linear System*, Proceedings of the 30th EPS (2003).

U. Fantz: *Emission Spectroscopy of Hydrogen and Hydrocarbons in Low Temperature Plasmas*, MAGNUM-PSI Workshop, Rijnhuizen, Netherlands, February 2003.

U. Fantz: *Summary of Spectroscopic Results from the Negative Ion Source BATMAN*, Max-Planck-Institut für Plasmaphysik, Garching, Seminar der Neutralteilcheninjektion, March 2003.

U. Fantz: *Compilation of Spectroscopic Data for Molecular Hydrogen and Diatomic Hydrocarbon Radicals*, CRP on „Data for Molecular Processes in Edge Plasmas“, IAEA Vienna, May 2003.

U. Fantz: *Diagnostics of Molecular Plasmas in Plasma Technology and Fusion Research*, Seminar at the Plasma Research Laboratory at DCU, Dublin, Ireland, March 2003.

U. Fantz: *Spectroscopic Characterisation of Negative Hydrogen Ion Sources*, Seminar at the Plasma Research Laboratory at DCU, Dublin, Ireland, March 2003.

U. Fantz: *Die farbige Natur von Regenbogen, Blitzen und Polarlichtern*, Nacht der Wissenschaft der Universität Augsburg, Augsburg, Juni 2003.

U. Fantz: *Emission Spectroscopy of Molecular Low Pressure Plasmas*, XXVI ICPIG, Greifswald, Germany, July 2003.

U. Fantz: *Die physikalische Natur von Regenbogen, Blitzen und Polarlichtern*, 7. Deutsche Physikerinnentagung, Augsburg, November 2003.

U. Fantz*: Wasserstoffplasmen – Eine Herausforderung für die Fusionsforschung und Technologie*, Physikalisches Kolloquium der Universität Stuttgart, Oktober 2003.

U. Fantz: *Spectroscopic Characterisation of a RF-Source for Negative Ions*, Combined ITER NBI R&D Review and Coordinating Committee (7th EU - JA Workshop) on Neutral Beams, Moscow, RF, December 2003.

U. Fantz: *Plasmaphysik und Fusionsforschung I*, Lecture, University of Augsburg, WS2003/2004

U. Fantz: *Plasmaphysik und Fusionsforschung II*, Lecture, University of Augsburg, SS2003

Scientific Staff

K. Behringer, U. Fantz, S. Meir, P. Starke, D. Wünderlich, M. Berger, S. Dietrich, J. Günther, M. Regler , S. Riegg

Lehrstuhl für Experimentalphysik III der Universität Bayreuth

Head: Prof. Dr. Jürgen Küppers

1 Elementary reactions of hydrogen atoms with adsorbates and solid surfaces

Cooperation between IPP and the University of Bayreuth is concentrated on investigating fusion-relevant plasma-wall interaction processes. Accordingly, the hydrogen atom surface chemistry on possible reactor wall materials is the primary research topic.

A considerable fraction of the species impinging on the first wall of a fusion experimental vessel are neutrals and ions in the energy range below a kinetic energy of about 10 eV . These particles are not capable of causing physical sputtering, but can induce several processes, such as chemical erosion, abstraction etc, which contaminate the plasma. It is therefore desirable to understand the elemental processes and mechanisms of these processes. Recent work of the IPP/UBT collaboration was concentrated on investigating these issues. Since low-energy ions are neutralised in the immediate vicinity of a substrate by resonance neutralisation, it is sufficient to study the low-energy atom-surface interaction. For experimental reasons, the present work utilised only thermal atoms with energies in the range of a few tenth of an eV.

Despite the fact that impinging ions from the boundary plasma transform a considerable fraction of the surfaces of carbon tiled walls into hydrogenated a-C:H, it is of interest to know whether H atoms exhibit strong interaction with graphite surfaces. As reported in the IPP report of the year 2002 and published recently, we demonstrated for the first time that H adsorbs on the basal plane of graphite. The experimental adsorption energy and parallel and normal vibrational frequencies were in excellent agreement with theoretical predictions based on DFT calculations. Surprisingly, thermal desorption spectra of H on C(0001) revealed a complicated structure, not expected from a substrate as simple as graphite.

In Figure 1 deuterium desorption spectra recorded at a natural single crystalline graphite flake, highly oriented pyrolytic graphite (HOPG) of ZYA quality, air-etched HOPG-ZYH with numerous etch pits on the surface, and high-temperature annealed ZYH are shown. It is seen that irrespective of the substrate the principal features of the spectra are identical. This indicates that the structure of the deuterium desorption features are intrinsic and not defect oriented. As origin of this structure specific C-H, H-C-C-H, and like adsorbate structures are suggested. Energetic differences in these adsorbate configurations could result in the observed features. This surprising result leaves the question open, whether largescale defects on a graphite surface affect H or D adsorption at all. Theory suggests that H adsorption on C is connected with a local reconstruction which should be affected by small-scale defects like first-layer vacancies and interstitials underneath the top layer. Since this type of defect should be abundant on plasma facing C tiles, the relevance of the H /graphite-basalplane bond for fusion applications might be small.

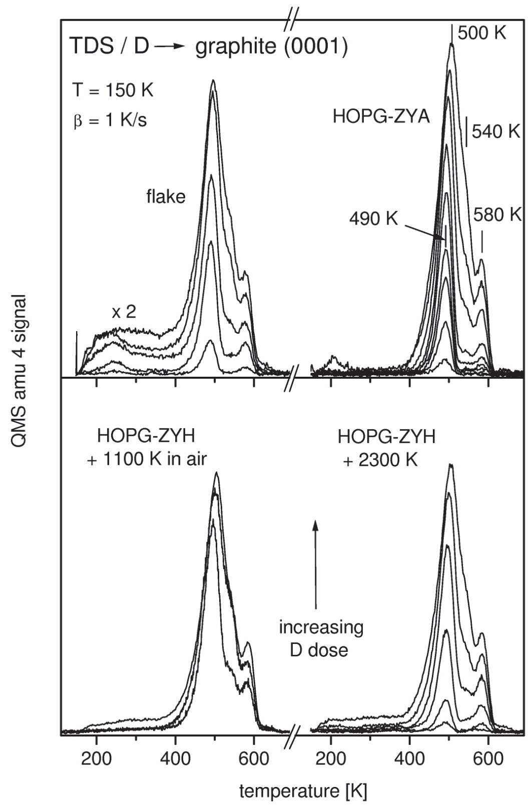

Figure 1: Thermal desorption spectra measured at various D atom exposed graphite surfaces. Heating rate 1 K/s.

2 Publications

D. Kolovos-Vellianitis and J. Küppers
Kinetics of abstraction of D and O on Cu(110) surfaces by gaseous H atoms.
J. Phys. Chem. B 107 (2003) 2559

T. Zecho, A. Güttler, and J. Küppers
Suppression of D adsorption and D by H abstraction on graphite (0001) surfaces by adsorbed water.
Chem. Phys. Lett. 370 (2003) 366

S. Wehner, F. Baumann, and J. Küppers
Kinetic hysteresis in the CO oxidation reaction on Ir(111) surfaces.
Chem. Phys. Lett. 370 (2003) 126

J. Biener, C. Lutterloh, M. Wicklein, A. Dinger, and J. Küppers
Thermal stability and hydrogen atom induced etching of nanometer-thick a-Si:H films grown by ion-beam deposition on Si(100) surfaces.
J. Vac. Sci. Technol. A 21 (2003) 831

S. Wehner, F. Baumann, M. Ruckdeschel, and J. Küppers
Kinetic Phase Transitions in the Reaction CO + O ˜ CO_2 on Ir(111) Surfaces.
J. Chem. Phys. 119 (2003) 6823

D. Kolovos-Vellianitis and J. Küppers
Abstraction of D on Ag(100) and Ag(111) surfaces by gaseous H atoms. The role of electron-hole excitations in hot atom reactions and the transition to Eley-Rideal kinetics.
Surf. Sci. 548 (2004) 67

A. Güttler, T. Zecho, and J. Küppers
Interaction of H (D) atoms with surfaces of glassy carbon: adsorption, abstraction, and etching.
Carbon in press

T. Zecho, A. Güttler, and J. Küppers
A TDS study of D adsorption on terraces and terrace edges of graphite (0001) surfaces Carbon in press

Y. Hayase, S. Wehner, J. Küppers, and H. R. Brand
External noise imposed on the reaction-diffusion system CO + O_2 ˜ CO_2 on Ir(111) surfaces: experiment and theory.
Phys. Rev. E in press

3 Conference contributions

J. Küppers, T. Zecho, A. Güttler
Adsorption and abstraction of H and D atoms on the (0001) graphite surface.
ACS National meeting, New Orleans, 24. März 2003

J. Küppers
Adsorption and abstraction of H atoms on graphite surfaces.
CEA Cadarache, 13. Juni 2003

Andreas Güttler, Thomas Zecho und Jürgen Küppers
Abstraktion von D auf Graphit (0001) durch thermische H Atome
DPG Frühjahrstagung Dresden, 24. März 2003

Thomas Zecho, Andreas Güttler, Clarissa Abetz, and Jürgen Küppers
Adsorption of thermal H on the basal plane and at step edges of graphite (0001) surfaces
DPG Frühjahrstagung Dresden, 26. März 2003

A. Güttler, Th. Zecho and J. Küppers
Interaction of H (D) atoms with surfaces of glassy carbon: adsorption, abstraction and etching ECOSS 22, Prag 11.9.2003

Frank Baumann, Stefan Wehner, Jürgen Küppers
CO-Oxidation auf einer Ir(111)-Oberfläche: Stationäre Reaktion und kinetischer Phasenübergang
DPG Frühjahrstagung Dresden, 24. März 2003

Stefan Wehner, Frank Baumann, Jürgen Küppers
CO oxidation reaction on Ir(111) surfaces: bistability and transient behavior
DPG Frühjahrstagung Dresden, 25. März 2003

Stefan Wehner, Frank Baumann, Jürgen Küppers
Kinetic phase transition and bistability in the CO oxidation reaction on Ir(111) surfaces
UC Symposium on Surface Science, Riverside CA, 13.2.2003

Stefan Wehner, Frank Baumann, Jürgen Küppers
Kinetic phase transition and bistability in the CO oxidation reaction on Ir(111) surfaces

Gordon Research Conference: Chemical Reactions At Surfaces, Ventura CA, 18.2.2003
T. Zecho, A. Güttler, C. Abetz, J. Küppers
Reactions of thermal H with graphite surfaces
Lehrstuhl für die Physikalische Chemie mikroskopischer Systeme TU Karlsruhe,
11.02.2003
T. Zecho, A. Güttler, C. Abetz, J. Küppers
Adsorption of thermal H on the basal plane and at step edges
of graphite (0001) surfaces
DPG Frühjahrstagung, 24-28 März 2003

T. Zecho and J. Küppers
Adsorption and recombination via abstraction of H(D) on graphite (0001) surfaces
Workshop on Solid State Astrochemistry of Star Forming Regions
14-17 April 2003, Leiden University, Netherlands

Scientific staff

A. Güttler, D. Kolovos-Vellianitis, T. Zecho

Lehrstuhl für Experimentelle Plasmaphysik

Head: Prof. Dr. Ulrich Stroth

1 Objectives

With the objective of a close experiment-theory comparison, this work focuses on plasma which complies, with respect to turbulence, with the most relevant requirements of a fusion experiment: the plasma in the torsatron TJ-K is toroidally confined and has centrally peaked pressure profiles. At the same time the complexity of the problem is reduced, since instabilities like the ion and electron-temperature-gradient driven modes are absent and electro-magnetic transport is not expected. With respect to earlier comparative studies, the stationary low-temperature plasma allows better diagnostics accessibility and the use of probe arrays with a large number of tips. Experiments in 2003 concentrated on turbulence measurements in discharges created with electron-cyclotron-resonance heating (ECRH) and diagnostics with arrays of 64 Langmuir probes. The experimental data are compared with simulations from the drift-Alfvén-wave code DALF3.

2 ECRH plasma parameters

A microwave source at 2.45 GHz and a power of 6 kW was used for plasma heating. The resonant magnetic field is about 90 mT. The wave is coupled in O-mode from a bottom flange to the plasma. Although the density cut-off at this frequency is at 7×10^{16} m^{-3}, centrally peaked density profiles with peak values up to 10^{18} m^{-3} are achieved. In Fig. 1, typical plasma parameters and profiles are depicted.

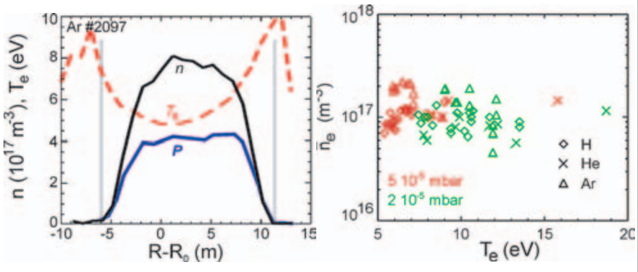

Figure 1: Left: Electron temperature, density and pressure profile of an Argon ECRH discharge measured with swept Langmuir probes. Right: Line averaged density and central electron temperature of ECRH discharges in different gases.

The electron temperature profile is slightly hollow with typical values of 5–15 eV depending on the working gas, which was Hydrogen, Helium or Argon. The ion temperature was measured with passive spectroscopy to be in the range 0.5–1 eV. Best results were obtained at neutral pressures in the range 2–5 10^{-5} mbar and heating powers of 0.7–2 kW. The hollow temperature profile indicates that most of the power is deposited outside or in the vicinity of the density cut-off. A standing wave might develop in the volume limited by the cut-off surface on one side and the vacuum vessel on the other. However, it is likely that a fraction of the wave is also transmitted to the plasma core by O-X-B mode conversion. Wave-field measurements will help to clarify this process.

3 Wave-number spectra

Systematic numerical studies carried out with DALF3 at TJ-K plasma parameters in equivalent tokamak geometry showed that drift-wave dynamics should clearly dominate interchange drive. The main signature of drift-wave turbulence is a cross-phase between density and potential fluctuations of $\gamma\approx 0$ on all spatial scales. In order to investigate the full spectral density of the fluctuations $P(\omega,k)$ in frequency and wave-number space as well as the cross-phase wave-number spectrum $\gamma(k)$, a poloidal Langmuir probe array was built. The 64 tips of the diagnostics were aligned on a flux surface at about half plasma radius with a poloidal probe separation of 7 mm. The tips were connected either to measure ion saturation current, floating potential or alternating to measure radial transport fluctuations.

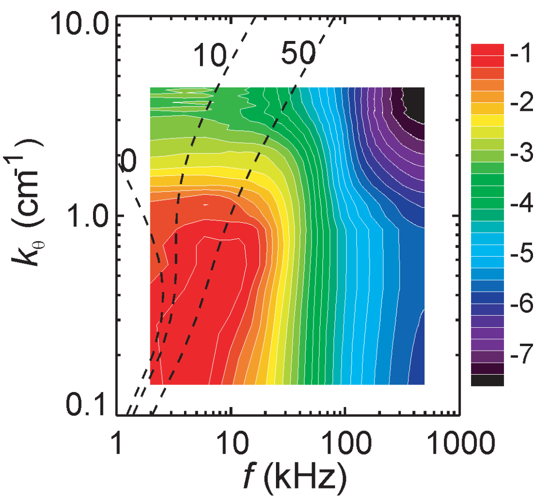

Figure 2: Spectral density of ion-saturation-current fluctuations of a Helium discharge. Dashed lines indicate the linear drift-wave dispersion relation corrected for $E_r\times B$ flow.

Fig. 2 shows the measured spectral density of ion-saturation-current fluctuations of a Helium discharge. Up to poloidal wave-numbers of k = 1 cm^{-1} and frequencies of f = 20 kHz the distribution is flat and has no simple relation $k(\omega)$. The broad distribution is typical for fully developed turbulence. The data is compared with the linear dispersion relation corrected for poloidal $E_r\times B$ background flow. Typical values in Helium discharges are of the order of 50

V/m. Hence the measured distribution is dominated by $E \times B$ flow.

A comparison of measured and simulated cross-phase spectra is depicted in Fig. 3. In both cases, broad distributions of the phase are centred on values close to zero. The cross-phase distributions from experiment and simulation agree very nicely. This is clear evidence that drift-wave dynamics is responsible for the drive of the turbulence in TJ-K.

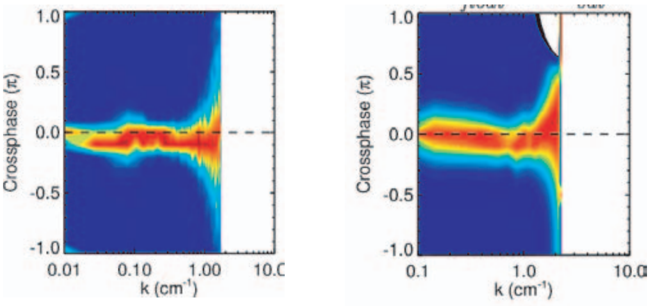

Figure 3: Cross-phase distribution as function of the poloidal wave-number for an Helium discharge (left) and a DALF3 simulation (right).

4 ρ_s scaling of turbulence

A linear scaling of the turbulent eddy size with the drift parameter $\rho_s \sim (T_e/m_i)^{1/2}/B$ is another robust prediction of theory. In TJ-K, ρ_s can be modified by a factor of 10 by changing the ion mass. In contrast to fusion experiments, on TJ-K the ρ_s scaling is studied directly on the size of the turbulent eddies and not on a deduced quantity like the diffusion coefficient. The correlation analysis of the data from the poloidal array gives the characteristic poloidal scale length L_{perp} of the most dominant turbulence structure.

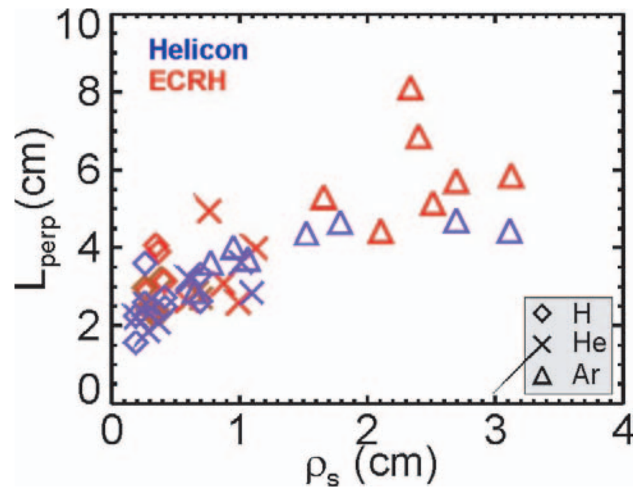

Figure 4: Poloidal correlation lengths for discharges in Hydrogen, Helium, and Argon at different drift scales.

In Fig. 4 the measured correlation lengths of discharges in different gases are plotted versus the drift parameter. The increase of the size of the dominant structure with ρ_s is apparent. Some of the scatter is due to variations in other parameters. However, further systematic variations were not found. The scaling can be fitted with a power law with an exponent between 1/3 and 1/2. More recently also Deuterium was used to study the isotopic effect in comparison with Hydrogen.

5 Publications

M. Ramisch, U. Stroth, S. Niedner, B. Scott, *On the Detection of Reynolds Stress as Driving and Damping Mechanism of Zonal Flows,* New J. of Phys. **5**, 12 (2003)

N. Mahdizadeh, U. Stroth, C. Lechte, M. Ramisch B. Scott, *Investigation of Intermittency in Simulated and Experimental Turbulence Data by Wavelet Analysis*, Phys. Plasmas, submitted

C. Lechte, N. Mahdizadeh, M. Ramisch, U. Stroth, *Spatial Structure of Drift-Wave Turbulence in a Toroidal Low-Temperature plasma,* Phys. Rev. Letter, submitted

U. Stroth, F. Greiner, C. Lechte, N. Mahdizadeh, K. Rahbarnia, M. Ramisch, *Study of Edge Turbulence in Dimensionally Similar Laboratory Plasmas*
Phys. Plasmas, 2004, in print

H.Yamada, K.Ida, S.Murakami, K.Y.Watanabe, S.Inagaki K.Tanaka, M.Goto, K.Narihara, S.Morita, S.Sakakibara, B.J.Peterson, R.Sakamto, J.Miyazawa, T.Morisaki, M.Osakabe, K.Toi, N.Tamura, K.Ikeda, K.Yamazaki, K.Kawahata, O.Kaneko, N.Ohyabu, A.Komori, E.Ascasibar2, A.Dinklage, J.H.Harris, S.Okamura, F.Sano, U.Stroth, *Configuration Effect of Energy Configuration Effect on Energy Confinement and Local Transport in LHD and Contribution to International Stellarator Database*, Proc. of 14th Int. Stellarator Workshop, Greifswald 2003

U. Stroth, C. Lechte, M. Ramisch, N. Mahdizadeh, M. Michel, *Dritwave Turbulence in the Torsatron TJ-K,* Proc. of 14th Int. Stellarator Workshop, Greifswald 2003

K. Rahbarnia, C. Beidler, F. Greiner, M. Ramisch, U. Stroth, *Neoclassical Transport and Radial Electric Fields in TJ-K ,* Proc. of 14th Int. Stellarator Workshop, Greifswald 2003

N. Mahdizadeh, C. Lechte, M. Ramisch, U. Stroth, *Scale Separation of Simulated and Measured Turbulence by Wavelet Analysis,* Proc. of 14th Int. Stellarator Workshop, Greifswald 2003

Scientific Staff

F.Greiner N. Krause, C. Lechte, N. Mahdizadeh, M. Michel, M. Ramisch, K.Rahbarnia, V. Senger, U. Stroth

Speckle metrology for time resolved surface diagnostics

Prof. Dr.-Ing. Alexander W. Koch

1 Introduction

The cooperation of IPP and Technische Universität München is concentrated on the development of Speckle measurement techniques to detect arc traces, deformation, erosion, surface roughness, surface structure, and surface contour in the divertor region of experimental fusion devices.

2 Interferometry of non-stationary objects

The proposed method of surface contouring using speckle-interferometry requires the detection of two interferograms generated at different wavelengths. The concept of a synchronous two-camera-system combined with a spatial phase-shifting technique prevents decorrelations of two interferograms with respect to each other. Furthermore disturbance of interferograms caused by movements are suppressed by short exposure times provided by the cameras. A new setup, shown in Fig 1., was developed using two separated, linearly polarised, tuneable laser sources. The polarisation direction of the lasers is adjusted perpendicular to each other. The separation of the two wavelengths in this setup is achieved by polarisation filters, adjusted according to the laser wavelengths polarization direction. The ability of tuning of the lasers permits a variation of the measurement sensitivity which is determined by the so called synthetic wavelength, calculated by:

$$\Lambda = \frac{\lambda_1 \cdot \lambda_2}{2 \cdot |\lambda_1 - \lambda_2|} \quad (1)$$

Moreover the use of separated laser sources permits the introduction of a tilt between the laser beams. This tilt can be used in order to compensate non-perpendicular observation angles. The detected position of the object in the first interferogram, generated by laser 1 is expressed by h. The tilt between the two lasers results in a different detection of positions in the second interferogram, expressed by Δh.
The difference of these two interferograms yields:

$$\begin{aligned} I_1 - I_2 = & -2 \cdot I_0 \cdot \lambda \cdot \\ & \cdot \sin\left(2\pi \cdot \left(\frac{\lambda_2 - \lambda_1}{|\lambda_1 \cdot \lambda_2|} \cdot h - \frac{1}{\lambda_2} \cdot \Delta h\right)\right) \\ & \cdot \sin\left(2\pi \cdot \left(\frac{\lambda_2 + \lambda_1}{|\lambda_1 \cdot \lambda_2|} \cdot h + \frac{1}{\lambda_2} \cdot \Delta h\right)\right) \end{aligned} \quad (2)$$

with I_1, I_2 representing the intensities of the first, and the second interferogram, respectively. Eq. (2) shows that small difference angles between the laser beams cause large changes in the detected phase. This effect can be used in order to compensate high fringe densities in the phase image.

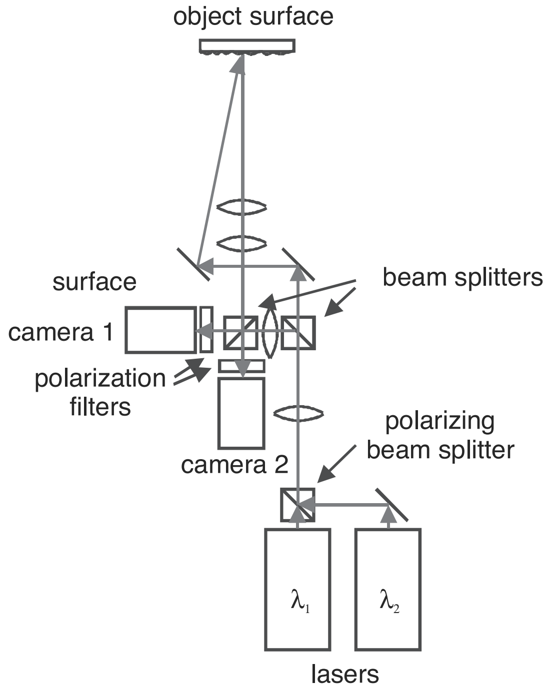

Figure 1: Two-camera-setup using the polarisation effect

The setup has been tested using moving measurement objects without vibration damping environment. First results show a high stability against movements resulting in a maximum shift of 60 μm during the exposure time of the cameras, permitting a velocity of 30 mm/s at an exposure time of 2 ms. An extrapolation of these results clearly exhibit that the acceptable velocity of the measurement object could be increased significantly by a further reduction of the cameras exposure time. Therefore intensified cameras can be used combined with increased laser power.

3 Scientific Staff

Martin Jakobi
Andreas Meixner
Andreas Purde
Thomas Zeh

Institut für Plasmaforschung (IPF) der Universität Stuttgart

Head: Prof. Dr. Uwe Schumacher

The Max-Planck-Institut für Plasmaphysik (IPP) at Garching and Institut für Plasmaforschung (IPF) at University of Stuttgart are collaborating closely for more than three decades on technological developments, measurements, and interpretations of heating and diagnostic systems. The main topics of the co-operation are applications of millimetre waves for heating, current drive, plasma stabilization and diagnostics - mainly for W7-X, ASDEX Upgrade and WENDELSTEIN 7-AS – and contributions to emission, absorption and LIF spectroscopy for bulk and divertor plasma diagnostics.

1 Plasma Heating and Diagnostics

The investigations of the application of millimetre waves to fusion plasmas for electron cyclotron resonance heating (ECRH), current drive, and neoclassical tearing mode stabilization were continued. On the technical side, work on the ECRH system of W7-X formed the major part. Nevertheless, technical support, research and development for W7-AS, ASDEX Upgrade and ITER was continued. Studies of the MHD stability of high-β discharges in ASDEX Upgrade and the use of ECRH / ECCD to control instabilities continued to be a major issue. Moreover, general developments in the field of millimetre wave technology as well as the study of microwaves as a plasma diagnostic tool are reported here.

1.1 Electron cyclotron resonance heating (ECRH)

1.1.1 ECRH system on ASDEX Upgrade

A new ECRH system with 4 gyrotrons, 1 MW each, is currently under construction at IPP Garching. The gyrotrons will allow operation at frequencies between 104 GHz and 140 GHz. Whereas the first tube emits only at these two frequencies, the others shall be step-tuneable. The transmission system is a combination of a quasi-optical mirror line (matching of gyrotron output beam, polarisation adjustment) and a HE_{11} corrugated waveguide (I.D. 87 mm, for the transmission from the gyrotron hall to the plasma), both operating at atmospheric pressure. The beam parameters have been defined, and the construction of the support structure for the mirrors is finished. Several mirrors for the first gyrotron have been manufactured and installed at ASDEX Upgrade. The antenna beams were optimized and the corresponding design of the launcher reflectors was performed.
The multi-frequency operation of this system requires broadband performance of the transmission lines. In particular the properties of elliptical polarisers and polarisation twisters have been studied numerically and experimentally. It has been verified that rotators with nearly perfect phase shift at two frequencies (104 GHz and 140 GHz) can be designed. However, for elliptical polarisers, only a monotonously increasing phase shift seems possible (see Fig. 1). Therefore, the phase shift of two polarisers in series will be used for the system, which gives acceptable frequency dependence (see IPP, technology part of this report, and see also 1.2.5, Wood's anomaly).

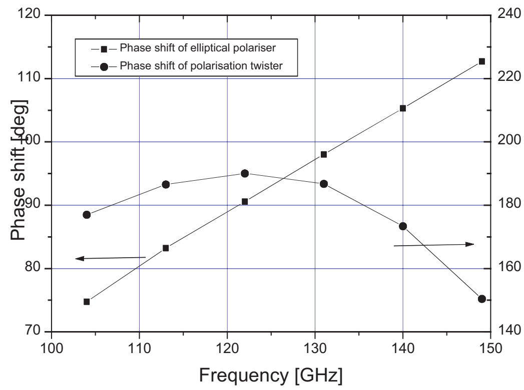

Figure 1: Frequency dependence of the phase shift difference of the two perpendicular E-field components.

1.1.2 MHD stability studies on ASDEX Upgrade

The occurrence of neoclassical tearing modes (NTM), driven by the gradients of the toroidal current density and the plasma pressure limits the energy content in a Tokamak plasma. To maximise the fusion power of a future machine the operation at high plasma pressure is foreseen – a regime where the occurrence of these modes is highly probable. Therefore, possibilities are explored to control or prevent such instabilities. The NTM's are associated with the development of magnetic islands with an initially relatively small width. Electron cyclotron current drive (ECCD) and electron cyclotron resonance heating (ECRH) which have a well localised power deposition to modify the current distribution within the islands are excellent candidates to stabilise the NTM's. On the tokamak ASDEX Upgrade both, ECCD and ECRH, are used to study the MHD stability of fusion plasmas.

1.1.2.1 Active control of neoclassical tearing modes using ECRH / ECCD on ASDEX Upgrade

Experiments have been conducted to investigate the possibilities of stabilising the m = 2, n = 1 mode. Fig. 2

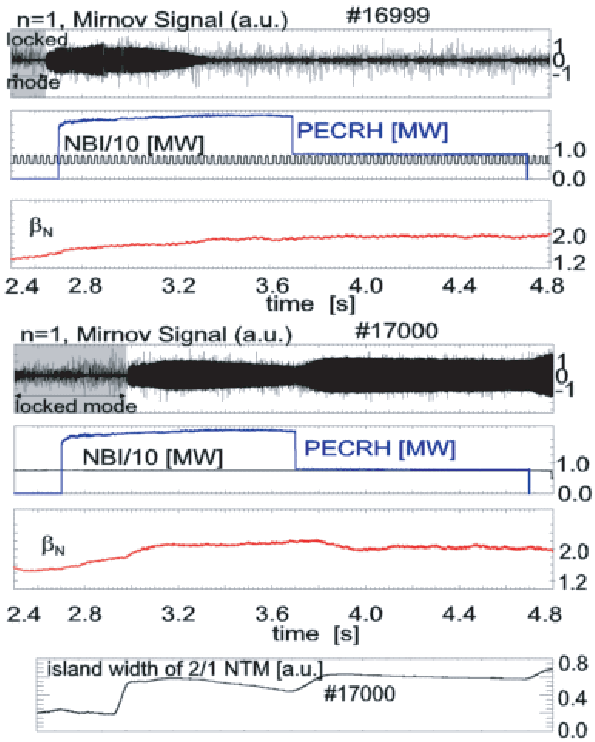

Figure 2: #16999, top: Complete suppression of 2/1 NTM. #17000, bottom: higher average NBI power, ECCD power is not sufficient for complete suppression.

illustrates a typical discharge where the 2/1 NTM is completely stabilised. In previous experiments on the suppression of the 3/2 NTM complete stabilisation in a steady state regime at $\beta_N \approx 2.6$ has been demonstrated. TORBEAM calculations predict a driven current at the q= 3/2 surface of up to 40 kA with 1.6 MW RF power. The total driven current and the current drive efficiency are considerably reduced in the case of 2/1 NTM at the q= 2 surface.

In Fig. 2 time traces showing the n=1 perturbation of the magnetic field, the heating power, and β_N are given for typical discharges. The discharge #16999 (Fig. 2, top) shows the successful suppression of the instability by ECCD.

In discharge #17000 (Fig. 2, bottom) the same parameters have been chosen, but the average NBI power and thus β_N have been increased by a small amount. In that case, the available ECCD power (1.9 MW, driven current up to 23 kA) is not sufficient to completely suppress the instability, and the island size shrinks only to 65 %.

1.1.3 ECR heating of high density plasmas using O2

ECRH at the second harmonic usually is launched in X-mode due to the nearly complete absorption of this mode. However, in plasmas with density above the X-mode cut-off density ($1.25 \cdot 10^{20}$ m^{-3} at 140 GHz), experiments with the O2 mode will be performed on ASDEX Upgrade.
The use of the O2 mode has the disadvantage, that absorption will be much less efficient, so that most of the launched wave will pass through the plasma and reach the inner wall. If this wave is reflected back in a controlled way and passes through the plasma a second time, heating efficiency will be increased by almost a factor of 2. Therefore, an in-vessel reflector will be designed at IPF to accomplish this task. To avoid high thermal loads on this mirror and/or on the rest of the inner wall, this mirror should have a geometry as similar as possible to the original wall tile that it will replace. For wave reflection in the optimal direction and polarisation under the condition of a predetermined large-scale geometric form, it is necessary to design the mirror surface as a holographic phase grating.
At present, numerical simulations are carried out to find the best grating geometry using the TORBEAM software package (to get the optimum injection angle and to get information about phase and amplitude distributions of the launched beam before reaching the mirror), and various electromagnetic field simulation tools were developed at IPF (to optimize the effect of the grated mirror to the wave).

1.1.4 ECRH system for WENDELSTEIN 7-X

As part of the work on the 140 GHz, 10 MW-CW ECRH system for the stellarator W7-X, IPF has taken responsibility for the quasi-optical transmission lines as well as for the development of the acceleration voltage modulator, the thyratron crowbars and the cathode heater supplies for the depressed collector gyrotrons which are under development at FZK Karlsruhe.

1.1.4.1 Multi-beam transmission system

In 2003, a major part of the mirrors for the transmission system on W7-X (Fig. 3) was fabricated and delivered. Most of these mirrors have been installed: The polarisers needed to adjust the proper polarisation of the beams, the beam combining optics which combine five 140 GHz beams each on the multi-beam waveguide (MBWG), and the MBWG mirrors themselves which guide the beams up to the end of the beam duct, where a distribution optics feeds the beams to various launcher ports on W7-X. The mirror blanks for the matching optics were fabricated as well, and the surface of the first MOU mirror pair was machined according to the beam parameters of the pre-prototype gyrotron "Maquette".

In the context of commissioning of this tube, a CW-version of a waveguide directional coupler is under test. Preliminary results show, that no loss of performance is expected for long pulses, however, the stray radiation level in the vicinity of the coupler should be lowered. The coupler is supplemented with calorimetry of the cooling water of the first mirror, which gives smooth power monitor signals for pulse lengths above 1 sec. For absolute power measurement in the short-pulse regime (<0.4 s), two different prototype calorimetric loads have been built, a load working with silicon oil as absorber and a load with water-cooled teflon pipes. As the tests of the teflon-pipe load are promising, this type is given priority; at present, the design is finalized.

In the frame of the development of prototype components, a novel design for a grating coupler was realised and investigated with good results. Drafting of special switching mirrors, absorbers, and other special components was completed. Thermal deformation tests on the prototype transmission line at IPF Stuttgart were performed confirming that a high transmission performance can be expected also for CW operation.

Figure 3: View into the transmission duct of the ECRH system on W7-X. The left picture shows matching optics and polarizers for one gyrotron, the upper picture is a view into the beam duct with two large multi-beam mirrors and the MD mirrors which can focus one beam at a time into the dummy loads seen at the bottom.

1.1.4.2 High-voltage system for gyrotron power control and tube protection

At IPP in Greifswald the first gyrotron pre-prototype (Maquette from Thales) was tested successfully starting Nov. 14th, 2003. For the power control of the gyrotron a regulator for the accelerating voltage was used similar to the device delivered from IPF to the gyrotron test facility at FZK. These regulators are improved and refurbished devices from the shut-down experiment W7-AS. For the application in Greifswald some special modifications were added like remote control by optical fibre link. Furthermore, a crowbar with thyratron and integrated cathode heater was tested successfully. This crowbar is used for the protection of the gyrotron and also for the test of the PSM high voltage supply from Thales.

The technical support of the high-voltage group at IPP in Greifswald was continued. Test of operation of the PSM-high-voltage supply has been supported by Pspice calculations. The main topics of these calculations were the noise and the transient behaviour of the high voltage at the gyrotron site. The equivalent circuit of the PSM-supply including parasitic capacitances and different lengths of the high-voltage cables was the basis for parametric studies. These studies revealed the need of compensation capacitors, which have to be connected at the PSM-supply site with capacity values matched for each gyrotron. Calculated and measured values for noise voltage and transient behaviour are in qualitative agreement.

The development of the prototypes of the high-voltage equipment (crowbar, cathode heater, high-voltage regulator for power modulation and monitoring) for the 140 GHz series gyrotrons has been continued. Especially the design of the PLC (Siemens SPS) and the related software development was done together with the ECRH group from IPP Greifswald.

The planned time schedule was delayed by several months due to technical reasons. Mainly the calculations of the modulator with Pspice showed that for obtaining the required slew rate additional elements like a variable high voltage capacitor and a transformer for neutralisation of the tube capacitance had to be added to the original design.

The prototypes are now ready for test. Preparations for the series production (definition of subcontractors, ordering of material etc.) are on the way.

1.1.5 ITER contributions: Development of a remote steering antenna

Among the activities for the remote steering antenna, computer codes developed at IPF to enable the calculation of the mode spectum, which is excited by the inclined gaussian beam at the input of the waveguide. With these mode amplitudes, it is possible to calculate the whole field structure inside the waveguide as well as the wall currents

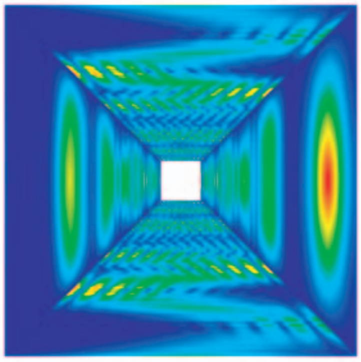

Figure 4: Distribution of the longitudinal magnetic fields inside a corrugated square waveguide used as a remote steering launcher.

due to the longitudinal magnetic fields (Fig. 4). Together with measurements of the reflection losses of a corrugated plate, which were done with a 3-mirror resonator, it is possible to determine the peak heat load in the waveguide walls as well as the total ohmic losses of the antenna.

Preparations are in progress for a high-power test of a remote steering launcher mock-up for ITER at IPP Greifswald. This activity is done under ITER task TW3-TPHE-ECHULA (Contract No. FU 06 CT 2003 – 00156).

In the W7-X ECRH beam duct, a beam will be coupled into the launcher mock-up by a beam shaping mirror and a movable steering mirror. The beam-shaping mirror is placed after mirror MD, which normally directs the beam into the dummy load (Fig. 3). It is planned to make calorimetric efficiency measurements as well as thermographic measurements of the radiation pattern and of the heat distribution at the waveguide walls. The necessary modifications of the waveguide as well as manufacturing of additional components are currently in progress.

1. 2 General developments in millimetre wave technology

1.2.1 Investigations of materials for in-vessel components and absorbers

Microwave properties of B_4C-coated in-vessel components of W7-X at 140 GHz (ECRH frequency) have been characterised. Investigations of samples with varying thickness (50µm ≤ d ≤ 300µm) on metallic substrates (Cu, Mo, TZM and SS) were carried out. The reflection coefficients R_p and R_s for polarisation parallel and perpendicular to the plane of incidence were measured at 140 GHz as a function of the angle of incidence α, and, for fixed α = 20°, as a function of frequency. From the measurements, the dielectric constant as well as angle- and polarisation-averaged reflection coefficients R_{av} were deduced. R_{av} is essential for the heat load induced by stray radiation from the ECRH heating system. Results for various coatings are listed in Table 1.

d (µm)	Substrate	ε_1	ε_2	$R(\alpha=0)$	R av.
50	TZM	-	-	1.0	0.92
100	TZM	6.9	20.8	0.54	0.58
150	Cu	5.9	6.0	0.33	0.49
190	TZM	22.5	7.6	0.63	0.60
300	Mo	10.9	16.6	0.47	0.50
300	SS	-	-	0.46	0.46
300	SS	29.	8.6	0.29	0.38

Table 1: Dielectric parameters ε_1, ε_2, reflection coefficients at perpendicular incidence as well as angle-averaged reflection coefficients for various samples.

For thin coatings (d < 200 µm), the parameters strongly depend on the thickness of the layer, which can be explained by the production process.

Due to the low reflection coefficient of the B_4C an incomplete absorption of the ECRH beams in the W7-X plasma will lead to high thermal loads of the B_4C- coated panels. Especially in the range 150 µm - 200 µm, resonant absorption up to 90% can occur. For this reason, wall protection elements with high reflectivity (like graphite) will be used close to the ECRH heating ports.

1.2.2 Frequency diplexers for oversized waveguides

The development of diplexers for combining and splitting microwaves at two different frequencies was continued. In addition to the diplexer based on the spatial Talbot effect in rectangular waveguides, another approach utilizes the angular Talbot effect. While the Talbot effect allows the prediction of optimum length for the diplexer, this can become very large, especially if the frequencies are close together.

By using an optimization algorithm, it is possible to find suitable small dimensions for diplexers, which have an overall efficiency of more than 95 % even for frequencies, which differ only slightly. As an example, Figure 5 shows the field distributions inside an optimized diplexer for 75 and 80 GHz, respectively. The length of the main waveguide is 1.09 m, the width is 3.72 cm, the mode conversion losses are 2.61% for 75 GHz and 3.38% for 80 GHz.

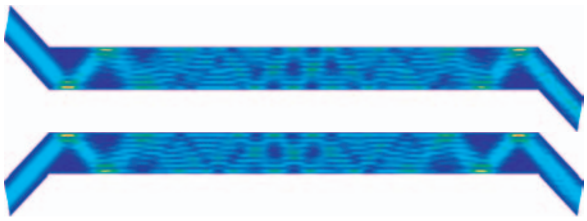

Figure 5: Field distributions inside an optimized diplexer for 80 GHz (top) and 75 GHz (bottom), respectively.

Another advantage of diplexers of this type is the bandpass characteristic, which makes them interesting for reflectometry systems.

1.2.3 Microwave beam propagation and diagnostics

Computer codes related to microwave beam propagation in free space and in quasi-optical waveguides were developed further and applied to actual problems, e.g. beam irradiation via a launcher mirror, improved mitre bend mirrors, reflectors for well defined power dispersion in microwave loads, and analysis of measured or calculated beam profiles for mode content.

The code for the beam profile analysis was extended to handle now also astigmatic beams. For example, the analysis of the electric field data from recent low-power measurements of the beam of the W7-X prototype gyrotron at the position of the window (z = 0) yields for the parameters of the desired TEM_{00} mode:

Beam waist: w_{0x} = 17.3 mm at z_{0x} = 112.0 mm,

w_{0y} = 19.8 mm at z_{0y} = 87.8 mm.

TEM_{00} content: 95.5 % of the total beam power.

Fig. 6 shows the x- and y-profiles of the amplitude of a measured electric field distribution compared with the corresponding profiles that result, when all the calculated contents of Hermite-Gaussian modes, TEM_{00} through TEM_{55}, are summed up.

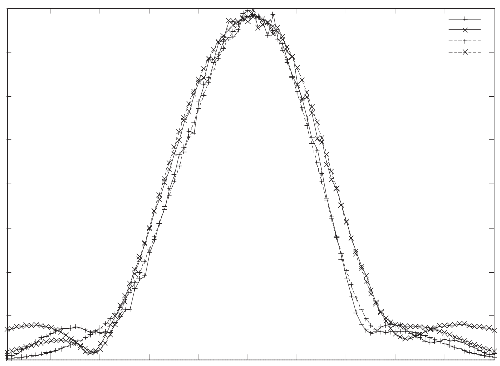

Figure 6: W7-X prototype gyrotron, low-power measurement at the window: Measured versus reconstructed amplitude profiles

1.2.4 Wood's anomaly in the design of corrugated mirrors

For broadband polarizers, where the groove period p is in the region $\lambda/2 < p < \lambda$, Wood's anomaly can occur, which leads to the almost total extinction of the 0^{th} order reflected power in a narrow frequency band. The lost power is converted into heat or radiated away as a leaky wave which can lead to serious problems at the MW levels considered.
In experiments, the occurrence of Wood's anomaly was found to be a function of frequency, geometry (depth, period length) and shape (rectangular, rounded) of the polarizing grating as well as the angle of incidence. Modelling was performed with the FDTD (Finite Difference Time Domain) method, and very good agreement with the measurements is found.
As an example Figure 7 shows the calculated phase difference for polarisation parallel and perpendicular to the grooves of the grating. For a finite angle of incidence (e.g. 5.5°) the anomaly is observed around 141 GHz. As expected for perpendicular incidence no anomaly is seen.

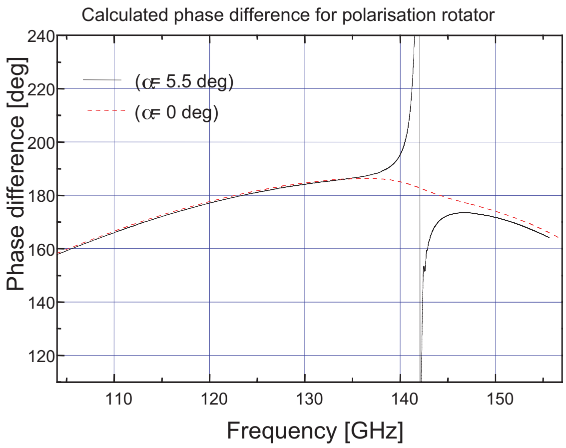

Figure 7: Calculated phase difference for two angles of incidence (0° and 5.5°).

1.3 Millimetre wave diagnostics

1.3.1 Doppler reflectometer for density fluctuation and plasma rotation studies

Doppler reflectometry is a diagnostic method for the investigation of propagating density perturbations. Whereas in a standard reflectometer transmitter and receiver antennas are oriented perpendicularly to the plasma surface the Doppler reflectometer probes the plasma by a microwave signal with a line of sight, which is non-perpendicular with respect to the reflecting layer. The diagnostic selects density perturbations with finite wave number $k_\perp$ in the reflecting layer defined by the tilt angle. For a given propagation velocity of these fluctuations this leads to a *Doppler shift* of the returning microwave. The accuracy in the measurement of both reflected power and its frequency shift is determined by the integration time and the statistical properties of the probed fluctuations.
Numerical simulations can optimise the antenna spot size with respect to plasma curvature effects in order to obtain maximum k-resolution. From the Doppler shift of the returning microwave the propagation velocity of the selected density perturbations $v_\perp$ can then be directly obtained.

It is found that a useful interpretation of the measurements in general is only possible if the design of the reflectometer (antenna geometry, receiver) and relevant plasma discharge parameters (density profile, magnetic field configuration) are taken in consideration. Specially developed computer programs (FDTD-code, equivalent network code) allow to calculate the propagation of the microwave in the inhomogenous plasma. These computations yield the *instrument function* of the reflectometer with respect to the input plasma parameters. The numerical code is being extended to include the effects of mode conversion on reflectometry experiments.

1.3.2 Microwave reflectometry on W7-AS

The final experimental campaign of W7-AS comprises the first island-divertor operation as well as externally triggered radial electric fields. For this campaign fast changes in the radial profile of turbulence level and propagation velocity were diagnosed. A total of seven homodyne reflectometers spanning the range of 70 GHz to 110 GHz were installed.
For an antenna with a fixed tilt angle of +14 deg with respect to the normal onto the reflecting layer values of up to 10 MHz were observed for the Doppler frequency shift which correspond to a local poloidal velocity of up to 70 km/s. A second symmetric antenna with -14 deg allows differential measurements if the orientation of the cut-off layer changes with the magnetic configuration. Evaluation of the experimental data is still under way. The main results are:

- Temporal and radial dependence of the signal power in discharges with different confinement properties. An example is given in the IPP part (W7-AS, Chapter 2.3).
- Dependence of poloidal propagation velocity of the turbulence in the gradient region and energy confinement. In cases where a comparison of the poloidal propagation velocity of the turbulence with the results from radial electric field measurements (CRX spectroscopy) were available agreement was found within the error bars of the diagnostics.
- *Time-of–flight*-measurements were performed with two poloidally separated antennas which measure the Doppler shift in addition. TOF is the second independent diagnostic method for the measurement of the propagation velocity of the turbulence. Fig. 8 shows the result from the cross-correlation of two reflectometers. The resulting velocity of 23 km/s agrees well with the value obtained from the Doppler frequency shift of the returning signal measured simultaneously. This demonstrates that the two methods are indeed complementary.

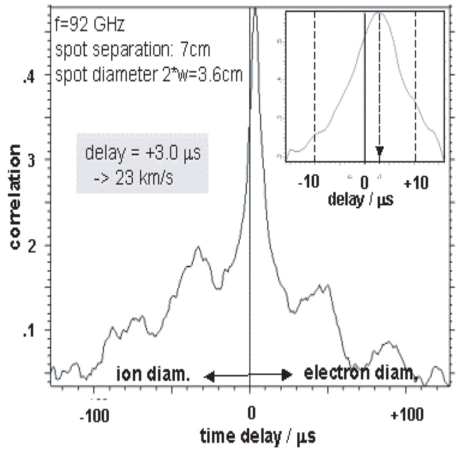

Figure 8 : Time-of-flight method to measure the propagation velocity of the turbulence. The inlay shows an enlargement of the peak maximum.

1.3.3 Microwave reflectometry on ASDEX Upgrade

For given discharge parameters the FDTD-code can calculate the instrument function for a given geometry of the reflectometer. In addition numerically calculated turbulence can be implemented into the numerical reflectometer. From the resulting time series the frequency spectra and statistical properties of these signals can be calculated. This allows to find out if and to what degree details of the turbulence can be observed by the instrument function of the Doppler reflectometer. The comparison of numerically generated time series of the numerical reflectometer with receiver signals in actual plasma experiments with corresponding discharge parameters also allows conclusions about the relevance of numerical turbulence codes.

Staff

W. Kasparek, P. Brand, G. Gantenbein, M. Grünert, H. Hailer, E. Holzhauer, H. Kumric, G. A. Müller, R. Munk, U. Niethammer, B. Plaum, K. Schwörer, R. Wacker, in collaboration with IPP Garching, FZK Karlsruhe, IAP Nizhny Novgorod and NIFS Toki.

2 Plasma Edge Diagnostics

2.1 Spectroscopic measurements of plasma parameters in the divertor of ASDEX Upgrade

Laser induced fluorescence (LIF) via fiber is a new diagnostic on ASDEX Upgrade for the investigation of space resolved temperature and density profiles of hydrogen isotopes, wall materials and impurities.

The frequency doubled Nd:YAG-Laser (λ=532 nm, τ_{pulse}=7ns) is used as a pump laser for the dye laser. The spectral ranges of the system depend on the applied dye. The measurement was done with the DCM dye with a specified spectral range between 640 and 670 nm. A new dye laser is used with a spectral resolution of $\lambda / \Delta\lambda \geq 3 \cdot 10^5$, which will allow to determine the velocity distribution of the detected species.

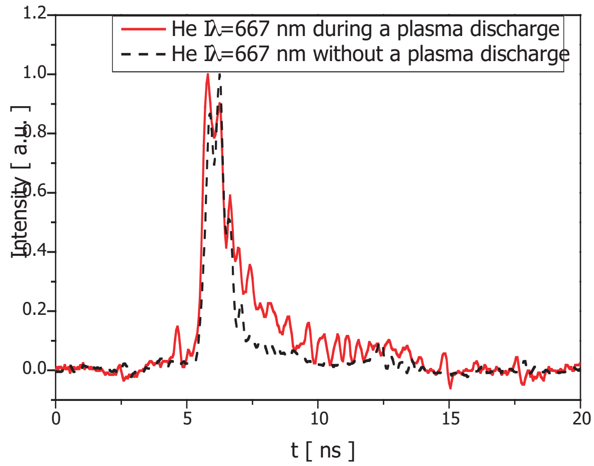

Figure 9: LIF signal of a He I line in an ECR plasma discharge.

Fig. 9 shows an example of a LIF signal in a laboratory ECR He plasma. The spectral tuning with this high resolution DYE-Laser system allows the determination of the velocity distribution. The result of the wavelength scan is shown in Fig. 10. The line is determined by the Doppler broadening with a gas temperature of 350 K. The measurement requires that the excited atomic level is not saturated by the laser. The opto-galvanic effect on a hydrogen filled hollow cathode lamp is used to calibrate the dye laser wavelength by tuning with the grating. This calibration was done with an accuracy of ± 3.5 pm.

Furthermore, is it possible to saturate the atomic level and determine the density. This assumes an intensity calibration of the detection system which was done by the Rayleigh scattering in N_2 gas. The experimental results of an ECR plasma show a helium density in a range of 10^{11} cm^{-3}. The density is related to the 1s2p $^1P^o$ atomic level.

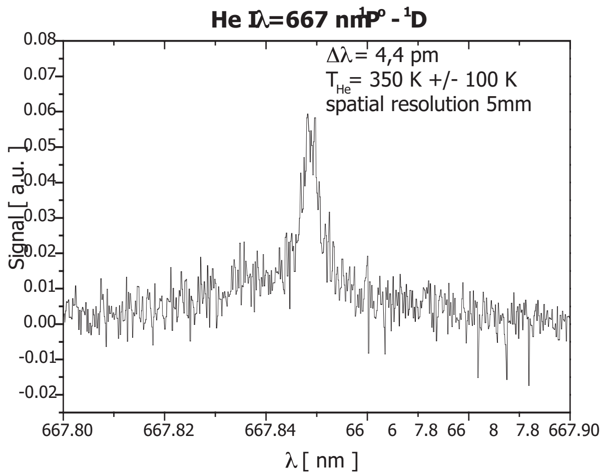

Figure. 10: Doppler broadening dominated velocity distribution of the He I line at a wavelength of 667 nm

The whole system was transferred to IPP Garching and was set up at ASDEX Upgrade. The experimental set up was implemented into the ASDEX Upgrade timing and data acquisition. Furthermore, investigations were performed to examine the influence of the magnetic field on the laser and diagnostic system, which shows no interferences between the magnetic field, and the experimental set up.

During the shut down phase of ASDEX Upgrade the optical path of the laser system to the torus was improved and re-calibrated. As the result of this improvement in the divertor region we measured laser energy of up to 8 mJ on a spot of 7 mm diameter, which is an enhancement of one order of magnitude.

The experimental set up will now be started with the measurements and improvements of the detection system and the coupling of the laser into the fibre.

2.2 Erosion studies from emission and absorption spectroscopy

The determination of erosion mechanisms and erosion rates as a function of the plasma parameters and surface temperature is of major importance not only for tests of thermal protection materials for reusable space transportation systems but also for plasma facing components in thermonuclear fusion devices. Plasma jets interacting with targets of the material in question are applied for these measurements and material tests. One of the methods is to study the erosion of a C/C-SiC target in such a plasma jet by high resolution emission and absorption spectroscopy of Si I resonance spectra of the multiplet lines at 251 nm and the singlet lines at 263 nm, 288 nm or 390 nm, respectively. The silicon is eroded by the plasma jet and forms a disc like radiating cloud in front of the target. Further improvement of the experimental set up was done to measure the silicon density as a function of time and surface temperature. This established method was adapted to the Ti I resonance spectra at 365 nm. Fig. 11 shows the experimental results in which the ratios of the measured intensity (straight line) is compared to the NIST database (stars).

The results show a self-absorption with which it is possible to determine the ground state density of the titanium. In addition to the determination of the spatial distribution of the ground state density of silicon from the line ratios of the Si I multiplet at 251 nm the determination of the electron temperature and electron density from the line ratios was

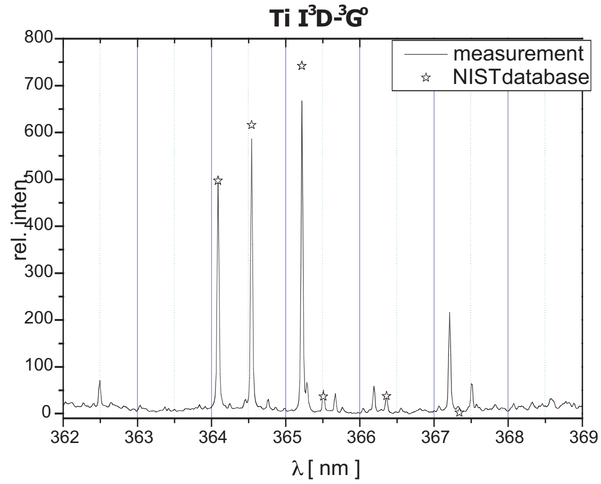

Figure 11: Measurements of titanium neutral density

further improved. The determination of this plasma parameter requires an atomic model for silicon. The atomic model and the electron collisional excitation coefficients to the relevant energy levels were calculated in a co-operation with H.P. Summers, Strathclyde University (Scotland), using modelling of the Si atom with the code SUPER STRUCTURE and R-Matrix calculations of the cross sections especially for low energies near threshold.

Tab. 2.1 shows a part of the comparison between the numerically calculated and the NIST database data. The numerical results are in good agreement with the NIST data.

configuratio n	term	J	level [cm $^{-1}$] NIST database	level [cm $^{-1}$] calculated
$3s^23p^2$	^3P	0	0	0
		1	77.1	136
		2	223.2	387
$3s^23p^2$	^1D	2	6298.8	8640
$3s^23p^2$	^1S	0	15394	15626
$3s^23p4s$	$^3P^o$	0	39683	34249
		1	39760	34636
		2	39955	34634
$3s^23p4s$	$^1P^o$	1	40991	36589

Tab. 2.1: Comparison between the numerically calculated energy values and the NIST database

Staff

U. Schumacher, G. Dodel, K. Hirsch, P. Lindner, T. Kubach, J. Schneider and R. Stirn

3 Publications, Conference Reports, Patents, Doctoral Theses, Diploma Theses, Reports, And Seminar Talks

3.1 Publications

B. Plaum, E. Holzhauer and W. Kasparek: Optimization of a Frequency Diplexer Based on the Talbot Effect in Oversized Rectangular Waveguides. Int. J. Infrared and Millimeter Waves **24** (2003), 311-326;

P. Brand and G.A. Müller, Circuit design and simulation of a HV-supply controlling the power of 140 GHz 1 MW gyrotrons for ECRH on W7-X. Fusion Eng. Design **66-68** (2003), 573 – 577.

Gantenbein, G., Keller, A., Leuterer, F., Maraschek, M., Suttrop, W., Zohm, H., ASDEX Upgrade Team, 2003, Neoclassical tearing mode suppression with ECRH and current drive in ASDEX Upgrade. AIP Conference Proceedings **694** (2003), 317-320.

W. Kasparek, H. Idei, S. Kubo and T. Notake: Beam Waveguide Reflector with Integrated Direction-Finding Antenna for In-Situ Alignment. Int. J. Infrared and Millimeter Waves **24** (2003) 451-472.

W. Kasparek, G. Gantenbein, B. Plaum, R. Wacker, A.V. Chirkov, G.G. Denisov, S.V. Kuzikov, K. Ohkubo, F. Hollmann, D. Wagner: Performance of a remote steering antenna for ECRH/ECCD applications in ITER using four-wall corrugated square waveguide. Nucl. Fusion **43** (2003), 1505 - 1512.

H. Hailer, G. Dammertz, V. Erckmann, G. Gantenbein, F. Hollmann, W. Kasparek, W. Leonhardt, M. Schmid, P.G. Schüller, M. Thumm, M. Weissgerber: Mirror Development for the 140 GHz ECRH System of the Stellarator W7-X. Fusion Eng. Des. **66-68** (2003), 639 – 644.

K. Ohkubo, S. Kubo, T. Shimozuma, H. Idei, Y. Yoshimura, T. Notake and W. Kasparek: Extension of steering angle in a square corrugated waveguide antenna. Fusion Eng. Des. **65** (2003) 657 – 672.

V. Erckmann, H.P. Laqua, H. Maaßberg, N.B. Marushchenko, W. Kasparek and G.A. Müller: 20 years of ECRH at W7-A and W7-AS. Nucl. Fusion **43** (2003) 1313-1323.

H.P. Laqua, H. Maassberg, F. Volpe, W7-AS Team and ECRH-Group IPF Stuttgart: Electron Bernstein wave heating and current drive in overdense plasmas at the W7-AS stellarator. Nucl. Fusion **43** (2003) 1324-1328.

V. Erckmann, H. Braune, H.P. Laqua, G. Michel, G,. Dammertz, M. Thumm, G. Gantenbein, W. Kasparek, G.A. Müller: The 10 MW ECRH and CD System for W7-X. High Energy-Density And High-Power RF: 6th Workshop, Berkeley Springs, USA, ed. S.H. Gold and G.S. Nusinovich, AIP Conf. Proc. **691** (2003) 213.

V. Erckmann, U. Gasparino, H.P. Laqua, H. Maaßberg, N.B. Marushchenko, H. Renner, M. Rome, W7-AS-team, W. Kasparek, G.A. Müller: 20 years of ECRH at W7-A and W7-AS. Strong Microwaves in Plasmas, ed. A.G. Litvak, ISBN 5-8048-0039-6, Nizhny Novgorod, Russia (2003), Vol. 1, 281 – 295.

W. Kasparek, G. Dammertz, V. Erckmann, G. Gantenbein, H. Hailer F. Hollmann, L. Jonitz, H.P. Laqua, W. Leonhardt, G. Michel, M. Schmid, P.G. Schüller, K. Schwörer, R. Wacker, M. Weissgerber: The transmission system for ECRH on the Stellarator W7-X: Design issues and test of prototype components. Strong Microwaves in Plasmas, ed. A.G. Litvak, ISBN 5-8048-0039-6, Nizhny Novgorod, Russia (2003), Vol. 1, 333 – 339.

G. Dammertz, S. Alberti, A. Arnold, E. Borie, V. Erckmann, G. Gantenbein, E. Giguet, R. Heidinger, J.P. Hogge, S. Illy, W. Kasparek, K. Koppenburg, M. Kuntze, H.P. Laqua, G. LeCloarec, Y. LeGoff, W. Leonhardt, C. Lievin, R. Magne, G. Michel, G. Müller, G. Neffe, B. Piosczyk, M. Schmid, M. Thumm, M.Q. Tran: Status of the 1 MW, 140 GHz, CW Gyrotron for W7-X. Strong Microwaves in Plasmas, ed. A.G. Litvak, ISBN 5-8048-0039-6, Nizhny Novgorod, Russia (2003), Vol. 1, 16 – 28.

M. Wanner, V. Erckmann, J.H.Feist, W. Gardebrecht, D. Hartmann, R. Krampitz, H. Niedermeyer, H. Renner, Th. Rummel, F. Schauer, L. Wegener, F. Wesner, G.A. Müller, W. Kasparek, M. Thumm, G. Dammertz: Status of Wendelstein W7-X construction. Nucl. Fusion **43** (2003) 416 - 424.

Günter, S., Gantenbein, G., Gude, A., Idochine, V., Maraschek, M., Mück, A., Saarelma, S., Sauter, O., Sips, A.C.C., Zohm, H., ASDEX Upgrade Team, 2003, Neoclassical tearing modes on ASDEX Upgrade: improved scaling laws, high confinement at high β_N and new stabilization experiments. Nucl. Fusion **43** (2003), 161-167.

F. Leuterer, R. Dux, G. Gantenbein, J. Hobirk, A. Keller, K. Kirov, M. Maraschek, A. Mück, R. Neu, A.G. Peeters, G. Pereverzev, F. Ryter, J. Stober, W. Suttrop, G. Tardini, H. Zohm and AUG Team, 2003, Recent ECRH results in ASDEX Upgrade. Nucl. Fusion **43** (2003), 1329-1342.

Leuterer, F., Kirov, K., Monaco, F., Münich, M., Schütz, H., Ryter, F., Wagner, D., Wilhelm, R., Zohm, H., Franke, T., Voigt, K., Thumm, M., Heidinger, R., Dammertz, Koppenburg, K., Gantenbein, G., Hailer, H., Kasparek, Müller, G.A., Bogdashov, A., Denisov, G., Kurbatov, V., Kuftin, A., Litvak, A., Malygin, S., Tai, E., Zapevalov, V., 2003, Plans for a new ECRH system at ASDEX upgrade. Fusion Eng. Design **66-68** (2003), 537-542.

Zohm, H., Gantenbein, G., Isayama, A., Keller, A., La Haye, R.J., Maraschek, M., Mück, A., Nagasaki, K., Pinches, S.D., Strait, E.J., 2003, MHD limits to tokamak operation and their control. Plasma Phys. Control. Fusion **45** (2003), 163-173.

3.2 Conference Reports

US/EU/JP Workshop on RF Technology, Los Angeles, 12. – 14. 2. 2003:

W. Kasparek, G. Gantenbein, B. Plaum, R. Wacker, A.V. Chirkov, G.G. Denisov, S.V. Kuzikov, K. Ohkubo, F. Hollmann, D. Wagner: Performance of a remote steering antenna for ECRH/ECCD applications using four-wall corrugated square waveguide.

US/EU/JP Workshop on RF Technology, Tokai, Japan, 24. – 26. 9. 2003:

G. Dammertz, H. Braune, V. Erckmann, G. Gantenbein, W. Kasparek, H. P. Laqua, W. Leonhardt, G. Michel, G. Mueller, G. Neffe, B. Piosczyk, M. Schmid, M. Thumm, Design and Experimental Results of the 10 MW, 140 GHz ECRH-System for the Stellarator W7-X.

15th Topical Conference on Radio Frequency Power in Plasmas, Moran, Wyoming 19. – 21. 5. 2003:

Gantenbein, G., Keller, A., Leuterer, F., Maraschek, M., Suttrop, W., Zohm, H., ASDEX Upgrade Team: Neoclassical tearing mode suppression with ECRH and current drive in ASDEX Upgrade. AIP Conference Proceedings 694, 317-320.

30th EPS Conference on Controlled Fusion and Plasma Physics, St. Peterburg, 7. – 11. 7. 2003

Zohm, H., Gantenbein, G., Isayama, A., Keller, A., La Haye, R.J., Maraschek, M., Mück, A., Nagasaki, K., Pinches, S.D., Strait, E.J., 2003, MHD limits to tokamak operation and their control. Plasmas Physics and Controlled Fusion, 45, A163-A173.

Int. Conf. on Plasma Science, Jeju, Korea, 2. - 5. 6. 2003:

G. Dammertz, H. Braune, V. Erckmann, G. Gantenbein, W. Kasparek, H.P. Laqua, W. Leonhard, G. Michel, G.A. Müller, G. Neffe, B. Piosczyk, M. Schmid, M. Thumm: Progress in the 10 MW ECRH CD System for the Stellarator W7-X. Proeedings.

15th Joint Russian German Meeting on ECRH and Gyrotrons, Karlsruhe, Stuttgart and Garching, June 25-July 1, 2003:

G. Müller: Microwave Sintering of Ceramics at IPF Stuttgart: A Retrospective View.

P. Brand and G. Müller: HV-System for Power Control and Protection of the W7-X Gyrotrons: Circuit Simulation and Optimization.

G. Gantenbein et al.: Optimisation of broadband polarizers for high power mm-wave transmission systems.

H. Kumric et al.: Development of transmission line components at frequencies of 14 – 35 GHz for application with ECR ion sources.

W. Kasparek et al.: Status of the 140 GHz / 10 MW CW Transmission System for ECRH on the Stellarator W7-X.

B. Plaum et al.: Design and Characterization of a Diplexer based on the Talbot Effect in Rectangular Waveguides.

B. Plaum et al.: Characterization of a Remote Steering Antenna for ECRH/ECCD in ITER .

E. Holzhauer, and M. Hirsch: Doppler-Reflectometry: Resolution in Space and Time.

Workshop on Microwave Reflectometry, San Diego, 5 - 8 May 2003:

M. Hirsch, E. Holzhauer, Doppler reflectometry with optimized temporal resolution for the measurement of turbulence and its propagation velocity, Proceedings.

IAEA-Technical Meeting on ECRH Physics and Technology for ITER, Seeon, Germany, 14. – 16. 7. 2003:

W. Kasparek, G. Dammertz, V. Erckmann, G. Gantenbein, H. Hailer F. Hollmann, L. Jonitz, H.P. Laqua, W. Leonhardt, G. Michel, G. Neffe, M. Schmid, K. Schwörer, R. Wacker, M. Weissgerber: The Multi-Megawatt Transmission System for the Stellarator W7-X and its Relevance for ITER ECRH Design. Proceedings, ed. H. Zohm, IPP Garching.

28th Int. Conf. on Infrared and Millimeter Waves, Otsu, Japan, 29..9. – 2. 10. 2003:

B. Plaum, G. Gantenbein, M. Grünert, W. Kasparek, H. Kumric, K. Schwörer, R. Wacker, A.V. Chirkov, G.G. Denisov, S.V. Kuzikov, K. Ohkubo, D. Wagner: Performance of a remote steering antenna for ECRH/ECCD applications Proceedings, ed. N. Hiromoto (2003), 383-384.

K. Ohkubo, W. Kasparek, Extension of the operating rage of a remote steering antenna. Proceedings, ed. N. Hiromoto (2003), 381 -382.

W. Kasparek, G. Dammertz, V. Erckmann, G. Gantenbein, H. Hailer F. Hollmann, L. Jonitz, H.P. Laqua, W. Leonhardt, G. Michel, G. Neffe, M. Schmid, K. Schwörer, J. Shi, R. Wacker, M. Weissgerber: Status of the 140 GHz / 10 MW CW Transmission System for ECRH on the Stellarator W7-X. Proceedings, ed. N. Hiromoto (2003), 367 - 368.

T. Notake, H. Idei, S. Kubo, T. Shimozuma, S. Kobayashi, Y. Mizuno, S. Ito, Y. Yoshimura, Y. Takita, K. Ohkubo, W. Kasparek, R. Kumazawa, and T. Watari, Polarization Monitor of high-power mm-wave for ECR/ECCD in LHD. Proceedings, ed. N. Hiromoto (2003), 411 – 412.

G. Dammertz, S. Alberti, A. Arnold, E. Borie, V. Erckmann, G. Gantenbein, E. Giguet, R. Heidinger, J.P. Hogge, S. Illy, W. Kasparek, K. Koppenburg, M. Kuntze, H.P. Laqua, G. LeCloarec, F. Legrand, W. Leonhardt, C. Lievin, R. Magne, G. Michel, G. Müller, G. Neffe, B. Piosczyk, M. Schmid, K. Schwörer, M. Thumm, M.Q. Tran: Prototype of a 1 MW, CW Gyrotron at 140 GHz for Wendelstein7-X. Proceedings, ed. N. Hiromoto (2003), 121 - 122.

Frühjahrstagung der Deutschen Physikalischen Gesellschaft, Fachausschuß Plasmaphysik, Aachen, März 18–21, 2003:

R. Stirn, K. Hirsch, P. Lindner, B. Roth und U. Schumacher: Determination of electron temperatur and electron density from inensity ratios of Si I. Verhandl. DPG P 10 33/2003 (2003) Poster P.10.25.

R. Stirn, K. Hirsch, P. Lindner, B. Roth und U. Schumacher: Silicon erosion behavior of coated and uncoated C/C-SiC heat shielding materials for the re-entry process into the earth atmosphere. Verhandl. DPG P 19 48/2003 (2003) Vortragr P.19.2.

3rd Inter. Symp. on Atmospheric Reentry Vehicles and Systems, Arcachon (France), 24-27 March 2003:

P. Lindner, K. Hirsch, B. Roth, J. Schneider, R. Stirn, U. Schumacher: In Situ Determination of the Erosion Rate of Heat Shield Materials in Re-entry Simulation Experiments. Paper in print

3.3 Doctoral Thesis

Julius Pretterebner: Kompakte quasi-optische Antennen im überdimensionierten Rundhohlleiter

3.4 Diploma Theses

Uwe Niethammer: Entwicklung eines Hohlleiterdiplexers basierend auf dem Talboteffekt im Winkelraum

Timo Kubach: Untersuchungen von gepulsten Mikrowellen-erzeugten Plasmen

3.5 Seminar Talks

G. Gantenbein: Remote Steering – Ein Antennenkonzept für ECRH und ECCD. IHM-Kolloquium, Forschungszentrum Karlsruhe, 17. 7. 2003

W. Kasparek: Developments for the ITER remote steering antenna and plans for high-power tests at the ECRH installation of W7-X. Kolloquium at FIR Center, Fukui University, 10.10.2003

B. Plaum: Optimierungsalgorithmen für HF-Komponenten.
IHM-Kolloquium, FZ Karlsruhe, 05. 06. 2003.

P. Lindner : Plasma beim Wiedereintritt – Hitzeschutzschild, Haus der Wirtschaft Stuttgart, 20 February 2003

U. Schumacher: Plasma – Zustand der Materie im Weltraum, Haus der Wirtschaft Stuttgart, 20. Februar 2003

U. Schumacher: Materialprobleme in der Fusionsforschung, Max-Planck-Institut für Metallforschung, Stuttgart-Büsnau, 24. Juni 2003

U. Schumacher: Von der Mikrowelle zur Fusion, NTI Karlsruhe, 5. August 2003

U. Schumacher: Grundlagen der Plasmaphysik, WE-Heraeus-Ferienkurs für Physik, Greifswald, 6. Oktober

Department of Electrical and Electronic Engineering

Head: Prof. Harald Weber

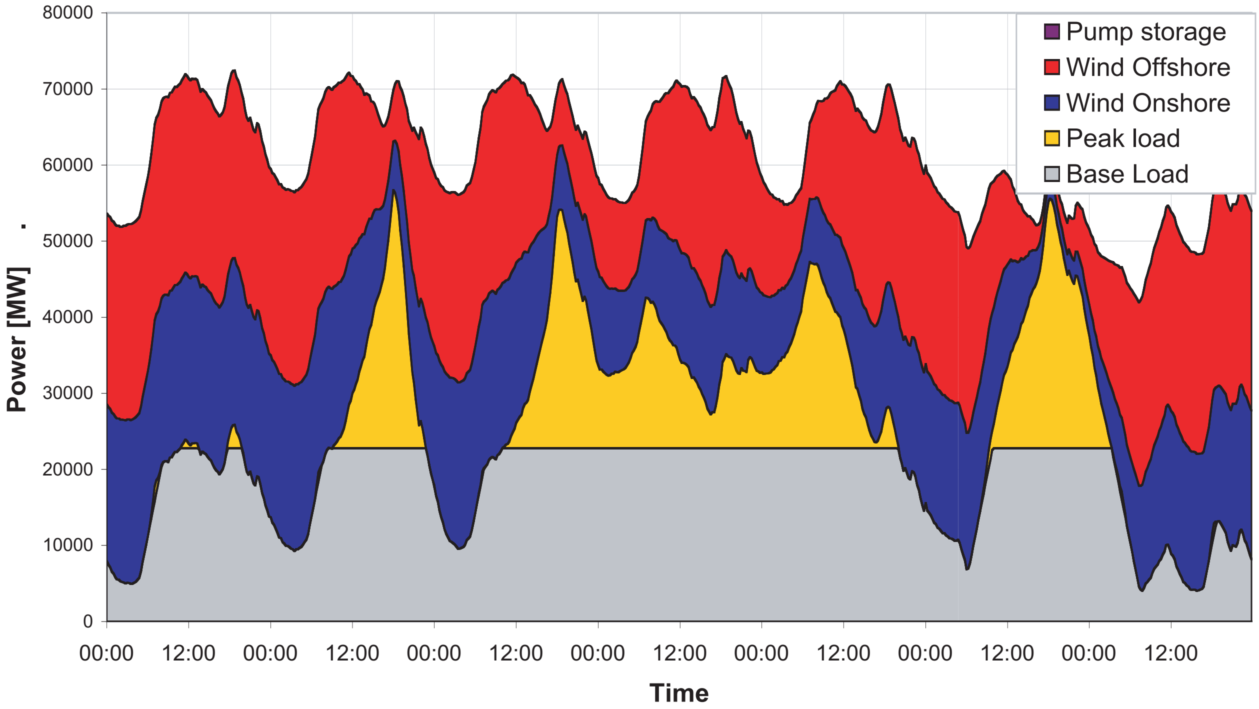

Figure 1: In picture presented a strong wind scenario over one week. As depicted, the base load power plants are displaced by the wind.

1. Future electricity networks

Especially the introduction of intermittent electricity sources and the diffusion of distributed generation will make it necessary to improve the electricity network capacities and control mechanisms and will make the introduction of completely new dispatching philosophies necessary. In the centre of the investigation is the question, which costs the development of the wind energy in Germany for the power plant park and the electricity net has? Basis for the technical analysis is the software tool DIgSILENT PowerFactory. Technical requirements, like availability of primary and secondary control, available power plants for regulation of voltage and reactive power as well as enough short-circuit power are investigated with DIgSILENT.

For the economical investigations the software tool GAMS is used, which is the leading tool for the development, solution, and management of large-scale optimisation problems. In the economic model all lines and power plants (coal, natural gas, water) are as implemented in the technical model. Further are considered efficiencies, capital costs as well as variable costs (fuel costs) of the lines and power plants. The economic model determines the cost-minimal driving fashion of the power plants and the electricity net. First test results of the economic model are: Development of the interconnect capacitances in the net particularly in the northern RWE and e.on area, displacement of base load power plants and development of the power plant park, particularly the peak load power plants (natural gas). Furthermore the power plants drive more frequently in the economically unfavourable partial load range, increased losses during transmission of the energy and increased need of control power due to the high feed of wind energy. As summary can be determined: The costs of the energy production and transmission are increasing by high feed of wind energy.

Scientific Staff

Dipl.-Ing. T. Haase, Dipl.-Ing A. Holst, Prof. H. Weber

Publications

Publications and Conference Reports

1. *Abdullaev*, S.S., K.H. Finken*, M.W. Jakubowski*, M. Kobayashi*, D. Reiser*, A.M. Runov and D. Reiter*:* Overview of magnetic structure induced by the TEXTOR-DED and the related transport. In: Proceedings of the 19th Fusion Energy Conference, Lyon 2002, (Ed.) M.Spak. IAEA, Vienna 2003, IC/P-02.

2. *Allfrey*, S.J. and R. Hatzky:* A revised _f algorithm for nonlinear PIC simulation. Computer Physics Communications **154**, 98-104 (2003).

3. *Andreev*, V.F., K. Kirov, A.V. Sushkov*, Yu.N. Dnestrovskij*, F. Leuterer G. Pereverzev, K.A. Rzumova*, F. Ryter and ASDEX Upgrade Team:* Analysis of ECRH Switch On/Off Events in ASDEX Upgrade. In: Proceedings of the 30th EPS Conference on Controlled Fusion and Plasma Physics, St. Petersburg 2003, (Eds.) R.Koch, S.Lebedev. ECA 27A, European Physical Society, Geneva 2003, P-1.186.

4. *Andreeva, T., C.D. Beidler, Yu. Igitkhanov, E. Harmeyer, F. Herrnegger, J. Kisslinger, E. Polunovskiy and H. Wobig:* Burn Control in a Helias Power Reactor. In: Proceedings of the 30th EPS Conference on Plasma Physics and Controlled Fusion, St. Petersburg 2003, (Eds.) R.Koch, S.Lebedev. ECA 27A. European Physical Society, Geneva 2003, P-1.8.

5. *Andreeva, T., C.D. Beidler and J. Kisslinger:* Equilibrium, Stability and Transport Analysis for Reduced and Controlled Fusion. In: Proceedings of the 30th EPS Conference on Plasma Physics and Controlled Fusion, St. Petersburg 2003, (Eds.) R.Koch, S.Lebedev. ECA 27A. European Physical Society, Geneva 2003, P-1.7.

6. *Andrew*, P., J.P. Coad*, T. Eich, E. Gauthier*, A. Herrmann, G.F. Matthews*, V. Riccardo*, M. Stamp* and Contributors to the EFDA-JET Work Programme:* Thermal Effects of Surface Layers on Divertor Target Plates. Journal of Nuclear Materials **313-316**, 135-139 (2003).

7. *Angioni, C., T.P. Goodman*, M.A. Henderson* and O. Sauter*:* Effects of Localized Electron Heating and Current Drive on the Sawtooth Period. Nuclear Fusion **43**, 455-468 (2003).

8. *Angioni, C., A.G. Peeters, X. Garbet*, F. Ryter, M. Apostoliceanu, A. Manini, G.V. Pereverzev, G. Tardini and ASDEX Upgrade Team:* Theoretical Understanding of Density Peaking: Dependence on Collisionality and on Heating Profiles. In: Proceedings of the 30th EPS Conference on Plasma Physics and Controlled Fusion, St. Petersburg 2003, (Eds.) R.Koch, S.Lebedev. ECA 27A. European Physical Society, Geneva 2003, O-3.3A.

9. *Angioni, C., A.G. Peeters, G.V. Pereverzev, F. Ryter, G. Tardini and ASDEX Upgrade Team:* Density Peaking, Anomalous Pinch, and Collisionality in Tokamak Plasmas. Physical Review Letters **90**, 205003 (2003).

10. *Angioni, C., A.G. Peeters, G.V. Pereverzev, F. Ryter, G. Tardini and ASDEX Upgrade Team:* Theory-based modeling of particle transport in ASDEX Upgrade H-mode plasmas, peaking, anomalous pinch and collisionality. Physics of Plasmas **10**, 3225-3239 (2003).

11. *Asakura*, N., A. Loarte*, G. Porter*, V. Philipps*, B. Lipschultz*, A. Kallenbach, G. Matthews*, G. Federici*, A. Kukushkin*, A. Mahdavi*, A.W. Leonard*, D. Whyte*, K. Itami*, H. Takenaga*, A.V. Chankin*, S. Higashijima*, T. Nakano*, A. Herrmann, T. Eich and B. LaBombard*:* Studies of ELM heat load, SOL flow and carbon erosion from existing Tokamak experiments, and projections for ITER. In: Proceedings of the 19th Fusion Energy Conference, Lyon 2002, (Ed.) M.Spak. IAEA, Vienna 2003, CT/P-01.

12. *Atanasiu*, C.V., S. Günter, K. Lackner and I.G. Miron*:* Analytical Solutions to the Grad-Shafranov Equation for Diverted Plasmas. In: Proceedings of the 30th EPS Conference on Plasma Physics and Controlled Fusion, St. Petersburg 2003, (Eds.) R.Koch, S.Lebedev. ECA 27A. European Physical Society, Geneva 2003, P-2.104.

13. *Azarenkov*, N.A., A.A. Bizyukov*, I.A. Bizyukov, V.V. Bobkov*, A.Y. Kashaba*, K. Krieger, K.N. Sereda* and I.K. Tarasov*:* Solid Ion Source Based on Hollow-Cylindrical Magnetron Sputtering Discharge. Voprosy atomnoj nauki i techniki, Serijya Fizika plazmy **9**, 125-127 (2003).

14. *Azarenkov*, N.A., I.A. Bizyukov, A.Y. Kashaba* and K.N. Sereda*:* Solid Ion Accelerator Based on Magnetron Sputtering Discharge. In: Proceedings of the 18th International Seminar on Accelerators of Charged Particles, Alusta, Crimea 2003. National Scientific Center Kharkov Institute of Physics and Technology, Kharkov 2003, 140-141.

15. *Azarenkov*, N.A., I.A. Bizyukov, A.Y. Kashaba*, K.N. Sereda*, I.K. Tarasov* and E.V. Romashenko*:* Surface Wave Ion Source for Producing Lange Area Coatings (Report). In: Proceedings of the 10th Anniversary Scientifical Technical Conference Vacuum Science and Technology 1, Sudak, Crimea 2003. Moscow National Institute of Electronics and Mathematics, Moscow 2003, 362-366.

16. *Baar*, C, M. Eppinger*, G. Raddatz*, J. Simon*, C. Lanz*, O. Klimmek*, R. Nandakumar*, R. Gross*, A. Rosinus*, H. Keller*, P. Jagtap*, B. Linke*, F. Meyer*, H. Lederer and S.C. Schuster*:* Complete genome sequence and analysis of Wolinella succinogenes. Proceedings of the National Academy of Sciences of the United States of America **100**, 11690-11695 (2003).

17. *Bachmann, P., D. Hildebrandt and D. Sünder:* Heat Propagation in Anisotropic Targets Irradiated by Laser Pulses. In: Proceedings of the 30th EPS Conference on Controlled Fusion and Plasma Physics, St. Petersburg 2003, (Eds.) R.Koch, S.Lebedev. ECA 27A, European Physical Society, Geneva 2003, P-3.190.

18. *Balden, M., E. Oyarzabal*, E. de Juan Pardo, K. Durocher*, J. Roth and C. García-Rosales*:* Deuterium Retention by Implantation in Carbide-Doped Graphites. Physica Scripta **T103**, 38-42 (2003).

19. *Balden, M., J. Roth, E. de Juan Pardo and A. Wiltner:* Chemical Erosion of Atomically Dispersed Doped Hydro-Carbon Layers by Deuterium. Journal of Nuclear Materials **313-316**, 348-353 (2003).

20. *Bäumel, S., G. Michel, H.J. Hartfuß, M. Rodriguéz-Girones Arboli and H.L. Hartnagel:* Two-Dimensional Correlation Measurements of Electron Cyclotron Emission Fluctuations on the Stellarator Wendelstein 7-AS. Review of Scientific Instruments **74**, 1441-1444 (2003).

21. *Bécoulet*, M., G. Huysmans*, Y. Sarazin*, X. Garbet*, Ph. Ghendrih*, F. Rimini*, E. Joffrin*, X. Litaudon*, P. Monier-Garbet*, J.-M. Ané*, P. Thomas*, A. Grosman*, V. Parail*, H. Wilson*, P. Lomas*, P. de Vries*, K.-D. Zastrow*, G.F. Matthews*, J. Lonnroth*, S. Gerasimov*, S. Sharapov*, M. Gryaznevich*, G. Counsell*, A. Kirk*, M. Valovic*, R. Buttery*, A. Loarte*, G. Saibene*, R. Sartori*, A. Leonard*, P. Snyder*, L.L. Lao*, P. Gohil*, T.E. Evans*, R.A. Moyer*, Y. Kamada*, A. Chankin*, N. Oyama*, T. Hatae*, N. Asakura*, O. Tudisco*, E. Giovannozzi*, F. Crisanti*, C.P. Perez*, H.R. Koslowski*, T. Eich, A.C.C. Sips, L.D. Horton, A. Herrmann, P.T. Lang, J. Stober, W. Suttrop, P. Beyer*, S. Saarelma* and Contributors to JET-EFDA Workprogramme:* Edge Localized Mode Physics and

Operational Aspects in Tokamaks. Plasma Physics and Controlled Fusion **45**, A93-A113 (2003).

22. *Behrisch, R., G. Federici*, A. Kukushkin* and D. Reiter*:* Material Erosion at the Vessel Walls of Future Fusion Devices. Journal of Nuclear Materials **313-316**, 388-392 (2003).

23. *Beidler C.D., S.V. Kasilov*, W. Kernbichler*, H. Maassberg, D.R. Mikkelsen*, S. Murakami*, V.V. Nemov*, M. Schmidt, D.A. Spong*, V. Tribaldos*, A. Wakasa* and R.B. White*:* Neoclassical Transport in Stellarators - Results from an International Collaboration. In: Proceedings of the 30th EPS Conference on Plasma Physics and Controlled Fusion, St. Petersburg 2003, (Eds.) R.Koch, S.Lebedev. ECA 27A. European Physical Society, Geneva 2003, P-3.2.

24. *Bergmann, A., E. Poli and A.G. Peeters:* Monte Carlo _f Simulations of Neoclassical Phenomena in Tokamak Plasmas. In: Proceedings of the 19th Fusion Energy Conference, Lyon 2002, (Ed.) M.Spak. IAEA, Vienna 2003, TH/P1-01.

25. *Bergmann, A., E. Poli, A.G. Peeters, S.D. Pinches and E. Strumberger:* Monte Carlo _f Calculation of the Ion Polarization Current at a Rotating Island and of the Bootstrap Current at a Large Pressure Gradient. In: Proceedings of the 30th EPS Conference on Plasma Physics and Controlled Fusion, St. Petersburg 2003, (Eds.) R.Koch, S.Lebedev. ECA 27A. European Physical Society, Geneva 2003, P-3.130.

26. *Biberacher*, M., T. Hamacher, H. Reisinger* and A. Reuter*:* Szenarien künftiger Energiesysteme. VEÖ Journal, September, 14-17 (2003).

27. *Biberacher*, M., T. Hamacher, H. Reisinger* and A. Reuter*:* Szenarien künftiger Energiesysteme, Teil 2. VEÖ Journal, Oktober, 18-20 (2003).

28. *Biedermann, C., R. Radtke and K. Fournier*:* Line Ratios and Wavelengths of Helium-like Argon n=2 Satellite Transitions and Resonance Lines. Nuclear Instruments and Methods in Physics Research B **205**, 255-259 (2003).

29. *Biener*, J., C. Lutterloh*, M. Wicklein*, A. Dinger* and J. Küppers:* Thermal stability and hydrogen atom induced etching of nanometer-thick a-Si:H films grown by ion-beam deposition on Si(100) surfaces. Journal of Vacuum Science and Technology A **21**, 831-837 (2003).

30. *Bilato, R. and M. Brambilla:* Fast Wave Current Drive in the Ion Cyclotron Frequency Range from the Single-particle Point of View. Physics of Plasmas **10**, 179-186 (2003).

31. *Bobkov, V., J.-M. Noterdaeme, F. Wesner, R. Wilhelm and ASDEX Upgrade Team:* Influence of the Plasma on ICRF Antenna Voltage Limits. Journal of Nuclear Materials **313-316**, 956-961 (2003).

32. *Bobkov*, V., M. Azarenkov*, O. Bizyukov*, Vl.V. Bobkov, J.-M. Noterdaeme and R. Wilhelm:* Development of Coatings to Improve RF Voltage Stand-off. Surface and Coatings Technology **174-175**, 176-180 (2003).

33. *Bobkov*, V.V., S.S. Alimov*, Vl.V. Bobkov, Yu.V. Slyusarenko* and R.I. Starovoitov*:* Growth of Metal Newborn Formations on Cathode Surface under Influence of Plasma Flow. Surface and Coatings Technology **174-175**, 1271-1275 (2003).

34. *Bobkov, Vl.V., D.A. Hartmann, J. Neuhauser, J.-M. Noterdaeme, F. Wesner, R. Wilhelm and ASDEX Upgrade Team:* Interaction of ICRF Electric Fields and the SOL Plasma. In: Proceedings of the 30th EPS Conference on Controlled Fusion and Plasma Physics, St. Petersburg 2003, (Eds.) R.Koch, S.Lebedev. ECA 27A, European Physical Society, Geneva 2003, P-1.165.

35. *Bohmeyer, W., G. Fussmann, C. Ibbott*, A. Markin* and H.-D. Reiner:* Formation of Hydrocarbon Films in the Plasma Generator PSI-2. In: Proceedings of the 30th EPS Conference on Controlled Fusion and Plasma Physics, St. Petersburg 2003, (Eds.) R.Koch, S.Lebedev. ECA. 27A, European Physical Society, Geneva 2003, P-3.184.

36. *Bolzonella*, T., G. Pautasso, V. Riccardo*, ASDEX Upgrade Team and JET EFDA Contributors:* Compared Characterisation of Vertical Displacement Events in ASDEX Upgrade and JET. In: Proceedings of the 30th EPS Conference on Plasma Physics and Controlled Fusion, St. Petersburg 2003, (Eds.) R.Koch, S.Lebedev. ECA 27A. European Physical Society, Geneva 2003, P-2.86.

37. *Bonnin, X., D. Coster, C.S. Pitcher*, R. Schneider, D. Reiter*, V. Rozhansky*, S. Voskoboynikov* and H. Bürbaumer*:* Improved Modelling of Detachment and Neutral-Dominated Regimes Using the B2.5-SOLPS Code. Journal of Nuclear Materials **313-316**, 909-913 (2003).

38. *Bonnin, X., A. Mutzke, C. Nührenberg, J. Nührenberg and R. Schneider:* Calculation of Magnetic Coordinates for Stellarator Fields. In: Proceedings of the 30th EPS Conference on Plasma Physics and Controlled Fusion, St. Petersburg 2003, (Eds.) R.Koch, S.Lebedev. ECA 27A. European Physical Society, Geneva 2003, P-4.10.

39. *Borba*, D., G.D. Conway, S. Günter, G.T.A. Huysmans*, S. Klose, M. Maraschek, A. Mück, I. Nunes*, S.D. Pinches, F. Serra* and ASDEX Upgrade Team:* Destabilisation of TAE Modes Using ICRH in ASDEX Upgrade. In: Proceedings of the 30th EPS Conference on Plasma Physics and Controlled Fusion, St. Petersburg 2003, (Eds.) R.Koch, S.Lebedev. ECA 27A. European Physical Society, Geneva 2003, P-1.115.

40. *Borchardt, M., J. Riemann and R. Schneider:* Numerics in BoRiS. In: Parallel Computational Fluid Dynamics - New Frontiers and Multi-Disciplinary Applications, (Eds.) K.Matsuno, A.Ecer, J.Periaux, N.Satofuka, P.Fox. Elsevier Science, Amsterdam 2003, 459-465.

41. *Boscary, J., H. Greuner, M. Czerwinski, B. Mendelevitch, K. Pfefferle and H. Renner:* Water-Cooled Target Modules for Steady-State Operation of the W7-X Divertor. Nuclear Fusion **43**, 831-834 (2003).

42. *Bozhko, Y. and F. Schauer:* Refrigeration System for W7-X. Nuclear Fusion **43**, 835-841 (2003).

43. *Bradshaw, A.M. and T. Hamacher:* Die Fusion – Energiequelle der Zukunft. In: Energie und Umwelt - Verantwortung für die Zukunft, 10. Pfingstsymposium, Benediktbeuren 2003, (Eds.) Zentrum für Umwelt und Kultur Benediktbeuren, Deutsche Bundesstiftung Umwelt (DBU) Osnabrück. Don Bosco Verlag, München 2003, 68-77.

44. *Brakel, R., P. Grigull, K. McCormick, R. Burhenn, Y. Feng, F. Sardei, J. Baldzuhn, H. Ehmler, F. Gadelmeier, L. Giannone, D. Hildebrandt, K. Ida*, R. Jaenicke, J. Kisslinger, T. Klinger, J.P. Knauer, R. König, G. Kühner, H.P. Laqua, D. Naujoks, H. Niedermeyer, E. Pasch, N. Ramasubramanian, N. Rust, F. Wagner, A. Weller, U. Wenzel, A. Werner and W7-AS Team:* Improved Performance of the W7-AS Stellarator with New Island Divertor. In: Proceedings of the 19th Fusion Energy Conference, Lyon 2002, (Ed.) M.Spak. IAEA, Vienna 2003, EX/C5-4.

45. *Brambilla, M.:* Iterative Solution of the Grad-Shafranov Equation in Symmetric Magnetic Coordinates. Physics of Plasmas **10**, 3674-3683 (2003).

46. *Breizman*, B.N., H.L. Berk*, M.S. Pekker*, S.E. Sharapov*, N.C. Hawkes*, D.N. Borba* and S.D. Pinches:* Alfvén Eigenmodes in Shear Reversed Plasmas. In: Proceedings of the

19th Fusion Energy Conference, Lyon 2002, (Ed.) M.Spak. IAEA, Vienna 2003, TH/4-3.

47. *Brendel, A., C. Popescu, C. Leyens*, J. Woltersdorf*, E. Pippel* and H. Bolt:* Metall-Matrix-Verbundwerkstoffe als Wärmesenkenmaterial in Fusionsreaktoren: Verbundwerkstoffe. In: Proceedings of the 14th Symposium Verbundwerkstoffe und Werkstoffverbunde, Wien 2003, (Ed.) H.P.Degischer. Wiley VCH Verlag, Weinheim 2003, 189-194.

48. *Brendel, A., C. Popescu, C. Leyens*, J. Woltersdorf*, E. Pippel* and H. Bolt*: SiC-Fibre Reinforced Copper Matrix Composites. In: Proceedings of the International Conference on Advanced Metallic Materials, Smolenice 2003, (Eds.) J.Jerz, P._ebo, M.Zemánková. Institute of Materials & Machine Mechanics, Slovak Academy of Science, Bratislava 2003, 24-27.

49. *Brill, R., F. Koch, J. Mazurelle, D. Levchuk, M. Balden, Y. Yamada-Takamura*, H. Maier and H. Bolt:* Crystal Structure Characterisation of Filtered Arc Deposited Alumina Coatings. Temperature and Bias Voltage. Surface and Coatings Technology **174-175**, 606-610 (2003).

50. *Bruschi*, A., N. Muzzini*, N. Spinicchia*, R. Benocci*, G. Carcano*, S. Cirant*, F. Gandini*, G. Gittini*, G. Granucci*, F. Leuterer, V. Mellera*, F. Monaco, M. Münich, A. Nardone*, H. Schütz, E. Signorelli*, A. Simonetto* and C. Sozzi*:* Matched Calorimetric Loads for High Power Millimetre Wave Gyrotrons. Fusion Engineering and Design **66-68**, 549-554 (2003).

51. *Budny*, R.V., R. Andre*, C.D. Challis*, W. Dorland*, R. Dux, D.R. Ernst*, C. Giroud*, C.W. Gowers*, C.M. Greenfield*, N. Hawkes*, G.W. Hammett*, W.A. Houlberg*, T.C. Luce*, M.A., Makowski*, D. Mikkelsen*, M. Murakami*, R. Prentice*, G. Staebler*, B. Stratton*, M.R. Wade*, W.P. West* and Contributors to the EFDA-JET and DIII-D Work Programs:* Microturbulence, Heat and Particle Fluxes in JET and DIII-D ITB Plasmas with Highly Reversed Magnetic Shear. In: Proceedings of the 30th EPS Conference on Plasma Physics and Controlled Fusion, St. Petersburg 2003, (Eds.) R.Koch, S.Lebedev. ECA 27A, European Physical Society, Geneva 2003, 0-3.4A.

52. *Campbell*, D.J., P. Barabaschi*, M. Bécoulet*, G. Federici*, T. Hellsten*, A. Loarte*, G. Pautasso and H. Wilson:* Report on the 9th European Fusion Physics Workshop, Leysin, Switzerland. Plasma Physics and Controlled Fusion **45**, 505-520 (2003).

53. *Campbell*, D.J., D. Borba*, J. Bucalossi*, D. Moreau*, O. Sauter*, J. Stober and G. Vayakis*:* Report on the 10th European Fusion Physics Workshop, Vaals, The Netherlands. Plasma Physics and Controlled Fusion **45**, 1051-1068 (2003).

54. *Cortes*, S.R., N.C. Hawkes*, P. Lotte*, C. Fenzi*, B.C. Stratton*, J. Hobirk, R. De Angelis*, F. Orsitto* and C.A.F. Varandas*:* Measurement of the Plasma Radial Electric Field by the Motional Stark Effect Diagnostic on JET Plasmas. Review of Scientific Instruments **74**, 1596-1600 (2003).

55. *Coster, D.P.:* Time Dependent SOL Modelling with SOLPS. In: Proceedings of the 30th EPS Conference on Plasma Physics and Controlled Fusion, St. Petersburg 2003, (Eds.) R.Koch, S.Lebedev. ECA 27A. European Physical Society, Geneva 2003, P-1.169.

56. *Coster, D.P., X. Bonnin, B. Braams*, H. Bürbaumer*, E. Kveeva*, J.-W. Kim, A. Kukushkin*, Y. Nishimura, D. Reiter*, V. Rozhansky*, R. Schneider, B.D. Scott, S. Voskoboynikov* and ASDEX Upgrade Team:* Further Developments of the Edge Transport Simulation Package, SOLPS. In: Proceedings of the 19th Fusion Energy Conference, Lyon 2002, (Ed.) M.Spak. IAEA, Vienna 2003, TH/P2-13.

57. *Coster, D.P., X. Bonnin, G. Corrigan*, R. Dejarnac*, M. Fenstermacher*, W. Fundamenski*, A. Geier, J. Hogan*, A. Kallenbach, A. Kirschner*, K. Krieger, A. Loarte*, G.F. Matthews*, R.A. Pitts*, G. Porter*, R. Pugno, D. Reiser*, D. Reiter*, S. Sipila*, J. Spence*, P.C. Stangeby*, E. Tsitrone*, D. Tskhakaya*, M. Wischmeier* and Contributors to the EFDA-JET Workprogramme:* An Overview of JET Edge Modelling Activities. Journal of Nuclear Materials **313-316**, 868-872 (2003).

58. *Dammertz*, G., S. Alberti*, A. Arnold*, E. Borie*, V. Erckmann, G. Gantenbein*, E. Giguet*, R. Heidinger*, J.P. Hogge*, S. Illy*, W. Kasparek*, K. Koppenburg*, M. Kuntze*, H.P. Laqua, G. LeCloarec*, Y. LeGoff*, W. Leonhardt*, C. Lievin*, R. Magne*, G. Michel, G. Müller*, G. Neffe*, B. Piosczyk*, M. Schmid*, M. Thumm* and M.Q. Tran*:* Status of the 1 MW, 140 GHZ, CW gyrotron for W7-X. In: Proceedings of the 5th International Workshop on Strong Microwaves in Plasmas, Nizhny Novgorod 2002, (Ed.) A.G.Litvak. Russian Academy of Sciences, Institute of Applied Physics, Nizhny Novgorod 2003, 16-28.

59. *Dinklage, A., R. Fischer, J. Geiger, S. Gori, G. Kühner, H. Maaßberg, J. Svensson and U. von Toussaint:* From Off-line to Real-time Analysis: Acceleration Bayesian Analysis Codes. In: Proceedings of the 30th EPS Conference on Plasma Physics and Controlled Fusion, St. Petersburg 2003, (Eds.) R.Koch, S.Lebedev. ECA 27A. European Physical Society, Geneva 2003, P-4.80.

60. *Dinklage, A., R. Fischer, M. Hirsch, E. Pasch, A. Weller and W7-AS Team:* Increasing the Significance of Thomson Scattering Data by Bayesian Modelling. In: Proceedings of the 30th EPS Conference on Plasma Physics and Controlled Fusion, St. Petersburg 2003, (Eds.) R.Koch, S.Lebedev. ECA 27A. European Physical Society, Geneva 2003, P-1.52.

61. *Dolan*, T. J., D.F. Düchs, R. Kirkpatrick*, D. Kraft*, E. Landman*, C. Orth*, R.F. Post*, J.R. Roth, M.J. Sadowski* and G. Van Oost*:* Summary of the 4th Symposium on Current Trends in International Fusion Research, Washington,D.C. 2001. Fusion Science and Technology **43**, 138-142 (2003).

62. *Dose, V.:* Bayesian inference in physics: case studies. Reports on Progress in Physics **66**, 1421-1461 (2003).

63. *Dose, V.:* Hyperplane priors. In: Proceedings of the 22nd International Workshop on Bayesian Inference and Maximum Entropy Methods in Science and Engineering, Moscow,ID 2002, (Ed.) C.J.Williams. AIP Conference Proceedings 659, American Institute of Physics, Melville,NY 2003, 350-357.

64. *Draxler*, M., R. Beikler, E. Taglauer, K. Schmid, R. Gruber*, S.N. Ermolov* and P. Bauer*:* Comprehensive study of the surface peak in charge-integrated low-energy ion scattering spectra. Physical Review A **68**, 022901 (2003).

65. *Draxler*, M., R. Beikler, E. Taglauer, K. Schmid, R. Gruber*, S.N. Ermolov* and P. Bauer*:* Explanation of the surface peak in charge integrated LEIS spectra. Nuclear Instruments and Methods in Physics Research B **203**, 218-224 (2003).

66. *Drevlak, M., M.F. Heyn*, S.V. Kasilov*, W. Kernbichler*, D. Monticello*, V.V. Nemov*, C. Nührenberg, J. Nührenberg and A. Reiman*:* Bootstrap Current for Neoclassically Optimized Stellarator Systems. In: Proceedings of the 30th EPS Conference on Plasma Physics and Controlled Fusion, St. Petersburg 2003, (Eds.) R.Koch, S.Lebedev. ECA 27A. European Physical Society, Geneva 2003, P-4.15.

67. *Drevlak, M., M.F. Heyn*, V.N. Kalyuzhnyj*, S.V. Kasilov*, W. Kernbichler*, D. Monticello*, V.V. Nemov*, J. Nührenberg and A. Reiman*:* Effective Ripple for the W7-X Magnetic Field Calculated by the PIES Code. In: Proceedings of the 30th EPS

Conference on Plasma Physics and Controlled Fusion, St. Petersburg 2003, (Eds.) R.Koch, S.Lebedev. ECA 27A. European Physical Society, Geneva 2003, P-1.12.

68. *Dux, R.:* Impurity Transport in ASDEX Upgrade. Fusion Science and Technology **44**, 708-715 (2003).

69. *Dux, R., K. Kirov, R. Neu, G. Pereverzev, A.G. Peeters and J. Stober:* Dependence of Impurity Transport on the Heating Profile in ASDEX Upgrade. In: Proceedings of the 30th EPS Conference on Plasma Physics and Controlled Fusion, St. Petersburg 2003, (Eds.) R.Koch, S.Lebedev. ECA 27A, European Physical Society, Geneva 2003, P-1.132.

70. *Dux, R., R. Neu, A.G. Peeters, G. Pereverzev, A. Mück, F. Ryter, J. Stober and ASDEX Upgrade Team:* Influence of the Heating Profile on Impurity Transport in ASDEX Upgrade. Plasma Physics and Controlled Fusion **45**, 1815-1825 (2003).

71. *Dyckhoff, W. and A.M. Bradshaw:* Stand der Fusionsforschung. In: Zukunft der Energieversorgung, (Eds.) Innovationsbeirat der Landesregierung von Baden-Württemberg, Wissenschaftlich-Technischer Beirat der Bayerischen Staatsregierung. Springer Verlag, Heidelberg 2003, 69-83.

72. *Eckstein, W. and R. Preuss:* New fit formulae for the sputtering yield. Journal of Nuclear Materials **320**, 209-213 (2003).

73. *Eich, T., A. Herrmann, P. Andrew*, A. Loarte* and Contributors to the EFDA-JET Workprogramme:* Power Deposition Measurements in Deuterium and Helium Discharges in JET MKIIGB Divertor by IR-Thermography. Journal of Nuclear Materials **313-316**, 919-924 (2003).

74. *Eich, T., A. Herrmann, J. Neuhauser and ASDEX Upgrade Team:* Nonaxisymmetric Energy Deposition Pattern on ASDEX Upgrade Divertor Target Plates during Type-I Edge-Localized Modes. Physical Review Letters **91**, 195003 (2003).

75. *Eich, T., A. Herrmann, J. Neuhauser, S. Günter and ASDEX Upgrade Team:* Type-I ELM Mode Structure Observed by Divertor Thermography in ASDEX Upgrade. In: Proceedings of the 30th EPS Conference on Plasma Physics and Controlled Fusion, St. Petersburg 2003, (Eds.) R.Koch, S.Lebedev. ECA 27A. European Physical Society, Geneva 2003, P-1.126.

76. *Erckmann, V., H. Braune, H.P. Laqua, G. Michel, G. Dammertz*, M. Thumm*, G. Gantenbein*, W. Kasparek* and G.A. Müller*:* The 10 MW ECRH and CD System for W7-X, High Energy Density and High Power RF. In: High Energy Density and High Power RF, (Eds.) S.H.Gold, G.S.Nusinovich. AIP Press, Berkeley Springs,CA 2003, 213-223.

77. *Erckmann, V., U. Gasparino, H.P. Laqua, H. Maassberg, N.B. Marushchenko, H. Renner, M. Romé, W7-AS Team, W. Kasparek* and G.A. Müller*:* 20 years ECRH at W7-A and W7-AS. In: Proceedings of the 5th International Workshop on Strong Microwaves in Plasmas, Nizhny Novgorod 2002, (Ed.) A.G.Litvak. Russian Academy of Sciences, Institute of Applied Physics, Nizhny Novgorod 2003, 281-295.

78. *Erckmann, V., H.P. Laqua, H. Maassberg, N.B. Marushchenko, W. Kasparek and G.A. Müller*:* 20 years of ECRH at W7-A and W-7-AS. Nuclear Fusion **43**, 1313-1323 (2003).

79. *Erckmann, V., H.P. Laqua, H. Maassberg, N.B. Marushchenko, M. Romé, F. Volpe, W. Kasparek*, G.A. Müller* and W7-AS Team:* ECRH at W7-AS. In: Proceedings of the 19th Fusion Energy Conference, Lyon 2002, (Ed.) M.Spak. IAEA, Vienna 2003, EX/W-3.

80. *Ezumi*, N., T. Lunt, B. Koch, W. Bohmeyer and G. Fußmann:* Measurement of Plasma Flow Passing through a Magnetic Nozzle in the Stationary Linear Plasma Device PSI-2. In: Proceedings of the 30th EPS Conference on Controlled Fusion and Plasma Physics, St. Petersburg 2003, (Eds.) R.Koch, S.Lebedev. ECA 27A, European Physical Society, Geneva 2003, P-2.165.

81. *Fattorini*, L., M.E. Manso*, I. Nunes* and ASDEX Upgrade Team:* Effects of Magnetic Field Perturbations on the Reconstruction of Density Profiles from X-mode and Combined O/X-mode Reflectometry. In: Proceedings of the 30th EPS Conference on Plasma Physics and Controlled Fusion, St. Petersburg 2003, (Eds.) R.Koch, S.Lebedev. ECA 27A. European Physical Society, Geneva 2003, P-1.78.

82. *Federici*, G., P. Andrew*, P. Barabaschi*, J. Brooks*, R. Dörner*, A. Geier, A. Herrmann, G. Janeschitz*, K. Krieger, A. Kukushkin*, A. Loarte*, R. Neu, G. Saibene*, M. Shimada*, G. Strohmayer* and M. Sugihara*:* Key ITER plasma edge and plasma-material interaction issues. Journal of Nuclear Materials **313-316**, 11-22 (2003).

83. *Feist, J.-H. and W7-X Construction Team:* Status of Wendelstein 7-X Construction. In: Proceedings of the 30th EPS Conference on Plasma Physics and Controlled Fusion, St. Petersburg 2003, (Eds.) R.Koch, S.Lebedev. ECA 27A. European Physical Society, Geneva 2003, P-1.11.

84. *Feng, Y, F. Sardei, P. Grigull, K. McCormick, L. Giannone*, J. Kisslinger, D. Reiter*, Y. Igitkhanov and U. Wenzel:* Modelling of Island Divertor Physics and Comparison to W7-AS Experimental Results. Journal of Nuclear Materials **313-316**, 857-862 (2003).

85. *Feng, Y., F. Sardei, P. Grigull, K. McCormick, J. Kisslinger, D. Reiter*, T. Bindemann and H. Ehmler:* Impact of Island Geometry on Island Divertor Performance. In: Proceedings of the 30th EPS Conference on Plasma Physics and Controlled Fusion, St. Petersburg 2003, (Eds.) R.Koch, S.Lebedev. ECA 27A. European Physical Society, Geneva 2003, O-4.4C.

86. *Fischer, R., A. Dinklage and E. Pasch:* Bayesian modelling of fusion diagnostics. Plasma Physics and Controlled Fusion **45**, 1095-1111 (2003).

87. *Franck, C.M., R. Kleiber, G. Bonhomme*, O. Grulke and T. Klinger:* Transition from Unbounded to Bounded Whistler Wave Dispersion: Reconsidered. Physics of Plasmas **10**, 3817-3822 (2003).

88. *Franzen, P., J. Sielanko*, H.P.L. De Esch*, E. Speth, B. Heinemann and R. Riedl:* A magnetic residual ion removal system with in-line ion dumps for the ITER neutral beam injection system. Fusion Science and Technology **44**, 776-790 (2003).

89. *Franzen, P., J. Sielanko*, H.P.L. De Esch*, E. Speth, B. Heinemann and R. Riedl:* In-Line Magnetic Residual Ion Dump for the ITER Neutral Beam System. Fusion Engineering and Design **66-68**, 585-590 (2003).

90. *Galutschek*, E., M. Proschek*, H.D. Falter*, H. Anderson*, Y. Andrew*, M. De Baar*, M. Brix*, S. Cox*, P. Franzen, C. Giroud*, C. Maggi, A. Meigs*, A. Stäbler, J. Schweinzer, E. Wolfrum, F. Aumayr*, H.P. Winter* and EFDA JET Contributors:* Development of Fast Helium Beam Emission Spectroscopy for Tokamak Plasma Density- and Temperature Diagnostics. In: Proceedings of the 30th EPS Conference on Plasma Physics and Controlled Fusion, St. Petersburg 2003, (Eds.) R.Koch, S.Lebedev. ECA 27A, European Physical Society, Geneva 2003, P-1.54.

91. *Gantenbein*, G., A. Keller, M. Maraschek, W. Suttrop, H. Zohm and ASDEX Upgrade Team:* Investigations on m=2, n=1 Tearing Mode Stabilisation with ECRH at ASDEX Upgrade. In: Proceedings of the 30th EPS Conference on Plasma Physics and

Controlled Fusion, St. Petersburg 2003, (Eds.) R.Koch, S.Lebedev. ECA 27A. European Physical Society, Geneva 2003, P-1.187.

92. *Garbet*, X., Y. Baranov*, G. Bateman*, S. Benkada*, P. Beyer*, R. Budny*, F. Crisanti*, B. Esposito*, C. Figarella*, C. Fourment*, Ph. Ghendrih*, F. Imbeaux, E. Joffrin*, J. Kinsey*, A. Kritz*, X. Litaudon*, P. Maget*, P. Mantica*, D. Moreau*, Y. Sarazin*, A. Pankin*, V. Parail*, A.G. Peeters, T. Tala*, G. Tardini, A. Thyagaraja*, I. Voitsekhovitch*, J. Weiland* and R. Wolf:* Micro-stability and transport modeling of internal transport barriers on JET. In: Proceedings of the 19th Fusion Energy Conference, Lyon 2002, (Ed.) M.Spak. IAEA, Vienna 2003, TH/2-1.

93. *Garbet*, X., Y. Baranov*, G. Bateman*, S. Benkadda*, P. Beyer*, R. Budny*, F. Crisanti*, B. Esposito*, C. Figarella*, C. Fourment*, Ph. Ghendrih*, F. Imbeaux*, E. Joffrin*, J. Kinsey*, A. Kritz*, X. Litaudon*, P. Maget*, P. Mantica*, D. Moreau*, Y. Sarazin*, A. Pankin*, V. Parail*, A.G. Peeters, T. Tala*, G. Tardini, A. Thyagaraja*, I. Voitsekhovitch*, J. Weiland*, R. Wolf* and Contributors to the EFDA-JET Workprogramme:* Micro-stability and Transport Modelling of Internal Transport Barriers on JET. Nuclear Fusion **43**, 975-981 (2003).

94. *Garbet*, X., L. Garzotti*, P. Mantica*, H. Nordman*, M. Valovic*, H. Weisen* and C. Angioni:* Turbulent Particle Transport in Magnetized Plasmas. Physical Review Letters **91**, 0350014 (2003).

95. *Garzotti*, L., X. Garbet*, P. Mantica*, V. Parail*, M. Valovic*, G. Corrigan*, D. Heading*, T.T.C. Jones*, P.T. Lang, H. Nordman*, B. Pegourie*, G. Saibene*, J. Spence*, P. Strand*, J. Weiland* and Contributors to the EFDA-JET Workprogramme:* Particle Transport and Density Profile Analysis of Different JET Plasmas. Nuclear Fusion **43**, 1829-1836 (2003).

96. *Geier, A., D.P. Coster, J.D. Elder*, K. Krieger, R. Pugno, V. Rohde, R. Neu and ASDEX Upgrade Team:* Modeling of Tungsten Erosion, Deposition and Scrape-off Layer Transport in ASDEX Upgrade. In: Proceedings of the 30th EPS Conference on Plasma Physics and Controlled Fusion, St. Petersburg 2003, (Eds.) R.Koch, S.Lebedev. ECA 27A. European Physical Society, Geneva 2003, P-1.156.

97. *Geier, A., K. Krieger, J.D. Elder*, R. Pugno, V. Rohde and ASDEX Upgrade Team:* Modeling of tungsten transport in the SOL for sources at the central column of ASDEX Upgrade using DIVIMP. Journal of Nuclear Materials **313-316**, 1216-1220 (2003).

98. *Geiger, J., N. Marushchenko, H. Maassberg, A. Dinklage, M. Schmidt, A. Werner and N. Rust:* Analysis of High-ß Equilibria with Toroidal Net-Current Densities. In: Proceedings of the 30th EPS Conference on Plasma Physics and Controlled Fusion, St. Petersburg 2003, (Eds.) R.Koch, S.Lebedev. ECA 27A. European Physical Society, Geneva 2003, P-1.3.

99. *Geraud*, A., L. Garzotti*, P.T. Lang, A. Lorenz, B. Pegourie*, G.L. Schmidt*, B. Alper*, T.T.C. Jones*, P. Monier-Garbet*, J. Strachan*, M. Stamp*, P. Bennett*, J.L. Marechal*, R. Mooney*, J. Ongena*, M.J. Watson*, D.J. Wilson* and Contributors to the EFDA-JET Workprogramme:* Experimental Comparison of Different Configurations of Injection for Pellet Fuelling on JET. In: Proceedings of the 30th EPS Conference on Plasma Physics and Controlled Fusion, St. Petersburg 2003, (Eds.) R.Koch, S.Lebedev. ECA 27A. European Physical Society, Geneva 2003, P-1.97.

100. *Giannone, L., R. Brakel, R. Burhenn, H. Ehmler, Y. Feng, P. Grigull, K. McCormick, F. Wagner, J. Baldzuhn, Y. Igitkhanov, J. Knauer, K. Nishimura*, E. Pasch, B.J. Peterson*, N. Ramasubramanian, N. Rust, A. Weller, A. Werner and W7-AS Team:* Bolometer Tomography at the Density Limit of the HDH Mode in the W7-AS Stellarator. Plasma Physics and Controlled Fusion **45**, 1713-1732 (2003).

101. *Girka*, I.O., V.I. Lapshin* and R. Schneider:* Resonant Influence of Helicity on Alfven Heating of Plasma in Stellarators. Plasma Physics and Controlled Fusion **45**, 121-132 (2003).

102. *Gohil*, P., J. Kinsey*, V. Parail*, X. Litaudon*, T. Fukuda*, T. Hoang*, J. Connor*, E. Doyle*, Y. Esipchuk*, T. Fujita*, S. Lebedev*, V. Mukhovatov*, J. Rice*, E. Synakowski*, K. Toi*, B. Unterberg*, V. Vershkov*, M. Wakatani*, J. Weiland*, T. Aniel*, Y. Baranov*, E. Barbato*, A. Bécoulet*, C. Bourdelle*, G. Bracco*, R.V. Budny*, P. Buratti*, L. Ericsson*, B. Esposito*, C. Greenfield*, M. Greenwald*, T. Hahm*, T. Hellsten*, D. Hogeweij*, S. Ide*, F. Imbeaux*, Y. Kamada*, N. Kirneva*, P. Maget*, A.G. Peeters, K. Razumova*, F. Ryter, Y. Sakamoto*, H. Shirai*, G. Sips, T. Suzuki*, T. Takizuka* and R. Wolf:* Increased understanding of the dynamics and transport in ITB plasmas from multi-machine comparisons. In: Proceedings of the 19th Fusion Energy Conference, Lyon 2002, (Ed.) M.Spak. IAEA, Vienna 2003, CT/P-05.

103. *Goodman*, T.P., S.M. Ahmed*, S. Alberti*, Y. Andrèbe*, C. Angioni, K. Appert*, G. Arnoux*, R. Behn*, P. Blanchard*, P. Bosshard*, Y. Camenen*, R. Chavan*, S. Coda*, I. Condrea*, A. Degeling*, B.P. Duval*, P. Etienne*, D. Fasel*, A. Fasoli*, J.-Y. Favez*, I. Furno*, M. Henderson*, F. Hofmann*, J.-P. Hogge*, J. Horacek*, P. Isoz*, B. Joye*, A. Karpushov*, I. Klimanov*, P. Lavanchy*, J.B. Lister*, X. Llobet*, J.-C. Magnin*, A. Manini, B. Marlétaz*, P. Marmillod*, Y. Martin*, A. Martynov*, J.-M. Mayor*, J. Mlynar*, J.-M. Moret*, E. Nelson-Melby*, P. Nikkola*, P.J. Paris*, A. Perez*, Y. Peysson*, R.A. Pitts*, A. Pochelon*, L. Porte*, D. Raju*, H. Reimerdes*, O. Sauter*, A. Scarabosio*, E. Scavino*, S.H. Seo*, U. Siravo*, A. Sushkov*, G. Tonetti*, H. Weisen*, M. Wischmeier*, A. Zabolotsky* and G. Zhuang*:* An overview of recent results from the TCV Tokamak. In: Proceedings of the 19th Fusion Energy Conference, Lyon 2002, (Ed.) M.Spak. IAEA, Vienna 2003, OV/4-2.

104. *Goodman*, T.P., A. Mück, C. Angioni, M.A. Henderson*, O. Sauter*, F. Ryter, E. Westerhof*, H. Zohm and ASDEX Upgrade Team:* Control of the Sawtooth Instability by Electron Cyclotron Heating and Current Drive in the TCV and ASDEX Upgrade Tokamak. In: Proceedings of the 19th Fusion Energy Conference, Lyon 2002, (Ed.) M.Spak. IAEA, Vienna 2003, EX/P5-11.

105. *Granucci*, G., A. Ekedahl*, J. Mailloux*, K. Erents*, M. Hron*, E. Joffrin*, P.J. Lomas*, M. Mantsinen*, J.-M. Noterdaeme, V. Pericoli-Ridolfini*, V. Petrzilka*, K. Rantamäki*, R. Sartori*, C. Silva*, A.A. Tuccillo*, D. McDonald* and JET-EFDA Contributors:* Recent Results of LHCD Coupling Experiments with Near Gas Injection in JET. In: Proceedings of the 30th EPS Conference on Controlled Fusion and Plasma Physics, St. Petersburg 2003, (Eds.) R.Koch, S.Lebedev. ECA 27A, European Physical Society, Geneva 2003, P-1.191.

106. *Greuner, H., B. Böswirth, J. Boscary, G. Hofmann*, B. Mendelevitch, H. Renner and R. Rieck*:* Final Design of W7-X Divertor Plasma Facing Components - Tests and Thermo-Mechanical Analysis of Baffle Prototypes. Fusion Engineering and Design **66-68**, 447-452 (2003).

107. *Grigull, P., K. McCormick, Y. Feng, A. Werner, R. Brakel, H. Ehmler, F. Gadelmeier, D. Hartmann, D. Hildebrandt, R. Jaenicke, J. Kisslinger, T. Klinger, R. König, D. Naujoks, H. Niedermeyer, N. Ramasubramanian, F. Sardei, F. Wagner, U. Wenzel and W7-AS Team:* Influence of Magnetic Field Configurations on Divertor Plasma Parameters in the W7-AS Stellarator. Journal of Nuclear Materials **313-316**, 1287-1291 (2003).

108. *Grigull, P., K. McCormick, H. Renner, S. Masuzaki*, R. König, J. Baldzuhn, S. Bäumel, R. Burhenn, R. Brakel, H. Ehmler, Y. Feng, F. Gadelmeier, L. Giannone, D. Hartmann, D. Hildebrandt, M. Hirsch, R. Jaenicke, J. Kisslinger, T. Klinger, J. Knauer, D. Naujoks, H. Niedermeyer, E. Pasch, N. Ramasubramanian, F. Sardei, F. Wagner, U. Wenzel, A. Werner and W7-AS Team:* Divertor operation in stellarators: results from W7-AS and implications for future devices. Fusion Engineering and Design **66-68**, 49-58 (2003).

109. *Grote, H., J. Kisslinger, H. Renner, J. Boscary, H. Greuner, F.-W. Hoffmann and B. Mendelevitch:* Neutral Particle Modelling and Particle Exhaust in the Wendelstein 7-X Stellarator. Journal of Nuclear Materials **313-316**, 1298-1303 (2003).

110. *Gruber, O., S. Günter, A. Herrmann, L.D. Horton, P.T. Lang, M. Maraschek, S. Saarelma*, A.C.C. Sips, J. Stober, W. Suttrop, H. Zohm and ASDEX Upgrade Team:* Tolerable ELMs in Conventional and Advanced Scenarios at ASDEX Upgrade. In: Proceedings of the 19th Fusion Energy Conference, Lyon 2002, (Ed.) M.Spak. IAEA, Vienna 2003, EX/C2-1.

111. *Günter, S., G. Gantenbein*, A. Gude, V. Igochine, M. Maraschek, A. Mück, S. Saarelma*, O. Sauter*, A.C.C. Sips, H. Zohm and ASDEX Upgrade Team:* Neoclassical Tearing Modes on ASDEX Upgrade: Improved Scaling Laws, High Confinement at High $_N$ and New Stabilization Experiments. Nuclear Fusion **43**, 161-167 (2003).

112. *Günter, S., G. Gantenbein*, A. Gude, V. Igochine, M. Maraschek, O. Sauter*, A.C.C. Sips, H. Zohm and ASDEX Upgrade Team:* Neoclassical Tearing Modes on ASDEX Upgrade: Improved Scaling Laws, High Confinement at High $_N$ and New Stabilization Experiments. In: Proceedings of the 19th Fusion Energy Conference, Lyon 2002, (Ed.) M.Spak. IAEA, Vienna 2003, EX/S1-4.

113. *Günter, S. and H. Zohm:* Performance-Limiting MHD Activity and Possibilities for its Stabilization in ASDEX Upgrade. Fusion Science and Technology **44**, 682-691 (2003).

114. *Hacquin*, S., D. Wagner, M. Manso*, J. Borreicho* and L. Farinha*:* Optimization of the FM-CW Reflectometry W-Band Antenna for Core Density Profile Measurements on ASDEX Upgrade. Review of Scientific Instruments **74**, 1485-1488 (2003).

115. *Hagino*, Y., N. Ohno*, S. Takamura* and M.Y. Ye:* Experimental Evaluation of Space Charge Limited Emission Current from Tungsten Surface in High Density Helium Plasma. Journal of Nuclear Materials **313-316**, 675-678 (2003).

116. *Hailer*, H., G. Dammertz*, V. Erckmann, G. Gantenbein*, F. Hollmann, W. Kasparek*, W. Leonhardt*, M. Schmid*, P.G. Schüller*, M. Thumm* and M. Weissgerber:* Mirror development for the 140 GHz ECRH system of the stellarator W7-X. Fusion Engineering and Design **66-68**, 639-644 (2003).

117. *Hallatschek, K. and P.H. Diamond*:* Modulational instability of drift waves. New Journal of Physics **5**, 29 (2003). http://www.iop.org/EJ/article/1367-2630/5/1/329/nj3129.pdf.

118. *Hallberg*, B., K. Aquilonius*, Y. Lechón*, H. Cabal*, R.M. Sáez*, T. Schneider*, S. Lepicard*, D. Ward*, T. Hamacher and R. Korhonen*:* External Costs of Material Recycling Strategies for Fusion Power Plants. Fusion Engineering and Design **69**, 699-703 (2003).

119. *Hamacher, T.:* Energie für die Zukunft - Stand und Perspektiven der Fusion. In: ETG Fachbericht: Energietechnik für die Zukunft, (Ed.) VDE, VDE Verlag, Berlin, 2003, 205-218.

120. *Hamacher, T., M. Biberacher* and the VLEEM Consortium:* The VLEEM Bach-Casting Approach: a Sketch of the Methodology. In: Annual Meeting of the International Energy Workshop IEW, Laxenburg 2003. http://www.iiasa.ac.at/Research/ECS/IEW2003/Papers/2003P_hamacher.pdf.

121. *Hamacher, T., T. Haase*, H. Weber* and D. Ward*:* Netzanforderung an fortschrittliche Kraftwerkskonzepte: Beispiel Kernfusion. In: Sichere und zuverlässige Systemführung von Kraftwerken und Netz im Zeichen der Deregulierung, Tagung München 2003, (Ed.) VDI-Gesellschaft Mess- u. Automatisierungstechnik. VDI Verlag, Düsseldorf 2003, 141-151.

122. *Hamacher T., R.P. Shukla* and A.J. Seebregts*:* The Possible Role of Fusion in the Indian Energy System of the Future. Fusion Engineering and Design **69**, 733-737 (2003).

123. *Harmeyer, E and J. Kisslinger:* Improved Support Concept for the Helias Reactor Coil System. Fusion Engineering and Design **66-68**, 1025-1028 (2003).

124. *Hartfuss, H.J., V. Erckmann, M. Hirsch and H. Laqua:* Problems with ECRH Stray Radiation in Wendelstein 7-X. In: Proceedings of the 30th EPS Conference on Plasma Physics and Controlled Fusion, St. Petersburg 2003, (Eds.) R.Koch, S.Lebedev. ECA 27A. European Physical Society, Geneva 2003, O-3.2C.

125. *Hatayama*, A., K. Hoshino*, K. Miyamoto*, N. Komatsu*, K. Itami*, S. Sakurai*, N. Asakura*, Y. Miura*, K. Shimizu*, R. Schneider and D.P. Coster:* High Mach flow associated with plasma detachment in JT-60U. In: Proceedings of the 19th Fusion Energy Conference, Lyon 2002, (Ed.) M.Spak. IAEA, Vienna 2003, TH/P2-15.

126. *Hender*, T.C., O. Sauter*, B. Alper*, C. Angioni, M.R. De Baar*, M. De Benedetti*, P. Belo*, M. Bigi*, D.N. Borba*, T. Bolzonella*, R. Budny*, R.J. Buttery*, A. Gondhalekar*, N.N. Gorelenkov*, A. Gude, S. Günter, T. Hellsten*, D.F. Howell*, R. Koslowski*, R.J. La Haye*, A.W. Hyatt*, P. Lamalle*, E. Lazzaro*, M.J. Mantsinen*, M. Maraschek, M.L. Mayoral*, K.G. McClements*, F. Milani*, F. Nabais*, M.F.F. Nave*, F. Nguyen*, S. Nowak*, A.-L. Pecquet*, C. Perez*, C.C. Petty*, S.D. Pinches, A. Pochelon*, S. Podda*, J. Rapp*, F. Salzedas*, F. Sartori*, S.E. Sharapov*, M. Stamp*, D. Testa*, E. Westerhof*, P. de Vries*, P. Zanca* and JET EFDA Contributors:* Sawtooth, neo-classical tearing mode and error field studies in JET. In: Proceedings of the 19th Fusion Energy Conference, Lyon 2002, (Ed.) M.Spak. IAEA, Vienna 2003, EX/S1-2.

127. *Henderson*, M.A., S. Alberti*, C. Angioni, G. Arnoux*, R. Behn*, P. Blanchard*, P. Bosshard*, Y. Camenen*, S. Coda*, I. Condrea*, T.P. Goodman*, F. Hofmann*, J.-P. Hogge*, A. Karpushov*, A. Manini*, A. Martynov*, J.-M. Moret*, P. Nikkola*, E. Nelson-Melby*, A. Pochelon*, L. Porte*, O. Sauter*, S.M. Ahmed*, Y. Andrèbe*, K. Appert*, R. Chavan*, A. Degeling*, B.P. Duval*, P. Etienne*, D. Fasel*, A. Fasoli*, J.-Y. Favez*, I. Furno*, J. Horacek*, P. Isoz*, B. Joye*, I. Klimanov*, P. Lavanchy*, J.B. Lister*, X. Llobet*, J.-C. Magnin*, B. Marlétaz*, P. Marmillod*, Y. Martin*, J.-M. Mayor*, J. Mylnar*, P.J. Paris*, A. Perez*, Y. Peysson*, R.A. Pitts*, D. Raju*, H. Reimerdes*, A. Scarabosio*, E. Scavino*, S.H. Seo*, U. Siravo*, A. Sushkov*, G. Tonetti*, M.Q. Tran*, H. Weisen*, M. Wischmeier*, A. Zabolotsky* and G. Yhuang*:* Recent results from the electron cyclotron heated plasmas in Tokamak à Configuration Variable (TCV). Physics of Plasmas **10**, 1796-1802 (2003).

128. *Hergenhahn, U., A. Rüdel*, K. Maier*, A.M. Bradshaw, R.F. Fink* and A.T. Wen*:* The Resonant Auger Spectra of Formic Acid, Acetaldehyde, Acetic Acid and Methyl Formate. Chemical Physics **289**, 57-67 (2003).

129. *Herrmann, A., T. Eich, S. Jachmich*, M. Laux, P. Andrew*, A. Bergmann, A. Loarte*, G.F. Matthews*, J. Neuhauser, ASDEX Upgrade Team and Contributors to EFDA-JET Work Programme:*

Stationary and Transient Divertor Heat Flux Profiles and Extrapolation to ITER. Journal of Nuclear Materials **313-316**, 759-767 (2003).

130. *Herrmann, A., T. Eich, V. Rohde, C.J. Fuchs, J. Neuhauser and ASDEX Upgrade Team:* Power Deposition outside the Divertor in ASDEX Upgrade. In: Proceedings of the 30th EPS Conference on Plasma Physics and Controlled Fusion, St. Petersburg 2003, (Eds.) R.Koch, S.Lebedev. ECA 27A. European Physical Society, Geneva 2003, P-1.155.

131. *Herrmann, A. and O. Gruber:* ASDEX Upgrade - Introduction and Overview. Fusion Science and Technology **44**, 569-577 (2003).

132. *Herrnegger, F., J. Junker, A. Weller and H. Wobig:* Neutron Field in the Wendelstein-7-X Hall. In: Fusion Engineering and Design **66-68**, 849-853 (2003).

133. *Hildebrandt, D., F. Gadelmeier, P. Grigull, K. McCormick, D. Naujoks, D. Sünder and W7-AS Team:* Thermographic observation of the divertor target plates in the stellarators W7-AS and W7-X. Journal of Nuclear Materials **313-316**, 738-742 (2003).

134. *Hobirk, J., T. Oikawa*, T. Fujita*, T. Fukuda*, S. Günter, O. Gruber, A. Isayama*, Y. Kamada*, M. Kikuchi*, M. Maraschek, Y. Miura*, A.G. Peeters, G.V. Pereverzev, A. Polevoi*, A.C.C. Sips, A. Stäbler, J. Stober, T. Suzuki*, K. Ushigusa*, ASDEX Upgrade Team and JT-60U Team:* Off-axis Neutral Beam Current Drive Experiments on ASDEX Upgrade and JT-60U. In: Proceedings of the 30th EPS Conference on Plasma Physics and Controlled Fusion, St. Petersburg 2003, (Eds.) R.Koch, S.Lebedev. ECA 27A. European Physical Society, Geneva 2003, P-4.49.

135. *Hogan*, J., R. Colchin*, D.P. Coster, L. Baylor*, M. Fenstermacher*, M. Groth* and M. Wade*:* Modeling of ELM events and their effect on impurity enrichment. Journal of Nuclear Materials **313-316**, 1221-1228 (2003).

136. *Hopf, C., A. von Keudell and W. Jacob:* Chemical sputtering of hydrocarbon films. Journal of Applied Physics **94**, 2373-2380 (2003).

137. *Hopf, C., A. von Keudell and W. Jacob:* Direct verification of the ion-neutral synergism during hydrocarbon film growth. Journal of Applied Physics **93**, 3352-3358 (2003).

138. *Hopf, C., A. von Keudell and W. Jacob:* The influence of hydrogen ion bombardment on plasma-assisted hydrocarbon film growth. Diamond and Related Materials **12**, 85-89 (2003).

139. *Huber*, A., P. Coad*, D.P. Coster, L.C. Ingesson*, K. Itami*, S. Jachmich*, A. Kirschner*, M. Lehnen*, G.F. Matthews*, Ph. Mertens*, V. Philipps*, A. Pospieszczyk*, B. Schweer*, G. Sergienko*, M. Stamp* and Contributors to the EFDA-JET Programme:* Tomographic reconstruction of 2D line radiation distribution in the JET MkIIGB divertor. Journal of Nuclear Materials **313-316**, 925-930 (2003).

140. *Hutton*, R., Y. Zou*, J. Reyna Almandos*, C. Biedermann, R. Radtke, A. Greier and R. Neu:* EBIT Spectroscopy of Pm-like Tungsten. Nuclear Instruments and Methods in Physics Research B **205**, 114-118 (2003).

141. *Idehara*, T., S. Mitsudo*, R. Pavlichenko*, I. Ogawa*, D. Wagner and M. Thumm*:* Development of Submillimeter Wave Gyrotron FU Series. In: Proceedings of the 5th International Workshop on Strong Microwaves in Plasmas, Nizhny Novgorod 2003, (Ed.) A.G.Litvak, Russian Academy of Sciences, Institute of Applied Physics, Nizhny Novgorod 2003, 116-128.

142. *Igochine, V., S. Günter, M. Maraschek and ASDEX Upgrade Team:* Investigation of Complex MHD Activity by a Combined Use of Various Diagnostics. Nuclear Fusion **43**, 1801-1812 (2003).

143. *Igochine, V., S. Günter, M. Maraschek and ASDEX Upgrade Team:* Investigation of Complex MHD Instabilities on ASDEX Upgrade. In: Proceedings of the 30th EPS Conference on Plasma Physics and Controlled Fusion, St. Petersburg 2003, (Eds.) R.Koch, S.Lebedev. ECA 27A. European Physical Society, Geneva 2003, P-1.133.

144. *Isaev*, M.Yu., S.E. Grebenshchikov*, S.V. Shchepetov*, J. Nührenberg and W.A. Cooper*:* Compact Torsatron with Improved _-Particle Confinement. Plasma Physics Reports **29**, 727-729 (2003).

145. *Isaev*, M.Yu., J. Nührenberg, M.I. Mikhailov*, W.A. Cooper*, K.Y. Watanabe*, M. Yokoyama*, K. Yamazaki*, A.A. Subbotin* and V.D. Shafranov*:* A New Class of Quasi-Omnigenous Configurations. Nuclear Fusion **43**, 1066-1071 (2003).

146. *Jacchia*, A., F. DeLuca*, F. Ryter, A. Bruschi*, F. Leuterer, R. Neu, G. Pereverzev, W. Suttrop, D. Wagner and ASDEX Upgrade Team:* Perturbative Electron Transport Studies by Means of Laser Blow Off Induced Cold Pulses in ASDEX Upgrade. In: Proceedings of the 30th EPS Conference on Controlled Fusion and Plasma Physics, St. Petersburg 2003, (Eds.) R.Koch, S.Lebedev. ECA 27A, European Physical Society, Geneva 2003, P-1.117.

147. *Jacob, W., C. Hopf, A. von Keudell, M. Meier and T. Schwarz-Selinger:* Particle-beam experiment to study heterogeneous surface reactions relevant to plasma-assisted thin film growth and etching. Review of Scientific Instruments **74**, 5123-5136 (2003).

148. *Jauregi*, E., D. Ganuza*, I. García*, J.M. Del Río*, T. Rummel and F. Füllenbach:* Power Supply of the Control Coils of Wendelstein 7-X Experiment. Fusion Engineering and Design **66-68**, 1125-1132 (2003).

149. *Jenko, J., B. Scott, W. Dorland*, A. Kendl and D. Strintzi:* Simulations of Finite _ Turbulence in Tokamaks and Stellarators. In: Proceedings of the 19th Fusion Energy Conference, Lyon 2002, (Ed.) M.Spak. IAEA, Vienna 2003, TH/1-2.

150. *Joffrin*, E., C.D. Challis*, G.D. Conway, X. Garbet*, A. Gude, S. Günter, N.C. Hawkes*, T.C. Hender*, D.F. Howell*, G.T.A. Huysmans*, E. Lazzaro*, P. Maget*, M. Maraschek, A.G. Peeters, S.D. Pinches, S.E. Sharapov* and EFDA-JET Workprogramme Contributors:* Internal Transport Barrier Triggering by Rational Magnetic Flux Surfaces in Tokamaks. Nuclear Fusion **43**, 1167-1174 (2003).

151. *Kallenbach, A., Y. Andrew*, M. Beurskens*, G. Corrigan*, T. Eich, S. Jachmich*, M. Kempenaars*, A. Korotkov*, A. Loarte*, G. Matthews*, P. Monier-Garbet*, G. Saibene*, J. Spence*, W. Suttrop and EFDA-JET Workprogramme Contributors:* EDGE2D Modelling of Edge Profiles Obtained in JET Diagnostic Optimised Configuration. In: Proceedings of the 30th EPS Conference on Plasma Physics and Controlled Fusion, St. Petersburg 2003, (Eds.) R.Koch, S.Lebedev. ECA 27A, European Physical Society, Geneva 2003, P-159.

152. *Kallenbach, A., R. Dux, J. Gafert, G. Haas, L.D. Horton, M. Jakobi, B. Kurzan, H.W. Müller, R. Neu, J. Neuhauser, R. Pugno, T. Pütterich, V. Rohde, W. Sandmann, S.-W. Yoon and ASDEX Upgrade Team:* Edge Transport and its Interconnection with Main Chamber Recycling in ASDEX Upgrade. Nuclear Fusion **43**, 573-578 (2003).

153. *Kamada*, Y., H. Takenaga*, H. Urano, T. Takizuka*, T. Hatae* and Y. Miura*:* Enhanced pedestal pressure and parameter-linkages determining edge pedestal structure in JT-60U Type I and Type II ELMy H-mode. In: Proceedings of the 19th

Fusion Energy Conference, Lyon 2002, (Ed.) M.Spak. IAEA, Vienna 2003, EX/P2-04.

154. *Kang, H.D. and V. Dose:* Radical detection in a methane plasma. Journal of Vacuum Science and Technology A **21**, 1978-1980 (2003).

155. *Kang*, J.-H., R.L. Toomes*, M. Polcik*, M. Kittel*, J.-T. Hoeft*, V. Efstathiou*, D.P. Woodruff* and A.M. Bradshaw:* Structural Investigation of Glycine on Cu(100) and Comparison to Glycine on Cu(110). Journal of Chemical Physics **118**, 6059-6071 (2003).

156. *Kardaun, O., D. Salome*, W. Schaafsma*, A.G.M. Steerneman*, J.C. Willems* and D.R. Cox*:* Reflections on Fourteen Cryptic Issues Concerning the Nature of Statistical Inference. International Statistical Review **71**, 277-303 (2003).

157. *Käsemann, C.-P., L. Van Lieshout*, M. Huart and C. Sihler:* 145 MVA Modular Thyristor Converter System with Neutral Control for ASDEX Upgrade. Fusion Engineering and Design **66-68**, 1133-1137 (2003).

158. *Kasparek*, W., G. Dammertz*, V. Erckmann, G. Gantenbein*, H. Hailer*, F. Hollmann, L. Jonitz, H.P. Laqua, W. Leonhardt*, G. Michel, M. Schmid*, P.G. Schüller*, K. Schwörer*, R. Wacker* and M. Weissgerber:* The transmission system for ECRH on the stellarator W7-X: design issues and tests of prototype components. In: Proceedings of the 5th International Workshop on Strong Microwaves in Plasmas, Nizhny Novgorod 2002, (Ed.) A.G.Litvak. Russian Academy of Sciences, Institute of Applied Physics, Nizhny Novgorod 2003, 333-339.

159. *Kasparek*, W., G. Gantenbein*, B. Plaum*, R. Wacker*, A.V. Chirkov*, G.G. Denisov*, S.V. Kuzikov*, K. Ohkubo*, F. Hollmann and D. Wagner:* Performance of a Remote Steering Antenna for ECRH/ECCD Applications in ITER Using a Four-Wall Corrugated Square Waveguide. Nuclear Fusion **43**, 1505-1512 (2003).

160. *Kasparek*, W., G. Gantenbein*, B. Plaum*, R. Wacker*, E. Filipovic*, A.V. Chirkov*, G.G. Denisov*, S.V. Kuzikov*, K. Ohkubo*, F. Hollmann and D. Wagner:* Performance of a remote steering antenna for ECRH/ECCD applications using 4-Wall corrugated square wave-guide. In: Proceedings of the 12th Joint Workshop on Electron Cyclotron Emission and Electron Cyclotron Heating, Aix-en-Provence 2002, (Ed.) G.Giruzzi. World Scientific Publ., New Jersey, NJ 2003, 481-487.

161. *Kaufmann, M. (Ed.):* Plasmaphysik und Fusionsforschung. Teubner, Stuttgart 2003, 288 p.

162. *Keller, A., F. Leuterer, M. Maraschek, W. Suttrop, H. Zohm and ASDEX Upgrade Team:* Analysis Methods and Conditions for Feedback Controlled NTM Stabilization. In: Proceedings of the 30th EPS Conference on Plasma Physics and Controlled Fusion, St. Petersburg 2003, (Eds.) R.Koch, S.Lebedev. ECA 27A. European Physical Society, Geneva 2003, P-1.130.

163. *Kendl, A.:* Linear Aspects of Streamer Formation in Electron Temperature Gradient Turbulence. Physics of Plasmas **10**, 317-318 (2003).

164. *Kendl, A. and B.D. Scott:* Magnetic shear damping of dissipative drift wave turbulence. Physical Review Letters **90**, 035006 (2003).

165. *Kendl, A., B.D. Scott, R. Ball* and R.L. Dewar*:* Turbulent Edge Structure Formation in Complex Configurations. Physics of Plasmas **10**, 3684-3691 (2003).

166. *Khudoleev*, A.V., H.-U. Fahrbach and ASDEX Upgrade Team:* Isotope Effect in Hydrogen Ion Distribution Function. In: Proceedings of the 30th EPS Conference on Plasma Physics and Controlled Fusion, St. Petersburg 2003, (Eds.) R.Koch, S.Lebedev. ECA 27A. European Physical Society, Geneva 2003, P-2.124.

167. *Kiss'ovski*, Zh., W. Bohmeyer and G. Fußmann:* An Optical Probe for Local Ion Temperature Measurements in a Plasma. Contributions to Plasma Physics **43**, 456-463 (2003).

168. *Kiviniemi*, T.P., S.K. Sipilä*, V.A. Rozhansky*, S.P. Voskoboynikov*, E.G. Kaveeva*, J.A. Heikkinen*, D.P. Coster, R. Schneider and X. Bonnin:* Neoclassical Nature of the Radial Electric Field at the Low-to-High Confinement Transition. Physics of Plasmas **10**, 2604-2607 (2003).

169. *Klages, K.U., A. Wiltner, J. Luthin* and Ch. Linsmeier:* Deuterium bombardment of carbon and carbon layers on titanium. Journal of Nuclear Materials **313-316**, 56-61 (2003).

170. *Knauer, J.P., E. Pasch, G. Kühner and W7-AS Team:* High-Resolution Ruby Laser Thomson Scattering Diagnostic for the W7-AS Stellarator. Review of Scientific Instruments **74**, 1679-1682 (2003).

171. *Koch, B., W. Bohmeyer and G. Fußmann:* Angular Dependence of the Floating Potential in a Magnetized Plasma. Journal of Nuclear Materials **313-316**, 1114-1118 (2003).

172. *Kocsis*, G., S. Kalvin*, P.T. Lang and ASDEX Upgrade Team:* Observation of Cyrogenic Hydrogen Pellet Cloud Distribution in ASDEX Upgrade Plasmas. In: Proceedings of the 30th EPS Conference on Plasma Physics and Controlled Fusion, St. Petersburg 2003, (Eds.) R.Koch, S.Lebedev. ECA 27A. European Physical Society, Geneva 2003, P-1.116.

173. *Koebbel*, A., M. Polcik*, D.R. Lloyd*, I.T. McGovern*, O. Schaff*, R. Lindsay*, A.J. Patchett*, A.M. Bradshaw and D.P. Woodruff*:* Local Structure of OH Adsorbed on the Ge(001)(2x1) Surface Using Scanned-Energy Mode Photoelectron Diffraction. Surface Science **540**, 246-254 (2003).

174. *König, R., N. Ramasubramanian, K. McCormick, P. Grigull, F. Gadelmeier, U. Wenzel, B. Schweer* and M. Brix*:* Island divertor spectroscopy at the Wendelstein W7-AS stellarator. Review of Scientific Instruments **74**, 2052-2055 (2003).

175. *Koniges*, A.E., A. Grossman*, M. Fenstermacher*, J. Kisslinger, P. Mioduszewski*, T. Rognlien*, E. Strumberger and M. Umansky*:* Magnetic Topology of a Candidate NCSX Plasma Boundary Configuration. Nuclear Fusion **43**, 107-118 (2003).

176. *Kornilov, V., R. Kleiber, R. Hatzky, A. Bottino* and S.J. Allfrey*:* Structure of Ion-Temperature-Gradient (ITG) Modes in the W7-X Stellarator. In: Proceedings of the 30th EPS Conference on Plasma Physics and Controlled Fusion, St. Petersburg 2003, (Eds.) R.Koch, S.Lebedev. ECA 27A. European Physical Society, Geneva 2003, P-1.17.

177. *Koslowski*, H.R., C.P. Perez*, B. Alper*, T. Eich, T.C. Hender*, G.T.A Huysmans*, S.E. Sharapov*, P. Smeulders*, E. Westerhof* and JET EFDA Contributors:* Observations of pre- and postcursor modes of type-I ELMs on JET. In: Proceedings of the 19th Fusion Energy Conference, Lyon 2002, (Ed.) M.Spak. IAEA, Vienna 2003, EX/P1-14.

178. *Kraus, W., P. McNeely, P. Franzen, A. Encheva, M. Bandyopadhyay, B. Heinemann, R. Riedl, E. Speth and R. Wilhelm:* Development of Large RF Driven Negative Ion Sources for Neutral Beam Injection. Fusion Engineering and Design **66-68**, 491-495 (2003).

179. *Krieger, K., A. Geier, X. Gong*, H. Maier, R. Neu, V. Rohde and ASDEX Upgrade Team:* Erosion and migration of tungsten employed at the main chamber first wall of ASDEX Upgrade. Journal of Nuclear Materials **313-316**, 327-332 (2003).

180. *Kugeler, O., S. Marburger and U. Hergenhahn:* Calculation and Experimental Verification of the Time-of-Flight Spread in a Hemispherical Electron Energy Analyser. Review of Scientific Instruments **74**, 3955-3961 (2003).

181. *Kukushkin*, A.S., H.D. Pacher*, G.W. Pacher*, G. Janeschitz*, D.P. Coster and A. Loarte*:* ITER divertor plasma modelling with consistent core-edge parameters. In: Proceedings of the 19th Fusion Energy Conference, Lyon 2002, (Ed.) M.Spak. IAEA, Vienna 2003, CT/P-05.

182. *Kukushkin*, A.S., H.D. Pacher*, G.W. Pacher*, G. Janeschitz*, D.P. Coster, A. Loarte* and D. Reiter*:* Scaling Laws for Edge Plasma Parameters in ITER from Two-dimensional Edge Modelling. Nuclear Fusion **43**, 716-723 (2003).

183. *Lackner, K. and N. Aschenbrenner:* In hundert Jahren benötigt Europa 200 Fusionskraftwerke. Interview. Spektrum der Wissenschaft **4**, 90-91 (2003).

184. *Lang, P.T., P. Cierpka, O. Gehre, M. Reich, C. Wittmann, ASDEX Upgrade Team, A. Lorenz, D. Frigione*, S. Kalvin*, G. Kocsis* and S. Maruyama*:* A System for Cryogenic Hydrogen Pellet High Speed Inboard Launch into a Fusion Device via Guiding Tube Transfer. Review of Scientic Instruments **74**, 3974-3983 (2003).

185. *Lang, P.T., A. Kallenbach, L. Fattorini*, L.D. Horton, J. Neuhauser, H. Urano and ASDEX Upgrade Team:* Active Edge Locallized Mode (ELM) Frequency Control with Pellets. In: Proceedings of the 30th EPS Conference on Plasma Physics and Controlled Fusion, St. Petersburg 2003, (Eds.) R.Koch, S.Lebedev. ECA 27A. European Physical Society, Geneva 2003, P-1.129.

186. *Lang, P.T., J. Neuhauser, L.D. Horton, T. Eich, L. Fattorini*, J.C. Fuchs, O. Gehre, A. Herrmann, P. Ignacz*, M. Jakobi, S. Kalvin*, M. Kaufmann, G. Kocsis*, B. Kurzan, C. Maggi, M.E. Manso*, M. Maraschek, V. Mertens, A. Mück, H.D. Murmann, R. Neu, I. Nunes*, D. Reich*, M. Reich, S. Saarelma*, W. Sandmann, J. Stober, U. Vogl and ASDEX Upgrade Team:* ELM Frequency Control by Continuous Small Pellet Injection in ASDEX Upgrade. Nuclear Fusion **43**, 1110-1120 (2003).

187. *Laqua, H., H. Niedermeyer and J. Schacht:* Control System of Wendelstein 7-X Experiment. Fusion Engineering and Design **66-68**, 669-673 (2003).

188. *Laqua, H.P., V. Erckmann, F. Volpe, H. Maassberg, W7-AS Team and ECRH Group:* Electron Bernstein wave heating and current drive in overdense plasmas at the Wendelstein 7-AS-Stellarator. In: Proceedings of the 12th Joint Workshop on Electron Cyclotron Emission and Electron Cyclotron Heating, (Ed.) G.Giruzzi. World Scientific Publ., New Jersey,NJ 2003, 403-406.

189. *Laqua, H.P., H. Maassberg, N.B. Marushchenko, F. Volpe, A. Weller, W7-AS Team, W. Kasparek and ECRH Group:* Electron-Bernstein-Wave Current Drive in an Overdense Plasma at the Wendelstein 7-AS Stellarator. Physical Review Letters **90**, 075003 (2003).

190. *Laux, M., W. Schneider, P. Wienhold*, B. Jüttner*, A. Huber*, M. Balden, J. Linke*, H. Kostial*, M. Mayer, M. Rubel*, A. Herrmann, A. Pospieszczyk*, S. Jachmich*, B. Schweer*, D. Hildebrandt, J. Rossignol* and H. Bolt:* Arcing at B_4C-Covered Limiters Exposed to a SOL-Plasma. Journal of Nuclear Materials **313-316**, 62-66 (2003).

191. *Lechón*, Y., H. Cabal*, R.M. Sáez*, B. Hallberg*, K. Aquilonius*, T. Schneider*, S. Lepicard*, D. Ward*, T. Hamacher and R. Korhonen*:* External Costs of Silicon Carbide Fusion Power Plants Compared to Other Advanced Generation Technologies. Fusion Engineering and Design **69**, 683-688 (2003).

192. *Lehto*, S., J. Likonen*, J.P. Coad*; T. Ahlgren*; D.E. Hole*, M. Mayer, H. Maier, P. Andrew* and J. Kolehmainen*:* Tungsten Coating on JET Divertor Tiles for Erosion/Deposition Studies. Fusion Engineering and Design **66-68**, 241–245 (2003).

193. *Leuterer, F., R. Dux, G. Gantenbein*, J. Hobirk, A. Keller, K. Kirov, M. Maraschek, A. Mück, R. Neu, A.G. Peeters, G. Pereverzev, F. Ryter, J. Stober, W. Suttrop, G. Tardini, H. Zohm and ASDEX Upgrade Team:* Recent ECRH Results in ASDEX Upgrade. Nuclear Fusion **43**, 1329-1342 (2003).

194. *Leuterer, F., K. Kirov, F. Monaco, M. Münich, H. Schütz, F. Ryter, D. Wagner, R. Wilhelm, H. Zohm, T. Franke, K. Voigt, M. Thumm*, R. Heidinger*, G. Dammertz*, K. Koppenburg*, G. Gantenbein*, H. Hailer*, W. Kasparek*, G.A. Müller*, A. Bogdashov*, G. Denisov*, V. Kurbatov*, A. Kuftin*, A. Litvak*, S. Malygin*, E. Tai* and V. Zapevalov*:* Plans for a New ECRH System for ASDEX Upgrade. Fusion Engineering and Design **66-68**, 537-542 (2003).

195. *Leuterer, F., K. Kirov, G. Pereverzev, F. Ryter and D. Wagner:* Modulated ECRH Power Deposition in ASDEX Upgrade. Nuclear Fusion **43**, 744-748 (2003).

196. *Liang*, J.H., M. Mayer, J. Roth and W. Eckstein:* Computer Simulation of the Chemical Erosion of Graphite due to Hydrogen Ion Bombardment. Nuclear Instruments and Methods B **202**, 195–200 (2003).

197. *Lingertat, J., K. Horvath, H. Laqua, M. Otte, Y. Podoba and F. Wagner:* First Results from the WEGA Stellarator. In: Proceedings of the 30th EPS Conference on Plasma Physics and Controlled Fusion, St. Petersburg 2003, (Eds.) R.Koch, S.Lebedev. ECA 27A. European Physical Society, Geneva 2003, P-1.10.

198. *Linsmeier, Ch., J. Roth und K. Schmid:* Formation and Erosion of Mixed Materials. Atomic and Plasma-Material Interaction Data for Fusion **12**, 79-96 (2003).

199. *Litaudon*, X., A. Bécoulet*, F. Crisanti*, R.C. Wolf*, Yu.F. Baranov*, E. Barbato*, M. Bécoulet*, R. Budny*, C. Castaldo*, R. Cesario*, C.D. Challis*, G.D. Conway, M.R. De Baar*, P. De Vries*, R. Dux, L.G. Eriksson*, B. Esposito*, R. Felton*, C. Fourment*, D. Frigione*, X. Garbet*, R. Giannella*, C. Giroud*, G. Gorini*, N.C. Hawkes*, T. Hellsten*, T.C. Hender*, P. Hennequin*, G.M.D. Hogeweij*, G.T.A. Huysmans*, F. Imbeaux*, E. Joffrin*, P.J. Lomas*, P. Lotte*, P. Maget*, J. Mailloux*, P. Mantica*, M.J. Mantsinen*, D. Mazon*, D. Moreau*, V. Parail*, V. Pericoli*, E. Rachlew*, M. Riva*, F. Rimini*, Y. Sarazin*, B.C. Stratton*, T.J.J. Tala*, G. Tresset*, O. Tudisco*, L. Zabeo*, K.-D. Zastrow* and Contributors to the EFDA-JET Workprogramme:* Progress towards Steady-state Operation and Real-time Control of Internal Transport Barriers in JET. Nuclear Fusion **43**, 565-572 (2003).

200. *Litaudon*, X., A. Bécoulet*, F. Crisanti*, R. Wolf*, Yu.F. Baranov*, E. Barbato*, M. Bécoulet*, R. Budny*, C. Castaldo*, R. Cesario*, C.D. Challis*, G.D. Conway, M.R. De Baar*, P. De Vries*, R. Dux, L.G. Eriksson*, B. Esposito*, R. Felton*, C. Fourment*, D. Frigione*, X. Garbet*, R. Giannella*, C. Giroud*, G. Gorini*, N.C. Hawkes*, T. Hellsten*, T.C. Hender*, P. Hennequin*, G.M.D. Hogeweij*, G.T.A. Huysmans*, F. Imbeaux*, E. Joffrin*, P.J. Lomas*, P. Lotte*, P. Maget*, J. Mailloux*, P. Mantica*, M.J. Mantsinen*, D. Mazon*, D. Moreau*, V. Parail*, V. Pericoli*, E. Rachlew*, M. Riva*, F. Rimini*, Y. Sarazin*, B.C. Stratton*, T.J.J. Tala*, G. Tresset*, O. Tudisco*, L. Zabeo*, K.-D. Zastrow* and JET EFDA Contributors:* Progress towards steady-state operation and real time control of internal transport barriers in JET. In: Proceedings of the 19th Fusion Energy Conference, Lyon 2002, (Ed.) M.Spak. IAEA, Vienna 2003, EX/C3-4.

201. *Loarte*, A., G. Saibene*, R. Sartori*, M. Bécoulet*, L.D. Horton, T. Eich, A. Herrmann, M. Laux, G.F. Matthews*, S. Jachmich*, N. Asakura*, A. Chankin*, A. Leonard*, G. Porter*, G. Federici, M. Shimada*, M. Sugihara* and G. Janeschitz*:* ELM energy and particle losses and their extrapolation to burning plasma experiments. Journal of Nuclear Materials **313-316**, 962-966 (2003).

202. *Loarte*, A., G. Saibene*, R. Sartori*, M. Bécoulet*, P.J. Lomas*, S. Ali-Arshad*, B. Alper*, M. Beurskens*, M. Kempenaars*, R. Koslowski*, C.P. Perez*, A. Kallenbach, W. Suttrop and Contributors to the EFDA-JET Workprogramme:* Correlation of Type I ELM Energy Losses with Pedestal Plasma Characteristics and Global Discharge Parameters in JET ELMy H-Modes. In: Proceedings of the 30th EPS Conference on Plasma Physics and Controlled Fusion, St. Petersburg 2003, (Eds.) R.Koch, S.Lebedev. ECA 27A, European Physical Society, Geneva 2003, P-1.96.

203. *Loarte*, A., G. Saibene*, R. Sartori*, D.J. Campbell*, M. Bécoulet*, L.D. Horton, T. Eich, A. Herrmann, G.F. Matthews*, N. Asakura*, A. Chankin*, A. Leonard*, G. Porter*, G. Federici*, G. Janeschitz*, M. Shimada* and M. Sugihara*:* Characteristics of Type I ELM Energy and Particle Losses in Existing Devices and their Extrapolation to ITER. Plasma Physics and Controlled Fusion **45**, 1549-1569 (2003).

204. *Lorenz, A., S. Combs*, M. Reich, P.T. Lang, W. Watson*, D. Wilson* and C. Wittmann:* Mass Transfer in Long Pellet Guiding Systems at ASDEX Upgrade and JET. Fusion Engineering and Design **69**, 15-20 (2003).

205. *Lortz, D.:* On the structure of the electron. Zeitschrift für Naturforschung A **58a**, 491-493 (2003).

206. *Lutsenko*, V.V., Ya.I. Kolesnichenko*, A. Weller, A. Werner, H. Wobig, Yu.V. Yakovenko* and O.P. Fesenyuk*:* Peculiarities of destabilization of alfven modes by energetic ions in stellarators. In: Proceedings of the 19th Fusion Energy Conference, Lyon 2002, (Ed.) M.Spak. IAEA, Vienna 2003, TH/P3-16.

207. *Maddison*, G.P., M. Brix*, R. Budny*, M. Charlet*, I. Coffey*, J.G. Cordey*, P. Dumortier*, S.K. Erents*, N.C. Hawkes*, M. von Hellermann*, D.L. Hillis*, J. Hogan*, L.D. Horton, L.C. Ingesson*, S. Jachmich*, G.L. Jackson*, A. Kallenbach, H.R. Koslowski*, K.D. Lawson*, A. Loarte*, G.F. Matthews*, D. McDonald*, G.R. McKee*, A. Meigs*, A.M. Messiaen*, F. Milani*, P. Monier-Garbet*, M. Murakami*, M.F.F. Nave*, J. Ongena*, M.E. Puiatti*, E. Rachlew*, J. Rapp*, S. Sharapov*, G.M. Staebler*, M. Stamp*, J.D. Strachan*, W. Suttrop, G. Telesca*, M.Z. Tokar*, B. Unterberg*, M. Valisa*, K.-D. Zastrow* and Contributors to the EFDA-JET Work-programme:* Impurity-seeded Plasma Experiments on JET. Nuclear Fusion **43**, 49-62 (2003).

208. *Maggi, C.F., L.D. Horton, B. Zaniol*, P. Franzen, H. Meister, D. Nishijima, A. Stäbler and ASDEX Upgrade Team:* Neutral Beam Energy Scan Experiments in ASDEX Upgrade for Impurity Ion Density Evaluation with CXRS. In: Proceedings of the 30th EPS Conference on Plasma Physics and Controlled Fusion, St. Petersburg 2003, (Eds.) R.Koch, S.Lebedev. ECA 27A, European Physical Society, Geneva 2003, P-1.63.

209. *Manini, A., J.-M. Moret*, F. Ryter and ASDEX Upgrade Team:* Signal Processing Techniques Based on Singular Value Decomposition Applied to Modulated ECH Experiments. Nuclear Fusion **43**, 490-511 (2003).

210. *Manini, A., F. Ryter, J. Stober, C. Angioni, K.K. Kirov, F. Leuterer, C. Maggi, W. Suttrop, D. Wagner and ASDEX Upgrade Team:* Electron Heat Transport in Low Density H-mode Plasmas with Dominant Ion Heating in ASDEX Upgrade. In: Proceedings of the 30th EPS Conference on Plasma Physics and Controlled Fusion, St. Petersburg 2003, (Eds.) R.Koch, S.Lebedev. ECA 27A. European Physical Society, Geneva 2003, P-1.127.

211. *Mantica*, P., C. Capuano*, F. Ryter, A. Thyagaraja*, J. Weiland*, C. Angioni, P. Knight*, F. Leuterer, G. Tardini, D. Wagner and ASDEX UpgradeTeam:* Investigation of Heat Pinch Effects in ASDEX Upgrade. In: Proceedings of the 30th EPS Conference on Controlled Fusion and Plasma Physics, St. Petersburg 2003, (Eds.) R.Koch, S.Lebedev. ECA 27A, European Physical Society, Geneva 2003, P-1.119.

212. *Mantica*, P., I. Coffey*, R. Dux, X. Garbet*, L. Garzotti*, G. Gorini*, F. Imbeaux*, E. Joffrin*, J. Kinsey*, M. Mantsinen*, R. Mooney*, V. Parail*, Y. Sarazin*, C. Sozzi*, W. Suttrop, G. Tardini, D. Van Eester* and JET EFDA Contributors:* Transient heat transport studies in JET conventional and advanced tokamak plasmas. In: Proceedings of the 30th EPS Conference on Plasma Physics and Controlled Fusion, St. Petersburg 2003, (Eds.) R.Koch, S.Lebedev. ECA 27A, European Physical Society, Geneva 2003, EX/P1-04.

213. *Mantica*, P., X. Garbet*, F. Imbeaux*, M. Mantsinen*, D. Van Eester*, M. De Baar*, P. Knight*, V. Parail*, F. Ryter, G. Saibene*, R. Sartori*, C. Sozzi*, A. Thyagaraja* and JET EFDA Contributors:* Heat Wave Propagation Experiments and Modelling at JET: L-Mode, H-Mode and ITBS. In: Proceedings of the 30th EPS Conference on Plasma Physics and Controlled Fusion, St. Petersburg 2003, (Eds.) R.Koch, S.Lebedev. ECA 27A. European Physical Society, Geneva 2003, O-3.1A.

214. *Mantsinen*, M.J., L.-G. Eriksson*, E. Gauthier*, G.T. Hoang*, E. Joffrin*, R. Koch*, X. Litaudon*, A. Lyssoivan*, P. Mantica*, M.F.F. Nave*, J.-M. Noterdaeme, C.C. Petty*, O. Sauter* and S.E. Sharapov*:* Application of ICRF Waves in Tokamaks beyond Heating. Plasma Physics and Controlled Fusion **45**, A445-A456 (2003).

215. *Maraschek, M., O. Sauter, S. Günter, H. Zohm and ASDEX Upgrade Team:* Scaling of the Marginal $_p$ of Neoclassical Tearing Modes during Power Ramp-down Experiments in ASDEX Upgrade. In: Proceedings of the 30th EPS Conference on Plasma Physics and Controlled Fusion, St. Petersburg 2003, (Eds.) R.Koch, S.Lebedev. ECA 27A. European Physical Society, Geneva 2003, P-1.120.

216. *Maraschek, M., O. Sauter*, S. Günter, H. Zohm and ASDEX Upgrade Team:* Scaling of the Marginal $_p$ of Neoclassical Tearing Modes during Power Ramp-down Experiments in ASDEX Upgrade. Plasma Physics and Nuclear Fusion **7**, 1369-1384 (2003).

217. *Marburger, S., O. Kugeler, U. Hergenhahn and T. Möller*:* Experimental Evidence for Interatomic Coulombic Decay in Ne Clusters. Physical Review Letters **90**, 203401 (2003).

218. *Marmar*, E.S., B. Bai*, R.L. Boivin*, P.T. Bonoli*, C. Boswell*, R. Bravanec*, B. Carreras*, D. Ernst*, C. Fiore*, S. Gangadhara*, K. Gentle*, J. Goetz*, R. Granetz*, M. Greenwald*, K. Hallatschek, J. Hastie*, J. Hosea*, A. Hubbard*, J.W. Hughes*, I. Hutchinson*, Y. In*, J. Irby*, T. Jennigs*, D. Kopon*, G. Kramer*, B. LaBombard*, W.D. Lee*, Y. Lin*, B. Lipschultz*, J. Liptac*, A. Lynn*, K. Marr*, R. Maqueda*, E. Melby*, D. Mikkelsen*, D. Mossessian*, R. Nazikian*, W.M. Nevins*, R. Parker*, T.S. Pedersen*, C.K. Phillips*, P. Phillips*, C.S. Pitcher*, M. Porkolab*, J. Ramos*, M. Redi*, J. Rice*, B.N. Rogers*, W.L. Rowan*, M. Sampsell*, G. Schilling*, J. Snipes*, P. Snyder*, D. Stotler*, G. Taylor*, J.L. Terry*, H. Wilson*, J.R. Wilson*, S.M. Wolfe*, S. Wukitch*, X.Q. Xu*, B. Youngblood*, H. Yuh*, K. Zhurovich* and S. Zweben*:* Overview of recent Alcator C-Mod research. In: Proceedings on Fusion Energy, Lyon 2002, (Ed.) M.Spak. IAEA, Vienna 2003, OV/4-1.

219. *Marushchenko, N.B., F. Volpe, V. Erckmann, H.P. Laqua, H. Maassberg and W7-AS Team:* Estimation of electron Bernstein current drive efficiency on the W7-AS stellarator. In: Proceedings of the 5th International Workshop on Strong Microwaves in Plasmas, Nizhny Novgorod 2002, (Ed.) A.G.Litvak. Russian Academy of Sciences, Institute of Applied Physics, Nizhny Novgorod 2003, 378-383.

220. *Matthews*, G.F, P. Andrew*, T. Eich, W. Fundamenski*, A. Herrmann, A. Loarte*, V. Riccardo* and Contributors to the EFDA-JET Workprogramme:* Steady-state and Transient Power Handling in JET. Nuclear Fusion **43**, 999-1005 (2003).

221. *Matthews*, G.F., G. Corrigan*, S.K. Erents*, W. Fundamenski*, A. Kallenbach, T. Kurki-Suonio*, S. Sipilä*, J. Spence* and Contributors to the EFDA-JET Workprogramme:* The effect of ion orbit losses on JET edge plasma simulations. Journal of Nuclear Materials **313-316**, 986-989 (2003).

222. *Matyash, K.V. and R. Schneider:* Kinetic Modelling of Dusty Plasmas. In: Proceedings of the 30th EPS Conference on Plasma Physics and Controlled Fusion, St. Petersburg 2003, (Eds.) R.Koch, S.Lebedev. ECA 27A. European Physical Society, Geneva 2003, P-4.115.

223. *Matyash, K., R. Schneider, A. Bergmann, W. Jacob, U. Fantz* and P. Pecher*:* Modeling of hydrocarbon species in ECR methane plasmas. Journal of Nuclear Materials **313-316**, 434-438 (2003).

224. *Mayer, M., B. Diaz-Herrera* and M. Schneider:* Back-scattering of ^{6}Li and ^{7}Li Ions from oxygen below 6 MeV. Nuclear Instruments and Methods in Physics Research B **207**, 263-267 (2003).

225. *Mayer, M., A. von Keudell, V. Rohde, P. Coad* and JET-EFDA Contributors:* Mechanism of Hydrocarbon Layer Formation in Remote Areas of Fusion Devices. In: Proceedings of the 30th EPS Conference on Plasma Physics and Controlled Fusion, St. Petersburg 2003, (Eds.) R.Koch, S.Lebedev. ECA 27A. European Physical Society, Geneva 2003, O-2.6A.

226. *Mayer, M., V. Rohde, A. von Keudell and ASDEX Upgrade Team:* Characterisation of deposited hydrocarbon layers below the divertor and in the pumping ducts of ASDEX Upgrade. Journal of Nuclear Materials **313-316**, 429-433 (2003).

227. *Mayer, M., P. Wienhold*, D. Hildebrandt and W. Schneider:* Erosion and deposition at the ALT-II limiter of TEXTOR. Journal of Nuclear Materials **313-316**, 377-382 (2003).

228. *McCarthy*, P.J., L.D. Horton, A. Kallenbach, B. Kurzan and ASDEX Upgrade Team:* ELM-resolved Interpretive MHD Equilibria on ASDEX Upgrade Using SOL Tile Currents and Kinetic Data. In: Proceedings of the 30th EPS Conference on Plasma Physics and Controlled Fusion, St. Petersburg 2003, (Eds.) R.Koch, S.Lebedev. ECA 27A. European Physical Society, Geneva 2003, P-1.64.

229. *McCormick, K., R. Burhenn, P. Grigull, J. Baldzuhn, S. Bäumel, R. Brakel, H. Ehmler, F. Gadelmeier, L. Giannone, M. Hirsch, E. Holzhauer*, R. Jaenicke, S. Klose, J.P. Knauer, E. Pasch, H. Thomsen, A. Werner, W7-AS Team, ECRH Team and NBI Team:* The Wendelstein 7-AS High Density H-Mode, A Mode for the Future? In: Proceedings of the 30th EPS Conference on Plasma Physics and Controlled Fusion, St. Petersburg 2003, (Eds.) R.Koch, S.Lebedev. ECA 27A. European Physical Society, Geneva 2003, P-1.1.

230. *McCormick, K., P. Grigull, R.Burhenn, R. Brakel, H. Ehmler, Y. Feng, R. Fischer, F. Gadelmeier, L. Giannone, D. Hildebrandt, M. Hirsch, E. Holzhauer, R. Jaenicke, J. Kisslinger, T. Klinger, S. Klose, J.P. Knauer, R. König, G. Kühner, H.P. Laqua, D. Naujoks, H. Niedermeyer, E. Pasch, N. Ramasubramanian , N. Rust, F. Sardei, F. Wagner, A. Weller, U. Wenzel and A. Werner:* Island Divertor Experiments on the Wendelstein 7-AS Stellarator. Journal of Nuclear Materials **313-316**, 1131-1140 (2003).

231. *McKee*, G.R., R.J. Fonck*, M. Jakubowski*, K.H. Burrell*, T.N. Carlstrom*, C. Fenzi*, R.J. Groebner*, K. Hallatschek, R.A. Moyer*, W. Nevins*, T.L. Rhodes*, C. Rost*, D. Rudakov* and X. Xu*:* Turbulence regulation and stabilization by equilibrium and zonal flows. In: Proceedings on Fusion Energy, Lyon 2002, (Ed.) M.Spak. IAEA, Vienna 2003, EX/C4-1Ra.

232. *McKee*, G.R., R.J. Fonck*, M. Jakubowski*, K.H. Burrell*, K. Hallatschek, R.A. Moyer*, W. Nevins*, D.L. Rudakov* and X. Xu*:* Observation and characterization of radially sheared zonal flows in DIII-D. Plasma Physics and Controlled Fusion **45**, A477-A485 (2003).

233. *McKee*, G.R., R.J. Fonck*, M. Jakubowski*, K.H. Burrell*, K. Hallatschek, R.A. Moyer*, D.L. Rudakov*, W. Nevins*, G.D. Porter*, P. Schoch* and X. Xu*:* Experimental characterization of coherent, radially-sheared zonal flows in the DIII-D tokamak. Physics of Plasmas **10**, 1712-1719 (2003).

234. *Meier, M. and A. von Keudell:* Assessment of Ion Surface Scattering (ISS) as in-situ real-time diagnostic tool in low temperature plasmas. In: Proceedings of the Workshop Frontiers in Low Temperature Plasma Diagnostics V, (Eds.) S.DeBenedictis, G.Dilecce. Organizing Comittee Workshop FLTPDV, Bari 2003, 126-129.

235. *Meier, M., A. von Keudell and W. Jacob:* Consequences of the temperature and flux dependent sticking coefficient of methyl radicals for nuclear fusion experiments. Nuclear Fusion **43**, 25-29 (2003).

236. *Meier, M., R. Preuss and V. Dose:* Interaction of CH_3 and H with amorphous hydrocarbon surfaces: estimation of reaction cross sections using Bayesian probability theory. New Journal of Physics **5**, 133 (2003). http://www.iop.org/EJ/article/1367-2630/5/1/133/njp3_1_133.pdf.

237. *Meister, H., R. Dux, L.D. Horton, B. Kurzan, P.J. McCarthy*, H. Zohm and ASDEX Upgrade Team:* An Integrated System to Measure the Effective Charge of Fusion Plasmas in the ASDEX Upgrade Tokamak. Review of Scientific Instruments **74**, 4625-4633 (2003).

238. *Meister, H., L.D. Horton, B. Kurzan, W. Suttrop, H. Zohm and ASDEX Upgrade Team:* Z_{eff} Behaviour in ASDEX Upgrade H-mode Discharges. In: Proceedings of the 30th EPS Conference on Plasma Physics and Controlled Fusion, St. Petersburg 2003, (Eds.) R.Koch, S.Lebedev. ECA 27A. European Physical Society, Geneva 2003, P-1.136.

239. *Merkl, D., J. Hobirk, P.J. McCarthy*, L. Giannone, O. Gruber, V. Igochine, M. Maraschek, G.V. Pereverzev, W. Schneider, A.C.C. Sips, E. Strumberger and ASDEX Upgrade Team:* 'Current Holes' at ASDEX Upgrade. In: Proceedings of the 30th EPS Conference on Plasma Physics and Controlled Fusion, St. Petersburg 2003, (Eds.) R.Koch, S.Lebedev. ECA 27A. European Physical Society, Geneva 2003, P-1.134.

240. *Mertens, V., G. Haas, V. Rohde and ASDEX Upgrade Team:* Hydrogen Gas Balance in ASDEX Upgrade with DIV IIB. In: Proceedings of the 30th EPS Conference on Plasma Physics and Controlled Fusion, St. Petersburg 2003. (Eds.) R.Koch, S.Lebedev. ECA 27A. European Physical Society, Geneva 2003, P-1.128.

241. *Mertens, V., J. Hobirk, A. Kallenbach, P.T. Lang, A. Mück, G. Pautasso, G. Raupp, A.C.C. Sips, J. Stober, H. Zohm and ASDEX Ugprade Team:* Development of Active Control Systems on ASDEX Upgrade in View of ITER Discharge Scenarios. Fusion Engineering and Design **66-68**, 119-127 (2003).

242. *Mertens, V., G. Raupp and W. Treutterer:* Plasma Control in ASDEX Upgrade. Fusion Science and Technology **44**, 593-604 (2003).

243. *Meyer-Spasche, R.:* Variable-Coefficient Difference Schemes for Quasilinear Evolution Problems. In: Numerical Methods and Applications, (Eds.) I.Dimov, I.Lirkov, S.Margenov, Z.Zlatev. Lecture Notes in Computer Science 2542, Springer Verlag, Berlin 2003, 36-47.

244. *Michel, G., P. Brand*, V. Erckmann, G. Gantenbein*, F. Hollmann, L. Jonitz, W. Kasparek*, H.P. Laqua, W. Leonhardt*, G. Müller*, F. Purps, M. Schmid*, T. Schulz, M. Thumm*, ECRH Team at Forschungszentrum Karlsruhe and ECRH Team at Institut für Plasmaforschung Stuttgart:* Progress of the 10 MW ECRH System for W7-X. In: Proceedings of the 12th Joint Workshop on Electron Cyclotron Emission and Electron Cyclotron Heating, Aix-en-Provence 2002, (Ed.) G.Giruzzi. World Scientific Publ., New Jersey,NJ 2003, 493-497.

245. *Milch, I.:* Fusion nucléaire - Etat et perspectives. Énergie panorama - Bulletin bimensuel d'economie énergétique **475**, 5-7 (2003).

246. *Milch, I.:* Kernfusion - Stand und Perspektiven. ew - Das Magazin für die Energiewirtschaft **102** (21), 48-51 (2003).

247. *Milch, I.:* Kernfusion - Stand und Perspektiven. SVA-Bulletin **45** (20), 11-15 (2003).

248. *Milch, I. and A. Rother*:* Wie die Sonne Energie erzeugen ... auf der Erde. HGF-Jahresheft 2003. (Ed.) Helmholtz-Gemeinschaft Deutscher Forschungszentren. Trio Verlag, Königswinter 2003, 20-23.

249. *Miri*, A.M. and C. Sihler:* Damping of Resonances at Energization of Power Transformers in an Isolated Network. In: Proceedings of the 38th Annual Meeting of IEEE Industry Applications Society, Salt Lake City,UT 2003, IEEE Service Center, Piscataway,NJ 2003, P-23.3.

250. *Mönnich, T. and T. Rummel:* Protection System for the Superconducting Coils in Wendelstein 7-X. Fusion Engineering and Design **66-68**, 1041-1044 (2003).

251. *Morozov*, D.K., V.I. Gervids*, I.Y. Senichenkov*, I.Y. Veselova*, V.A. Rozhansky*, L.L. Lengyel and R. Schneider:* Ionization - Recombination Processes in a Carbon Cloud Surrounding a Carbon Pellet. In: Proceedings of the 30th EPS Conference on Plasma Physics and Controlled Fusion, St. Petersburg 2003, (Eds.) R.Koch, S.Lebedev. ECA 27A. European Physical Society, Geneva 2003, P-2.65.

252. *Mück, A., C. Angioni, T.P. Goodman*, M. Maraschek, G.V. Pereverzev, F. Ryter, H. Zohm and ASDEX Upgrade Team:* NTM Control via Sawtooth Tailoring in ASDEX Upgrade. In: Proceedings of the 30th EPS Conference on Plasma Physics and Controlled Fusion, St. Petersburg 2003, (Eds.) R.Koch, S.Lebedev. ECA 27A. European Physical Society, Geneva 2003, P-1.131.

253. *Mukhovatov*, V., M. Shimada*, A. Chudnovskiy*, A.E. Costley*, Y. Gribov*, G. Federici*, O. Kardaun, A.S. Kukushkin*, A. Polevoi*, V.D. Pustovitov*, Y. Shimomura*, T. Sugie*, M. Sugihara*, and G. Vayakis*:* Overview of Physics Basis for ITER. Plasma Physics and Controlled Fusion **45**, A235-A252 (2003).

254. *Mukhovatov*, V., Y. Shimomura*, A. Polevoi*, M. Shimada*, M. Sugihara*, G. Bateman*, J.G. Cordey*, O. Kardaun, G.V. Pereverzev, I. Voitsekhovich*, J. Weiland*, O. Zolotukhin*, A. Chudnovskiy*, A.H. Kritz*, A. Kukushkin*, T. Onjun*, A. Pankin* and F.W. Perkins*:* Comparison of ITER Performance Predicted by Semi-Empirical and Theory-Based Transport Models. Nuclear Fusion **43**, 942-948 (2003).

255. *Müller, W.-C. and D. Biskamp:* The Evolving Phenomenological View on Magnetohydrodynamic Turbulence. In: Turbulence and Magnetic Fields in Astrophysics, (Eds.) E.Falgarone, T.Passot. Lecture Notes in Physics 614, Springer Verlag, Berlin 2003, 3-27.

256. *Müller, W.-C., R. Grappin* and D. Biskamp:* Statistical Anisotropy of Magnetohydrodynamic Turbulence. Physical Review E **67**, 066302 (2003).

257. *Murakami*, S., H. Yamada*, A. Wakasa*, M. Sasao*, M. Isobe*, T. Ozaki*, P. Goncharov*, T. Saida*, J.F. Lyon*, M. Osakabe*, K. Narihara*, K. Tanaka*, H. Inagaki*, S. Morita*, K. Ida*, J. Miyazawa*, P. Idei*, K. Ikeda*, S. Kubo*, R. Kumazawa*, T. Mutoh*, Y. Oka*, K. Saito*, T. Seki*, Y. Takeiri*, Y. Torii*, K. Tumori*, T. Watari*, K.Y. Watanabe*, H. Funaba*, M. Yokoyama*, H. Maassberg, C.D. Beidler, K. Itoh*, O. Kaneko*, A. Komori*, T. Akiyama*, N. Ashikawa*, M. Emoto*, M. Goto*, K. Kawahata*, H. Kawazome*, K. Khlopenkov*, T. Kobuchi*, A. Kostrioukov*, Y. Liang*, S. Masuzaki*, T. Minami*, T. Morisaki*, S. Muto*, Y. Nagayama*, Y. Nakamura*, H. Nakanishi*, Y. Narushima*, K. Nishimura*, N. Noda*, T. Notake*, H. Nozato*, S. Ohdachi*, N. Ohyabu*, B.J. Peterson*, A. Sagara*, S. Sakakibara*, R. Sakamoto*, K. Sato*, M. Sato*, T. Shimozuma*, M. Shoji*, H. Suzuki*, N. Takeuchi*, N. Tamura*, K. Toi*, T. Tokuzawa*, Y. Xu*, I. Yamada*, S. Yamamoto*, T. Yamamoto*, Y. Yoshimura*, M. Yoshinuma*, M.Y. Tanaka*, S. Okamura*, S. Yoshimura*, K. Nagaoka*, T. Satow*, S. Imagawa*, T. Mito*, I. Ohtake*, T. Uda*, K. Ohkubo*, S. Sudo*, K. Yamazaki*, K. Matsuoka*, O. Motojima*, Y. Hamada* and M. Fujiwara*:* A demonstration of magnetic field optimization in LHD. In: Proceedings of the 19th Fusion Energy Conference, Lyon 2002, (Ed.) M.Spak. IAEA, Vienna 2003, EX/C5-3.

258. *Murmann, H.D., M. Jakobi, B. Kurzan and H.B. Schilling:* Dynamic Laser Alignment Control for Thomson Scattering on ASDEX Upgrade. Review of Science Instruments **74**, 4310-4313 (2003).

259. *Na, Y.-S., A.C.C. Sips, X. Garbet*, J. Hobirk, X. Litaudon*, D. Moreau*, T.J.J. Tala, W. Treutterer, ASDEX Upgrade Team and EFDA-JET Contributors:* Modelling of the Current Profile Control with Neutral Beam Injection at ASDEX Upgrade and Comparison to JET. In: Proceedings of the 30th EPS Conference on Plasma Physics and Controlled Fusion, St. Petersburg 2003, (Eds.) R.Koch, S.Lebedev. ECA 27A. European Physical Society, Geneva 2003, P-1.128.

260. *Nagel, M. and F. Schauer:* Cooling of the W7-X Superconducting Coils. In: Proceedings of the 19th International Cryogenic Engineering Conference, Grenoble 2002, (Eds.) G.G.Baguer, P.Seyfert. Narosa Publishing House, New Dehli 2003, 677-680.

261. *Nakamura*, Y., R. Yoshino*, R.S. Granetz*, G. Pautasso, O. Gruber and S.C. Jardin*:* Characterization of axisymmetric disruption dynamics toward VDE avoidance in Tokamaks. In: Proceedings of the 19th Fusion Energy Conference, Lyon 2002, (Ed.) M.Spak. IAEA, Vienna 2003, EX/P4-13.

262. *Nave*, M.F.F., J. Rapp*, T. Bolzonella*, R. Dux, M.J. Mantsinen*, R. Budny*, P. Dumortier*, M. von Hellermann*, S. Jachmich*, H.R. Koslowski*, G.P. Maddison*, A.M. Messiaen*, P. Monier-Garbet*, J. Ongena*, M.E. Puiatti*, J. Strachan*, G. Telesca*, B. Unterberg*, M. Valisa*, P. de Vries* and Contributors to the JET-EFDA Workprogramme:* Role of sawtooth in avoiding impurity accumulation and maintaining good confinement in JET radiative mantle discharges. Nuclear Fusion **43**, 1204-1213 (2003).

263. *Nemov*, V.V., S.V. Kasilov*, C. Nührenberg, J. Nührenberg, W. Kernbichler* and M.F. Heyn*:* Study of Neoclassical

Transport Properties of W7-X Using the Integration along Magnetic Field Lines. Plasma Physics and Controlled Fusion **45**, 43-52 (2003).

264. *Neu, R., R. Dux, A. Geier, H. Greuner, K. Krieger, H. Maier, R. Pugno, V. Rohde, S.-W. Yoon and ASDEX Upgrade Team:* New Results from the Tungsten Programme at ASDEX Upgrade. Journal of Nuclear Materials **313-316**, 116-126 (2003).

265. *Neu, R., R. Dux, A. Geier, O. Gruber, A. Kallenbach, K. Krieger, H. Maier, R. Pugno, V. Rohde, S. Schweizer and ASDEX Upgrade Team:* Tungsten as Plasma-Facing Material in ASDEX Upgrade. Fusion Engineering and Design **65**, 367-374 (2003).

266. *Neu, R., A. Kallenbach, K. Krieger, V. Rohde and J. Roth:* Plasma Wall Interaction and First-Wall Materials in ASDEX Upgrade. Fusion Science and Technology **44**, 692-707 (2003).

267. *Neu, R., J.C. Fuchs, A. Kallenbach, C. Maggi, V. Rohde, F. Ryter, T. Eich, J. Gafert, O. Gruber, G. Haas, A. Herrmann, M. Kaufmann, M. Laux, V. Mertens, H.W. Müller, J. Neuhauser, T. Pütterich, J. Stober, S.-W. Yoon and ASDEX Upgrade Team:* The ASDEX Upgrade Divertor IIB - A Closed Divertor for Strongly Shaped Plasmas. Nuclear Fusion **43**, 1191-1196 (2003).

268. *Neu, R., R. Pugno, V. Rohde, R. Dux, T. Eich, H.-U. Fahrbach, A. Geier, A. Herrmann, D. Hildebrandt, A. Kallenbach, P.T. Lang, C. Maggi, T. Pütterich, F. Ryter, W. Schneider, U. Seidel and ASDEX Upgrade Team:* Assessment of Intrinsic Impurity Behaviour in ASDEX Upgrade. In: Proceedings of the 30th EPS Conference on Plasma Physics and Controlled Fusion, St. Petersburg 2003, (Eds.) R.Koch, S.Lebedev. ECA 27A, European Physical Society, Geneva 2003, P-1.123.

269. *Neuhauser, J., H.-S. Bosch, D.P. Coster, A. Herrmann and A. Kallenbach:* Edge and Divertor Physics in ASDEX Upgrade. Fusion Science and Technology **44**, 659-681 (2003).

270. *Neuner, U. and W7-X Diagnostics Team:* Design of Diagnostics in the Steady State Environment of W7-X. In: Proceedings of the 30th EPS Conference on Plasma Physics and Controlled Fusion, St. Petersburg 2003, (Eds.) R.Koch, S.Lebedev. ECA 27A. European Physical Society, Geneva 2003, P-4.84.

271. *Nishijima, D., M.Y. Ye, N. Ohno* and S. Takamura*:* Incident ion energy dependence of bubble formation on tungsten surface with low energy and high flux helium plasma irradiation. Journal of Nuclear Materials **313-316**, 97-101 (2003).

272. *Nishijima, D., M.Y. Ye, N. Ohno* and S. Takamura*:* Surface Morphology of Tungsten Irradiated by Low-Energy and High-Flux Steady State Helium Plasma. In: Proceedings of the 30th EPS Conference on Plasma Physics and Controlled Fusion, St. Petersburg 2003, (Eds.) R.Koch, S.Lebedev. ECA 27A. European Physical Society, Geneva 2003, P-2.163.

273. *Noterdaeme, J.-M., R. Budny*, A. Cardinali*, C. Castaldo*, R. Cesario*, F. Crisanti*, J. deGrassie*, D.A. D'Ippolito*, F. Durodié*, A. Ekedahl*, A. Figueiredo*, C. Ingesson*, E. Joffrin*, D. Hartmann, J. Heikkinen*, T. Hellsten*, T. Jones*, V. Kitpily*, Ph. Lamalle*, X. Litaudon*, F. Nguyen*, J. Mailloux*, M. Mantsinen*, M. Mayoral*, D. Mazon*, F. Meo, I. Monakhov*, J.R. Myra*, J. Pamela*, V. Pericoli*, Yu. Petrov*, O. Sauter*, Y. Sarazin*, S.E. Sharapov*, A.A. Tuccillo*, D. Van Eester* and JET-EFDA Contributors:* Heating, Current Drive and Energetic Particle Studies on JET in Preparation of ITER Operation. Nuclear Fusion **43**, 202-209 (2003).

274. *Noterdaeme, J.-M., E. Righi*, V. Chan*, J. deGrassie*, K. Kirov, M.J. Mantsinen*, M.F.F. Nave*, D. Testa*, K.-D. Zastrow*, R. Budny*, R. Cesario*, A. Gondhalekar*, N. Hawkes*, T. Hellsten*, Ph. Lamalle*, F. Meo, F. Nguyen* and JET-EFDA Contributors:* Spatially Resolved Toroidal Plasma Rotation with ICRF on JET. Nuclear Fusion **43**, 274-289 (2003).

275. *Nowak*, S., A. Bruschi*, G. Ramponi*, S. Cirant*, E. Lazzaro*, A.G.A. Verhoeven* and H. Zohm:* Impact of ECRH launcher flexibility on NTM stabilization and advanced scenarios in large toroidal configurations as JET plasmas. In: Proceedings of the 12th Joint Workshop on Electron Cyclotron Emission and Electron Cyclotron Heating, Aix-en-Provence 2002. (Ed.) G.Giruzzi. World Scientific Publ., New Jersey, NJ 2003, 329-334.

276. *Nührenberg, C.:* Physical Growth Rates for Global Ballooning Modes in W7-X. In: Proceedings of the 30th EPS Conference on Plasma Physics and Controlled Fusion, St. Petersburg 2003, (Eds.) R.Koch, S.Lebedev. ECA 27A. European Physical Society, Geneva 2003, P-1.16.

277. *Nührenberg, C. and A.H. Boozer*:* Magnetic Islands and Perturbed Plasma Equilibria. Physics of Plasmas **10**, 2840-2851 (2003).

278. *Nührenberg, J., W.A. Cooper*, M.Yu. Isaev*, M.F. Heyn*, V.N. Kalyuzhnyi*, S.V. Kasilov*, W. Kernbichler*, A.Yu. Kuyanov*, M.I. Mikhailov*, V.V. Nemov*, M.A. Samitov*, V.D. Sahfranov*, A.A. Skovoroda*, A.A. Subbotin*, R. Zille and A.V. Zvonkov*:* New Schemes for Confinement of Fusion Products in Stellarators. In: Proceedings of the 19th Fusion Energy Conference, Lyon 2002, (Ed.) M.Spak. IAEA, Vienna 2003, IC/P-06.

279. *Nunes*, I., G.D. Conway, A. Loarte*, M.E. Manso*, G. Saibene*, R. Sartori*, F. Serra*, W. Suttrop, CFN Team and ASDEX Upgrade Team:* Study of ELM Density Crash in ASDEX Upgrade. In: Proceedings of the 30th EPS Conference on Plasma Physics and Controlled Fusion, St. Petersburg 2003, (Eds.) R.Koch, S.Lebedev. ECA 27A. European Physical Society, Geneva 2003, P-1.157.

280. *Ogorodnikova, O.V., J. Roth and M. Mayer:* Deuterium retention in tungsten in dependence of the surface conditions. Journal of Nuclear Materials **313-316**, 469-477 (2003).

281. *Ongena*, J., P. Monier-Garbet*, W. Suttrop, P. Andrew*, M. Bécoulet*, R. Budny*, Y. Corre*, G. Cordey*, P. Dumortier*, T. Eich, L. Garzotti*, D.L. Hillis*, J. Hogan*, L.C. Ingesson*, S. Jachmich*, E. Joffrin*, P.T. Lang, A. Loarte*, P. Lomas*, G.P. Maddison*, D. McDonald*, A. Messiaen*, M.F.F. Nave*, G. Saibene*, R. Sartori*, O. Sauter*, J.D. Strachan*, B. Unterberg*, M. Valovic*, I. Voitsekhovitch*, M. von Hellermann*, B. Alper*, Y. Baranov*, M. Beurskens*, G. Bonheure*, J. Brzozowski*, J. Bucalossi*, M. Brix*, M. Charlet*, I. Coffey*, M. De Baar*, P. De Vries*, C. Giroud*, C. Gowers*, N.C. Hawkes*, G.L. Jackson*, C. Jupen*, A. Kallenbach, H.R. Koslowski*, K.D. Lawson*, M. Mantsinen*, G. Matthews*, F. Milani*, M. Murakami*, A. Murari*, R. Neu, V. Parail*, S. Podda*, M.E. Puiatti*, J. Rapp*, E. Righi*, R. Sartori*, Y. Sarazin*, A. Stäbler, M. Stamp*, G. Telesca*, M. Valisa*, B. Weyssow*, K.-D. Zastrow* and EFDA-JET Workprogramme Contributors:* Towards the Realization of JET of an Integrated H-Mode Scenario for ITER. In: Proceedings of the 19th Fusion Energy Conference, Lyon 2002, (Ed.) M.Spak. IAEA, Vienna 2003, EX/C2-4.

282. *Osborne*, T.H., J.G. Cordey*, R.J. Groebner*, T. Hatae*, A.E. Hubbard*, L.D. Horton, Y. Kamada*, A. Kritz*, L.L. Lao*, A.W. Leonard*, A. Loarte*, M.A. Mahdavi*, D. Mossessian*, T. Onjun*, M. Ossenpenko*, T.D. Rognlien*, G. Saibene*, P.B. Snyder*, M. Sugihara*, R. Shurygin*, K. Thomsen*, M.R. Wade*, H.R. Wilson*, X.Q. Xu*, K. Yatsu* and International Tokamak Physics Activity H Mode Pedestal Working Group:* Characteristics of the H-mode pedestal and extrapolation to ITER. In: Proceedings of the 19th Fusion Energy Conference, Lyon 2002, (Ed.) M.Spak. IAEA, Vienna 2003, CT-3.

283. *Otte, M., J. Lingertat and F. Wagner:* Operation of the WEGA Stellarator with Vertical Field and Compensation. In: Proceedings of the 30th EPS Conference on Plasma Physics and Controlled Fusion, St. Petersburg 2003, (Eds.) R.Koch, S.Lebedev. ECA 27A. European Physical Society, Geneva 2003, P-1.9.

284. *Pacher*, G.W., H.D. Pacher*, A.S. Kukushkin*, G. Janeschitz* and G.V. Pereverzev:* Core plasma operation consistent with SOL parameters in ITER. Nuclear Fusion **43**, 188-195 (2003).

285. *Pautasso, G., S. Egorov*, K.H. Finken*, O. Gruber, A. Herrmann, C.J. Fuchs, M. Maraschek, G. Neu, Y. Nakamura*, V. Rohde, A. Savtchkov*, S. Schweizer, U. Seidel, B. Streibl, C. Tichmann and ASDEX Upgrade Team:* Disruption Studies on ASDEX Upgrade. In: Proceedings of the 19th Fusion Energy Conference, Lyon 2002, (Ed.) M.Spak. IAEA, Vienna 2003, EX/P4-14.

286. *Pautasso, G. and O. Gruber:* Study of Disruptions in ASDEX Upgrade. Fusion Science and Technology **44**, 716-729 (2003).

287. *Pautasso, G., A. Herrmann, T. Eich, J.C. Fuchs, O. Gruber, A. Kallenbach and ASDEX Upgrade Team:* Analysis of the Power Deposition in the ASDEX Upgrade Divertor during Disruptions. In: Proceedings of the 30th EPS Conference on Plasma Physics and Controlled Fusion, St. Petersburg 2003, (Eds.) R.Koch, S.Lebedev. ECA 27A. European Physical Society, Geneva 2003, P-1.135.

288. *Pedemonte*, L., G. Bracco*, R. Beikler, E. Taglauer, A. Robin* and W. Heiland*:* A low-energy ion scattering study of Al(110) surface melting. Surface Science **532-535**, 13-18 (2003).

289. *Peeters, A.G., A.C.C. Sips, E. Quigley*, O. Gruber, V. Igochine, P.J. McCarthy*, F. Ryter, R. Wolf and ASDEX Upgrade Team:* Internal Transport Barriers in ASDEX Upgrade. In: Proceedings of the 19th Fusion Energy Conference, Lyon 2002, (Ed.) M.Spak. IAEA, Vienna 2003, EX/P4-03.

290. *Pereverzev, G.V. and O.V. Zolotukhin*:* Predictive Simulation of ITER Performance with Theory-based Transport Models. In: Proceedings of the 30th EPS Conference on Plasma Physics and Controlled Fusion, St. Petersburg 2003, (Eds.) R.Koch, S.Lebedev. ECA 27A. European Physical Society, Geneva 2003, P-1.138.

291. *Pericoli*, V. E. Joffrin*, R. Neu, M. De Baar*, T. Bolzonella*, J. Brzozowski*, V. Cocilovo*, E. De La Luna*, R. Giannella*, C. Groud*, F. Nave*, L. Zabeo* and EFDA JET Contributors:* Progress towards Long Lasting Steady Internal Transport Barriers at JET. In: Proceedings of the 30th EPS Conference on Plasma Physics and Controlled Fusion, St. Petersburg 2003, (Eds.) R.Koch, S.Lebedev. ECA 27A, European Physical Society, Geneva 2003, P-2.89.

292. *Pinches, S.D.:* MHD in JET Advanced Scenarios. In: Proceedings of the 30th EPS Conference on Plasma Physics and Controlled Fusion, St. Petersburg 2003, (Eds.) R.Koch, S.Lebedev. ECA 27A. European Physical Society, Geneva 2003, P-1.93.

293. *Pitts*, R.A., P. Andrew*, Y. Andrew*, M. Bécoulet*, I. Coffey*, D.P. Coster, D.C. McDonald*, T. Eich, S.K. Erents*, M. Fenstermacher*, W. Fundamenski*, G. Haas, A. Herrmann, C. Hidalgo*, D.L. Hillis*, A. Huber*, L.C. Ingesson*, S. Jachmich*, A. Kallenbach, A. Korotkov*, K.D. Lawson*, P. Lomas*, T. Loarer*, A. Loarte*, G.F. Matthews*, G. McCracken*, A. Meigs*, Ph. Mertens*, M. O'Mullane*, V. Philipps*, G. Porter*, A. Pospieszczyk*, J. Rapp*, D. Reiter*, V. Riccardo*, G. Saibene*, R. Sartori*, M.F. Stamp*, E. Tsitrone*, M. Wischmeier*, J. Gafert and Contributors to the EFDA-JET Workprogramme:* Comparing scrape-off layer and divertor physics in JET pure He and D discharges. Journal of Nuclear Materials **313-316**, 777-786 (2003).

294. P*olevoi*, A.R., M. Sugihara*, H. Takenaga*, A. Isayama*, N. Oyama*, A. Loarte*, G. Saibene* and G.V. Pereverzev:* Pellet Injection as a Possible Tool for Plasma Performance Improvement. Nuclear Fusion **43**, 1072-1076 (2003).

295. *Poli, E., A.G. Peeters, A. Bergmann, S. Günter and S.D. Pinches:* Monte Carlo _f Simulation of the Bootstrap Current in the Presence of a Magnetic Island. Plasma Physics and Controlled Fusion **45**, 71-87 (2003).

296. *Pospieszczyk*, A., B. Schweer*, V. Philipps*, A. Huber*, G. Sergienko*, U. Samm*, H. Reimer*, M. Freisinger*, M. Rubel*, A. Herrmann, S. Kötterl, M. Laux, H. Renner and H. Bolt:* B_4C-limiter experiments at TEXTOR. Journal of Nuclear Materials **313-316**, 223-229 (2003).

297. *Powis*, I., E.E. Rennie*, U. Hergenhahn, O. Kugeler and R. Bussy-Socrate*:* Investigation of the Gas-Phase Amino Acid Alanine by Synchrotron Radiation Photoelectron Spectroscopy. Journal of Physical Chemistry A **107**, 25-34 (2003).

298. *Preuss, R., M. Maraschek, H. Zohm and V. Dose:* Bayesian analysis of magnetic island dynamics. In: Proceedings of the 22nd International Workshop on Bayesian Inference and Maximum Entropy Methods in Science and Engineering, Moscow,ID 2002, (Ed.) C.J.Williams. AIP Conference Proceedings 659, American Institute of Physics, Melville,NY 2003, 124-131.

299. *Preuss, R., A. Schwab*, H.-J. Schnittler* and P. Dieterich*:* Bayesian analysis of cell migration - linking experimental data and theoretical models. In: Foundations of Statistical Inference, (Ed.) Y.Haitovsky. Econometric Series. Physica Verlag, Heidelberg 2003, 107-114.

300. *Pugno, R., A. Kallenbach, B. Heger, A. Carlson and ASDEX Upgrade Team:* Hydrocarbon Puff Experiment in the ASDEX Upgrade Divertor. In: Proceedings of the 30th EPS Conference on Plasma Physics and Controlled Fusion, St. Petersburg 2003, (Eds.) R.Koch, S.Lebedev. ECA 27A, European Physical Society, Geneva 2003, P-1.153.

301. *Puiatti*, M.E., M. Valisa*, M. Mattioli*, T. Bolzonella*, A. Bortolon*, I. Coffey*, R. Dux, M. von Hellermann*, P. Monier-Garbet*, M.F.F. Nave*, J. Ongena* and Contributors to the EFDA-JET Workprogramme:* Simulation of the Time Behaviour of Impurities in JET Ar-seeded Discharges and its Relation with Sawtoothing and RF Heating. Plasma Physics and Controlled Fusion, **45**, 2011-2024 (2003).

302. *Pütterich, T., R. Dux, J. Gafert, A. Kallenbach, R. Neu, R. Pugno, S.-W. Yoon and ASDEX Upgrade Team:* Carbon Influx Studies in the Main Chamber of ASDEX Upgrade. Plasma Physics and Controlled Fusion **45**, 1873-1892 (2003).

303. *Radtke, R. and C. Biedermann:* Sawtooth Activity of the Ion Cloud in an Electron-Beam Ion Trap. Physical Review E **67**, 032705 (2003).

304. R*adtke, R., C. Biedermann and P. Bachmann:* Sawtooth-like X-ray Emission Observed in EBIT. Nuclear Instruments and Methods in Physics Research B **205**, 250-254 (2003).

305. *Ramisch*, M., U. Stroth, S. Niedner and B.D. Scott:* On the detection of Reynolds stress as a driving and damping mechanism of geodesic acoustic modes and zonal flows. New Journal of Physics **5**, 12 (2003). http://www.iop.org/EJ/article/1367-2630/5/1/312/nj3112.pdf.

306. *Rapp*, J., W. Fundamenski*, J. Gafert, A. Huber*, S. Jachmich*, G.F. Matthews*, M. Stamp* and JET-EFDA Contributors:* L-Mode Density Limits at JET: Effect of Septum

Removal in the Mk-II Gas Box Divertor. In: Proceedings of the 30th EPS Conference on Plasma Physics and Controlled Fusion, St. Petersburg 2003, (Eds.) R.Koch, S.Lebedev. ECA 27A, European Physical Society, Geneva 2003, P-1.160.

307. *Rapp*, J., P. Monier-Garbet*, P. Andrew*, P. Dumortier*, T. Eich, W. Fundamenski*, M. von Hellermann*, J. Hogan*, L.C. Ingesson*, S. Jachmich*, H.R. Koslowski*, A. Loarte*, G.P. Maddison*, G.F. Matthews*, D.C. McDonald*, A.M. Messiaen*, J. Ongena*, V. Parail*, V. Philipps*, G. Saibene*, R. Sartori*, B. Unterberg* and JET-EFDA Contributors:* Reduction of divertor heat load in JET ELMy H-modes using impurity seeding techniques. In: Proceedings of the 19th Fusion Energy Conference, Lyon 2002, (Ed.) M.Spak. IAEA, Vienna 2003, EX/P1-09.

308. *Raupp, G., R. Cole*, K. Behler, M. Fitzek*, P. Heimann, A. Lohs, K. Lüddecke*, G. Neu, J. Schacht, W. Treutterer, D. Zasche, T. Zehetbauer, M. Zilker and ASDEX Upgrade Team:* A "Universal Time" System for ASDEX Upgrade. Fusion Engineering and Design **66-68**, 947-951 (2003).

309. *Reich, J., W. Gardebrecht, B. Hein, B. Missal, F. Starke and K.-U. Seidler:* Manufacture of Cryostat Components for Wendelstein 7-X. Fusion Engineering and Design **69**, 345-348 (2003).

310. *Renner, H., J. Boscary, H. Greuner, H. Grote, D. Hildebrandt, J. Kisslinger, R. Schneider and D. Sharma:* Divertor concept for the WENDELSTEIN 7-X stellarator. Theoretical studies of the boundary and engineering. In: Proceedings of the 19th Fusion Energy Conference, Lyon 2002, (Ed.) M.Spak. IAEA, Vienna 2003, FT/P2-04.

311. *Ribeiro*, T., B.D. Scott, D.P. Coster and F. Serra*:* Flux Surface Geometry for Turbulence Computation on Open Field Lines. In: Proceedings of the 30th EPS Conference on Plasma Physics and Controlled Fusion, St. Petersburg 2003, (Eds.) R.Koch, S.Lebedev. ECA 27A. European Physical Society, Geneva 2003, P-1.152.

312. *Richter, S.:* Das Stadtentwicklungsmodul in der integralen Methode URBS - Beschreibung und erste Ergebnisse am Beispiel Augsburg. Beiträge zur Stadtentwicklung, Stadtforschung und Statistik, Heft 22, (2003), 73 S.

313. *Richter, S. and T. Hamacher:* Die integrale Methode URBS zur Beschreibung und Optimierung urbaner Energiesysteme. In: Optionen für die Energie der Zukunft, DPG-Physikertagung, Arbeitskreis Energie, Hannover 2003, (Ed.) M.Keilhacker. Deutsch Physikalische Gesellschaft 2003, 133-170.

314. *Richter S. and T. Hamacher:* URBS - A Model for Investigations On Future Urban Energy Systems. In: Proceedings PowerGen Europe, International Conference and Fair, Düsseldorf 2003. Penn Well Verlag 2003.

315. *Riemann, J., M. Borchardt, R. Schneider, X. Bonnin, A. Mutzke, T. Rognlien* and M. Umansky*:* Hierarchy Tests of Edge Transport Models (BoRiS, UEDGE). Journal of Nuclear Materials **313-316**, 1030-1035 (2003).

316. *Riemann, J., M. Borchardt, R. Schneider, A. Mutzke, T.D. Rognlien* and M.V. Umansky*:* Navier-Stokes Neutral and Plasma Fluid Modelling in 3D. In: Proceedings of the 30th EPS Conference on Plasma Physics and Controlled Fusion, St. Petersburg 2003, (Eds.) R.Koch, S.Lebedev. ECA 27A. European Physical Society, Geneva 2003, P-2.151.

317. *Riße, K., T. Rummel, L. Wegener, R. Holzthüm, N. Jaksic, F. Kerl and J. Sapper:* Fabrication of the Superconducting Coils for Wendelstein 7-X. Fusion Engineering and Design **66-68**, 965-969 (2003).

318. *Rohde, V. and ASDEX Upgrade Team:* On the Influence of Parasitic Plasma below the Divertor Structure of ASDEX Upgrade on the Formation of a-C:H Layers. In: Proceedings of the 30th EPS Conference on Plasma Physics and Controlled Fusion, St. Petersburg 2003, (Eds.) R.Koch, S.Lebedev. ECA 27A. European Physical Society, Geneva 2003, P-1.154.

319. *Rohde, V., M. Mayer and ASDEX Upgrade Team:* Characterisation and Formation of a-C:D Layers below the Divertor of ASDEX Upgrade. Physica Scripta **T103**, 25-28 (2003).

320. *Rohde, V., M. Mayer and ASDEX Upgrade Team:* On the formation of a-C:D layers and parasitic plasma underneath the roof baffle of the ASDEX Upgrade divertor. Journal of Nuclear Materials **313-316**, 337-341 (2003).

321. *Rohde, V., R. Neu, R. Dux, A. Geier, X. Gong, A. Kallenbach, K. Krieger, S. Lindig, H. Maier, W. Müller, R. Pugno, W. Schneider and ASDEX Upgrade Team:* Operation of ASDEX Upgrade with Tungsten Coated Walls. In: Proceedings of the 19th Fusion Energy Conference, Lyon 2002, (Ed.) M.Spak. IAEA, Vienna 2003, EX/D1-4.

322. *Romé, M., V. Erckmann, H.P. Laqua, H. Maassberg and N.B. Marushchenko:* Comparison of high-field-side and low-field-side launch ECCD in the W7-AS stellarator. Plasma Physics and Controlled Fusion **45**, 783-792 (2003).

323. *Rozhansky*, V., E. Kaveeva*, S. Voskoboynikov*, A.H. Bekheit*, D. Coster, X. Bonnin and R. Schneider:* Impact of *E x B* Drifts on the Distribution of Impurities in the Tokamak Plasma Edge. Journal of Nuclear Materials **313-316**, 1141-1149 (2003).

324. *Rozhansky*, V., E. Kaveeva*, S. Voskoboynikov*, D.P. Coster, X. Bonnin and R. Schneider:* Potentials and currents in the edge tokamak plasma: simplified approach and comparison with two-dimensional modelling. Nuclear Fusion **43**, 614-621 (2003).

325. *Rozhansky*, V.A., E.G. Kaveeva*, S. Voskoboynikov*, G. Counsell*, A. Kirk*, D.P. Coster, X. Bonnin and R. Schneider:* First Results from B2SOLPS5.0 Plasma Edge Modeling for the MAST Spherical Tokamak. In: Proceedings of the 30th EPS Conference on Plasma Physics and Controlled Fusion, St. Petersburg 2003, (Eds.) R.Koch, S.Lebedev. ECA 27A. European Physical Society, Geneva 2003, P-3.91.

326. *Rozhansky*, V.A., I.Y. Senichenkov*, I.Y. Veselova*, L.L. Lengyel and R. Schneider:* Mass Deposition after Pellet Injection into a Tokamak. In: Proceedings of the 30th EPS Conference on Plasma Physics and Controlled Fusion, St. Petersburg 2003, (Eds.) R.Koch, S.Lebedev. ECA 27A. European Physical Society, Geneva 2003, P-3.155.

327. *Rubel*, M., P. Wienhold* and D. Hildebrandt:* Ion Beam Analysis Methods in the Studies of Plasma Facing Materials in Controlled Fusion Devices. Vaccum **70**, 423-428 (2003).

328. *Rummel, T., F. Füllenbach and T. Mönnich:* Power Supplies for the Wendelstein 7-X Stellarator. Fusion Engineering and Design **66-68**, 1115-1118 (2003).

329. *Runov, A., S. Kasilov*, D. Reiter*, N. McTaggart, X. Bonnin and R. Schneider:* Transport in Complex Magnetic Geometries: 3-Dimensional Modelling of Ergodic Edge Plasmas in Fusion Experiments. Journal of Nuclear Materials **313-316**, 1292-1297 (2003).

330. *Runov, A.M., N. McTaggart, S. Kasilov*, R. Schneider, X. Bonnin and D. Reiter*:* Transport Modelling for Ergodic Configurations. In: Proceedings of the 30th EPS Conference on Plasma Physics and Controlled Fusion, St. Petersburg 2003, (Eds.) R.Koch, S.Lebedev. ECA 27A. European Physical Society, Geneva 2003, P-2.149.

331. *Ryan*, P.M., A.L. Rosenberg*, D.W. Swain*, J.R. Wilson*, D.B. Batchelor*, M.G. Bell*, R.E. Bell*, S. Bernabei*, J.M.*

Bitter, P.T. Bonoli*, M. Brambilla, A. Cardinali*, M.D. Carter*, D. Darrow*, E. Fredrickson*, D. Gates*, J.C. Hosea*, E.F. Jaeger*, S.M. Kaye*, B.P. LeBlanc*, R. Maingi*, T.K. Mau*, S.S. Medley*, J.E. Menard*, D. Mueller*, M. Ono*, F. Paoletti*, Y.-K.M. Peng*, C.K. Phillips*, R.I. Pinsker*, D.A. Rasmussen*, S.A. Sabbagh*, E.J. Synokowski*, J.B. Wilgen* and NSTX Team:* RF heating and current drive on NSTX with high harmonic fast waves. In: Proceedings of the 19th Fusion Energy Conference, Lyon 2002, (Ed.) M.Spak. IAEA, Vienna 2003, EX/P2-13.

332. *Ryter, F., A. Stäbler and G. Tardini:* Core Energy Transport in Conventional Scenarios in ASDEX Upgrade. Fusion Science and Technology **44**, 618-634 (2003).

333. *Ryter, F., W. Suttrop, H.-U. Fahrbach, K. Kirov, F. Leuterer, A.G. Peeters, G. Pereverzev, G. Tardini and ASDEX Upgrade Team:* Diagnosing Electron Heat Transport in ASDEX Upgrade with ECH Power Modulation. In: Proceedings of the 11th International Congress on Plasma Physics, Sydney 2002, (Eds.) I.S.Falconer, R.L.Dewar, J.Khachan. AIP Conference Proceedings 669, American Institute of Physics, Melville,NY 2003, 199-202.

334. *Ryter, F., G. Tardini, F. De Luca*, H.-U. Fahrbach, F. Imbeaux*, A. Jacchia*, K. Kirov, F. Leuterer, P. Mantica*, A.G. Peeters, G. Pereverzev, W. Suttrop and ASDEX Upgrade Team:* Electron Heat Transport in ASDEX Upgrade: Experiment and Modelling. Nuclear Fusion **43**, 1396-1404 (2003).

335. *Saarelma*, S., S. Günter, L.D. Horton and ASDEX Upgrade Team:* MHD Stability Analysis of Type II ELMs in ASDEX Upgrade. Nuclear Fusion **43**, 262-267 (2003).

336. *Saarelma*, S., S. Günter, L.D. Horton, T. Kurki-Suonio*, P.T. Lang, W. Suttrop and ASDEX Upgrade Team:* MHD Stability Analysis of ASDEX Upgrade H-mode Plasmas in Various ELMy and ELM-free Regimes. In: Proceedings of the 30th EPS Conference on Plasma Physics and Controlled Fusion, St. Petersburg 2003, (Eds.) R.Koch, S.Lebedev. ECA 27A. European Physical Society, Geneva 2003, P-1.122.

337. *Santos*, J., M.E. Manso*, P. Varela, J. Neuhauser and ASDEX Upgrade Team:* Plasma position measurements from ordinary FM-CW reflectometry on ASDEX Upgrade. Review of Scientific Instruments **74**, 1489-1492 (2003).

338. *Scavino*, E., J.S. Bakos*, R. Dux, H. Weisen* and TCV Team:* Effects of Plasma Shape on Laser Blow-off Injected Impurity Transport in TCV. Plasma Physics and Controlled Fusion **45**, 1961-1974 (2003).

339. *Schauer, F., H. Bau, Y. Bozhko, R. Brockmann, M. Nagel, M. Pietsch and S. Raatz:* Cryotechnology for Wendelstein 7-X. Fusion Engineering and Design **66-68**, 1045-1048 (2003).

340. *Schmid, K. and J. Roth:* Comparison of Surface Modification and Erosion of High-Z Metals due to Carbon Ion Implantation. Surface Coatings and Technology **158-159**, 81-86 (2003).

341. *Schmid, K. and J. Roth:* Erosion of high-Z metals with typical impurity ions. Journal of Nuclear Materials **313-316**, 302-310 (2003).

342. *Schmidt, M. and A. Werner:* NBI Heating Simulations in W7-X with the “Advanced” _f Method. In: Proceedings of the 30th EPS Conference on Plasma Physics and Controlled Fusion, St. Petersburg 2003, (Eds.) R.Koch, S.Lebedev. ECA 27A. European Physical Society, Geneva 2003, P-1.15.

343. *Schwarz-Selinger, T., W. Jacob, R. Preuss and V. Dose:* Determination of the Electron Temperature in Hydrogen Discharges with Energy Dispersive Mass Spectrometry. In: Proceedings of the Workshop Frontiers in Low Temperature Plasma Diagnostics V, (Eds.) S.DeBenedictis, G.Dilecce. Organizing Comittee Workshop FLTPDV, Bari 2003, 192-195.

344. *Schwarz-Selinger, T., M. Meier, C. Hopf, A. von Keudell and W. Jacob:* Can plasma experiments unravel microscopic surface processes in thin film growth and erosion? Implications of particle-beam experiments on the understanding of a-C:H growth. Vacuum **71**, 361-376 (2003).

345. *Scott, B.D.:* Computation of Electromagnetic Turbulence and Anomalous Transport Mechanisms in Tokamak Plasmas. Plasma Physics and Controlled Fusion **45**, A385-A398 (2003).

346. Scott, B.D.: The Character of Transport Caused by *E x B* Drift Turbulence. Physics of Plasmas **10**, 963-976 (2003).

347. *Sengupta*, A., P.J. McCarthy*, J. Geiger and A. Werner:* Fast Recovery of Vacuum Magnetic Configuration of W7-X Stellarator Using Function Parametrization and Neutral Nets. In: Proceedings of the 30th EPS Conference on Plasma Physics and Controlled Fusion, St. Petersburg 2003, (Eds.) R.Koch, S.Lebedev. ECA 27A. European Physical Society, Geneva 2003, P-1.13.

348. *Shafranov*, V.D., W.A. Cooper*, M.Yu. Isaev*, M.I. Mikhailov*, J. Nührenberg, M.A. Samitov*, A.A. Skovoroda*, A.A. Subbotin* and R. Zille:* Optimized Poloidal Pseudosymmetry for Toroidal Systems. In: Proceedings of the 30th EPS Conference on Plasma Physics and Controlled Fusion, St. Petersburg 2003, (Eds.) R.Koch, S.Lebedev. ECA 27A. European Physical Society, Geneva 2003, P-4.17.

349. *Shalashov*, A.G., H. Maassberg, E. Holzhauer*, W. Kasparek*, L.V. Lubyako*, E.V. Suvorov* and W7-AS Team:* NBI-driven ion cyclotron instability in the lower hybrid frequency range in the W7-AS experiment. In: Proceedings of the 5th International Workshop on Strong Microwaves in Plasmas, Nizhny Novgorod 2002, (Ed.) A.G.Litvak. Russian Academy of Sciences, Institute of Applied Physics, Nizhny Novgorod 2003, 372-377.

350. *Sharma, D., Y. Feng, F. Sardei, H. Grote, P. Grigull and H. Renner:* Optimization of the W7-X Pumping System. In: Proceedings of the 30th EPS Conference on Plasma Physics and Controlled Fusion, St. Petersburg 2003, (Eds.) R.Koch, S.Lebedev. ECA 27A. European Physical Society, Geneva 2003, P-1.14.

351. *Sharpe*, J.P., V. Rohde, ASDEX Upgrade Team, A. Sagara*, H. Suzuki*, A. Komori*, O. Motojima* and LHD Experimental Group:* Characterization of dust collected from ASDEX-Upgrade and LHD. Journal of Nuclear Materials **313-316**, 455-459 (2003).

352. *Shishkin*, A., O. Shyshkin*, H. Wobig, Yu. Igitkhanov, O. Motojima*, S. Morimoto*, K. Yamazaki* and S. Inagaki*:* The Effect of Magnetic Field Modification on Heavy Ion Movement in Advanced Stellarators and Helical Devices. Journal of Nuclear Materials **313-316**, 1192-1196 (2003).

353. *Sihler, C., M. Huart, C.-P. Käsemann, B. Streibl and ASDEX Upgrade Team:* Operational Experience with Reactive Power Control Methods Optimized for Tokamak Power Supplies. Fusion Engineering and Design **66-68**, 1139-1142 (2003).

354. *Sihler, C., M. Huart, F. Stobbe, B. Streibl, W. Treutterer and A. Joswig*:* Excitation of Torsional Oscillations in Generator Shaft Lines by Plasma Feedback Control. Fusion Engineering and Design **66-68**, 1061-1064 (2003).

355. *Sihler, C., A.M. Miri*, A. Harada* and ASDEX Upgrade Team:* Damping of Torsional Resonances in Generator Shafts Using a Feedback Controlled Buffer Storage of Magnetic Energy. In: 5th International Conference on Power Systems Transients, New Orleans,LA 2003, 6b-3. http://www.ipst.org/TechPapers/2003/IPST03Paper6b-3.pdf.

356. *Sips, A.C.C., J. Hobirk and A.G. Peeters:* Advanced Tokamak Studies in ASDEX Upgrade. Fusion Science and Technology **44**, 605-617 (2003).

357. *Sips, A.C.C., E. Joffrin*, M. De Baar*, R. Barnsley*, R. Budny*, R.J. Buttery*, C.D. Challis*, C. Giroud*, O. Gruber, T.C. Hender*, J. Hobirk, X. Litaudon*, C.F. Maggi, Y.-S. Na, S.D. Pinches, A. Stäbler, ASDEX Upgrade Team and EFDA-JET Contributors:* Improved H-mode Identity Experiments in JET and ASDEX Upgrade. In: Proceedings of the 30th EPS Conference on Plasma Physics and Controlled Fusion, St. Petersburg 2003, (Eds.) R.Koch, S.Lebedev. ECA 27A. European Physical Society, Geneva 2003, P-1.87.

358. *Spies, G. O.:* Relaxed plasma-vacuum systems with pressure. Physics of Plasmas **10**, 3030-3031 (2003).

359. *Spies, G.O. and J.A. Tataronis*:* The Accumulation Continua in Ideal Magnetohydrodynamics. Physics of Plasmas **10**, 413-418 (2003).

360. *Spring, A., R. Brakel and H. Niedermeyer:* Wall Conditioning for Wendelstein 7-X by Glow Discharge. Fusion Engineering and Design **66-68**, 371-375 (2003).

361. *Stäbler, A., J. Hobirk, F. Leuterer, F. Meo and J.-M. Noterdaeme:* Current Drive in ASDEX Upgrade. Fusion Science and Technology **44**, 730-742 (2003).

362. *Stache, K., F. Kerl, J. Sapper, B. Sombach and L. Wegener:* The Superconducting Busbar System of Wendelstein 7-X. Fusion Engineering and Design **66-68**, 1119-1123 (2003).

363. *Stober, J., P.T. Lang and V. Mertens:* High-Density H-mode Operation in ASDEX Upgrade. Fusion Science and Technology **44**, 650-658 (2003).

364. *Stober, J., R. Dux, O. Gruber, L.D. Horton, P.T. Lang, R. Lorenzini*, C. Maggi, F. Meo, R. Neu, J.-M. Noterdaeme, A.G. Peeters, G.V. Pereverzev, F. Ryter, A.C.C. Sips, A. Stäbler, H. Zohm and ASDEX Upgrade Team:* Dependence of Particle Transport on Heating Profiles in ASDEX Upgrade. Nuclear Fusion **43**, 1265-1271 (2003).

365. *Stober, J., R. Dux, O. Gruber, L.D. Horton, P.T. Lang, R. Lorenzini**, C. Maggi, F. Meo, R. Neu, J.-M. Noterdaeme, A.G. Peeters, G.V. Pereverzev, F. Ryter, A.C.C. Sips, A. Stäbler, H. Zohm and ASDEX Upgrade Team:* Dependence of Particle Transport on Heating Profiles in ASDEX Upgrade. In: Proceedings of the 19th Fusion Energy Conference, Lyon 2002, (Ed.) M.Spak. IAEA, Vienna 2003, EX/C3-7Rb.

366. *Strachan*, J.D., W. Fundamenski*, M. Charlet*, G. Corrigan*, K. Erents*, J. Gafert, C. Giroud*, C. Gowers*, M. von Hellermann*, L.D. Horton, G.F. Matthews*, G. McCracken*, V. Philipps*, J. Spence*, M.F. Stamp*, K.-D. Zastrow* and EFDA-JET Work Programme Collaborators:* JET carbon screening experiments using methane gas puffing and its relation to intrinsic carbon impurities. Nuclear Fusion **43**, 922-941 (2003).

367. *Stratton*, B.C., N.C. Hawkes*, G.T.A. Huysmans*, J.A. Breslau*, L.E. Zakharov*, B. Alper*, R.V. Budny*, C.D. Challis*, R. De Angelis*, V. Drozdov*, C. Fenzi*, C. Giroud*, T.C. Hender*, J. Hobirk, S.C. Jardin*, E. Joffrin*, P.J. Lomas*, P. Lotte*, J. Mailloux*, W. Park*, E. Rachlew*, S. Reyes-Cortes*, E. Solano*, T. Tala*, K.-D. Zastrow* and EFDA-JET Contributors:* Equilibria and stability of JET discharges with zero core current density. In: Proceedings of the 19th Fusion Energy Conference, Lyon 2002, (Ed.) M.Spak. IAEA, Vienna 2003, EX/C3-1Rb.

368. *Streibl, B., N. Berger, U. Brendel, T. Härtl, V. Rohde and G. Schall:* Hydrogen Frosting Scenarios with the ASDEX Upgrade In-vessel Cyro Pump. Fusion Engineering and Design **69**, 103-108 (2003).

369. *Streibl, B., P.T. Lang, F. Leuterer, J.-M. Noterdaeme and A. Stäbler:* Machine Design, Fueling, and Heating in ASDEX Upgrade. Fusion Science and Technology **44**, 578-592 (2003).

370. *Subbotin*, A.A., W.A. Cooper*, M.I. Mikhailov*, J. Nührenberg, M.A. Samitov*, V.D. Shafranov* and R. Zille:* Elimination of the Bootstrap Current Factor in Stellarators with Poloidally Closed Contours of the Magnetic Field Strength. In: Proceedings of the 30th EPS Conference on Plasma Physics and Controlled Fusion, St. Petersburg 2003, (Eds.) R.Koch, S.Lebedev. ECA 27A. European Physical Society, Geneva 2003, P-4.16.

371. *Suttrop, W., A. Herrmann, F. Ryter and J. Stober:* H-Mode and Pedestal Physics in ASDEX Upgrade. Fusion Science and Technology **44**, 636-649 (2003).

372. *Suttrop, W., L.D. Horton, A.E. Hubbard*, D. McDonald*, R. Barnsley*, M. Beurskens*, P. Bonoli*, J.-M. Chareau*, J.G. Cordey*, J.W. Hughes*, P.J. Lomas*, G. Maddison*, A. Meigs*, F. Meo, D. Mossessian*, R. Neu, J.-M. Noterdaeme, V.V. Parail*, F. Ryter, J. Schweinzer, M. Stamp*, J.D. Strachan*, J. Stober, S. Wukitch*, ASDEX Upgrade Team, ALCATOR C-Mod Team and JET EFDA Contributors:* Parameter Similarity Studies in JET, ASDEX Upgrade and ALCATOR C-Mod. In: Proceedings of the 19th Fusion Energy Conference, Lyon 2002, (Ed.) M.Spak. IAEA, Vienna 2003, EX/P5-07.

373. *Suttrop, W., M. Maraschek, G.D. Conway, H.-U. Fahrbach, L. Fattorini*, G. Haas, L.D. Horton, S. Klose, T. Kurki-Suonio*, C.F. Maggi, P.J. McCarthy*, H. Meister, A. Mück, R. Neu, I. Nunes*, T. Pütterich, M. Reich, A.C.C. Sips and ASDEX Upgrade Team:* ELM-free Stationary H-mode Plasmas in ASDEX Upgrade. In: Proceedings of the 30th EPS Conference on Plasma Physics and Controlled Fusion, St. Petersburg 2003, (Eds.) R.Koch, S.Lebedev. ECA 27A. European Physical Society, P-1.125.

374. *Suttrop, W., M. Maraschek, G.D. Conway, H.-U. Fahrbach, G. Haas, L.D. Horton, T. Kurki-Suonio*, C.J. Lasnier*, A.W. Leonard*, C.F. Maggi, H. Meister, A. Mück, R. Neu, I. Nunes*, T. Pütterich, M. Reich, A.C.C. Sips and ASDEX Upgrade Team:* ELM-free Stationary H-mode Plasma in the ASDEX Upgrade Tokamak. Plasma Physics and Controlled Fusion **45**, 1399-1416 (2003).

375. *Svensson, J., A. Dinklage, J. Geiger and R. Fischer:* An Integrated Data Analysis Model for the W7- AS Stellarator. In: Proceedings of the 30th EPS Conference on Plasma Physics and Controlled Fusion, St. Petersburg 2003, (Eds.) R.Koch, S.Lebedev. ECA 27A. European Physical Society, Geneva 2003, P-1.65.

376. *Tasso, H. and G.N. Throumoulopoulos*:* Cross-helicity and Magnetized Trkal Flows. Physics of Plasmas **10**, 4897-4898 (2003).

377. *Tasso, H. and G.N. Throumoulopoulos*:* Two-Step Control of Wall Mode and the Monodromy Matrix. Physics Letters A **307**, 304-312 (2003).

378. *Terry*, J.L., S.J. Zweben*, K. Hallatschek, B. LaBombard*, R.J. Maqueda*, B. Bai*, C.J. Boswell*, M. Greenwald*, D. Kopon*, W.M. Nevins*, C.S. Pitcher*, B.N. Rogers*, D.P. Stotler* and X.Q. Xu*:* Observations of the turbulence in the scrape-off-layer of Alcator C-Mod and comparisons with simulation. Physics of Plasmas **10**, 1739-1747 (2003).

379. *Terry*, J.L., S.J. Zweben*, D.L. Rudakov*, J.A. Boedo*, K. Hallatschek, R.J. Maqueda*, R.A. Moyer*, B. Bai*, C.J. Boswell*, M. Greenwald*, S. Krasheninnikov*, B. LaBombard*, D. Kopon*, A.W. Leonard*, M.A. Mahdavi*, G.R. McKee*, W.M. Nevins*, B.N. Rogers*, P.C. Stangeby*, D. Stotler*, J.G. Watkins*, W.P. West*, D.G. Whyte* and X.Q. Xu*:* Experimental / theoretical

comparisons of the turbulence in the scrape-off-layers of Alcator C-Mod, DIII-D, and NSTX. In: Proceedings of the 19th Fusion Energy Conference, Lyon 2002, (Ed.) M.Spak. IAEA, Vienna 2003, EX/P5-10.

380. *Throumoulopoulos*, G.N., G. Poulipoulis*, G. Pantis* and H. Tasso:* Exact Magnetohydrodynamic Equilibria with Flow and Effects on the Shafranov Shift. Physics Letters A **317**, 463-469 (2003).

381. *Throumoulopoulos*, G.N. and H. Tasso:* On Axisymmetric Resistive Magnetohydrodynamic Equilibria with Flow Free of Pfirsch-Schlüter Diffusion. Physics of Plasmas **10**, 2382-2388 (2003).

382. *Thumm*, M., A. Arnold*, E. Borie*, G. Dammertz*, O. Drumm*, R. Heidinger*, M.V. Kartikeyan*, K. Koppenburg*, A. Meier*, B. Piosczyk*, D. Wagner and X. Yang*:* Development of Frequency Step-Tunable 1 MW Gyrotrons in D-Band. In: Proceedings of the 4th IEEE International Vacuum Electronics Conference (IVEC), Seoul 2003, IEEE, Piscataway,NJ 2003, 30-31.

383. *Treutterer, W., K. Behler, R. Cole*, J. Hobirk, M. Jakobi, A. Lohs, K. Lüddecke*, G. Neu, G. Raupp, W. Suttrop, D. Zasche, T. Zehetbauer, M. Zilker and ASDEX Upgrade Team:* The New ASDEX Upgrade Real-Time Control and Data Acquisition System. Fusion Engineering and Design **66-68**, 755-760 (2003).

384. *Turnbull*, A.D., L.L. Lao*, T.H. Osborne*, O. Sauter*, E.J. Strait*, T.S. Taylor*, M.S. Chu*, J.R. Ferron*, C.M. Greenfield*, A.W. Leonard*, R.L. Miller*, P.B. Snyder*, H.R. Wilson* and H. Zohm:* Edge Localized Modes in DIII-D High Performance Discharges. Plasma Physics and Controlled Fusion **45**, 1845-1872 (2003).

385. *Umansky*, M.V., T.D. Rognlien*, M.E. Fenstermacher*, M. Borchardt, A. Mutzke, J. Riemann, R. Schneider and L.W. Owen*:* Modeling of Localized Neutral Particle Sources in 3D Edge Plasmas. Journal of Nuclear Materials **313-316**, 559-563 (2003).

386. *Urano, H., W. Suttrop, L.D. Horton, A. Herrmann, J.C. Fuchs and ASDEX Upgrade Team:* Energy and Particle Losses during Type-I ELMy H-mode in ASDEX Upgrade. Plasma Physics and Controlled Fusion **45**, 1571-1596 (2003).

387. *Urano, H., W. Suttrop, L.D. Horton, A. Herrmann, J.C. Fuchs and ASDEX Upgrade Team:* The Influence of Plasma Density, Heating Power and Plasma Shape on Type-I ELM Energy and Particle Losses in ASDEX Upgrade. In: Proceedings of the 30th EPS Conference on Plasma Physics and Controlled Fusion, St. Petersburg 2003, (Eds.) R.Koch, S.Lebedev. ECA 27A. European Physical Society, Geneva 2003, P-1.121.

388. *Valovic*, M., R. Budny*, L. Garzotti*, X. Garbet*, A.A. Korotkov*, J. Rapp*, R. Neu*, O. Sauter*, H. Weisen*, P. de Vries*, B. Alper*, M. Beurskens*, J. Brzozowski*, D. McDonald*, H. Leggate*, V. Parail* and JET EFDA Contributors:* Density Peaking in ELMy H-Mode in JET. In: Proceedings of the 30th EPS Conference on Plasma Physics and Controlled Fusion, St. Petersburg 2003, (Eds.) R.Koch, S.Lebedev. ECA 27A, European Physical Society, Geneva 2003, P-1.105.

389. *Varela, P., M.E. Manso*, G.D. Conway, W. Suttrop, H. Zohm and ASDEX Upgrade Team:* High resolution edge density measurements in ASDEX Upgrade H-mode discharges with broadband reflectometry. Review of Scientific Instruments **74**, 1493-1496 (2003).

390. *Verhoeven*, A.G.A., W.A. Bongers*, B.S.Q. Elzendoorn*, M. Graswinckel*, P. Hellingman*, W. Kooijman*, O.G. Kruijt*, J. Maagdenberg*, D. Ronden*, J. Stakenborg*, A.B. Sterk*, J. Tichler*, S. Alberti*, T.P. Goodman*, M. Henderson*, J.A. Hoekzema*, J.W. Oosterbeek*, A. Fernandez*, K. Likin*, A. Bruschi*, S. Cirant*, S. Novak*, B. Piosczyk*, M. Thumm*, H. Bindslev*, A. Kaye*, C. Fleming* and H. Zohm:* The design of an ECRH system for JET-EP. Nuclear Fusion **43**, 1477-1486 (2003).

391. *Verhoeven*, A.G.A., W.A. Bongers*, B.S.Q. Elzendoorn*, M. Graswinckel*, P. Hellingman*, W. Kooijman*, O.G. Kruijt*, J. Maagdenberg*, D. Ronden*, J. Stakenborg*, A.B. Sterk*, J. Tichler*, S. Alberti*, M.A. Henderson*, J.A. Hoekzema*, A. Fernandez*, K. Likin*, A. Bruschi*, S. Cirant*, S. Novak*, B. Piosczyk*, M. Thumm*, A. Guigon*, C. Damiani*, J. Pamela*, A. Kaye*, C. Fleming* and H. Zohm:* Design and R&D of an ECRH system on JET. Fusion Engineering and Design **66-68**, 645-649 (2003).

392. *Verhoeven*, A.G.A., W.A. Bongers*, B.S.Q. Elzendoorn*, M. Graswinckel*, P. Hellingman*, W. Kooijman*, O.G. Kruijt*, J. Maagdenberg*, D. Ronden*, J. Stakenborg*, A.B. Sterk*, J. Tichler*, S. Alberti*, M.A. Henderson*, J.A. Hoekzema*, A. Fernandez*, K. Likin*, A. Bruschi*, S. Cirant*, S. Novak*, B. Piosczyk*, M. Thumm*, A. Guigon*, C. Damiani*, J. Pamela*, A. Kaye*, C. Fleming* and H. Zohm:* The design of the JET-ECRH system and design considerations for ITER. In: Proceedings of the 5th International Workshop on Strong Microwaves in Plasmas, Nizhny Novgorod 2002. (Ed.) A.G.Litvak. Russian Academy of Sciences, Institute of Applied Physics, Nizhny Novgorod 2003, 340-346.

393. *Volpe, F., H.P. Laqua and W7-AS Team:* BXO mode-converted electron Bernstein emission diagnostic (invited). Review of Scientific Instruments **74**, 1409-1413 (2003).

394. *Volpe, F., H.P. Laqua and W7-AS Team:* Electron Bernstein emission diagnostic of electron temperature profiles at W7-AS Stellarator. In: Proceedings of the 12th Joint Workshop on Electron Cyclotron Emission and Electron Cyclotron Heating, Aix-en-Provence 2002, (Ed.) G.Giruzzi. World Scientific Publ., New Jersey,NJ 2003, 221-226.

395. *Wagner F., R. Burhenn, F. Gadelmeier, J. Geiger, M. Hirsch, H.P. Laqua, A. Weller, A. Werner, S. Bäumel, J. Baldzuhn, R. Brakel, A. Dinklage, P. Grigull, M. Endler, V. Erckmann, H. Ehmler, Y. Feng, R. Fischer, L. Giannone, H.-J. Hartfuss, D. Hildebrandt, E. Holzhauer, Y. Igitkhanov, R. Jaenicke, M. Kick, A. Kislyakov*, A. Kreter*, J. Kisslinger, T. Klinger, S. Klose, J.P. Knauer, G. Kühner, H. Maaßberg, K. McCormick, D. Naujoks, H. Niedermeyer, C. Nührenberg, E. Pasch, N. Ramasubramanian, N. Rust, E. Sallander, F. Sardei, U. Wenzel, H. Wobig, E. Würsching, M. Zarnstorff*, S. Zoletnik* and W7-AS Team:* Major Results from Wendelstein 7-AS Stellarator, In: Proceedings of the 19th Fusion Energy Conference, Lyon 2002, (Ed.) M.Spak. IAEA, Vienna 2003, OV/2-4.

396. *Wanner, M., V. Erckmann, J.-H. Feist, W. Gardebrecht, D. Hartmann, R. Krampitz, H. Niedermeyer, H. Renner, T. Rummel, F. Schauer, L. Wegener, F. Wesner, G.A. Müller*, W. Kasparek*, M. Thumm* and G. Dammertz*:* Status of Wendelstein 7-X Construction. Nuclear Fusion **43**, 416-424 (2003).

397. *Warrier, M., X. Bonnin, R. Schneider and D.P. Coster:* Improved Plasma-Wall Interaction Model for B2-solps5.0. In: Proceedings of the 30th EPS Conference on Plasma Physics and Controlled Fusion, St. Petersburg 2003, (Eds.) R.Koch, S.Lebedev. ECA 27A. European Physical Society, Geneva 2003, P-2.150.

398. *Wehner*, S., F. Baumann* and J. Küppers:* Kinetic hysteresis in the CO oxidation reaction on Ir(111) surfaces. Chemical Physics Letters **370**, 126-131 (2003).

399. *Weller, A., J. Geiger, M. Zarnstorff*, E. Sallander, S. Klose, A. Werner, J. Baldzuhn, R. Brakel, R. Burhenn, A. Dinklage, H. Ehmler, R. Fischer, E. Fredrickson*, G.Y. Fu*, F. Gadelmeier, L. Giannone, P. Grigull, D. Hartmann, R. Jaenicke, J. Knauer,*

H.P. Laqua, H. Maassberg, S. Murakami, K. McCormick, D. Monticello*, C. Nührenberg, M. Osakabe*, E. Pasch, A. Reiman*, N. Rust, D.A. Spong*, F. Wagner, U. Wenzel, W7-AS Team and NBI Group:* Experiments Close to the Beta-Limit in Wendelstein W7-AS. Plasma Physics and Controlled Fusion **45**, A285-A308 (2003).

400. *Wenzel, U., K. McCormick, N. Ramasubramanian, P. Grigull and R. König:* A new plasma condensation phenomenon in the W7-AS island divertor. Journal of Nuclear Materials **313-316**, 1098-1102 (2003).

401. *Wesner, F., F. Braun, D.A. Hartmann, D. Birus, F. Braun and J. Wendorf:* ICRF Heating for Wendelstein 7-X. Fusion Engineering and Design **66-68**, 561-566 (2003).

402. *Wienhold*, P., V. Philipps*, A. Kirschner*, A. Huber*, J. von Seggern*, H.G. Esser*, D. Hildebrandt, M. Mayer, M. Rubel* and W. Schneider:* Short and long range transport of materials eroded from wall components in fusion devices. Journal of Nuclear Materials **313-316**, 311-320 (2003).

403. *Wilhelm, R.:* Compression Effects in Inductively Coupled, High-Power RF Discharges for Negative Hydrogen Ion Production. Physics of Plasmas **10**, 513-520 (2003).

404. *Wischmeier*, M., D.P. Coster, X. Bonnin, T. Eich, A. Huber*, L.C. Ingesson*, S. Jachmich*, A. Kukushkin*, A. Loarte*, G.F. Matthews*, R.A. Pitts*, J. Rapp*, D. Reiter*, E. Tsitrone* and Contributors EFDA JET Work Programme:* Divertor Detachment during Pure Helium Plasmas in JET. Journal of Nuclear Materials **313-316**, 980-985 (2003).

405. *Wobig, H., T. Andreeva, C.D. Beidler, E. Harmeyer, F. Herrnegger, Yu. Igitkhanov, J. Kisslinger, Ya.I. Kolesnichenko*, V.V. Lutsenko*, V.S. Marchenko*, C. Nührenberg, I.N. Sidorenko, Y. Turkin, A. Wieczorek* and Yu.V. Yakovenko*:* Concept of a Helias Ignition Experiment. Nuclear Fusion **43**, 889-898 (2003).

406. *Wobig, H., T. Andreeva, C.D. Beidler, E. Harmeyer, F. Herrnegger, Yu. Igitkhanov, J. Kisslinger, Ya.I. Kolesnichenko*, V.V. Lutsenko*, V.S. Marchenko*, C. Nührenberg, Y. Turkin*, A. Wieczorek* and Yu.V. Yakovenko*:* Recent development in Helias reactor studies. In: Proceedings of the 19th Fusion Energy Conference, Lyon 2002, (Ed.) M.Spak. IAEA, Vienna 2003, FT/1-6.

407. *Wolf*, R.C.:* Internal Transport Barriers in Tokamak Plasmas. Plasma Physics and Controlled Fusion **45**, R1-R91 (2003).

408. *Wolf*, R.C., Y. Baranov*, X. Garbet*, N.C. Hawkes*, A.G. Peeters, C.D. Challis*, M. De Baar*, C. Giroud*, E. Joffrin*, M.J. Mantsinen*, D. Mazon*, H. Meister, W. Suttrop, K.-D. Zastrow*, ASDEX Upgrade Team and Contributors to the EFDA-JET Workprogramme:* Characterization of Ion Heat Conduction in JET and ASDEX Upgrade Plasmas with and without Internal Transport Barriers. Plasma Physics and Controlled Fusion **45**, 1757-1778 (2003).

409. *Yang*, X., E. Borie*, G. Dammertz*, R. Heidinger*, K. Koppenburg*, F. Leuterer, B. Piosczyk*, D. Wagner and M. Thumm*:* The Influence of Window Parameters on the Transmission Characteristics of Millimeter Waves. International Journal of Infrared and Millimeter Waves **24**, 1805-1813 (2003).

410. *Yang*, X., E. Borie*, G. Dammertz*, R. Heidinger*, K. Koppenburg*, B. Piosczyk*, D. Wagner and M. Thumm*:* A CVD-Diamond Disk Brewster Window for a Frequency Step-Tunable 1 MW Gyrotron. International Journal of Infrared and Millimeter Waves **24**, 2017-2024 (2003).

411. *Yang*, X., O. Drumm*, A. Arnold*, E. Borie*, G. Dammertz*, K. Koppenburg*, B. Piosczyk*, D. Wagner and M. Thumm*:* Design of a Quasi-Optical Mode Converter for a Frequency Step-Tunable Gyrotron. International Journal of Infrared and Millimeter Waves **24**, 1599-1608 (2003).

412. *Yang*, X., D. Wagner, B. Piosczyk*, K. Koppenburg*, E. Borie*, R. Heidinger*, F. Leuterer, G. Dammertz* and M. Thumm*:* Analysis of Transmission Characteristics for Single and Double Disk Windows. International Journal of Infrared and Millimeter Waves **24**, 619-628 (2003).

413. *Ye, M.Y., H. Kanehara*, S. Fukuta*, N. Ohno* and S. Takamura*:* Blister Formation on Tungsten Surface under Low Energy and High Flux Hydrogen Plasma Irradiation in NAGDIS-I. Journal of Nuclear Materials **313-316**, 72-76 (2003).

414. *You, J.H. and H. Bolt:* Thermal Stress Intensity Factor of Interfacial Cracks of a Plasma-Facing Component under High Heat Flux Loading. Fusion Engineering and Design **65**, 483-492 (2003).

415. *You, J.H., O. Poznansky and H. Bolt:* A Comparative Study on Two Elasto-Plastic Mean Field Methods. Materials Science and Engineering A **344**, 201-208 (2003).

416. *Yu, Q., S. Günter and B.D. Scott:* Numerical Modeling of Linear Drift-Tearing Mode Stability. Physics of Plasmas **10**, 797-810 (2003).

417. *Yu, Q., S. Günter and B.D. Scott:* Numerical Modelling of Tearing Mode Stability. In: Proceedings of the 30th EPS Conference on Plasma Physics and Controlled Fusion, St. Petersburg 2003, (Eds.) R.Koch, S.Lebedev. ECA 27A. European Physical Society, Geneva 2003, P-1.113.

418. *Zalking*, V.M., V.V. Bobkov*, S.S. Alimov*, Vl.V. Bobkov, A.V. Onyshchenko* and R.I. Starovoitov*:* Modified Method for Measurement of Plasma Temperature with Double Langmuir Probe. In: Proceedings of the 30th EPS Conference on Plasma Physics and Controlled Fusion, St. Petersburg 2003, (Eds.) R.Koch, S.Lebedev. ECA 27A, European Physical Society, Geneva 2003, P-4.100.

419. *Zaniol*, B., C.F. Maggi, L. Carraro*, R. Dux, L.D. Horton, D. Nishijima, M.E. Puiatti*, F. Sattin*, P. Scarin*, M. Valisa* and ASDEX Upgrade Team:* Effect of ICRH on Impurity Transport in Improved H-Mode Discharges in ASDEX Upgrade. In: Proceedings of the 30th EPS Conference on Plasma Physics and Controlled Fusion, St. Petersburg 2003, (Eds.) R.Koch, S.Lebedev. ECA 27A, European Physical Society, Geneva 2003, P-1.118.

420. *Zohm, H., C. Angioni, R. Arslanbekov*, C.V. Atanasiu*, G. Becker, W. Becker, K. Behler, K. Behringer, A. Bergmann, R. Bilato, V. Bobkov, D. Bolshukhin*, T. Bolzonella*, K. Borrass, M. Brambilla, F. Braun, A. Buhler, A. Carlson, G.D. Conway, D.P. Coster, R. Drube, R. Dux, S. Egorov*, T. Eich, K. Engelhardt, H.-U. Fahrbach, U. Fantz*, H. Faugel*, K.H. Finken*, M. Foley*, P. Franzen, J.C. Fuchs, J. Gafert, K.B. Fournier*, G. Gantenbein*, O. Gehre, A. Geier, J. Gernhardt, T.P. Goodman*, O. Gruber, A. Gude, S. Günter, G. Haas, D. Hartmann, B. Heger, B. Heinemann, A. Herrmann, J. Hobirk, F. Hofmeister, H. Hohenöcker, L.D. Horton, V. Igochine, A. Jacchia*, M. Jakobi, F. Jenko, A. Kallenbach, O. Kardaun, M. Kaufmann, A. Keller, A. Kendl, J.-W. Kim, K.K. Kirov, R. Kochergov, H. Kollotzek, W. Kraus, K. Krieger, T. Kurki-Suonio*, B. Kurzan, P.T. Lang, C.J. Lasnier*, P. Lauber, M. Laux, A.W. Leonard*, F. Leuterer, A. Lohs, A. Lorenz, R. Lorenzini*, C. Maggi, H. Maier, K. Mank, M.E. Manso*, P. Mantica*, M. Maraschek, E. Martines*, K.-F. Mast, P. McCarthy*, D. Meisel, H. Meister, F. Meo, P. Merkel, R. Merkel, D. Merkl, V. Mertens, F. Monaco, A. Mück, H.W. Müller, M. Münich, H. Murmann, Y.-S. Na, G. Neu, R. Neu, J. Neuhauser, F. Nguyen*, D. Nishijima, Y. Nishimura, J.-M. Noterdaeme, I. Nunes*, G. Pautasso, A.G. Peeters, G.V. Pereverzev, S.D. Pinches, E. Poli, M. Proschek*, R. Pugno, E. Quigley*, G. Raupp,

M. Reich, T. Ribeiro, R. Riedl, V. Rohde, J. Roth, F. Ryter, S. Saarelma*, W. Sandmann, A. Savtchkov*, O. Sauter*, S. Schade, H.-B. Schilling, W. Schneider, G. Schramm, E. Schwarz, J. Schweinzer, S. Schweizer, B.D. Scott, U. Seidel, F. Serra*, S. Sesnic*, C. Sihler, A. Silva*, A.C.C. Sips, E. Speth, A. Stäbler, K.-H. Steuer, J. Stober, B. Streibl, E. Strumberger, W. Suttrop, A. Tabasso, A. Tanga, G. Tardini, C. Tichmann, W. Treutterer, M. Troppmann, H. Urano, P. Varela*, O. Vollmer, D. Wagner, U. Wenzel, F. Wesner, E. Westerhof*, R. Wolf*, E. Wolfrum, E. Würsching, S.-W. Yoon, Q. Yu, D. Zasche, T. Zehetbauer andH.-P. Zehrfeld:* Overview of ASDEX Upgrade results. In: Proceedings of the 19th Fusion Energy Conference, Lyon 2002, (Ed.) M.Spak. IAEA, Vienna 2003, OV/2-1.

421. *Zohm, H., C. Angioni, R. Arslanbekov*, C.V. Atanasiu*, G. Becker, W. Becker, K. Behler, K. Behringer, A. Bergmann, R. Bilato, V. Bobkov, D. Bolshukhin*, T. Bolzonella*, K. Borrass, M. Brambilla, F. Braun, A. Buhler, A. Carlson, G.D. Conway, D.P. Coster, R. Drube, R. Dux, S. Egorov*, T. Eich, K. Engelhardt, H.-U. Fahrbach, U. Fantz*, H. Faugel*, K.H. Finken*, M. Foley*, P. Franzen, J.C. Fuchs, J. Gafert, K.B. Fournier*, G. Gantenbein*, O. Gehre, A. Geier, J. Gernhardt, T. Goodman*, O. Gruber, A. Gude, S. Günter, G. Haas, D. Hartmann, B. Heger, B. Heinemann, A. Herrmann, J. Hobirk, F. Hofmeister, H. Hohenöcker, L.D. Horton, V. Igochine, A. Jacchia*, M. Jakobi, F. Jenko, A. Kallenbach, O. Kardaun, M. Kaufmann, A. Keller, A. Kendl, J.-W. Kim, K.K. Kirov, R. Kochergov, H. Kollotzek, W. Kraus, K. Krieger, T. Kurki-Suonio*, B. Kurzan, P.T. Lang, C.J. Lasnier*, P. Lauber, M. Laux, A.W. Leonard*, F. Leuterer, A. Lohs, A. Lorenz, R. Lorenzini*, C. Maggi, H. Maier, K. Mank, M.-E. Manso*, P. Mantica*, M. Maraschek, E. Martines*, K.-F. Mast, P. McCarthy*, D. Meisel, H. Meister, F. Meo, P. Merkel, R. Merkel, D. Merkl, V. Mertens, F. Monaco, A. Mück, H.W. Müller, M. Münich, H. Murmann, Y.-S. Na, G. Neu, R. Neu, J. Neuhauser, F. Nguyen*, D. Nishijima, Y. Nishimura, J.-M. Noterdaeme, I. Nunes*, G. Pautasso, A.G. Peeters, G.V. Pereverzev, S.D. Pinches, E. Poli, M. Proschek*, R. Pugno, E. Quigley*, G. Raupp, M. Reich, T. Ribeiro*, R. Riedl, V. Rohde, J. Roth, F. Ryter, S. Saarelma*, W. Sandmann, A. Savtchkov*, O. Sauter*, S. Schade, H.-B. Schilling, W. Schneider, G. Schramm, E. Schwarz, J. Schweinzer, S. Schweizer, B.D. Scott, U. Seidel, F. Serra*, S. Sesnic*, C. Sihler, A. Silva*, A.C.C. Sips, E. Speth, A. Stäbler, K.-H. Steuer, J. Stober, B. Streibl, E. Strumberger, W. Suttrop, A. Tabasso, A. Tanga, G. Tardini, C. Tichmann, W. Treutterer, M. Troppmann, H. Urano, P. Varela*, O. Vollmer, D. Wagner, U. Wenzel, F. Wesner, E. Westerhof*, R. Wolf*, E. Wolfrum, E. Würsching, S.-W. Yoon, Q. Yu, D. Zasche, T. Zehetbauer and H.-P. Zehrfeld:* Overview of ASDEX Upgrade Results. Nuclear Fusion **43**, 1570-1582 (2003).

422. *Zohm, H., G. Gantenbein*, A. Isayama*, A. Keller, R.J. La Haye*, M. Maraschek, A. Mück, K. Nagasaki*, S.D. Pinches and E.J. Strait*:* MHD Limits to Tokamak Operation and their Control. Plasma Physics and Controlled Fusion **45**, A163-A174 (2003).

423. *Zohm, H., G. Gantenbein*, A. Keller, F. Leuterer, M. Maraschek, A. Mück, R. Neu, F. Ryter, J. Stober, W. Suttrop and ASDEX Upgrade Team:* Confinement and Stability Studies with ECRH in ASDEX Upgrade. In: Strong Microwaves in Plasmas, Nizhny Novgorod 2002, (Ed.). A.G.Litvak. Russian Academy of Sciences, Institute of Applied Physics, Nizhny Novgorod 2003, 296-306.

424. *Zurro*, B., A. Ochando*, A. Baciero*, R. Dux, K.J. McCarthy*, F. Medina*, A. López-Sánchez*, D. Rapisard*, A. Fernandez*, I. Pastor*, J. Herranz* and TJ-II Team:* Transport Analysis of Impurities Injected by Laser Ablation in the TJ-II Stellarator. In: Proceedings of the 30th EPS Conference on Plasma Physics and Controlled Fusion, St. Petersburg 2003, (Eds.) R.Koch, S.Lebedev. ECA 27A, European Physical Society, Geneva 2003, P-2.79.

Diploma Theses

425. *Dreier, H.:* Optische Spektroskopie von hochgeladenen Ionen an der EBIT. Humboldt-Universität Berlin 2003.

426. *Fink, M.:* Untersuchung der Fluktuationen des Plasmapotentials mit emissiven und nichtemissiven elektrostatischen Sonden. Universität Greifswald 2003.

427. *Garcia Munoz, M.:* Modelling of Fast Ion Losses in Tokamaks. Universität München 2003.

428. *Lunt, T.:* Experimental Investigation on the Bohm Criterion behind a Magnetic Laval Nozzle. Humboldt-Universität Berlin 2003.

429. *Morlaine, L.:* Oxidation of W and WSi_2 Coatings - Influence of Cromium Addition. Ecole Nationale Superieure de Chimie de Paris 2003.

430. *Waldmann, B.:* Interpretation der sichtbaren Bremsstrahlung einiger ASDEX Ugrade-Entladungen. TU Augsburg 2003.

431. *Windisch, T.:* Untersuchung der Sägezahn-Aktivität von Ionen in EBIT. Humboldt-Universität Berlin 2003.

Doctoral Theses

432. *Bobkov, V.:* Studies of High Voltage Breakdown Phenomena on ICRF Antennas. TU München 2003.

433. *Franck, C.:* Experiments on Whistler Ware Dispersion in Bounded Magnetised Plasmas. Universität Greifswald 2003.

434. *Hopf, C.:* Chemische Zerstäubung und ionenunterstütztes Wachstum amorpher Kohlenwasserstoffschichten - Experimente mit Teilchenstrahlen. Universität Bayreuth 2003.

435. *Kochergov, R.:* Wave Equations for Low Frequency Waves in Hot Magnetically Confined Plasmas. Universität München 2003.

436. *Kugeler, O.:* Elektronenkoinzidenzmessungen an kleinen Molekülen mit hoher Energieauflösung. TU Berlin 2003.

437. *Lauber, P.:* Linear Gyrokinetic Description of Fast Particle Effects on the MHD Stability in Tokamaks. Universität München 2003.

438. *Ludvik, J.:* FE-analysis of the Stellarator W7-X with Regard to Static and Dynamic Loads. Universität Pilsen 2003.

439. *Matyash, K.:* Kinetic Modelling of Multi-Component Edge Plasmas. Universität Greifswald 2003.

440. *McTaggart, N.:* Higher Order Methods for Conduction-Convection Problems with High Anisotropy. Universität Greifswald 2003.

441. *Na, Y.-S.:* Modelling of Current Profile Control in Tokamak Plasmas. TU München 2003.

442. *Schröder, C.:* Experimental Investigations on Drift Waves in Linear Magnetized Plasmas. Universität Greifswald 2003.

443. *Tardini, G.:* Validation of Theory Based Transport Models in Tokamak Plasmas. Universität München 2003.

444. *Volpe, F.:* Electron Bernstein Emission Diagnostic of Electron Temperature Profile at W7-AS Stellarator. Universität Greifswald 2003.

445. *Yoon, S.-W.:* The Relation of Carbon Influxes and Core Carbon Concentrations in ASDEX Upgrade. TU München 2003.

Habilitations

446. *Peeters, A.G.:* Kinetic Effects and Transport in Tokamak Plasma. TU München 2003.

447. *Neu, R.:* Tungsten as a Plasma Facing Material in Fusion Devices. Universität Tübingen 2003.

Patents

448. *Haas, G.:* Heißkathoden-Ionisationsmanometer II. Ende der deutschen Gebrauchsmuster-Schutzdauer: 13.04.2003

449. *Sihler, C.:* Verfahren zur aktiven elektromagnetische Dämpfung von Torsionsschwingungen im Wellenstrang von großen elektrischen Maschinen. Erfindungsmeldung: 03.03.2003. Erfindung wurde unbeschränkt in Anspruch genommen: 20.05.2003. Anmeldung der Erfindung und Stellung des Prüfantrags: 13.06.2003. Amtl. Aktenzeichen 103 26 816.2. Meldung einer Weiterentwicklung der Erfindung 24.11.2003.

450. *Küppers, J. and Th. Zecho*:* Wasserstoffspeicherung auf Kohlenstoff-Nanoröhrchen. Erfindungsmeldung: 18.03.2003. Freigabe der Erfindung: 17.06.2003.

451. *Schacht, J. and H. Niedermeyer:* Verfahren und Vorrichtung zum Synchronisieren und Steuern von technischen Systemen. Offenlegung der Patentschrift: 30.01.2003. Erteilung des deutschen Patentes DE 101 34 194.A1: 26.06.2003.

452. *Mast, K.-F., G. Schramm and M. Münch:* Folienmanometer. Aufgabe des deutschen Patentes: 16.04.2003.

453. *Dose, V., A. Golan* and U. von Toussaint:* Decomposition of Quadrupole Mass Spectra. Erfindungsmeldung: 06.05.2003. Freigabe der Erfindungsmeldung: 17.06.2003.

454. *Schaer, F.:* Abstandhalter mit extrem niedriger Wärmeleitung. Erfindungsmeldung: 22.09.2003.

455. *Allen, F., C. Biedermann and R. Radtke:* Extraction of Highly Charged Ions at the Berlin EBIT. Frühjahrstagung Hannover. Verhandl. DPG (VI) **38** (6), A 11.1 (2003).

456. *Allfrey*, S.J. and R. Hatzky:* Recent advances in nonlinear gyrokinetic simulation. 18th International Conference on Numerical Simulation of Plasmas, Cape Cod,MA 2003.

457. *Andreeva, T., C.D. Beidler, E. Harmeyer, F. Herrnegger, Yu. Igitkhanov, J. Kisslinger, Ya.I. Kolesnichenko*, V.V. Lutsenko*, C. Nührenberg, A. Shishkin* and H. Wobig:* The Helias Reactor Concept: Comparison of Different Field Period Configurations. 14th InternationalStellarator Workshop, Greifswald 2003.

458. *Andreeva, T., J. Kisslinger and Yu. Igitkhanov:* Analysis of Magnetic Field Perturbations during the Assembly of W7-X. 14th International Stellarator Workshop, Greifswald 2003.

459. *Arnold*, A., G. Dammertz*, K. Koppenburg*, D. Wagner and M. Thumm*:* Low Power Measurements on a Mode Converter System of Step-Tunable Gyrotrons. 28th International Conference on Infrared and Millimeter Waves, Otsu, Shiga 2003.

460. *Bachmann, P., D. Hildebrandt and D. Sünder:* Nonlinear Heat Transport in Anisotropic Targets Irradiated by Laser Pulses. 9th International Workshop on Plasma Edge Theory in Fusion Devices , San DiegoCA 2003.

461. *Bakhareva*, O.A., B.V. Kuteev*, V.Yu. Sergeev*, V.G. Skokov*, V.M. Timokhin*, R. Burhenn and W7-AS Team:* Studies of C Pellet Ablation Cloud Structure in W7-AS Plasmas. Russian Annual Conference on Plasma Physics and Controlled Fusion, Zwenigorod 2003.

462. *Balden, M., H. Bolt, A.F. Bardamid*, A.I. Belyaeva*, K.A. Slatin*, J.W. Davis*, A.A. Haasz*, M. Poon*, V.G. Konovalov*, I.V. Ryzhkov*, A.N. Shapoval* and V.S. Voitsenya*:* Surface Roughening and Grain Orientation Dependence of the Erosion of Polycrystalline Stainless Steel by Hydrogen Irradiation. 11th International Conference on Fusion Reactor Materials, Kyoto 2003.

463. *Balden, M., E. de Juan Pardo, H. Maier, P. Starke and U. Fantz*:* Chemical Erosion Behaviour of Doped Graphites under Hydrogen Impact - A Comparison of Ion Beam Experiments and Planar Inductively Coupled RF Plasmas. 10th International Workshop on Carbon Materials for Fusion Application, Jülich 2003.

464. *Balden, M., J. Roth, E. de Juan Pardo, A. Weghorn and C. García-Rosales*:* Chemical Erosion of Carbon by Hydrogen Bombardment Potential of Mitigation by Doping. University of Toronto, Institute for Aerospace Studies, Toronto 2003.

465. *Balden, M., J. Roth, E. de Juan Pardo, A. Weghorn and C. García-Rosales*:* Chemical Erosion of Carbon Materials by Hydrogen - Reduction by Doping and Morphology Changes. PISCES, University of California, San Diego,CA 2003.

466. *Baldzuhn, J, L.R. Baylor*, J.F. Lyon* and W7-AS Team:* Penetration Studies for Deuterium Pellets in W7-AS. 14th International Stellarator Workshop, Greifswald 2003.

467. *Bandyopadhyay, M., A. Tanga, P. McNeely and V. Yaroshenko*:* Comparative Measurements between Langmuir Probe and Ion-Acoustic Wave Detection in a Radio Source. 5th International Workshop on Electrical Devices in Magnetical Plasma, Greifswald 2003.

468. *Bandyopadhyay, M. and R. Wilhelm:* Simulation of Negative Hydrogen Ion Production and Transport in a Negative Ion Source. 10th International Conference on Ion Sources, JINR, Dubna 2003.

469. *Bauer, M.:* Oberflächenprozesse beim Wachstum von a-C:H-Schichten in gepulsten Plasmen. 11. Bundesdeutsche Fachtagung Plasmatechnologie, Ilmenau 2003.

470. *Bäumel S.:* Energetic Ion Loss Diagnostic for Fusion Plasmas. MIT, Cambridge 2003.

471. *Bäumel, S.:* Investigation of Fluctuations in the HDH and H* Regime of Wendelstein 7-AS. 14th International Stellarator Workshop, Greifswald 2003.

472. *Bäumel S., A. Werner, R. Semler, D. Darrow*, E. Cecil*, L. Pedrick*, H. Altmann and V. Kiptily*:* Lost Alpha Particle Diagnostic Design Review. JET, Culham 2003.

473. *Bäumel S., A. Werner, R. Semler, D. Darrow*, E. Cecil*, L. Pedrick*, H. Altmann and V. Kiptily*:* Lost Alpha Particle Diagnostic Progress. General Review Meeting, JET, Culham 2003.

474. *Bäumel S., A. Werner, R. Semler, D. Darrow*, E. Cecil*, L. Pedrick*, H. Altmann and V. Kiptily*:* Lost Alpha Particle Project - Scintillator Probe. Final Design Review, JET, Culham 2003.

475. *Bäumel S., A. Werner, R. Semler, D. Darrow*, E. Cecil*, L. Pedrick*, H. Altmann and V. Kiptily*:* Lost Alpha Particle Project - Scintillator Probe. General Review Meeting, JET, Culham 2003.

476. *Bäumel S., A. Werner, R. Semler, D. Darrow*, E. Cecil*, L. Pedrick*, H. Altmann and V. Kiptily*:* Lost Alpha Particle Project - Scintillator Probe. Preliminary Design Review, JET, Culham 2003.

477. *Bäumel, S., A. Werner, R. Semler, D. Darrow*, E. Cecil*, L. Pedrick*, H. Altmann and V. Kiptily*:* Scintillator Probe Alpha-Loss Diagnostic for JET. APS, Division of Plasma Physics, 45th Annual Meeting, Albuquerque,NM 2003. Bulletin of the American Physical Society **48** (7), 204 (2003).

478. *Behler, K., H. Blank, A. Buhler, R. Drube, K. Engelhardt, M. Jacobi, A. Lohs, R. Merkel, G. Raupp, M. Zilker, ASDEX Upgrade Control Team and XDV Team:* Integration of Real-Time Data Acquisition Systems into the ASDEX Upgrade Diagnostic and Control Architecture. 4th IAEA TCM on Control, Data Acquisition and Remote Participation for Fusion Research, San Diego,CA 2003.

479. *Behler, K., U. Schwenn and W. Suttrop:* Video-Conferencing and Remote Participation Features at ASDEX Upgrade - Report of Recent Experiences. 4th IAEA TCM on Control, Data Acquisition and Remote Participation for Fusion Research, San Diego,CA 2003.

480. *Behringer, K.:* Aktuelle Fragen der Plasmaphysik. Seminar, Universität Augsburg, SS 2003.

481. *Behringer, K.:* Atomic Data for Present and Next Generation in Fusion Research. NIST Symposium for Atomic Physics, Gaithersburg 2003.

482. *Behringer, K.:* Einführung in die Plasmaspektroskopie. Vorlesung, Universität Augsburg, WS 2003/2004.

483. *Behringer, K.:* Spektroskopie von Nichtgleichgewichts-plasmen. Vorlesung, Universität Augsburg, SS 2003.

484. *Behringer, K. and U. Fantz*:* Physikalisches Praktikum für Fortgeschrittene Teil B. Seminar, Universität Augsburg, SS 2003.

485. *Behringer, K., U. Fantz* and T. Hamacher:* Physikalische Grundlagen der Energiewandlung und Verteilung. Seminar, Universität Augsburg, WS 2003/2004.

486. *Behringer, K., U. Fantz* and T. Hamacher:* Probleme der zukünftigen Energieversorgung. Seminar, Universität Augsburg, SS 2003.

487. *Behringer, K., U. Fantz* and M. Schreck*:* Anwendungen und Diagnostik von Niederdruckplasmen. Seminar, Universität Augsburg, SS 2003.

488. *Behringer, K., M. Stritzker*, U. Fantz* and H. Schreck*:* Diagnostik von Niederdrucktemperaturplasmen als industrielle Schlüsseltechnologie. Seminar, Universität Augsburg, WS 2003/2004.

489. *Behrisch, R.:* Plasma Materials Interaction in Fusion Research. International Conference on Ion Surface Interactions (ISI), Zvenigorod 2003.

490. *Beidler, C.D., S.V. Kasilov*, W. Kernbichler*, H. Maaßberg, D.R. Mikkelsen*, S. Murakami*, V.V. Nemov*, M. Schmidt, D.A. Spong*, V. Tribaldos*, A. Wakasa* and R.B. White*:* Neoclassical Transport in Stellarators - Further Results from an International Collaboration. 14th International Stellarator Workshop, Greifswald 2003.

491. *Bessenrodt-Weberpals, M.:* Diagnostik heißer Laborplasmen. Vorlesung, Universität Düsseldorf, SS 2003.

492. *Biedermann, C. and R. Radtke:* Spectroscopy of Highly Charged Argon for Plasma Diagnostics. 23rd ICPEAC, Stockholm 2003.

493. *Biel, W. and R. Burhenn:* Design of Optimised VUV / XUV Spectrometers for Impurity Studies on W7-X. Spring Meeting Aachen. Verhandl. DPG (VI) **38** (4), P 17.30 (2003).

494. *Bohmeyer, W., G. Fußmann, B. Koch, D. Naujoks and H.-D. Reiner:* Plasmagenerator PSI-2. Magnum-PSI-Seminar, Garching 2003.

495. *Bohmeyer, W., D. Naujoks, A. Markin*, I. Arkhipov*, P. Carl*, B. Koch, D. Schröder and G. Fußmann:* Transport and Deposition of Hydrocarbons in the Plasmagenerator PSI-2. 11th European Fusion Physics Workshop, Heraklion 2003.

496. *Bolt, H.:* Development of Plasma-Facing Materials. UKAEA Brainstorming Meeting on Future Materials Activities, UKAEA, Culham 2003.

497. *Bolt, H.:* Dünne Schichten. Vorlesung, Technische Universität München, SS 2003.

498. *Bolt, H.:* Materialien für die plasmabelasteten Komponenten von Fusionsanlagen. Materials Colloquium, Technische Universität Wien 2003.

499. *Bolt, H.:* Materials for Extreme Environments, JAERI, Naka 2003.

500. *Bolt, H.:* Materials for Fusion Energy Systems. Technical University of Warzaw 2003.

501. *Bolt, H.:* Materials for the Plasma-Facing Components of Fusion Devices. Max-Planck-Institut für Eisenforschung, Düsseldorf 2003.

502. *Bolt, H.:* Oberflächentechnik. Vorlesung, Technische Universität München, WS 2003/2004.

503. *Bolt, H.:* Some Views on the EU Fusion Programme besides ITER. Atomic Energy Commission of Japan, Tokyo 2003.

504. *Bolt, H., V. Barabash, W. Kraus, J. Linke*, R. Neu, S. Suzuki*, N. Yoshida* and ASDEX Upgrade Team:* Materials for the Plasma Facing Components of Fusion Reactors. 11th International Conference on Fusion Reactor Materials, Kyoto 2003.

505. *Boozer*, A.H. and C. Nührenberg:* Delta-W Calculation of Magnetic Islands in Plasma Equilibria. 30th EPS Conference on Plasma Physics and Controlled Fusion, St. Petersburg 2003.

506. *Boozer*, A.H. and C Nührenberg:* Delta-W Calculation of Magnetic Islands in Plasma Equilibria. International Sherwood Fusion Theory Conference, Corpus Christi 2003.

507. *Boscary, J., H. Greuner, J. Kisslinger, B. Mendelevitch, K. Pfefferle, H. Renner and B. Streibl:* Modification of the Target Design of the W7-X Divertor for Steady-State Operation. 20th IEEE-NPSS Symposium on Fusion Engineering, San Diego,CA 2003.

508. *Bradshaw, A.M.:* Fusionsforschung. Deutsch-französiches Kolloquium 'Energie in Europa'. Paris 2003.

509. *Bradshaw, A.M.:* Hochtemperaturplasmaphysik: Der Weg zu einem Fusionskraftwerk. Festkolloquium Plasmaforschung, Stuttgart 2003.

510. *Bradshaw, A.M.:* ITER in Europe and its Benefits. Meeting on 'A Candidate Site for the International Tokamak Experimental Reactor', Vandellós 2003.

511. *Bradshaw, A.M.:* Kernfusion: Prinzip, Stand der Forschung und zukünftige Entwicklungen. Leopoldina, Halle 2003.

512. *Bradshaw, A.M.:* Possible Cooperation / Consortia between Industrie and IPP. Workshop on the Opportunities for German Industry in ITER, Karlsruhe 2003.

513. *Bradshaw, A.M.:* Recent Advances in Fusion Research. Summer School, Karlsruhe 2003.

514. *Bradshaw, A.M.:* Stand und Zukunft der Fusionsforschung. Parlamentarischer Abend, Berlin 2003.

515. *Bräuer, T., T. Andreeva, M. Endler and J. Kisslinger:* Accuracy Requirements for the Fabrication and Assembly of Wendelstein 7-X. 14th International Stellarator Workshop, Greifswald 2003.

516. *Brendel, A.:* Herstellung und Charakterisierung von SiC-faserverstärkten Kupfermatrix-Verbundwerkstoffen. Deutsches Zentrum für Luft- und Raumfahrt, Köln 2003.

517. *Brendel, A., C. Popescu, C. Leyens*, J. Woltersdorf*, E. Pippel* and H. Bolt:* Metall-Matrix-Verbundwerkstoffe als Wärmesenkenmaterial in Fusionsreaktoren. 14th Symposium Verbundwerkstoffe und Werkstoffverbunde, Wien 2003.

518. *Brendel, A., C. Popescu, C. Leyens*, J. Woltersdorf*, E. Pippel* and H. Bolt:* SiC-Fibre Reinforced Copper as Heat Sink Material for Fusion Applications. 11th International Conference on Fusion Reactor Materials, Kyoto 2003.

519. *Brendel, A., C. Popescu , C. Leyens*, J. Woltersdorf*, E. Pippel* and H. Bolt:* SiC-Fibre Reinforced Copper Matrix Composites. International Conference Advanced Metallic Materials, Smolenice 2003.

520. *Burhenn, R., J. Baldzuhn, R. Brakel, H. Ehmler, L. Giannone, P. Grigull, J. Knauer, M.Krychowiak, M. Hirsch, K. Ida*, H. Maaßberg, K. McCormick, E. Pasch, H. Thomsen, A. Weller, W7-AS Team, ECRH Group and NI Group:* Impurity Transport in the W7-AS Stellarator. 14th International Stellarator Workshop, Greifswald 2003.

521. *Burhenn, R., W7-AS Team, ECRH Group and NI Group:* Impurity Transport Studied by Tracer Injection. Spring Meeting Aachen. Verhandl. DPG (VI) **38** (4), P V (2003).

522. *Camenen*, Y., A. Pochelon*, F. Ryter and S. Coda*:* Electron Heat Transport Studies under Intense EC Heating in TCV. IAEA Technical Meeting on ECRH Physics and Technology for ITER, Kloster Seeon 2003.

523. *Chankin, A.:* Drift Flows in the SOL and their Influence on Divertor Asymmetries. 11th European Fusion Physics Workshop, Heraklion 2003.

524. *Chung, J., R. König, R. Narayanan, T. Klinger and J. Howard*:* Time Resolved 2-D Doppler Imaging of the W7-AS Divertor Plasma Using a MOSS Spectrometer. Spring Meeting Aachen. Verhandl. DPG (VI) **38** (4), P 4.30 (2003).

525. *Danilov*, I., A. Meier*, R. Heidinger*, X. Yang*, F. Leuterer and D. Wagner:* Design of a Tunable Double Disk Window. 15th Joint Russian-German STC Meeting on ECRH and Gyrotrons, Karlsruhe/Stuttgart/Garching 2003.

526. *De Juan Pardo, E., M. Balden, B. Cieciwa, C. García-Rosales* and J. Roth:* Erosion Processes of Carbon Materials under Hydrogen Bombardment and their Mitigation by Doping. 10th International Workshop on Carbon Materials for Fusion Application, Jülich 2003.

527. *Dewar*, R.L., C. Nührenberg, B.F. McMillan* and T. Tatsuno*:* The Statistical Characterization of the Spectrum of Ideal-MHD Instabilities in Toroidal Plasmas. 5th International Congress on Industrial and Applied Mathematics, Sydney 2003.

528. *Dewar*, R.L., C. Nührenberg and T. Tatsuno*:* Quantum Chaos Theory and the Spectrum of Ideal-MHD Instabilities in Toroidal Plasmas. 13th International Toki Conference on Plasma Physics and Controlled Fusion, Toki 2003.

529. *Dinklage, A.:* Data Mining in der Fusionsphysik. Fachhochschule Stralsund 2003.

530. *Dinklage, A.:* Integrierte Datenanalyse. Universität Greifswald 2003.

531. *Dinklage, A.:* Topics and Methods for Steady- State Data Validation. 14th International Stellarator Workshop, Greifswald 2003.

532. *Dinklage, A., R. Fischer and J. Svensson:* Bayesian Methods for Integrated Data Analysis. Plasma-2003 International Conference, Warsaw 2003.

533. *Dinklage, A. and R. König:* Practical Spectroscopy. IMPRS, Universität Greifswald 2003.

534. *Dose, V.:* Bayesian Data Analysis. Kolloquium, Universität Bochum 2003.

535. *Dose, V.:* Bayesian Data Analysis. Kolloquium, Universität Konstanz 2003.

536. *Dose, V. and A. Menzel*:* Cherry Blossom and Plasma Turbulence. 23rd International Conference on Bayesian Methods and Maximum Entropy in Science and Engineering, Jackson Hole 2003.

537. *Düchs, D.:* Contribution to the Control of Plasma-Wall Interaction. Eingeladener Beitrag, 5th Symposium on Current Trends in International Fusion Research, Washington,D.C. 2003.

538. *Düchs, D.:* Plasma, ein komplexes und nichtlineares System; Methoden zur theoretischen Beschreibung. Vorlesung, Ruhr-Universität Bochum, SS 2003.

539. *Düchs, D.:* Wozu ist die Erforschung von Fusionsplasmen noch gut? Vorlesung, Ruhr-Universität Bochum, WS 2002/2003.

540. *Ehmler, H., Y. Turkin, K. McCormick, M. Reich, E. Wolfrum, W7-AS Team and ASDEX Upgrade Team:* Progress in Edge Measurements of Ion Temperature and Radial Electric Field. APS, Division of Plasma Physics, 45th Annual Meeting, Albuquerque 2003.

541. *Eich, T.:* ELM Transport in the SOL and Divertor. 11th European Fusion Physics Workshop, Heraklion 2003.

542. *Eich, T.:* Power Deposition in JET and ASDEX Upgrade. JET/EFDA Seminar, Abingdon 2003.

543. *Eich, T., J. Neuhauser and A. Herrmann:* Target Heat Load Pattern as Finger Points of Magnetic Edge Perturbation during Type ELMs in ASDEX Upgrade. 1st International Workshop on Stochasticity in Fusion Edge Plasmas, Jülich 2003.

544. *Ekedahl*, A., L. Colas*, M.-L. Mayoral*, B. Beaumont*, Ph. Bibet*, S. Brémond*, F. Kazarin*, J. Mailloux*, J.-M. Noterdaeme, A.A. Tuccillo* and EFDA-JET Contributors:* Density Convection near Radiating ICRH Antennas and its Effect on the Coupling of Lower Hybrid Waves. 15th Topical Conference on RF Power in Plasmas, Moran,WY 2003.

545. *Ekedahl*, A.G. Grancucci*, J. Mailloux*, V. Petrzilka*, K. Rantamäki*, Y. Baranov*, K. Erents*, M. Goniche*, E. Joffrin*, P.J. Lomas*, M.J. Mantsinen*, D. McDonald*, J.-M. Noterdaeme, V. Pricoli*, R. Sartori*, C. Silva*, M. Stamp*, A.A. Tuccillo*, F. Zacek* and EFDA-JET Contributors:* Long Distance Coupling of Lower Hybrid Waves in ITER Relevant Edge Conditions in JET Reversed Shear Plasmas. 15th Topical Conference on RF Power in Plasmas, Moran,WY 2003.

546. *Erckmann, V., H. Braune, G. Dammertz*, G. Gantenbein*, W. Kasparek*, H. Laqua, G. Michel, G. Iller*, M. Thumm* and W7-X ECRH Team at IPP, FZK and IPF:* The 10 MW ECRH and CD System for W7-X. 6th Workshop on High Energy Density and High Power RF, Berkeley,CA 2003.

547. *Eriksson*, L.-G., T. Johnson*, T. Hellsten*, C. Giroud*, V.G. Kiptily*, K. Kirov, J. Brozowski*, M. De Baar*, J. DeGrassie*, M.J. Mantsinen*, A. Meigs*, J.-M. Noterdaeme, A. Stäbler, A. Tuccillo*, H. Weisen*, K.-D. Zastrow* and JET-EFDA Contributors:* Evidence for the Influence of Fast Ions on Toroidal Plasma Rotation. 8th IAEA Technical Meeting on Energetic Particles in Magnetic Confinement Systems, San Diego,CA 2003.

548. *Eriksson*, L.-G., J.-M. Noterdaeme, S. Assas*, C. Giroud*, J. DeGrassie*, T. Hellsten*, T. Johnson*, V.G. Kiptily*, K. Kirov, M.J. Mantsinen*, K.-D. Zastrow*, M. De Baar*, J. Brozowski*, R. Budny*, R. Cesario*, V. Chan*, A.G. Gondhalekar*, N. Hawkes*, G.T. Hoang*, Ph. Lamalle*, A. Meigs*, F. Meo, F. Nguyen*, E. Righi*, A. Stäbler, D. Testa*, A. Tuccillo*, H. Weisen* and EFDA-JET Contributors:* Bulk Plasma Rotation in the Presence of Waves in the Ion Cyclotron Range of Frequencies. 15th Topical Conference on RF Power in Plasmas, Moran,WY 2003.

549. *Feist, J.-H. and W7-X Construction Team:* Status of Wendelstein 7-X Construction. 14th International Stellarator Workshop, Greifswald 2003.

550. *Feng, Y., F. Sardei and J. Kisslinger:* Essential Features of the Reversible Field-Line Mapping Technique. 9th International Workshop on Plasma Edge Theory in Fusion Devices, San Diego,CA 2003.

551. *Feng, Y., F. Sardei and J. Kisslinger:* Essential Features of the Reversible Field-Line Mapping Technique. 1st International Workshop on Stochasticity in Fusion Edge Plasmas, Jülich 2003.

552. *Feng, Y., F. Sardei, J. Kisslinger, P. Grigull, K. McCormick and D. Reiter:* 3D Modelling and Island Divertor. 9th International Workshop on Plasma Edge Theory in Fusion Devices, San Diego,CA 2003.

553. *Feng, Y., F. Sardei, J. Kisslinger, P. Grigull, K. McCormick and D. Reiter:* Physics and Modelling of the W7-AS Island Divertor. 14th International Stellarator Workshop, Greifswald 2003.

554. *Fink, M.A., M. Endler and T. Klinger:* New Developments of Self-emitting Electrostatic Probes for Use in High Temperature Plasmas. 5th International Workshop on Electrical Probes in Magnetized Plasmas, Greifswald 2003.

555. *Fischer, R.:* Bayesian Methods for Diagnostics Applications. Four Lectures and Three Seminars, Greifswald 2003.

556. *Fischer, R.:* Bestimmung der relativen biologischen Wirksamkeit von Neutronen. Seminar "Anwendung kernphysikalischer Methoden in der Interdisziplinären Forschung", Fakultät für Physik der Technischen Universität München und Sektion Physik der Universität München, Garching 2003.

557. *Fischer, R.:* Grundlagen der Bayes'schen Wahrscheinlichkeitstheorie. Seminar, Strahlenbiologisches Institut, Universität München 2003.

558. *Fischer, R., Ch. Räth and V. Dose:* Bayesian Group Analysis in Plasma Physics and Texture Analysis. Practical Bayesian Statistics 5, Milton Keynes 2003.

559. *Fußmann, G.:* Atom- und Molekülphysik. Vorlesung, Humboldt-Universität Berlin, SS 2003.

560. *Fußmann, G.:* Plasmaphysik und Fusionsforschung (Plasmaphysik II). Vorlesung, Humboldt-Universität Berlin, WS 2003/04.

561. *Fußmann, G.:* Plasmaspektroskopie an kosmischen Objekten. Vortrag, Gemeinschaftsseminar zur Experimentalphysik: Plasmen, Teilchen, Weltall, Humboldt-Universität Berlin 2003.

562. *Fußmann, G.:* Spektroskopie an Laborplasmen und kosmischen Objekten. Festvortrag, Institut für Plasmaforschung, Universität Stuttgart 2003.

563. *Fussmann, G., W. Bohmeyer, P. Carl*, B. Koch, A. Markin*, D. Naujoks, H.-D. Reiner and D. Schröder:* Abschlussbericht Transport and Deposition of Hydrocarbons in the Plasma Generator PSI-2: Experiment and Modelling. Technology Task TW2-TVM-CFC2, 2003.

564. *Gadelmeier, F. and J. Kisslinger:* The Influence of the Magnetic Field Perturbation onto the Divertor Target Deposition in W7-AS. 14th International Stellarator Workshop, Greifswald 2003.

565. *Geiger, J., A. Weller, M. Zarnstorff*, C. Nührenberg, A. Werner, Ya. Kolesnichenko*, W7-AS Team and NBI Group:* Equilibrium and Stability of High-ß Plasmas in W7-AS. 14th International Stellarator Workshop, Greifswald 2003.

566. *Greuner, H., M. Balden, B. Böswirth, H. Bolt, P. Grigull, G. Hofmann*, T. Huber*, W. Kasparek*, A. Killinger*, M. Mayer, R. Neu and H. Renner:* Evaluation of Vacuum Plasma-Sprayed Boron Carbide Protection for the Stainless Steel First Wall of W7-X. 11th International Conference on Fusion Reactor Materials, Kyoto 2003.

567. *Greuner, H., B. Böswirth, S. Lindig, G. Matern and H. Bolt:* Plasma Sprayed Tungsten Coatings on Steel. ITER Divertor Meeting, Naka 2003.

568. *Grigull, P., K. McCormick, Y. Feng, A. Werner, R. König, R. Brakel, R. Burhenn, H. Ehmler, F. Gadelmeier, L. Giannone, D. Hildebrandt, M. Hirsch, R. Jaenicke, J. Kisslinger, T. Klinger, R. Narayanan, D. Naujoks, H. Niedermeyer, H. Thomsen, F. Sardei, F. Wagner and W7-AS Team:* Behaviour of the W7-AS Island Divertor. 14th International Workshop on Stellarators, Greifswald 2003.

569. *Grote, H., J. Boscary, H. Greuner, J. Kisslinger, B. Mendelevitch, H. Renner and D. Sharma:* Operation and Engineering of the Power and Particle Exhaust in Wendelstein 7-X. 14th International Stellarator Workshop, Greifswald 2003.

570. *Grote, H., J. Kisslinger, F.W. Hoffmann*, H. Greuner, B. Mendelevitch, R. Brockmann, O. Volzke, R. Konwitschny* and W7-X Construction Team:* The Vacuum Systems of the Stellarator Wendelstein 7-X. R&D Conference, Alcatel Vacuum Technology, Annecy 2003.

571. *Gruber, O.:* ASDEX Upgrade Operation Plan and Experiment Planning in 2004. 2nd ITPA-IEA Workshop on "Implementation of the ITPA Joint Experiment Recommendations", JAERI, Naka 2003.

572. *Gruber, O.:* Proposals from ITPA TG on MHD, Disruption and Control for ITPA/IEA Joint Experiments in 2004. 2nd ITPA-IEA Workshop on "Implementation of the ITPA Joint Experiment Recommendations", JAERI, Naka 2003.

573. *Gruber, O.:* Recent ITER Relevant Results from ASDEX Upgrade. Informal Meeting of the Japan Society of Plasma Science and Nuclear Fusion Research, Mito 2003.

574. *Gruber, O.:* Report of ITPA TG on MHD, Disruption and Control. 4th Meeting of the ITPA Coordinating Committee, General Atomics, San Diego,CA 2003.

575. *Gruber, O.:* Report on MHD, Disruption and Control ITPA/IEA Joint Experiments in 2003. 2nd ITPA-IEA Workshop on "Implementation of the ITPA Joint Experiment Recommendations", JAERI, Naka 2003.

576. *Gruber, O.:* Research Cooperation between KBSI and IPP Garching. 1st German-Korean Science and Technology Collaborative Committee Meeting, Bonn 2003.

577. *Gruber, O.:* Towards Integrated Advanced Scenarios at ASDEX Upgrade. 4th General Scientific Assembly of Asia Plasma & Fusion Association on New Development of Plasma Physics and Fusion Technology, Hangzhou 2003.

578. *Gruber, O. (presented for A. Mück and ASDEX Upgrade Team):* Sawtooth Control Methods for NTM Suppression on ASDEX Upgrade. 3rd Meeting of the ITPA Topical Group on MHD, Disruption and Control, St. Petersburg 2003.

579. *Günter, S.:* Chancen und Risiken der Fusionsforschung. Parlamentarischer Abend, Vertretung des Landes Mecklenburg-Vorpommern, Berlin 2003.

580. *Günter, S.:* Error Field Amplification: Modelling Results and Proposal for Textor Experiments. 1st International Workshop on Stochasticity in Fusion Edge Plasmas, Jülich 2003.

581. *Günter, S.:* FIR-NTMs on ASDEX Upgrade and JET - Active Control of (2,1) NTMs on ASDEX Upgrade. Workshop on Active Control of MHD Stability: Extension to the Burning Plasma, Austin,TX 2003.

582. *Günter, S.:* Recent Work on the Control of MHD Instabilities at ASDEX Upgrade. Workshop on Active Control of MHD Stability: Extension to the Burning Plasma, Austin,TX 2003.

583. *Günter, S., C. Angioni, F. Jenko, M. Maraschek, A.G. Peeters, S.D. Pinches, B.D. Scott, G. Tardini, H. Zohm and ASDEX Upgrade Team:* Magnetic Confinement: How to Replace Simple Scaling Laws by Physics Understanding? Spring Meeting Aachen. Verhandl. DPG (VI) **38** (4), PV III (2003).

584. *Günter, S., M. Maraschek, M. De Baar*, ASDEX Upgrade Team and JET-EFDA Contributors Collaboration:* Active Control of (3,2) NTMs by Triggering the Transition into the FIR Regime. APS, Division of Plasma Physics, 45th Annual Meeting, Albuquerque,NM 2030. Bulletin of the American Physical Society **48** (7), 204 (2003).

585. *Günter, S., Q. Yu and K. Lackner:* Ergodic Heat Transport Analysis in Non-Aligned Coordinate Systems. 1st International Workshop on Stochasticity in Fusion Edge Plasmas, Jülich 2003.

586. *Guglielmetti, F., R. Fischer, V. Dose, W. Voges* and G. Boese*:* Source Detection with Bayesian Inference on ROSAT

All-Sky Survey Data Sample. Astronomical Data Analysis Software and Systems ADASS XIII Conference, Strasbourg 2003.

587. *Hamacher, T.:* Energie für die Zukunft - Stand und Perspektiven der Fusion. Internationaler ETG-Kongress, Hamburg, 2003.

588. *Hamacher, T.:* Sichere und zuverlässige Systemführung von Kraftwerken und Netz im Zeichen der Deregulierung. VDI-VDE Tagung, München 2003.

589. *Hamacher, T.:* Städtische Energiesysteme. WZU-Tag, Augsburg 2003.

590. *Hamacher, T.:* The VLEEM Bach-casting approach: a sketch of the methodology. International Energy Workshop (IEW), Wien 2003.

591. *Hamacher, T.:* Das VLEEM-Projekt. Forschungsforum der Verbund, Wien 2003.

592. *Hartfuß, H.-J.:* ECRH Stray Radiation Problems with W7-X. 15th Joint Russian-German STC Meeting, Garching 2003.

593. *Hartfuß, H.-J.:* Hochtemperaturplasmadiagnostik. Lehrveranstaltungen, Universität Greifswald 2003.

594. *Hartfuß, H.-J.:* Mikrowellendiagnostik. Lehrveranstaltungen, Universität Greifswald 2003.

595. *Hartfuß, H.-J.:* Status of Diagnostic Development for W7-X. Seminar on Status of W7-X, NIFS, Nagoya 2003.

596. *Hartfuß, H.-J., A. Dinklage and R. Fischer:* Integrated Data Analysis for Burning Plasma Experiments. ITPA Meeting on Diagnostics, St. Petersburg 2003.

597. *Hartmann, D.A.:* ICRH on W7-X. International Workshop on Technical Issues of RF Heating, Moran,WY 2003.

598. *Hartmann, D.A.:* Lohnt sich das Warten auf die Kernfusion? Hanns-Seidel-Stiftung, München 2003.

599. *Hartmann, D.A.:* Stellarators. 6th Carolus Magnus Summer School, Brussels 2003.

600. *Hartmann, D.A., R. Bilato, D. Birus, M. Brambilla, F. Braun, J.-M. Noterdaeme and F. Wesner:* Measurements and Calculations of Electrical Properties of ICRF Atennnas. 15th Conference on RF Power in Plasmas, Moran,WY 2003.

601. *Hartmann, D.A. and J.-M. Noterdaeme:* Studies of Antenna Voltage Limitations on AUG. International Workshop on Technical Issues of RF Heating, Moran,WY 2003.

602. *Hatzky, R.:* Optimization of a Particle-in-Cell (PIC) Code on the IBM "Regatta" Hardware. 7. Treffen der internationalen Benutzergruppe für wissenschaftliches Rechnen auf IBM-Systemen (ScicomP7), Göttingen 2003.

603. *Heger, B., R. Pugno, A. Kirschner*, D. Coster and ASDEX Upgrade Team:* Hydrocarbons in the Divertor IIb of ASDEX Upgrade. Spring Meeting Aachen. Verhandl. DPG (VI) **38** (4), P 10.28 (2003).

604. *Heimann, P., S. Heinzel, C. Hennig, H. Kühntopf, H. Kroiss, G. Kühner, J. Maier, J. Reetz and M. Zilker:* Status Report on the Data Acquisiton System of Wendelstein 7X. IAEA Technical Committee Meeting on Control, Data Acquisition and Remote Participation for Fusion Research, San Diego,CA 2003.

605. *Hein, B., W. Gardebrecht, B. Missal, J. Tretter and F. Leher*:* Manufacture of the Plasma Vessel for Wendelstein 7-X. 14th International Stellarator Workshop, Greifswald 2003.

606. *Hellsten*, T., T. Johansson*, F. Meo, F. Nguyen*, D. Van Eester*, C. Challis*, J.-M. Noterdaeme, J. Mailloux*, M.-L. Mayoral*, M.J. Mantsinen*, F. Sartori*, A. Stäbler, A.A. Tuccillo* and EFDA-JET Contributors:* Fast Wave Current Drive in JET. 15th Topical Conference on RF Power in Plasmas, Moran,WY 2003.

607. *Hennig, C.:* Die etwas andere Netzwerkprogrammierung mit Java. Informatica feminale, Universität Bremen 2003.

608. *Hennig, C., P. Heimann, S. Heinzel, H. Kroiss, G. Kühner, H. Kühntopf, J. Maier, J. Reetz and M. Zilker:* A Concept of Online Monitoring for the Wendelstein 7-X Experiment. 4th IAEA Technical Meeting on Control, Data Acquisition, and Remote Participation for Fusion Research, San Diego,CA 2003.

609. *Hergenhahn, U.:* Energy and Charge Transfer in Weakly Bound Systems. Workshop on Free, Neutral Clusters Studied by Synchrotron Radiation, Sigtuna 2003.

610. *Hergenhahn, U.:* Experimental Evidence for Interatomic Coulombic Decay in Ne Clusters. BESSY Users' Meeting, Berlin 2003.

611. *Hergenhahn, U.:* Innerschalen-Photoionisation chiraler Moleküle. SFB 276 Seminar, Universität Freiburg 2003.

612. *Hergenhahn, U.:* New directions in inner-shell photoionisation of molecules. Hasylab-Seminar, DESY, Hamburg 2003.

613. *Hergenhahn, U.:* Non-local autoionization of van-der-Waals clusters. Seminar 'Electron and Ion Driven Reactions', Institut für Chemie, Freie Universität Berlin 2003.

614. *Herrmann, A., D. Hildebrandt, M. Balden and W. Bohmeyer:* Investigation of IR Emission from Carbon Microstructure on a 30 Micron Scale. 10th International Workshop on Carbon Materials for Fusion Application, Jülich 2003.

615. *Herrnegger, F., R. Burhenn, J. Sallander, A. Weller and J. Junker:* Angular Distribution of the Neutron Field and Energy Spectra in the Wendelstein-7-X Hall. 14th International Stellarator Workshop, Greifswald 2003.

616. *Hildebrandt, D., D. Sünder and A. Herrmann:* Temperature Measurements of Carbon Materials in Fusion Devices at High Heat Fluxes. Inframation 2003, Las Vegas,NV 2003.

617. *Hirsch, M. and E. Holzhauer:* Doppler Reflectrometry with Optimized Temporal Resolution for the Measurement of Turbulence and its Propagation Velocity. Workshop on Microwave Reflectrometry, San Diego,CA 2003.

618. *Hopf, C., W. Jacob and A. von Keudell:* Chemical Sputtering of Hydrocarbon Films. 10th International Workshop on Carbon Materials for Fusion Application, Jülich 2003.

619. *Horvath, K., M. Laux and J. Lingertat:* Langmuir Probe Measurements in the WEGA Stellarator. Spring Meeting Aachen. Verhandl. DPG (VI) **38** (4), P 4.27 (2003).

620. *Horvath, K., J. Lingertat, T. Bindemann, U. Fantz*, R. König, M. Otte, Y. Podoba and F. Wagner:* Characterization of WEGA Plasma. 14th International Stellarator Workshop, Greifswald 2003.

621. *Horvath, K., J. Lingertat, M. Laux and F. Wagner:* Langmuir Probe Measurements in the WEGA Stellarator. 5th International Workshop on Electrical Probes in Magnetized Plasma, Greifswald 2003.

622. *Horvath, K., J. Lingertat and F. Wagner:* Improvement of the WEGA Performance. Doktorandenkolloquium, Greifswald 2003.

623. *Höschen, T.:* Erkenntnisgewinn durch die am Plasmagenerator installierte Messtechnik. Lehrstuhlseminar, Lehrstuhl für Feststoff- und Grenzflächenverfahrenstechnik, Technische Universität München 2003.

624. *Igitkhanov, Yu.:* Density Limit Dependence in Stellarator and Tokamak Plasmas. Theory Meeting, Zinnowitz 2003.

625. *Igitkhanov, Yu.:* IPP Stellarator Reactor Perspective. ARIES-CS Project Meeting, Princeton,NJ 2003.

626. *Igitkhanov, Yu., K. McCormick and P. Grigull:* On the High Density Modes of Operation in W7-AS. 14th International Stellarator Workshop, Greifswald 2003.

627. *Jacob, W., C. Hopf and A. von Keudell:* Chemical Sputtering oder Was treiben Wasserstoffatome und Ionen gemeinsam auf der Oberfläche von a-C:H-Schichten? 10. Erfahrungsaustausch "Oberflächentechnologie mit Plasmaprozessen", Mühlleithen 2003.

628. *Jacob, W., C. Hopf, A. von Keudell, M. Meier and T. Schwarz-Selinger:* Chemical Sputtering of Hydrocarbon Layers. ASEVA Workshop 14: Reactive Plasmas - Physical and Chemical Processes in Reactive Hydrocarbon Plasmas in Contact with Surfaces, Avila 2003.

629. *Jacob W., C. Hopf, A. von Keudell, M. Meier and T. Schwarz-Selinger:* Elementary Surface Processes during Growth and Erosion of Amorphous Hydrogenated Carbon Films. 5th Meeting on Diamond, Amorphous Carbon, Nanotubes, and Related Materials, Rio de Janeiro 2003.

630. *Jaenicke, R.:* Summary of W7-AS Results after 14 Years of Operation. 14th International Stellarator Workshop, Greifswald 2003.

631. *Jaenicke, R.:* Wendelstein 7-AS ein erfolgreiches Stellarator-experiment. IPF Stuttgart 2003.

632. *Jaenicke, R.:* Wendelstein 7-AS ein erfolgreiches Stellarator-experiment. Universität Greifswald 2003.

633. *Kallenbach, A.:* Energieszenarien für das 21. Jahrhundert. Vorlesung, Universität Hannover, SS 2003, WS 2003/2004.

634. *Kang, H.D. and V. Dose:* Decomposition of Multicomponent Mass Spectra. 23rd International Conference on Bayesian Methods and Maximum Entropy in Science and Engineering, Jackson Hole 2003.

635. *Kaufmann, M.:* Angewandte Physik: Plasmaphysik und Fusionsforschung. Vorlesung, Universität Bayreuth, SS 2003.

636. *Kaufmann, M.:* Energie der Sterne - Kernfusion. Deutsches Patentamt, München 2003.

637. *Kaufmann, M.:* Fusion: Energie der Zukunft. 6. Internationaler Münchner Sommer, München 2003.

638. *Kaufmann, M.:* "ITER: Getting Close to Ignition". Brussels 2003.

639. *Keudell, A. von, C. Hopf, M. Meier, T. Schwarz-Selinger and W. Jacob:* Elementary Surface Processes during Growth of a-C:H Films. ASEVA Workshop 14: Reactive Plasmas - Physical and Chemical Processes in Reactive Hydrocarbon Plasmas in Contact with Surfaces, Avila 2003.

640. *Kirov, K., F. Leuterer, G. Pereverzev, E. Poli and F. Ryter:* ECRH Power Deposition Studies in ASDEX Upgrade. 15th Joint Russian-German STC Meeting on ECRH and Gyrotrons, Karlsruhe/Stuttgart/Garching 2003.

641. *Kirov, K., F. Leuterer, G. Pereverzev, F. Ryter, V. Andreev*, Y. Dnestrovski* and A. Sushkov*:* Analysis of ECRH Switch On/Off Events in ASDEX Upgrade. 15th Joint Russian-German STC Meeting on ECRH and Gyrotrons, Karlsruhe/Stuttgart/Garching 2003.

642. *Kirov, K., F. Leuterer, F. Ryter and ASDEX Upgrade Team:* ECRH Power Deposition Profile in ASDEX Upgrade. Spring Meeting Aachen. Verhandl. DPG (VI) **38** (4), P 4.17 (2003).

643. *Klages, K.U. and Ch. Linsmeier:* Carbidbildung von Beryllium durch Deuterium-Beschuss. Frühjahrstagung Dresden. Verhandl. DPG (VI) **38** (5), O 3.7 (2003).

644. *Klages, K.U. and Ch. Linsmeier:* Deuterium Bombardment of Beryllium and Carbon Layers on Beryllium. 4th German-Brazilian Workshop on Applied Surface Science, Ringberg 2003.

645. *Klages, K.U. and Ch. Linsmeier:* Deuterium Ion Induced Carbide Formation on Beryllium. The Ion Beam Centre, 12th Annual User Workshop, University of Surrey, Guildford 2003.

646. *Kleiber, R.:* Edge Turbulence Simulations for Axisymmetric and Stellarator Equilibria. Theory Meeting, Zinnowitz 2003.

647. *Kleiber, R.:* Turbulence Simulations for Axisymmetric Configurations and Stellarators. IAEA Technical Meeting on Innovative Concepts and Theory of Stellarators, Greifswald 2003.

648. *Klinger, T., J. Baldzuhn, S. Bäumel, R. Brakel, R. Burhenn, A. Dinklage, M. Endler, H. Ehmler, V. Erckmann, Y. Feng, F. Gadelmeier, J. Geiger, L. Giannone, P. Grigull, D. Hildebrandt, M. Hirsch, R. Jaenicke, J. Kisslinger, R. König, G. Kühner, J. Knauer, H.-P. Laqua, H. Maaßberg, K. McCormick, R. Narayanan, D. Naujoks, E. Pasch, F. Sardei, H. Thomsen, U. Wenzel, F. Wagner, A. Weller, A. Werner, D. Zang and W7-AS Team:* Wendelstein 7-AS Results Relevant for Wendelstein7-X. 14th International Stellarator Workshop, Greifswald 2003.

649. *Klose, S., M. Zarnstorff*, A. Weller and W7-AS Team:* Determination of the Toroidal Current Density- and Iota-Profile in the W7-AS Using Soft X-Ray Measurements. 14th International Stellarator Workshop, Greifswald 2003.

650. *Koch, B., W. Bohmeyer and G. Fußmann:* Angular Resolved Energy Flux Measurements in a Magnetized Plasma. 5th International Workshop on Electrical Probes in Magnetized Plasmas, Greifswald 2003.

651. *Koch, B., W. Bohmeyer and G. Fußmann:* Angular Resolved Energy Flux Measurements in a Magnetized Plasma. Spring Meeting Aachen. Verhandl. DPG (VI) **38** (4), P 11.3 (2003).

652. *Koch, F., R. Brill, H. Maier, D. Levchuk, A. Suzuki*, T. Muroga* and H. Bolt:* Crystallization Behavior of Arc-Deposited Ceramic Barrier Coatings. 11th International Conference on Fusion Reactor Materials, Kyoto 2003.

653. *Kolesnichenko*, Ya.I, V.V. Lutsenko*, V.S. Marchenko*, A. Weller, A. Werner, H. Wobig, Y. Yakovenko* and K. Yamazaki*:* Fast Ion Confinement and Fast-Ion-Induced Effects in Stellarators. 14th International Stellarator Workshop, Greifswald 2003.

654. *Könies, A.:* A Perturbative Approach to the Destabilization of Alfvén Eigenmodes in Stellarators Using Kinetic MHD. IAEA Technical Meeting on Innovative Concepts and Theory of Stellarators, Greifswald 2003.

655. *Könies, A., O.P. Fesenyuk* and Yu.V. Yakovenko*:* Numerical Analysis of Kinetic Alfvén Eigenmodes in Stellarators. IAEA Technical Meeting on Innovative Concepts and Theory of Stellarators, Greifswald 2003.

656. *König, R., Y. Feng, P. Grigull, K. McCormick, H. Ehmler, F. Gadelmeier, L. Giannone, D. Hildebrandt, J. Kisslinger, T. Klinger, R. Narayanan, D. Naujoks, H. Thomsen, F. Sardei, F. Wagner, A. Werner and W7-AS Team:* Edge and Divertor Physics Issues for W7-X. 11th European Fusion Physics Workshop, Heraklion 2003.

657. *König, R., P. Grigull, K. McCormick, Y. Feng, H. Ehmler, F. Gadelmeier, L. Giannone, D. Hildebrandt, J. Kisslinger, T.*

Klinger, A. Komori, S. Masuzaki*, K. Matsuoka*, P. Mioduszewski*, T. Morisaki*, R. Narayanan, D. Naujoks, T. Obiki*, N. Ohyabo*, H. Renner, F. Sardei, H. Thomsen, F. Wagner, U. Wenzel and A. Werner:* Divertors for Helical Devices: Concepts, Plans, Results, and Problems. 14th International Stellarator Workshop, Greifswald 2003.

658. *König, R., O. Ogorodnikova*, A. Vorköper, H. Schmidt, C. von Sehren, J. Baldzuhn, R. Burhenn, H. Ehmler, K. Grosser, A. John, M. Krychowiak, P. Mertens, A. Pospieszczyk*, B. Schweer*, T. Klinger and W7-X Team:* Power Loaded Components. W7-X Seminar, National Institute for Fusion Science, Toki 2003.

659. *Kornilov, V. and R. Kleiber:* 3D Global Simulations of Ion-Temperature-Gradient (ITG) Modes in a Two-Fluid Model. IAEA Technical Meeting on Innovative Concepts and Theory of Stellarators, Greifswald 2003.

660. *Kraus, W.:* Hochfrequenz-Ionenquellen in der Neutralteilcheninjektion zur Aufheizung von Fusionsplasmen. Meeting "Elektrische Antriebe", Deutsches Zentrum für Luft- und Raumfahrt, Bonn 2003.

661. *Kraus, W., M. Bandyopadhyay, H. Falter, P. Franzen, B. Heinemann, P. McNeely, R. Riedl, E. Speth, A. Tanga and R. Wilhelm:* Progress in the Development of RF Driven Negative Ion Sources for Neutral Beam Injection. 10th International Conference on Ion Sources, JINR, Dubna 2003.

662. *Kreter, A., J. Baldzuhn, A. Dinklage, H. Ehmler, M. Kick, H. Maaßberg and W7-AS Team:* Plasma Profiles in Optimized Confinement Discharges with High Ion Temperatures after Installation of the Island Divertor in W7-AS. 14th International Stellarator Workshop, Greifswald 2003.

663. *Krieger, K.:* Methods of Surface Analysis. Vorlesung, Universität Greifswald, SS 2003.

664. *Krieger, K, A. Geier, X. Gong*, H. Maier, M. Mayer, R. Neu, R. Pugno, V. Rohde, W. Schneider and ASDEX Upgrade Team:* Tungsten Transport and Redeposition in ASDEX Upgrade. 11th European Fusion Physics Workshop, Heraklion 2003.

665. *Krieger, K., A. Geier, H. Maier, R. Neu, R. Pugno, V. Rohde and ASDEX Upgrade Team:* Erosion and Redeposition of Tungsten in the Tokamak ASDEX Upgrade. Spring Meeting Aachen. Verhandl. DPG (VI) **38** (4), P 1.1 (2003).

666. *Krieger, K., G. Matthews*, Ph. Mertens* and M. Stamp*:* Uniformity of Beryllium Sources in JET. JET Seminar, Culham 2003.

667. *Krychowiak, M., R. König, R. Burhenn, H. Ehmler, R. Fischer, J. Knauer, E. Pasch, A. Werner and T. Klinger:* Impurity Transport Studies in the Divertor Operation of the W7-AS Stellarator. Spring Meeting Aachen. Verhandl. DPG (VI) **38** (4), P 10.14 (2003).

668. *Krychowiak, M., R. König, R. Burhenn, H. Ehmler, R. Fischer, J. Knauer, E. Pasch, A. Weller, A. Werner and T. Klinger:* Impurity Transport Studies in the Divertor Operation of the W7-AS Stellarator. 14th International Stellarator Workshop, Greifswald 2003.

669. *Kugeler, O., S. Marburger and U. Hergenhahn:* Photoelectron - Auger-Electron Coincidence Measurements in N_2O K-shell Photoionisation. Frühjahrstagung Hannover. Verhandl. DPG (VI) **38** (6), MO 8.6 (2003).

670. *Kuteev*, B.V., V.Yu. Sergeev*, V.G. Skokov*, V.M. Timokhin*, R. Burhenn and W7-AS Team:* Studies of Carbon Pellet Ablation in W7-AS Stellarator Plasmas with Different ECR Power Launch. Russian Annual Conference on Plasma Physics and Controlled Fusion, Zwenigorod 2003.

671. *Laqua H.:* Electron Bernstein Wave Heating in Fusion Plasma. 15th Topical Conference on Radio Frequency Power in Plasmas, Moran,WY 2003.

672. *Laqua, H.:* Electron Bernstein Wave Heating in Overdense Stellarator Plasmas. 14th International Stellarator Workshop, Greifswald 2003.

673. *Laqua, H.P.:* Electron Cyclotron Resonance Heating in Fusion Plasmas. 5th International Workshop on Microwave Discharges: Fundamentals and Applications, Zinnowitz 2003.

674. *Laux, M.:* How to Interpret Triple Probe Measurements when none of the Tips Saturates? 5th International Workshop on Electrical Probes in Magnetized Plasmas, Greifswald 2003.

675. *Lederer, H.:* Bioinformatics Project Status Overview: From a test towards a production system. MPG Bioinformatics Meeting, Saarbrücken 2003.

676. *Lederer, H.:* Implementing the processing pipeline: project status and overview. MPG Bioinformatics Meeting: Microbial Genomes, Garching 2003.

677. *Lederer, H.:* Neues vom RZG: IBM Regatta Systeme, Linux Cluster, Globale Filesysteme. ZKI-Tagung, Hamburg 2003.

678. *Lederer, H., S. Heinzel and M. Panea:* 40 Years of Supercomputing: Rechenzentrum Garching (RZG) der Max-Planck-Gesellschaft. Supercomputer Conference, Heidelberg 2003.

679. *Lee, K., T. Bindemann, M. Hirsch and H.-J. Hartfuß:* Cotton-Mouton Polarimetry at the W7-AS Stellarator. Spring Meeting Aachen. Verhandl. DPG (VI) **38** (4), P 17.23 (2003).

680. *Leuterer, F., K. Kirov, F. Monaco, M. Münich, H. Schütz, F. Ryter, D. Wagner, R. Wilhelm, H. Zohm, T. Franke, K. Voigt, G. Dammertz*, R. Heidinger*, I. Danilov*, K. Koppenburg*, A. Meier*, M. Thumm*, X. Yang*, W. Kasparek*, G. Gantenbein*, H. Hailer*, G.A. Müller*, K. Schwörer*, G.G. Denisov*, A. Litvak* and V. Zapevalov*:* The New ECRH System for ASDEX Upgrade. IAEA Technical Meeting on ECRH Physics and Technology for ITER, Kloster Seeon 2003.

681. *Leuterer, F., K. Kirov, F. Monaco, M. Münich, H. Schütz, F. Ryter, D. Wagner, R. Wilhelm, H. Zohm, T. Franke, K. Voigt, G. Dammertz*, R. Heidinger*, I. Danilov*, K. Koppenburg*, A. Meier*, M. Thumm*, X. Yang*, W. Kasparek*, G. Gantenbein*, H. Hailer*, G.A. Müller*, K. Schwörer*, G.G. Denisov*, A. Litvak* and V. Zapevalov*:* Status of the New ECRH System. 15th Joint Russian-German STC Meeting on ECRH and Gyrotrons, Karlsruhe/Stuttgart/Garching 2003.

682. *Leuterer, F., K. Kirov, G. Pereverzev, F. Ryter and ASDEX Upgrade Team:* Modulated ECRH Power Deposition in ASDEX Upgrade. Spring Meeting Aachen. Verhandl. DPG (VI) **38** (4), P 8.6 (2003).

683. *Levchuk, D., F. Koch, H. Maier and H. Bolt:* Deuterium Permeation through Bare and Coated EUROFER. 11th International Conference on Fusion Reactor Materials, Kyoto 2003.

684. *Linsmeier, Ch.:* Beryllium Surface Reactions with Carbon and Oxygen. 4th German-Brazilian Workshop on Applied Surface Science, Ringberg 2003.

685. *Linsmeier, Ch.:* Formation and Erosion of Carbon-Containing Mixed Materials on Metals. 10th International Workshop on Carbon Materials for Fusion Application, Jülich 2003.

686. *Linsmeier, Ch.:* Surface Reactions on Beryllium with Carbon and Oxygen. University of San Diego,CA 2003.

687. *Ludvik, J.:* Seismic Analysis of the Fusion Experiment W7-X Using the Response Spectrum Method. Conference Applied Mechanics, Jaworzynka 2003.

688. *Lunt, T., N. Ezumi*, B. Koch and G. Fußmann:* Flow Velocity Measurements in a Magnetic Nozzle in PSI-2 and the Bohm Criterion. Spring Meeting Aachen. Verhandl. DPG (VI) **38** (4), P 1.5 (2003).

689. *Lutsenko*, V.V., Ya.I. Kolesnichenko*, Y.V. Yakovenko*, A. Weller, A. Werner, H. Wobig and J. Heikkinen*:* Numerical Simulation of Alfvén Instabilities in NBI Experiments on Wendelstein 7-AS. European Fusion Theory Conference, Helsinki 2003.

690. *Lyssoivan*, A., M.J. Mantsinen*, D. Van Eester*, R. Koch*, A. Salmi*, J.-M. Noterdaeme, I. Monakhov* and EFDA-JET Contributors:* Effect of ICRF Mode Conversion at the Ion-Ion Hybrid Resonance on Plasma Confinement in JET. 15th Topical Conference on RF Power in Plasmas, Moran,WY 2003.

691. *Maier, H. and H. Bolt:* Nuclear Fusion and its Implications on Materials Research for Extreme Environments. International Congress on Materials Science and Nanotechnologies, Brussels 2003.

692. *Manini, A., F. Ryter and ASDEX Upgrade Team:* Starting T_e / T_i Studies in ASDEX Upgrade. ITPA Meeting of Transport & ITB Physics and Confinement & Modelling Topical Groups, St. Petersburg 2003.

693. *Manini, A., F. Ryter, J. Stober, C. Angioni, A.G. Peeters, G. Tardini and ASDEX Upgrade Team:* Electron Transport Studies in Plasmas with $T_i > T_e$ in ASDEX Upgrade. ITPA Meeting of Transport & ITB Physics and Confinement & Modelling Topical Groups, San Diego,CA 2003.

694. *Manso*, M., J. Borreicho*, L. Farinha*, D. Wagner, S. Hacquin*, F. Silva* and P. Varela*:* Computer Based Techniques to Design Antennas in Microwave Diagnostics for Fusion Plasma. 9th International Conference on Enhancement and Promotion of Computational Methods in Engineering and Science, Macao 2003.

695. *Mantsinen*, M.J., M. Laxaback*, A. Salmi*, V. Kiptily*, D. Testa*, Y. Baranov*, R. Barnsley*, B. Beaumont*, S. Conroy*, P. de Vries*, C. Giroud*, C. Gowers*, T. Hellsten*, L.C. Ingesson*, T. Johnson*, H. Leggate*, M.-L. Mayoral*, I. Monakhov*, J.-M. Noterdaeme, P. Podda*, S. Sharapov*, A.A. Tuccillo*, D. Van Eester* and EFDA-JET Contributors:* Comparison of Monochromatic and Polychromatic ICRH on JET. 15th Topical Conference on RF Power in Plasmas, Moran,WY 2003.

696. *Marburger, S.:* Interatomic Coulombic Decay studied in Ne clusters. Workshop on Free, Neutral Clusters Studied by Synchrotron Radiation, Sigtuna 2003.

697. *Marburger, S., O. Kugeler and U. Hergenhahn:* A Molecular Beam Source for Electron Spectroscopy of Clusters. 8th International Conference on Synchrotron Radiation Instrumentation, San Francisco,CA 2003.

698. *Marburger, S., O. Kugeler, U. Hergenhahn and T. Möller*:* Experimental Evidence for Interatomic Coulombic Decay of Ne Clusters. Frühjahrstagung Hannover. Verhandl. DPG (VI) **38** (6), MO 13.5 (2003).

699. *Matern, G., A. Brendel and C. Popescu:* Metall-Matrix-Verbundwerkstoffe als Wärmesenkenmaterial in Fusionsreaktoren. 37. Metallographietagung, Berlin 2003.

700. *Mayer, M.:* Cross Section Data in SIMNRA 5.0. IAEA Technical Meeting on Database of Evaluated Cross Sections for Ion Beam Applications, Vienna 2003.

701. *Mayer, M.:* Nuclear Reaction Analysis. Workshop on Nuclear Data for Science and Technology: Materials Analysis. The Abdus Salam International Centre for Theoretical Physics, Trieste 2003.

702. *Mayer, M.:* Rutherford Backscattering Spectrometry. Workshop on Nuclear Data for Science and Technology: Materials Analysis. The Abdus Salam International Centre for Theoretical Physics, Trieste 2003.

703. *Mayer, M., V. Rohde, T. Pütterich, P. Coad*, JET-EFDA Contributors and ASDEX Upgrade Team:* Carbon Migration and Deposition in Divertor Machines. 11th European Fusion Physics Workshop, Heraklion 2003.

704. *Mayer, M., V. Rohde, T. Pütterich, P. Coad*, P. Wienhold*, JET-EFDA Contributors and ASDEX Upgrade Team:* Carbon Erosion and Migration in Fusion Devices. 10th International Workshop on Carbon Materials for Fusion Application, Jülich, 2003.

705. *Mayoral*, M., R. Buttery*, T. Jones*, V.G. Kiptily*, S. Sharapov*, M.J. Mantsinen* S. Coda*, O. Sauter*, L.-G. Eriksson*, D. Borba*, A. Mück, S. Pinches and J.-M. Noterdaeme:* Studies of Burning Plasma Physics in the Joint European Torus. APS, Division of Plasma Physics, 45th Annual Meeting, Albuquerque,NM 2003. Bulletin of the American Physical Society **48** (7), 126 (2003).

706. *McCormick, K.:* High Performance Regimes in Wendelstein 7-AS. 14th International Stellarator Workshop, Greifswald 2003.

707. *McCormick, K., R. Burhenn, P. Grigull, J. Baldzuhn, S. Bäumel, R. Brakel, H. Ehmler, F. Gadelmeier, L. Giannone, M. Hirsch, E. Holzhauer*, Yu. Igitkhanov, R. Jaenicke, S. Klose, J.P. Knauer, E. Pasch, H. Thomsen, A. Werner, W7-AS Team, ECRH Team and NBI Team:* Essential Elements of the High Density H-Mode on W7-AS. 14th International Stellarator Workshop, Greifswald 2003.

708. *Meier, M. and A. von Keudell:* Assessment of Ion Surface Scattering (ISS) as In-situ Real-time Diagnostic Tool in Low Temperature Plasmas. Workshop "Frontiers in Low Temperature Plasma Diagnostics V", Speccia 2003.

709. *Meir, S., U. Fantz* and K. Behringer:* Influence of Wall Materials at Different Temperatures on the Vibrational Population of Molecular Hydrogen. Spring Meeting Aachen. Verhandl. DPG (VI) **38** (4), P 18.5 (2003).

710. *Meyer-Spasche, R.:* Dynamical Properties of Difference Schemes. AbiTUMath 4: "Chaotische Systeme", Elite-Förderungsprogramm der Universität München, Kloster Neustift bei Brixen 2003.

711. *Meyer-Spasche, R.:* Frauen in Mathematik und Naturwissenschaften. Öffentlicher Vortrag zur Eröffnung der Ausstellung "Women in Maths", Universität München 2003.

712. *Meyer-Spasche, R.:* Gelüftete Tarnkappen: Wissenschaftlerinnen seit Aristoclea, der Lehrerin von Pythagoras. Ferien-Akademie für Studentinnen und junge Wissenschaftlerinnen, Junges Forum, Evangelische Akademie Tutzing 2003.

713. *Meyer-Spasche, R.:* Nicht-lineare Dynamik. Herbst-Universität für Oberstufenschülerinnen an Gymnasien, Universität München 2003.

714. *Meyer-Spasche, R.:* Numerical Analysis and Dynamical Systems. Vorlesung, Universität München, WS 2003/2004.

715. *Meyer-Spasche, R.:* Variable-Coefficient Difference Schemes for Quasilinear Evolution Problems. European Advanced Studies Conference 4: "Chaos and Complex Systems", Kloster Neustift bei Brixen 2003.

716. *Michel G.:* Another Variant of the Katzenelenbaum - Semenov Algorithm. 28th International Conference on Infrared and Millimeter Waves, Otsu, Shiga 2003.

717. *Mikhailov*, M.I., W.A. Cooper*, M.Yu. Isaev*, J. Nührenberg, M.A. Samitov*, A.A. Skovoroda*, V.D. Shafranov*, A.A. Subbotin* and R. Zille:* The Effect of Fulfilling the Quasi-isodynamicity Condition on the Bootstrap and the Pfirsch-Schlüter Currents. IAEA Technical Meeting on Innovative Concepts and Theory of Stellarators, Greifswald 2003.

718. *Müller, W.-C.:* Anisotropy, Intermittency, and Energy Cascades in MHD. University of Maryland 2003.

719. *Müller, W.-C.:* Magnetohydrodynamic Turbulence: Simulations and Developments in Theory. Festival de Théorie, Université de Provence, Aix-en-Provence 2003.

720. *Müller, W.-C.:* Magnetohydrodynamic Turbulence: Simulations and Developments in Theory. Universität Hannover 2003.

721. *Müller, W.-C.:* Simulations and Theory of Magnetohydrodynamic Turbulence. CRPP Lausanne 2003.

722. *Müller, W.-C.:* Two Lectures on MHD Turbulence. University of Tabriz 2003.

723. *Nakajima*, N., C. Nührenberg and J. Nührenberg:* Growth Rates and Structures of MHD Modes in Stellarator/Heliotron. 13th International Toki Conference on Plasma Physics and Controlled Fusion, Toki 2003.

724. *Narayanan, R. and R. König:* Recombination Dominated Hydrogenic Emission from the Detached Plasmas in W7-AS. 14th International Stellarator Workshop, Greifswald 2003.

725. *Naujoks, D.:* Investigation on Plasma Transport via Particle Simulation. Spring Meeting Aachen. Verhandl. DPG (VI) **38** (4), P 12.1 (2003).

726. *Naujoks, D.:* Sonnenfeuer auf der Erde. Ausstellung „Energie der Sterne", Europäisches Patentamt, Berlin 2003.

727. *Naujoks, D., W. Bohmeyer, A. Markin*, I. Arkhipov*, P. Carl*, B. Koch, T. Lunt, H.-D. Reiner, D. Schröder and G. Fußmann:* Transport and Deposition of Hydrocarbons in the Plasma Generator PSI-2. 10th International Workshop on Carbon Materials for Fusion Application, Jülich 2003.

728. *Neu, R.:* Plasmaphysik. Vorlesung, Universität Tübingen, SS 2003, WS 2003/2004.

729. *Nishijima*, D., M.Y. Ye, N. Ohno* and S. Takamura*:* Formation Mechanism of Bubbles on Tungsten Surface with Low Energy and High Flux Helium Plasma Irradiation in NAGDIS-II. 11th International Conference on Fusion Reactor Materials, Kyoto 2003.

730. *Noterdaeme, J.-M.:* Controlled Nuclear Fusion, a Challenging Task with a Big Payoff. GENES4/ANP2003, Kyoto 2003.

731. *Noterdaeme, J.-M.:* Nuclear Reactor Theory - Part II**.** Belgian Nuclear Higher Education Network and European Nuclear Higher Education, Gent University, WS 2003/2004.

732. *Noterdaeme, J.-M.:* Plasmaheizung. Technische Universität München 2003.

733. *Noterdaeme, J.-M.:* Recent ICRF Developments for AUG, JET, W7-X. NIFS, Toki 2003.

734. *Noterdaeme, J.-M.:* Theorie van de kernreactor, vermogensverdeling. Vorlesung, Gent University, SS 2003.

735. *Noterdaeme, J.-M., W. Becker, V. Bobkov, F. Braun, D. Hartmann and F. Wesner:* Status and Development of the ICRF Antennas on ASDEX Upgrade. 15th Topical Conference on RF Power in Plasmas, Moran,WY 2003.

736. *Nührenberg, C. and A.H. Boozer*:* Error-Field-Induced Islands in W7-X. IAEA Technical Meeting on Innovative Concepts and Theory of Stellarators, Greifswald 2003.

737. *Nührenberg, J.:* Stellarator Confinement of Plasmas. APS, Division of Plasma Physics, 45th Annual Meeting, Albuquerque,NM 2003. Bulletin of the American Physics Society **48** (7), 197 (2003).

738. *Nührenberg, J., W.A. Cooper*, A.A. Ivanov*, M.Yu. Isaev*, V.N. Kalyuzhnyj*, S.V. Kasilov*, A.A. Martynov*, S.Yu. Medvedev*, M.I. Mikhailov*, V.V. Nemov*, Yu.Yu. Poshekhonov*, M.A. Samitov*, V.D. Shafranov*, A.A. Subbotin* and R. Zille:* INTAS Project 592: Novel Approaches to Improve Confinement in 3D Plasma Magnetic Systems. 14th International Stellarator Workshop, Greifswald 2003.

739. *Ogawa*, I., T. Idehara*, Y. Itakura*, D. Wagner and M. Thumm*:* High Purity Mode Operation of Gyrotron FU VA and Generation of Intense Gaussian Beam. 28th International Conference on Infrared and Millimeter Waves, Otsu, Shiga 2003.

740. *Ogawa*, I., H. Nozu*, Y. Itakura*, T. Idehara*, R. Pavlichenko*, D. Wagner and M. Thumm*:* Generation of High Mode Purity Output of a Gyrotron and its Conversion to a Gaussian Beam. 30th IEEE International Conference on Plasma Science, Jeju 2003.

741. *Ordás*, N., R. Cemboráin*, C. García-Rosales*, S. Lindig and M. Balden:* Influence of Manufacturing Parameters on the Thermo-Mechanical Properties of Carbide-Doped Fine-Grain Graphites. Carbon Conference, Carbon Community of Spain, Oviedo 2003.

742. *Ordás*, N., R. Cemboráin*, S. Lindig, M. Balden, H. Wang* and C. García-Rosales*:* Effect of Catalytic Graphitization on the Thermo-Mechanical Properties of Isotropic Graphite Doped with Metallic Carbides. 10th International Workshop on Carbon Materials for Fusion Application, Jülich 2003.

743. *Otte, M.:* Magnetic Flux Surface Measurement with Vertical Field and Compensation Coils at the WEGA. 14th International Stellarator Workshop, Greifswald 2003.

744. *Pasch, E., A. Dinklage, R. Fischer and J.P. Knauer:* Topics of Thomson Scattering at the Stellarator Wendelstein 7-AS. Laser-Aided Plasma Diagnostics, Les Houches 2003.

745. *Pautasso, G., A. Savtchov* and C. Tichmann:* Avoidance, Prediction and Mitigation of Disruptions in Tokamaks. Spring Meeting Aachen. Verhandl. DPG (VI) **38** (4), P III (2003).

746. *Piosczyk*, B., S. Alberti*, A. Arnold*, D. Bariou*, A. Beunas*, H. Budig*, G. Dammertz*, O. Dumbrajs*, O. Drumm*, D. Fasel*, T. Goodman*, M. Henderson*, J.P. Hogge*, S. Illy*, J. Jin*, C. Lievin*, M. Thumm*, M.Q. Tran*, D. Wagner and I. Yovchev*:* A 2MWm cw, 170 GHz Coaxial Cavity Gyrotron for ITER. IAEA Technical Meeting on ECRH Physics and Technology for ITER, Kloster Seeon 2003.

747. *Piosczyk*, B., H. Budig*, G. Dammertz*, O. Drumm*, S. Illy*, J. Jin*, M.V. Kartikeyan*, W. Leonhardt*, M. Schmid*, M. Thumm*, X. Yang*, D. Wagner, O. Dumbrajs*, V. Manilov* and A. Pavelyav*:* A Coaxial Cavity Gyrotron - Recent Results and Future Plans. 15th Joint Russian-German STC Meeting on ECRH and Gyrotrons, Karlsruhe/Stuttgart/Garching 2003.

748. *Piosczyk*, B., H. Budig*, G. Dammertz*, O. Dumbrajs*, O. Drumm*, S. Illy*, J. Jin*, M. Thumm* and D. Wagner:* Coaxial Cavity Gyrotron - Recent Results and Ongoing Development Work. 28th International Conference on Infrared and Millimeter Waves, Otsu, Shiga 2003.

749. *Plaum*, B., G. Gantenbein*, M. Grünert*, W. Kasparek*, H. Kumric*, K. Schwörer*, R. Wacker*, G.G. Denisov*, S.V. Kuzikov*, K. Ohkubo*, F. Hollmann and D. Wagner:* Characterization of a Remote Steering Antenna for ECRH / ECCD in ITER. 15th Joint Russian-German STC Meeting on ECRH and Gyrotrons, Karlsruhe/Stuttgart/Garching 2003.

750. *Plaum*, B., G. Gantenbein*, M. Grünert*, W. Kasparek*, H. Kumric*, K. Schwörer*, R. Wacker*, G.G. Denisov*, S.V. Kuzikov*, K. Ohkubo* and D. Wagner:* Performance of a Remote Steering Antenna for ECRH/ECCD Applications. 28th International Conference on Infrared and Millimeter Waves, Otsu, Shiga 2003.

751. *Plaum*, B., G. Gantenbein*, M. Grünert*, W. Kasparek*, R. Wacker*, G.G. Denisov*, S.V. Kuzikov*, K. Ohkubo*, F. Hollmann and D. Wagner:* Characterization of a Remote Steering Antenna for ECRH / ECCD in ITER. IAEA Technical Meeting on ECRH Physics and Technology for ITER, Kloster Seeon 2003.

752. *Podoba, Y., K. Horvath, H.P. Laqua, J. Lingertat and F. Wagner:* Electron Cyclotron Heating at the WEGA Stellarator. 14th International Stellarator Workshop, Greifswald 2003.

753. *Poli, E., A. Bergmann and A.G. Peeters:* Drift Kinetic Simulations of the Polarisation Current in the Presence of a Magnetic Island. 10th European Fusion Theory Conference, Helsinki 2003.

754. *Poli, E., A.G. Peeters, A. Bergmann, S. Günter and S.D. Pinches:* Drift Kinetic Simulations of the Current Driving and Damping the Neoclassical Tearing Mode. Kolloquium, IFP/CNR Milan 2003.

755. *Popescu, C., A. Brendel, C. Leyens* and H. Bolt:* Metal Matrix Composites as Heat Sink Material for Fusion Applications. European Congress on Advanced Materials and Processes, EUROMAT, Lausanne 2003.

756. *Poulipoulis*, G., G.N. Throumoulopoulos* and H. Tasso:* Two-Fluid Tokamak Equilibria with Reversed Magnetic Shear and Sheared Flow. 10th European Fusion Theory Conference, Helsinki 2003.

757. *Preuss, R.:* Bayes'sche Datenanalyse für voneinander abweichende Datengruppen. Kolloquium der PTB, Braunschweig 2003.

758. *Pütterich, T., R. Neu, M. O'Mullane*, A. Whiteford*, R. Dux and ASDEX Upgrade Team:* Investigations on Spectroscopic Diagnostics for High-Z Elements in Fusion Plasmas. Spring Meeting Aachen. Verhandl. DPG (VI) **38** (4), P 17.21 (2003).

759. *Radtke, R., F. Allen, C. Biedermann and G. Fußmann:* Overview of the Berlin Electron Beam Ion Trap Project. 2nd IAEA Research Coordinating Meeting, Vienna 2003.

760. *Reetz, J., P. Heimann, S. Heinzel, C. Hennig, H. Kroiss, G. Kühner, H. Kühntopf, J. Maier and M. Zilker:* Image Data Acquisition in the Scope of Long Duration Discharges. IAEA Technical Meeting on Control, Data Acquisition, and Remote Participation for Fusion Research, San Diego,CA 2003.

761. *Regler*, M., U. Fantz* and K. Behringer:* Investigation of Neon Plasmas with Admixtures of Hydrogen in ECR and ICP Reactors. Spring Meeting Aachen. Verhandl. DPG (VI) **38** (4), P 10.31 (2003).

762. *Reich, M., E. Wolfrum, J. Schweinzer, H. Ehmler*, H.-U. Fahrbach, J. Neuhauser and ASDEX Upgrade Team:* Edge Ion Temperature Profile Measurements with Li Beam CXRS on ASDEX Upgrade. Spring Meeting Aachen. Verhandl. DPG (VI) **38** (4), P 17.15 (2003).

763. *Renner, H.:* Wege zur kontrollierten Kernfusion: Magnetischer Plasmaeinschluss im Max-Planck-Institut für Plasmaphysik. Vortragsreihe des Elektrotechnischen Vereins, Bezirksverein Berlin-Brandenburg im VDE, Frankfurt/Oder 2003.

764. *Renner, H., D. Sharma, J. Kisslinger, J. Boscary, H. Grote and R. Schneider:* Physical Aspects for the W7-X Divertor Design. 14th International Stellarator Workshop, Greifswald 2003.

765. *Richter, S.:* Die Methode URBS zur integralen Beschreibung und Optimierung urbaner Energiesysteme. RENEXPO, Internationale Fachmesse und Kongress für Regenerative Energiesysteme und Energieeffizienz, Teilkongress: "Wie optimiert man urbane Energiesysteme?", Augsburg 2003.

766. *Richter, S. and T. Hamacher:* Die integrale Methode URBS zur Beschreibung und Optimierung urbaner Energiesysteme. Frühjahrstagung Hannover. Verhandl. DPG (VI) **48** (6), AKE 3.3 (2003).

767. *Richter, S. and T. Hamacher:* URBS - A Method for Investigation urban energy systems. PowerGen Europe, Conference and Fair, Track "Low CO_2 Future: What are the actions?", Düsseldorf 2003.

768. *Riegg*, S., U. Fantz* and K. Behringer:* Helium Line Ratios for Diagnostics of Plasma Parameters in Different Types of Discharges. Spring Meeting Aachen. Verhandl. DPG (VI) **38** (4), P 10.22 (2003).

769. *Riße, K., H. Viebke and W7-X Construction Team:* Fabrication of the Superconducting Coils for Wendelstein 7-X. 14th International Stellarator Workshop, Greifswald 2003.

770. *Roth, J.:* Comparison of Exiting Measurements for the Flux Dependence of Chemical Erosion. ITPA Director and SOL Physics, St. Petersburg 2003.

771. *Roth, J.:* Erosion Processes. Atomic and Molecular Data for Fusion Energy Research. Workshop on the International Atomic Energy Agency (IAEA) and the International Centre for Theoretical Physics (ICTP), Trieste 2003.

772. *Roth, J.:* EU-Plasma Wall Interaction Task Force and EFDA Plasma Edge: Technology Programme. 2nd EU Task Force Meeting, JET, Culham 2003.

773. *Roth, J.:* EU Task Force on Plasma Wall Interactions. Scientific and Technical Advisory Committee Meeting (STAC), Brussels 2003.

774. *Roth, J.:* Flux Dependence of Chemical Erosion and its Implications for ITER. 11th European Fusion Physics Workshop, Heraklion 2003.

775. *Roth, J.:* Materialforschung am IPP - Bezug auf ITER. Plasmakolloquium, Institut für Plasmaforschung, Universität Stuttgart 2003.

776. *Roth, J.:* Plasma-Wall Interaction in Magnetically Confined Fusion. Atomic and Molecular Data for Fusion Energy Research. Workshop on the International Atomic Energy Agency (IAEA) and the International Centre for Theoretical Physics (ICTP), Trieste 2003.

777. *Roth, J.:* Tritium Inventory. Atomic and Molecular Data for Fusion Energy Research. Workshop on the International Atomic Energy Agency (IAEA) and the International Centre for Theoretical Physics (ICTP), Trieste 2003.

778. *Rummel, T., K. Riße, H. Viebke, T. Bräuer and J. Kisslinger:* Accuracy of Construction of the Superconducting Coils for Wendelstein 7-X. 18th International Conference on Magnet Technology, Morioka-City 2003.

779. *Rummel, T. and W7-X Construction Team:* The Magnet System of the Fusion Experiment Wendelstein 7-X. Jahrestagung Kerntechnik, Berlin 2003.

780. *Ryter, F., C. Angioni, M. Apostoliceanu, A. Manini, A.G. Peeters and ASDEX Upgrade Team:* Studies of Electron Thermal Transport in ASDEX Upgrade. Theory Seminar, CEA-DRFC Cadarache 2003.

781. *Ryter, F., M. Apostoliceanu, S. Cirant*, J. DeBoo*, X. Garbet*, K. Gentle*, L. Giannone, C.M. Greenfield*, G.T. Hoang*, A. Jacchia*, S.M. Kaye*, X. Litaudon*, T.C. Luce*, P. Mantica*, A.G. Peeters, U. Stroth, G. Tardini, J. Weiland* and H. Yamada*:* Electron Thermal Transport: An Experimental Perspective. Invited Preview Talk, 9th Joint US-European Transport Force Meeting, Madison,WS 2003.

782. *Ryter, F. and ASDEX Upgrade Team:* Electron Heat Transport in ASDEX Upgrade. 15th Joint Russian-German STC Meeting on ECRH and Gyrotrons, Karlsruhe/Stuttgart/Garching 2003.

783. *Ryter, F., K. Kirov, F. Leuterer, F. Monaco, M. Münich, G. Pereverzev, H. Schütz, W. Suttrop, ASDEX Upgrade Team and IPF-Stuttgart ECRH-Group:* Transport Studies with ECRH in ASDEX Upgrade. 15th Joint Russian-German STC Meeting on ECRH and Gyrotrons, Karlsruhe/Stuttgart/Garching. 2003.

784. *Ryter, F., S. Lebedev*, M. Reich and ASDEX Upgrade Team:* Recent Studies of LH Transition at Low Density in ASDEX Upgrade. 4th ITPA Meeting of Transport and ITB Physics and Confinement and Modeling Topical Groups, St. Petersburg 2003.

785. *Samitov*, M.A., W.A. Cooper*, M.Yu. Isaev*, M.I. Mikhailov*, J. Nührenberg, V.D. Shafranov*, A.A. Subbotin*, K. Yamazaki* and R. Zille:* Quasi-isodynamic Configuration with Poloidally Closed Contours of B and Small Number of Periods. 13th International Toki Conference on Plasma Physics and Controlled Fusion, Toki 2003.

786. *Samitov*, M.A., W.A. Cooper*, M.I. Mikhailov*, J. Nührenberg, V.D. Shafranov*, A.A. Subbotin* and R. Zille:* Numerical Optimisation of a Three-Period Stellarator Configuration with Respect to Quasi-isodynamicity. IAEA Technical Meeting on Innovative Concepts and Theory of Stellarators, Greifswald 2003.

787. *Sardei F.:* Magnetohydrodynamik. Universität der Bundeswehr München 2003.

788. *Sardei F.:* Rechneranwendungen in der Fluiddynamik. Universität der Bundeswehr München 2003.

789. *Schacht, J., H. Niedermeyer, H. Laqua, J. Hildebrandt* and K. Gleu**: Structure and Properties of the Trigger-Time-Event System for the W7-X Experiment. 13th IEEE-NPSS Real Time Conference, Montreal 2003.

790. *Schirmer, J., G.D. Conway, W. Suttrop, S. Klenge, H. Zohm and ASDEX Upgrade Team: E x B* Velocity Measurements from Doppler Reflectometry. Spring Meeting Aachen. Verhandl. DPG (VI) **38** (4), P 8.5 (2003).

791. *Schmid, K.:* Erosion of Carbon by Simultaneous Impact of Deuterium and Beryllium and Enhanced Erosion of Be at Elevated Temperatures. 11th European Fusion Program Workshop, Heraklion 2003.

792. *Schmid, K., A. Wiltner and Ch. Linsmeier:* Measurement of Beryllium Depth Profiles in Carbon. Ion Beam Analysis Workshop, Albuquerque,NM 2003.

793. *Schmidt, M.:* Advanced Δ-f Monte Carlo Simulations of the NBI Heating in W7-X. Theory Meeting, Zinnowitz 2003.

794. *Schmidt, M. and A. Werner:* “Advanced” Delta-f Simulation of the NBI Heating in Wendelstein 7-X. 14th International Stellarator Workshop, Greifswald 2003.

795. *Schneider, R.:* Comprehensive Suite of Codes for Plasma-Edge Modelling. International Conference on Numerical Simulation of Plasmas, Cape Cod 2003.

796. *Schneider, R.:* Computational Plasma Physics. Heraeus Sommerschule, Greifswald 2003.

797. *Schneider, R.:* Edge Physics in Tokamaks: Theory, Methods and Results. Universität Innsbruck, WS 2002/2003.

798. *Schneider, R.:* Generalized Coordinates, Basic Concepts and Applications. Universität Greifswald, WS 2002/2003.

799. *Schneider, R.:* Kinetic Modeling of Dusty Plasmas. 9th International Workshop on Plasma Edge Theory in Fusion Devices, San Diego,CA 2003.

800. *Schneider, R.:* New Developments in Plasma Edge Modelling. Frontiers in Plasma Theory, Greifswald 2003.

801. *Schneider, R.:* Plasma-Edge Modelling at IPP-Greifswald. Colloquium, University of Bari 2003.

802. *Schröder, C., O. Grulke and T. Klinger:* Investigations on Drift Waves in a Helicon Discharge. Spring Meeting Aachen. Verhandl. DPG (VI) **38** (4), P 10.13 (2003).

803. *Schröder, D., U. Wenzel, B. Koch and W. Bohmeyer:* Measurement of the Electron Temperature and Density in Recombining Plasmas. Spring Meeting Aachen. Verhandl. DPG (VI) **38** (4), P 10.33 (2003).

804. *Schubert, M. and M. Endler:* Spatially Resolved Fast Swept Langmuir Probe Measurements at the Wendelstein 7-AS Stellarator. Spring Meeting Aachen. Verhandl. DPG (VI) **38** (4), P 7.6 (2003).

805. *Schwarz-Selinger, T.:* Growth and Erosion of Hydrogenated Carbon Films: Interplay between Ions and Radicals. Invited Seminar Talk, Plasma Research Laboratory, Dublin City University, Dublin 2003.

806. *Schwarz-Selinger, T., C. Hopf, M. Meier and W. Jacob:* Deposition of Hydrogenated Carbon Films from Nitrogen Containing Methane Plasmas. 10th International Workshop on Carbon Materials for Fusion Application, Jülich 2003.

807. *Schwarz-Selinger, T. and W. Jacob:* Deposition of Hydrogenated Carbon Films from Nitrogen Containing Methane Plasmas. ASEVA Workshop 14: Reactive Plasmas - Physical and Chemical Processes in Reactive Hydrocarbon Plasmas in Contact with Surfaces, Avila 2003.

808. *Schwarz-Selinger, T., W. Jacob, R. Preuss and V. Dose:* Determination of the Electron Temperature in Hydrogen Discharges with Energy Dispersive Mass Spectrometry. Workshop "Frontiers in Low Temperature Plasma Diagnostics V", Speccia 2003.

809. *Schwarz-Selinger, T., H.D. Kang, R. Preuss and V. Dose:* Decomposition of Multicomponent Mass Spectra Applying Bayesian Data Analysis. ASEVA Workshop 14: Reactive Plasmas - Physical and Chemical Processes in Reactive Hydrocarbon Plasmas in Contact with Surfaces, Avila 2003.

810. *Schwarz-Selinger, T., B. Plöckl and W. Jacob:* Bestimmung des Ionenflusses aus einem Wasserstoff-ICP-Plasma mit energiedispersiver Massenspektrometrie: erste Erfahrungen mit dem PPM 422. 10. Erfahrungsaustausch "Oberflächentechnologie mit Plasmaprozessen", Mühlleithen 2003.

811. *Schweinzer, J.:* Atomic Processes and Density Reconstruction Algorithm for the Lithium-Beam Diagnostic. NIFS, Nagoya 2003.

812. *Schweinzer, J.:* ITER - der nächste Schritt zum Kernfusionsreaktor. Institut für Angewandte Physik, Technische Universität Wien 2003.

813. *Schweinzer, J.:* Plasmaphysik II. Vorlesung, Universität Ulm, SS 2003.

814. *Schwenn, U.:* Trends in Videoconferencing in Max-Planck-Gesellschaft. Seminar DRFC Salle Gravier, CEA, Cadarache 2003.

815. *Schwenn, U.:* Video over IP - Establishing an H.323 Videoconferencing Infrastructure for the German Max-Planck-Gesellschaft. IMTC/Wainhouse Research European Forum, Geneva 2003.

816. *Schwenn, U.:* Video over IP - Videoconferencing Infrastructur, Max-Planck-Gesellschaft & IPP. Seminar, KFKI Research Institute for Particle and Nuclear Physics of the Hungarian Academy of Sciences, Budapest 2003.

817. *Schwenn, U.:* Videokonferenzen in der MPG und dem IPP - DFNVC Serice des DFN. 20. DV Treffen der MPG, Göttingen 2003.

818. *Schwenn, U.:* Videokonferenzszenarien: RZG - IPP – MPG. VIKTAS-Tag, Berlin, Dresden, Essen, Garching 2003.

819. *Schwenn, U. and K. Stoeckigt:* Videoconferencing New Zealand - Germany: Experiences in Collaborative Research and Work for the Max-Planck-Gesellschaft. Presentation Megaconference V, Hamilton, New Zealand 2003.

820. *Scott, B.D.:* Understanding of Plasma Boundary Turbulence. Spring Meeting Aachen. Verhandl. DPG (VI) **38** (4), P IV (2003).

821. *Shafranov*, V.D., W.A. Cooper*, A.A. Ivanov*, M.Yu. Isaev*, A.A. Martynov*, S.Yu. Medvedev*, M.I. Mikhailov*, J. Nührenberg, C. Nührenberg, Yu.Yu. Poshekhonov*, M.A. Samitov*, A.A. Skovoroda*, A.A. Subbotin* and R. Zille:* Optimized N=9 Stellarator Configuration with Poloidally Closed Contours of B on the Magnetic Surfaces. IAEA Technical Meeting on Innovative Concepts and Theory of Stellarators, Greifswald 2003.

822. *Shimizu, T., W. Jacob, H. Thomas, G. Morfill*, N. Sato* and T. Abe*:* Particles Behavior in Methane-Hydrogen Plasmas. 56th Gaseous Electronics Conference, San Francisco,CA 2003.

823. *Shyshkin*, O., R. Schneider and Yu. Igitkhanov:* Stochastic Diffusion Tensor and Tungsten Ion Fluxes in Drift Optimized Plasma Configuration. 14th International Stellarator Workshop, Greifswald 2003.

824. *Shishkin*, A., H. Wobig, R. Schneider and Yu. Igitkhanov:* Impurity Flow in Helical Plasma under the Resonant Magnetic Field. 14th International Stellarator Workshop, Greifswald 2003.

825. *Soddemann, T.:* BladeCenter: Alternative zum herkömmlichen Linux Cluster? Linux Workshop der MPG, Leipzig 2003.

826. *Soddemann, T.:* Design der BioInfo Pipeline. Treffen der BioInfo Initiative, Garching 2003.

827. *Soddemann, T.:* Erweitertes Design der BioInfo Pipeline. Treffen der BioInfo Initiative, Saarbrücken 2003.

828. *Soddemann, T.:* Vorstellung des Designs der BioInfo Pipeline. Projektmeeting BioInfo Initiative, Tübingen 2003.

829. *Soddemann, T.:* Vorstellung des RZG. ZebraFish Models-Treffen, Tübingen 2003.

830. *Sorge, S.:* Investigation of ITG-Driven Turbulence in Pinch-Geometry within Nonlinear PIC-Calculations. IAEA Technical Meeting on Innovative Concepts and Theory of Stellarators, Greifswald 2003.

831. *Sorge, S. and R. Hatzky:* Investigation of ion-temperature-gradient-driven turbulence in a pinch configuration within a gyrokinetic global nonlinear particle-in-cell simulation. IAEA Technical Meeting on Innovative Concepts and Theory of Stellarators, Greifswald 2003.

832. *Speth, E. and NBI Team:* Development of Powerful RF Plasma Sources for Present and Future NBI Systems. 4th General Scientific Assembly of Asia Plasma and Fusion Technology, Hangzhou 2003.

833. *Starke, P., U. Fantz* and K. Behringer:* Interaction and Influence of Hydrogen and Deuterium on Chemical Erosion of Carbon. Spring Meeting Aachen. Verhandl. DPG (VI) **38** (4), P 1.2 (2003).

834. *Stoeckigt, K.:* Advantages of GnuGK. MPG-HGF VC Meeting, Seminar RZG, Garching 2003.

835. *Stoeckigt, K.:* Gatekeepers in general - A short introduction. Seminar via VC RZG, Auckland 2003.

836. *Subbotin*, A.A., W.A. Cooper*, M.Yu. Isaev*, M.I. Mikhailov*, V.N. Kalyuzhnyj*, S.V. Kasilov*, V.V. Nemov*, J. Nührenberg, M.A. Samitov*, V.D. Shafranov* and R. Zille:* Modification of the Stellarator Optimization Procedure by Including the Effective Ripple and Bootstrap Current Structural Factor Calculations. IAEA Technical Meeting on Innovative Concepts and Theory of Stellarators, Greifswald 2003.

837. *Suttrop, W.:* Introduction to ASDEX Upgrade Data. Seminar at the Advanced Energy Systems Laboratory, Helsinki University of Technology, Helsinki 2003.

838. *Suttrop, W.:* Physics of the H-mode Pedestal. 11th European Fusion Physics Workshop, Heraklion 2003.

839. *Suttrop, W.:* Physik der Transportbarriere am Rand von Fusionsplasmen. Kolloquium, Universität Stuttgart 2003.

840. *Suttrop, W.:* Stationary ELM-free H-mode in ASDEX Upgrade. Seminar at the Advanced Energy Systems Laboratory, Helsinki University of Technology, Helsinki 2003.

841. *Suttrop, W.:* Technische Plasmen. Vorlesung, Universität Bayreuth, WS 2003/2004.

842. *Takamura*, S., N. Ohno*, M.Y. Ye and T. Kuwabara*:* Space-Charge Limited Current from Plasma-Facing Material. 9th International Workshop on Plasma Edge Theory, San Diego,CA 2003.

843. *Tasso, H. and G.N. Throumoulopoulos*:* Two-Step Control of Wall Mode and the Monodromy Matrix. 5th International Congress on Industrial and Applied Mathematics, Sydney 2003.

844. *Thomsen, H., Y. Feng, P. Grigull, R. König, K. McCormick, R. Narayanan, U. Wenzel and W7-AS Team:* Spatio-Temporal Behaviour of Asymmetric Non-Stationary Radiation in the Wendelstein 7-AS Stellarator. 14th International Stellarator Workshop, Greifswald 2003.

845. *Thomsen, H. and R. König:* Spatio-Temporal Behaviour of Radiative Instabilities in Wendelstein 7-AS Stellarator. Spring Meeting Aachen. Verhandl. DPG (VI) **38** (4), P 8.1 (2003).

846. *Throumoulopoulos*, G.N., G. Poulipoulis*, G. Pantis* and H. Tasso:* Exact Magnetohydrodynamic Equilibria with Flow and Effects on the Shafranov Shift. 5th International Congress on Industrial and Applied Mathematics, Sydney 2003.

847. *Thumm*, M., A. Arnold*, E. Borie*, G. Dammertz*, O. Drumm*, R. Heidinger*, S. Illy*, J. Jin*, K. Koppenburg*, B. Piosczyk*, T. Rzesnicki*, D. Wagner and X. Yang*:* Development of Advanced High Power Gyrotrons for ECH&CD Applications in Fusion Plasmas. Joint Workshop of Annual US-JA-Workshop on RF Heating Technology and the 6th EU-JA-Workshop on RF Antenna and Related Technology, Tokai 2003.

848. *Toussaint, U. von:* Modelling from a Bayesian Perspective. Meeting on Material Research and Modelling, Ringberg 2003.

849. *Toussaint, U. von, S. Gori and V. Dose:* Neural Networks and Hyperplane Priors. 23rd International Conference on Bayesian Methods and Maximum Entropy in Science and Engineering, Jackson Hole 2003.

850. *Treutterer, W., K. Behler, A. Lohs, G. Neu, G. Raupp, D. Zasche, T. Zehetbauer, R. Cole* and K. Lüddecke*:* Software Structure and Real-Time Signal Exchange for the ASDEX Upgrade Tokamak Control System. International Conference of Accelerator and Large Experimental Physics Control Systems (ICALEPCS), Gyeongju 2003.

851. *Turkin, Y.:* Predictive Transport Code for W7-X. Theory Meeting, Zinnowitz 2003.

852. *Van Eester*, D., F. Imbeaux*, P. Mantica*, M.J. Mantsinen*, M. de Baar*, P. de Vries*, L.-G. Eriksson*, R. Felton*, A. Figueiredo*, J. Harling*, E. Joffrin*, K. Lawson*, H. Leggate*, X. Litaudon*, V. Kiptily*, J.-M. Noterdaeme, V. Pericoli*, E. Rachlew*, A. Tuccillo*, K.-D. Zastrow* and EFDA-JET Contributors:* Recent ^{3}He Radio Frequency Heating Experiments on JET. 15th Topical Conference on RF Power in Plasmas, Moran,WY 2003.

853. *Wagner, D., A. Arnold*, T. Rzesnicki* and M. Thumm*:* Low Power Mode Excitation for the Cold Test of Next Generation Fusion. 28th International Conference on Infrared and Millimeter Waves, Otsu, Shiga 2003.

854. *Wagner, D., K. Kirov, F. Leuterer, F. Monaco, M. Münich, H. Schütz, F. Ryter, R. Wilhelm, H. Zohm, T. Franke, K. Voigt, G. Dammertz*, H. Heidinger*, I. Danilov*, K. Koppenburg*, A. Meier*, M. Thumm*, X. Yang*, W. Kasparek*, G. Gantenbein*, H. Hailer*, G.A. Müller*, K. Schwörer*, G. Denisov*, A. Litvak* and V. Zapevalov*:* A New ECRH System for ASDEX. 28th International Conference on Infrared and Millimeter Waves, Otsu, Shiga 2003.

855. *Wagner, D., F. Leuterer, F. Monaco, M. Münich and H. Schütz:* Polarisation Mirrors with Nonideal Geometry. 15th Joint Russian-German STC Meeting on ECRH and Gyrotrons, Karlsruhe/Stuttgart/Garching 2003.

856. *Wagner, F.:* Achievements of the Wendelstein-Stellarator Line. 4th General Scientific Assembly of Asia Plasma and Fusion Association on New Development of Plasma Physics and Fusion Technology, Hangzhou 2003.

857. *Wagner, F.:* Experimentelle Plasmaphysik I. Vorlesung, Universität Greifswald, SS 2003.

858. *Wagner, F.:* Experimentelle Plasmaphysik II. Vorlesung, Universität Greifswald, WS 2003/2004.

859. *Wagner, F.:* Kernfusion als nachhaltige Energiequelle. Vortragsreihe des Physikalischen Vereins „Aus Naturwissenschaft und Technik“, Frankfurt/Main 2003.

860. *Wagner, F.:* Major Results from Wendelstein 7-AS Stellarator. Board of Councillors Meeting, Japan 2003.

861. *Wagner, F.:* Progress in Fusion Research. Lecture Programme at UCC Cork, QUB Belfast, DCU Dublin 2003.

862. *Wagner, F.:* Die Sonne als Vorbild - Energiegewinnung aus kontrollierter Kernfusion. Fachhochschule Stralsund 2003.

863. *Wagner, F.:* Stand und Zukunft der Fusionsforschung mit magnetischem Einschluss. Kolloquiumvortrag, Universität Regensburg 2003.

864. *Wagner, F.:* The Stellarator Concept - an Option for a Fusion Power Plant. BNN Symposium, Leipzig 2003.

865. *Warrier, M.:* Modeling of the Diffusion of Hydrogen in Porous Graphite. Workshop on Hydrogen in Condensed Matter, Helsinki 2003.

866. *Watanabe*, K.Y., A. Weller, S. Sakakibara*, Y. Narushima*, S. Ohdachi*, K. Toi*, H. Yamada*, Y. Suzuki*, O. Kaneko*, K. Narihara*, K. Ida* and LHD, W7-AS Experimental Group:* Progress of High Beta Experiments in Stellarator/Heliotron. 14th International Stellarator Workshop, Greifswald 2003.

867. *Weller, A.:* High-Beta Experiments in W7-AS. APS, Division of Plasma Physics, 45th Annual Meeting, Albuquerque,NM 2003. Bulletin of the American Physics Society **48** (7), 198 (2003).

868. *Weller, A.:* The High-Density/High-Beta Regime in W7-AS. Colloquium, PPPL, Princeton 2003.

869. *Wenzel, U., K. McCormick, R. Narayanan, F. Gadelmeier, P. Grigull, R. König and H. Thomsen:* Spectroscopic Study of the Detachment Phases in the W7-AS Stellarator with Island Divertors. 14th International Stellarator Workshop, Greifswald 2003.

870. *Wenzel, U. and D. Schröder:* The H_- Minimum at the Transition from a Recombining to an Ionizing Plasma. Spring Meeting Aachen. Verhandl. DPG (VI) **38** (4), P 16.4 (2003).

871. *Wieczorek*, A., E. Harmeyer and G. Linhofer*:* Computer Simulations of the Power Supply for the Superconduction Coils of Helias Stellarator Fusion Reactors. 10th European Conference on Power Electronics and Applications, Toulouse 2003.

872. *Wieczorek*, A., E. Harmeyer and G. Linhofer*:* Simulation Studies of the Power Supply and the Protection System for the Helias Reactor Coils. 14th International Stellarator Workshop, Greifswald 2003.

873. *Wieczorek* A., E. Harmeyer and G. Linhofer*:* Simulation Studies of the Protection Systems for the Superconducting Coils of Helias Stellarator Fusion Reactors. 20th IEEE/NPSS Symposium on Fusion Engineering, San Diego,CA 2003.

874. *Wilhelm, R.:* Basic Procedures and Technology of Negative Ion Sources for Fusion Applications. Master Class: Electro-negative Plasmas, Bad Honnef 2003.

875. *Wilhelm, R.:* Entwicklung einer HF-Quelle für negative Wasserstoffionen - ein ITER Projekt. Kolloquium, Institut für Niedertemperatur-Plasmaphysik, Greifswald 2003.

876. *Wilhelm, R.:* Der Knick im Hohlleiter. Festkolloquium Prof. Thumm, Universität Karlsruhe 2003.

877. *Wilhelm, R.:* Plasmaphysik I. Vorlesung, Technische Universität München, WS 2002/2003.

878. *Wilhelm, R.:* Plasmaphysik II. Vorlesung, Technische Universität München, SS 2003.

879. *Wiltner, A. and Ch. Linsmeier:* Formation of Endothermic Carbides on Iron and Nickel. 4th German-Brazilian Workshop on Applied Surface Science, Ringberg 2003.

880. *Wiltner, A. and Ch. Linsmeier:* Thermally Induced Carbide Formation on Metals. Gordon Research Conference, Chemical Reactions at Surfaces, Ventura 2003.

881. *Wiltner, A. and Ch. Linsmeier:* Untersuchung der Carbidbildung auf Eisen und Nickel. Frühjahrstagung Dresden. Verhandl. DPG (VI) **38** (5), O 23.10 (2003).

882. *Wobig H.:* On Electric Fields in Stellarator Equilibria. 14th International Stellarator Workshop, Greifswald 2003.

883. *Wünderlich, D., U. Fantz* and K. Behringer:* An Adaptive Radiative Model: Theory and Application for Low Temperature Plasmas. Spring Meeting Aachen. Verhandl. DPG (VI) **38** (4), P 10.12 (2003).

884. *Yakovenko*, Y. V., Y. I. Kolesnichenko*, A. Könies, A. Weller, A. Werner and S. Zegenhagen:* Peculiarities of the Alfvén Continuum in Stellarators. IAEA TCM on Innovative Concepts and Theory of Stellarators, Greifswald 2003.

885. *Yang*, X., O. Drumm*, A. Arnold*, E. Borie*, G. Dammertz*, K. Koppenburg*, B. Piosczyk*, D. Wagner and M. Thumm*:* Design of a Quasi Optical Mode Converter for a Frequency Step-Tunable Gyrotron. 28th International Conference on Infrared and Millimeter Waves, Otsu, Shiga 2003.

886. *Yang*, X, O. Drumm*, A. Arnold*, E. Borie*, G. Dammertz*, R. Heidinger*, K. Koppenburg*, B. Piosczyk*, M. Thumm* and D. Wagner:* Quasi Optical Mode Converter and Window System for a Step-Tunable 1 MW Gyrotron. 15th Joint Russian-German STC Meeting on ECRH and Gyrotrons, Karlsruhe/Stuttgart/Garching 2003.

887. *You, J.-H. and H. Bolt:* Structural Analysis of a Plasma-Facing Component Reinforced with Fibrous Metal Matrix Composite Laminate. 11th International Conference on Fusion Reactor Materials, Kyoto 2003.

888. *Zalach, J., O. Grulke and T. Klinger:* ECR Heating of a Linearly Magnetized Helicon Plasma. Spring Meeting Aachen. Verhandl. DPG (VI) **38** (4), P 10.1 (2003).

889. *Zohm, H.:* Magneto Hydro Dynamics. Guest Lecture, International Max-Planck Research School, Garching 2003.

890. *Zohm, H.:* Magnetohydrodynamics - Plasma Physics on the Road to a Fusion Reactor. Kolloquium, Magdeburg 2003.

891. *Zohm, H.:* Magnetohydrodynamik (MHD) heißer Plasmen. Vorlesung, Universität München, WS 2003/2004.

892. *Zohm, H.:* New Results from NTM Stabilisation by ECCD in ASDEX Upgrade. Joint German-Russian Workshop on ECRH and Gyrotrons, Garching 2003.

893. *Zohm, H.:* Optimisation of the ITER ECRH Launcher. Joint German-Russian Workshop on ECRH and Gyrotrons, Garching 2003.

894. *Zohm, H.:* Physics of Hot Plasmas. Heraeus Sommerschule, Greifswald 2003.

895. *Zohm, H.:* Plasmaphysik. Vorlesung, Universität München, SS 2003.

896. *Zohm, H.:* Recent Results from ASDEX Upgrade. Seminar, General Atomics, San Diego,CA 2003.

897. *Zymara*, A., U. Fantz* and K. Behringer:* Analysis of the Intensity Ratio C_2/CH Radiation from Different Plasmas in Hydrocarbons. Spring Meeting Aachen. Verhandl. DPG (VI) **38** (4), P 17.8 (2003).

Internal Laboratory Reports

IPP 1/330
Bosch, H.-S. and M. Jung (Eds.): ASDEX Upgrade Results in 2002. Publications and Conference Contributions.

IPP 1/331
Na, Y.-S.: Modelling of Current Profile Control in Tokamak Plasmas.

IPP II/5
*Bosch, H.-S. and M. Jung (Eds.):*ASDEX Upgrade Results in 2002. Publications and Conference Contributions.

IPP II/6
Munoz, M.G.: Modelling of Fast Ion Losses in Tokamak.

IPP 4/281
Franzen, P., J. Sielanko, H.P.L. De Esch*, E. Speth, B. Heinemann and R. Riedl:* Design Studies for an Alternative Magnetic Residual Ion Removal System for the ITER Neutral Beam Injection System.

IPP 4/282
Bobkov, V., ICRF Team and ASDEX Upgrade Team.: Studies of High Voltage Breakdown Phenomena on ICRF (Ion Cyclotron Range of Frequencies) Antennas.

IPP 5/102
Tardini, G.: Validation of Theory Based Transport Models in Tokamak Plasmas.

IPP 5/103
Bosch, H.-S. and M. Jung (Eds.): ASDEX Upgrade Results in 2002. Publications and Conference Contributions.

IPP 5/104
Kochergov, R.: Wave Equations for Low Frequency Waves in Hot Magnetically Confined Plasmas.

IPP 9/134
Hopf, C.: Chemische Zerstäubung und ionenunterstütztes Wachstum amorpher Kohlenwasserstoffschichten- Experimente mit Teilchenstrahlen.

IPP 10/23
Bosch, H.-S. and M. Jung (Eds.): ASDEX Upgrade Results in 2002. Publications and Conference Contributions.

IPP 10/24
Yoon, S.-W.: The Relation of Carbon Influces and Core Carbon Concentrations in ASDEX Upgrade.

IPP 10/25
Neu, R.: Tungsten as a Plasma Facing Material in Fusion Devices.

IPP 12/2
Mutzke, A., X. Bonnin, J. Nührenberg and R. Schneider: Calculation of Magnetic Coordinates for Stellarator Fields.

IPP 13/1
Volpe, F.: Electron Bernstein Emission Diagnostic of Electron Temperature Profile at W7-AS Stellarator

IPP 13/2
Andreeva, T. and E. Harmeyer: Das magnetische Streufeld in der Maschinenhalle von Wendelstein 7-X.

IPP 15/3
Fink, M.: Untersuchung der Fluktuationen des Plasmapotentials mit emissiven und nichtemissiven elektrostatischen Sonden.

IPP 15/4
Franck, C.: Experiments on Whistler Wave Dispersion in Bounded Magnetised Plasmas.

IPP Z/4
Jaksic, N. and J. Simon-Weidner: Summary of Static and Buckling Calculations of the W7-X Plasma Vessel.

External Laboratory Reports

LRP-747
Henderson, M.A., S. Alberti*, C. Angioni, G. Arnoux*, R. Behn*, P. Blanchard*, P. Bosshard*, Y. Camenen*, S. Coda*, I. Condrea*, T.P. Goodman*, F. Hofmann*, J.-P. Hogge*, A. Karpushov*, A. Manini*, A. Martynov*, J.-M. Moret*, P. Nikkola*, E. Nelson-Melby*, A. Pochelon*, L. Porte*, O. Sauter*, S.M. Ahmed*, Y. Andrebe*, K. Appert*, R. Chavan*, A. Degeling*, B.P. Duval*, P. Etienne*, D. Fasel*, A. Fasoli*, J.-Y. Favez*, I. Furno*, J. Horacek*, P. Isoz*, B. Joye*, I. Klimanov*, P. Lavanchy*, J.B. Lister*, X. Llobet*, J.-C. Magnin*, B. Marletaz*, P. Marmillod*, Y. Martin*, J.-M. Mayor*, J. Mlynar*, P.J. Paris*, A. Perez*, Y. Peysson*, R.A. Pitts*, D. Raju*, H. Reimerdes*, A. Scarabosio*, E. Scavino*, S.H. Seo*, U. Siravo*, A. Sushkov*, G. Tonetti*, M.Q. Tran*, H. Weisen*, M. Wischmeier*, A. Zabolotsky* and G. Yhuang*:* Recent results from the electron cyclotron heated plasmas in TVC. Centre de Recherches en Physique des Plasmas, Lausanne(CH).

LRP-749
Allfrey, S.J. and R. Hatzky:* A revised δ f algorithm for nonlinear PIC simulation. Centre de Recherches en Physique des Plasmas, Lausanne(CH).

LRP-763
Villar,L., S.J. Allfrey*, A. Bottino*, M. Brunetti*, G.L. Falchetto*, V. Grandgirard*, R. Hatzky, J. Nührenberg, A.G. Peeters, O. Sauter*, S. Sorge and J. Vaclavik:* Full radius linear and nonlinear gyrokinetic simulations for Tokamaks and Stellarators: Zonal flows, applied E x B Flows, trapped electrons and finite beta. Centre de Recherches en Physique des Plasmas, Lausanne(CH).

Author Index

Teams

ASDEX Upgrade Team

C.Angioni, M. Apostoliceanu, M.Balden, W.Becker, G.Becker, K.Behler, K.Behringer, A.Bergmann, R.Bilato, I.Bizyukov, V.Bobkov, T.Bolzonella*, D.Borba*, K.Borrass, M.Brambilla, F.Braun, A.Buhler, A.Carlson, A.Chankin, J.Chen, Y.Chen, S.Cirant*, G.Conway, D.P.Coster, T.Dannert, K.Dimova, R.Drube, R.Dux, T.Eich, K.Engelhardt, H.-U.Fahrbach, U.Fantz, L.Fattorini*, M.Foley*, P.Franzen, J.C.Fuchs, J.Gafert, G.Gantenbein*, M.Garcia Munoz, O.Gehre, A.Geier, L.Gianonne, O.Gruber, S.Günter, G.Haas, D.Hartmann, B.Heger, B.Heinemann, A.Herrmann, J.Hobirk, H.Hohenöcker, L.D.Horton, M.Huart, V.Igochine, D.Jacobi, A.Jacchia*, M.Jakobi, F.Jenko, A.Kallenbach, S.Kalvin*, O.Kardaun, M.Kaufmann, A.Keller, A.Kendl, M.Kick, J.-W.Kim, K.Kirov, S.Klose, R.Kochergov, G.Kocsis*, H.Kollotzek, C.Konz, W.Kraus, K.Krieger, T.Kurki-Suonio*, B.Kurzan, K.Lackner, P.T.Lang, P.Lauber, M.Laux, F.Leuterer, J.Likonen*, A.Lohs, A.Lyssoivan*, C.Maggi, H.Maier, K.Mank, A.Manini, M.-E.Manso*, P.Mantica, M.Maraschek, K.-F.Mast, H.Mayer, M.Mayer, P.McCarthy*, D.Meisel, H.Meister, F.Meo*, P.Merkel, R.Merkel, D.Merkl, V.Mertens, F.Monaco, A.Mück, H.W.Müller, M.Münich, H.Murmann, Y.-S.Na, R.Narayanan, G.Neu, R.Neu, J.Neuhauser, D.Nishijima, Y.Nishimura, J.-M.Noterdaeme, I.Nunes*, M.Pacco-Düchs, G.Pautasso, A.G.Peeters, G.Pereverzev, S.D.Pinches, E.Poli, E.Posthumus-Wolfrum, T.Pütterich, R.Pugno, E.Quigley*, I.Radivojevic, G.Raupp, R.Riedl, S.Riondato, V.Rohde, J.Roth, F.Ryter, S.Saarelma*, W.Sandmann, J.Santos*, G.Schall, H.-B.Schilling, J.Schirmer, W.Schneider, G.Schramm, J.Schweinzer, S.Schweizer, B.D.Scott, U.Seidel, F.Serra*, C.Sihler, A.Silva*, A.C.C.Sips, E.Speth, A.Stäbler, K.-H.Steuer, J.Stober, B.Streibl, D.Strintzi, E.Strumberger, W.Suttrop, G.Tardini, C.Tichmann, W.Treutterer, M.Troppmann, H.Urano, P.Varela*, D.Wagner, F.Wesner, E.Würsching, M.Y.Ye, S.-W.Yoon, Q.Yu, B.Zaniol, D.Zasche, T.Zehetbauer, M.Zilker, H.Zohm.

ECRH Group (WENDELSTEIN 7-AS)

H.Braune, V.Erckmann, J.Hofner, F.Hollmann, J.Jonitz, H.Laqua, G.Michel, F.Noke, F.Purps, T.Schulz.

WENDELSTEIN 7-AS Team

T.Andreeva, S.Bäumel, J.Baldzuhn, C.Beidler, T.Bindemann, R.Brakel, H.Braune, R.Burhenn, A.Dinklage, A.Dodhy, D.Dorst, H.Ehmler, M.Endler, V.Erckmann, Y.Feng, F.Gadelmeier, J.Geiger, L.Giannone, P.Grigull, O.Grulke, E.Harmeyer, H.-J.Hartfuss, D.Hartmann, F.Herrnegger, M.Hirsch, E.Holzhauer*, K.Horvath, Yu.L.Igitkhanov, R.Jaenicke, F.Karger, W.Kasparek*, J.Kisslinger, T.Klinger, J.Knauer, R.König, G.Kühner, A.Kus, H.Laqua, J.Lingertat, R.Liu, H.Maaßberg, S.Marsen, N.B.Marushchenko, K.McCormick, G.Michel, G.Müller*, R.Narayanan, U.Neuner, M.Otte, E.Pasch, Y.Podoba, A. Reichert, N.Ruhs, N.Rust, J.Saffert, E.Sallander, J.Sallander, F.Sardei, F.Schneider, M.Schmidt, M.Schubert, J.Svensson, H.Thomsen, Y.Turkin, F.Volpe, F.Wagner, A.Weller, A.Werner, H.Wobig, D.Zhang.

WENDELSTEIN 7-X

Construction Division Engineering Team

Y.Bozhko, J.Boscary, T.Bräuer, Ch.P.Dhard, J.-H.Feist, W.Gardebrecht, M.Gasparotto, H.Grote, B.Hein, H.Laqua, J.Ludvik, H.Modrow, M.Nagel, H.Niedermeyer, J.Reich, H.Renner, K.Riße, K.Rummel, T.Rummel, J.Schacht, F.Schauer, D.Sharma, S.Y.Shim, A.Spring, M.Wanner, L.Wegener.

Construction Division Technical Team

H.Bau, A.Benndorf, A.Berg, H.-J.Bramow, R.Brockmann, A.Brückner, M.Czerwinski, H.Dutz, M.Fricke, F.Füllenbach, G.Gliege, M.Gottschewsky, S.Heinrich, A.Hölting, U.Kamionka, T.Kluck, E.Köster, C.Kopplin, U.Krybus, F.Kunkel, K.Lang, H.Lentz, B.Missal, T.Mönnich, I.Müller, F.Nankemann, A.Opitz, M.Pietsch, S.Pingel, S.Raatz, D.Schinkel, A.Schütz, U.Schultz, M.Schweitzer, K.-U.Seidler, F.Starke, H.Viebke, O.Volzke, A.Vorköper, A.Wölk.

Appendix

Organisational structure of Max-Planck-Institut für Plasmaphysik

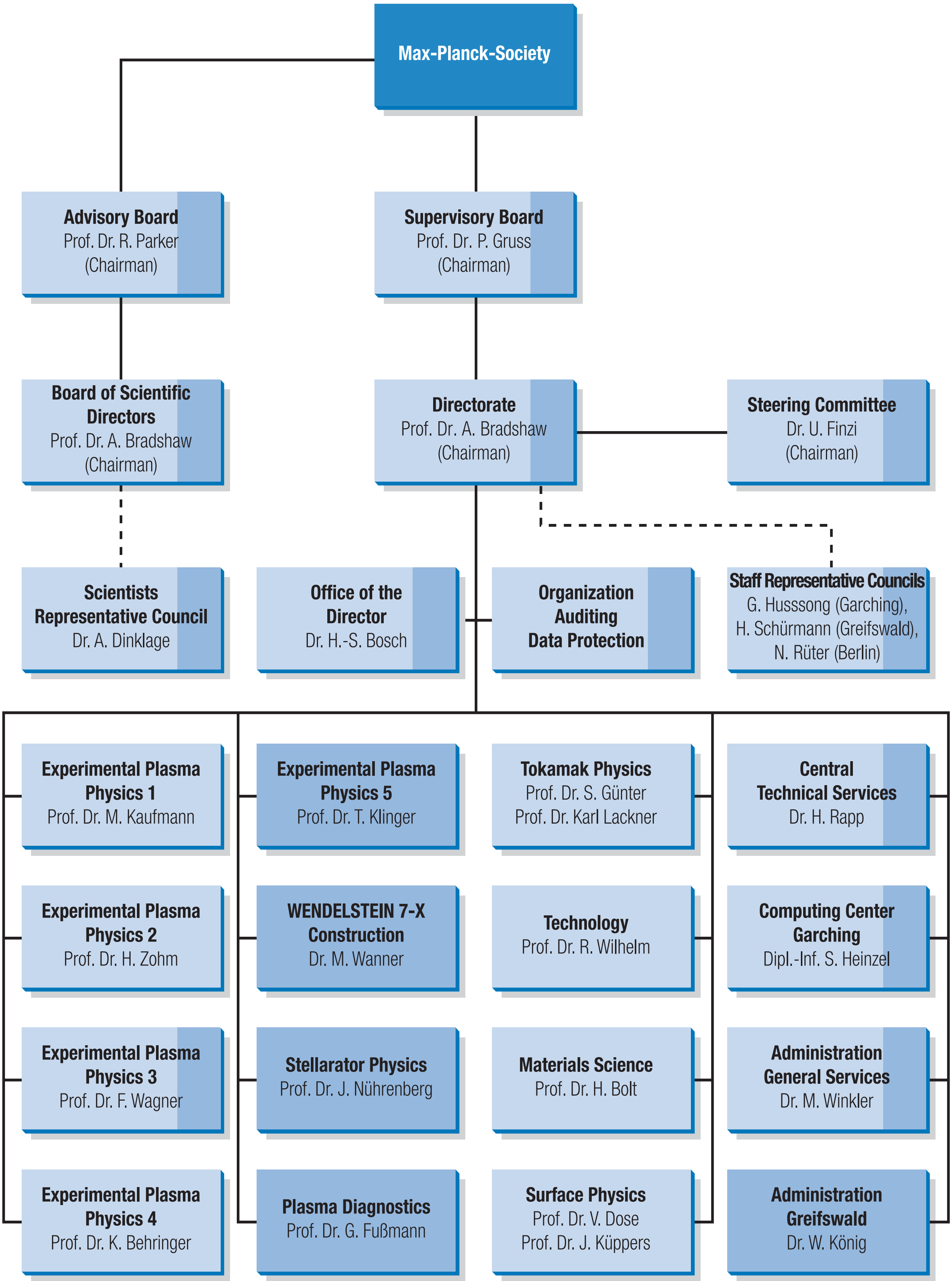

Scientific division of IPP

Experimental Plasma Physics Division 1

Director: Prof. Michael Kaufmann

ASDEX Upgrade (Divertor Tokamak)
- operation of ASDEX Upgrade
- investigation of ITER plasma boundary in a reactor-relevant divertor
- advanced tokamak studies
- investigation of energy transport, MHD stability, beta limit, density limit and disruptions

JET collaboration
- participation in experiments on JET under EFDA
- operation of special discharge scenarios at JET
- comparative studies together with ASDEX Upgrade

Experimental Plasma Physics Division 2

Director: Prof. Hartmut Zohm

ASDEX Upgrade
- Analysis and control of MHD instabilities
- Diagnostics
- Control and data acquisition

ITER
- Physics integration of ECRH sytem design

JET
- Contributions to task forces S1, S2 and M

Experimental Plasma Physics Division 3

Director: Prof. Friedrich Wagner

- Experiment-orientated stellarator theory
- interpretation of WENDELSTEIN 7-AS experimental results
- Stellarator power plant system studies along the HELIAS concept
- Preparation of the WENDELSTEIN 7-X diagnostics
- Preparation of ECRH for WENDELSTEIN 7-X
- operation of the WEGA device
- Development of Greifswald site

Experimental Plasma Physics Division 4

Director: Prof. Kurt Behringer

Experimental and theoretical investigations of plasma boundary and divertor physics, impurity transport, chemical impurity production and plasma radiation in ASDEX Upgrade and WENDELSTEIN 7-AS

- spectroscopic diagnostics on ASDEX Upgrade
- spectroscopic diagnostics on WENDELSTEIN 7-AS laboratory experiments at the University of Augsburg, Experimental Plasma Physics

Experimental Plasma Physics Division 5

Director: Prof. Thomas Klinger

dynamical behaviour of stellarator plasmas physics of the plasma edge and divertor region stellarator magnetohydrodynamics data acquisition and control

WENDELSTEIN 7-AS
- development and optimization of diagnostics

WENDELSTEIN 7-X
- preparation of the experiment program

VINETA
- basic behaviour of plasmas waves and plasma instabilities

INTERNATIONAL MAX-PLANCK RESEARCH SCHOOL "BOUNDED PLASMAS"
- training of PhD students

Stellarator Theory Division

Director: Prof. Jürgen Nührenberg

General stellarator theory
- Further development of the stellarator concept and computational as well as analytical methods to investigate equilibrium, stability and transport problems in three-dimensional toroidal configurations.

Plasma edge physics
- Theoretical work on 3D plasma edge physics

Scientific division of IPP

WENDELSTEIN 7-X Construction

Director: Dr. Manfred Wanner

WENDELSTEIN 7-X Construction

- engineering, construction and installation of the WENDELSTEIN 7-X device incl. system control, plasma heating, in-vessel components, and auxiliary systems
- project control and quality management

Technology Division

Director: Prof. Rolf Wilhelm

Neutral injection

- development, constuction and operation of the injectionsystems for ASDEX Upgrade and WENDELSTEIN 7-X
- development of RF-driven negative ion sources for ITER

Electron cyclotron resonance heating

- construction and operation of an ECRH system for ASDEX Upgrade

Ion cyclotron resonance heating

- development, construction and operation of ICRH systems for ASDEX Upgrade and WENDELSTEIN 7-X

Surface Physics Division

Directors: Prof. Volker Dose, Prof. Jürgen Küppers

Surface physics

- atomistic characterisation of surfaces Plasma-wall interactions
- interactions of atoms, ions and electrons with solid surfaces

Low temperature plasma physics

- preparation and characterisation of thin-film coatings for plasma devices and plasma diagnostics

Data analysis*

- application of Bayesian techniques to experimental data
  *Part of Centre for Interdisciplinary Plasma Science

Plasma Diagnostics Division

Director: Prof. Gerd Fussmann

Edge plasma physics

- experimental and theoretical work relating to fusion devices

Plasma generator PSI-II

- basic plasma physics
- plasma interaction with solid surfaces
- development and testing of plasma diagnostics Electron Beam Ion Trap (EBIT)
- production of highly charged ions
- X-ray spectroscopy and atomic physics measurements
- ITER collaboration

Materials Research Division

Director: Prof. Harald Bolt

- Characterisation of fusion relevant properties of plasma facing materials; development and qualification of plasma facing materials for present fusion devices, esp. ASDEX Upgrade and WENDELSTEIN 7-X
- Design and development of materials for plasma facing components in fusion reactors
- interaction of atoms, ions and electrons with solid surfaces
- wall fluxes in the boundary layer of plasma devices
- limiter and wall analyses

Tokamak Physics

Directors: Prof. Sibylle Günter, Prof. Karl Lackner

Theoretical support for the tokamak activities of IPP as well as study of fundamental plasma physics in toroidal magnetic confinement devices:

- plasma edge physics
- nonlinear plasma dynamics and turbulence
- heat and particle transport in tokamaks
- large scale instabilities in tokamaks including MHD and kinetic effects
- wave propagation and absorption in inhomogeneous plasmas

How to reach IPP in Garching

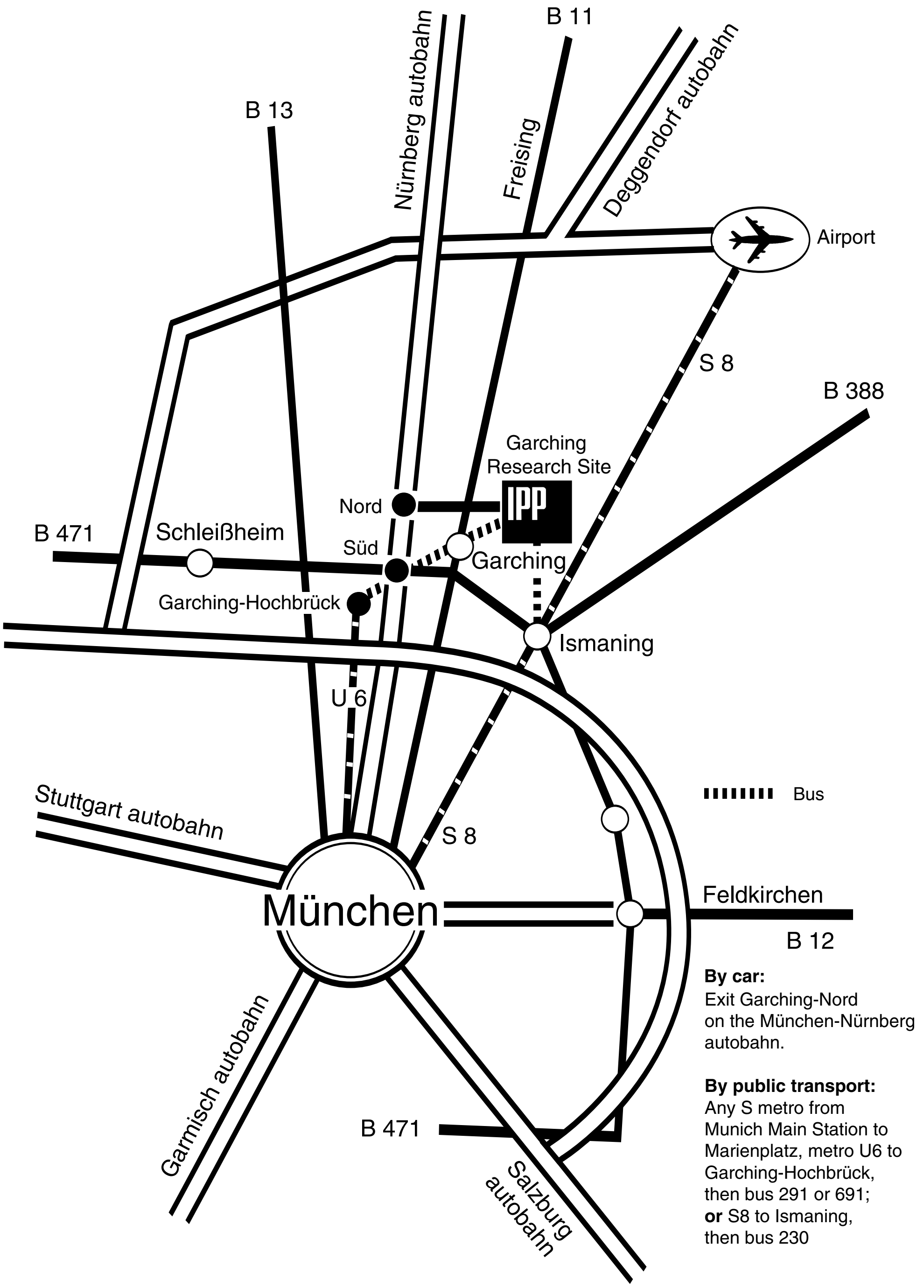

By car:
Exit Garching-Nord
on the München-Nürnberg
autobahn.

By public transport:
Any S metro from
Munich Main Station to
Marienplatz, metro U6 to
Garching-Hochbrück,
then bus 291 or 691;
or S8 to Ismaning,
then bus 230

How to reach Greifswald Branch Institute of IPP

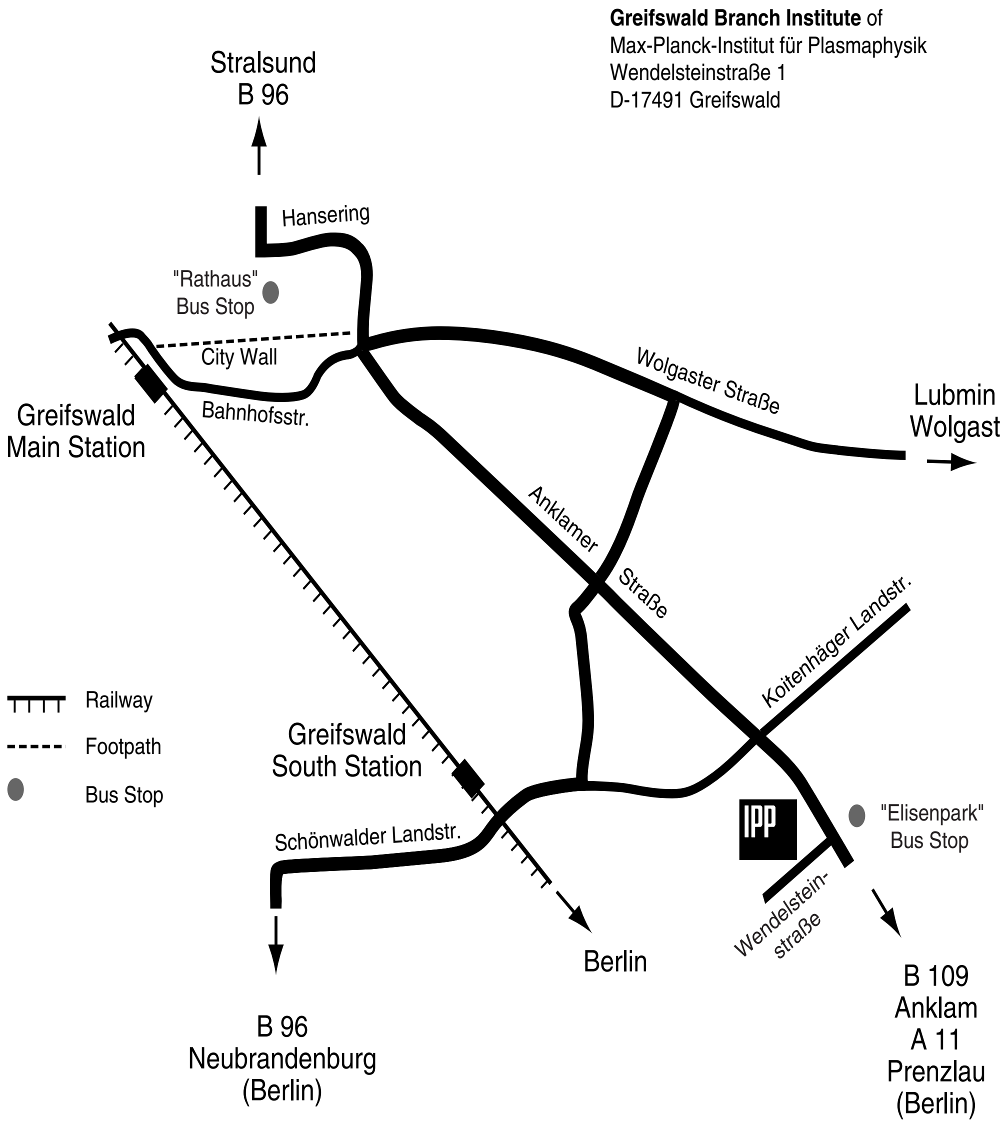

By air:
Via Berlin: from Berlin Tegel Airport by bus No. X9 to Zoologischer Garten, by train to Greifswald
Via Hamburg: from the airport to Main Railway Station, by train to Greifswald.

By car:
Via Berlin, Neubrandenburg to Greifswald **or** via Hamburg, Lübeck, Stralsund to Greifswald,
in Greifswald follow the signs "Max-Planck-Institut".

By bus:
From Greifswald Railway Station walking distance of 10 minutes to the "Rathaus" (Town Hall).
Then from "Rathaus's" stop by bus No. 2 or 3 to the "Elisenpark's" stop.

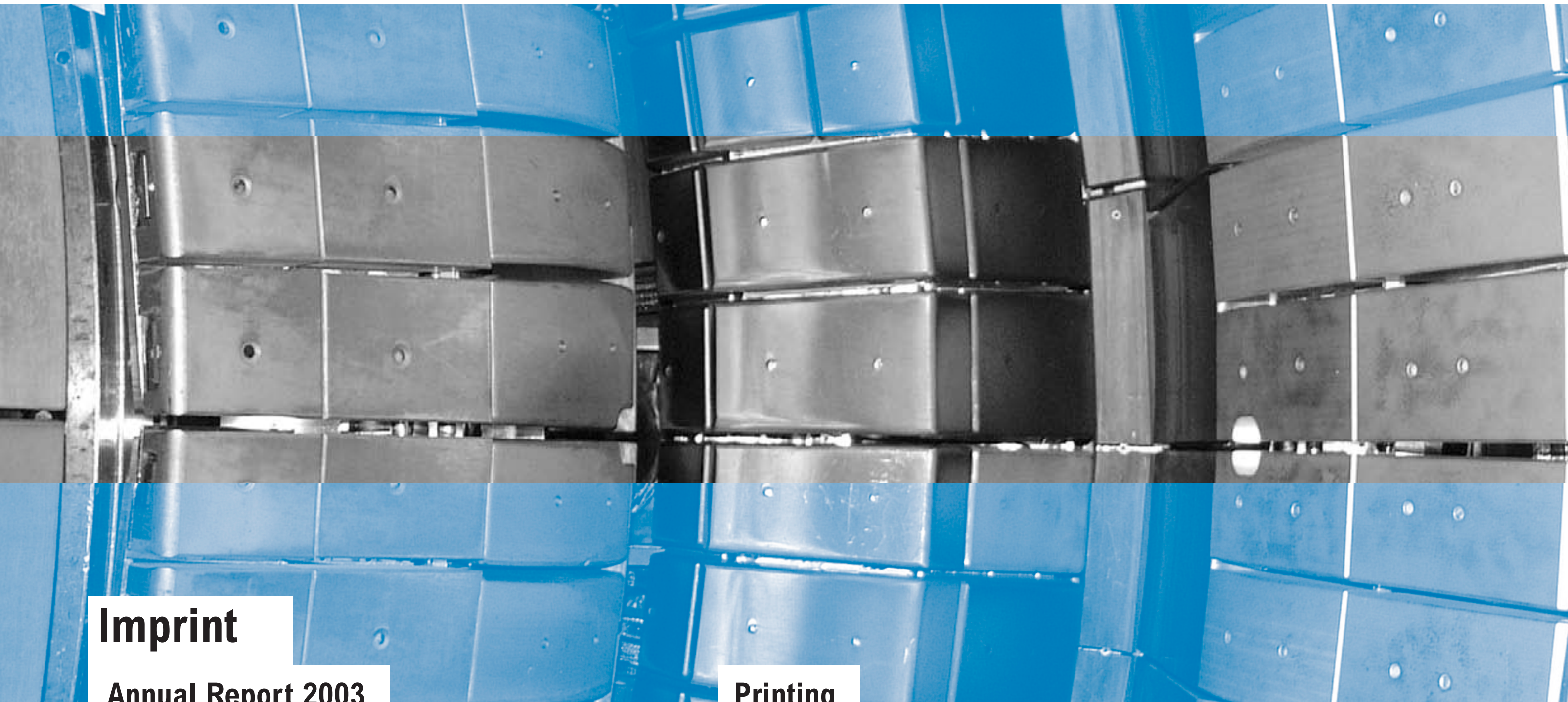

Imprint

Annual Report 2003

Max-Planck-Institut für Plasmaphysik (IPP)
Boltzmannstrasse 2
85748 Garching bei München
Telephone (0 89) 32 99-01
Telefax (0 89) 32 99-22 00
http://www.ipp.mpg.de

Printing

Druckerei Behr, Scheyern-Fernhag

Printed in Germany
ISSN 0179-9347

Further Information
This work was performed under the terms of the agreement between Max-Planck-Institut für Plasmaphysik and the European Atomic Energy Community to conduct joint research in the field of plasma physics.